



RESEARCH REPORT

HEALTH
EFFECTS
INSTITUTE

Number 178
October 2013

National Particle Component Toxicity (NPACT) Initiative Report on Cardiovascular Effects

Sverre Vedal, Matthew J. Campen, Jacob D. McDonald,
Joel D. Kaufman, Timothy V. Larson, Paul D. Sampson,
Lianne Sheppard, Christopher D. Simpson,
and Adam A. Szpiro

Section 1. NPACT Epidemiologic Study of Components of Fine Particulate Matter and Cardiovascular Disease in the MESA and WHI-OS Cohorts

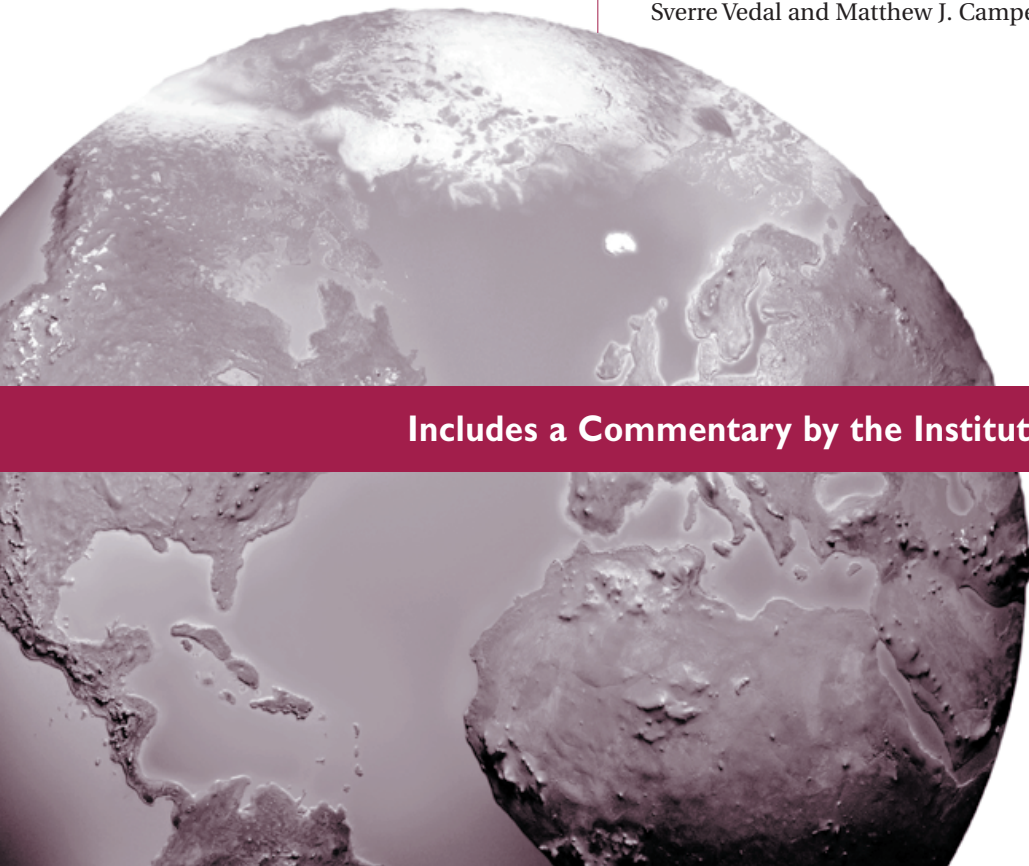
Sverre Vedal, Sun-Young Kim, Kristin A. Miller,
Julie Richman Fox, Silas Bergen, Timothy Gould,
Joel D. Kaufman, Timothy V. Larson, Paul D. Sampson,
Lianne Sheppard, Christopher D. Simpson,
and Adam A. Szpiro

Section 2. NPACT Animal Toxicologic Study of Cardiovascular Effects of Mixed Vehicle Emissions Combined with Non-vehicular Particulate Matter

Matthew J. Campen, Amie K. Lund, Steven K. Seilkop,
and Jacob D. McDonald

Section 3. Integrated Discussion

Sverre Vedal and Matthew J. Campen

A grayscale image of a globe showing the continents of North and South America, serving as a background for the bottom half of the page.

Includes a Commentary by the Institute's NPACT Review Panel

National Particle Component Toxicity (NPACT) Initiative Report on Cardiovascular Effects

Sverre Vedal, Matthew J. Campen, Jacob D. McDonald, Joel D. Kaufman,
Timothy V. Larson, Paul D. Sampson, Lianne Sheppard,
Christopher D. Simpson, and Adam A. Szpiro

with a Commentary by the NPACT Review Panel

Research Report 178
Health Effects Institute
Boston, Massachusetts

Trusted Science • Cleaner Air • Better Health

Publishing history: This document was posted at www.healtheffects.org in October 2013.

Citation for Research Report 178 in its entirety:

Vedal S, Campen MJ, McDonald JD, Kaufman JD, Larson TV, Sampson PD, Sheppard L, Simpson CD, Szpiro AA. 2013. National Particle Component Toxicity (NPACT) Initiative Report on Cardiovascular Effects. Research Report 178. Health Effects Institute, Boston, MA.

Citation for Section 1 only:

Vedal S, Kim S-Y, Miller KA, Fox JR, Bergen S, Gould T, Kaufman JD, Larson TV, Sampson PD, Sheppard L, Simpson CD, Szpiro AA. 2013. Section 1. NPACT epidemiologic study of components of fine particulate matter and cardiovascular disease in the MESA and WHI-OS cohorts. In: National Particle Component Toxicity (NPACT) Initiative Report on Cardiovascular Effects. Research Report 178. Health Effects Institute, Boston, MA.

Citation for Section 2 only:

Campen MJ, Lund AK, Seilkop SK, McDonald JD. 2013. Section 2. NPACT animal toxicologic study of cardiovascular effects of mixed vehicle emissions combined with non-vehicular particulate matter. In: National Particle Component Toxicity (NPACT) Initiative Report on Cardiovascular Effects. Research Report 178. Health Effects Institute, Boston, MA.

© 2013 Health Effects Institute, Boston, Mass., U.S.A. Asterisk Typographics, Barre, Vt., Compositor. Printed by Recycled Paper Printing, Boston, Mass. Library of Congress Catalog Number for the HEI Report Series: WA 754 R432.

♻️ Cover paper: made with at least 55% recycled content, of which at least 30% is post-consumer waste; free of acid and elemental chlorine. Text paper: made with 100% post-consumer waste recycled content; acid free; no chlorine used in processing. The book is printed with soy-based inks and is of permanent archival quality.

CONTENTS

About HEI	vii
About This Report	ix
Contributors	xi
PREFACE: HEI's Research Program on Particle Component Toxicity	xiii
HEI STATEMENT	1
INVESTIGATORS' REPORT <i>by Vedal et al.</i>	5
OVERALL ABSTRACT	5
OVERALL INTRODUCTION	6
SECTION I. NPACT Epidemiologic Study of Components of Fine Particulate Matter and Cardiovascular Disease in the MESA and WHI-OS Cohorts	9
ABSTRACT	9
OVERVIEW	10
SPECIFIC AIM	12
THE MESA ANALYSES	12
Introduction and Study Design	12
The MESA Cohort	12
MESA Exposure Data	13
Source Apportionment	24
Building and Validating the Spatiotemporal Exposure Model	43
Building and Validating the National Spatial Exposure Model	64
Secondary Estimates of Exposure	69
Analysis of Health Effects	69
THE WHI-OS ANALYSES	91
Introduction and Study Design	91
The WHI-OS Cohort	92
National Spatial Model Predictions	94
Secondary Exposure Estimates	96
Analysis of Health Effects	97
DISCUSSION	110
Main Health Effects Findings	110
Estimation of Exposure	111
Interpretation and Limitations of the Findings	115
CONCLUSIONS	119
ACKNOWLEDGMENTS	120

Research Report 178

REFERENCES	120
APPENDIX A: HEI Quality Assurance Statement	122
APPENDICES AVAILABLE ON THE WEB	123
ABOUT THE AUTHORS	123
Contributors	125
OTHER PUBLICATIONS RESULTING FROM THIS RESEARCH	126
ABBREVIATIONS AND OTHER TERMS	126
SECTION 2. NPACT Animal Toxicologic Study of Cardiovascular Effects of Mixed Vehicle Emissions Combined with Non-vehicular Particulate Matter	129
ABSTRACT	129
Background	129
Methods	129
Results	129
Conclusions	130
INTRODUCTION	130
SPECIFIC AIMS	132
METHODS AND STUDY DESIGN	132
Exposure Atmospheres	132
Biologic Endpoints	137
QUALITY ASSURANCE	140
RESULTS	140
Exposure Atmosphere Composition	140
Biologic Responses	144
Multiple Additive Regression Tree Analysis	154
DISCUSSION	160
IMPLICATIONS OF FINDINGS	164
ACKNOWLEDGMENTS	165
REFERENCES	165
APPENDICES AVAILABLE ON THE WEB	167
ABOUT THE AUTHORS	168
OTHER PUBLICATION RESULTING FROM THIS RESEARCH	168
ABBREVIATIONS AND OTHER TERMS	168

Research Report 178

SECTION 3. Integrated Discussion	171
INTEGRATING THE EPIDEMIOLOGIC AND TOXICOLOGIC STUDIES	171
TOXICOLOGIC AND EPIDEMIOLOGIC EXPOSURES	171
TOXICOLOGIC AND EPIDEMIOLOGIC ENDPOINTS	173
INTEGRATING EPIDEMIOLOGIC AND TOXICOLOGIC FINDINGS	173
Sulfate	174
Nitrate	175
Mixed Vehicular Engine Emissions	175
Road Dust and Crustal Sources	176
Organic Carbon	176
Sulfur Dioxide	176
SUMMARY AND SUGGESTIONS FOR IMPROVING INTEGRATION	176
REFERENCES	177
ABBREVIATIONS AND OTHER TERMS	178
COMMENTARY <i>by the NPACT Review Panel</i>	179
INTRODUCTION	179
SCIENTIFIC AND REGULATORY BACKGROUND	180
PM Characteristics, Components, and Sources	180
Epidemiologic Evidence	182
Toxicologic Evidence	183
Integrating Epidemiologic and Toxicologic Approaches in NPACT	184
Specific Aims	184
SECTION I: EPIDEMIOLOGY STUDY	186
Introduction	186
Exposure Modeling for the MESA and WHI-OS Studies	186
Evaluation of the MESA and WHI-OS Exposure Assessment	188
Overview of the MESA Cohort Study	189
Key Results for the MESA Cohort	191
Evaluation of the MESA Cohort Study	193
WHI-OS Cohort Overview	195
Key Results from the WHI-OS Cohort	197
Evaluation of the WHI-OS Cohort Study	199
WHI-OS Study Conclusions	202

Research Report 178

SECTION 2: TOXICOLOGY STUDY	202
Specific Aims	202
Approach	202
Summary of Key Toxicologic Results	204
Evaluation of the Toxicology Study	207
OVERALL EVALUATION OF THE VEDAL REPORT	213
PM _{2.5} Components and Cardiovascular Outcomes in Humans	213
MVE and PM _{2.5} Components and Cardiovascular Outcomes in Mice	215
Summary and Conclusions for the Vedal Report	215
ACKNOWLEDGMENTS	216
REFERENCES	216
ABBREVIATIONS AND OTHER TERMS	221
SYNTHESIS OF THE NPACT INITIATIVE <i>by the NPACT Review Panel</i>	223
INTRODUCTION	223
INITIAL OBJECTIVES OF THE NPACT INITIATIVE	223
DATA AND STUDY DESIGN	224
PM Composition Data	224
Linking PM Components and Sources to Health Outcomes	225
Estimating Exposure Using Air Quality Data	226
Single-Pollutant and Multipollutant Models	227
Approaches to Animal Inhalation Exposures	227
COMPARING KEY FINDINGS ACROSS THE STUDIES	228
REFLECTIONS ON THE MAIN FINDINGS	231
ACKNOWLEDGMENTS	232
REFERENCES	232
ABBREVIATIONS AND OTHER TERMS	233
Related HEI Publications	235
HEI Board, Committees, and Staff	237

ABOUT HEI

The Health Effects Institute is a nonprofit corporation chartered in 1980 as an independent research organization to provide high-quality, impartial, and relevant science on the effects of air pollution on health. To accomplish its mission, the institute

- Identifies the highest-priority areas for health effects research;
- Competitively funds and oversees research projects;
- Provides intensive independent review of HEI-supported studies and related research;
- Integrates HEI's research results with those of other institutions into broader evaluations; and
- Communicates the results of HEI's research and analyses to public and private decision makers.

HEI typically receives half of its core funds from the U.S. Environmental Protection Agency and half from the worldwide motor vehicle industry. Frequently, other public and private organizations in the United States and around the world also support major projects or research programs. For the research funded under the National Particle Component Toxicity initiative, HEI received additional funds from the American Forest & Paper Association, American Iron and Steel Institute, American Petroleum Institute, ExxonMobil, and Public Service Electric and Gas.

HEI has funded more than 280 research projects in North America, Europe, Asia, and Latin America, the results of which have informed decisions regarding carbon monoxide, air toxics, nitrogen oxides, diesel exhaust, ozone, particulate matter, and other pollutants. These results have appeared in the peer-reviewed literature and in more than 200 comprehensive reports published by HEI.

HEI's independent Board of Directors consists of leaders in science and policy who are committed to fostering the public–private partnership that is central to the organization. The Health Research Committee solicits input from HEI sponsors and other stakeholders and works with scientific staff to develop a Five-Year Strategic Plan, select research projects for funding, and oversee their conduct. The Health Review Committee, which has no role in selecting or overseeing studies, works with staff to evaluate and interpret the results of funded studies and related research. For the NPACT studies, a special NPACT Review Panel — comprising Review Committee members and outside experts — fulfilled that role.

All project results and accompanying comments by the Health Review Committee are widely disseminated through HEI's Web site (www.healtheffects.org), printed reports, newsletters and other publications, annual conferences, and presentations to legislative bodies and public agencies.

ABOUT THIS REPORT

Research Report 178, *National Particle Component Toxicity (NPACT) Initiative Report on Cardiovascular Effects*, presents a research project funded by the Health Effects Institute and conducted by Dr. Sverre Vedal of the Department of Environmental and Occupational Health Sciences, University of Washington School of Public Health, Seattle, and his colleagues (Section 1), and Dr. Matthew J. Campen of the University of New Mexico College of Pharmacy, and collaborators at the Lovelace Respiratory Research Institute, both in Albuquerque, New Mexico (Section 2). This report contains the following sections:

The HEI Statement, prepared by staff at HEI, is a brief, nontechnical summary of the study and its findings; it also briefly describes the HEI NPACT Review Panel's comments on the study.

The Investigators' Report comprises Section 1 (the epidemiologic studies), prepared by Vedal and colleagues, and Section 2 (the toxicologic study), prepared by Campen and colleagues. Each describes the scientific background, aims, methods, results, and conclusions of that portion of the study. Also included is an integrated discussion of the studies (Section 3) authored by Drs. Vedal and Campen.

The Commentary, prepared by members of the HEI NPACT Review Panel (see below) with the assistance of HEI staff, places the study in a broader scientific context, points out its strengths and limitations, and discusses remaining uncertainties and implications of the study's findings for public health and future research.

The Synthesis, also prepared by the HEI NPACT Review Panel, provides a summary evaluation of the NPACT initiative, including this Research Report and the accompanying HEI Research Report 177 by Dr. Morton Lippmann and colleagues, and puts the results of the NPACT initiative in a broader context.

This report has gone through HEI's rigorous review process. When an HEI-funded study is completed, the investigators submit a draft final report presenting the background and results of the study. This draft report was evaluated by the HEI NPACT Review Panel, an independent panel of distinguished scientists, including some members of the HEI Health Review Committee, who had no involvement in selecting or overseeing these studies. Comments from the Panel were sent to the investigators, who revised their report as they considered appropriate. The revised report was again evaluated by the Panel, which then prepared the Commentary based on the final version of the report.

CONTRIBUTORS

HEI NPACT Oversight Committee

Mark Utell (Chair), *University of Rochester Medical Center; former chair, HEI Research Committee*

Wayne Cascio, *East Carolina University; currently at U.S. Environmental Protection Agency National Health and Environmental Effects Research Laboratory (resigned from the Committee in spring 2012)*

Kenneth Demerjian, *State University of New York at Albany; former member, HEI Research Committee*

Francesca Dominici, *Harvard School of Public Health*

Uwe Heinrich, *Fraunhofer Institute of Toxicology and Experimental Medicine; member, HEI Research Committee*

Petros Koutrakis, *Harvard School of Public Health*

Grace LeMasters, *University of Cincinnati College of Medicine; member, HEI Research Committee*

Ira Tager, *University of California–Berkeley School of Public Health; former member, HEI Research Committee*

HEI NPACT Review Panel

Bert Brunekreef (Cochair), *University of Utrecht Institute of Risk Assessment Sciences; member, HEI Review Committee*

Armistead Russell (Cochair), *Georgia Institute of Technology School of Civil and Environmental Engineering; member, HEI Review Committee*

Jesus Araujo, *David Geffen School of Medicine at University of California–Los Angeles*

Ben Armstrong, *London School of Hygiene and Tropical Medicine; member, HEI Review Committee*

Aruni Bhatnagar, *University of Louisville School of Medicine*

Jeff Brook, *Environment Canada*

Eric Edgerton, *Atmospheric Research and Analysis*

John Godleski, *Harvard School of Public Health and Harvard Medical School*

Gerard Hoek, *University of Utrecht Institute of Risk Assessment Sciences*

Barbara Hoffmann, *Heinrich Heine University Leibniz Research Institute for Environmental Medicine*

Neil Pearce, *London School of Hygiene and Tropical Medicine*

Jennifer Peel, *Colorado State University–Fort Collins*

Jay Turner, *Washington University School of Engineering*

Antonella Zanobetti, *Harvard School of Public Health*

PREFACE

HEI's Research Program on Particle Component Toxicity

INTRODUCTION

Findings from epidemiologic and controlled-exposure studies about the health effects of particulate matter (PM) have led the U.S. Environmental Protection Agency (EPA) and other regulatory agencies to establish mass-based ambient air quality standards for PM within a specific size range. PM with an aerodynamic diameter $\leq 2.5 \mu\text{m}$ (PM_{2.5}) is considered to be particularly important because the small particles can be easily inhaled. Because the composition of PM is complex, there has long been a question as to whether some components of the PM mixture are of greater public health concern than others. Obtaining this information would help focus efforts to reduce people's exposure by enabling the control of those sources that contribute most of the toxic components in the PM mixture.

Detailed information on PM_{2.5} composition began to be collected systematically in the year 1999, in what was then called the Speciation Trends Network (currently the Chemical Speciation Network [CSN]). In an effort to consolidate the available data from several data sources and make them more accessible to researchers, HEI funded the company Atmospheric and Environmental Research (AER) through a December 2003 Request for Proposals (RFP) (titled *To Create a Database of Air Pollutant Components*) to set up and maintain such a database. The resulting HEI Air Quality Database (<https://hei.aer.com>) was launched by AER in September 2005 and comprises data from the EPA's monitoring networks, particularly concentrations of PM_{2.5} components and gaseous pollutants at and near sites in the CSN and state, local, and tribal air monitoring stations. Currently, the database contains information on speciated PM components and gaseous pollutants at these sites for the years 2000 to the present.

While the Air Quality Database was under construction, HEI issued Request for Applications (RFA) 05-1-A, *Conducting Full Studies to Compare Characteristics of PM Associated with Health Effects*. Its goal was to

support integrated multidisciplinary studies — including epidemiology, toxicology, exposure science, and statistics — to investigate the health effects of PM components in humans and animal models at locations across the United States where PM sources and components differ. The comparison of PM component effects was to be made in the context of the contribution of gaseous copollutants to the air pollution mixture and its health effects, as well as to PM-related toxicity and health effects.

RFA 05-1-A was accompanied by RFA 05-1-B, *Conducting Planning or Demonstration Studies to Design a Major Study to Compare Characteristics of PM Associated with Health Effects*, in order to provide a smaller amount of funding to multidisciplinary study teams that had not previously worked together. These teams would then conduct planning or demonstration studies to gather and analyze the data necessary to design a full study of the toxicity of PM components, similar to those funded under RFA 05-1-A.

DESCRIPTION OF THE NATIONAL PARTICLE COMPONENT TOXICITY INITIATIVE

HEI's National Particle Component Toxicity (NPACT) initiative was launched in view of emerging evidence that the composition of PM is different in different places as well as that there are geographic differences in the toxicity of PM across the country. Given the complexity and importance of these issues, HEI organized several workshops and held extensive discussions and consultations about the best approaches to investigate these questions. These deliberations resulted in the publication of several RFAs and the funding of two major studies. The primary goal of the NPACT initiative was to determine if components of PM from various sources are equally toxic to health, or if some components are more toxic than others. A summary of the studies funded under the NPACT initiative is provided in the table.

Preface

HEI's NPACT Studies^a

RFA/RFP Investigator (Institution)	Study or Report Title	Citation or PI
RFP December 2003: To Create a Database of Air Pollutant Components		
Christian Seigneur (AER)	Creation of an Air Pollutant Database for Epidemiologic Studies	https://hei.aer.com
RFA 04-2: Walter A. Rosenblith New Investigator Award		
Michelle Bell (Yale University)	Assessment of the Health Impacts of Particulate Matter Characteristics	Bell 2012
RFA 05-I-A: Conducting Full Studies to Compare Characteristics of PM Associated with Health Effects		
Morton Lippmann (New York University)	National Particle Component Toxicity (NPACT) Initiative: Integrated Epidemiologic and Toxicologic Studies of the Health Effects of Particulate Matter Components	
	NPACT Study 1. Subchronic Inhalation Exposure of Mice to Concentrated Ambient PM _{2.5} from Five Airsheds	Chen
	NPACT Study 2. In Vitro and In Vivo Toxicity of Exposure to Coarse, Fine, and Ultrafine PM from Five Airsheds	Gordon
	NPACT Study 3. Time-Series Analysis of Mortality, Hospitalizations, and Ambient PM _{2.5} and Its Components	Ito
Sverre Vedal (University of Washington)	NPACT Study 4. Mortality and Long-Term Exposure to PM _{2.5} and Its Components in the American Cancer Society's Cancer Prevention Study II Cohort	Thurston
	National Particle Component Toxicity (NPACT) Initiative Report on Cardiovascular Effects. Section 1. NPACT Epidemiologic Study of Components of Fine Particulate Matter and Cardiovascular Disease in the MESA and WHI-OS Cohorts	Vedal
	National Particle Component Toxicity (NPACT) Initiative Report on Cardiovascular Effects. Section 2. NPACT Animal Toxicologic Study of Cardiovascular Effects of Mixed Vehicle Emissions Combined with Non-vehicular Particulate Matter	Campen
RFA 05-I-B: Conducting Planning or Demonstration Studies to Design a Major Study to Compare Characteristics of PM Associated with Health Effects		
JoAnn Lighty (University of Utah)	A planning study to investigate the impacts of dust and vehicles on acute cardiorespiratory responses in the arid Southwest.	Lighty et al. 2008 (unpublished report)

^a RFA indicates request for applications; RFP request for proposals.

HEI funded two major NPACT studies under RFA 05-I-A, which combined coordinated efforts in (1) exposure assessment using advanced techniques, (2) epidemiology focusing on PM components and long-term health effects, and (3) toxicology focusing on endpoints that are relevant to the cardiovascular and other health effects observed in epidemiologic studies. Each main study comprised several studies, led by co-investigators, looking at different aspects of the questions regarding the cardiovascular and other health effects of short- and long-term exposure to PM components, using exposure

assessment, epidemiologic approaches, and toxicologic approaches that would complement each other.

The two major NPACT studies were led by Dr. Morton Lippmann at New York University and Dr. Sverre Vedal at the University of Washington. Dr. Lippmann's study comprised two toxicologic studies led by Drs. Lung-Chi Chen and Terry Gordon and two epidemiologic studies led by Drs. Kazuhiko Ito and George Thurston. Dr. Vedal's study comprised an epidemiologic study of two cohorts, as described below, and a toxicologic study conducted by Drs. Matt Campen

at the University of New Mexico and Jacob McDonald at the Lovelace Respiratory Research Institute.

At the time of funding for the two integrated NPACT studies, HEI was already supporting a time-series epidemiologic study of PM components by Dr. Michelle Bell at Yale University (RFA 04-2, *Walter A. Rosenblith New Investigator Award*). Because the topic was very relevant to the NPACT initiative, HEI decided to include this study under the broader umbrella of NPACT (although the study was reviewed separately and published earlier).

Oversight of the NPACT Studies

Given the complexity of the NPACT studies, the HEI Research Committee formed an NPACT Oversight Committee composed of Research Committee members and additional technical experts. The Oversight Committee met approximately annually with the investigator teams during the conduct of the study and provided advice and feedback on the study design, analytical plans, and progress. The Oversight Committee members are listed on the Contributors page of this report.

In addition, HEI formed an NPACT Advisory Group, which included representatives from the EPA and industry sponsors of the NPACT studies, as well as other interested stakeholders. The advisory group met with the NPACT investigators to discuss study designs, progress, and other key issues.

Study by Lippmann et al.

In one of the two toxicologic studies, Drs. Chen and Lippmann used an animal inhalation approach to evaluate the effect of PM components on cardiovascular endpoints in vivo. They selected a mouse model of the development of atherosclerosis, the underlying cause of most chronic cardiovascular disease. The mice were exposed for 6 months to fine concentrated ambient particles (CAPs) collected at five different sites across the United States. These CAPs represented ambient pollutant mixtures from diverse locations that are dominated by different source categories, including coal combustion, wood smoke, and traffic. For their comprehensive assessment of the cardiovascular toxicity of PM_{2.5} components, Chen and Lippmann chose two cardiovascular endpoints (atherosclerotic plaque progression and heart rate variability) to represent the long- and short-term effects of CAPs exposure, respectively,

as well as a number of additional markers of inflammation, oxidative stress, and cardiovascular changes.

In the second toxicologic study, Dr. Gordon and colleagues used a combined in vitro and in vivo approach to analyze acute toxicity of a large number of PM samples collected at five locations identical or in close proximity to the sites studied by Chen and Lippmann. The overall goal was to examine the toxicity of exposure to PM of varying composition and size. At each location, daily PM filter samples were collected in three size fractions (coarse, fine, and ultrafine) over a 2-week period during two seasons. Each individual sample was tested in a cell culture or administered to mice by aspiration into the lung. In addition, the investigators conducted a longer-term study in two of the five locations, in which 100 daily samples were collected and administered to mice by aspiration.

In the first epidemiologic study, Dr. Ito and colleagues examined associations between short-term exposure to ambient air pollution and mortality (for all ages) and hospital admissions among people 65 years or older, using a multicity two-stage time-series study design. The investigators based their analyses on exposure to ambient concentrations of individual components of PM_{2.5}, using CSN data from 150 cities in the United States and a subset of 64 cities where gaseous pollutant data were also available. The investigators also conducted source apportionment, partitioning the daily PM_{2.5} mass into separate factors attributed to different source categories. Mortality data were available for the years 2000 to 2006, and hospitalization data for the years 2000 to 2008. The investigators ran city-specific analyses and combined the results using second-stage random effects models.

In the second epidemiologic study, Dr. Thurston and colleagues expanded previous analyses of the American Cancer Society's Cancer Prevention Study II (CPS-II) cohort. They used data from the cohort to evaluate associations between long-term exposure to speciated components of PM_{2.5} and all-cause, cardiovascular, and pulmonary mortality during the years 1982 to 2004. This analysis included approximately 450,000 members of the cohort residing in the 100 metropolitan statistical areas for which measurement data for PM_{2.5} components were available. In primary analyses, the investigators averaged all available measurements of 24-hour PM_{2.5} component concentrations obtained from the CSN for the years 2000 to 2005. In secondary analyses,

they constructed source categories using the PM_{2.5} component data. They also applied a novel approach to estimate the relative impacts of component mixtures in a multipollutant environment, using a total relative risk impact method.

Study by Vedal et al.

Dr. Vedal's epidemiologic study assessed the effects of long-term exposure to fine PM components and emission sources on cardiovascular endpoints, using data from two established cohort studies sponsored by the National Heart, Lung, and Blood Institute (specifically, the Women's Health Initiative-Observational Study [WHI-OS] and the Multi-Ethnic Study of Atherosclerosis [MESA]). The WHI-OS cohort included more than 93,000 postmenopausal women, between 50 and 79 years old, from 46 U.S. cities. They were evaluated at baseline between 1994 and 1998 for cardiovascular disease risk factors and followed annually through 2005. In addition, two five-year extension studies were initiated in 2005 and 2010. The MESA cohort study recruited more than 6000 participants without known heart disease between 2000 and 2002. Participants were from diverse ethnic or racial groups (major categories were white non-Hispanic, African American, Chinese American, and Hispanic), were between 45 and 84 years old, and lived in one of six metropolitan areas: New York, New York; Los Angeles, California; Chicago, Illinois; Winston-Salem, North Carolina; St. Paul, Minnesota; and Baltimore, Maryland.

The specific aim of the Vedal team's analyses within both cohorts was to identify the chemical components of ambient PM that contribute to the incidence of cardiovascular events. The major hypothesis was that PM_{2.5} components in primary emissions from motor vehicles have a greater effect on long-term cardiovascular toxicity than do inorganic or crustal components in secondary PM.

In the WHI-OS analyses, Vedal and colleagues assessed associations of concentrations of PM_{2.5} and four major components — elemental carbon, organic carbon, sulfur, and silicon measured at government monitoring sites across the United States — with cardiovascular health outcomes. These outcomes included myocardial infarction, stroke, mortality due to cardiovascular or cerebrovascular diseases, hospitalization for coronary heart disease or angina pectoris, and

coronary revascularization procedures including bypass surgery and angioplasty.

In the MESA analyses, Vedal and colleagues assessed associations of concentrations of PM_{2.5} and its components and subclinical markers of atherosclerosis, primarily coronary artery calcification and carotid intima-media thickness. The investigators developed a spatiotemporal exposure model that included estimates at the individual home level and a national spatial exposure model that used data from numerous monitoring sites to estimate spatial variability of specific PM_{2.5} components in the six metropolitan areas. The investigators focused some of their analyses on data from MESA-Air, an ancillary MESA study funded in 2004 by the EPA, which included monitoring at three additional locations: along the coast in Los Angeles, California; inland in Riverside, California; and in Rockland County, New York, a suburban area outside New York City.

The toxicology component of the Vedal study consisted of an animal inhalation study in which Apo-E knockout mice were exposed to a mixture of diesel and gasoline engine exhaust (MVE) or to non-vehicular particles (specifically, sulfate, nitrate, and road dust filtered to include only fine PM), or to combinations of MVE and non-vehicular particles. In addition, the investigators evaluated mice exposed to MVE gases only — with the particles filtered out — or to combinations of MVE gases with each of the non-vehicular particles listed above. The mice were exposed for 50 days and evaluated for markers of oxidative stress, inflammation, and cardiovascular outcomes. Responses were compared among mice exposed to the various mixtures and mice exposed to filtered air, providing an indication of which mixtures may be more toxic than others. In addition, the investigators used a statistical approach to evaluate the role of individual components of the mixtures.

Study by Bell

Dr. Bell evaluated short-term effects of PM components on mortality in 187 counties across the United States (as reported in her study *Assessment of the Health Impacts of Particulate Matter Characteristics* [2012]). She was one of the first researchers to make use of the data that would later make up the CSN database, and she applied the time-series approach

developed in the National Morbidity, Mortality, and Air Pollution Study (Samet et al. 2000) to look for associations between PM component concentrations and mortality and morbidity outcomes. Bell obtained data on PM_{2.5} total mass and on the mass of 52 chemical components of PM_{2.5} for air monitored in 187 counties in the continental United States for the period 2000 through 2005. She also collected data on daily admissions to hospitals for cardiovascular- and respiratory-related illnesses for the period 1999 through 2005 for Medicare enrollees 65 years or older. She began by characterizing how the chemical composition of PM_{2.5} varies regionally and seasonally in the United States. Subsequently, she evaluated whether the associations between short-term exposure to PM total mass and health effects followed regional and seasonal patterns, and whether the observed effects could in turn be explained by regional and seasonal variations in the chemical composition of PM_{2.5} (Bell 2012).

REVIEW OF THE NPACT STUDIES

Given the breadth and depth of the two major NPACT studies, HEI convened a special NPACT Review Panel, chaired by members of the HEI Review Committee and comprising twelve experts in medicine,

epidemiology, toxicology, statistics, atmospheric chemistry, and exposure. The members of the Panel were not involved in either conducting or overseeing the studies, and they subjected the studies to intensive peer review. The Panel and HEI scientific staff then produced the detailed Commentaries published in the reports to discuss the strengths and weaknesses of the studies, as well as the relevance of the findings to major air quality public health policy questions.

REFERENCES

- Bell ML. 2012. Assessment of the Health Impacts of Particulate Matter Characteristics. Research Report 161. Health Effects Institute, Boston, MA.
- Lighty J, Wendt J, Kelly K, Li WW, Staniswalis J, Sarnat J, Sarnat S, Holguin F, Witten M. 2008. A planning study to investigate the impacts of dust and vehicles on acute cardiorespiratory responses in the arid Southwest. Health Effects Institute, Boston, MA. Unpublished Report; available on Request.
- Samet JM, Dominici F, Zeger SL, Schwartz J, Dockery DW. 2000. Part I. Methods and methodologic issues. In: The National Morbidity, Mortality, and Air Pollution Study. Research Report 94. Health Effects Institute, Cambridge, MA.

HEI STATEMENT

Synopsis of Research Report 178

National Particle Component Toxicity (NPACT) Initiative Report on Cardiovascular Effects

BACKGROUND

Extensive epidemiologic evidence, as well as toxicologic evidence, supports an association between air pollution and adverse health effects, in particular cardiovascular disease (CVD). Because detailed insight is needed into whether certain components of the particulate matter (PM) mixture may be responsible for its toxicity and human health effects, HEI funded the National Particle Component Toxicity (NPACT) initiative. The initiative consisted of coordinated epidemiologic and toxicologic studies to evaluate the relative toxicity of various chemical and physical properties of PM and selected gaseous copollutants. The lead investigators were Drs. Sverre Vedal (for this report) and Morton Lippmann (for HEI Research Report 177). Given the strong associations between ambient PM concentrations and cardiovascular mortality and morbidity, the NPACT studies focused primarily on health outcomes and biologic markers related to CVD.

APPROACH

Vedal and colleagues at the University of Washington hypothesized that the cardiovascular health effects associated with long-term exposure to PM_{2.5} (PM with an aerodynamic diameter $\leq 2.5 \mu\text{m}$) are driven in large part by traffic-related sources. They used data from the Multi-Ethnic Study of Atherosclerosis (MESA) and the Women's Health Initiative–Observational Study (WHI-OS) cohorts. The MESA cohort comprised approximately 6800 participants (45 to 84 years old) living in six U.S. cities. Endpoints evaluated were two subclinical markers of atherosclerosis, carotid intima-media thickness (CIMT) and coronary artery calcium (CAC), measured at baseline and follow-up visits. The WHI-OS cohort comprised

approximately 90,000 postmenopausal women (50 to 79 years old) living in 45 U.S. cities. Outcomes included deaths from total CVD and from atherosclerotic and cerebrovascular disease (including stroke), as well as time to the first event (fatal and nonfatal) associated with CVD, including coronary heart disease and stroke.

What This Study Adds

- Vedal and colleagues' coordinated epidemiologic and toxicologic studies of the cardiovascular effects of PM components, with a focus on traffic sources, are an important addition to air quality and health research. In their study, they evaluated data from the MESA and WHI-OS cohorts and exposed mice to combinations of mixed vehicle engine emissions and non-vehicular PM.
- The investigators found strong evidence for associations of PM_{2.5}, organic carbon, and sulfur with subclinical and clinical outcomes in the cohorts, with less evidence for elemental carbon. Their toxicologic study provided strong evidence for effects of mixed vehicular engine exhaust and to a lesser extent exhaust gases on vascular markers in mice; non-vehicular PM induced few effects.
- The study has added to the evidence about long-term exposure to particulate air pollution and cardiovascular events and mortality, although the relative importance of traffic sources remains unclear. Because pollutant concentrations are often correlated, interpretations about specific components and sources remain limited.

This Statement, prepared by the Health Effects Institute, summarizes a research project funded by HEI and conducted by Dr. Sverre Vedal, Department of Environmental and Occupational Health Sciences, University of Washington School of Public Health, Seattle, WA, and colleagues. Research Report 178 contains the detailed Investigators' Report, a Commentary on the study prepared by the Institute's NPACT Review Panel, and a Synthesis by the Panel discussing the results of this study and those of HEI Research Report 177.

The investigators obtained concentrations for PM_{2.5}, sulfur, organic carbon (OC), elemental carbon (EC), and silicon (used as markers for specific source categories) from the U.S. Environmental Protection Agency's Chemical Speciation Network (CSN). They then estimated long-term pollutant concentrations to which participants in both cohorts had been exposed (referred to as the *national spatial model*). They also used data from additional measuring campaigns in the MESA cities to estimate spatially and temporally resolved concentrations at the participants' residences in the MESA cohort (referred to as the *spatiotemporal model*). The investigators also conducted source apportionment, primarily to assist in interpreting the PM_{2.5} component health effect estimates.

In a parallel toxicologic study, Matthew Campen of the University of New Mexico and colleagues at the Lovelace Respiratory Research Institute evaluated the role of mixed vehicular engine emissions (MVE) and its gaseous components in contributing to the adverse health effects of PM. They generated a mixture of diesel and gasoline emissions and exposed mice that are prone to developing atherosclerotic plaques to whole MVE or MVE gases only (i.e., without PM). They also generated primary sulfate, nitrate, and fine road dust and exposed the mice to combinations of such non-vehicular PM and MVE or MVE gases. They then assessed biomarkers of oxidative stress and vascular inflammation in the exposed mice. Campen and colleagues used multiple additive regression tree (MART) analysis to evaluate associations between the hundreds of compounds measured in the generated atmospheres and various biologic markers.

RESULTS AND INTERPRETATION

MESA Study Vedal and colleagues reported CIMT was significantly associated with exposure to PM_{2.5}, OC, and sulfur in both the spatiotemporal and national spatial models, although the risk estimates were generally small (see Figure). Relative risks for OC and sulfur were higher than for PM_{2.5} for the spatiotemporal model, but in the national spatial model, this was true only for the city-adjusted model for sulfur. The investigators reported no significant associations of CAC with PM_{2.5} in any model. When the spatiotemporal model of exposure was used in an analysis adjusted for city, relative risks for sulfur, EC, and OC became significant. In analyses using the national spatial model, the relative risk of OC

was elevated, and the relative risks for sulfur, EC, and OC were significant in the city-adjusted analyses.

In its independent review of the study, the HEI NPACT Review Panel commented that the analysis of subclinical cardiovascular effects is a promising direction for air pollution epidemiology. However, the Panel noted that the longitudinal analyses of CAC and CIMT (i.e., over several follow-up visits) were hampered by the short period of time between evaluations, leaving only the cross-sectional evaluation (i.e., at one time point across cities) with interpretable results. Furthermore, the Panel thought that the spatiotemporal model did not fully represent the spatial variability of locally variable components such as EC, which may have further resulted in a lack of associations. Overall, the Panel thought that further follow-up of the MESA cohort would be useful, including analyses of subclinical endpoints that were not covered in the current study (e.g., markers of inflammation and coagulation and other biomarkers).

WHI-OS Study Vedal and colleagues reported that total deaths from CVD and from atherosclerotic disease showed the strongest associations with OC; associations with PM_{2.5} and EC were marginal (see the Figure). Associations between deaths from cerebrovascular disease and exposure to OC were significant but less strong; they were not significant for PM_{2.5} or any of the other components. Associations of total CVD events with PM_{2.5} and sulfur were statistically significant, although small; a negative and marginal association was found for silicon. The only significant associations for coronary heart disease events were with sulfur and PM_{2.5}. Cerebrovascular disease events were significantly associated with OC and PM_{2.5} and marginally associated with sulfur. A significant negative association was observed with silicon. Additional analyses to compare the relative contributions of within- and between-city variances found mixed results.

The Panel noted that the WHI-OS study was well conducted and included a wide set of cardiovascular outcomes, including cerebrovascular outcomes and non-fatal events. The Panel was not surprised that this study found that the regionally varying pollutants — sulfur and OC — were more prominently associated with outcomes than more locally variable pollutants, such as EC. However, the Panel cautioned that nonsignificant results for such locally variable pollutants are not evidence of a lack of associations, given the study design and high

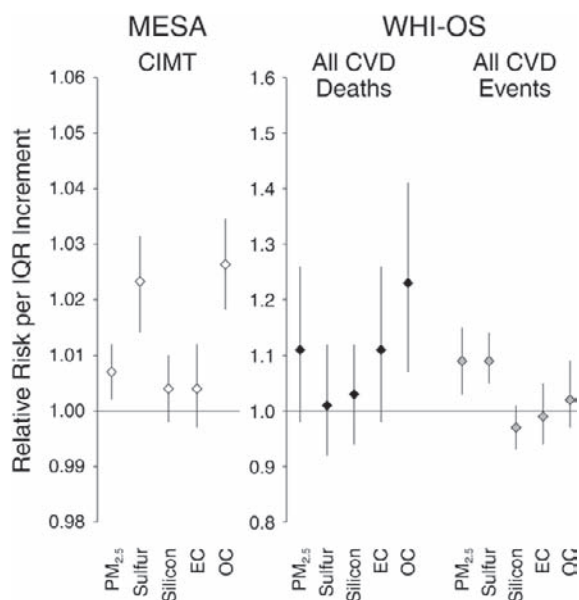


Figure. Associations found between selected pollutants and carotid intima-media thickness (CIMT) in the MESA cohort (left) and total cardiovascular disease mortality or events in the WHI-OS cohort (right). Data shown are relative risk estimates with 95% confidence intervals associated with an interquartile range (IQR) increment of baseline exposure using spatiotemporal model predictions (Model 3) for MESA data and national spatial model predictions for WHI-OS data. Note that the IQR varied by study, by pollutant, and by exposure model — for example, the IQRs for PM_{2.5} and sulfur were 3.9 µg/m³ and 0.25 µg/m³, respectively, in WHI-OS and 1.51 µg/m³ and 0.51 µg/m³, respectively, in MESA. Also note differences in the y-axis scales.

correlations between components (particularly, EC and OC). Overall, the Panel thought that the WHI-OS study had produced interesting results but that the data could be further explored with more locally focused exposure modeling strategies.

Exposure Assessment The Panel thought that the four components of interest were logical choices and that the focus on these markers was justified. The source apportionment provided reassurance that the selected components generally covaried with the factors, as expected, although none was unequivocally linked to vehicle emissions, which limited the investigators’ ability to assess the importance of traffic sources in the two cohorts.

The multiple exposure estimates used in the MESA study provided a good opportunity to gain new insight into how the choice of exposure model affected the results. The Panel noted that the ability of the models to predict national-scale patterns does not necessarily translate into an ability to predict patterns within a city and that developing a

reliable model is generally more difficult for within-city patterns.

Toxicologic Study Campen and colleagues reported that lipid peroxidation, a marker of oxidative stress, was increased in aortic tissue of mice exposed to various atmospheres, with the largest increase observed after exposure to MVE. Removing the particles from the atmosphere reduced these effects but did not fully eliminate them. In contrast, exposures to non-vehicular PM alone did not produce an effect. Infiltration of atherosclerotic plaques by macrophages increased after exposure to MVE and to MVE gases combined with either sulfate or nitrate. In contrast, plaque formation increased only after exposure to nitrate alone or nitrate combined with MVE gases, but not to the other atmospheres. The investigators reported less consistent changes in the other endpoints.

The Panel noted that Campen and colleagues had conducted a complex study with an impressive number of single and combined exposure atmospheres. The results suggested that the PM in MVE played a significant role in the induction of aortic lipid peroxidation, more so than MVE gases. These findings differ from those of previous studies from this laboratory, which found that the gaseous components in diesel or in gasoline exhaust induced oxidative stress. However, in the absence of exposures using MVE particles alone (i.e., without the gases), the role of MVE particles by themselves remains unclear.

Several caveats suggest a cautious interpretation of these results, including possible variability in aortic tissues because of sample collection procedures; small group sizes for certain endpoints resulting in insufficient power to find an effect; and some subjectivity in the method for assessing plaque densities. The Panel thought that the MART analysis was an interesting approach but that the interpretation remains limited because the number of independent atmospheres was small compared with the number of components measured and because daily variability in composition was not assessed.

CONCLUSIONS

The epidemiologic study by Vedal and colleagues has added to the evidence about long-term exposure to particulate air pollution and cardiovascular events and mortality, although the relative importance of traffic versus other sources of PM remains unclear. Given the often high correlations among pollutants

and the multiple sources of some components, interpretations about specific components and sources remain limited. The results of the toxicologic study support the notion that both particulate and gaseous components of vehicle exhaust play a role in the induction of various cardiovascular outcomes.

SYNTHESIS OF NPACT STUDIES BY LIPPMANN AND VEDAL

This section looks broadly at the approaches and results of the reports by Drs. Lippmann and Vedal and considers whether there is coherence and consistency in the epidemiologic and toxicologic results.

Both studies found that adverse health outcomes were consistently associated with sulfur and sulfate (markers primarily of coal and oil combustion) and with traffic-related pollutants, although the relative importance of the latter remains unclear, because exposure to traffic-related pollutants varies within metropolitan areas and thus is more subject to uncertainty than exposure to pollutants from other source categories. The results for sulfur and sulfate may have been more consistent because their concentrations were more accurately estimated (due to their spatial homogeneity) than concentrations of other pollutants.

Biomass combustion, crustal sources, and related components were not generally associated with short- or long-term epidemiologic findings in these studies, but there were only a limited number of cities where these sources and components were likely to be measured consistently. The possibility remains that biomass combustion contributed to OC concentrations and thus to its associations with cardiovascular outcomes. There were few consistent

associations with other components or sources, although the Panel cautioned that this is not conclusive evidence that these components and sources do not have adverse health effects. Further analyses of some of these sources are warranted.

Both studies highlight how important the CSN is to research on the health effects of components of air pollution and to air quality management. Neither study could have been performed without CSN data, although the studies highlighted some limitations that suggest that further efforts would be helpful to characterize EC, OC, and metals (i.e., combustion and traffic-related components); to lower the detection limits of some components; and to collect daily measurements.

The NPACT studies, which are to date the most systematic effort to combine epidemiologic and toxicologic analyses of these questions, found associations of secondary sulfate and, to a somewhat lesser extent, traffic sources with health effects. But the Panel concluded that the studies do not provide compelling evidence that any specific source, component, or size class of PM may be excluded as a possible contributor to PM toxicity. If greater success is to be achieved in isolating the effects of pollutants from mobile and other major sources, either as individual components or as a mixture, more advanced approaches and additional measurements will be needed so that exposure at the individual or population level can be assessed more accurately. Such enhanced understanding of exposure and health effects will be needed before it can be concluded that regulations targeting specific sources or components of PM_{2.5} will protect public health more effectively than continuing to follow the current practices of targeting PM_{2.5} mass as a whole.

National Particle Component Toxicity (NPACT) Initiative Report on Cardiovascular Effects

Sverre Vedal, Matthew J. Campen, Jacob D. McDonald, Joel D. Kaufman, Timothy V. Larson,
Paul D. Sampson, Lianne Sheppard, Christopher D. Simpson, and Adam A. Szpiro

Department of Environmental and Occupational Health Sciences, University of Washington, Seattle (S.V., J.D.K., T.V.L., L.S., C.D.S.); Department of Statistics, University of Washington, Seattle (P.D.S.); Department of Epidemiology and Medicine, University of Washington, Seattle (J.D.K.); Department of Civil and Environmental Engineering, University of Washington, Seattle (T.V.L.); Department of Biostatistics, University of Washington, Seattle (L.S., A.A.S.); Department of Pharmaceutical Sciences, University of New Mexico, Albuquerque (M.J.C.); Environmental Respiratory Health Program, and Chemistry and Inhalation Exposure Program, Lovelace Respiratory Research Institute, Albuquerque, New Mexico (J.D.M.)

OVERALL ABSTRACT

Epidemiologic and toxicologic studies were carried out in concert to provide complementary insights into the compositional features of ambient particulate matter (PM*) that produce cardiovascular effects. In the epidemiologic studies, we made use of cohort data from two ongoing studies — the Multi-Ethnic Study of Atherosclerosis (MESA) and the Women's Health Initiative–Observational Study (WHI-OS) — to investigate subclinical markers of atherosclerosis and clinical cardiovascular events. In the toxicologic study, we used the apolipoprotein E null (ApoE^{-/-}) hypercholesterolemic mouse model to assess cardiovascular effects of inhalation exposure to various atmospheres containing laboratory-generated pollutants.

This Investigators' Report is one part of Health Effects Institute Research Report 178, which also includes a Commentary by the NPACT Review Panel, an HEI Statement about the research project, and a Synthesis relating this report to Research Report 177. Correspondence concerning the Investigators' Report may be addressed to Dr. Sverre Vedal, 4225 Roosevelt Way NE, #100, Department of Environmental and Occupational Health Sciences, University of Washington School of Public Health, Seattle, WA 98105; svedal@uw.edu.

Although this document was produced with partial funding by the United States Environmental Protection Agency under Assistance Award CR-83234701 to the Health Effects Institute, it has not been subjected to the Agency's peer and administrative review and therefore may not necessarily reflect the views of the Agency, and no official endorsement by it should be inferred. For the research funded under the National Particle Component Toxicity initiative, HEI received additional funds from the American Forest & Paper Association, American Iron and Steel Institute, American Petroleum Institute, ExxonMobil, and Public Service Electric and Gas. The contents of this document also have not been reviewed by private party institutions, including those that support the Health Effects Institute; therefore, it may not reflect the views or policies of these parties, and no endorsement by them should be inferred.

* A list of abbreviations and other terms appears at the end of each section of the Investigators' Report.

In the epidemiologic studies, individual-level residential concentrations of fine PM, that is, PM with an aerodynamic diameter of 2.5 μm or smaller (PM_{2.5}), PM_{2.5} components (primarily elemental carbon [EC] and organic carbon [OC], silicon, and sulfur but also sulfate, nitrate, nickel, vanadium, and copper), and the gaseous pollutants sulfur dioxide and nitrogen dioxide were estimated using spatio-temporal modeling and other exposure estimation approaches. In the MESA cohort data, evidence for associations with increased carotid intima-media thickness (CIMT) was found to be strongest for PM_{2.5}, OC, and sulfur, as well as for copper in more limited analyses; the evidence for this was found to be weaker for silicon, EC, and the other components and gases. Similarly, in the WHI-OS cohort data, evidence for associations with incidence of cardiovascular mortality and cardiovascular events was found to be good for OC and sulfur, respectively, and for PM_{2.5}; the evidence for this was found to be weaker for EC and silicon. Source apportionment based on extensive monitoring data in the six cities in the MESA analyses indicated that OC represented secondary formation processes as well as primary gasoline and biomass emissions, that sulfur represented largely secondary inorganic aerosols, and that copper represented brake dust and diesel emissions.

In the toxicologic study, hypercholesterolemic mice were exposed for 50 days to atmospheres containing mixed vehicular engine emissions (MVE) consisting of mixed gasoline and diesel engine exhaust or to MVE-derived gases only (MVEG). Mice were also exposed to atmospheres containing sulfate, nitrate, or road dust, either alone or mixed with MVE or MVEG. Sulfate alone or in combination with MVE was associated with increased aortic reactivity. All

exposures to atmospheres containing MVE (including a combination of MVE with other PM) were associated with increases in plasma and aortic oxidative stress; exposures to atmospheres containing only sulfate or nitrate were not. Exposure to MVE and to MVEG combinations except those containing road dust resulted in increased monocyte/macrophage sequestration in aortic plaque (a measure of plaque inflammation). Exposure to all atmospheres except those containing nitrate was associated with enhanced aortic vasoconstriction. Exposure to the MVEG was an independent driver of lipid peroxidation, matrix metalloproteinase (MMP) activation, and vascular inflammation.

The epidemiologic and toxicologic study designs were intended to complement each other. The epidemiologic studies provided evidence in real-world human settings, and the toxicologic study directly assessed the biologic effects of various pollutant mixtures (in a way that is not possible in epidemiologic studies) by examining endpoints that probably underlie the subclinical and clinical cardiovascular endpoints examined in the epidemiologic studies. The epidemiologic studies were not suited to determining whether the observed associations were caused by direct effects of individual pollutants or by the mixtures in which individual pollutants are found. These studies were consistent in finding that OC and sulfate had the strongest evidence for associations with the cardiovascular disease endpoints, with much weaker evidence for EC and silicon. Both OC and sulfate reflected a large secondary aerosol component. Results from the toxicologic study indicated, for the most part, that MVE and mixtures of MVE and MVEG with other PM pollutants were important in producing the toxic cardiovascular effects found in the study. Further work on the effects of pollutant mixtures and secondary aerosols should allow better understanding of the pollution components and sources most responsible for the adverse cardiovascular effects of air pollution exposure.

OVERALL INTRODUCTION

Associations between estimates of long-term population exposures to fine airborne particulate matter (PM_{2.5}) and cardiovascular endpoints, especially mortality, have now been reported in several population cohort studies (Dockery et al. 1993; Pope et al. 1995; Abbey et al. 1999; McDonnell et al. 2000; Pope et al. 2002; Miller et al. 2007). Several other studies have reported that traffic-related pollutants are more strongly associated with these outcomes (Hoek et al. 2002; Jerrett et al. 2005; Künzli et al. 2005; Hoffmann et al. 2007; Sarnat et al. 2008). There are toxicologic data on long-term PM exposure that, in addition

to providing insight into some of the mechanisms of pathophysiology, have supported the plausibility of observational findings on PM (Suwa et al. 2002; Lippmann et al. 2005; Sun et al. 2005). It is likely that the chemical composition of airborne inhalable PM plays a role in determining its long-term toxicity, although physical characteristics of PM, such as its particle size, might also be relevant. Because composition is determined primarily by the source of the PM and by secondary atmospheric chemical reactions, different sources might be expected to emit PM with different degrees of toxicity.

The components of PM_{2.5} that are primarily responsible for the cardiovascular effects of long-term PM_{2.5} exposure have yet to be identified. Estimated mortality effects of long-term exposure to PM_{2.5} components (estimated from the nearest air pollution monitor) were recently reported for the California Teachers Study (Ostro et al. 2010; Ostro et al. 2011 [erratum]). Silicon, sulfate, and nitrate were associated with cardiopulmonary mortality in general; all PM_{2.5} components assessed in the study were associated with mortality from ischemic heart disease specifically. Although traffic-related pollutants have been implicated, as mentioned above, little is known about which features of these pollutants are responsible, including the role of gases versus PM. Although there is a modest increase in PM_{2.5} concentrations in areas within approximately 300 meters of large urban freeways, concentrations of ultra-fine PM (PM with an aerodynamic diameter of 100 nm or smaller), oxides of nitrogen, and hydrocarbon compounds increase dramatically (Rodes and Holland 1981; Zhu et al. 2002; Reponen et al. 2003; Zhang et al. 2004). It is therefore not clear whether PM_{2.5}, specific components of PM_{2.5}, or gases are solely responsible for the health effects of traffic-related pollutants. In addition, the roles of secondary inorganic aerosols and fugitive dust have not been elucidated.

Recent findings in our laboratory at the Lovelace Respiratory Research Institute suggest that whole combustion emissions (i.e., including both the particles and the gases) have a greater cardiovascular effect than the particles alone (Lund et al. 2007; Campen et al. 2010b). A number of studies over the past decade have suggested that ambient particle exposures affect atherosclerosis progression independently of effects from gaseous components. Sun and colleagues (2005) reported substantial plaque progression in ApoE^{-/-} mice after a 6-month exposure to concentrated ambient PM. Plaque progression associated with combustion emissions, such as diesel exhaust, has been reported (Bai et al. 2011). Our earlier work with diesel exhaust (Campen et al. 2010a) did not show plaque progression but did show substantial plaque composition changes, most notably an enhancement in macrophage staining.

Removal of combustion particles by filtration did not modify effects on vascular oxidative stress and inflammation, suggesting that the gas phase drove many of these effects. However, follow-up studies suggested that specific gases prominent in gasoline and diesel emissions, namely carbon monoxide and oxides of nitrogen, were unable to reproduce the complete panel of adverse vascular effects caused by whole diesel exhaust (Campen et al. 2010b).

The epidemiologic and toxicologic studies described here were designed in response to RFA 05-1A, a 2005 HEI request for applications (RFA) to investigate the health effects of PM components. The overall objective of this project was to further our understanding of the compositional features of ambient particulate air pollution that are most detrimental to human health and to gain insight into mechanisms that underlie the associated health effects. To address this objective, a program of research was carried out that combined observational epidemiology and animal toxicology and focused on cardiovascular disease.

Our study represents a multidisciplinary effort by investigators at the University of Washington who conducted the epidemiology part and at the Lovelace Respiratory Research Institute and the University of New Mexico who conducted the toxicology to identify chemical components and sources of PM_{2.5} that might be the most responsible for cardiovascular effects, with a focus on vehicle emissions. The regulatory significance of this program is substantial. Of the criteria pollutants, PM_{2.5} is the only one that is nonspecific, being neither a specific chemical compound nor an element. It is well understood that not all PM is equally toxic. Identification of the components of PM that are most toxic, and of the corresponding sources of these PM components, will allow more focused and efficient approaches to be considered in the regulation of PM.

The objectives of the HEI RFA were to “address questions about the health effects related to different components and characteristics of the ambient PM mixture” by (1) using a comprehensive program of research that took a systematic and comparative approach, (2) using, preferably, a combination of epidemiologic and toxicologic approaches, (3) accounting for the role of gaseous pollutants in affecting PM component toxicity, and (4) evaluating multiple PM characteristics. The program of study described here was highly responsive to these objectives. The epidemiologic studies focused on the comparison of several components of fine PM, with exposures estimated for individual cohort members. The toxicologic study, prompted by findings from earlier epidemiologic studies, took a systematic and comparative approach to investigating the effects of PM components strongly suspected of contributing to PM toxicity and to attempting to focus sequentially on the most toxic components. The roles of

gaseous pollutants, including vapors and gases in vehicular emissions as well as the gaseous criteria pollutants, were examined in qualitatively different but complementary ways in the two studies.

Section 1 of this report presents the epidemiologic studies. Section 2 presents the toxicologic study. Section 3 is an integrated discussion of the findings from all three studies.

REFERENCES

- Abbey DE, Nishino N, McDonnell WF, Burchette RJ, Knutsen SF, Lawrence Beeson W, Yang JX. 1999. Long-term inhalable particles and other air pollutants related to mortality in nonsmokers. *Am J Respir Crit Care Med* 159:373–382.
- Bai N, Kido T, Suzuki H, Yang G, Kavanagh TJ, Kaufman JD, Rosenfeld ME, van Breemen C, Eeden SF. 2011. Changes in atherosclerotic plaques induced by inhalation of diesel exhaust. *Atherosclerosis* 216:299–306.
- Campen MJ, Lund AK, Knuckles TL, Conklin DF, Bishop B, Young D, Sielkop SK, Seagrave JC, Reed MD, McDonald JD. 2010a. Inhaled diesel emissions alter atherosclerotic plaque composition in ApoE^{-/-} mice. *Toxicol Appl Pharmacol* 242:310–317.
- Campen MJ, Lund AK, Doyle-Eisele M, McDonald JD, Knuckles TL, Rohr A, Knipping E, Mauderly JL. 2010b. A comparison of vascular effects from complex and individual air pollutants indicates a toxic role for monoxide gases. *Environ Health Perspect* 118:921–927.
- Dockery DW, Pope CA III, Xu X, Spengler JD, Ware JH, Fay ME, Ferris BG, Speizer FE. 1993. An association between air pollution and mortality in six U.S. cities. *N Engl J Med* 329:1753–1759.
- Health Effects Institute. 2005. Request for Applications 05-1: Studies to Compare Components and Characteristics of Particulate Matter Associated with Health Effects. Health Effects Institute. Boston, MA.
- Hoek G, Brunekreef B, Goldbohm S, Fischer P, Van Den Brandt PA. 2002. Association between mortality and indicators of traffic-related air pollution in the Netherlands: A cohort study. *Lancet* 360:1203–1209.
- Hoffmann B, Moebus S, Mohlenkamp S, Stang A, Lehmann N, Dragano N, Schmermund A, Memmesheimer M, Mann K, Erbel R, Jockel KH. 2007. Residential exposure to traffic is associated with coronary atherosclerosis. *Circulation* 116:489–496.

- Jerrett M, Burnett RT, Ma R, Pope CA III, Krewski D, Newbold KB, Thurston G, Shi Y, Finkelstein N, Calle EE, Thun MJ. 2005. Spatial analysis of air pollution and mortality in Los Angeles. *Epidemiology* 16:727–736.
- Künzli N, Jerrett M, Mack WJ, Beckerman B, Labree L, Gilliland F, Thomas D, Peters J, Hodis HN. 2005. Ambient air pollution and atherosclerosis in Los Angeles. *Environ Health Perspect* 113:201–206.
- Lippmann M, Gordon T, Chen LC. 2005. Effects of subchronic exposures to concentrated ambient particles in mice. IX. Integral assessment and human health implications of subchronic exposures of mice to CAPs. *Inhal Toxicol* 17:255–261.
- Lund AK, Knuckles TL, Obat Akata C, Shohet R, McDonald JD, Seagrave JC, Campen MJ. 2007. Exposure to gasoline exhaust results in alterations of pathways involved in atherosclerosis. *Toxicol Sci* 95:485–494.
- McDonnell WF, Nishino-Ishikawa N, Petersen FF, Chen LH, Abbey DE. 2000. Relationships of mortality with the fine and coarse fractions of long-term ambient PM₁₀ concentrations in nonsmokers. *J Expo Anal Environ Epidemiol* 10:427–436.
- Miller KA, Siscovick DS, Sheppard L, Shepherd K, Sullivan JH, Anderson GL, Kaufman JD. 2007. Long-term exposure to air pollution and incidence of cardiovascular events in women. *N Engl J Med* 356:447–458.
- Ostro B, Lipsett M, Reynolds P, Goldberg D, Hertz A, Garcia C, Henderson KD, Bernstein L. 2010. Long-term exposure to constituents of fine particulate air pollution and mortality: Results from the California Teachers Study. *Environ Health Perspect* 118:363–369.
- Ostro B, Lipsett M, Reynolds P, Goldberg D, Hertz A, Garcia C, Henderson KD, Bernstein L. 2011. Erratum: Assessing long-term exposure in the California Teachers Study. *Environ Health Perspect* 119:A242–A243.
- Pope CA III, Burnett RT, Thun MJ, Calle EE, Krewski D, Ito K, Thurston GD. 2002. Lung cancer, cardiopulmonary mortality, and long-term exposure to fine particulate air pollution. *JAMA* 287:1132–1141.
- Pope CA III, Thun MJ, Namboodiri MM, Dockery DW, Evans JS, Speizer FE, Heath CW. 1995. Particulate air pollution as a predictor of mortality in a prospective study of U.S. adults. *Am J Respir Crit Care Med* 131:669–674.
- Reponen T, Grinshpun SA, Trakumas S, Martuzevicius D, Wang ZM, Lemasters G, Lockey JE, Biswas P. 2003. Concentration gradient patterns of aerosol particles near interstate highways in the Greater Cincinnati airshed. *J Environ Monit* 5:557–562.
- Rodes CE, Holland DM. 1981. Variations of NO, NO₂ and O₃ downwind of a Los Angeles freeway. *Atmos Environ* 15:243–250.
- Sarnat JA, Marmur A, Klein M, Kim E, Russell AG, Sarnat SE, Mulholland JA, Hopke PK, Tolbert PE. 2008. Fine particle sources and cardiorespiratory morbidity: An application of chemical mass balance and factor analytical source-apportionment methods. *Environ Health Perspect* 116:459–466.
- Sun Q, Wang A, Jin X, Natanzon A, Duquaine D, Brook RD, Aguinaldo JG, Fayad ZA, Fuster V, Lippmann M, Chen LC, Rajagopalan S. 2005. Long-term air pollution exposure and acceleration of atherosclerosis and vascular inflammation in an animal model. *JAMA* 294:3003–3010.
- Suwa T, Hogg JC, Quinlan KB, Ohgami A, Vincent R, Van Eeden SF. 2002. Particulate air pollution induces progression of atherosclerosis. *J Am Coll Cardiol* 39:935–942.
- Zhang KM, Wexler AS, Zhud YF, Hinds WC, Sioutas C. 2004. Evolution of particle number distribution near roadways. Part II: the ‘Road-to-Ambient’ process. *Atmos Environ* 38:6655–6665.
- Zhu Y, Hinds WC, Kim S, Sioutas C. 2002. Concentration and size distribution of ultrafine particles near a major highway. *J Air Waste Manage Assoc* 52:1032–1042.

Section I: NPACT Epidemiologic Study of Components of Fine Particulate Matter and Cardiovascular Disease in the MESA and WHI-OS Cohorts

Sverre Vedal, Sun-Young Kim, Kristin A. Miller, Julie Richman Fox, Silas Bergen, Timothy Gould, Joel D. Kaufman, Timothy V. Larson, Paul D. Sampson, Lianne Sheppard, Christopher D. Simpson, and Adam A. Szpiro

ABSTRACT

Understanding of the features of particulate matter (PM*) that underlie its effects on health is limited. There is evidence that PM from combustion sources, including vehicular emissions, may be more toxic than PM from other sources. In Section 1 of this report, we assess associations of predicted exposures to several components of fine PM (particulate matter $\leq 2.5 \mu\text{m}$ in aerodynamic diameter [PM_{2.5}]) with subclinical measures of atherosclerosis and incidence of cardiovascular events in individuals from two population cohorts. The working hypothesis of this study was that PM_{2.5} components produced from combustion processes would be associated with greater cardiovascular effects than components from other sources and processes, specifically crustal matter and secondary inorganic aerosol.

The two population cohorts were derived from the Multi-Ethnic Study of Atherosclerosis (MESA) and the Women's Health Initiative–Observational Study (WHI-OS). Approximately 6800 participants were recruited into MESA at baseline in 2000 through 2002 in six metropolitan areas in the United States: Baltimore, Maryland; Chicago, Illinois; Los Angeles, California; New York, New York; St. Paul, Minnesota; and Winston-Salem, North Carolina. Participants were without clinical cardiovascular disease (CVD) at enrollment and underwent initial and follow-up cardiovascular studies to identify subclinical predictors of CVD. The primary subclinical outcomes in MESA were carotid intima-media thickness (CIMT), as measured by ultrasound,

and coronary artery calcium (CAC), as measured by computed tomography (CT). Both were measured at the first examinations of all participants in 2000–2002, and subsets of the participants had repeated measurements at subsequent examinations. The WHI-OS cohort includes approximately 90,000 women in 45 U.S. cities for whom detailed information on risk factors for CVD is available and who have been followed regularly since the mid-1990s for clinical events, such as hospitalization or death, related to cardiovascular causes.

Estimation of exposure in the MESA participants was based on two separate prediction models, the spatiotemporal model and the national spatial model. The spatiotemporal model made use of a monitoring campaign dedicated to MESA that was carried out as part of the MESA Air Pollution Study (MESA Air) and of this study within the National Particle Component Toxicity (NPACT) initiative. PM_{2.5} and PM_{2.5} chemical components were measured in 2-week samples from a few fixed monitoring sites in each of the six cities over 1 to 4 years and in samples from approximately 50 outdoor sites at a rotating set of participants' homes, where 2-week samples were obtained in each of two seasons. The spatiotemporal model incorporated the MESA Air/NPACT monitoring data, geographic variables, and geostatistical smoothing that predicted levels of PM_{2.5} components at the residences of MESA participants. In the national spatial model, used to predict exposures for both the MESA cohort and the WHI-OS cohort, the approach was similar except that the monitoring data consisted of 1 year of data from the Chemical Speciation Network (CSN) of the U.S. Environmental Protection Agency (EPA) and from the Interagency Monitoring of Protected Visual Environments (IMPROVE) network. Performance of both models was assessed using cross-validation of predicted exposures against actual monitoring data. The PM_{2.5} components of primary interest were elemental carbon (EC), organic carbon (OC), silicon, and sulfur. Source apportionment using positive matrix factorization (PMF) was carried out using all NPACT samples from the fixed monitoring sites and from the home-outdoor sites.

In general, the spatiotemporal model for predicting the PM_{2.5} chemical components performed best in Los Angeles

This section is one part of Health Effects Institute Research Report 178, which also includes a section covering the animal toxicology portion of this study, a Commentary by the HEI NPACT Review Panel, an HEI Statement about the research project, and a Synthesis relating this report to Research Report 177. Correspondence concerning the Research Report may be addressed to Dr. Sverre Vedal, 4225 Roosevelt Way NE, #100, Department of Environmental and Occupational Health Sciences, University of Washington School of Public Health, Seattle, WA 98105; svedal@uw.edu.

Also contributing were Sara Dubowsky Adar, Cynthia L. Curl, Amanda Gasset, Anne Ho, Krystle Jumawan, Hil Lyons, Assaf Oron, Michael Paulsen, Mark Richards, and Min Sun. For authors' and contributing authors' affiliations, see About the Authors at the end of this section.

* A list of abbreviations and other terms appears at the end of the section.

and least well in Winston-Salem and was better for sulfur than for the other three components. The national spatial model performed best for sulfur (cross-validation $R^2 = 0.95$) and least well for silicon ($R^2 = 0.61$). In the MESA cohort, there was good evidence that OC and sulfur were associated cross-sectionally with CIMT using both the spatiotemporal model predictions (increase of 0.025 mm [95% CI, 0.017 to 0.033] for an interquartile range [IQR] increase in OC, and 0.021 mm [0.012 to 0.029] for an IQR increase in sulfur) and the national spatial model predictions, but little evidence that they were associated with CAC. There was much less evidence for associations of predicted exposures to either EC or silicon with either CIMT or CAC. Limited analyses of other PM_{2.5} components and gaseous pollutants showed evidence of associations between CIMT and sulfate (SO₄), as expected from the findings for sulfur, and between CIMT and copper. There was comparatively less evidence for associations with nitrate (NO₃), sulfur dioxide (SO₂), and nickel, and little evidence for associations with nitrogen dioxide (NO₂) or vanadium.

In the WHI-OS cohort, there was good evidence that OC exposure was associated with clinical CVD events due to cerebrovascular disease and stroke, but not with other event categories. For deaths, however, there was evidence that OC was associated with CVD deaths in general (hazard ratio [HR], 1.23; 95% CI, 1.07 to 1.41 for an IQR increase in OC) and with several subcategories, including deaths from atherosclerotic cardiac disease and deaths from cerebrovascular disease. Evidence was also good that predicted exposure to sulfur was associated with total incidence of CVD events (HR, 1.09; 95% CI 1.05 to 1.14) and with all of the CVD event subsets; however, the evidence for an association of sulfur with CVD deaths was weaker. For EC, there was little evidence of associations with total CVD events, but some evidence of associations with subsets of CVD deaths, except for death from cerebrovascular disease. There was little evidence for associations of silicon with either total CVD events or CVD deaths in the WHI-OS cohort.

Sensitivity analyses in the MESA cohort showed little sensitivity of findings to more extended covariate models or to control for copollutants. In contrast, most effect estimates were attenuated when results were adjusted for city (for example, the association of OC with CIMT), and all had wider CIs, as expected. In the WHI-OS cohort, the findings were largely insensitive to model specification or copollutant adjustment. In limited corrections of exposure measurement error in the MESA analyses, there was no indication that our use of predicted exposures biased

effect estimates, although there was loss of precision in some instances.

Source apportionment provided insight into the sources of the PM_{2.5} components in the MESA analyses. In all six cities OC had a large contribution from secondary aerosol-like factors, and in St. Paul and Winston-Salem there was an additional large contribution from a biomass-like factor. The largest contribution to sulfur in all of the cities except Los Angeles was from a secondary aerosol-like factor that was also enriched in arsenic and selenium. EC had large contributions from a diesel exhaust-like factor in four of the six cities. Silicon showed large contributions from a crustal-like factor in five of the six cities. Of the PM_{2.5} components of secondary interest, copper had a large contribution from a diesel exhaust/brake wear-like factor in all of the cities, and nickel had a substantial contribution from an oil combustion-like factor in all of the cities and a large contribution from another residual oil combustion-like factor in New York.

These observational findings provide further evidence that the chemical composition of PM_{2.5} is an important determinant of the health effects of PM_{2.5} exposure. Of the four PM_{2.5} components considered here to be of primary interest, evidence for associations with the CVD endpoints in both the MESA and WHI-OS cohorts was strongest for OC and sulfur (or SO₄) and less strong for EC and silicon. Of the components of secondary interest, the evidence was limited but strongest for copper. The source apportionment indicated that secondary PM_{2.5} mixtures contributed substantially to both OC and sulfur levels, motivating renewed interest in the effects of secondary mixtures.

OVERVIEW

Cohorts from two different studies, MESA and WHI-OS, were utilized for the epidemiologic work reported here. The methods and findings of analyses using the two cohorts are presented separately. We begin by introducing and describing the MESA cohort, followed by detailed descriptions of the exposure estimation and the analyses of health effects. The description of the WHI-OS cohort and the methods and findings for this cohort follow. Table 1 presents an overview comparison of the two cohorts.

The exposure estimation sections for the MESA participants begin with an initial overview, followed by descriptions of cohort geocoding and assignment of geographic covariates to be used for the estimations. Next, we describe the air monitoring methods and data, and the methods

Table 1. Comparison of Features of the Two Cohort Studies^a

Cohort	Study Design	Health Endpoints	Population Sample	Monitoring and Exposure Estimation
MESA	<ul style="list-style-type: none"> • Prospective cohort • Initial exam 2000–2002 	Subclinical CVD (CIMT, CAC)	<ul style="list-style-type: none"> • ~6800, 4 racial-ethnic groups (white, African American, Chinese American, Hispanic) • 6 cities: New York, Los Angeles, Chicago, Winston-Salem, St. Paul, Baltimore • Ages 45–84, no previous CVD 	<ul style="list-style-type: none"> • Regulatory (CSN/AQS) monitors in all cities • MESA Air/NPACT monitors (fixed site, rotating home-outdoor) • MESA Air/NPACT spatiotemporal prediction model • National spatial prediction model
WHI-OS	<ul style="list-style-type: none"> • Prospective cohort • Initial enrollment 1994–1998 	Cardiovascular events (MI, stroke, cardiac procedures, CVD deaths)	<ul style="list-style-type: none"> • ~90,000 postmenopausal women (87% white) • 45 cities: Northeast (8 cities), Southeast (11 cities), Midwest (13 cities), Southwest (3 cities), Southern California (4 cities), Northwest (6 cities) • Ages 50–79 	<ul style="list-style-type: none"> • 79% of subjects reside within 30 miles of a regulatory monitor • No supplemental monitoring • National spatial prediction model

^a CSN indicates Chemical Speciation Network; AQS, Air Quality System of the EPA; CIMT, carotid intima-media thickness; CAC, coronary artery calcium; MI, myocardial infarction; CVD, cardiovascular disease.

and findings of the source apportionment in MESA cities based on these data. We describe the exposure modeling and the predictions of our two primary exposure models, the MESA Air/NPACT spatiotemporal model and the national spatial model, as well as some less-sophisticated approaches to exposure estimation that are used in secondary health analyses. We then compare the exposure predictions based on the spatiotemporal and national spatial models, as well as those from the secondary approaches to exposure estimation.

For the analysis of health effects in the MESA participants, we begin with description of the modeling methods for our two primary endpoints, CIMT and CAC. We then describe results of cross-sectional and longitudinal analyses using individual-level exposure predictions from the spatiotemporal and national spatial models, and we finish with descriptions of findings from sensitivity analyses and secondary analyses.

An introduction and description of the WHI-OS cohort is followed by detailed descriptions of the exposure estimation using the national spatial model predictions and secondary exposure measures of citywide average exposures and distance to major roadways. The methods for the time-to-event analyses of health effects are described,

and the findings using individual-level exposure predictions from the national spatial model are presented, along with results of a within-city and between-city analysis. Results of sensitivity analyses and results using secondary exposure estimates are also presented.

Appendices to this section of the report (available on the HEI Web site), apart from including supplements to text, tables, and figures, include description of the NO₂ model and predictions (Appendix D), the methods and findings of the work on PM oxidative potential (Appendix E), supplemental monitoring methods and results aimed at validating our monitoring data (Appendix F), detailed cross-sectional analyses in the MESA population using secondary exposure estimates, specifically nearest-neighbor (nearest-monitor) and inverse-distance weighting (IDW) (Appendix H), and detailed time-to-event analyses for the WHI-OS cohort using our secondary citywide average estimates of exposure (Appendix I). A literature review that places the source-apportionment findings in context appears in Appendix J. Also presented are quality assessment and quality control reports for the NPACT monitoring data (Appendix K), for supplemental NPACT monitoring (Appendix L), for CAC data (Appendix O), and for CIMT measurements (Appendix P).

SPECIFIC AIM

The specific aim of this study was to identify the chemical components of ambient PM that contribute to the effects that long-term exposure has on the development and progression of atherosclerosis and incidence of cardiovascular events. The primary hypothesis of the study was that the chemical components of PM_{2.5} resulting from combustion processes would have more long-term cardiovascular toxicity, as reflected in measurements of atherosclerosis, incidence of cardiovascular events, and deaths from cardiovascular causes, than PM composed of either secondary inorganic aerosols or crustal components.

THE MESA ANALYSES

INTRODUCTION AND STUDY DESIGN

MESA is a relatively new cohort study, sponsored by the National Heart, Lung, and Blood Institute, that focuses on predictors of subclinical atherosclerosis and the relationship between subclinical disease and subsequent CVD events in a population comprising different racial or ethnic groups. Cohort members, all of whom were without prior CVD at enrollment, were largely recruited between 2000 and 2002. Due to the relatively small size of this cohort (compared with the WHI-OS cohort), it is premature to focus intensely on clinical cardiovascular events, though this will be possible in the future. Research on the health effects of air pollution in the MESA cohort has been initiated with analyses using markers of subclinical CVD and other biomarkers (Gill et al. 2011) and with increasingly sophisticated methods for estimating the exposures of individual participants. The MESA Air Pollution Study (MESA Air), funded by the EPA, was initiated in 2004 in an effort to better estimate individual-level exposures to air pollution, focusing on long-term exposure to PM_{2.5}, black (light-absorbing) carbon, and oxides of nitrogen (NO_x), in order to examine associations between these exposures and incidence and progression of atherosclerotic cardiac disease. It will end in 2014. The NPACT work with this cohort is designed to exploit the work of MESA and MESA Air in order to examine associations between exposure to particle components and markers of subclinical atherosclerosis measured in the early years of MESA. The intensive characterization of the cohort, the availability of specific consent for use of information on residential addresses and air pollution data, cohort-specific exposure monitoring and modeling, and the availability of measurements of subclinical atherosclerosis markers make this cohort especially well suited for study of subclinical atherosclerosis in association with air pollution.

THE MESA COHORT

Recruitment and Follow-Up

The original MESA cohort study included 6814 participants, selected on a population basis, who had no preexisting clinically apparent CVD. Participants were recruited from six U.S. communities: Baltimore City and Baltimore County, Maryland; Chicago, Illinois; Los Angeles County, California; St. Paul, Minnesota; New York, New York; and Forsyth County (Winston-Salem), North Carolina. Participants were 45 to 84 years of age at enrollment, with an approximately equal ratio of men to women. Four racial or ethnic groups were targeted for inclusion, and the recruitment protocol required overlapping ethnic groups among communities. The MESA cohort is 39% white, 28% African American, 22% Hispanic, and 12% Chinese American. Participants underwent intensive repeated clinical examinations over 10 years.

Data collection included extensive questionnaires about personal characteristics associated with risk of CVD, blood and urine analyses, and imaging measures of atherosclerosis and cardiovascular function. Questionnaire data and laboratory measurements also identified potential confounding risk factors for CVD. In this study we focused on two of these measurements: CIMT, as measured by carotid ultrasound, and CAC, as measured by rapid-acquisition CT of the chest. Detailed descriptions have been reported (Bild et al. 2002).

The original MESA cohort of 6814 subjects underwent the first set of measurements (exam 1) in 2000–2002. Exam 2 was completed in 2004, and exam 3 was completed 18 months later in 2005. At both exam 2 and exam 3, CAC and CIMT were measured in a random sample of 50% of the participants in exam 1. Exam 4, which extended from September 2005 through April 2007, included CAC and CIMT measurements in approximately 3300 of the subjects who had those measurements at exam 2. Exam 5 extended from April 2010 through February 2012, but findings from exam 5 were not available for the analyses included in this report. In addition, up to 15 years of retrospective residential data were available through collaboration with an EPA-funded ancillary study (MESA Neighborhood), led by Dr. Ana Diez Roux at the University of Michigan, Ann Arbor.

Participants in the main MESA study who consented to use of their address were included in the analyses presented here. Address consent was required for inclusion in both the MESA Neighborhood and the MESA Air studies. Of the 6814 original MESA participants, 6266 (92%) consented to use of their address in one of these ancillary studies.

MESA Air was started in 2004 to study associations between long-term exposure to $PM_{2.5}$ and CVD in the MESA cohort. MESA Air extended the population with the addition of 257 participants from three more study sites: two additional sites in the Los Angeles area (one in a coastal region of Los Angeles and the other in Riverside, California) and one additional nonurban site in the New York area, in Rockland County. An additional 491 participants were recruited from another MESA ancillary study, MESA Family (led by Dr. Jerome I. Rotter, Cedars-Sinai Medical Center, Los Angeles), in which the genetics of CVD in the MESA cohort is being studied. These participants, together with the 6266 MESA participants who consented to use of their address, constitute the MESA Air cohort that is being followed for cardiovascular events. Because measures of subclinical CVD were not available for the participants added in the MESA Air extension of MESA until after their recruitment in 2004, we did not include data for these individuals in the health analyses. Institutional review board approval was granted at each study site and written informed consent was obtained from all participants.

Health Endpoint and Covariate Data

Measures of CIMT and CAC, as markers for subclinical CVD, were used as the primary study endpoints. Participants' CIMT was measured at a study clinic in each city by B-mode ultrasound using a GE Logiq scanner. The protocol for image acquisition and analysis focused on reproducible measurements of intima-media thickness in the common carotid artery. The transducer was positioned relative to the patient's neck and artery in a consistent location defined by the plane of the internal jugular vein as it lines up on top of the common carotid artery.

CAC was assessed by chest CT using a cardiac-gated electron beam computed tomography (EBCT) scanner or a multi-detector computed tomography (MDCT) scanner. In MESA the CAC scores are calibrated regularly for each scanner by scanning torso phantoms that simulate the density of anatomic structures in average subjects. Two scans were obtained for each participant. An Agatston score was calculated for each scan that reflects the amount of calcium in the coronary arteries; the mean of the Agatston scores for the two scans was used in the analyses. The presence of CAC was defined as an Agatston score greater than zero.

Detailed questionnaires were used to collect a variety of data from participants, including medical history, personal history, demographic data, socioeconomic factors, medication use, psychosocial factors, diet, physical activity, and family history. Other measurements collected in

the MESA exams included blood pressure, ankle-brachial index, and measures of endothelial function, as well as measurements from anthropometry, electrocardiography, spot urine collection, phlebotomy, and magnetic resonance imaging (MRI).

MESA EXPOSURE DATA

Overview

We used sophisticated statistical models to predict individual-level exposure (outdoor concentration at the participant's residence) to components of ambient $PM_{2.5}$. We based our approach on the premise that estimating exposure at the individual level would result in less measurement error than other approaches that assign exposure at larger spatial scales and that the resulting estimates of health effects would be more valid and precise. This premise also guided the approach to exposure estimation in the MESA Air study, allowing us to exploit the exposure modeling done for MESA Air. The exposure model that generated predictions at the individual level for the MESA participants was developed by combining data from air pollution monitoring and individual-level geographic information and using geostatistical modeling methods to estimate exposure.

Monitoring data included both data obtained from the regulatory networks CSN and IMPROVE and data generated from a complex monitoring campaign specific to MESA Air. Original CSN data were 24-hour averages, typically from samples obtained every third day or every sixth day, while the MESA Air data were obtained from 2-week integrated samples. MESA Air data were generated from several fixed monitoring sites in each city that provided multiyear time series of 2-week samples, and from a rotating set of outdoor monitoring sites at participants' homes that provided 2-week samples in each of two seasons for approximately 50 sites in each city (Cohen et al. 2009). Also, a supplemental monitoring campaign was carried out using collocated monitors to compare results from CSN and MESA Air monitoring regimens (Appendix F, available on the HEI Web site). Monitoring results from a MESA Air ancillary "snapshot" study in three of the MESA cities allowed for further validation of prediction models for silicon and sulfur.

The CSN and IMPROVE data were utilized for the national spatial model of exposure to $PM_{2.5}$ components. Potentially, they could have also been used, along with the monitoring data generated specifically for MESA Air and NPACT, in the MESA Air/NPACT spatiotemporal exposure model. Unfortunately, for several reasons, as detailed below and in Appendix C (available on the HEI

Web site), we judged that it was inappropriate to incorporate the data obtained from regulatory monitoring and from MESA Air/NPACT monitoring together in the same exposure models. Therefore, we elected to only use data from the MESA Air/NPACT monitoring campaign to build the spatiotemporal model for predicting exposure to PM_{2.5} components.

The intent at the outset was to investigate and compare cardiovascular effects associated with several classes of selected PM_{2.5} components. To this end, we chose to focus on EC and OC because they reflect a variety of combustion processes, as well as secondary organic aerosols in the case of OC. We hypothesized that PM_{2.5} components produced from combustion processes would be associated with more cardiovascular effects than other PM_{2.5} components. The PM_{2.5} components silicon and SO₄ (with sulfur used as a surrogate for SO₄ in the MESA analyses) were selected to reflect other sources and processes, specifically airborne crustal matter and secondary inorganic aerosol, respectively.

Other PM_{2.5} components were also evaluated, including NO₃, nickel, vanadium, and copper. Predictions for exposure to these other components for the MESA cohort were developed using the national spatial model. Analyses of the gaseous pollutants NO₂ and SO₂ are also included in this report. Predictions from the NO₂ exposure model were available from work performed in MESA Air; NO₂ modeling is described in Appendix D (available on the HEI Web site). SO₂ predictions were provided from the national spatial model. This allowed assessment of potential confounding and effect modification by NO₂ and SO₂.

We also conducted PM source apportionment, which integrates information on the chemical composition of PM, exploiting correlations, in this case, of components over space and time, to estimate PM_{2.5} sources or PM_{2.5} processes. Insight into sources can be helpful in interpreting health effects related to specific PM components.

Our two primary exposure model frameworks were the MESA Air/NPACT spatiotemporal model and the national spatial model. Predictions from the national spatial model in the MESA analyses were compared with predictions from the MESA Air/NPACT spatiotemporal model and used as exposure estimates in the analyses of health effects. In addition to our primary models for individual-level exposure to PM_{2.5} components, we also produced several secondary estimates of exposure defined by nearest monitor (“nearest neighbor”), IDW, and citywide average concentrations. This allowed us to compare not only the exposure estimates across several approaches, but also the results of using the different exposure estimates on estimates of health effects.

Geocoding and Geographic Data Acquisition and Assignment

MESA Air participants’ residential addresses were obtained at follow-up exams and through the residential history questionnaire from MESA Neighborhood. These addresses were geocoded using TeleAtlas Dynamap 2000 according to standard procedures described in the MESA Air Data Organization and Operating Procedures (MESA Air Data Team 2013). Geocoded locations of agency monitoring sites were obtained from the EPA so that spatial profiles of these locations could be described in the same way.

Each location was linked to several geographic information system (GIS) layers. Layers included a Normalized Difference Vegetation Index (NDVI) term from satellite imagery, land cover from the U.S. Geological Survey, emissions based on the 2002 National Emissions Inventory, and variables based on the TeleAtlas road network (distance to road and the sums of road lengths within buffer distances). Table 2 describes the geographic covariates. Layers obtained from the original sources were clipped at 25 km around the borders of State Plane Coordinate System zones and then projected into the appropriate coordinates for those zones. Custom Python scripts allowed fast batch processing of the geographic linkages and calculation of the variables.

Pollutant Data from Regulatory Monitoring Networks

We evaluated two regulatory monitoring networks as potential data sources for our MESA analyses: CSN, including both the Speciation Trends Network (STN) and supplemental monitoring data, and the IMPROVE monitoring network. Differences in the protocols for monitoring, sampling, and analyzing data across the networks and across time periods within the networks made the inclusion of data from these sources problematic.

For our initial assessment, we used data from CSN and IMPROVE sites within 200-km radii of the MESA city centers. The number of network monitoring sites in these centers was relatively small, ranging from 6 in St. Paul to 27 in New York (Figure 1 of Appendix B, available on the HEI Web site). (The full set of monitoring sites considered is listed, along with collocated sites, in Table 1 of Appendix B, available on the HEI Web site.) Very few IMPROVE network sites were included, because they are mostly located near wilderness and rural areas far from MESA participants’ residences.

Differences in sampling frequency and sampling protocols drove our decision as to whether to include the CSN data in the spatiotemporal model for PM_{2.5} component

Table 2. Geographic Covariates^a

Category	Units	Buffer Radii (meters) ^b
Position Latitude, longitude	GPS	NA
Population	Sum of people	500, 1000, 1500, 2000, 2500, 3000, 5000, 10,000, 15,000
Emissions PM _{2.5} , PM ₁₀ , SO ₂ , CO, NO _x	Tons per year	3000, 15,000, 30,000
Land use resi, comm, industrial, transport, industcomm, mix_urban, oth_urban, crop, grove, feeding, oth_agri, herb_range, shrub, mix_range, forest, green, mix_forest, stream, lakes, reservoir, bays, wetland, nf_wetland, dry_salt, beach, sandy, rock, mine, transition, mix_barren, shrub_tun, herb_tun, bare_tun, wet_tun, mix_tun, snowfield, glacier, unspec	Percent	500, 1000, 1500, 3000, 5000, 10,000, 15,000
Vegetative index 25th, 50th, 75th quartile, summer average, winter average	NA	250, 500, 1000, 2500, 5000, 7500, 10,000
Roadway Sum of A1 lengths, sum of A2 + A3 lengths	Meters	50, 100, 150, 300, 400, 500, 750, 1000, 1500, 3000, 5000
Distance to features A1, A2, A3 road, railroad, railyard, large airport, commercial zone	Meters	NA

^a NA indicates not applicable; A1 is a primary road with limited access; A2, primary road without limited access; A3, secondary connecting road.

^b Buffer radii are the radii of a circle whose center is the point around which all of the data for a geographic variable within the circle circumference are summed.

predictions. With respect to sampling frequency, the EPA's regulatory Air Quality System (AQS) sites operated every third or sixth day. The 53 core CSN sites that make up the STN sample operated every third day, while about 190 supplemental CSN sites collected data every sixth day (U.S. EPA 2009). All IMPROVE sites operated every third day. In contrast, MESA Air/NPACT monitoring data were obtained as 2-week samples. These sampling differences induce differences in precision in the 2-week averages and need to be considered if the data are to be used in the same spatiotemporal model.

The protocols also differed between the two networks. (Sampling and analysis protocols for carbon at CSN and IMPROVE are shown in Table 2 of Appendix B, available on the HEI Web site.) The discrepancies in the data due to differences between the CSN and IMPROVE protocols at collocated sites have been well documented (Watson et al. 2005). Consequently, the EPA began to change sampling and analysis protocols at CSN sites to an IMPROVE-like method beginning in March 2007. All core CSN sites (STN sites) made changes simultaneously, while changes at

supplemental CSN sites were phased in over time. The new protocol is comparable to the MESA Air/NPACT protocol, with a few exceptions, most notably the monitor flow rate. We explored the comparability of the data across networks in considering whether to combine data from all networks in one statistical model (discussed below under "Building and Validating the Spatiotemporal Exposure Model").

The field monitoring campaign for MESA Air/NPACT relied on having PM_{2.5} monitors collocated with regulatory agency PM sampling monitors in at least one CSN site in each city. One of the CSN sites in each of the six metropolitan areas was a speciation site where chemical components of PM_{2.5} were quantified on a schedule of either 1 day in 6 days or 1 day in 3 days. (A list with descriptions of these collocated sites is presented in Table 3 of Appendix B, available on the HEI Web site.)

A supplemental monitoring campaign was performed to assess comparability of CSN and NPACT monitoring instrumentation and sampling regimens (described in Appendix F, available on the HEI Web site).

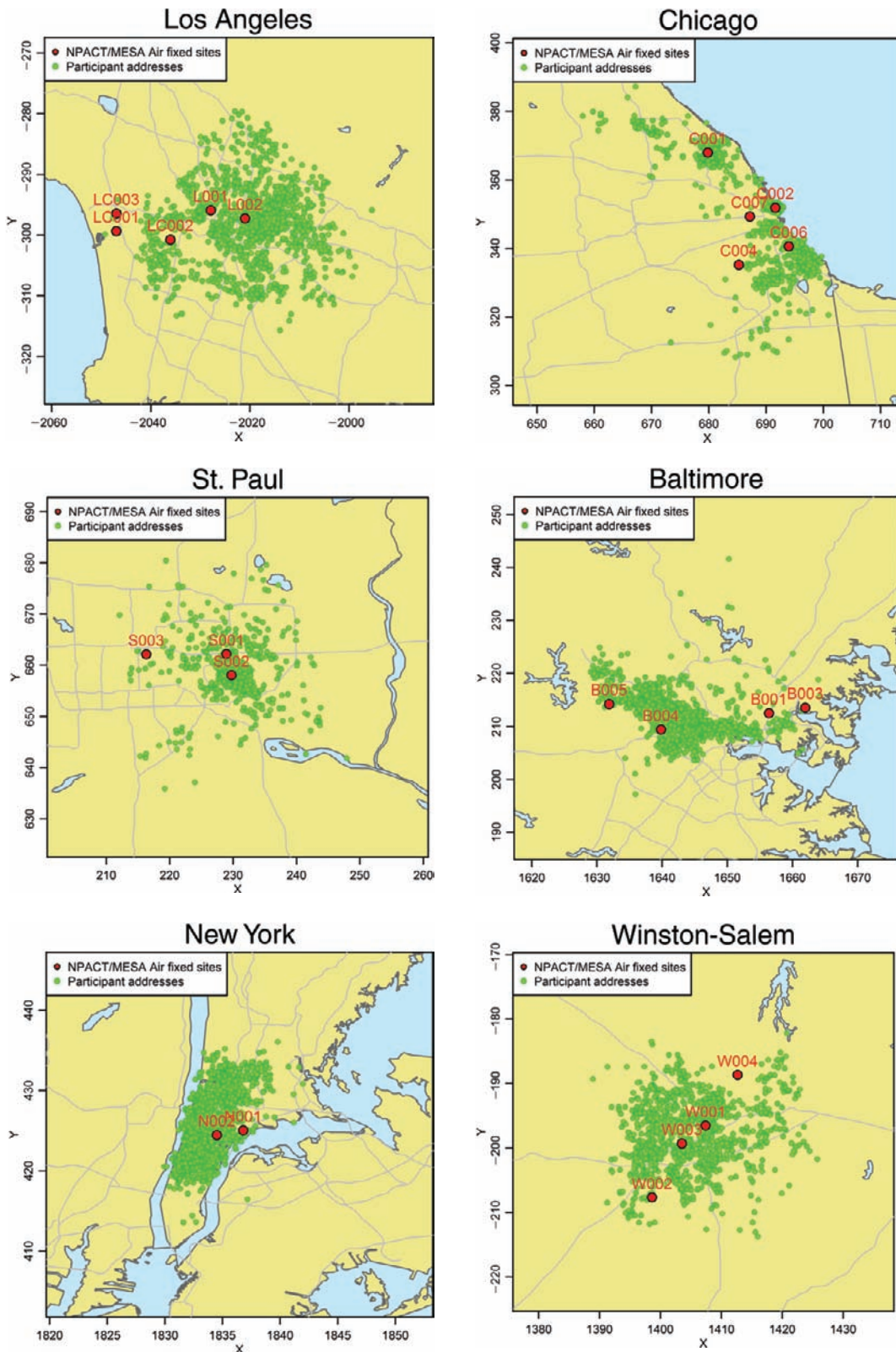


Figure 1. Maps showing locations of fixed monitoring sites in the six MESA cities. Monitoring sites are in red (numbers correspond to monitor identification numbers), study participants' residences are in green (jittered for confidentiality), and faint lines indicate interstate highways. The numbers on the axes indicate the X and Y map coordinates in kilometers.

Table 3. Distance of MESA Air Participant Residences from MESA Air/NPACT Fixed-Site Monitors

Location	Distance to Nearest Monitor (km)			Participant Proximity (%)	
	10th Percentile	Median	90th Percentile	< 2 km	< 5 km
Los Angeles	1.7	4.9	9.8	15	51
Coastal Los Angeles	0.8	3.2	12.2	25	69
Riverside	1.1	4.7	32.8	23	54
Chicago	0.3	2.0	7.5	50	84
St. Paul	0.7	1.3	5.9	65	87
Baltimore	1.5	3.1	6.5	24	77
New York	0.9	2.3	4.5	43	94
Rockland County	0.4	1.8	4.5	58	92
Winston-Salem	1.8	3.8	7.4	14	70

MESA Air and NPACT Pollutant Monitoring

PM_{2.5} and PM_{2.5} Component Sampling The pollutant measures of primary interest in MESA Air are PM_{2.5} and measures of traffic-generated pollution (NO_x, NO₂, and the light absorption coefficient [LAC]). NPACT data collection relied on the MESA Air field program that consisted of data from three to seven fixed monitoring sites in each of the six MESA cities where 2-week samples were being collected and from approximately 50 rotating home-outdoor sites in each city, where 2-week samples were collected in each of two seasons at each home.

The fixed-site monitors were located in libraries, schools, or other buildings in participant-dense areas underrepresented by the EPA's existing regulatory AQS network (Figure 1). Proximity of the fixed sites to residences of MESA Air participants is summarized in Table 3. The median distance from a participant's residence to an NPACT fixed monitoring site varied from 1.3 km in St. Paul to 4.9 km in Los Angeles.

One site in each metropolitan area was located within about 100 m of a major roadway to allow characterization of the temporal trends in air pollution created by proximity to the roadway relative to typical urban sites where AQS PM_{2.5} monitors are located and air pollution is well mixed. Actual distances from these near-road sites to the closest major highway are shown in Figure 2 for all six MESA cities, as well as two other sites in the Los Angeles area — a coastal site in Los Angeles and a site in Riverside — and a site close to New York City, in Rockland County. Except for the Rockland County site and the coastal Los Angeles site, each site was collocated with an AQS network site to allow calibration of the MESA

Air/NPACT measurements with Federal Reference Method (FRM) measurements (Table 3 of Appendix B, available on the HEI Web site).

PM_{2.5} mass concentrations were determined for 2-week integrated sampling events, typically starting and ending on Wednesdays, using Harvard personal environmental monitors (HPEMs) with a 2.5- μ m cut size when operated at a flow rate of 1.8 L/min. The sampling system drew the air sample through an HPEM using a personal sampling pump (TSI SidePak Model SP530) and collected a PM_{2.5} sample on Teflon filter media housed inside the HPEM. Teflon filters were used to determine total PM_{2.5} mass, and subsequently the LAC of the black carbon in the sample and the mass concentration of a suite of metals. Collection of these samples began with collocated monitors at AQS fixed monitoring sites in August 2005, was extended to home-outdoor sites from 2006 to 2008, and continued

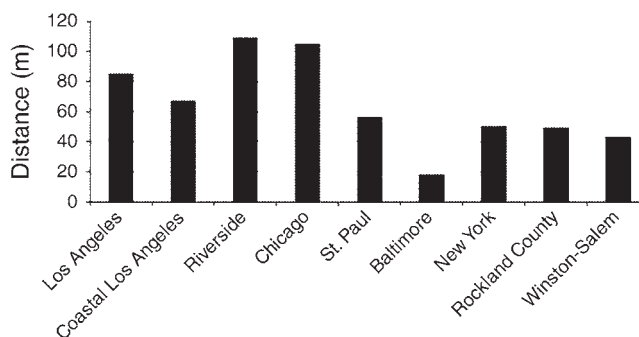


Figure 2. Distance from NPACT near-road fixed monitoring sites to a major roadway. For the Rockland County site, the distance is to an A3 roadway; for all other sites, the distance is to an A1 roadway.

City	Type	Number of Sites	Site ID	<i>n</i>	2005	2006	2007	2008	2009
Los Angeles	Fixed	1	L001	82					
		2	L002	75					
		3	LC001	81					
		4	LC002	74					
		5	LC003	78					
		6	LR001	71					
		7	LR002	75					
Home	1-61	L100-L841	1-2						
	1-16	LC200-LC302	1-2						
	1-32	LR201-LR303	1-2						
Chicago	Fixed	1	C001	83					
		2	C002	87					
		3	C004	72					
		4	C006	73					
		5	C007	62					
Home	1-127	C100-C832	1-3						
St. Paul	Fixed	1	S001	81					
		2	S002	86					
		3	S003	90					
Home	1-131	S100-S312	1-3						
Baltimore	Fixed	1	B001	85					
		2	B003	92					
		3	B004	82					
		4	B005	73					
Home	1-81	B100-B313	1-3						
New York	Fixed	1	N001	69					
		2	N002	79					
		3	NR001	46					
Home	1-82	N100-N316	1-3						
Home	1-25	NR200-NR304	1-3						
Winston-Salem	Fixed	1	W001	96					
		2	W002	91					
		3	W003	90					
		4	W004	78					
Home	1-114	W100-W814	1-3						

Figure 3. Monitoring using Teflon filters in the six MESA cities at fixed sites and a rotating set of home-outdoor sites. IDs in blue are sites collocated with EPA CSN sites; IDs in red are near-road sites; *n* is the number of samples per site.

at NPACT fixed monitoring sites through July 2009 (Figure 3). Parallel samplers containing prefired quartz-fiber filter media were used to collect samples at fixed and home-outdoor sites from March 2007 through August 2008 for quantification of OC and EC and subsequently of oxidative potential (Figure 4). NO₂ and NO_x were measured using Ogawa passive badge-style samplers deployed underneath rain shelters adjacent to the active HPEM.

While the NPACT data collection was largely concurrent with the collection of PM_{2.5} samples on both Teflon and quartz-fiber filter media from March 2007 through August 2008, additional MESA Air data consisting of total PM_{2.5} and metal species were collected both before and after collection of the quartz-fiber filter samples. Metal species data are therefore available from the fixed monitoring sites from August 2005 through July 2009, and from selected

home-outdoor sites during the times when samples were collected at those locations from February 2006 through October 2008 (Figure 3). The same type of sampling equipment and the same sampling schedule were employed throughout the entire MESA Air/NPACT field program, allowing for ease in comparing these data over time.

Gaseous Pollutant Sampling The NO₂ and NO_x passive badge samples were collected at fixed sites and home-outdoor sites during the same periods that PM_{2.5} samples were collected on Teflon filter media, and data for these combustion-related gases are concurrent with the total PM_{2.5} data for each sampling location.

Snapshot samples consisting of approximately 100 concurrent 2-week samples of NO₂, NO_x, and SO₂ were collected three times in each study area during seasons

City	Type	Number of Sites	Site ID	<i>n</i>	2007	2008	2009
Los Angeles	Fixed	1	L001	41	[Hatched]	[Hatched]	[Hatched]
		2	L002	30			
		3	LC001	32			
		4	LC002	31			
		5	LC003	30			
		6	LR001	23			
		7	LR002	37			
Home	1-61	L217-L309	1-2	[Hatched]	[Hatched]	[Hatched]	
	1-16	LC200-LC302	1-2				
	1-32	LR100-LR303	1-2				
Chicago	Fixed	1	C001	27	[Hatched]	[Hatched]	[Hatched]
		2	C002	24			
		3	C004	41			
		4	C006	29			
		5	C007	29			
Home	1-127	C107-C800	1-2	[Hatched]	[Hatched]	[Hatched]	
St. Paul	Fixed	1	S001	30	[Hatched]	[Hatched]	[Hatched]
		2	S002	33			
		3	S003	43			
Home	1-131	S125-S312	1-2	[Hatched]	[Hatched]	[Hatched]	
Baltimore	Fixed	1	B001	34	[Hatched]	[Hatched]	[Hatched]
		2	B003	46			
		3	B004	34			
		4	B005	33			
Home	1-81	B115-B313	1-2	[Hatched]	[Hatched]	[Hatched]	
New York	Fixed	1	N001	41	[Hatched]	[Hatched]	[Hatched]
		2	N002	27			
		3	NR001	23			
Home	1-82	N203-N316	1-2	[Hatched]	[Hatched]	[Hatched]	
	1-25	NR202-NR304	1-2	[Hatched]	[Hatched]	[Hatched]	
Winston-Salem	Fixed	1	W001	33	[Hatched]	[Hatched]	[Hatched]
		2	W002	24			
		3	W003	28			
		4	W004	29			
Home	1-114	W117-W814	1-2	[Hatched]	[Hatched]	[Hatched]	

Figure 4. Monitoring using quartz-fiber filters in the six MESA cities at fixed sites and a rotating set of home-outdoor sites. IDs in blue are sites collocated with EPA CSN sites; IDs in red are near-road sites; *n* is the number of samples per site.

with high, medium, and low ozone (O_3) levels. The resulting spatially rich data set was intended for use in identifying important geographic predictors of within-city concentration variability. Since traffic is a major source of this variability, the snapshot samples focused on concentration gradients associated with roadways, but also captured other local sources of pollution.

All snapshot samples were collected using Ogawa passive samplers attached to utility poles approximately 3 m above ground level. We selected a factorial design to sample near and far from major roadways and in areas of high and low population density. A roadway gradient design was used for most locations, with six samples collected along a trajectory perpendicular to a major roadway, defined by the U.S. Census Bureau's Census Feature Class Code (CFCC) as A1, A2, or A3 roads. Primary highways

with limited access are coded as A1, primary roads without limited access as A2, secondary connecting roads as A3, and local neighborhood roads or streets as A4 (U.S. Census Bureau 2007). Typical traffic volumes in major cities such as Los Angeles and Chicago are greater than 100,000 vehicles per day on A1 roads and less than 10,000 vehicles per day on A4 roads; in smaller cities like St. Paul or Winston-Salem, typical traffic volumes are greater than 50,000 vehicles per day on A1 roads and less than 5000 vehicles per day on A4 roads.

On either side of the major roadway, one sampler was situated between 0 and 50 m, one between 50 and 100 m, and one between 100 and 350 m from the road edge. Samplers were deployed in different orientations to capture concentration gradients in the direction of the prevailing wind and perpendicular to it.

Laboratory Analyses

PM and LAC Teflon filters were used to collect samples for determination of total PM_{2.5}, LAC, and concentrations of trace elements. Parallel measurements of samples collected with quartz-fiber filters were used to determine the presence of OC and EC and the oxidative potential of the PM. The Teflon filters were initially measured for reflectance and weighed at the University of Washington (UW), then shipped to the field centers in the six MESA metropolitan areas for assembly into HPEM samplers. Technicians based at the field centers deployed the samplers in the field and subsequently retrieved and disassembled them. These samples were shipped in coolers with freezer packs at 0°C back to the UW, where they were stored in laboratory freezers (−20°C to −10°C) after gravimetric and reflectance analyses. The quartz-fiber filters, which were not weighed, were shipped to field centers for sampling and subsequently returned to the UW for storage in laboratory freezers.

PM_{2.5} mass concentrations were gravimetrically determined at the UW with a microbalance (Mettler Toledo UMT2) from Teflon filter samples in an environment controlled for temperature and humidity (Allen et al. 2001) using standard filter-weighing procedures (U.S. EPA 1998). Reflectance was measured on the Teflon filter samples using a smoke stain reflectometer (EEL Model 43D) to determine the LAC, a surrogate for EC. Each filter was measured for reflectance before the pre-exposure filter weighing and after the post-exposure filter weighing. The light absorption coefficient by particle, b_{ap} (m^{−1}), of each sample was determined from its reflectance readings before and after exposure and adjusted by a city-specific average value from field blanks. The relationship between LAC and EC was developed empirically for each area. LAC data are not considered in this report, apart from their use in developing an adjusted EC value for use in a sensitivity analysis described in Appendix Q (available on the HEI Web site).

After gravimetric analysis and reflectometry, the Teflon filter samples were assigned to a category based on the location and type of site where they were collected and the other samples that were collected concurrently, then they were sent to a contract laboratory for elemental analysis.

Metals and Trace Elements Cooper Environmental Services of Portland, Oregon, conducted the x-ray fluorescence (XRF) analysis of the Teflon filter samples to determine the relative abundance of 48 elements. The method employed for this analysis is based on EPA Compendium Method IO-3.3 (U.S. EPA 1999). The interaction of photons produced in an x-ray tube with elements in a PM_{2.5} filter deposit is the basis of XRF spectrometry.

Table 4. Metal Elements Detected by XRF, Listed in Order of Atomic Weight^a

Na*	Cr*	Sr	La
Mg*	Mn*	Y	Ce
Al*	Fe*	Zr	Sm
Si*	Co	Nb	Eu
P	Ni*	Mo*	Tb
S*	Cu*	Ag	Hf
Cl*	Zn*	Cd*	Ta
K*	Ga	In	W
Ca*	As*	Sn	Ir
Sc	Se	Sb	Au
Ti	Br*	Cs	Hg
V*	Rb	Ba*	Pb*

^a Required detection limits were specified for those designated with (*) when selecting a laboratory for sample analysis. Cooper Environmental Services detection limits met all specified detection limits for these 21 elements.

Individual elements can be identified because of the dependence of the method's characteristic measurement on the atomic number.

The elements potentially identified by XRF are listed in Table 4; the elements for which required detection levels were specified are also identified.

Bulk Organic Species Sunset Laboratory of Tigard, Oregon, performed the analyses for EC, OC, and temperature-resolved carbon fractions. The IMPROVE_A thermal-optical reflectance (TOR) method was used to quantify the concentrations of OC, EC, and the carbon fractions. This method is consistent with the method now used by the EPA for analysis of samples from its CSN monitoring sites. When sampling using quartz-fiber filters started during the NPACT field program, the EPA was beginning its transition from use of the National Institute of Occupational Safety and Health (NIOSH)/STN thermal-optical transmittance (TOT) method to the IMPROVE_A TOR method and corresponding sampling equipment. Therefore, we selected the method that has been used in all subsequent EPA sampling and laboratory analysis protocols.

In this analysis method, a punch of approximately 1.5 cm² is removed from the quartz-fiber filter samples. Sunset Laboratory routinely conducted replicate analyses on 10% of the samples it analyzed, requiring the removal of a second punch from the filter sample. A known standard was analyzed during the course of an analysis batch to provide method quality control. Consistent with the analysis method, Sunset Laboratory provided results for OC and EC, as well as the four temperature-resolved OC peaks, three EC peaks, and pyrolytic carbon. A subset of

dynamic blank filter measurements was used in the development of a blank correction formula based on linear regression between the OC and EC filter values and their corresponding blank values. The blank-corrected OC and EC values were used in subsequent analyses. The quartz-fiber filter samples, minus the 1.5-cm² punch removed for carbon analysis, were returned. Some of these samples were subsequently extracted for determination of oxidative potential (described in Appendix E, available on the HEI Web site), and the others were archived at UW for potential later reanalysis.

Though we used the same thermal-optical protocol (IMPROVE_A) as the collocated EPA CSN sites, we observed some systematic differences between time-matched OC and EC measurements (Appendices F and L, available on the HEI Web site). From the results of the supplemental study, we concluded that our OC measurements were biased somewhat low and only moderately correlated with the EPA values. Loss of some of the more volatile or reactive OC components from our filter, compared with the EPA filter, is one possible reason. It is also possible that organic compounds were oxidized by reaction with hydroxyl radical in particles collected on our 2-week filter samples. Such oxidation is a complex process that has not been well documented with respect to reactions occurring on filters. The oxidation process can potentially not only increase the volatility of the particles on the filter, leading to loss of apparent OC (such as by production of carbon dioxide and loss of carbon), but also decrease the volatility of other compounds, leading to greater amounts of oxidized organic aerosol. Kessler et al. (2012) have recently shown that even highly oxidized organic species can undergo further oxidation by hydroxyl radical, although their studies were done in a reaction chamber, not on sampler-collected particles.

Another possible source of bias is that we overly adjusted for potential positive artifacts from gas-phase uptake on the quartz-fiber filters. Our adjustment for this effect was based on a city-specific model and a subset of filters for which there were paired backup filters. However, we observed relatively good agreement between our MESA Air/NPACT time-matched total carbon (TC) values and those at the collocated STN site: $TC_{STN} = (0.89 \pm 0.15) \times TC_{NPACT} + (0.53 \pm 0.38) \mu\text{g}/\text{m}^3$; $r^2 = 0.74$. The slight underestimate of our total carbon measurements is likely due to some loss of carbon from oxidation and volatilization. Interestingly, the intercept in the above relationship is essentially the correction that the EPA applied to all STN OC filters to account for sampling artifacts in the absence of a dynamic blank correction. The EPA's most recent recommendation, however, is to use a lower value, closer to $0.1 \mu\text{g}/\text{m}^3$, as a correction — consistent with our result (Frank 2012).

Given these results, it is most likely that our underestimate in OC is mainly due to differences in the OC/EC split obtained by thermal-optical analysis. Although the EPA-certified laboratory that conducted these filter analyses used the same protocol as the EPA used, we cannot completely rule out sampling or analytical bias. In this case, we used the IMPROVE_A filter analysis protocol that has a relatively low peak helium temperature (550°C) compared with the previous STN protocol. As such, it is more susceptible to potential positive EC bias from unpyrolyzed organics that might be formed by oxidation (Subramanian et al. 2006; Cheng et al. 2010). As discussed earlier, such further oxidation is possible on our 2-week filter samples compared with the 24-hour STN samples.

In any case, the good agreement of our total carbon values with EPA values motivated us to also estimate OC and EC exposures using both our total carbon measurements and our LAC measurements. We used this alternative set of OC and EC estimates in subsequent exposure and health models as a sensitivity analysis. (These results are discussed in detail in Appendix Q, available on the HEI Web site.)

Gaseous Pollutants Ogawa passive samplers were used to measure NO₂, NO_x, SO₂, and O₃; these were processed and analyzed in the Environmental Health Laboratories at the UW. Ion chromatography (IC) was used to analyze the sample extracts for nitrite, NO₃, and SO₄ for the quantification of NO₂, O₃, and SO₂, respectively. The IC system consisted of a Dionex ICS1000 with an AS40 autosampler and conductivity detector (Dionex, Sunnyvale, CA). A Dionex IonPac AS9-HC analytical column and AG9-HC guard column were used, along with an ASRS-ULTRA-II suppressor run in recycle mode at a current of between 37 and 45 mA. A 25- μL sample loop was used with a 9-mM sodium carbonate eluent, set to a flow rate of between 0.75 and 1.0 mL/min.

Ultraviolet spectroscopy was used for analysis of NO_x, and the mass of NO₂ was subtracted from the mass of NO_x to estimate the net mass of NO. A Spectromax 190 absorbance microplate reader (Molecular Devices, Sunnyvale, CA) was employed for the ultraviolet spectroscopy method. Nitrite ions were detected colorimetrically at a wavelength of 545 nm, and the instrument was calibrated during each analysis session using nitrite ion standards of varying concentrations (0.032 to 10 ppm). Ambient concentrations of NO, NO_x, O₃, and SO₂ were then calculated using the equations and tables provided by Ogawa.

Description of the PM_{2.5} Component Data

Table 5 shows the final mean concentrations of selected PM species (OC, EC, sulfur, silicon, aluminum, arsenic, copper, iron, potassium, nickel, vanadium, and zinc) at

Table 5. Concentrations (Mean ± SD) of Selected PM Species at MESA Air/NPACT Fixed-Site Monitors

Location/ Site No. ^a	n ^b	OC ^c (µg/m ³)	EC (µg/m ³)	n ^d	S (µg/m ³)	Si (ng/m ³)	Al (ng/m ³)
Los Angeles							
1	40	2.0 ± 0.82	2.0 ± 0.79	79	1.2 ± 0.66	144.2 ± 52.4	43.2 ± 27.6
2	29	2.2 ± 0.83	2.3 ± 0.61	78	1.1 ± 0.64	145.3 ± 58.4	44.2 ± 29.5
Coastal Los Angeles							
1	32	1.4 ± 0.71	1.4 ± 0.77	81	1.2 ± 0.60	107.8 ± 57.3	27.3 ± 20.2
2	33	1.8 ± 0.83	1.6 ± 0.73	76	1.3 ± 0.62	132.3 ± 67.6	31.9 ± 19.5
3	30	1.2 ± 0.51	1.3 ± 0.56	78	1.2 ± 0.59	119.8 ± 59.7	25.5 ± 19.0
Riverside							
1	27	2.5 ± 0.99	2.0 ± 0.62	73	1.0 ± 0.48	209.8 ± 71.8	63.5 ± 25.0
2	38	2.6 ± 1.43	1.6 ± 0.66	78	1.0 ± 0.51	238.5 ± 92.5	72.1 ± 32.4
Chicago							
1	29	1.3 ± 0.45	1.1 ± 0.29	86	1.1 ± 0.46	87.6 ± 37.3	29.2 ± 16.1
2	25	1.3 ± 0.39	1.3 ± 0.28	89	1.1 ± 0.48	108.3 ± 40.6	37.8 ± 16.5
4	39	1.4 ± 0.33	1.3 ± 0.37	69	1.2 ± 0.41	97.6 ± 38.8	38.3 ± 16.7
6	29	1.3 ± 0.42	1.3 ± 0.35	74	1.1 ± 0.40	115.7 ± 53.6	40.0 ± 17.3
7	28	1.5 ± 0.37	1.7 ± 0.35	61	1.1 ± 0.41	136.8 ± 185.2	39.0 ± 18.5
St. Paul							
1	34	1.5 ± 0.39	1.1 ± 0.20	88	0.8 ± 0.26	111.1 ± 51.4	30.8 ± 15.5
2	35	1.2 ± 0.34	0.7 ± 0.24	88	0.7 ± 0.24	91.2 ± 41.5	27.3 ± 13.5
3	44	1.3 ± 0.32	0.7 ± 0.21	91	0.7 ± 0.22	98.4 ± 44.7	30.3 ± 13.2
Baltimore							
1	35	2.2 ± 0.79	2.0 ± 0.45	87	1.6 ± 0.66	105.9 ± 44.9	35.8 ± 17.0
3	44	2.1 ± 0.82	1.3 ± 0.40	93	1.5 ± 0.62	80.7 ± 37.8	31.5 ± 16.1
4	35	1.9 ± 0.95	1.3 ± 0.27	83	1.5 ± 0.63	77.8 ± 79.4	26.6 ± 25.4
5	32	1.5 ± 0.91	0.9 ± 0.22	75	1.5 ± 0.60	62.9 ± 36.0	22.9 ± 14.6
New York							
1	44	1.6 ± 0.77	2.0 ± 0.63	83	1.4 ± 0.52	93.2 ± 40.3	36.5 ± 16.8
2	32	1.9 ± 1.19	3.1 ± 1.09	85	1.3 ± 0.60	130.8 ± 74.1	44.3 ± 20.8
Rockland County							
1	27	1.6 ± 0.75	1.2 ± 0.50	53	1.2 ± 0.53	67.9 ± 36.6	24.5 ± 14.6
Winston-Salem							
1	32	2.7 ± 2.01	1.1 ± 1.00	90	1.5 ± 0.83	83.8 ± 47.6	33.9 ± 22.2
2	25	2.4 ± 0.70	1.0 ± 0.32	91	1.5 ± 0.74	89.2 ± 53.3	34.8 ± 22.6
3	27	2.6 ± 0.66	1.2 ± 0.23	90	1.5 ± 0.76	82.9 ± 41.1	33.1 ± 22.8
4	30	2.5 ± 0.72	1.0 ± 0.23	79	1.5 ± 0.75	82.8 ± 46.8	32.1 ± 19.6

(Table continues on next page)

^a **Bold** indicates near-road site.

^b Sample counts shown are for OC and EC, which were measured over shorter intervals than elemental species obtained from Teflon filter samples.

^c Blank-corrected based on dynamic blanks (see Appendix F, available on the HEI Web site).

^d Sample counts are for elemental species.

Table 5 (Continued). Concentrations (Mean \pm SD) of Selected PM Species at MESA Air/NPACT Fixed-Site Monitors

Location/ Site No. ^a	As (ng/m ³)	Cu (ng/m ³)	Fe (ng/m ³)	K (ng/m ³)	Ni (ng/m ³)	V (ng/m ³)	Zn (ng/m ³)
Los Angeles							
1	0.83 \pm 0.45	12.7 \pm 8.1	246.4 \pm 107.7	125.8 \pm 197.8	4.7 \pm 7.3	5.0 \pm 2.3	20.9 \pm 8.0
2	0.88 \pm 0.57	14.3 \pm 11.5	223.8 \pm 77.9	158.3 \pm 346.7	1.8 \pm 0.8	4.6 \pm 2.2	18.6 \pm 8.0
Coastal Los Angeles							
1	0.65 \pm 0.44	8.4 \pm 7.0	143.4 \pm 104.7	90.4 \pm 46.1	2.4 \pm 0.9	6.7 \pm 2.7	9.8 \pm 6.6
2	0.71 \pm 0.48	10.8 \pm 7.2	187.4 \pm 111.9	128.4 \pm 144.9	2.3 \pm 0.9	6.2 \pm 2.5	18.1 \pm 13.3
3	0.66 \pm 0.47	11.3 \pm 8.5	176.5 \pm 118.9	91.0 \pm 60.4	2.4 \pm 1.1	6.4 \pm 2.6	10.4 \pm 6.9
Riverside							
1	0.92 \pm 0.51	7.5 \pm 5.0	194.6 \pm 69.6	148.7 \pm 156.0	1.6 \pm 0.7	3.9 \pm 1.8	18.3 \pm 9.0
2	0.90 \pm 0.53	8.5 \pm 5.3	199.6 \pm 83.3	163.5 \pm 163.8	1.4 \pm 0.7	3.8 \pm 1.9	19.4 \pm 11.1
Chicago							
1	0.90 \pm 0.41	3.8 \pm 2.9	79.3 \pm 23.7	75.0 \pm 89.3	0.3 \pm 0.4	0.3 \pm 0.2	16.2 \pm 5.1
2	0.93 \pm 0.56	5.5 \pm 1.9	138.2 \pm 63.2	76.0 \pm 37.4	0.4 \pm 0.2	0.3 \pm 0.3	33.4 \pm 12.1
4	1.03 \pm 0.48	4.4 \pm 3.7	101.1 \pm 33.9	94.3 \pm 156.1	0.5 \pm 0.4	0.2 \pm 0.2	24.6 \pm 7.8
6	0.93 \pm 0.52	4.2 \pm 3.1	115.1 \pm 33.8	78.3 \pm 74.7	0.4 \pm 0.2	0.3 \pm 0.3	30.7 \pm 11.6
7	0.93 \pm 0.56	8.9 \pm 4.5	154.6 \pm 39.7	97.7 \pm 149.6	0.4 \pm 0.2	0.3 \pm 0.3	46.9 \pm 19.4
St. Paul							
1	0.99 \pm 0.54	4.2 \pm 2.7	100.4 \pm 25.9	82.6 \pm 89.5	0.4 \pm 0.5	0.4 \pm 0.3	16.3 \pm 5.6
2	1.08 \pm 0.49	1.9 \pm 2.3	48.5 \pm 14.3	78.2 \pm 86.5	0.2 \pm 0.2	0.3 \pm 0.3	11.5 \pm 4.2
3	0.92 \pm 0.53	3.5 \pm 3.7	55.8 \pm 16.4	83.6 \pm 111.0	0.9 \pm 1.8	1.6 \pm 2.9	11.3 \pm 6.4
Baltimore							
1	1.19 \pm 0.51	7.6 \pm 2.6	184.8 \pm 57.0	105.3 \pm 65.1	1.1 \pm 0.6	2.4 \pm 1.1	26.5 \pm 13.7
3	1.44 \pm 0.55	4.3 \pm 3.2	102.9 \pm 32.3	141.0 \pm 110.4	1.0 \pm 0.4	2.1 \pm 0.9	18.9 \pm 7.7
4	1.00 \pm 0.42	5.5 \pm 5.7	114.2 \pm 134.8	75.4 \pm 54.6	0.6 \pm 0.8	1.1 \pm 0.9	14.2 \pm 8.2
5	1.00 \pm 0.49	2.3 \pm 1.0	51.4 \pm 15.2	63.0 \pm 34.5	0.4 \pm 0.3	0.8 \pm 0.5	10.2 \pm 4.1
New York							
1	0.73 \pm 0.51	5.7 \pm 2.1	125.4 \pm 30.3	59.0 \pm 36.7	9.8 \pm 5.7	3.8 \pm 1.5	39.4 \pm 16.9
2	0.84 \pm 0.52	10.2 \pm 2.8	243.4 \pm 67.6	61.2 \pm 32.0	10.4 \pm 9.9	4.0 \pm 1.6	37.8 \pm 19.1
Rockland County							
1	0.73 \pm 0.45	2.7 \pm 1.5	58.4 \pm 14.5	47.4 \pm 23.3	1.3 \pm 0.8	1.3 \pm 0.7	10.8 \pm 5.0
Winston-Salem							
1	1.11 \pm 0.51	3.1 \pm 2.4	54.3 \pm 21.4	75.8 \pm 33.2	0.3 \pm 0.9	0.5 \pm 0.3	9.0 \pm 3.7
2	1.03 \pm 0.53	2.2 \pm 1.3	51.9 \pm 17.8	75.6 \pm 29.0	0.2 \pm 0.2	0.5 \pm 0.3	8.3 \pm 3.1
3	0.92 \pm 0.43	4.3 \pm 2.4	77.7 \pm 21.5	74.2 \pm 27.3	0.2 \pm 0.3	0.5 \pm 0.3	9.7 \pm 3.7
4	1.02 \pm 0.48	2.0 \pm 1.1	45.4 \pm 15.3	73.1 \pm 26.1	0.2 \pm 0.2	0.4 \pm 0.3	7.8 \pm 2.9

^a **Bold** indicates near-road site.^b Sample counts shown are for OC and EC, which were measured over shorter intervals than elemental species obtained from Teflon filter samples.^c Blank-corrected based on dynamic blanks (see Appendix F, available on the HEI Web site).^d Sample counts are for elemental species.

each of the MESA Air/NPACT fixed monitoring sites. As expected, sulfur was higher in the east; silicon and aluminum, in Riverside, California; nickel, in New York; and vanadium, in New York and Los Angeles, especially coastal Los Angeles. The time periods over which the respective means were calculated are shown in Figures 3 and 4. As noted earlier, measurements of elements and metals were obtained over a longer time period than EC and OC measurements because Teflon filters were deployed during the entire period of MESA Air monitoring, while quartz-fiber filters were only deployed during the shorter period of NPACT monitoring.

The species concentration data reflect differences between monitoring sites within cities as well as differences between cities. The MESA Air monitoring campaign included both fixed and home-outdoor monitoring sites. The monitors at fixed sites were characterized as being either population-oriented monitors or roadside monitors. They were located in study areas underrepresented by the existing EPA regulatory monitoring network and were collocated with EPA CSN sites. One monitor was also placed within 100 m of a major roadway in each area. In general, as expected, the average concentrations of EC and copper were higher at the near-road sites than the other sites, although not dramatically higher. There were two exceptions, both in the Los Angeles area: EC was not highest at the near-road monitor for the coastal site, and copper was not highest at the near-road monitor for the Riverside site. For copper, this apparent discrepancy is explained by the source-apportionment (PMF) analysis. In Riverside, estimates of the average contribution to copper from the PMF-derived diesel exhaust/brake wear-like feature were higher at the near-road site than at the nonroad site, indicating that even though the mean copper concentration was lower, copper at that site was reflecting more of the diesel exhaust/brake wear-like feature than at the other site. The overall contribution to copper from all other PMF-derived features was greater at the nonroad site than at the near-road site, suggesting that other sources of copper contributed to the high copper level at the nonroad monitor. Why the near-road monitor in the Los Angeles coastal area did not have the highest EC concentration is not as clear; however, the monitoring site with the highest average EC concentration in the Los Angeles coastal area was also relatively near another major road. Furthermore, there were many source contributions to EC, so it is possible that these other sources contributed to EC at the nonroad sites.

The mean concentrations of the same selected PM species as for fixed sites are summarized for home-outdoor sites by city in Table 6. The results at the home-outdoor sites mirror those at the fixed monitoring sites, with sulfur

higher in the east, silicon and aluminum highest in Riverside, California, nickel higher in New York, and vanadium higher in New York and Los Angeles, especially coastal Los Angeles. The levels of iron and potassium were elevated at both the home-outdoor fixed monitoring sites in Riverside, but less so at the fixed sites.

SOURCE APPORTIONMENT

The primary focus of the NPACT initiative is on PM components; however, we used source apportionment to also gain insight into the sources in the MESA cities associated with the PM components we chose to be of primary interest: EC, OC, sulfur, and silicon.

We used the EPA's PMF tool based on the table-driven weighted least squares algorithm of Paatero (1999) to decompose the observed species concentrations into linear factors that are related to the underlying variability in the data, which is associated with both transport and transformation of source emissions. Our goal was not to use PMF to specifically apportion $PM_{2.5}$, but rather to explore whether there are species that are strongly associated with a given PMF factor, both within and between cities. Specifically, we wanted to know whether the species chosen for spatiotemporal modeling and subsequent epidemiologic analyses were associated with particular factors identifiable by PMF. Therefore, we included in our analyses both the particulate species, including trace metals and temperature-resolved organic fractions, and the gaseous components NO_2 , NO_x , and SO_2 .

Previous studies have examined the influence of sources in one or more of the six MESA cities. These studies focused primarily, but not exclusively, on the sources of $PM_{2.5}$. Not surprisingly, no previous studies have included all six of these cities in the same analysis. In Appendix J (available on the HEI Web site), we include a review of the literature on source-apportionment findings relevant to the six MESA cities. Information in Appendix J helps to place in context the source-apportionment findings described below.

Data and Methods

Investigators typically report PMF results that are based on daily, or sometimes even hourly, measurements of a given set of species taken at a given site. Our data set is somewhat different in that for each city we are using 2-week measurements sampled not only at several sites simultaneously within a given city, but also at other sites throughout the city at different times in two different seasons. This sampling strategy was dictated by the need for such data as inputs to the spatiotemporal model. In principle, this should not affect our PMF results, given that

Table 6. Concentrations (Mean \pm SD) of Selected PM Species at MESA Air/NPACT Home-Outdoor Sites

Location	n^a	OC ^b ($\mu\text{g}/\text{m}^3$)	EC ($\mu\text{g}/\text{m}^3$)			
Los Angeles	39	2.2 \pm 1.10	2.0 \pm 0.88			
Coastal Los Angeles	20	1.1 \pm 0.34	0.9 \pm 0.28			
Riverside	39	2.5 \pm 0.95	1.9 \pm 0.66			
Chicago	88	1.4 \pm 0.45	1.2 \pm 0.36			
St. Paul	94	1.3 \pm 0.34	0.8 \pm 0.23			
Baltimore	107	2.0 \pm 1.21	1.2 \pm 0.38			
New York	55	2.1 \pm 1.16	2.2 \pm 0.96			
Rockland County	36	2.1 \pm 1.21	1.1 \pm 0.53			
Winston-Salem	89	2.8 \pm 0.77	1.0 \pm 0.30			
	n^c	S ($\mu\text{g}/\text{m}^3$)	Si (ng/m^3)	Al (ng/m^3)	As (ng/m^3)	Cu (ng/m^3)
Los Angeles	101	1.1 \pm 0.61	120.7 \pm 55.5	29.4 \pm 20.9	0.90 \pm 0.58	8.9 \pm 5.2
Coastal Los Angeles	29	1.4 \pm 0.75	98.5 \pm 29.9	18.1 \pm 11.1	0.59 \pm 0.36	7.2 \pm 6.0
Riverside	51	0.8 \pm 0.45	238.8 \pm 146.2	66.8 \pm 49.8	0.74 \pm 0.42	5.8 \pm 2.2
Chicago	161	1.1 \pm 0.39	106.8 \pm 89.0	30.3 \pm 21.1	1.04 \pm 0.52	4.5 \pm 4.1
St. Paul	190	0.7 \pm 0.23	100.5 \pm 43.7	22.6 \pm 15.4	1.31 \pm 2.12	2.8 \pm 4.3
Baltimore	159	1.7 \pm 0.66	78.3 \pm 48.2	19.9 \pm 20.0	1.07 \pm 0.54	3.7 \pm 2.0
New York	170	1.4 \pm 0.60	109.2 \pm 73.9	34.9 \pm 24.9	0.89 \pm 0.55	7.7 \pm 3.7
Rockland County	55	1.2 \pm 0.56	85.2 \pm 175.8	10.9 \pm 10.0	0.90 \pm 0.70	2.7 \pm 1.1
Winston-Salem	177	1.7 \pm 0.72	99.7 \pm 53.1	31.2 \pm 24.6	1.16 \pm 0.57	2.3 \pm 1.3
	n^c	Fe (ng/m^3)	K (ng/m^3)	Ni (ng/m^3)	V (ng/m^3)	Zn (ng/m^3)
Los Angeles	101	175.6 \pm 78.2	88.7 \pm 35.2	2.2 \pm 1.2	5.4 \pm 2.7	16.8 \pm 8.4
Coastal Los Angeles	29	115.9 \pm 82.1	94.2 \pm 53.9	2.2 \pm 0.7	6.0 \pm 2.3	9.1 \pm 5.8
Riverside	51	201.3 \pm 95.1	113.2 \pm 47.9	1.2 \pm 0.6	3.1 \pm 1.5	18.3 \pm 8.6
Chicago	161	100.3 \pm 41.8	94.9 \pm 150.5	0.3 \pm 0.2	0.3 \pm 0.3	22.6 \pm 12.8
St. Paul	190	63.8 \pm 47.8	105.8 \pm 156.3	0.3 \pm 0.5	0.3 \pm 0.3	13.5 \pm 11.3
Baltimore	159	92.4 \pm 48.4	79.1 \pm 39.9	0.8 \pm 1.3	1.4 \pm 1.2	14.6 \pm 8.7
New York	170	234.4 \pm 561.3	73.8 \pm 48.4	14.4 \pm 11.1	5.7 \pm 3.5	48.8 \pm 30.2
Rockland County	55	58.6 \pm 17.3	56.0 \pm 32.3	1.5 \pm 1.0	1.3 \pm 0.6	11.3 \pm 5.7
Winston-Salem	177	55.7 \pm 22.5	83.2 \pm 29.0	0.1 \pm 0.2	0.5 \pm 0.3	8.1 \pm 2.8

^a Sample counts shown are for OC and EC, which were measured over shorter intervals than elemental species obtained from Teflon filter samples.

^b Blank-corrected based on dynamic blanks (see Appendix F, available on the HEI Web site).

^c Sample counts shown are for elemental species.

each sample contains measurements of the same species and the variability across samples in species concentrations is exploited by PMF.

However, measurement of volatile species, including OC and chloride and nitrate ions, is not optimal with 2-week samples. Compared with daily samples, there is greater opportunity for chloride species on the filter to be replaced by subsequently sampled nitric acid vapor over

the longer 2-week sampling period. There is also more opportunity for volatilization off the filters of previously sampled nitrate ion that has not reacted with chlorine species. Our low-volume samplers did not include an upstream denuder or backup filter to recapture volatilized nitrate and chloride ions. Therefore, we chose not to measure nitrate ion. Not surprisingly, the XRF-based chlorine measurements were most often below detection limits in

this data set, presumably due to volatilization of the chlorine, as previously discussed. We therefore chose not to include chlorine in our analyses. Implications of these choices are discussed under “PMF Results.”

Sample measurements from both the MESA Air/NPACT fixed monitoring sites and the home-outdoor sites were used for the PMF analysis. The species used in the PMF analysis are listed in Table 7.

Species for which the measurement was less than or equal to the limit of detection in more than 50% of samples were excluded from source-apportionment analysis: antimony, cadmium, cesium, chlorine, cobalt, gold, hafnium, indium, iridium, lanthanum, mercury, niobium, rubidium, samarium, scandium, silver, tantalum, tin, tungsten, and yttrium. An exception was that magnesium was included, though the measurement was less than or equal to the limit of detection in 54% of samples, because it is a relatively good marker of crustal sources. We excluded some species, even though they were above the limit of detection in more than 50% of samples, if we judged that they would not add further information to the model: cerium, europium, gallium, phosphorus, and terbium. Nitric oxide was excluded because this measure is already accounted for by the inclusion of NO_2 and NO_x . Peak 1 of the OC data was excluded because it was found to be an unstable measurement.

Of the XRF species that were kept in the model, negative values were replaced with half of their measurement uncertainty; the limit of detection was not used because this was often zero, and zero values of concentration cannot be computed in PMF. Negative values of carbon species and gaseous species were replaced with half of their limit of detection. Missing observations were replaced with the median species concentration for each city. For a given city, species with an average signal-to-noise ratio ($S/N = \text{measured concentration}/\text{measurement uncertainty}$) near or below 1 were excluded, and those with $1 \leq S/N < 2$ were downscaled by increasing their measurement uncertainties by a factor of 3. In all cities $\text{PM}_{2.5}$, total carbon, and NO_x were downscaled by a factor of 30 to adjust for the fact that these species are the sum of other species in the models.

Samples with strontium concentrations greater than the 95th percentile of strontium for each city were excluded. These high-concentration samples most often included those obtained on either the July 4 or the January 1 holidays and were observed at all sites, consistent with samples strongly influenced by fireworks. Samples with high chlorine, sodium, and potassium levels, defined as 6 times the SD of the mass fraction of each species for each city, were also excluded, as the high levels of these species may

be attributed to contamination from handling the samples. An attributed mass was reconstructed for each sample, defined as: $1.6 \times (\text{OC} + \text{EC}) + 2.2 \times \text{Aluminum} + 2.49 \times \text{Silicon} + 1.63 \times \text{Calcium} + 2.42 \times \text{Iron} + 1.94 \times \text{Titanium} + 3.6 \times \text{Sulfur} + \text{Sum of other elements}$. Samples were excluded if the ratio of the attributed mass to the measured mass ($\text{PM}_{2.5}$ concentration) was less than the 5th percentile or greater than the 99th percentile for each city.

The PMF analyses were implemented using the EPA software program PMF4.1, which includes tools not available in the PMF3.xx series, including rotational tools to examine the robustness of a given solution. We relied on these rotational analysis tools, notably the displacement method analyses, to assist in the choice of the number of factors (Norris et al. 2010). The final models met the stated criteria for a sufficiently constrained model, defined in terms of the number of factor swaps under predefined rotational freedom for all factors. In addition, the final models met the more general criterion that the robust value of the base-case objective function, Q , was near its theoretical value. It should be noted, however, that there is no absolute set of rules that one can use to specify a best final model. In addition to the quantitative criteria described above, we used judgment and previously published results from the cities of interest to choose the final model in each city.

PMF Results

In this summary of PMF results, factor loadings are presented by city without reference to a given associated source or sources. The average factor contributions across all samples in a given city are then presented along with the associated standard errors, based on 20 fits to the model with bootstrapping. Finally, we summarize the pairwise correlations between the factor contributions and the selected species by city.

Factor Loadings (Source Profiles) The factor loadings for each MESA city (frequently referred to as source profiles in the literature) are shown in Figures 5 through 10. The designated factor numbers represent the order in which the factors were generated by the PMF base-case solution and thus are not associated with a similarly numbered factor in another city. Not surprisingly, several source profiles were similar across two or more cities.

The identification of possible sources related to each of the extracted factors is challenging. However, all cities had some factors in common, even though the PMF analyses were done separately for each city. This implies that common sources were driving the variability captured by these factors. The possible underlying sources are discussed

Table 7. Median Measured Species Concentrations Used in PMF Analysis^{a,b}

Species	Baltimore			Chicago			Los Angeles			New York			St. Paul			Winston-Salem		
	Median	S/N	RMSE/ Mean ^c	Median	S/N	RMSE/ Mean ^c	Median	S/N	RMSE/ Mean ^c	Median	S/N	RMSE/ Mean ^c	Median	S/N	RMSE/ Mean ^c	Median	S/N	RMSE/ Mean ^c
PM _{2.5} ^d	14.00	0.43	0.08	13.59	0.49	0.12	14.30	0.30	0.17	13.65	0.34	0.10	8.16	0.40	0.17	12.51	0.40	0.08
Al	26.57	11.87	0.14	37.53	17.64	0.10	35.87	18.70	0.18	28.07	15.40	0.29	22.90	14.30	0.13	23.53	1.00	0.49
As	1.09	4.42	0.43	1.06	3.17	0.41	0.65	3.00	0.56	0.82	3.25	0.59	1.01	8.80	1.81	1.01	1.00	0.48
Ba	5.12	3.84	0.34	5.26	2.67	0.31	10.08	5.70	0.20	6.58	5.89	0.92	3.32	2.40	0.49	2.95	2.10	0.46
Br	3.50	15.09	0.12	3.26	13.37	0.17	4.72	17.50	0.17	2.86	12.31	0.15	2.29	11.40	0.25	3.85	15.10	0.08
Ca	43.69	24.98	0.38	92.13	25.74	0.03	84.43	25.80	0.17	93.27	25.54	0.15	59.85	25.30	0.30	28.87	23.20	0.04
Cr	0.66	9.33	2.36	1.06	4.96	0.45	0.94	4.60	0.30	0.88	8.30	1.63	0.41	1.90	0.49	0.32	10.40	3.99
Cu	3.74	10.87	0.16	4.13	17.02	0.06	6.89	20.40	0.09	5.96	10.49	0.30	2.35	6.00	0.50	2.48	7.40	0.55
Fe	90.88	25.19	0.09	111.03	26.25	0.07	155.06	26.30	0.05	128.44	26.50	2.69	54.67	20.00	0.12	52.92	22.40	0.10
K	71.41	23.76	0.03	67.30	20.22	0.13	83.71	23.90	0.19	55.32	21.17	0.31	65.52	23.00	0.26	77.25	24.70	0.07
Mg	8.09	5.27	0.34	44.33	9.28	0.15	8.95	6.80	0.28	17.72	6.34	0.30	18.21	8.60	0.23	1.12	3.80	1.60
Mn	2.45	9.75	0.18	3.77	13.10	0.29	3.36	14.30	0.26	3.38	15.96	1.28	2.09	8.40	0.20	1.67	4.90	0.31
Mo	0.48	0.73	—	0.55	0.99	0.83	0.56	1.00	0.54	0.94	2.08	0.48	0.52	0.60	—	0.41	0.70	—
Na	3.33	0.78	—	0.39	0.50	—	117.32	14.90	0.10	3.24	2.55	—	3.30	2.30	—	3.36	0.50	—
Ni	0.61	5.38	1.47	0.38	2.73	0.60	1.91	16.40	1.62	5.81	13.78	0.15	0.19	1.70	1.31	0.16	2.80	2.38
Pb	3.31	9.42	0.53	4.69	10.18	0.25	2.58	7.40	0.37	2.93	6.97	0.32	2.82	24.00	5.04	2.24	3.40	0.40
S ^d	1.46	27.16	0.07	1.06	27.08	0.04	1.14	27.10	0.06	1.22	27.11	0.02	0.67	26.90	0.04	1.47	27.20	0.02
Se	1.33	7.39	0.24	1.00	5.12	0.27	0.65	4.60	0.51	0.70	3.51	0.37	0.61	3.40	0.48	1.65	1.10	0.24
Si	86.15	24.80	0.12	113.23	26.23	0.09	144.81	26.50	0.08	103.40	25.80	0.27	92.19	25.90	0.08	93.40	24.70	0.08
Sr	0.23	1.43	0.85	0.66	2.61	0.56	1.39	5.80	0.43	0.61	2.17	0.54	0.23	1.40	0.97	0.21	0.60	—
Ti	4.74	14.86	0.39	4.02	11.36	0.14	8.11	17.60	0.13	4.11	12.50	0.31	2.63	14.50	0.96	3.72	9.60	0.13
V	1.30	5.72	0.38	0.25	0.72	—	4.73	13.60	0.21	3.01	10.85	0.26	0.29	3.30	1.54	0.38	1.30	0.49
Zn	12.96	21.29	0.03	25.67	25.53	0.03	12.78	22.90	0.04	29.04	21.86	0.09	10.96	13.50	0.34	7.87	13.40	0.11
Zr	0.62	2.00	0.52	0.81	2.14	0.42	1.30	4.90	0.30	1.04	3.03	0.42	0.30	1.00	0.72	0.29	0.80	—
LAC ^e	0.63	8.87	0.14	0.72	7.73	0.18	1.01	12.30	0.12	1.11	12.03	0.22	0.41	8.10	0.18	0.45	6.60	0.17
TC ^d	3.42	0.34	0.14	3.05	0.25	0.08	4.46	0.60	0.11	4.31	0.44	0.06	2.78	0.20	0.12	3.62	0.30	0.06
OC ^d	2.10	8.60	0.20	1.76	6.65	0.15	2.73	10.50	0.15	2.22	8.37	0.16	1.98	8.10	0.15	2.50	8.60	0.09
Pk2 ^d	0.85	5.98	0.21	0.79	5.22	0.18	1.11	6.70	0.15	1.09	6.90	0.17	0.66	4.40	0.20	0.98	6.20	0.17
Pk3 ^d	0.37	2.89	0.25	0.38	3.20	0.29	0.79	6.00	0.17	0.45	3.65	0.23	0.45	3.50	0.23	0.43	3.60	0.20
Pk4 ^d	0.21	4.64	0.22	0.19	4.38	0.32	0.28	5.90	0.20	0.25	5.25	0.19	0.20	4.50	0.21	0.22	4.90	0.15
Pyrol ^d	0.82	4.06	0.23	0.52	2.60	0.27	0.54	3.00	0.42	0.70	3.59	0.36	0.63	2.90	0.21	1.13	4.80	0.11
EC ^d	1.23	8.07	0.17	1.31	8.03	0.14	1.63	9.90	0.19	1.97	10.34	0.17	0.78	5.50	0.21	1.04	6.70	0.18
EC1 ^d	1.69	13.89	0.15	1.63	13.41	0.08	1.74	14.50	0.20	2.15	14.68	0.09	1.04	11.70	0.15	1.71	13.90	0.08
EC2 ^d	0.37	2.80	0.48	0.27	2.21	0.55	0.43	2.70	0.41	0.48	3.91	0.49	0.35	2.30	0.39	0.36	2.50	0.46
EC3 ^d	0.013	1.58	1.37	0.04	0.46	—	0.02	0.90	—	0.03	1.22	0.87	0.01	0.90	—	0.01	1.00	0.96
NO _x ^f	17.47	0.37	0.21	25.52	0.29	0.32	30.65	0.60	0.32	38.27	0.44	0.33	14.69	0.40	0.34	9.45	0.50	0.25
NO ₂ ^f	11.54	13.25	0.14	16.76	16.43	0.16	18.13	13.60	0.22	22.48	12.26	0.25	9.71	8.30	0.24	6.17	6.60	0.22
SO ₂ ^f	1.06	5.22	0.68	0.67	5.31	0.91	0.32	0.40	—	1.28	7.63	0.60	0.31	4.00	1.55	0.37	3.90	0.68

^a S/N indicates measured concentration/measurement uncertainty; RMSE, root mean squared error; —, species excluded from analysis. Pk2, Pk3, Pk4 are the temperature-resolved OC peaks; EC1, EC2, EC3, the EC peaks; Pyrol, pyrolytic carbon.

^b Data are expressed in ng/m³ unless specified otherwise.

^c All species means in µg/m³ except NO_x, NO₂, and SO₂ means in ppbv.

^d Data are expressed in µg/m³.

^e Data are expressed in µg/m³ estimated from conversion of units of 10⁻⁵ m⁻¹.

^f Data are expressed in ppbv.

■ = S/N ≥ 2 ■ = 1 ≤ S/N < 2 ■ = Downscaled by 30× Uncertainty ■ = S/N < 1, excluded

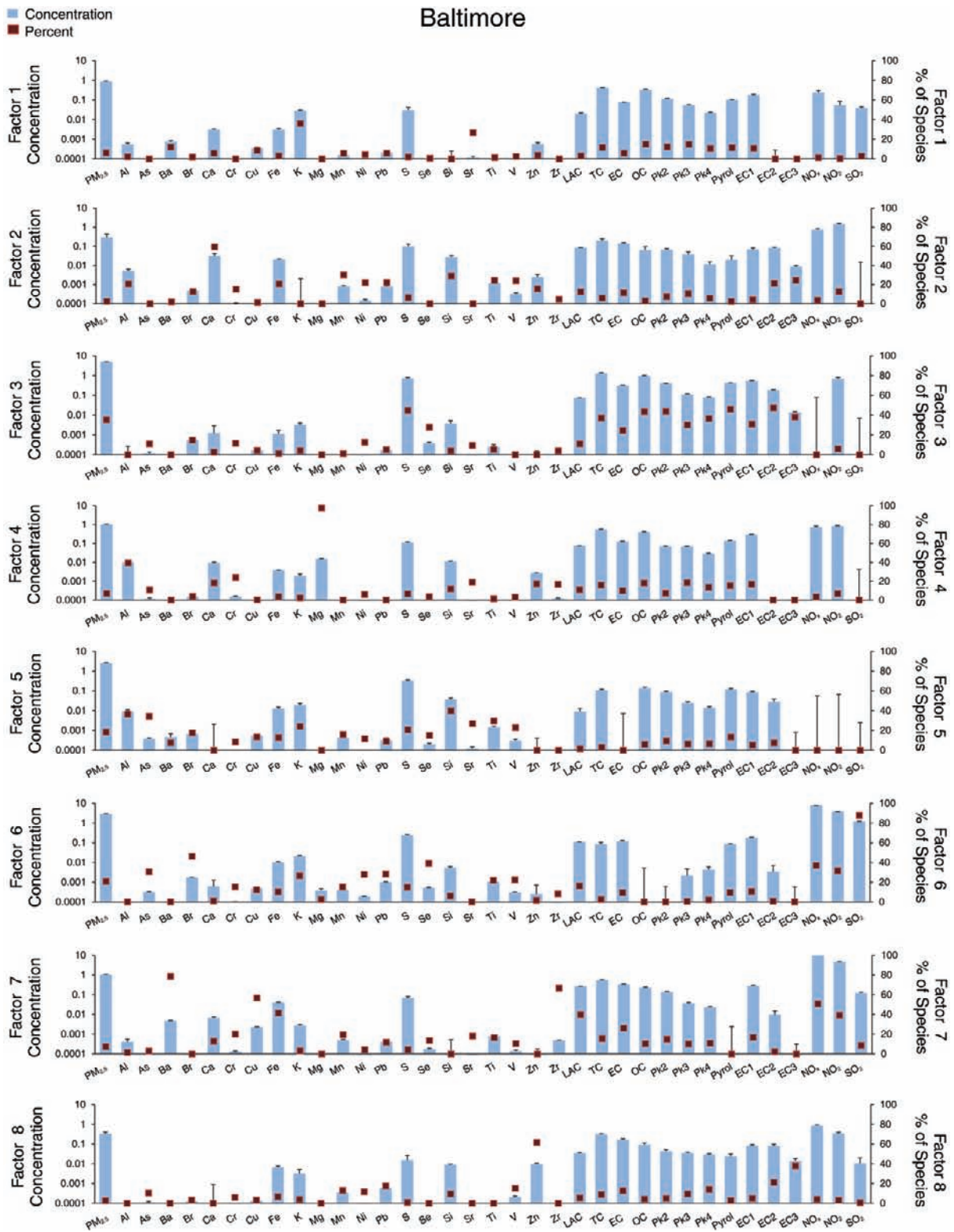
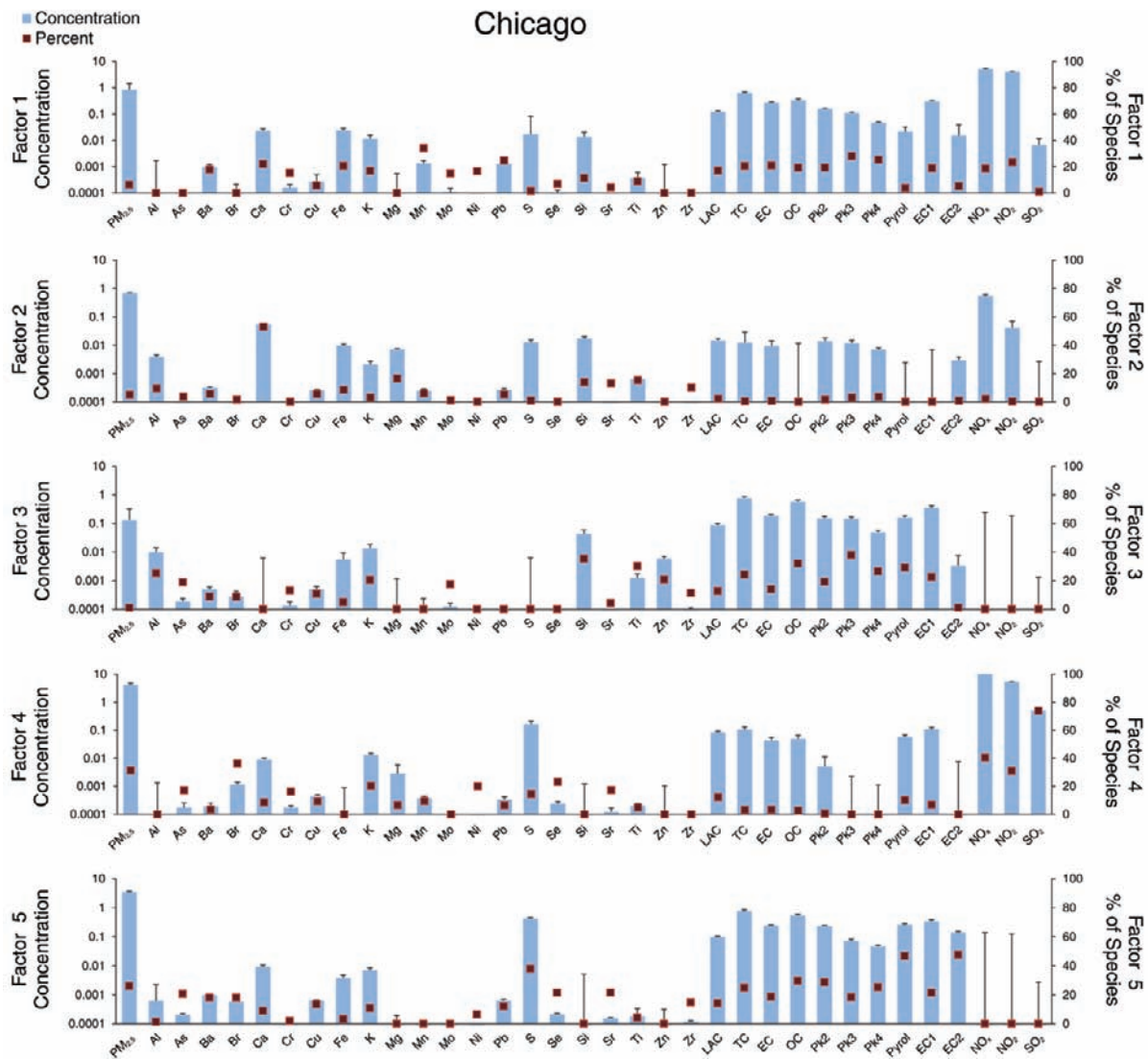


Figure 5. PMF-derived factor profiles for Baltimore. Average species concentrations (blue bars and scale on left) include bootstrapped estimates of the respective uncertainties (standard errors shown). Concentration units are $\mu\text{g}/\text{m}^3$, except for NO_x , NO_2 , and SO_2 units, which are ppbv. The average percent contribution to the overall predicted species concentrations is also shown for each factor (red dots and scale on right). Factor 1 is biomass-like; 2, road dust-like; 3, secondary SO_4 ; 4, magnesium-rich; 5, crustal-like; 6, oil combustion-like; 7, diesel exhaust/brake wear-like; 8, zinc-rich.



(Figure continues on next page.)

Figure 6. PMF-derived factor profiles for Chicago. Average species concentrations (blue bars and scale on left) include bootstrapped estimates of the respective uncertainties (standard errors shown). Concentration units are $\mu\text{g}/\text{m}^3$, except for NO_x , NO_2 , and SO_2 units, which are ppbv. The average percent contribution to the overall predicted species concentrations is also shown for each factor (red dots and scale on right). Factor 1 is gasoline-like; 2, crustal-like; 3, biomass-like; 4, oil combustion-like; 5, secondary SO_4 and secondary organic; 6, diesel exhaust/brake wear-like; 7, magnesium-rich; 8, industrial; 9, zinc-rich.

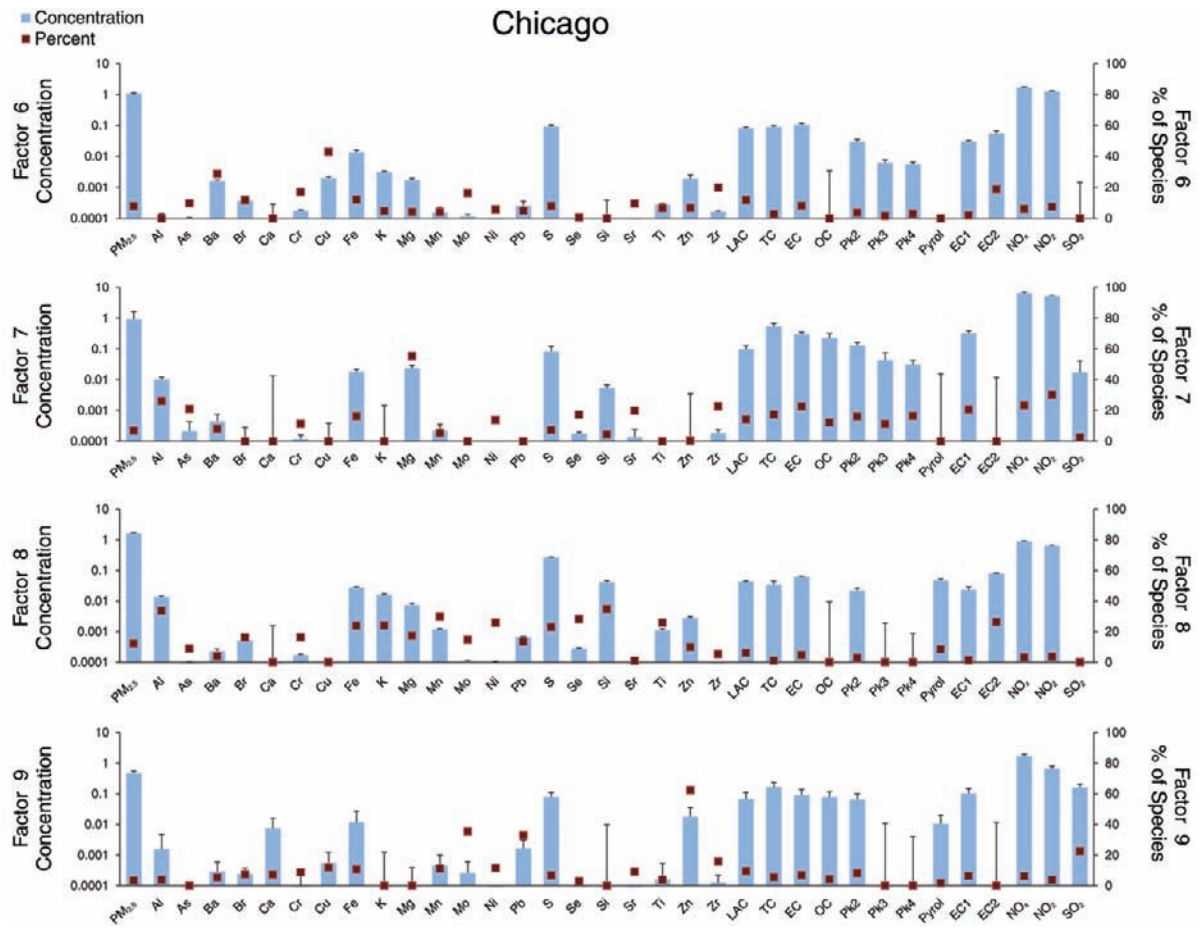


Figure 6 (Continued).

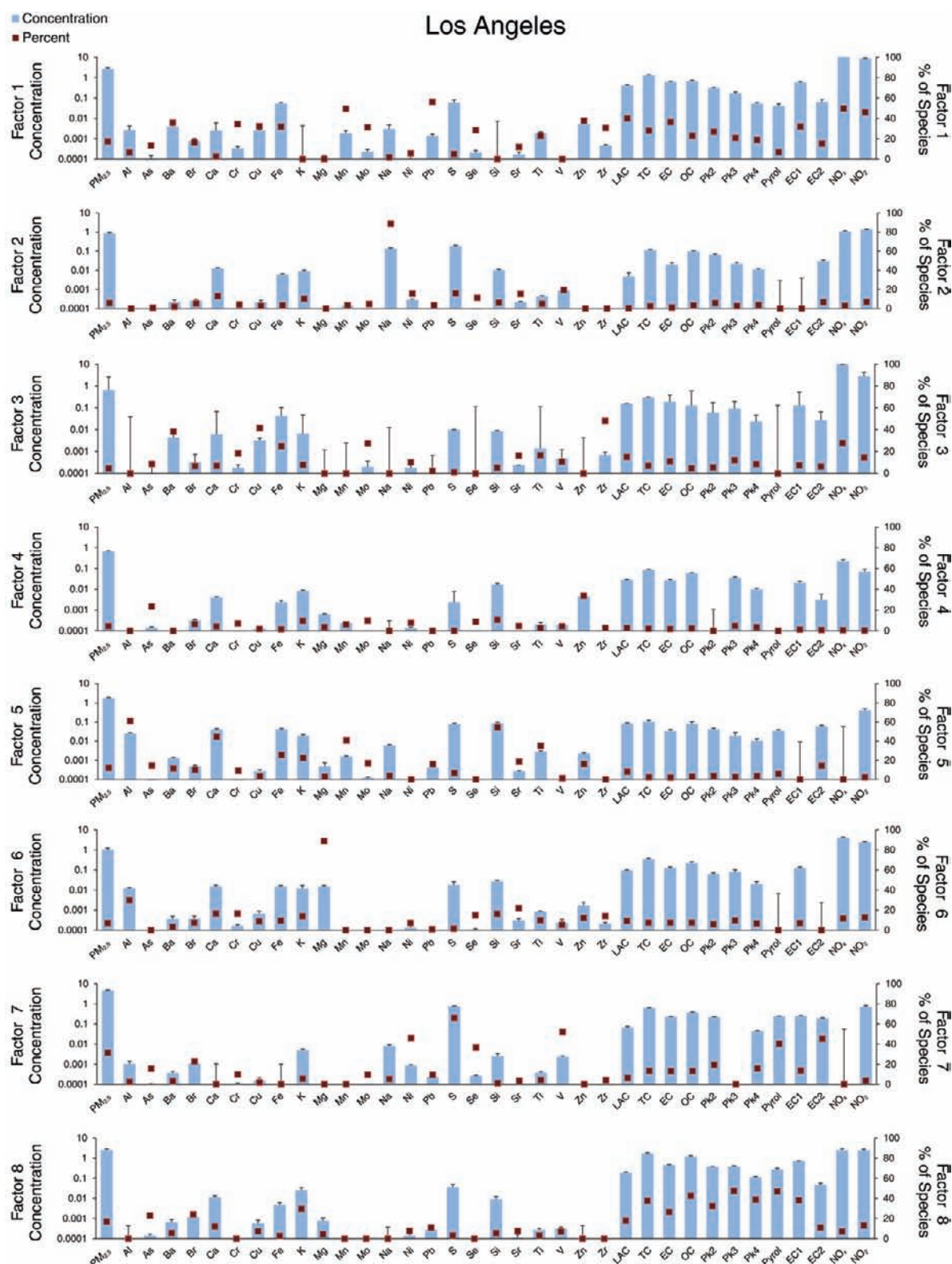
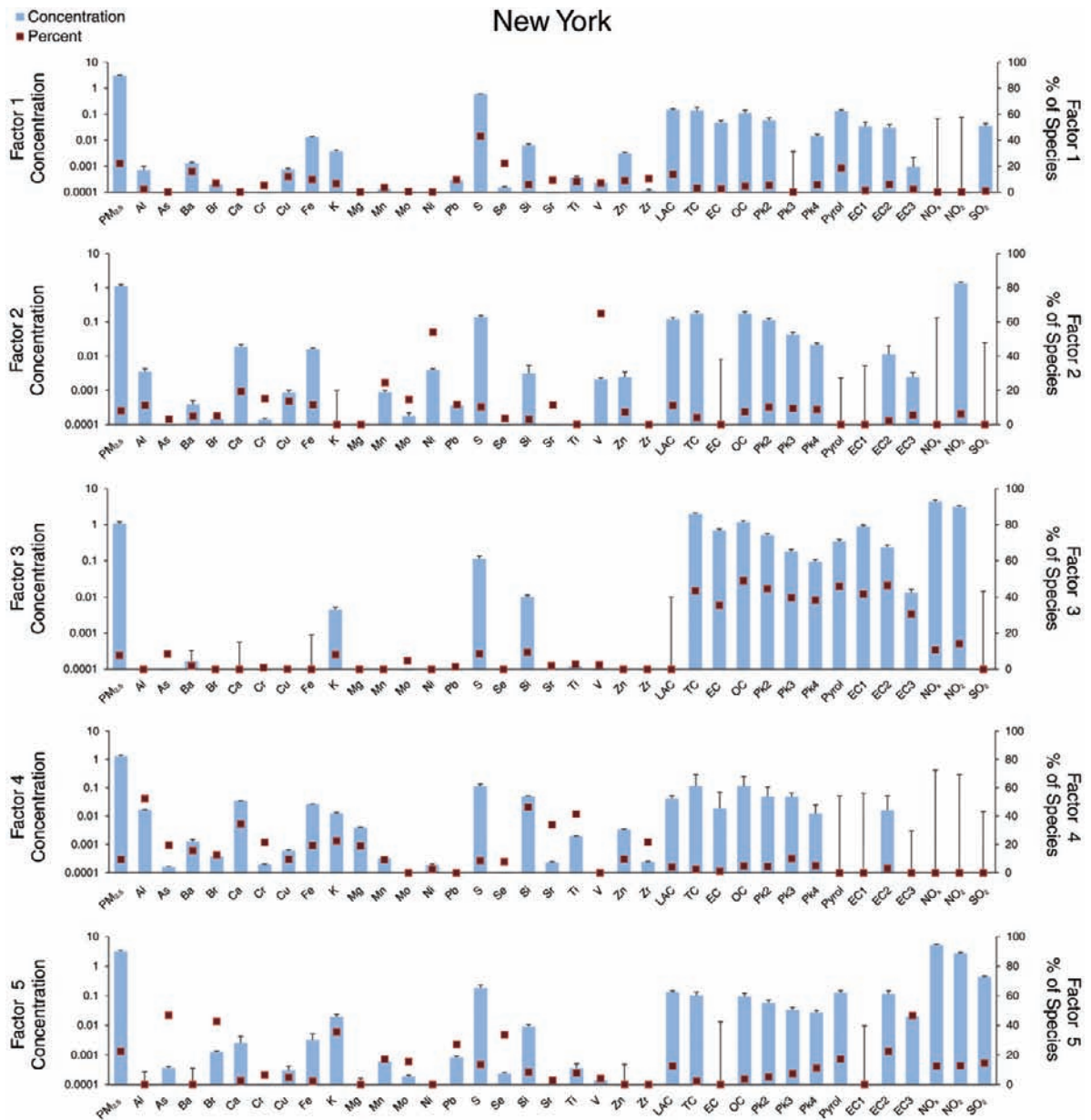


Figure 7. PMF-derived factor profiles for Los Angeles. Average species concentrations (blue bars and scale on left) include bootstrapped estimates of the respective uncertainties (standard error shown). Concentration units are $\mu\text{g}/\text{m}^3$, except for NO_x , NO_2 , and SO_2 units, which are ppbv. The average percent contribution to the overall predicted species concentrations is also shown for each factor (red dots and scale on right). Factor 1 is diesel exhaust/brake wear-like; 2, aged sea salt-like; 3, winter NO_x ; 4, zinc-rich; 5, crustal-like; 6, magnesium-rich; 7, oil combustion/secondary SO_4 ; 8, secondary organic.



(Figure continues on next page.)

Figure 8. PMF-derived factor profiles for New York. Average species concentrations (blue bars and scale on left) include bootstrapped estimates of the respective uncertainties (standard error shown). Concentration units are $\mu\text{g}/\text{m}^3$, except for NO_x , NO_2 , and SO_2 units, which are ppbv. The average percent contribution to the overall predicted species concentrations is also shown for each factor (red dots and scale on right). Factor 1 is secondary SO_4 ; 2, residual oil combustion-like; 3, secondary organic; 4, crustal-like; 5, local area sources; 6, zinc-rich; 7, oil combustion-like; 8, magnesium-rich; 9, diesel exhaust/brake wear-like.

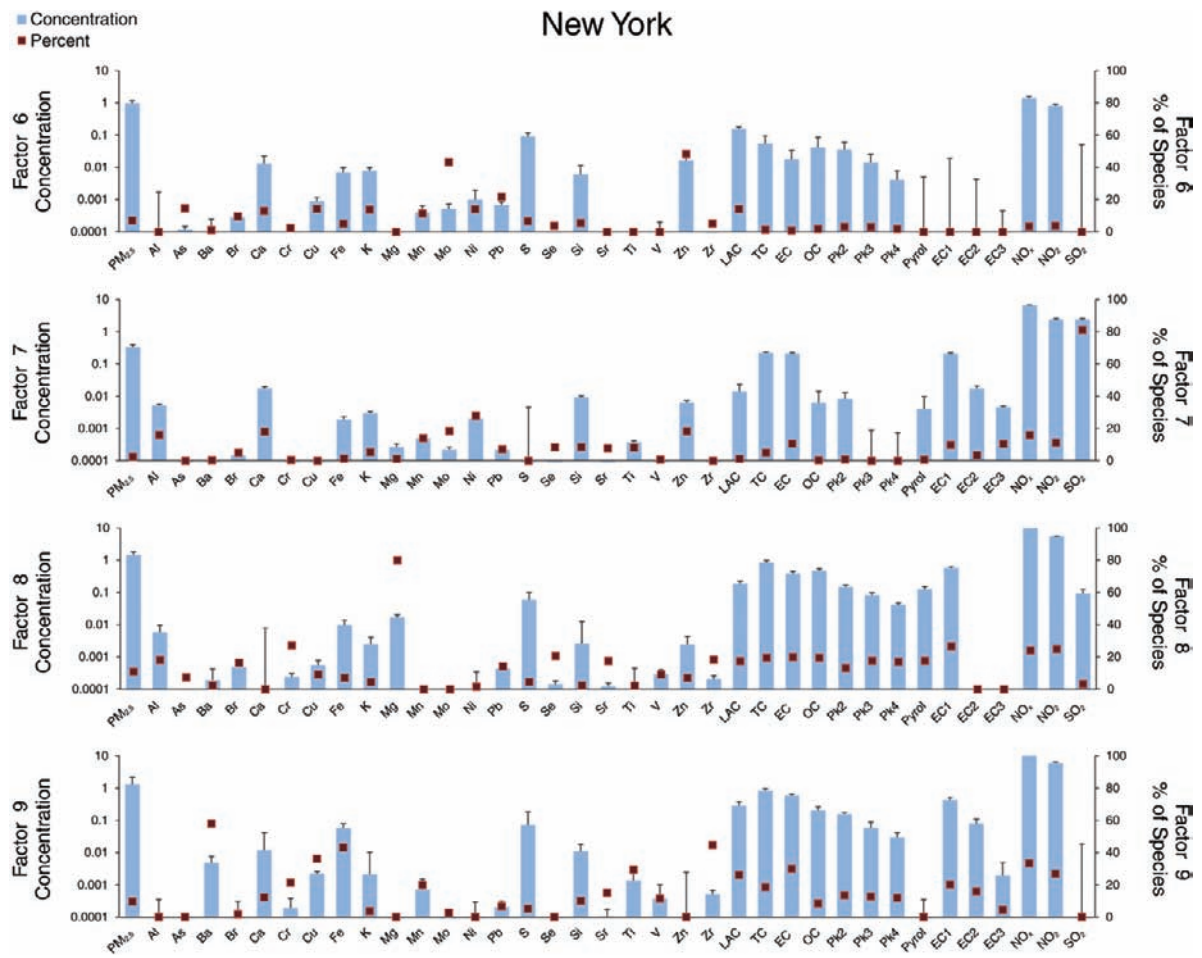


Figure 8 (Continued).

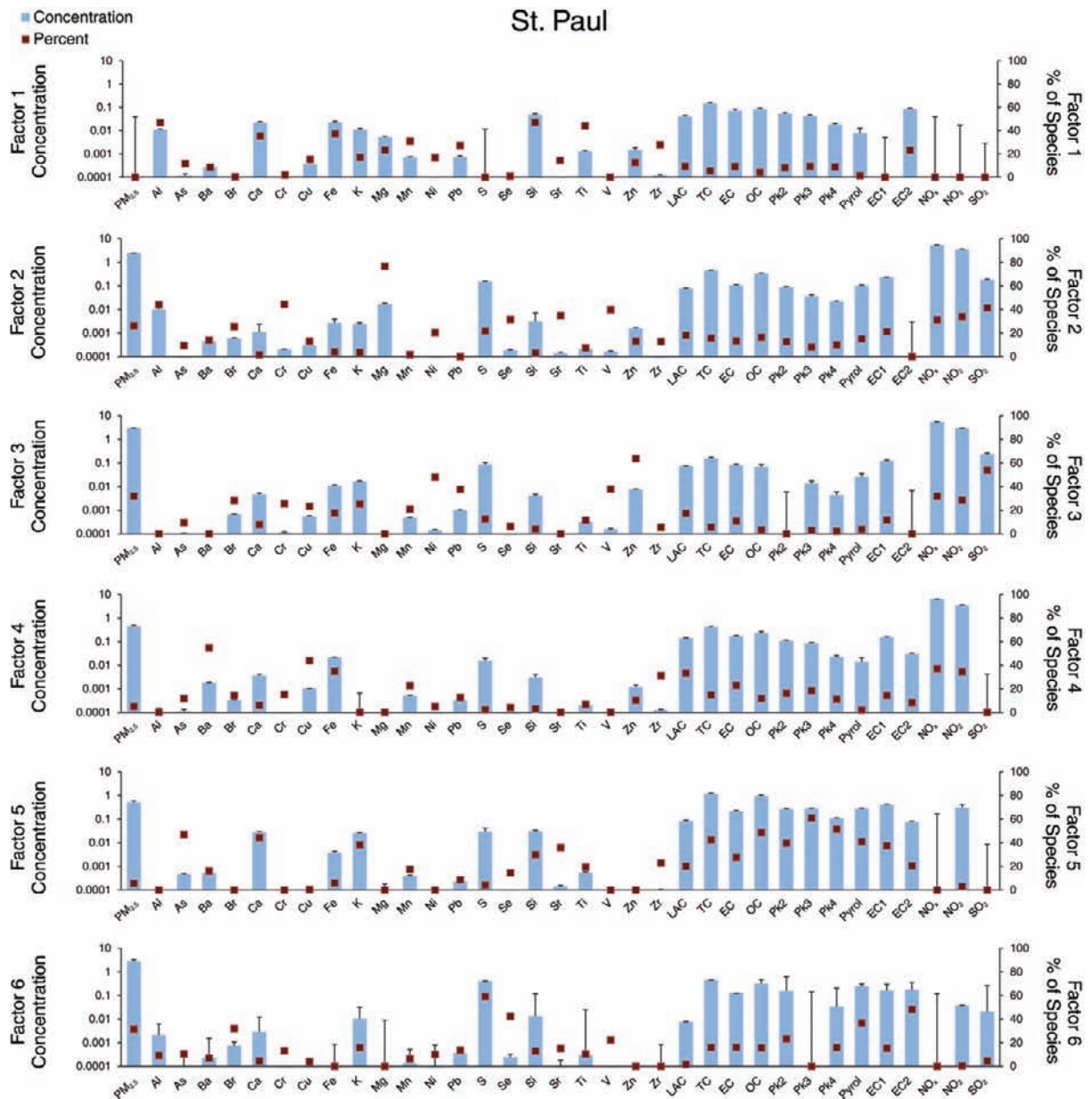


Figure 9. PMF-derived factor profiles for St. Paul. Average species concentrations (blue bars and scale on left) include bootstrapped estimates of the respective uncertainties (standard errors shown). Concentration units are $\mu\text{g}/\text{m}^3$, except for NO_x , NO_2 , and SO_2 units, which are ppbv. The average percent contribution to the overall predicted species concentrations is also shown for each factor (red dots and scale on right). Factor 1 is crustal-like; 2, magnesium-rich; 3, oil combustion-like; 4, diesel exhaust/brake wear-like; 5, biomass-like; 6, secondary SO_4 and secondary organic.

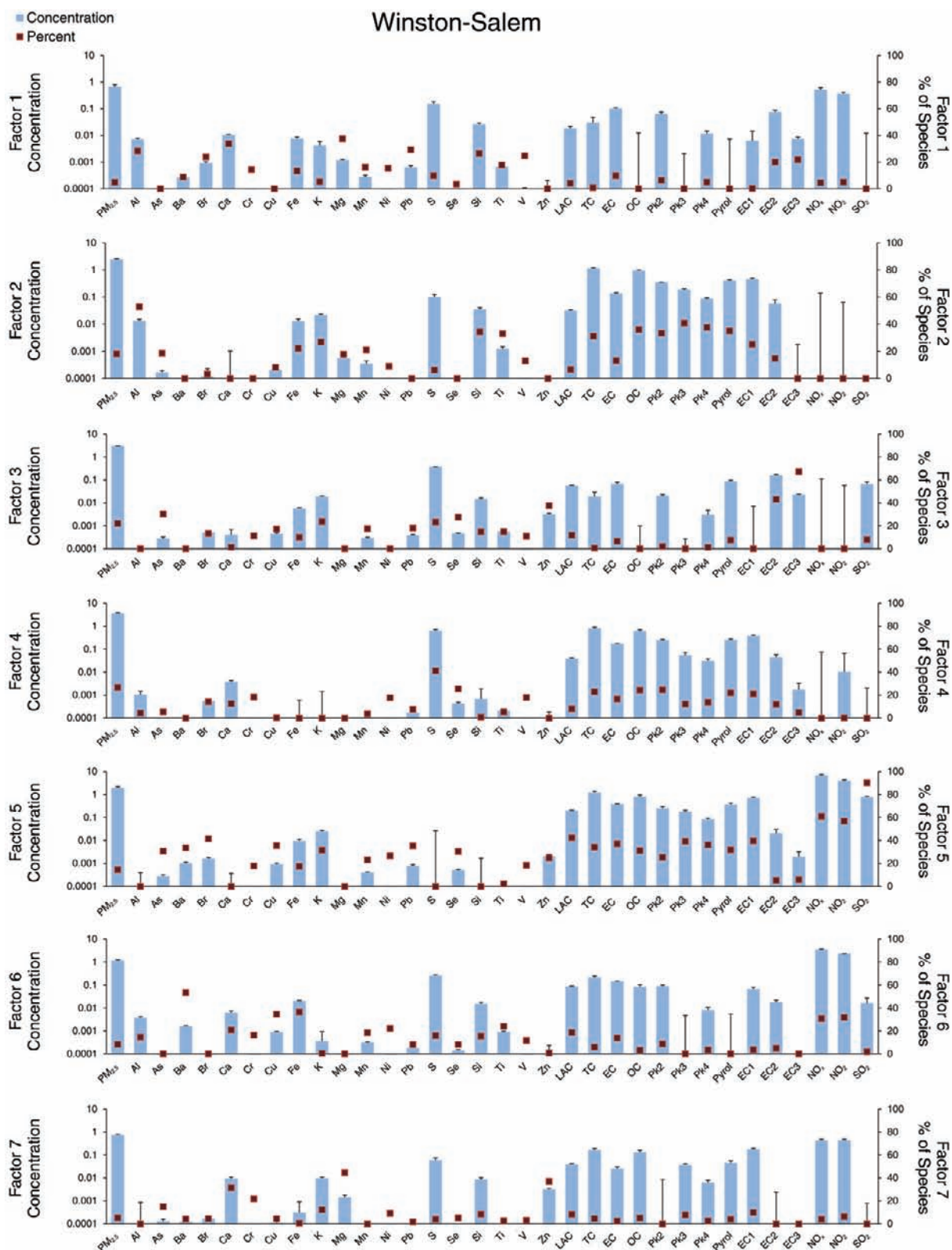


Figure 10. PMF-derived factor profiles for Winston-Salem. Average species concentrations (blue bars and scale on left) include bootstrapped estimates of the respective uncertainties (standard error shown). Concentration units are $\mu\text{g}/\text{m}^3$, except for NO_x , NO_2 , and SO_2 units, which are ppbv. The average percent contribution to the overall predicted species concentrations is also shown for each factor (red dots and scale on right). Factor 1 is crustal-like; 2, biomass-like; 3, road dust-like; 4, secondary SO_4 ; 5, oil combustion-like; 6, diesel exhaust/brake wear-like; 7, magnesium-rich.

briefly below (and in more detail in Appendix J, available on the HEI Web site). In this discussion we refer to each city by letter (B is for Baltimore; C, Chicago; L, Los Angeles; N, New York; S, St. Paul; and W, Winston-Salem) and group the factors by hypothesized source categories.

The diesel exhaust/break wear–like feature (factors 7B, 6C, 1L, 9N, 4S, and 6W) was consistent with a combination of particles from diesel exhaust and brake wear. Its contributions were correlated with the length of A1 roads within 300 m (Pearson correlation = 0.67). The ratio of NO_x to $\text{PM}_{2.5}$ is consistent with diesel emissions under engine load. According to the EPA SPECIATE Database, diesel exhaust particles are also relatively enriched in chromium, copper, iron, manganese, and EC (www.epa.gov/ttnchie1/software/speciate/), whereas brake wear particles are enriched in barium, copper, and iron (Thorpe and Harrison 2008; Geitl et al. 2010; see also the EPA SPECIATE Database link cited above).

The oil combustion–like feature (factors 6B, 4C, 7L, 7N, 3S, and 5W) was typically enriched in nickel and vanadium and sometimes in SO_2 . In general, the feature contributions were higher in the winter heating season, consistent with residential or commercial heating sources. This feature was also associated with summertime secondary SO_4 formation in Los Angeles, presumably from SO_2 emissions of ships nearby (Ault et al. 2009), and with the combustion of oil used for electrical generation in Baltimore (Ogulei et al. 2006). In Los Angeles, the association with SO_2 was not as evident as elsewhere, perhaps due to relatively rapid summertime transformation to SO_4 . The SO_2 level was very low in Los Angeles and usually below the analytical detection limit. The attribution of two factors to the oil combustion–like source in New York (2N and 7N) was based on the observations by Peltier and colleagues (2009, 2010) of a spatial pattern of nickel that is not correlated with vanadium and a separate nickel–vanadium spatial pattern.

The secondary SO_4 feature (factors 3B, 5C, 7L, 1N, 6S, and 4W) was also enriched in both selenium and arsenic, which is indicative of long-range transport and transformation of emissions from coal combustion and is consistent with our regional model predictions — except in Los Angeles, where it was mixed with the marker species for oil combustion. It was also typically depleted in primary NO_x , but enriched in NO_2 , indicative of secondary formation processes. Its contributions increased systematically with distance from the coast in Los Angeles, consistent with SO_2 precursors from port emissions. In the other cities, however, the within-city variability of the long-term average of this factor at the fixed monitoring sites was low.

The sources underlying the secondary organic feature (factors 5C, 8L, 3N, and 6S) are not easily separated. Previous studies have implicated primary gasoline emissions

(see Appendix J, available on the HEI Web site), although there is also strong evidence for an independent secondary feature driven by atmospheric processes in several of these cities. There is also strong published evidence for the importance of biomass combustion as a contributor to both the primary organic component in the winter and the secondary organic component in the summer in several of these cities (notably, Chicago and New York).

The magnesium-rich feature (factors 4B, 7C, 6L, 8N, 2S, and 7W) was enriched in soil components and magnesium. Its contributions were significant across all fixed monitoring sites. There was a moderate correlation with chlorine (not shown because of an abundance of chlorine values below the limit of detection in this data set), indicating possible use of road salt in the winter, or dust suppression on unpaved roads in the summer, or both. Both sources are consistent with this feature's lack of seasonal dependence. Magnesium is also used as an additive to improve combustion and inhibit corrosion in large boilers and oil-fired turbines, including the engines of railroad trains and marine vessels (www.chevron.com/products/prodserv/fuels/documents/Diesel_Fuel_Tech_Review.pdf).

The crustal-like feature (factors 5B, 2C, 5L, 4N, 1S, and 1W) was enriched in silicon, calcium, iron, titanium, aluminum, and potassium in proportions that varied with local soil conditions. It was higher in spring and summer in New York, St. Paul, Chicago, and Baltimore, but showed no obvious seasonal dependence in Los Angeles.

The biomass-like feature (factors 1B, 3C, 5S, and 2W) was mixed with particles from fireworks (enriched with strontium) in Baltimore and St. Paul. This feature was more distinct in Baltimore and Winston-Salem, but showed less seasonal dependence than could be deduced from either previous PMF analyses or studies with organic markers and carbon isotopes (Appendix J, available on the HEI Web site). Previous studies (discussed in Appendix J) also did not find substantial biomass contributions in Los Angeles. Nor did they see contributions in New York, although no studies with specific organic markers have been published, to our knowledge.

The zinc-rich feature (factors 8B, 9C, 4L, and 6N) was enriched in zinc and lead and displayed peaks in the contribution time series indicative of incinerators at fixed locations nearby. However, the production of zinc by tire wear could also have contributed to the low but consistent baseline levels across seasons and sites.

Factor Scores (Source Contributions) The average contributions of each factor to selected species for the entire sampling period, as well as by heating season versus non-heating season, are summarized in Tables 8 through 19. The seasonal contrasts are presented as normalized factor

Table 8. Average Factor Contributions for Selected Species in Baltimore^{a,b}

Species	Factor 1 (Biomass- Like)	Factor 2 (Road Dust-Like)	Factor 3 (Secondary SO ₄)	Factor 4 (Mg-Rich)	Factor 5 (Crustal-Like)	Factor 6 (Oil Combustion- Like)	Factor 7 (Diesel Exhaust/ Brake Wear-Like)	Factor 8 (Zn-Rich)
PM _{2.5}	0.88 (0.39 to 1.51)	0.31 (0.17 to 2.27)	4.87 (3.12 to 7.37)	1 (0.8 to 1.68)	2.56 (1.58 to 2.84)	2.88 (1.51 to 3.1)	1.03 (0.27 to 1.38)	0.34 (0.03 to 1.06)
Cu ^c	0.35 (0.06 to 0.86)	0.04 (0 to 0.57)	0.17 (0.02 to 0.63)	0.01 (0 to 0.25)	0.54 (0.07 to 2.16)	0.5 (0.33 to 0.67)	2.31 (1.86 to 3.43)	0.13 (0.01 to 0.91)
Ni ^c	0.03 (0 to 0.06)	0.15 (0.01 to 0.29)	0.08 (0.01 to 0.27)	0.04 (0 to 0.07)	0.08 (0 to 0.26)	0.19 (0.1 to 0.28)	0.03 (0 to 0.11)	0.08 (0 to 0.33)
S	0.03 (0 to 0.2)	0.1 (0 to 0.55)	0.73 (0.32 to 1.51)	0.11 (0.04 to 0.22)	0.34 (0.2 to 0.46)	0.24 (0 to 0.35)	0.07 (0 to 0.14)	0.01 (0 to 0.19)
Si ^c	0 (0 to 4.08)	27.35 (2.32 to 101.8)	3.74 (0 to 24.77)	11.06 (5.58 to 22.25)	37.72 (5.51 to 118.1)	5.46 (0.13 to 10.84)	0 (0 to 7.47)	8.97 (2.55 to 16.6)
V ^c	0.03 (0 to 0.09)	0.32 (0.07 to 0.74)	0 (0 to 0.44)	0.04 (0 to 0.11)	0.31 (0.12 to 1.13)	0.31 (0.18 to 0.45)	0.14 (0 to 0.28)	0.21 (0.1 to 0.73)
LAC ^d	0.02 (0 to 0.03)	0.08 (0 to 0.1)	0.07 (0.03 to 0.1)	0.08 (0.05 to 0.07)	0.01 (0 to 0.06)	0.11 (0.1 to 0.15)	0.27 (0.25 to 0.31)	0.03 (0.02 to 0.07)
EC	0.08 (0.03 to 0.07)	0.14 (0 to 0.14)	0.31 (0.13 to 0.36)	0.13 (0.08 to 0.16)	0 (0 to 0.1)	0.12 (0.08 to 0.26)	0.34 (0.24 to 0.43)	0.16 (0.07 to 0.51)
OC	0.34 (0.03 to 0.39)	0.06 (0 to 0.53)	0.97 (0.29 to 1.12)	0.4 (0.24 to 0.52)	0.13 (0 to 0.28)	0 (0 to 0.08)	0.23 (0.12 to 0.4)	0.09 (0 to 0.27)
NO _x ^e	0.25 (0 to 0.89)	0.74 (0 to 1.46)	0 (0 to 1.12)	0.74 (0 to 1.28)	0 (0 to 0.86)	7.82 (7.23 to 8.61)	10.8 (9.7 to 11.48)	0.86 (0 to 1.35)
NO ₂ ^e	0.05 (0 to 0.48)	1.5 (0.01 to 2.2)	0.7 (0 to 1.62)	0.84 (0.47 to 0.92)	0 (0 to 0.85)	3.76 (3.71 to 4.31)	4.67 (4.1 to 5.78)	0.36 (0 to 0.63)
SO ₂ ^e	0.04 (0 to 0.11)	0 (0 to 0.23)	0 (0 to 0.13)	0 (0 to 0.06)	0 (0 to 0.05)	1.2 (0.92 to 1.28)	0.12 (0 to 0.23)	0.01 (0 to 0.16)

^a Data are expressed in $\mu\text{g}/\text{m}^3$ unless specified otherwise. Numbers in parentheses indicate 95% CIs via bootstrapping.

^b Factor number is followed by possible source(s) associated with the factor. See Figure 5 for factor profiles.

^c Data are expressed in ng/m^3 .

^d Data are expressed in $\mu\text{g}/\text{m}^3$ estimated from conversion of units of 10^{-5} m^{-1} .

^e Data are expressed in ppbv.

Table 9. Factor Contributions by Heating vs. Nonheating Season in Baltimore^{a,b}

Season	Factor 1 (Biomass- Like)	Factor 2 (Road Dust-Like)	Factor 3 (Secondary SO ₄)	Factor 4 (Mg-Rich)	Factor 5 (Crustal- Like)	Factor 6 (Oil Combustion- Like)	Factor 7 (Diesel Exhaust/ Brake Wear- Like)	Factor 8 (Zn-Rich)
Spring/ Summer ^c	0.94 ± 0.99	1.16 ± 0.88	1.29 ± 0.85	1.01 ± 1.05	1.33 ± 0.67	0.48 ± 0.40	0.97 ± 0.67	0.89 ± 0.79
Autumn/ Winter ^d	1.11 ± 1.38	0.70 ± 0.48	0.47 ± 0.38	0.99 ± 1.13	0.39 ± 0.38	1.95 ± 0.78	1.05 ± 0.84	1.19 ± 0.49

^a Values are mean ± SD. Overall mean factor contribution = 1.0.

^b Factor number is followed by possible source(s) associated with the factor.

^c April–September.

^d October–March.

Table 10. Average Factor Contributions for Selected Species in Chicago^{a,b}

Species	Factor 1 (Gasoline- Like)	Factor 2 (Crustal- Like)	Factor 3 (Biomass- Like)	Factor 4 (Oil Combustion- Like)	Factor 5 (Secondary SO ₄ & Secondary Organic)	Factor 6 (Diesel Exhaust/Brake Wear-Like)	Factor 7 (Mg-Rich)	Factor 8 (Industrial)	Factor 9 (Zn-Rich)
PM _{2.5}	1.79 (0.55 to 9.23)	0.49 (0.09 to 0.61)	0.88 (0.23 to 3.51)	4.28 (2.2 to 13.8)	3.2 (0.81 to 3.92)	1.01 (0.06 to 0.67)	0.82 (0.01 to 10.9)	0.97 (0.15 to 1.06)	0 (0 to 1.45)
Cu ^c	0.33 (0 to 3.45)	0.05 (0 to 0.41)	1.11 (0 to 2.04)	0.23 (0 to 1.02)	0.12 (0 to 0.74)	2.08 (0.24 to 3.71)	0.68 (0 to 7.22)	0 (0 to 0.61)	0.02 (0 to 10.5)
Ni ^c	0.13 (0.05 to 0.6)	0 (0 to 0.01)	0.02 (0 to 0.38)	0.09 (0.02 to 0.33)	0.03 (0 to 0.07)	0.02 (0 to 0.02)	0.01 (0 to 0.1)	0.06 (0 to 0.06)	0.04 (0.02 to 0.84)
S	0.21 (0 to 1.04)	0.01 (0 to 0.04)	0 (0 to 0.09)	0.21 (0.02 to 1.02)	0.41 (0.09 to 0.56)	0.1 (0 to 0.19)	0 (0 to 0.64)	0.17 (0.02 to 0.21)	0.03 (0 to 0.41)
Si ^c	9.41 (0 to 129)	14.35 (2.24 to 45.4)	39.88 (4.73 to 286)	0 (0 to 20.2)	0.35 (0 to 82.7)	1.47 (0 to 6.64)	2.21 (0 to 20.5)	53.22 (0.01 to 81.4)	0.13 (0 to 170)
LAC ^d	0.09 (0.03 to 0.31)	0.01 (0 to 0.05)	0.12 (0.06 to 0.27)	0.09 (0.05 to 0.22)	0.1 (0.05 to 0.12)	0.08 (0.02 to 0.15)	0.12 (0.04 to 0.52)	0.03 (0 to 0.04)	0.07 (0.04 to 0.67)
EC	0.18 (0.13 to 0.42)	0.01 (0 to 0.09)	0.23 (0 to 0.49)	0.06 (0 to 0.18)	0.26 (0.07 to 0.36)	0.08 (0.02 to 0.22)	0.3 (0.03 to 0.99)	0.04 (0 to 0.05)	0.15 (0.04 to 0.76)
OC	0 (0 to 0.62)	0.01 (0 to 0.16)	0.55 (0.12 to 1.37)	0.09 (0 to 0.31)	0.62 (0.05 to 1.24)	0 (0 to 0.05)	0.31 (0 to 1.72)	0 (0 to 0.17)	0.21 (0 to 0.71)
NO _x ^e	5.4 (0 to 5.57)	0.63 (0 to 0.8)	1.59 (0 to 3.37)	11.1 (5.66 to 12.4)	0 (0 to 2.21)	0.33 (0 to 1.07)	6.8 (0 to 8.92)	0 (0 to 0.76)	1.76 (0 to 2.42)
NO ₂ ^e	3.72 (0 to 3.9)	0 (0 to 0.39)	1.81 (0 to 2.59)	5.06 (0.46 to 6.44)	0 (0 to 1.55)	0.24 (0.22 to 0.76)	4.68 (0 to 5.13)	0 (0 to 0.65)	1.34 (0 to 1.8)
SO ₂ ^e	0 (0 to 0.09)	0 (0 to 0.05)	0 (0 to 0.02)	0.54 (0.04 to 0.84)	0 (0 to 0.05)	0 (0 to 0.02)	0.06 (0 to 0.38)	0 (0 to 0)	0.11 (0 to 0.66)

^a Data are expressed in µg/m³ unless specified otherwise. Numbers in parentheses indicate 95% CIs via bootstrapping.

^b Factor number is followed by possible source(s) associated with the factor. See Figure 6 for factor profiles.

^c Data are expressed in ng/m³.

^d Data are expressed in µg/m³ estimated from conversion of units of 10⁻⁵ m⁻¹.

^e Data are expressed in ppbv.

Table 11. Factor Contributions by Heating vs. Nonheating Season in Chicago^{a,b}

Season	Factor 1 (Gasoline- Like)	Factor 2 (Crustal- Like)	Factor 3 (Biomass- Like)	Factor 4 (Oil Combustion- Like)	Factor 5 (Secondary SO ₄ & Secondary Organic)	Factor 6 (Diesel Exhaust/Brake Wear-Like)	Factor 7 (Mg-Rich)	Factor 8 (Industrial)	Factor 9 (Zn-Rich)
Spring/ Summer ^c	1.05 ± 0.61	1.07 ± 1.58	1.13 ± 0.72	0.61 ± 0.46	1.28 ± 0.94	0.96 ± 0.88	0.96 ± 0.57	1.13 ± 0.72	0.94 ± 0.81
Autumn/ Winter ^d	0.91 ± 0.55	0.88 ± 0.81	0.78 ± 0.62	1.67 ± 0.70	0.52 ± 0.46	1.07 ± 0.78	1.07 ± 0.57	0.79 ± 0.38	1.10 ± 1.00

^a Values are mean ± SD. Overall mean factor contribution = 1.0.

^b Factor number is followed by possible source(s) associated with the factor.

^c April–September.

^d October–March.

Table 12. Average Factor Contributions for Selected Species in Los Angeles^{a,b}

Species	Factor 1 (Diesel Exhaust/ Brake Wear– Like)	Factor 2 (Aged Sea Salt–Like)	Factor 3 (Winter NO _x)	Factor 4 (Zn-Rich)	Factor 5 (Crustal-Like)	Factor 6 (Mg-Rich)	Factor 7 (Oil Combustion/ Secondary SO ₄)	Factor 8 (Secondary Organic)
PM _{2.5}	2.59 (1.59 to 9.65)	0.95 (0.42 to 1.58)	0.66 (0.41 to 4.8)	0.65 (0.16 to 0.82)	1.78 (0.55 to 2.03)	1.09 (0.81 to 3.67)	4.65 (3.92 to 5.24)	2.6 (1.22 to 5.74)
Cu ^c	2.54 (0.22 to 4.66)	0.22 (0 to 0.81)	3.27 (2.05 to 8.38)	0.13 (0.02 to 0.56)	0.27 (0.06 to 0.93)	0.69 (0.04 to 4.04)	0.15 (0 to 1.16)	0.58 (0.28 to 4.48)
Ni ^c	0.1 (0 to 0.63)	0.3 (0.02 to 0.66)	0.18 (0.04 to 1.54)	0.13 (0.02 to 0.18)	0 (0 to 0.13)	0.13 (0.02 to 0.85)	0.81 (0.53 to 2.51)	0.15 (0 to 0.44)
S	0.06 (0 to 0.32)	0.2 (0.08 to 0.34)	0.01 (0 to 0.03)	0 (0 to 0.07)	0.08 (0.03 to 0.12)	0.02 (0 to 0.12)	0.75 (0.6 to 0.9)	0.04 (0 to 0.18)
Si ^c	0 (0 to 112)	10.29 (3.38 to 22.2)	8.7 (0 to 256)	17.18 (2.27 to 31.1)	89.26 (39.6 to 131)	26.79 (0.69 to 66.6)	2.73 (1.47 to 15.8)	9.46 (0 to 50)
V ^c	0 (0 to 0.85)	0.92 (0.16 to 1.7)	0.48 (0.03 to 4.12)	0.18 (0.01 to 0.42)	0.06 (0 to 0.48)	0.24 (0 to 1.98)	2.28 (1.61 to 6.86)	0.32 (0 to 1.05)
LAC ^d	0.42 (0.3 to 0.85)	0 (0 to 0.04)	0.16 (0.13 to 0.6)	0.03 (0.01 to 0.03)	0.08 (0.01 to 0.13)	0.1 (0.07 to 0.15)	0.07 (0.04 to 0.2)	0.19 (0.16 to 0.36)
EC	0.62 (0.18 to 0.92)	0.02 (0 to 0.07)	0.19 (0.17 to 0.66)	0.03 (0 to 0.05)	0.03 (0 to 0.11)	0.13 (0 to 0.21)	0.22 (0.16 to 0.38)	0.46 (0.24 to 0.6)
OC	0.66 (0 to 1.27)	0.1 (0.07 to 0.27)	0.13 (0.09 to 1.65)	0.06 (0.01 to 0.07)	0.08 (0.01 to 0.36)	0.22 (0.11 to 0.87)	0.38 (0.28 to 0.45)	1.22 (0.57 to 2.01)
NO _x ^e	17.85 (13 to 20.4)	1.04 (0 to 1.57)	0 (0.89 to 11.3)	0.25 (0.08 to 0.69)	0 (0 to 0.74)	4.23 (1.98 to 4.67)	0 (0 to 0.86)	2.52 (0 to 5.63)
NO ₂ ^e	8.79 (3.95 to 11)	1.38 (1 to 1.76)	2.76 (0 to 3.4)	0.09 (0 to 0.33)	0.4 (0 to 1)	2.49 (0.16 to 3.22)	0.66 (0 to 1.53)	2.5 (0 to 3.32)

^a Data are expressed in $\mu\text{g}/\text{m}^3$ unless specified otherwise. Numbers in parentheses indicate 95% CIs via bootstrapping.

^b Factor number is followed by possible source(s) associated with the factor. See Figure 7 for factor profiles.

^c Data are expressed in ng/m^3 .

^d Data are expressed in $\mu\text{g}/\text{m}^3$ estimated from conversion of units of 10^{-5} m^{-1}

^e Data are expressed in ppbv.

Table 13. Factor Contributions by Heating vs. Nonheating Season in Los Angeles^{a,b}

Season	Factor 1 (Diesel Exhaust/Brake Wear–Like)	Factor 2 (Aged Sea Salt–Like)	Factor 3 (Winter NO _x)	Factor 4 (Zn-Rich)	Factor 5 (Crustal- Like)	Factor 6 (Mg-Rich)	Factor 7 (Oil Combustion/ Secondary SO ₄)	Factor 8 (Secondary Organic)
Spring/ Summer ^c	0.68 ± 0.62	1.40 ± 1.16	0.64 ± 0.52	0.95 ± 0.93	1.02 ± 0.90	0.85 ± 1.17	1.28 ± 0.62	0.88 ± 0.63
Autumn/ Winter ^d	1.53 ± 0.84	0.34 ± 0.57	1.60 ± 1.25	1.08 ± 0.78	0.96 ± 0.87	1.25 ± 1.28	0.54 ± 0.57	1.20 ± 0.81

^a Values are mean ± SD. Overall mean factor contribution = 1.0.

^b Factor number is followed by possible source(s) associated with the factor.

^c April–September.

^d October–March.

Table 14. Average Factor Contributions for Selected Species in New York^{a,b}

Species	Factor 1 (Secondary SO ₄)	Factor 2 (Residual Oil Combustion- Like)	Factor 3 (Secondary Organic)	Factor 4 (Crustal- Like)	Factor 5 (Local Area Sources)	Factor 6 (Zn-Rich)	Factor 7 (Oil Combustion- Like)	Factor 8 (Mg-Rich)	Factor 9 (Diesel Exhaust/Brake Wear-Like)
PM _{2.5}	3.21 (1.78 to 3.55)	1.17 (0.21 to 2.09)	0.99 (0.39 to 2.41)	1.14 (0.44 to 1.16)	2.97 (1.07 to 6.26)	1.02 (0 to 2.36)	0.35 (0.1 to 0.87)	1.6 (0.71 to 5.77)	1.41 (0.79 to 14.5)
Cu ^c	0.78 (0.06 to 0.87)	0.72 (0 to 2.44)	0 (0 to 0.68)	0.53 (0.01 to 1.57)	0.28 (0 to 2.51)	1.04 (0.19 to 5.55)	0 (0 to 0.55)	0.62 (0.01 to 4.08)	2.3 (0 to 5.63)
Ni ^c	0 (0 to 1.12)	3.43 (0.41 to 7.59)	0 (0 to 0.18)	0.19 (0 to 1.13)	0 (0 to 0.63)	1.25 (0.2 to 18.9)	2.29 (0.34 to 3.6)	0.04 (0 to 4.66)	0 (0 to 5.31)
S	0.61 (0.29 to 0.68)	0.15 (0 to 0.22)	0.1 (0 to 0.27)	0.08 (0 to 0.17)	0.16 (0 to 0.78)	0.1 (0 to 0.4)	0 (0 to 0.07)	0.09 (0 to 0.56)	0.09 (0 to 1.8)
Si ^c	6.75 (1.2 to 13)	3.22 (0 to 35.4)	9.98 (1.57 to 17.7)	50.1 (5.31 to 85.4)	9 (0 to 23.5)	6.88 (0 to 99.9)	8.61 (0 to 13)	3.07 (0 to 188)	10.95 (3.43 to 115)
V ^c	0.24 (0.11 to 1.23)	2.02 (0.49 to 3.77)	0.06 (0 to 0.29)	0 (0 to 0.64)	0.12 (0 to 0.6)	0 (0 to 3.54)	0.2 (0 to 1.01)	0.26 (0 to 1.98)	0.38 (0 to 10.1)
LAC ^d	0.15 (0.03 to 0.18)	0.1 (0.03 to 0.27)	0 (0 to 0.14)	0.03 (0 to 0.09)	0.13 (0.09 to 0.29)	0.17 (0.03 to 0.42)	0.01 (0 to 0.11)	0.2 (0.13 to 0.81)	0.29 (0.21 to 1.8)
EC	0.06 (0 to 0.13)	0 (0 to 0.13)	0.7 (0.32 to 1.2)	0.02 (0 to 0.17)	0 (0 to 0.18)	0.02 (0 to 0.21)	0.2 (0.09 to 0.29)	0.41 (0 to 0.68)	0.59 (0.12 to 1.22)
OC	0.14 (0.02 to 0.52)	0.17 (0.02 to 0.34)	1.15 (0.28 to 2.36)	0.12 (0 to 0.25)	0.08 (0 to 0.43)	0.04 (0 to 0.82)	0 (0 to 0.13)	0.48 (0.01 to 1.51)	0.19 (0 to 0.94)
NO _x ^e	0 (0 to 1.2)	0 (0 to 1.48)	4.56 (1.16 to 7.07)	0 (0 to 0.71)	5.26 (1.05 to 7.12)	1.36 (0 to 2.35)	6.55 (6.07 to 7.69)	10.14 (4.66 to 11.1)	13.77 (0 to 15.3)
NO ₂ ^e	0 (0 to 0.95)	1.3 (0 to 1.99)	3.1 (0.04 to 5.25)	0 (0 to 0.55)	2.82 (1.75 to 3.67)	0.77 (0 to 1.14)	2.49 (1.82 to 4)	5.45 (2.82 to 6.66)	5.82 (0 to 7.85)
SO ₂ ^e	0.02 (0 to 0.13)	0 (0 to 0.38)	0 (0 to 0.18)	0 (0 to 0.16)	0.45 (0 to 0.27)	0 (0 to 0.76)	2.46 (0.4 to 2.4)	0.09 (0 to 0.5)	0 (0 to 0.25)

^a Data are expressed in µg/m³ unless specified otherwise. Numbers in parentheses indicate 95% CIs via bootstrapping.

^b Factor number is followed by possible source(s) associated with the factor. See Figure 8 for factor profiles.

^c Data are expressed in ng/m³.

^d Data are expressed in µg/m³ estimated from conversion of units of 10⁻⁵ m⁻¹.

^e Data are expressed in ppbv.

Table 15. Factor Contributions by Heating vs. Nonheating Season in New York^{a,b}

Season	Factor 1 (Secondary SO ₄)	Factor 2 (Residual Oil Combustion- Like)	Factor 3 (Secondary Organic)	Factor 4 (Crustal- Like)	Factor 5 (Local Area Sources)	Factor 6 (Zn-Rich)	Factor 7 (Oil Combustion- Like)	Factor 8 (Mg-Rich)	Factor 9 (Diesel Exhaust/Brake Wear-Like)
Spring/ Summer ^c	1.16 ± 0.90	1.15 ± 0.89	1.29 ± 0.88	1.26 ± 0.96	0.97 ± 0.57	0.83 ± 0.76	0.29 ± 0.62	0.77 ± 0.97	1.09 ± 1.09
Autumn/ Winter ^d	0.75 ± 0.45	0.78 ± 0.80	0.55 ± 0.58	0.60 ± 0.54	1.04 ± 0.68	1.27 ± 1.29	2.10 ± 2.09	1.36 ± 0.91	0.86 ± 0.77

^a Values are mean ± SD. Overall mean factor contribution = 1.0.

^b Factor number is followed by possible source(s) associated with the factor.

^c April–September.

^d October–March.

Table 16. Average Factor Contributions for Selected Species in St. Paul^{a,b}

Species	Factor 1 (Crustal-Like)	Factor 2 (Mg-Rich)	Factor 3 (Oil Combustion– Like)	Factor 4 (Diesel Exhaust/Brake Wear–Like)	Factor 5 (Biomass-Like)	Factor 6 (Secondary SO ₄ & Secondary Organic)
PM _{2.5}	0.23 (0 to 0.46)	0.72 (0.2 to 1.06)	3.2 (2.23 to 4.51)	0.64 (0.44 to 1.05)	0.6 (0.14 to 1.5)	3.75 (3.08 to 6.21)
Cu ^c	0.51 (0.02 to 1.22)	0.03 (0 to 0.35)	0.57 (0.19 to 0.69)	0.94 (0.83 to 1.31)	0 (0 to 0.38)	0.3 (0 to 0.38)
Ni ^c	0.08 (0 to 0.14)	0.05 (0 to 0.09)	0.14 (0.05 to 0.19)	0.01 (0 to 0.08)	0 (0 to 0.05)	0.02 (0 to 0.08)
S	0.11 (0 to 0.18)	0.03 (0 to 0.13)	0.11 (0.05 to 0.32)	0.02 (0 to 0.06)	0.04 (0 to 0.15)	0.38 (0.17 to 0.82)
Si ^c	49.9 (13.2 to 73.4)	23.4 (1.38 to 75.8)	0 (0 to 8.35)	0.68 (0 to 14.1)	30.2 (0.71 to 34.6)	0.63 (0 to 55.3)
V ^c	0 (0 to 0.05)	0.09 (0 to 0.13)	0.18 (0.09 to 0.26)	0 (0 to 0.08)	0 (0 to 0.07)	0.14 (0 to 0.24)
LAC ^d	0.04 (0 to 0.08)	0.03 (0.02 to 0.07)	0.08 (0.03 to 0.11)	0.14 (0.13 to 0.18)	0.08 (0.02 to 0.12)	0.06 (0.02 to 0.14)
EC	0.1 (0.01 to 0.2)	0.03 (0.02 to 0.14)	0.09 (0.04 to 0.14)	0.18 (0.13 to 0.26)	0.2 (0 to 0.25)	0.18 (0.07 to 0.46)
OC	0.05 (0 to 0.18)	0.14 (0.09 to 0.3)	0.1 (0 to 0.36)	0.29 (0.03 to 0.68)	0.91 (0.11 to 1.03)	0.51 (0.13 to 1.51)
NO _x ^e	0.01 (0 to 0.51)	2.09 (1.42 to 2.57)	6.49 (5.23 to 7.47)	6.29 (4.89 to 6.79)	0 (0 to 2.02)	2.24 (0 to 4.2)
NO ₂ ^e	0 (0 to 0.23)	1.63 (1.23 to 1.76)	3.44 (2.66 to 3.82)	3.51 (3.26 to 3.88)	0.16 (0 to 1.34)	1.62 (0 to 2.13)
SO ₂ ^e	0 (0 to 0.04)	0.11 (0.03 to 0.16)	0.28 (0.11 to 0.4)	0 (0 to 0.07)	0 (0 to 0.11)	0.06 (0 to 0.19)

^a Data are expressed in $\mu\text{g}/\text{m}^3$ unless specified otherwise. Numbers in parentheses indicate 95% CIs via bootstrapping.

^b Factor number is followed by possible source(s) associated with the factor. See Figure 9 for factor profiles.

^c Data are expressed in ng/m^3 .

^d Data are expressed in $\mu\text{g}/\text{m}^3$ estimated from conversion of units of 10^{-5} m^{-1} .

^e Data are expressed in ppbv.

Table 17. Factor Contributions by Heating vs. Nonheating Season in St. Paul^{a,b}

Season	Factor 1 (Crustal-Like)	Factor 2 (Mg-Rich)	Factor 3 (Oil Combustion– Like)	Factor 4 (Diesel Exhaust/Brake Wear–Like)	Factor 5 (Biomass-Like)	Factor 6 (Secondary SO ₄ & Secondary Organic)
Spring/ Summer ^c	1.20 ± 0.85	1.02 ± 0.69	0.65 ± 0.47	0.94 ± 0.90	1.07 ± 0.52	1.00 ± 0.54
Autumn/ Winter ^d	0.63 ± 0.58	0.95 ± 0.85	1.65 ± 0.77	1.10 ± 0.85	0.87 ± 0.63	1.00 ± 0.57

^a Values are mean ± SD. Overall mean factor contribution = 1.0.

^b Factor number is followed by possible source(s) associated with the factor.

^c April–September.

^d October–March.

Table 18. Average Factor Contributions for Selected Species in Winston-Salem^{a,b}

Species	Factor 1 (Crustal-Like)	Factor 2 (Biomass-Like)	Factor 3 (Road Dust-Like)	Factor 4 (Secondary SO ₄)	Factor 5 (Oil Combustion- Like)	Factor 6 (Diesel Exhaust/Brake Wear-Like)	Factor 7 (Mg-Rich)
PM _{2.5}	2.67 (1.12 to 2.95)	1.98 (1.22 to 3.17)	1.37 (0.31 to 1.45)	4.82 (2.2 to 6.15)	1.15 (0.65 to 5.83)	1.21 (0.46 to 2.05)	0.43 (0.18 to 1.45)
Cu ^c	0.02 (0 to 0.82)	0.22 (0 to 1.03)	0.56 (0 to 0.65)	0.23 (0 to 0.69)	0.68 (0 to 1.74)	0.9 (0.29 to 1.01)	0 (0 to 0.26)
Ni ^c	0.02 (0 to 0.05)	0.02 (0 to 0.11)	0 (0 to 0.04)	0.03 (0 to 0.09)	0.06 (0 to 0.12)	0.05 (0 to 0.1)	0.03 (0 to 0.06)
S	0.48 (0.08 to 0.54)	0 (0 to 0.37)	0 (0 to 0.12)	0.76 (0.01 to 1.03)	0 (0 to 0.45)	0.27 (0.05 to 0.45)	0.08 (0 to 0.2)
Si ^c	26.8 (0.49 to 56.9)	37.6 (6.45 to 102)	8.59 (0 to 20.1)	0 (0 to 17.2)	0 (0 to 25.7)	15.12 (0 to 39)	12.24 (4.88 to 30.4)
V ^c	0.12 (0.03 to 0.17)	0.05 (0.02 to 0.22)	0 (0 to 0.09)	0.05 (0.01 to 0.13)	0.08 (0.02 to 0.21)	0.05 (0.01 to 0.14)	0.04 (0.01 to 0.11)
LAC ^d	0.03 (0.02 to 0.07)	0.03 (0.03 to 0.06)	0.06 (0.02 to 0.05)	0.06 (0.05 to 0.1)	0.18 (0.14 to 0.24)	0.09 (0.07 to 0.12)	0.04 (0.01 to 0.05)
EC	0.15 (0.04 to 0.2)	0.12 (0.09 to 0.23)	0 (0.02 to 0.18)	0.17 (0.12 to 0.26)	0.39 (0.27 to 0.55)	0.14 (0.11 to 0.2)	0.04 (0 to 0.07)
OC	0 (0 to 0.19)	0.89 (0.01 to 0.9)	0.01 (0 to 0.01)	0.82 (0.19 to 1.22)	0.74 (0 to 2.19)	0.09 (0 to 0.35)	0.05 (0 to 0.34)
NO _x ^e	0 (0 to 1.39)	0 (0 to 2.09)	0.47 (0 to 1.72)	0 (0 to 1.13)	7.09 (0.69 to 8.95)	3.49 (2.87 to 4.14)	0.51 (0 to 0.79)
NO ₂ ^e	0 (0 to 0.68)	0 (0 to 0.93)	0.1 (0 to 0.69)	0 (0 to 0.91)	4.28 (0.9 to 5.41)	2.26 (1.72 to 2.59)	0.51 (0 to 0.69)
SO ₂ ^e	0 (0 to 0.16)	0 (0 to 0)	0.22 (0 to 0.23)	0 (0 to 0.03)	0.63 (0.29 to 1.36)	0 (0 to 0.14)	0 (0 to 0.01)

^a Data are expressed in µg/m³ unless specified otherwise. Numbers in parentheses indicate 95% CIs via bootstrapping.

^b Factor number is followed by possible source(s) associated with the factor. See Figure 10 for factor profiles.

^c Data are expressed in ng/m³.

^d Data are expressed in µg/m³ estimated from conversion of units of 10⁻⁵ m⁻¹.

^e Data are expressed in ppbv.

Table 19. Factor Contributions by Heating vs. Nonheating Season in Winston-Salem^{a,b}

Season	Factor 1 (Crustal-Like)	Factor 2 (Biomass-Like)	Factor 3 (Road Dust-Like)	Factor 4 (Secondary SO ₄)	Factor 5 (Oil Combustion- Like)	Factor 6 (Diesel Exhaust/Brake Wear-Like)	Factor 7 (Mg-Rich)
Spring/ Summer ^c	1.15 ± 0.56	1.48 ± 0.72	0.61 ± 0.44	1.24 ± 0.86	0.53 ± 0.41	1.10 ± 0.81	1.20 ± 0.87
Autumn/ Winter ^d	0.79 ± 0.57	0.34 ± 0.34	1.54 ± 0.52	0.67 ± 0.34	1.66 ± 0.71	0.87 ± 0.78	0.71 ± 0.41

^a Values are mean ± SD. Overall mean factor contribution = 1.0.

^b Factor number is followed by possible source(s) associated with the factor.

^c April–September.

^d October–March.

scores, with the overall mean for all seasons set to a value of 1.0. Therefore, a value of 1.5 for a given season means that the average factor score for that season is 50% higher than the overall average for all seasons. For example, factor 5 in Baltimore contributes significantly more to samples collected in the spring and summer than to samples collected in autumn and winter. The opposite pattern is observed for factor 6 in Baltimore.

Factor-vs.-Species Correlations Tables 20 through 25 summarize the pairwise correlation coefficients between each factor's contributions and selected species. Values greater than 0.80 are shown in bold type.

Summary of Source Apportionment

The purpose of this positively constrained factor analysis was to examine whether the species used in our health analyses (primarily, OC, EC, silicon, and sulfur; and secondarily, nickel, vanadium, and copper) were strong markers of particular source-related features. Sulfur was correlated ($r > 0.8$) with a single secondary SO_4 factor in all six cities. The secondary SO_4 factor contributed to $\text{PM}_{2.5}$ mass primarily in the spring and summer in five of the six cities (excluding St. Paul), and these contributions were nearly equal across all fixed sites within each city except Los Angeles, where there was an additional contribution from sources within the region associated with oil combustion. Silicon was strongly correlated with a single factor in three of the cities (Los Angeles, St. Paul, and Winston-Salem). Copper was strongly correlated with a single factor in

Baltimore, Chicago, and Los Angeles, but not in New York, St. Paul, and Winston-Salem. Nickel only had a strong correlation with a single factor in New York. OC also showed moderate correlations with a single factor that is related to a secondary formation process, as either secondary SO_4 or secondary organic (Baltimore, Chicago, Los Angeles, New York, and Winston-Salem) or biomass emissions (Chicago, St. Paul, and Winston-Salem). In Chicago, gasoline vehicle emissions appeared to be important, and in Baltimore, Chicago, St. Paul, and Winston-Salem, there was evidence for important contributions from biomass combustion. EC was moderately correlated with primary emissions from vehicles in all cities except Chicago and Winston-Salem, but no strong correlations were evident with any particular factor.

BUILDING AND VALIDATING THE SPATIOTEMPORAL EXPOSURE MODEL

Model Overview and General Approach

Our approach was based on the model specification, fitting approach, and technical details for the spatiotemporal prediction model described in Lindström et al. (2011b), with some additional details provided in Sampson et al. (2011). Briefly, we modeled the 2-week average log concentration measurements $C(s, t)$, and we fit a separate model in each city for each component. The spatiotemporal model is decomposed into a mean model $\mu(\cdot)$ and a variance model $\varepsilon(\cdot)$:

$$C(s, t) = \mu(s, t) + \varepsilon(s, t)$$

Table 20. Pairwise Correlation of Species with Factors in Baltimore^a

Species	Factor 1 (Biomass-Like)	Factor 2 (Road Dust-Like)	Factor 3 (Secondary SO_4)	Factor 4 (Mg-Rich)	Factor 5 (Crustal-Like)	Factor 6 (Oil Combustion-Like)	Factor 7 (Diesel Exhaust/Brake Wear-Like)	Factor 8 (Zn-Rich)
$\text{PM}_{2.5}$	0.37	0.05	0.64	0.17	0.38	-0.12	0.18	-0.08
Cu	0.36	0.21	-0.19	0.18	0.05	0.17	0.90	0.30
Ni	0.04	0.14	-0.04	-0.03	-0.01	0.07	0.06	0.15
S	0.10	0.15	0.87	-0.02	0.51	-0.46	0.04	-0.21
Si	0.13	0.59	0.11	0.20	0.77	-0.43	0.19	0.09
V	0.27	0.48	-0.14	0.05	0.13	0.26	0.38	0.43
LAC	0.30	0.28	-0.17	0.32	-0.11	0.32	0.84	0.38
EC	0.33	0.31	0.17	0.15	-0.01	0.07	0.69	0.39
OC	0.37	0.06	0.62	0.28	0.41	-0.34	0.16	-0.14
NO_x	0.25	0.10	-0.47	0.23	-0.40	0.64	0.74	0.45
NO_2	0.25	0.22	-0.40	0.22	-0.35	0.60	0.74	0.44
SO_2	0.21	-0.13	-0.45	0.09	-0.51	0.80	0.11	0.30

^a Factor number is followed by possible source(s) associated with the factor. Values greater than 0.80 are in bold.

Table 21. Pairwise Correlation of Species with Factors in Chicago^a

Species	Factor 1 (Gasoline- Like)	Factor 2 (Crustal- Like)	Factor 3 (Biomass- Like)	Factor 4 (Oil Combustion- Like)	Factor 5 (Secondary SO ₄ & Secondary Organic)	Factor 6 (Diesel Exhaust/Brake Wear-Like)	Factor 7 (Mg-Rich)	Factor 8 (Industrial)	Factor 9 (Zn-Rich)
PM _{2.5}	0.12	0.22	-0.03	0.35	0.36	0.13	0.03	0.19	0.25
Cu	0.30	0.15	0.30	-0.09	-0.15	0.89	0.25	-0.16	0.45
Ni	0.23	-0.02	-0.06	0.08	-0.08	0.25	-0.04	0.05	0.14
S	0.36	0.13	-0.07	-0.22	0.81	0.10	-0.08	0.45	0.12
Si	0.23	0.55	0.50	-0.34	0.21	-0.05	-0.09	0.67	0.01
V	0.21	0.24	0.20	-0.16	0.12	0.18	-0.15	0.14	0.20
LAC	0.28	0.20	0.33	-0.08	0.17	0.40	0.25	-0.07	0.54
EC	0.30	0.15	0.41	-0.34	0.46	0.22	0.36	-0.03	0.46
OC	0.04	0.11	0.58	-0.30	0.67	-0.10	0.22	0.06	0.27
NO _x	0.03	0.04	-0.03	0.59	-0.37	0.13	0.30	-0.19	0.32
NO ₂	0.14	0.03	0.10	0.54	-0.33	0.24	0.43	-0.23	0.47
SO ₂	-0.10	-0.04	-0.05	0.68	-0.29	0.11	0.15	-0.19	0.31

^a Factor number is followed by possible source(s) associated with the factor. Values greater than 0.80 are in **bold**.

Table 22. Pairwise Correlation of Species with Factors in Los Angeles^a

Species	Factor 1 (Diesel Exhaust/Brake Wear-Like)	Factor 2 (Aged Sea Salt- Like)	Factor 3 (Winter NO _x)	Factor 4 (Zn-Rich)	Factor 5 (Crustal- Like)	Factor 6 (Mg-Rich)	Factor 7 (Oil Combustion/ Secondary SO ₄)	Factor 8 (Secondary Organic)
PM _{2.5}	0.36	-0.14	-0.04	0.05	0.27	0.26	0.23	0.35
Cu	0.72	-0.31	0.87	0.20	0.03	0.24	-0.49	0.21
Ni	0.04	0.18	-0.09	0.14	-0.01	-0.04	0.14	-0.11
S	-0.39	0.42	-0.48	-0.10	-0.21	-0.06	0.92	-0.36
Si	0.08	-0.11	0.05	0.06	0.91	0.24	-0.36	0.42
V	-0.39	0.47	-0.20	0.05	-0.30	-0.01	0.71	-0.29
LAC	0.87	-0.48	0.50	0.11	0.23	0.32	-0.48	0.46
EC	0.79	-0.42	0.38	0.07	0.17	0.27	-0.34	0.54
OC	0.60	-0.30	0.19	0.06	0.35	0.19	-0.28	0.78
NO _x	0.79	-0.41	0.62	0.12	-0.05	0.28	-0.47	0.22
NO ₂	0.85	-0.37	0.48	0.03	0.04	0.29	-0.43	0.28
SO ₂	-0.23	0.13	-0.28	-0.03	0.14	-0.08	0.22	-0.03

^a Factor number is followed by possible source(s) associated with the factor. Values greater than 0.80 are in **bold**.

Table 23. Pairwise Correlation of Species with Factors in New York^a

Species	Factor 1 (Secondary SO ₄)	Factor 2 (Residual Oil Combustion- Like)	Factor 3 (Secondary Organic)	Factor 4 (Crustal- Like)	Factor 5 (Local Area Sources)	Factor 6 (Zn-Rich)	Factor 7 (Oil Combustion- Like)	Factor 8 (Mg-Rich)	Factor 9 (Diesel Exhaust/Brake Wear-Like)
PM _{2.5}	0.49	0.45	0.32	0.27	0.34	0.18	0.09	-0.07	0.35
Cu	-0.13	0.48	0.00	0.40	-0.18	0.51	0.22	0.07	0.71
Ni	-0.27	0.67	-0.14	-0.09	-0.15	0.79	0.83	-0.01	0.25
S	0.86	0.32	0.48	0.14	0.33	-0.06	-0.14	-0.26	0.08
Si	-0.07	0.34	0.06	0.75	-0.06	0.25	0.10	0.11	0.46
V	-0.06	0.90	0.15	0.13	0.05	0.49	0.28	-0.13	0.40
LAC	-0.11	0.45	0.03	0.26	-0.04	0.48	0.33	0.18	0.68
EC	-0.06	0.31	0.35	0.15	-0.09	0.36	0.31	0.02	0.70
OC	0.32	0.24	0.80	0.15	0.16	0.04	-0.22	-0.16	0.20
NO _x	-0.34	0.19	-0.06	0.05	-0.12	0.38	0.51	0.22	0.63
NO ₂	-0.26	0.29	-0.05	0.06	-0.11	0.42	0.50	0.26	0.57
SO ₂	-0.24	0.11	-0.26	-0.29	-0.10	0.44	0.91	0.16	0.10

^a Factor number is followed by possible source(s) associated with the factor. Values greater than 0.80 are in **bold**.

Table 24. Pairwise Correlation of Species with Factors in St. Paul^a

Species	Factor 1 (Crustal-Like)	Factor 2 (Mg-Rich)	Factor 3 (Oil Combustion- Like)	Factor 4 (Diesel Exhaust/Brake Wear-Like)	Factor 5 (Biomass-Like)	Factor 6 (Secondary SO ₄ & Secondary Organic)
PM _{2.5}	-0.14	0.00	0.68	0.06	-0.07	0.54
Cu	0.25	0.05	0.22	0.44	-0.01	-0.16
Ni	0.09	0.05	0.22	0.07	-0.05	0.05
S	0.30	-0.08	0.24	-0.15	-0.19	0.90
Si	0.83	0.32	-0.43	0.07	0.26	-0.10
V	-0.09	0.10	0.19	-0.01	-0.04	0.14
LAC	0.02	0.07	0.28	0.78	0.21	-0.10
EC	0.17	0.00	0.13	0.54	0.33	0.16
OC	-0.07	0.09	0.00	0.37	0.71	0.13
NO _x	-0.16	0.16	0.55	0.57	-0.09	0.05
NO ₂	-0.20	0.21	0.54	0.61	0.02	0.02
SO ₂	-0.16	0.09	0.38	-0.06	-0.03	0.16

^a Factor number is followed by possible source(s) associated with the factor. Values greater than 0.80 are in **bold**.

Table 25. Pairwise Correlation of Species with Factors in Winston-Salem^a

Species	Factor 1 (Crustal-Like)	Factor 2 (Biomass-Like)	Factor 3 (Road Dust-Like)	Factor 4 (Secondary SO ₄)	Factor 5 (Oil Combustion-Like)	Factor 6 (Diesel Exhaust/Brake Wear-Like)	Factor 7 (Mg-Rich)
PM _{2.5}	0.23	0.56	-0.32	0.85	-0.30	0.08	0.08
Cu	-0.08	-0.23	0.30	0.07	0.23	0.47	-0.20
Ni	0.04	0.14	0.07	-0.04	-0.06	0.30	-0.09
S	0.40	0.49	-0.45	0.84	-0.51	0.18	0.01
Si	0.42	0.87	-0.59	0.22	-0.71	0.31	0.54
V	0.13	0.26	-0.20	0.21	-0.16	0.02	0.10
LAC	-0.48	-0.33	0.57	0.01	0.72	0.29	-0.16
EC	-0.29	-0.04	0.25	0.29	0.51	0.18	-0.11
OC	-0.24	0.64	-0.32	0.77	0.00	-0.07	0.31
NO _x	-0.56	-0.53	0.65	-0.32	0.80	0.33	-0.20
NO ₂	-0.56	-0.49	0.60	-0.26	0.80	0.34	-0.19
SO ₂	-0.38	-0.56	0.67	-0.22	0.78	-0.03	-0.34

^a Factor number is followed by possible source(s) associated with the factor. Values greater than 0.80 are in **bold**.

where s denotes the spatial coordinates of a subject’s residential address. In general, we write $\mu(s, t) = \sum_{l=1}^L \gamma_l M_l(s, t) + \sum_{i=0}^m \beta_i(s) f_i(t)$ where the $f_i(t)$ are temporal basis functions of possible seasonal trend patterns with $f_0(t) = \mathbf{1}$, so $\beta_0(s) f_0(t) = \beta_0(s)$. With T observations at N MESA Air fixed monitoring sites, we compute the temporal trends empirically as smooth representations of the temporal singular vectors of the $T \times N$ data matrix (rather than assuming parametric forms such as trigonometric functions). $M_l(s, t)$ denotes spatiotemporal covariates. The final component, the variance model $\varepsilon(s, t)$, represents spatiotemporal variation at the 2-week time scale of the fixed and home-outdoor monitoring sites. The hierarchical structure of our spatiotemporal model can account for complex spatiotemporal dependencies by modeling spatially varying temporal trends as a linear combination of the mean-zero empirical seasonal basis functions $f_i(t)$. Our modeling is done at the 2-week time scale, which is consistent with the averaging period of the MESA Air monitoring data. The spatial field of coefficients $\beta_i(s)$ for each temporal trend is described by a universal kriging model that incorporates dependence on geographic covariates $X_i(s)$ and spatial correlation in the residuals described by a covariance function, $\Sigma(\theta_j)$, with the parameter θ_j incorporating the range (ϕ_j), partial sill (σ^2_j), and nugget (τ^2_j) for a prespecified geostatistical model. The spatiotemporal residual field is modeled as spatially correlated but temporally independent because the seasonal trend basis functions account for autocorrelation in the 2-week average data. The spatial covariance model for the residual field is

$\Sigma_\varepsilon(\theta_\varepsilon)$, with the parameter θ_ε including the range, partial sill, and nugget for a geostatistical model. This hierarchical model can exploit temporally sparse monitoring data with different sampling times at a large number of locations to improve predictions. Efficient computation is possible with maximum likelihood methods and has been implemented in the R package SpatioTemporal, available on the Comprehensive R Archive Network (CRAN) (Lindström et al. 2011a).

Of the kriging parameters τ^2 , σ^2 , and ϕ , known as the nugget, partial sill, and range, respectively, the partial sill and the nugget together give the total amount of residual variation. The partial sill is the amount of that variation that is due to spatial correlation and can thus be exploited to improve predictions. The presence of large values of the partial sill relative to nugget values indicates that the predictions can be significantly improved by exploiting the spatial correlation. The range is interpreted as the distance at which observations are essentially independent.

To validate the model, we assess its prediction ability by cross-validation. For instance, 10-fold cross-validation splits the data from home-outdoor sites into 10 groups, fits 10 models, each time leaving one group out, and then predicts for the left-out group. Prediction summary statistics such as mean squared error (MSE) and cross-validated prediction R^2 compare observed and predicted values. The cross-validated R^2 is computed as

$$\max \left\{ 0, 1 - \frac{MSE[C(s, t)]}{VAR[C(s, t)]} \right\}.$$

Our applications of the cross-validation approach appear below under “Exposure Predictions: Distributions, Model Fit, and Validation.”

Data Assessment and Inclusion Criteria for Spatiotemporal Modeling

EPA AQS monitoring data have been a common resource for many studies of short-term exposure to $PM_{2.5}$ components and health (Ostro et al. 2009; Peng et al. 2009; Ito et al. 2011; Zhou et al. 2011) and for some long-term studies (Thurston et al. 2009; Ostro et al. 2010, 2011). We considered using these existing data sources for our spatiotemporal model of $PM_{2.5}$ components, specifically the EPA AQS monitoring data collected at CSN sites, as well as the IMPROVE sites, in addition to our MESA Air monitoring data. As we discuss at length in this section (and in Appendix C, available on the HEI Web site), we found serious discrepancies between measurements obtained from these three sources of data, which led us to abandon our original plan of utilizing all available data to fit a spatiotemporal model. We found that these data inconsistencies between networks were due to differences in the protocols for monitoring, sampling, and sample analysis. After extensive exploratory data analyses, we concluded that it would be unwise to combine data across platforms in the spatiotemporal model. We then fit the spatiotemporal model to only the $PM_{2.5}$ component data collected under the MESA Air platform.

Approach to the $PM_{2.5}$ Component Data

We modified the approach used to fit the spatiotemporal model developed for MESA Air to the $PM_{2.5}$ component data collected by the NPACT study. Modifications were necessary because the $PM_{2.5}$ component data available to the NPACT study were much more limited in both space and time than the $PM_{2.5}$ mass and NO_x data used in MESA Air. (Table 1.B in Appendix C, available on the HEI Web site, summarizes the procedure for fitting a city-specific spatiotemporal prediction model for $PM_{2.5}$ components.)

For the spatiotemporal model of $PM_{2.5}$ components, we concentrated on EC, OC, silicon, and sulfur. EC and OC are markers of combustion, silicon is a marker of crustal material, and sulfur reflects SO_4 , a secondary aerosol. Since we restricted the data used in our exposure prediction modeling to MESA Air monitoring data, the data for our spatiotemporal model were all available 2-week average concentrations of sulfur and silicon collected in MESA cities between August 2005 and August 2009, and concentrations of EC and OC collected between March 2008 and August 2009. The 2-week concentrations of the four $PM_{2.5}$

components were log-transformed values (after adding 1), with silicon values converted to nanograms per cubic meter from micrograms per cubic meter.

Given the relatively limited data for $PM_{2.5}$ components, our approach (outlined in Table 26) was more ad hoc than the one described for the MESA Air prediction model. Specifically, we assumed that the log 2-week average component concentration $C(s, t)$ consists of a long-term mean, $\beta_0(s)$, a single temporal trend, $\beta_1 f_1(t)$, and a spatiotemporal residual, $\varepsilon(s, t)$. We assumed that there is a single temporal trend within each city, because there are not enough long-running monitors in each city to allow us to estimate several site-specific temporal trends. The characterization of the trend coefficient (β_1) for the single temporal trend was simplified as being modeled with one geographic covariate and error excluding spatial correlation structure. We did not include any spatiotemporal covariates, $M_l(s, t)$, in our models. In addition, we found the temporal trends and land-use characteristics differed between the Riverside and central Los Angeles sites, and between the Rockland County and central New York sites in our preliminary analysis. Thus, we fitted some parts of our models separately in eight areas (the six cities plus Riverside and Rockland County), rather than six areas. In the following sections, we provide details of the main model-fitting tasks outlined in Table 26.

Data Cleaning For the $PM_{2.5}$ component data, extensive data cleaning was conducted under the auspices of the MESA Air study and its quality assurance protocols. We made a few more data deletions from the final analysis file. Specifically, we excluded one or two measurements for each component that were flagged due to equipment problems. In addition, we excluded two silicon measurements that were unreasonably high, possibly because of greases on the sampling devices. (Further details about these data exclusions are provided in Appendix C, available on the HEI Web site.)

There were 852 candidate GIS variables for our models. We eliminated, log-transformed, and recoded some geographic variables using the protocol outlined in Table 1 of Appendix C (available on the HEI Web site). Variables were excluded if they did not meet our minimum variability requirements. After this area-specific data processing, the number of candidate geographic variables in each area ranged between 52 and 116 (Table 27).

Temporal Basis Function Estimation We computed the temporal basis function by smoothing the first temporal component from a singular value decomposition (SVD) using the cleaned $PM_{2.5}$ component data at the three to seven fixed monitoring sites in each of the six cities.

Table 26. Prediction Model Procedure

Procedure	Formula ^a
Spatiotemporal model specification (city-specific)	$C(s, t) = \beta_0(s) + \beta_1(s)f_1(t) + \varepsilon(s, t),$ where $\beta_0(s) \sim N[X\alpha_{\beta_0}, \Sigma_{\beta_0}(\varphi_{\beta_0}, \sigma_{\beta_0}^2, \tau_{\beta_0}^2)]$ $\beta_1(s) \sim N(X\alpha_{\beta_1}, \tau_{\beta_1}^2)$ $\varepsilon(s, t) \sim N[0, (\varphi_{\varepsilon}, \sigma_{\varepsilon}^2, \tau_{\varepsilon}^2)]$
Data cleaning	
Temporal trend estimation	
Estimate the trend function ($f_1(t)$) using measurements only at MESA Air fixed sites by smoothing the first temporal component from SVD	
Variable selection	
Compute a provisional temporal basis function ($\tilde{f}_1(t)$) by SVD using 2-week measurements only at MESA Air fixed sites ($C_{\text{fixed}}(s, t)$) and estimate the provisional coefficients ($\tilde{\beta}_0, \tilde{\beta}_1$)	$C_{\text{fixed}}(s, t) = \tilde{\beta}_0 + \tilde{\beta}_1\tilde{f}_1(t) + \varepsilon(s, t)$
Temporally adjust the data by subtracting the temporal trend from 2-week concentrations at MESA Air home-outdoor sites	
Average the home-outdoor site trend-removed 2-week concentrations over time to obtain long-term average concentrations for model selection purposes	$C_{\text{home}}^*(s) = E_t(C_{\text{home}}[s, t] - \tilde{\beta}_1\tilde{f}_1[t])$
Select 12 variables (X) by lasso using the temporally averaged concentrations	$C_{\text{home}}^*(s) \sim N(X\alpha_{\beta_0}^*, \Sigma_{\beta_0}^*)$
Perform all subset selection in a universal kriging structure and select at most 5 variables	
Estimate provisional site-specific coefficients ($\tilde{\beta}_0(s), \tilde{\beta}_1(s)$) at each fixed site	$C_{\text{fixed}}(s, t) = \tilde{\beta}_0(s) + \tilde{\beta}_1(s)\tilde{f}_1(t) + \varepsilon(s, t)$
Select one covariate to model the trend coefficient from selected variables based on relationships with the estimated provisional site-specific trend coefficient ($\tilde{\beta}_1(s)$) across fixed sites	$\tilde{\beta}_1(s) \sim N(X\alpha_{\beta_1}^*, \Sigma_{\beta_1}^*)$
Parameter estimation	
Estimate parameters ($\hat{\alpha}, \hat{\varphi}, \hat{\sigma}^2, \hat{\tau}^2$) given the selected covariates and covariance structures using measurements at MESA Air fixed and home-outdoor sites for various spatiotemporal models with different spatial structures (shown in Appendix C, Table 3.1, available on the HEI Web site)	
Evaluate the models across home-outdoor sites by computing R^2 and MSE in 10-fold cross-validation following Lindström et al. (2011b)	
Choose the final model based on estimated parameters and cross-validated statistics	
Prediction at participant addresses	
Predict 2-week concentrations at participant addresses using estimated parameters and covariate data for participants	

^a Equations shown for an example of the spatiotemporal model with one trend component.

Variable Selection We performed variable selection for the long-term mean $\beta_0(s)$ using “long-term average” $\text{PM}_{2.5}$ component concentrations computed as the temporal averages of the 2-week trend-removed concentrations only at home-outdoor sites in each city. (Note that home-outdoor sites provide much more uncertain estimates of these

long-term averages than fixed monitoring sites.) To obtain “long-term average” concentrations, we recomputed the provisional temporal basis function $\tilde{f}_0(t)$ from an SVD (without smoothing in order to avoid losing spatial variability) and estimated a provisional trend coefficient, $\tilde{\beta}_1$, across fixed sites in each city. Here, we separately estimated

Table 27. Description of Candidate Geographic Variables

Category	Measure	Variable Description
Traffic	Distance to the nearest road Sum within buffers of 0.05–15 km	Any road, A1, intersection A1, A2+A3, truck route, intersections
Population	Sum within buffers of 0.5–3 km	Population in block groups
Land use, urban	Percent within buffers of 0.05–15 km	Urban or built-up land (residential, commercial, industrial, transportation, urban) Developed low, medium, and high density Developed open space
Land use, rural	Percent within buffers of 0.05–15 km	Agricultural land (cropland, groves, feeding) Rangeland (herbaceous, shrub) Forest land (deciduous, evergreen, mixed) Water (streams, lakes, reservoirs, bays) Wetland Barren land (beaches, dry salt flats, sand, mines, rock) Tundra Perennial snow or ice
Position	Coordinates	Longitude, latitude
Source	Distance to the nearest source	Coastline, rough coastline Commercial area Railroad Railyard Airport Major airport Large port City hall
Emission	Sum within buffers of 3–30 km	PM _{2.5} PM ₁₀ CO SO ₂ NO _x
Vegetation	Quantiles within buffers of 0.5–10 km	Normalized Difference Vegetation Index (NDVI)
Imperviousness	Percent within buffers of 0.05–5 km	Impervious surface value
Elevation	Elevation above sea level Counts of points above or below a threshold within buffers of 1–5 km	Elevation value
Residual oil	Distance to the nearest boiler Sum within buffers of 0.1–3 km	Residual oil grade 4 or 6 Total residual oil active heating capacity

trend coefficients by subregions in Los Angeles (central Los Angeles, coastal Los Angeles, and Riverside) and New York (central New York and Rockland County) to reflect the possible variation in amplitude of the temporal trends due to different pollution characteristics in these nearby areas. Then, we multiplied the provisional trend function by the provisional trend coefficient and obtained one estimated temporal trend for each area. Finally, we subtracted the provisional temporal trends from the 2-week

concentrations only at home-outdoor sites and averaged 2-week trend-removed concentrations over time.

Using these “long-term average” concentrations as our outcome measure, we implemented the least absolute shrinkage and selection operator (lasso) to select 12 candidate geographic covariates in each city from the reduced set of candidate geographic variables. Lasso shrinks some coefficients and sets others to zero to balance variance and bias (Tibshirani 1996). All subset kriging was then performed

by examining all subsets of a maximum 5 variables for sulfur and silicon and 4 variables for EC and OC (out of the 12 candidate variables) and calculating 5-fold cross-validated performance statistics such as R^2 and MSE. Because the best subset with the highest R^2 was based on one specific random assignment of sites into five cross-validation groups, we examined whether selected variable subsets were consistent when cross-validation groups were resampled. For Los Angeles and New York, variable selection was performed separately for central Los Angeles and Riverside and central New York and Rockland County, as well as for the combined areas. In the variable selection for the trend coefficient $\beta_1(s)$, we estimated provisional site-specific trend coefficients, $\tilde{\beta}_1(s)$, at each fixed site using the provisional trend functions described above, fit regressions on each variable selected for the long-term mean, and selected one variable for our final model based on P values and coefficients.

Model Parameter Estimation We used all 2-week concentrations, the selected geographic covariates, and the estimated trend function for each $PM_{2.5}$ component and area to estimate the spatiotemporal model parameters in the full city-specific data sets. The parameters we estimated include the regression parameters for the long-term mean field $\beta_0(s)$ and the trend coefficient field $\beta_1(s)$, as well as the variance parameters for the long-term mean field, the trend field, and the spatiotemporal residual field $\varepsilon(s, t)$. The variance parameters include the range, partial sill, and nugget for the long-term mean field and the spatiotemporal residual field, but only the nugget for the trend coefficient field. When estimated parameters for the range and partial sill were extremely small or their 95% CIs were unreasonably large, we assumed that there was no spatial structure and fitted a spatiotemporal model without those parameters (Appendix C, available on the HEI Web site).

Model Evaluation The spatiotemporal model was evaluated at home-outdoor sites using 10-fold cross-validation. We found that the traditional R^2 statistic, calculated as 1 minus the ratio of the MSE to data variance for the 2-week concentrations, was generally too large because it included the temporal variability from the home-outdoor sites. Since our primary goal for this model was prediction of spatial contrasts, we calculated a “temporally adjusted R^2 ” taking into account temporal variability by using either estimated trend or spatial averages of fixed sites at each time (mathematical details are given in Appendix C, available on the HEI Web site; for further background, also see the discussion in Lindström et al. 2011b). The temporally adjusted R^2 is intended to represent an estimate of

the model’s spatial prediction ability, although because of the imbalanced data structure, it is not possible to completely separate spatial and temporal variability. We also used this statistic to guide our selection of the final spatiotemporal model from various spatial correlation models (Table 3 in Appendix C, available on the HEI Web site). We also evaluated our prediction model using some additional snapshot monitoring data for sulfur and silicon that were collected from home-outdoor sites in three cities for an ancillary study to MESA Air. This snapshot sampling campaign, as distinguished from the monitoring carried out at the rotating set of home-outdoor sites in the main MESA Air study, simultaneously collected samples from approximately 30 home sites in each of three MESA cities (Chicago, St. Paul, and Winston-Salem) for two seasons in 2009. We also calculated R^2 and MSE for predictions at these snapshot locations.

Predicting Concentrations at Participants’ Addresses

Using the estimated spatiotemporal model parameters and the covariate data at participants’ addresses, we predicted log-transformed 2-week average concentrations and used exponentiation to obtain 2-week concentrations, converting silicon values back to the original unit of micrograms per cubic meter, and finally averaged the 2-week average predicted concentrations for 1 year, from May 2007 through April 2008. For the Los Angeles and New York areas, because newly recruited MESA Air participants living in Riverside and in Rockland County were not included in our health analysis, we focused on evaluating the performance of our prediction model for central and coastal Los Angeles and central New York by including or excluding monitoring data and geographic variables selected for Riverside and Rockland County, and we chose different approaches by using $PM_{2.5}$ components based on the magnitude of the cross-validated temporally adjusted R^2 (described in Appendix C, available on the HEI Web site). In a few cases there were unreasonably large or small predictions at a participant’s address because the value for a particular covariate at that address was far outside the range of values for that covariate across monitoring locations, resulting in unrealistically large (or small) predictions given the regression coefficient for the corresponding covariate. Those subject locations were excluded from the analysis.

Exposure Predictions: Distributions, Model Fit, and Validation

Trend Estimation As an example of a portion of the temporal trend estimation step in the model-fitting process (Table 26), Figure 11 shows the computed SVD and

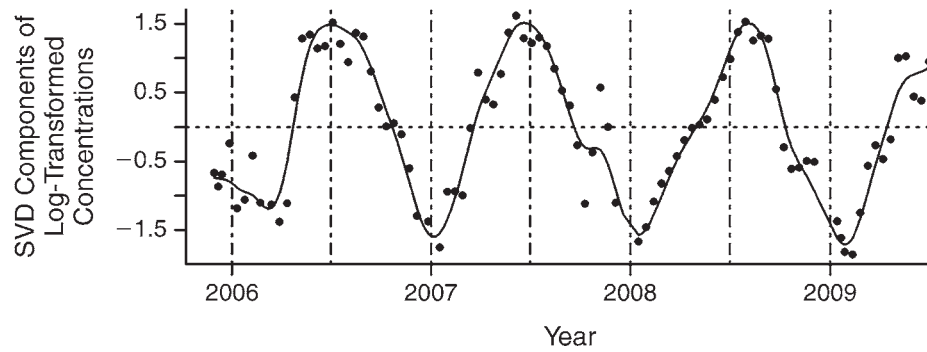


Figure 11. Estimated temporal trend function of SVD components of log-transformed sulfur concentrations in Los Angeles.

smoothed trend function $f_1(t)$ for $\log(\text{sulfur} + 1)$ in Los Angeles. In this example, the SVD component explains most of the variability in the data, as is evident in the good fits at two Los Angeles fixed monitoring sites shown in Figure 12. Site-specific estimated temporal trends, obtained by multiplying the trend functions by site-specific estimated trend coefficients, were more homogenous across fixed monitoring sites for sulfur than for the other components shown in Figure 13.

Variable Selection Table 28 gives the classes of geographic covariates included in the final selected models for each component and area. For most pollutants and areas, the final models included covariates for traffic and urban and rural land-use characteristics. The inclusion in the models of population, geographic coordinates, distances to sources, emission variables, vegetation, imperviousness of the land surface, and elevation varied across $\text{PM}_{2.5}$ components and areas. The vegetation index was

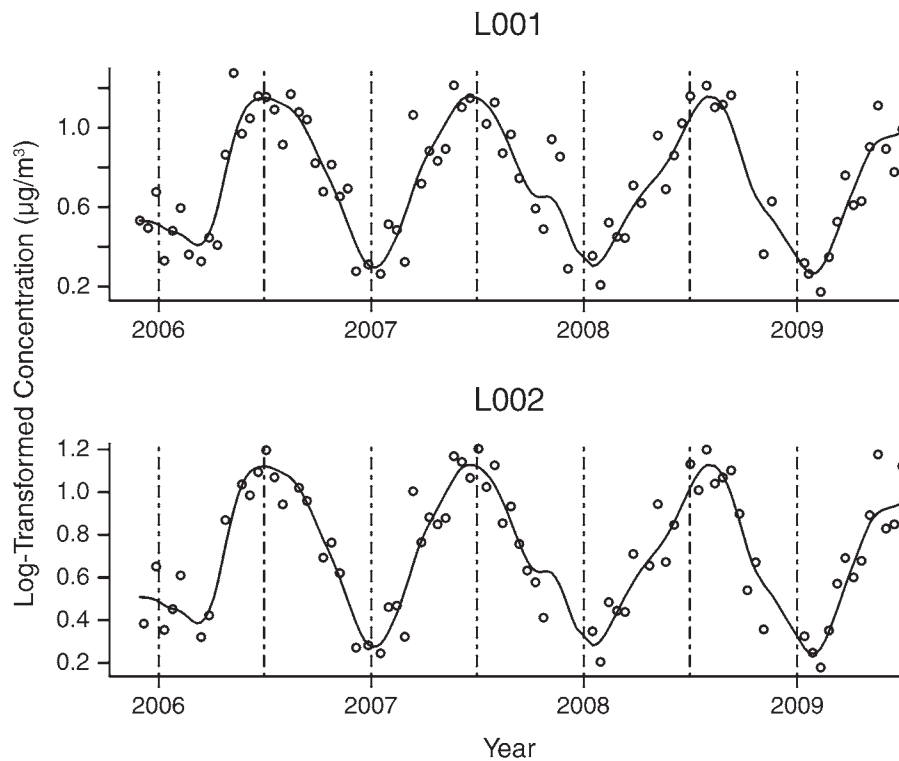


Figure 12. Trend fits for the estimated temporal trend of log-transformed sulfur concentrations at two MESA Air fixed monitoring sites (L001 and L002) in Los Angeles.

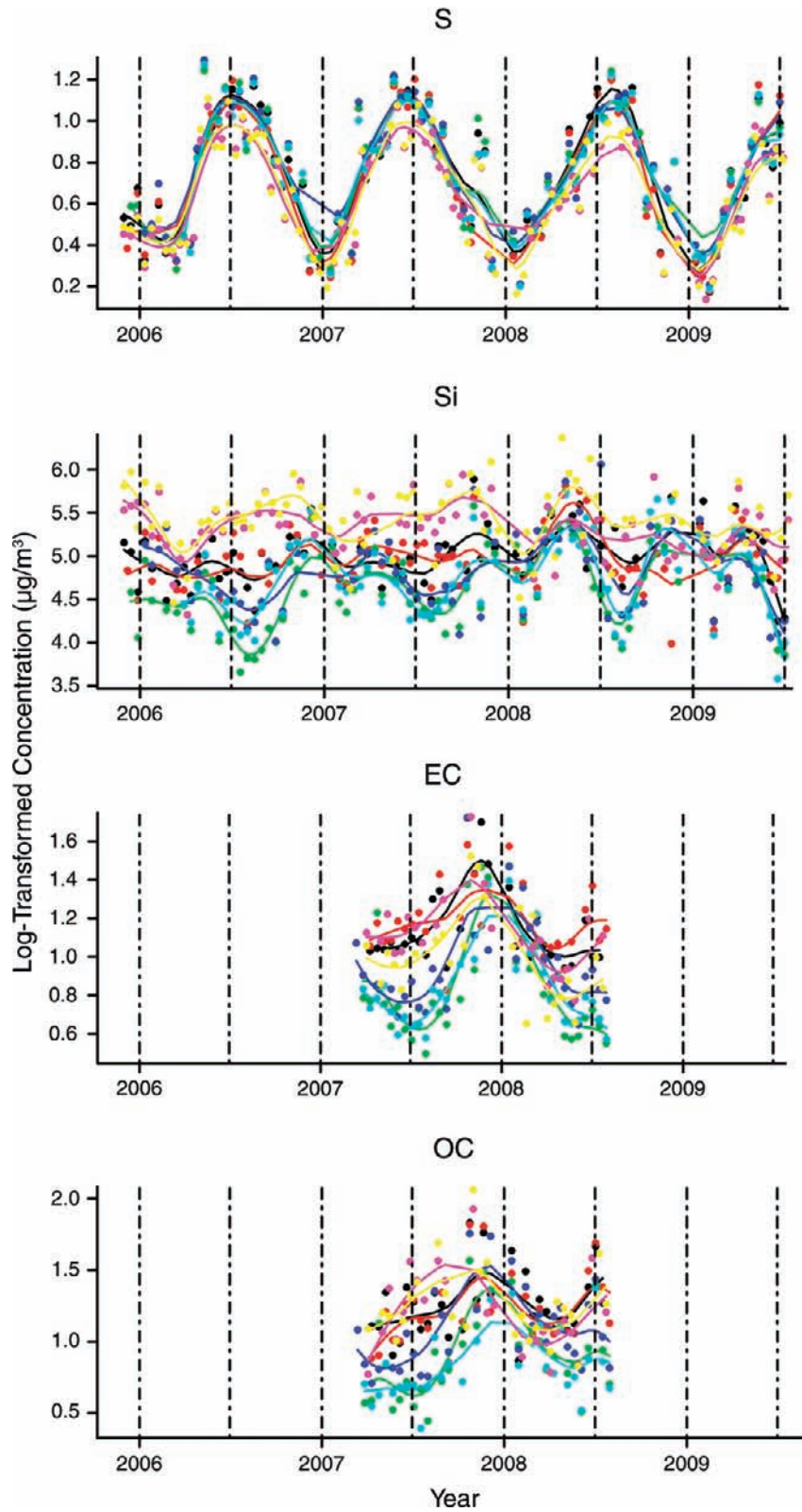


Figure 13. Trend fits for the estimated temporal trend of log-transformed sulfur, silicon, EC, and OC concentrations at seven MESA Air fixed monitoring sites in Los Angeles. Black indicates L001; red, L002; green, LC001; blue, LC002; light blue, LC003; pink, LR001; yellow, LR002.

Table 28. Provisional Cross-Validation Statistics and Selected Variables from Trend-Adjusted Long-Term Average Concentrations at Home-Outdoor Sites

City/ Pollutant	Cross-Validation Statistic ^a		Geographic Variable ^b									
	MSE	R ²	Traffic	Urban Land Use	Rural Land Use	Position	Source	Emission	Vegetation	Impervi- ousness	Elevation	Residual Oil ^c
Los Angeles												
S	0.006	0.21	X	X	—	—	X	—	—	—	X	—
Si	0.051	0.38	X	—	X	—	—	—	—	—	—	—
EC	0.010	0.78	X	X	X	—	—	—	—	—	X	—
OC	0.041	0.24	—	X	X	—	—	—	—	—	X	—
Chicago												
S	0.006	0.35	X	—	X	—	X	—	—	—	—	—
Si	0.058	0.22	X	X	X	—	—	—	—	—	—	—
EC	0.006	0.51	X	—	X	—	X	—	—	—	—	—
OC	0.016	0.43	X	X	—	—	X	—	—	—	—	—
St. Paul												
S	0.002	0.16	X	—	—	—	X	—	X	X	X	—
Si	0.053	0.10	—	X	X	—	—	—	X	—	—	—
EC	0.004	0.42	X	X	—	—	—	—	X	—	—	—
OC	0.002	0.60	X	X	X	—	—	—	—	—	—	—
Baltimore												
S	0.004	0.14	—	X	X	—	—	—	—	—	—	—
Si	0.031	0.54	—	—	—	X	X	—	X	—	X	—
EC	0.006	0.59	X	—	X	—	—	—	—	—	X	—
OC	0.005	0.63	X	—	X	—	—	X	X	—	—	—
New York												
S	0.029	0.16	—	X	X	—	—	—	—	—	X	—
Si	0.090	0.09	—	—	—	—	—	—	—	—	X	X
EC	0.039	0.51	—	X	X	—	—	—	—	—	—	—
OC	0.015	0.49	X	X	X	—	—	—	—	—	—	—
Winston-Salem												
S	0.007	0.29	—	X	X	—	—	—	—	—	—	—
Si	0.023	0.21	X	—	—	X	—	—	—	—	X	—
EC	0.004	0.41	—	X	X	—	—	—	—	—	X	—
OC	0.011	0.19	—	X	X	—	X	—	—	—	—	—

^a Provisional cross-validation approach (lasso variable selection followed by all subset universal kriging) is described in the text under “Variable Selection” and in Table 26.

^b List of geographic variables for each category is shown in Table 27.

^c Considered only for New York.

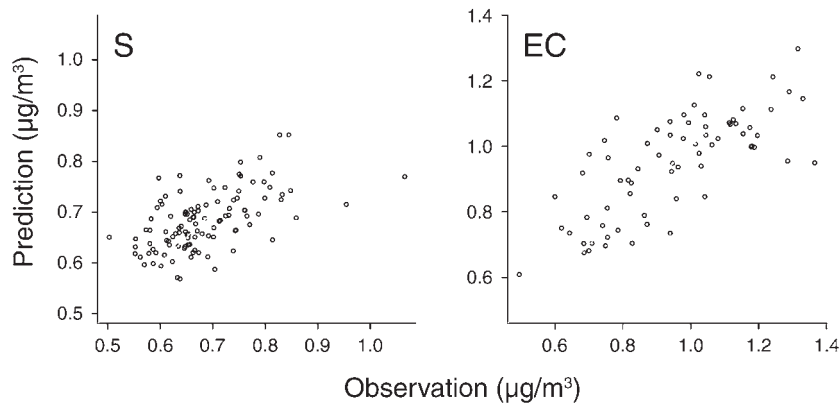


Figure 14. Scatter plots of observed and predicted trend-removed and log-transformed long-term concentrations of sulfur (cross-validated $R^2 = 0.21$) and EC (cross-validated $R^2 = 0.78$) determined by universal kriging with selected covariates across home-outdoor monitoring sites in Los Angeles.

selected only in St. Paul and Baltimore, and imperviousness was chosen only in St. Paul. The provisional R^2 values from our cross-validation approach using selected variables for the regression of long-term average $PM_{2.5}$ component concentrations are shown in Table 28. They were generally higher in all areas for EC and OC than for sulfur and silicon. As an example, Figure 14 compares observed and predicted trend-removed long-term average concentrations for sulfur and EC in Los Angeles. It shows a stronger relationship for EC than for sulfur. The low cross-validated provisional R^2 values (below 0.2) for sulfur and silicon in St. Paul and New York and for sulfur in Baltimore (Table 28) may be due to less spatial variability of $PM_{2.5}$ components or to the absence of other important geographic covariates.

Model Parameter Estimates As an example of the results, the estimates for the regression parameters (the covariates were rescaled to have common mean and unit variance) and variance model parameters for log(sulfur) in Chicago are shown in Figure 15. The full set of parameter estimates is provided in Figures 4 to 7 of Appendix C (available on the HEI Web site). Variance model parameters are shown on the log scale.

Los Angeles and Chicago tended to show stronger spatial correlation structure than the other areas (Table 4 in Appendix C, available on the HEI Web site). The estimated regression parameters for EC and OC tended to be significantly different from zero, whereas the regression parameter estimates for silicon and sulfur were not (comparisons not shown).

Model Evaluation Table 29 shows cross-validated statistics of predictions for 2-week concentrations across

home-outdoor sites by city. Many of the temporally adjusted R^2 values (with adjustment based on either the estimated unsmoothed trend or spatial means of fixed sites) were much lower than the overall (unadjusted) values. The lower temporally adjusted R^2 values suggest that some of these model predictions capture less spatial variation in long-term average $PM_{2.5}$ components than could be

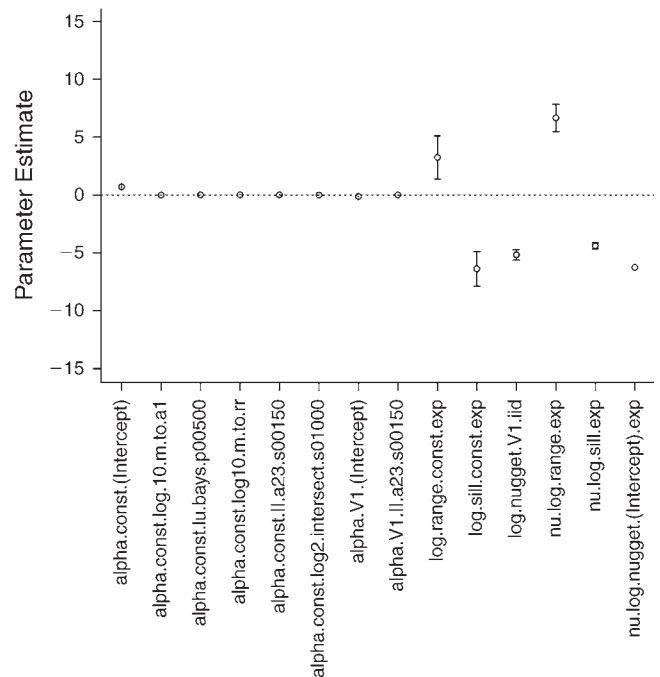


Figure 15. Estimated parameters for the selected covariates (scaled) and covariance structure in the spatiotemporal model for log(sulfur) concentrations in Chicago.

Table 29. Cross-Validation Statistics for Predicted 2-Week Concentrations Across Home-Outdoor Sites for Final Spatiotemporal Model in MESA Cities

City/ Pollutant	MSE	Overall R^2	Temporally Adjusted \bar{R}^2	
			Estimated Trend ^a	Average ^b
Los Angeles^c				
S	0.002	0.98	0.84	0.46
Si	0.040	0.64	0.65	0.46
EC	0.018	0.82	0.67	0.64
OC	0.027	0.70	0.53	0.40
Chicago				
S	0.009	0.70	0.49	0.14
Si	0.109	0.52	0.18	0.00
EC	0.006	0.69	0.49	0.47
OC	0.023	0.52	0.25	0.24
St. Paul				
S	0.001	0.93	0.77	0.59
Si	0.041	0.73	0.48	0.18
EC	0.006	0.58	0.34	0.34
OC	0.003	0.86	0.49	0.48
Baltimore				
S	0.002	0.97	0.75	0.51
Si	0.032	0.87	0.64	0.52
EC	0.009	0.62	0.58	0.60
OC	0.008	0.89	0.46	0.46
New York^c				
S	0.016	0.68	0.19	0.00
Si	0.074	0.38	0.29	0.39
EC	0.040	0.13	0.57	0.49
OC	0.022	0.44	0.58	0.47
Winston-Salem				
S	0.007	0.89	0.40	0.10
Si	0.034	0.83	0.30	0.05
EC	0.010	0.43	0.18	0.15
OC	0.015	0.68	0.13	0.13
Six Cities Combined				
S	0.006	0.92	0.86	0.84
Si	0.054	0.72	0.53	0.43
EC	0.012	0.79	0.81	0.81
OC	0.016	0.76	0.60	0.56

^a Adjusted temporal trend was defined by the temporal trend estimated using measurements across fixed sites without smoothing.

^b Adjusted temporal trend was defined by the mean of measurements across fixed sites at each time.

^c Unsmoothed trend and average were computed by subregions.

inferred from the overall R^2 . As a graphical example of this finding, Figure 16 compares, by $PM_{2.5}$ component, the observed concentrations and cross-validated predicted concentrations in Los Angeles. The 2-week concentrations show reasonable correlation between observations and predictions without adjustment for temporal variability. In contrast, the 2-week concentrations after adjustment for temporal variability show similar or less correlation between observations and predictions.

In some areas, such plots highlight that there is little remaining spatial variability, resulting in the lower temporally adjusted R^2 estimates shown in Table 29. These low temporally adjusted R^2 values suggest that our prediction models do not capture much spatial variability in some areas. Across all areas, the temporally adjusted R^2 values were generally higher for EC and OC than for sulfur and silicon, particularly when spatial averages were used. Temporally adjusted R^2 values across all six cities were generally higher than the city-specific values because of the contribution of between-city variability to this estimate (Figure 17, Table 29). Table 30 shows the proportion of the total variance of the set of cross-validated predictions at home-outdoor sites; the larger temporally adjusted R^2 values for EC and OC are consistent with larger proportions of the variances attributed to the regression part of the models. Similarly, the variability in the predictions of sulfur and silicon are dominated by the temporal trends or the spatiotemporal residuals in most areas. The limited spatial predictive ability for sulfur and silicon was also demonstrated by an evaluation using external data for sulfur and silicon from the snapshot campaign in Chicago, St. Paul, and Winston-Salem. In this evaluation, the R^2 estimates were close to zero in each season (Figure 18). Although data from the snapshot campaign are limited to three cities and two components, the small R^2 estimates from these purely spatial external data sets indicate that the prediction ability of our spatiotemporal model is limited, at least for sulfur and silicon.

Predicted Concentrations at Participants' Addresses

Figure 19 shows predicted long-term average concentrations of $PM_{2.5}$ components at MESA Air participants' addresses in the six cities. Predicted long-term concentrations were generally more variable in Los Angeles and New York and less variable in St. Paul and Winston-Salem (Figure 20, Table 31). A full discussion of these exposure modeling results and their implications is provided below under "Discussion and Conclusions/Estimation of Exposure."

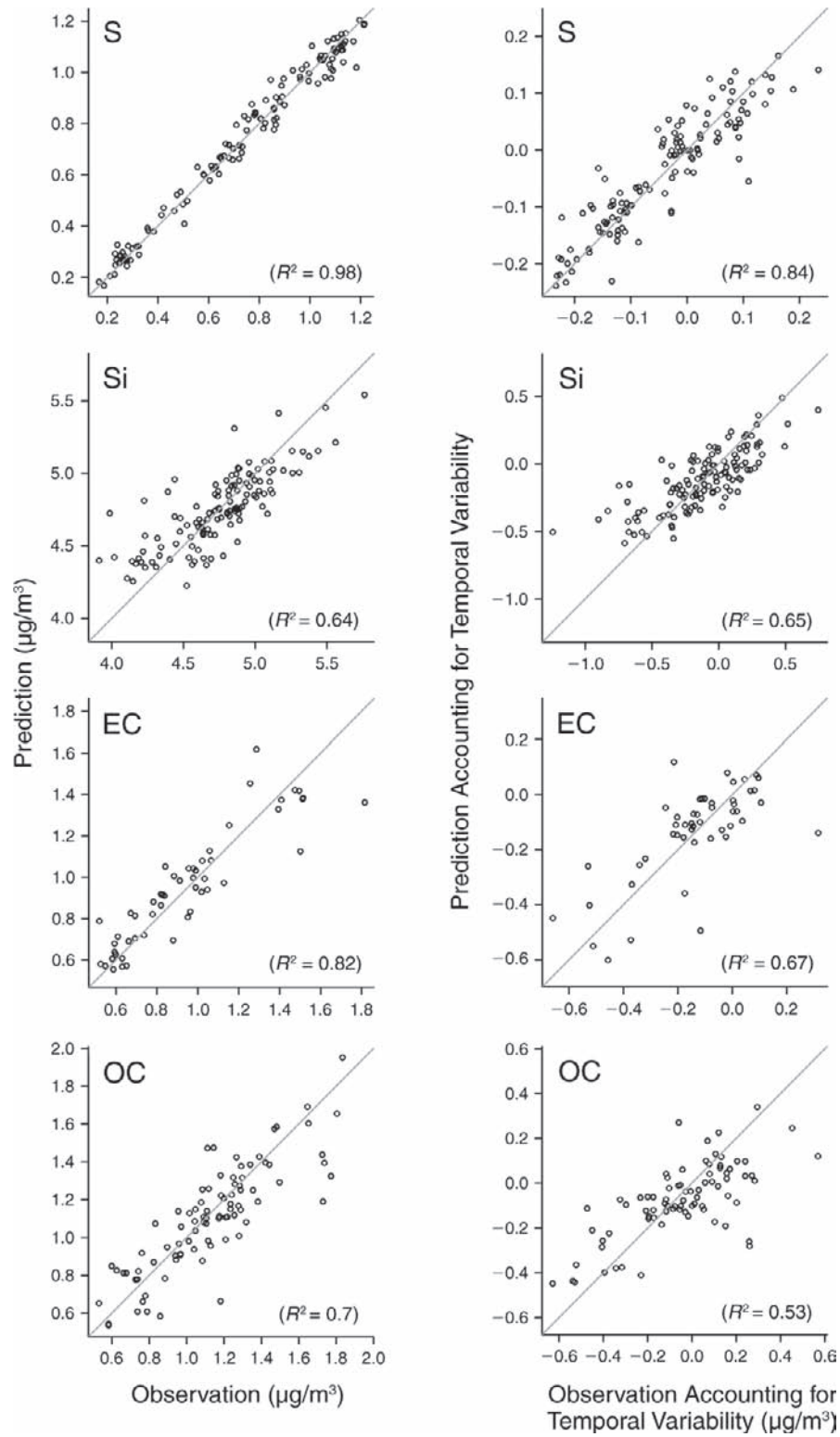


Figure 16. Scatter plots of observations vs. predictions (from the spatiotemporal model) for log-transformed 2-week concentrations of sulfur, silicon, EC, and OC across home-outdoor monitoring sites in Los Angeles, without accounting for temporal variability (left column) and accounting for temporal variability (right column). The diagonal (unity) line depicts perfect agreement between observed and predicted values.

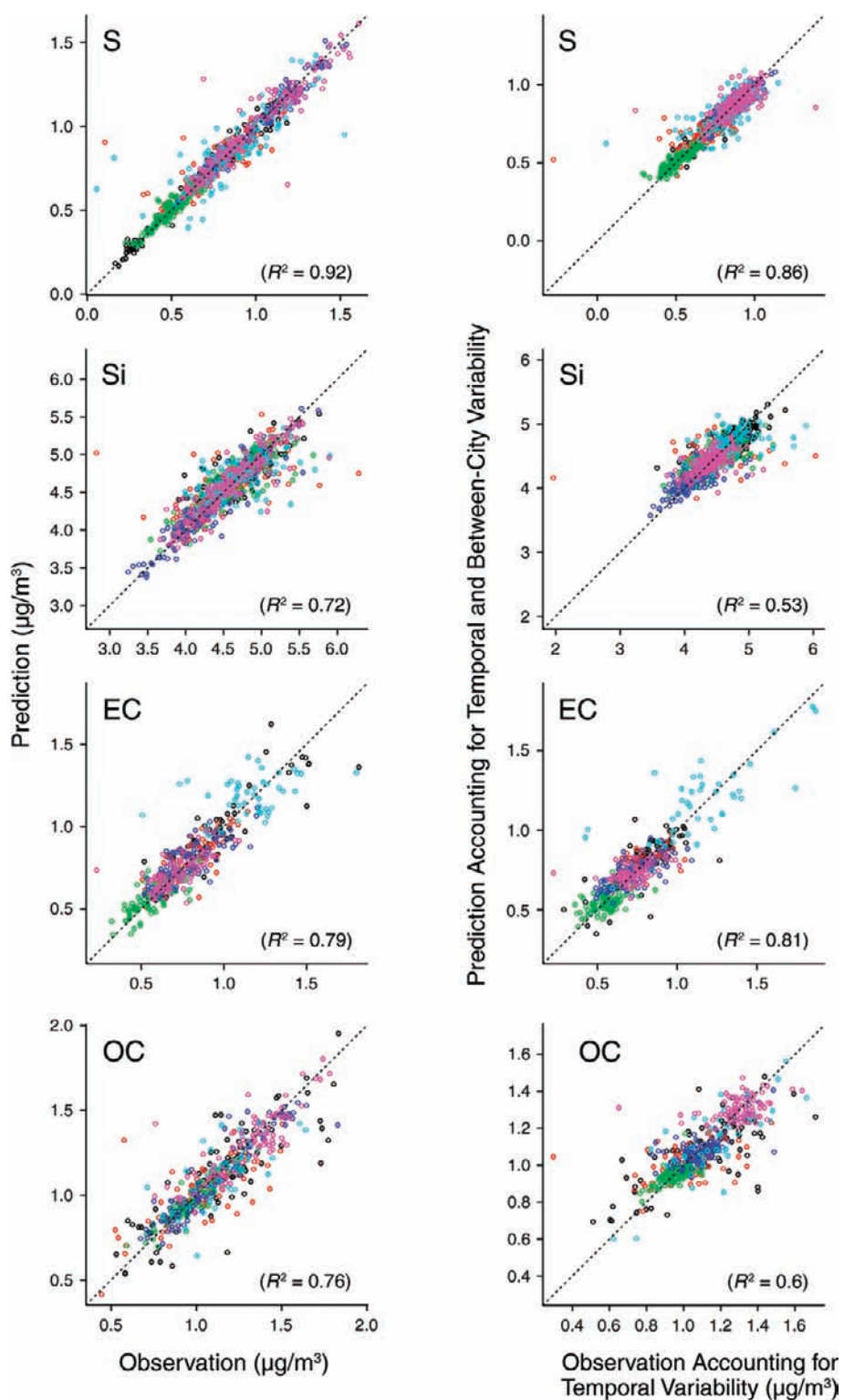
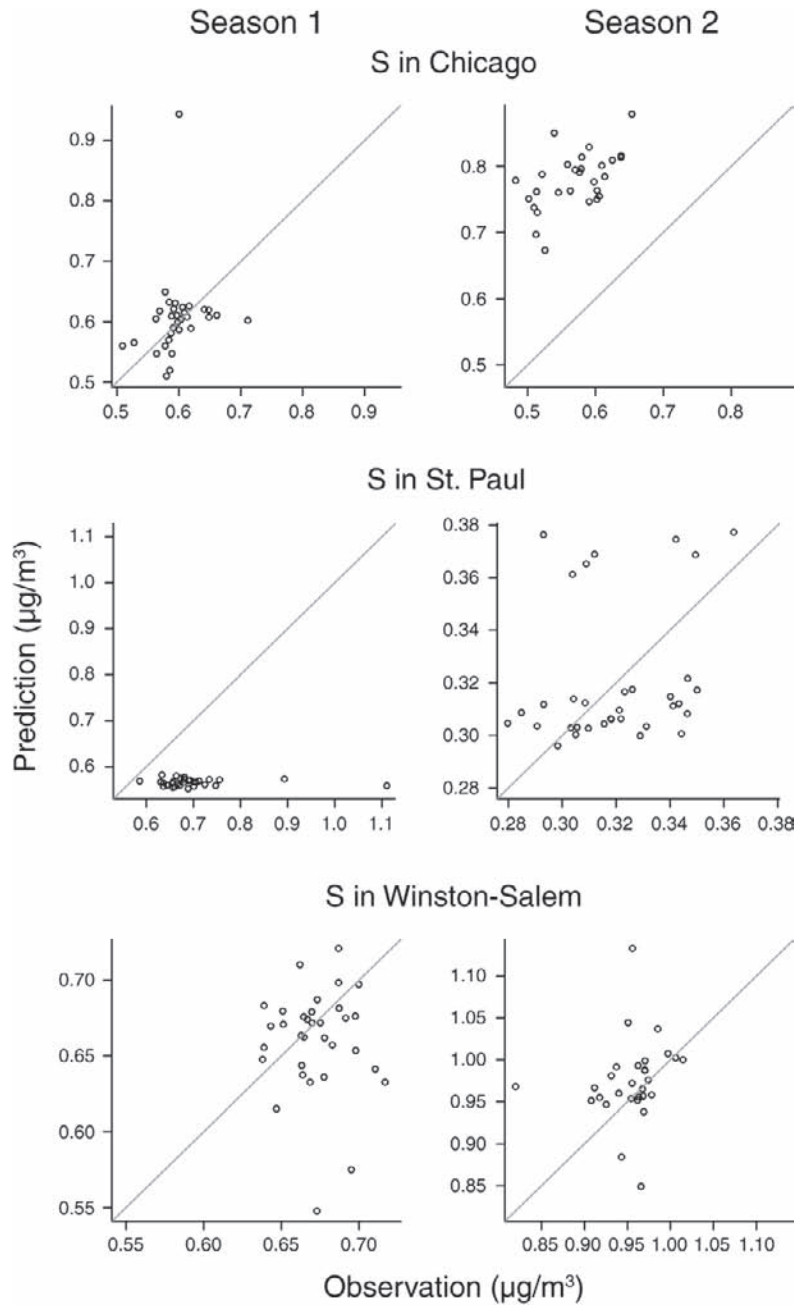


Figure 17. Scatter plots of observations vs. predictions (from the spatiotemporal model) for log-transformed 2-week concentrations of sulfur, silicon, EC, and OC across home-outdoor monitoring sites in the six MESA cities, without accounting for temporal variability (left column) and accounting for temporal variability by subtracting estimated temporal trend without smoothing (right column). Estimated city-specific long-term means were added to the temporal trends to allow between-city comparisons. Data are color-coded by city: black indicates Los Angeles; red, Chicago; green, St. Paul; blue, Baltimore; light blue, New York; and pink, Winston-Salem. The diagonal (unity) line depicts perfect agreement between observed and predicted values.



(Figure continues on next page.)

Figure 18. Scatter plots of observations vs. predictions (from the spatiotemporal model) for log-transformed sulfur and silicon concentrations across the snapshot campaign sites in Chicago, St. Paul, and Winston-Salem in two seasons. Season 1 is January, March, and April; Season 2, June, July, and August. The diagonal (unity) line depicts perfect agreement between observed and predicted values.

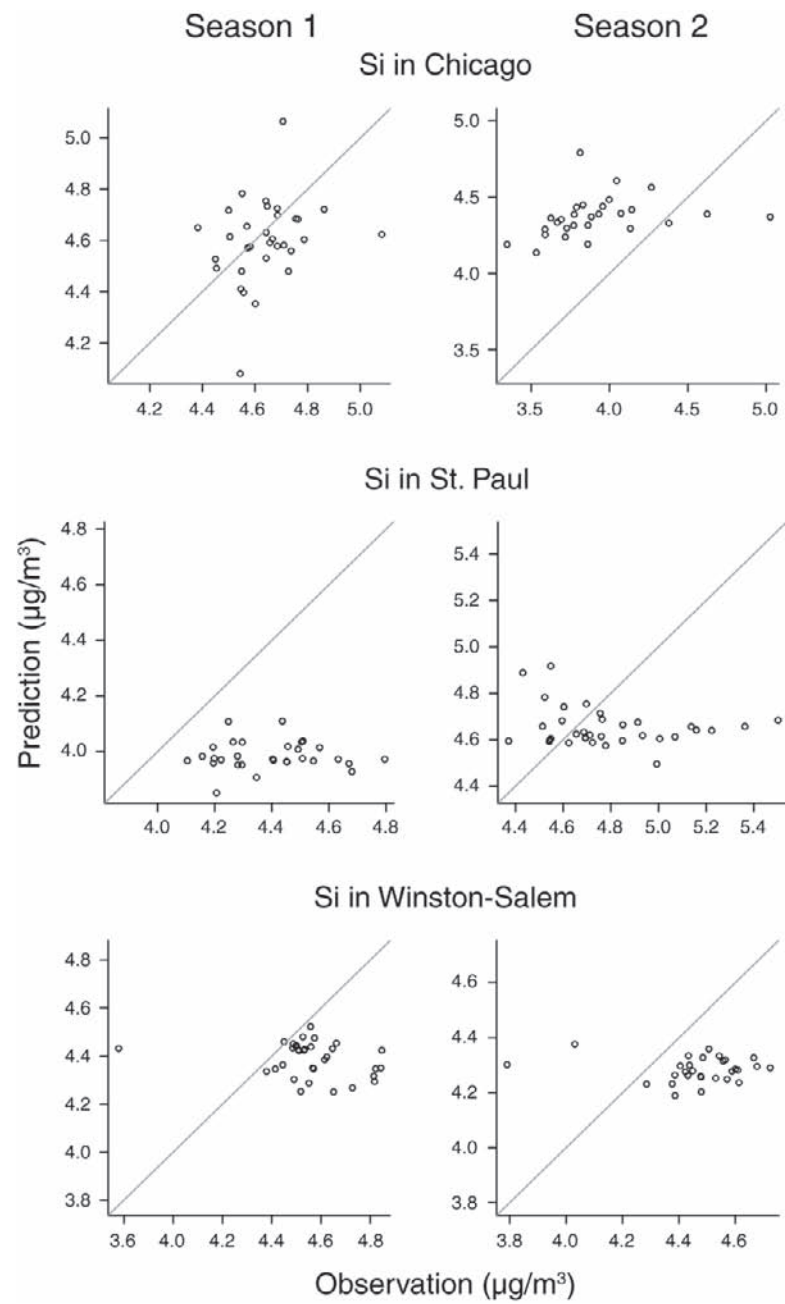
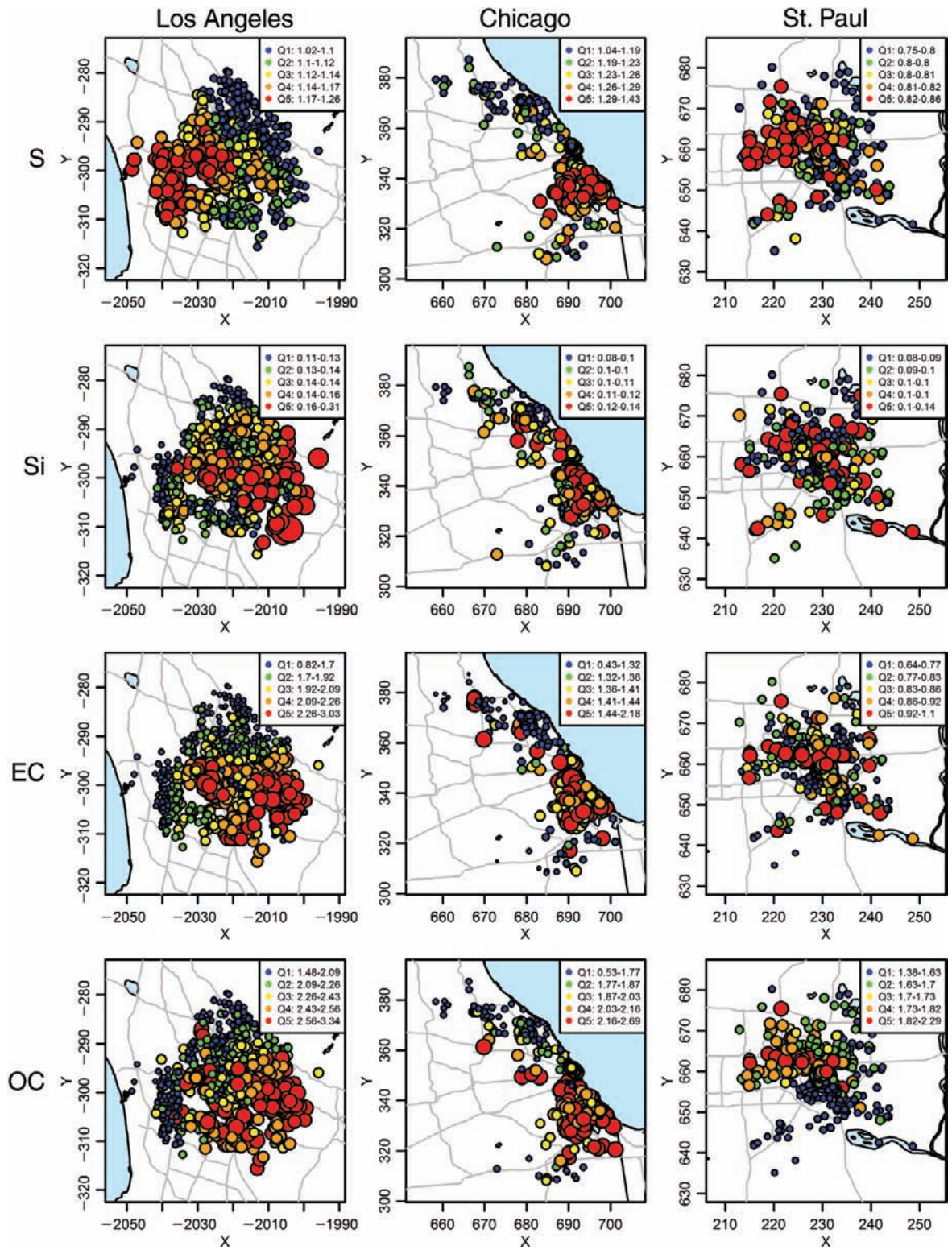


Figure 18 (Continued).



(Figure continues on next page.)

Figure 19. Predicted long-term concentrations (from the spatiotemporal model) of sulfur, silicon, EC, and OC at participants' addresses in the six MESA cities. Different colors represent quintiles of the range of concentrations ($\mu\text{g}/\text{m}^3$), shown in inset boxes, for a component in each city: blue, green, yellow, orange, and red display 1st, 2nd, 3rd, 4th, and 5th quintiles, respectively. The numbers on the axes indicate the X and Y map coordinates in kilometers.

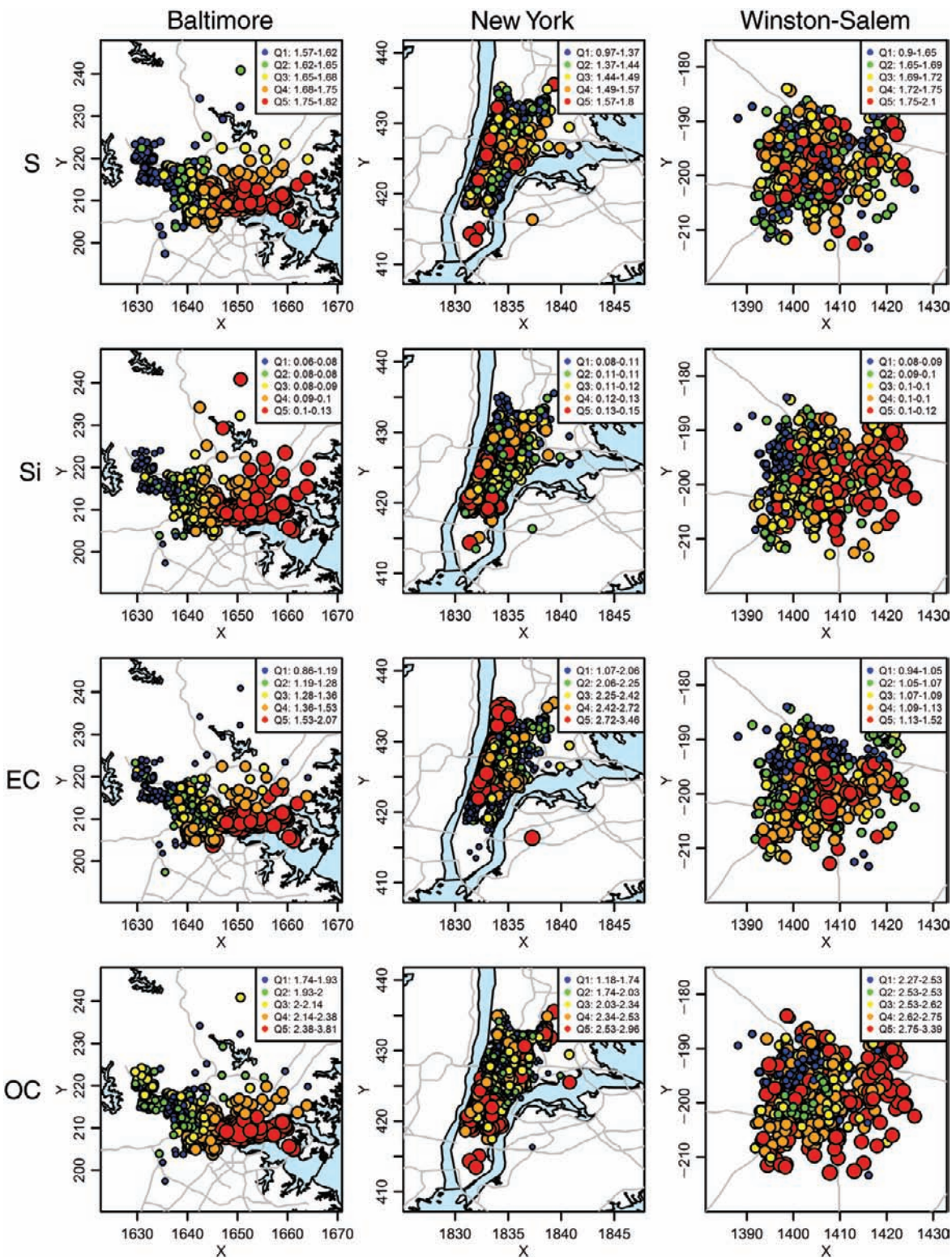


Figure 19 (Continued).

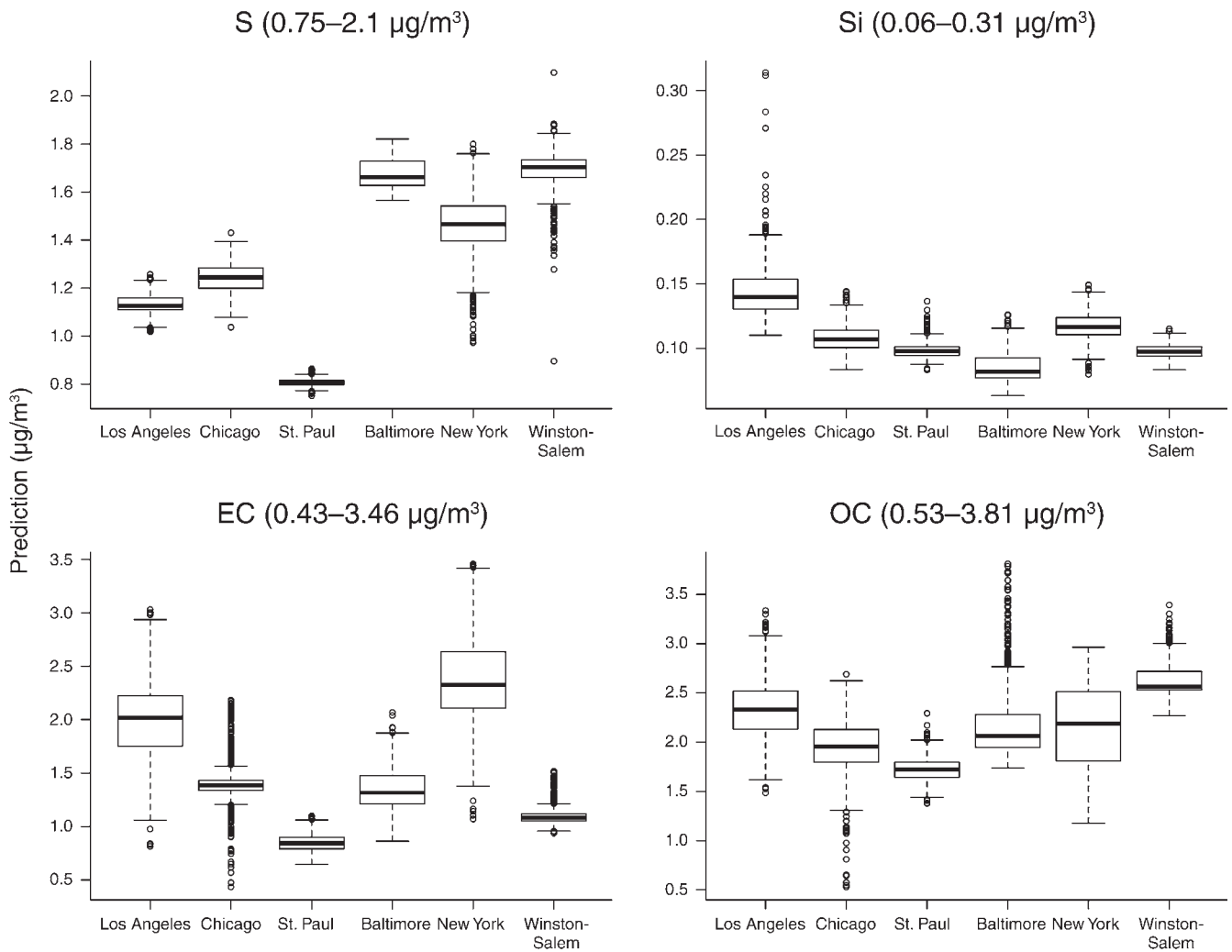


Figure 20. Box plots of predicted long-term concentrations (from the spatiotemporal model) of sulfur, silicon, EC, and OC at participants' addresses in the six MESA cities. Boxes outline 25th to 75th percentile, with middle bar showing the median. Dotted lines represent the 5th to 95th percentile, with outliers shown as circles above and below. The concentration measurements in parentheses represent the full range for all cities.

Table 30. Proportion of Total Variance of the Predictions Captured by the Long-Term Mean, Temporal Trend, and Spatiotemporal Residuals Across Home-Outdoor Sites

City/ Pollutant	Long-Term Mean ^a			
	Regression ^b	Regression + Kriging + Error	Temporal Trend ^a	Spatio- temporal Residual ^a
Los Angeles				
S	0.00	0.01	0.82	0.17
Si	0.10	0.20	0.32	0.48
EC	0.04	0.35	0.50	0.15
OC	0.04	0.28	0.36	0.36
Chicago				
S	0.02	0.04	0.52	0.43
Si	0.07	0.08	0.76	0.15
EC	0.26	0.31	0.54	0.16
OC	0.19	0.19	0.60	0.22
St. Paul				
S	0.00	0.00	0.56	0.44
Si	0.02	0.02	0.60	0.38
EC	0.39	0.41	0.41	0.18
OC	0.12	0.13	0.71	0.15
Baltimore				
S	0.01	0.01	0.79	0.20
Si	0.11	0.11	0.69	0.19
EC	0.48	0.48	0.35	0.17
OC	0.10	0.10	0.72	0.18
New York				
S	0.09	0.09	0.54	0.37
Si	0.11	0.11	0.39	0.51
EC	0.66	0.64	0.36	0.00
OC	0.46	0.46	0.43	0.11
Winston-Salem				
S	0.01	0.01	0.84	0.15
Si	0.02	0.02	0.74	0.24
EC	0.17	0.21	0.57	0.22
OC	0.06	0.06	0.43	0.51

^a Sum of ratios of long-term mean including regression, kriging, and error, temporal trend, and spatiotemporal residual = 1. Total variance used as denominator for calculating ratios was sum of variances of long-term mean, temporal trend, and spatiotemporal residual instead of variance of predictions given correlation structure between the three parts.

^b Ratio of regression part for long-term mean is presented separately to show its contribution to total variability.

Table 31. Predicted Long-Term Average Pollutant Concentrations for MESA Air Participants^a

City/ Pollutant	<i>n</i> ^b	Minimum	Median	Maximum	Mean	SD
Los Angeles						
S	2879	1.02	1.13	1.26	1.14	0.04
Si	2879	0.10	0.14	0.54	0.14	0.03
EC	2854	0.82	1.99	3.24	1.96	0.35
OC	2854	1.07	2.35	3.34	2.34	0.33
Chicago						
S	2781	1.04	1.24	1.50	1.24	0.06
Si	2781	0.08	0.11	0.15	0.11	0.01
EC	2705	0.43	1.38	2.18	1.39	0.21
OC	2705	0.23	1.96	3.00	1.93	0.30
St. Paul						
S	2697	0.75	0.81	0.88	0.81	0.02
Si	2697	0.08	0.10	0.14	0.10	0.01
EC	2682	0.54	0.84	1.13	0.84	0.09
OC	2682	1.26	1.72	2.34	1.71	0.13
Baltimore						
S	1954	1.53	1.67	1.83	1.68	0.07
Si	1954	0.06	0.08	0.13	0.09	0.01
EC	1954	0.85	1.32	2.09	1.35	0.21
OC	1954	1.65	2.09	3.81	2.19	0.35
New York						
S	2005	0.88	1.47	1.83	1.47	0.13
Si	2005	0.06	0.12	0.17	0.12	0.01
EC	1992	0.64	2.32	4.37	2.38	0.45
OC	2003	1.18	2.22	2.96	2.18	0.40
Winston-Salem						
S	1980	0.90	1.70	2.10	1.68	0.10
Si	1980	0.08	0.10	0.12	0.10	0.01
EC	1967	0.94	1.09	1.52	1.10	0.08
OC	1967	2.24	2.56	3.91	2.62	0.16

^a Data are expressed as $\mu\text{g}/\text{m}^3$.

^b Number of participants differed by component because we restricted our analyses to buffer areas within 10 km from any MESA Air/NPACT monitors, which varied by component.

NO₂ Exposure Model

A spatiotemporal NO₂ exposure model was developed in MESA Air using all available NO₂ monitoring data, including AQS data and MESA Air snapshot data, and geographic predictors that included a covariate for dispersion of emissions from traffic, from the California Line Source Dispersion model (CALINE). Classes of geographic variables that contributed to the NO₂ predictions included population density and measures of traffic. We used exposure predictions for MESA participants from this model to assess associations of NO₂ with the subclinical endpoint measures and the potential confounding effects of NO₂. (The NO₂ exposure model is described in Appendix D, available on the HEI Web site.)

BUILDING AND VALIDATING THE NATIONAL SPATIAL EXPOSURE MODEL

CSN and IMPROVE PM_{2.5} Component Data

Data on EC, OC, silicon, and sulfur were collected to fit and cross-validate the national spatial model for exposure to PM_{2.5} components. These consisted of 1-year averages of data measured by the EPA’s IMPROVE (Eldred et al. 1988) and CSN (U.S. EPA 2010) networks in 2009 and 2010 and housed in the AQS database. The IMPROVE monitors, located mostly in national parks and other similarly remote areas nationwide, were put in place to assess and regulate visibility in these vicinities. The CSN monitors are in areas that are more urban, and the combination of CSN and IMPROVE monitors provides a collection of pollution measurements that are evenly dispersed throughout the lower 48 states. The CSN monitors measure pollution on every third day or every sixth day; the pollutant data from those monitors that had at least 10 data points per quarter and a maximum of 45 days between measurements were included in calculating averages.

For EC and OC measurements collected between January 1 and December 31, 2009, there were 157 IMPROVE monitors and 47 CSN monitors that met these criteria. Before May 2009, many CSN monitors used a temperature protocol to measure EC and OC concentrations that was incompatible with that used by IMPROVE; in May 2009 CSN changed the protocol for several of these monitors to match the IMPROVE monitors. As a result, 95 additional annual averages from CSN monitors that met the inclusion criteria described above were calculated from May 1, 2009, through April 30, 2010. Of these, 44 also had averages available for January 1 through December 31, 2009. These 44 averages calculated over different periods were strongly correlated; for these monitors the averages calculated over the period from January 1 through December

Table 32. CSN Monitoring Periods for OC and EC in the National Spatial Exposure Model

Available Time Series	Monitors <i>n</i>	Time Series Used ^a
01/01/2009–12/31/2009 only	3	01/01/2009–12/31/2009
01/01/2009–04/30/2010	44	01/01/2009–12/31/2009
05/01/2009–04/30/2010 only	51	05/01/2009–04/30/2010

^a Time series used in calculation of 1-year averages for EC and OC.

31, 2009, were included in the modeling. In addition, we included the 51 monitors that only had averages calculated from measurements made between May 1, 2009, and April 30, 2010.

This resulted in a final data set of 255 monitors: 157 IMPROVE monitors with averages calculated from the 2009 time series, and 98 STN monitors with averages calculated either over all of 2009 or from May 1, 2009, through April 30, 2010 (Table 32). For silicon and sulfur, there were no compatibility problems between the network protocols; all 155 IMPROVE and 89 CSN monitors (a total of 244 monitors) had averages available for the period from January 1 through December 31, 2009.

The National Spatial Exposure Model

A flexible and efficient approach to handling the large amount of often-collinear GIS data in spatial modeling is partial least squares (PLS) (Abdi 2003; Sampson et al. 2011). This machine learning type of method finds the linear combinations of the GIS covariates that are most correlated with the outcome. The linear combinations, known as “scores,” effectively reduce the dimension of the covariate space to a much smaller number (since typically the first two or three scores are selected for further analysis) and take into account the multicollinearity of the GIS covariates. Although the PLS procedure is based on the assumption of independent residuals, the resulting scores can be used as covariates to parameterize the mean structure in a universal kriging model, instead of using multiple separate GIS covariates (as was done in the spatiotemporal model selection described above under “Exposure Predictions: Distributions, Model Fit, and Validation”). A 10-fold cross-validation procedure was implemented to determine the effectiveness of coupling PLS and universal kriging on a nationwide scale to predict long-term average

concentrations of components of $PM_{2.5}$. The land-use regression covariates were preprocessed to eliminate uninformative homogenous variables (using a procedure similar to the one outlined in Table 1 of Appendix C, available on the HEI Web site) and were mean-centered and scaled. In addition, the long-term average concentrations were square-root-transformed to reduce skewness. For each $PM_{2.5}$ component, part of the data (a “test set”) was left out, and the rest of the data (a “training set”) was used to fit the model and make predictions for the test set. Observations were randomly assigned to 1 of 10 groups, with each group being treated as a test set until predictions were obtained for the entire data set. At each iteration, the following steps were followed until the predictions were complete:

1. PLS was fit using the training set, and 10 scores were computed.
2. Universal kriging was used to smooth the residuals accounting for spatial correlation. The first n scores from the PLS were used for the mean structure, for $n = 1, \dots, 10$.
3. The test set was predicted using only the first n PLS components and using the first n PLS components plus the corresponding spatial smoothing.

This cross-validation procedure thus produced two sets of predicted square-root-transformed long-term averages for each pollutant: one set that was made using only PLS and one set that used both PLS and spatial smoothing from universal kriging. This allowed for comparisons between the types of predictions and gave insight into the level of spatial correlation inherent in each pollutant.

Figures 21 through 24 display the results of the cross-validation and the impact that universal kriging had on improving predictions. For each pollutant, the root mean-squared error of the predictions (RMSEP) is shown for each PLS score, both for predictions made using only PLS and for predictions made using PLS and universal kriging. Each figure displays a semivariogram of the residuals from a PLS fit on the entire data set, along with the likelihood fit from the corresponding universal kriging; this is the universal kriging model that would be fit following PLS on the entire data set to make predictions at truly unobserved locations. The semivariograms were computed for residuals resulting from PLS models that used a small number of PLS scores: for EC, the residuals were from a model with three PLS scores; for OC, silicon, and sulfur, the universal kriging model used only two PLS scores. These semivariograms further depict the extent to which

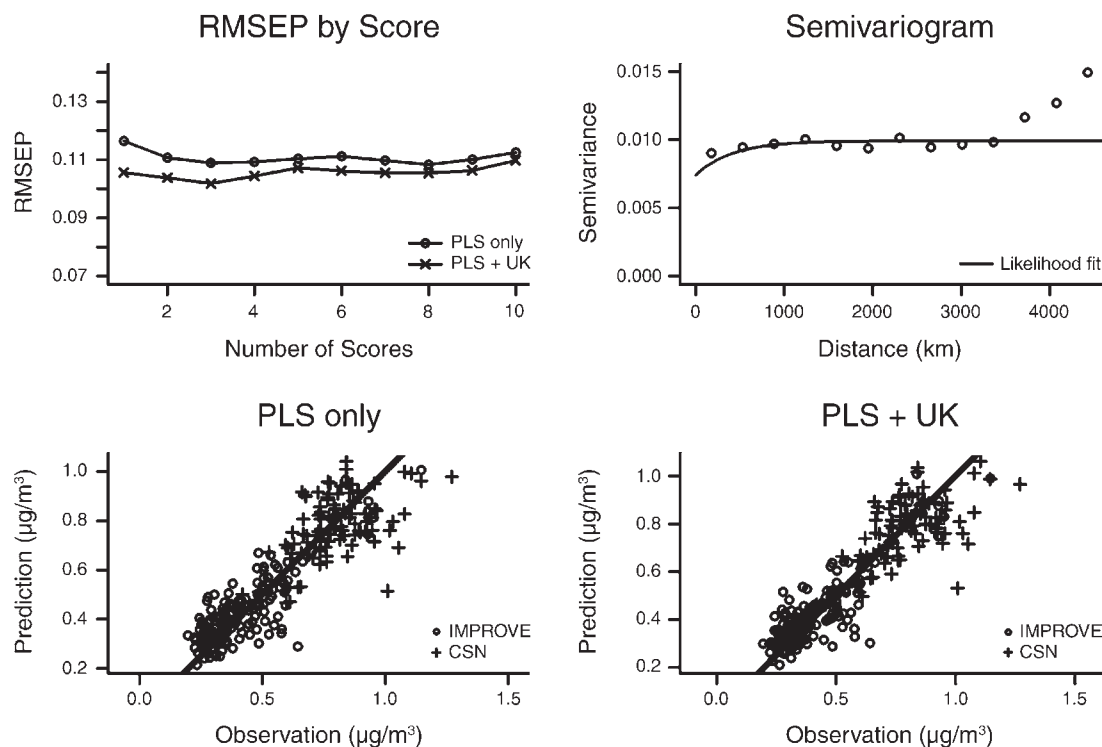


Figure 21. Tenfold cross-validation results for predicted EC concentrations on square-root scale. PLS indicates partial least squares; RMSEP, root mean-squared error of the prediction; UK, universal kriging. The diagonal (unity) line (lower graphs) depicts perfect agreement between observed and predicted values.

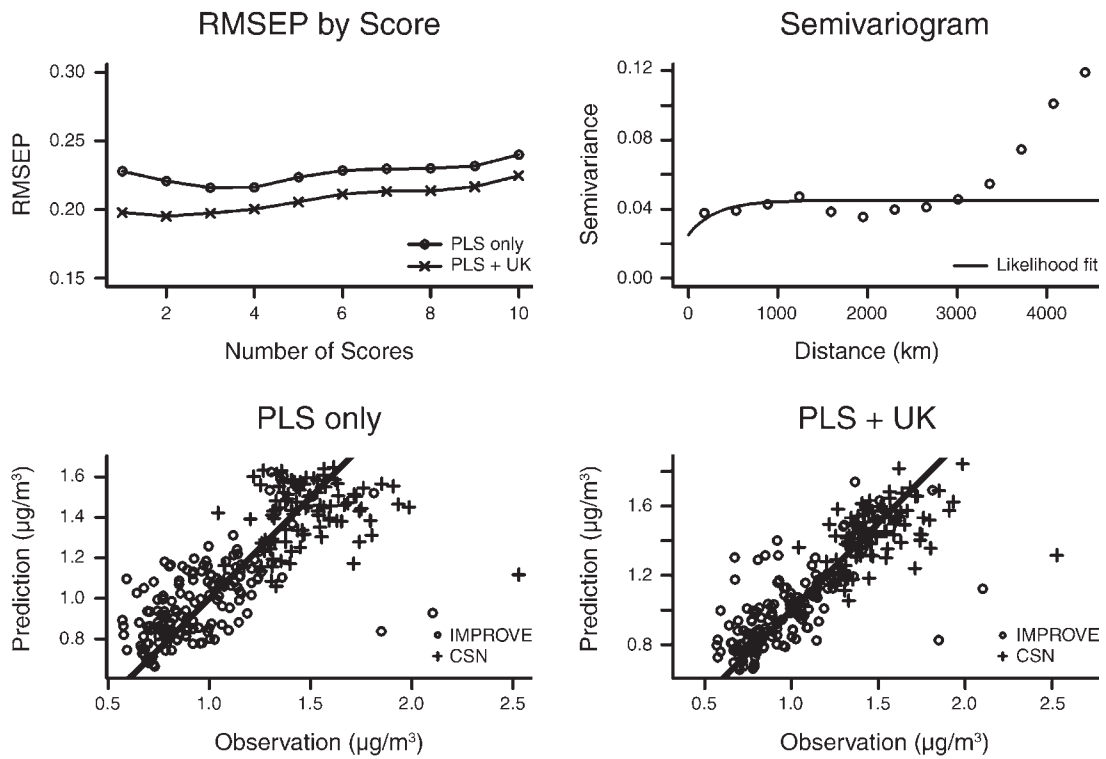


Figure 22. Tenfold cross-validation results for predicted OC concentrations on square-root scale. (For details, see Figure 21.)

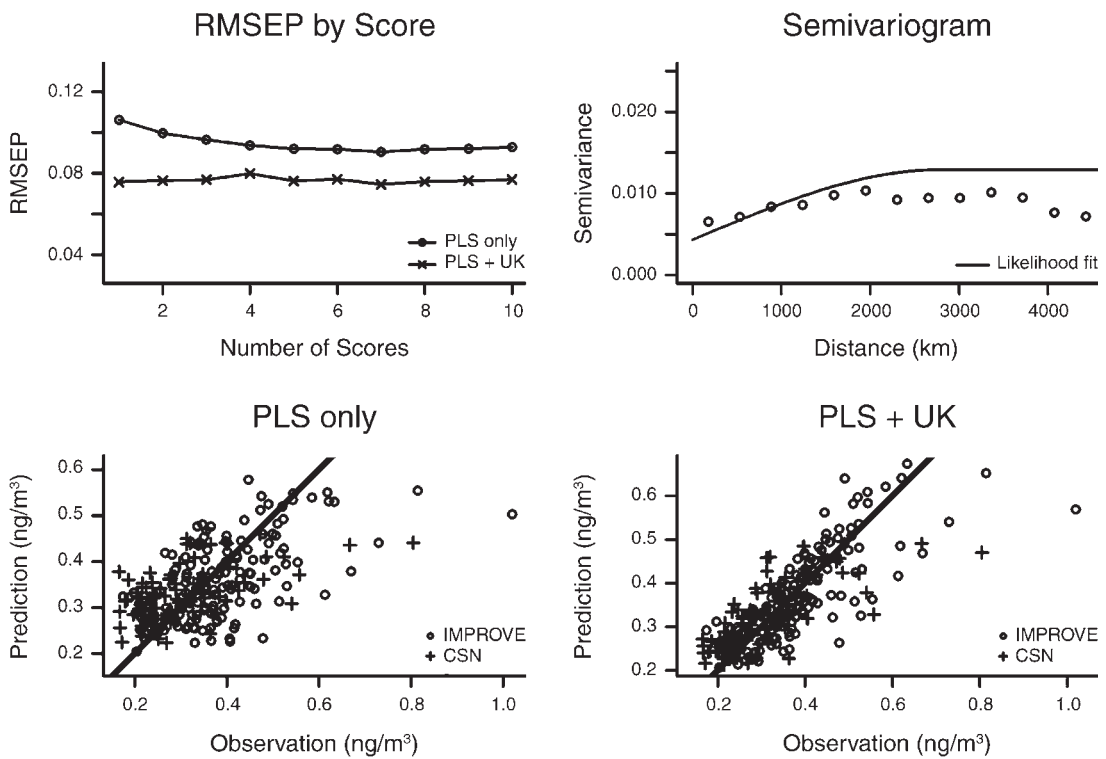


Figure 23. Tenfold cross-validation results for predicted silicon concentrations on square-root scale. (For details, see Figure 21.)

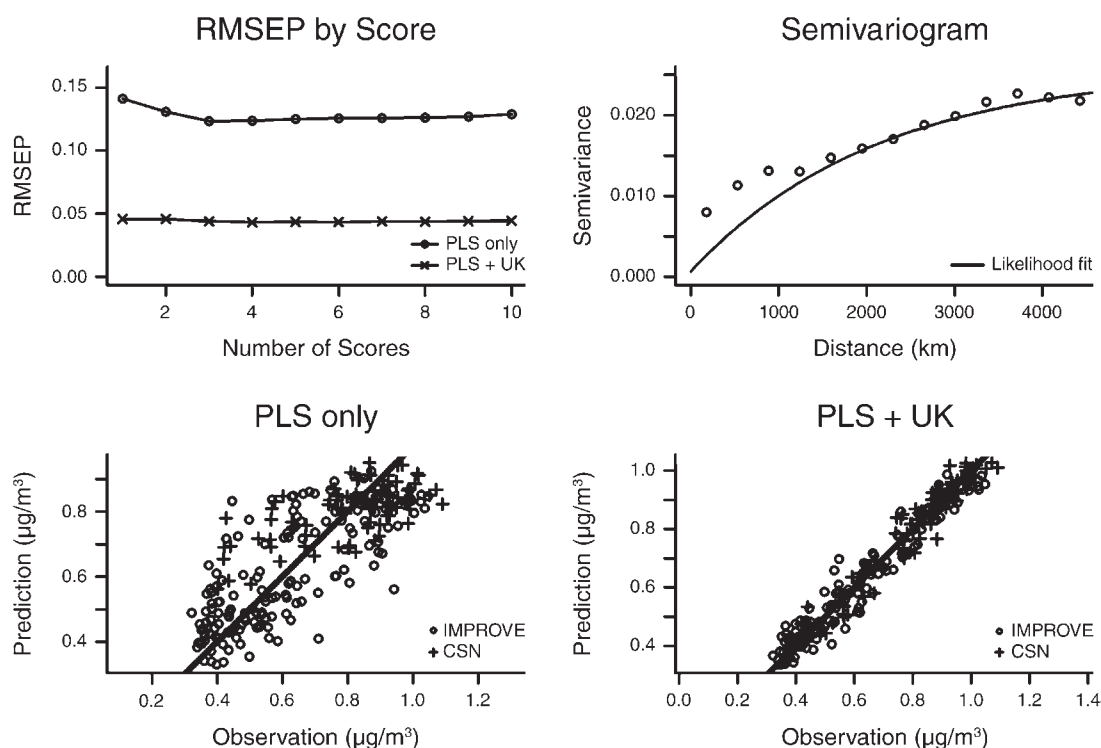


Figure 24. Tenfold cross-validation results for predicted sulfur concentrations on square-root scale. (For details, see Figure 21.)

spatial smoothing can be used to improve predictions for each pollutant. Plots of predicted concentrations versus observed square-root-transformed annual averages can also be seen in Figures 21–24. Table 33 gives cross-validated R^2 and RMSEP for the different pollutants for a given number of PLS scores, as well as the estimated kriging parameters used in spatial smoothing.

Figures 21–24 and Table 33 convey varying results for different pollutants. The scores presented in Table 33 are based on the plots of RMSEP in Figures 21–24. From these plots, EC predictions had the lowest RMSEP when PLS and universal kriging were used with three scores; for OC, the lowest RMSEP was obtained when two scores were used. Silicon and sulfur had relatively unchanging RMSEP values for low numbers of scores; thus, we chose to use two scores for each of these pollutants for the sake of consistency and low dimensionality. The predicted-versus-observed plots in Figures 21–24 are also based on three scores for EC and two scores for OC, silicon, and sulfur. For EC predictions, using three PLS scores alone was sufficient to make accurate predictions; the additional smoothing done by universal kriging did not greatly increase the accuracy in terms of R^2 and RMSEP. For OC, although the kriging range was smaller than for EC, the

partial sill was not quite so trivial relative to the nugget as it was for EC; as a result, kriging slightly improved the predictions and only two PLS scores were needed. For silicon and sulfur, the impact of kriging on improving predictions was much less trivial, and for both of these pollutants only two scores were needed. The sulfur predictions, in particular, were greatly improved by kriging, with a cross-validated R^2 of 0.95 when both kriging and PLS were used, compared with 0.63 when PLS alone was used. This drastic improvement was due to the large-scale spatial structure present in the results for sulfur, which accordingly could be very well exploited in a national model.

We also developed a national model for SO_2 and other selected PM components: nickel, vanadium, copper, SO_4 , and NO_3 . SO_4 and NO_3 modeling included data from 167 monitors across the lower 48 states; SO_2 modeling, from 386 AQS monitors; and nickel, vanadium, and copper modeling, from 323 AQS monitors. The same preprocessing procedure that was applied to EC, OC, silicon, and sulfur was applied to these other pollutants to eliminate uninformative or homogenous land-use regression covariates. The same 10-fold cross-validation was done to determine the number of PLS components to use in making predictions

Table 33. Cross-Validation Statistics and Universal Kriging Parameters^a

Pollutant	Scores <i>n</i>	<i>R</i> ²		RMSEP		UK Parameters		
		PLS Only	PLS + UK	PLS Only	PLS + UK	τ^2	σ^2	φ
EC	3	0.79	0.82	0.11	0.10	0.0074	0.0025	413
OC	2	0.60	0.69	0.22	0.20	0.0251	0.0199	304
Si	2	0.35	0.62	0.10	0.08	0.0043	0.0172	3635
S	2	0.63	0.95	0.13	0.05	0.0007	0.0251	2145
SO ₄	2	0.47	0.93	0.22	0.08	0.0036	0.0721	2214
SO ₂	2	0.31	0.45	0.41	0.36	0.0873	0.0701	123
NO ₃	2	0.06	0.76	0.34	0.17	0.000	0.1040	346
Ni	2	0.71	0.73	0.84	0.80	0.5208	0.1856	428
V	2	0.54	0.74	0.009	0.007	0.000	0.0001	593
Cu	2	0.68	0.75	0.74	0.65	0.3254	0.3748	1467

^a All metrics are on the modeling scale. PLS indicates partial least squares; RMSEP, root mean-squared error of the predictions; UK, universal kriging.

and to assess the effectiveness of universal kriging in incorporating spatial structure in the pollutant analyses. SO₄, SO₂, NO₃, and vanadium values were square-root transformed for modeling, and nickel and copper values were log transformed. The log transformation was used for nickel and copper because we encountered problems finding a true likelihood maximum in estimating the kriging semivariogram when the square-root transformation was used. The results of the 10-fold cross-validation can be seen in appendices available on the HEI Web site: Appendix H for SO₄, SO₂, and NO₃ and Appendix N for nickel, vanadium, and copper. The figures in these appendices show that SO₄ and NO₃ were well predicted by our national models, and that kriging dramatically improved the model’s performance. Two PLS scores were sufficient for making predictions. Kriging moderately improved SO₂ and vanadium predictions, but only slightly improved nickel and copper predictions. These results are echoed in Table 33, which presents the cross-validation statistics and universal kriging parameters used to make predictions for unobserved locations.

Since we used predictions from the national spatial exposure model to estimate health effects in the MESA cohort, we conducted an additional cross-validation calculation restricted to monitors within 200 km of MESA cities. The results are given in Table 34. The most notable differences were that for silicon *R*² was only 0.33 for monitors near MESA cities, but 0.62 overall, and that for copper *R*² was only 0.36 for monitors near the cities, but 0.75 overall. This implies that in all cases a significant fraction of the predicted variability was between cities, but our

national spatial model also provided valid estimates of within-city contrasts, except for silicon and copper.

The above describes the approach to building and validating the national spatial model for exposure to PM_{2.5} components. A generally similar approach was used to build a national model in MESA Air using AQS and IMPROVE network data to obtain an annual average PM_{2.5} exposure concentration for the year 2000. For that PM_{2.5} model, the cross-validated *R*² was 0.86. We used predictions from that model in the health effects analyses for the WHI-OS cohort. No further description of the PM_{2.5} model is included here.

Table 34. Cross-Validation Statistics for Monitors Within 200 km of MESA Cities^a

Pollutant	<i>n</i>	<i>R</i> ²	RMSEP
EC	36	0.80	0.11
OC	36	0.75	0.13
Si	41	0.33	0.07
S	41	0.87	0.05
SO ₄	47	0.86	0.06
SO ₂	78	0.35	0.30
NO ₃	47	0.79	0.15
Ni	61	0.63	0.74
V	61	0.71	0.01
Cu	61	0.36	0.75

^a All metrics are on the modeling scale.

Exposure Predictions for the MESA Cohort

Figure 25 shows the spatial distributions of the four $PM_{2.5}$ chemical components, as predicted by the national spatial model, at participants' addresses for each of the six MESA cities. Box-plot distributions of predicted concentrations of each component for each city are shown in Figure 26. Figures 25 and 26 can be compared with the analogous figures for the MESA Air/NPACT spatiotemporal model predictions (Figures 19 and 20). Additional summary statistics for the national spatial model predictions are presented in Table 35.

SECONDARY ESTIMATES OF EXPOSURE

Exposure estimates for $PM_{2.5}$ components were developed and applied using the nearest-monitor and IDW approaches for MESA Air participants (detailed descriptions are provided in Appendix H, available on the HEI Web site). Citywide average estimates for the six MESA cities are also presented.

To gain insight into the performance of different exposure prediction models, we compared the predicted long-term concentrations for the four $PM_{2.5}$ components from the citywide average, nearest-monitor, IDW, national spatial, and spatiotemporal models. As shown in Figure 27, predictions between the five exposure models were generally well correlated but mostly driven by between-city differences. Sulfur and silicon were more correlated across exposure models (correlation coefficient, 0.92 to 1.00 for sulfur and 0.59 to 0.98 for silicon) than EC and OC were (0.71 to 0.99 for EC and 0.03 to 0.91 for OC). In general, predictions from the national spatial model were less correlated with predictions from the other models. This discrepancy between estimates reflects intrinsic differences resulting from different data sources, in addition to differences in modeling approaches. The citywide average, nearest-monitor, IDW, and spatiotemporal models used only the MESA Air monitoring data, whereas the national spatial model used the EPA monitoring data from the entire United States. The lower predictions of silicon, sulfur, and EC from the national spatial model compared with predictions from the spatiotemporal model across cities (Figure 28, Table 35) were largely driven by lower concentrations at EPA monitoring sites compared with those at MESA Air sites. The within-city variability of predictions from the national spatial model may be lower than the variability of predictions from the city-specific spatiotemporal model (Table 35), in part, because the EPA monitors are located such that only a limited number of them capture spatial variability within cities.

ANALYSIS OF HEALTH EFFECTS

Statistical Methods and Data Analysis

Models for Effects on CIMT and CAC The two primary outcomes for the analysis of health effects in the MESA participants were CAC measured by Agatston score units and CIMT measured in millimeters. Analyses using baseline data only are purely cross-sectional; analyses using baseline and follow-up data are longitudinal. For the longitudinal analyses of continuous outcomes, we used a mixed-effects model with a random subject-specific intercept and a random slope term for the effect of time since baseline (exam 1). Our approach to parameterizing the model allowed us to obtain cross-sectional effect estimates directly from the longitudinal model. The cross-sectional effect estimates from the longitudinal model and those from purely cross-sectional models were very similar. (The detailed analysis plan for the longitudinal analyses is given in Appendix G, available on the HEI Web site.) The longitudinal model and parameters of interest are summarized here. The purely cross-sectional model is obtained by fitting model term A_{ki} to baseline data. Our longitudinal model is given as

$$Y_{kit} = A_{ki} + \sum_{t'=1}^t B_{kit}(v_{kit'} - v_{kit(t'-1)}) + C_{kit} + \varepsilon_{kit}$$

$$A_{ki} = \alpha_0 + \alpha_1 X_{ki} + \alpha_2 Z_{ki0} + a_{ki}$$

$$B_{kit} = \beta_0 + \beta_1 X_{ki} + \beta_2 W_{kit} + b_{ki}$$

$$C_{kit} = \gamma_2 U_{kit}$$

where Y_{kit} is the CIMT measurement for the i th person in the k th area at the t th follow-up visit, X_{ki} is the participant's predicted long-term average exposure to the component, Z_{ki0} is a vector of baseline covariates, W_{kit} is a vector of possibly time-varying covariates, v_{kit} is the time of the t th follow-up visit, and U_{kit} is a vector of time-varying covariates for adjustment of transient effects. Term A_{ki} captures the cross-sectional component of the model (including the estimated baseline effect of pollution), term B_{kit} captures the longitudinal (rate-of-change) component of the model, and term C_{kit} includes any transient time-varying covariates for the current visit. The parameter β_1 is the longitudinal exposure effect parameter of interest, while α_1 is the cross-sectional exposure effect parameter. The longitudinal parameter is presented as outcome units per year for a one-unit change in the pollutant, while the cross-sectional parameter is presented as outcome units without any prespecified time period for a one-unit change in the pollutant. Since the exposure time period necessary to obtain the cross-sectional effect is unknown, there is good reason to believe these parameters are scientifically distinct.

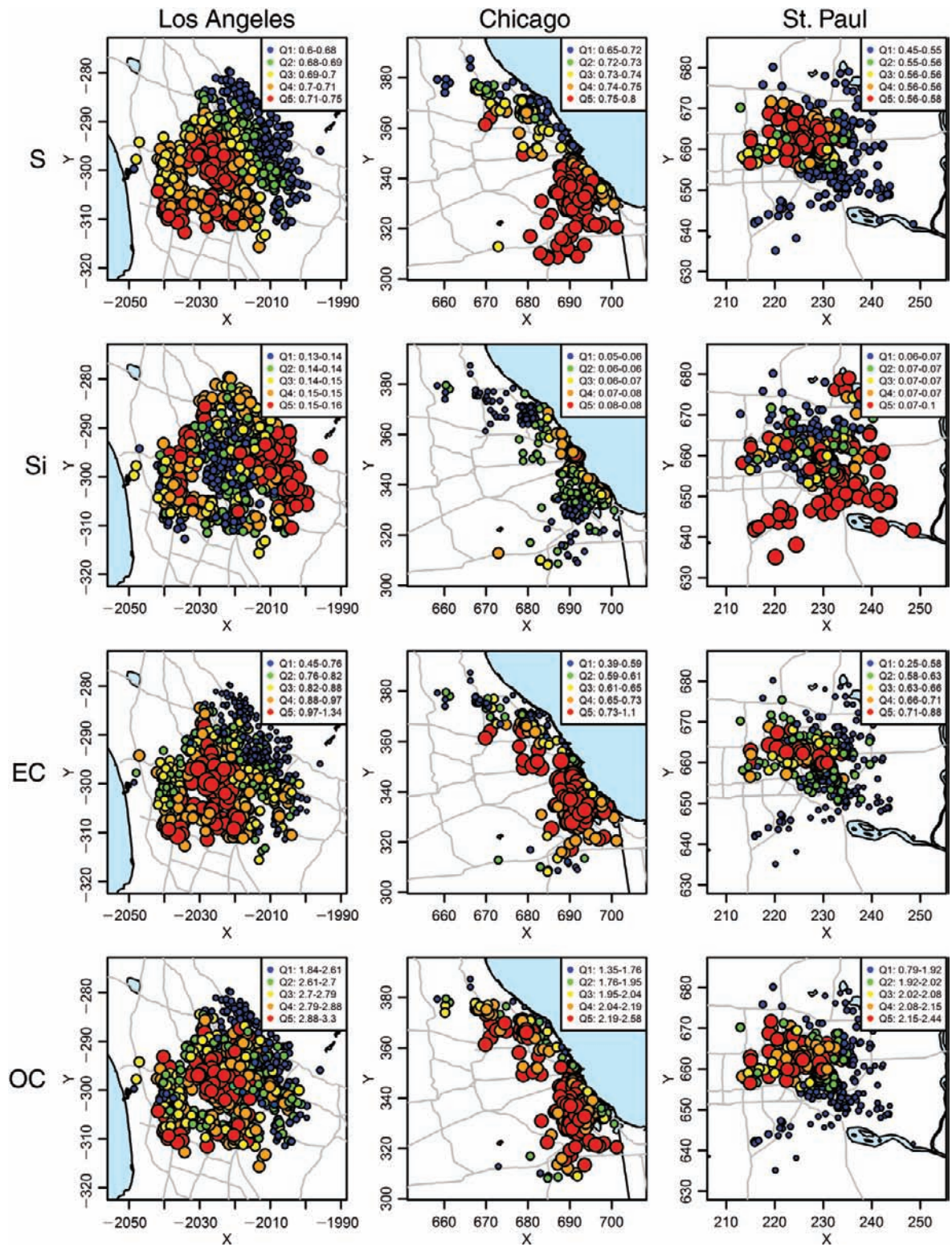


(Figure continues on next page.)

Figure 25. Predicted long-term concentrations (from the national spatial model) of sulfur, silicon, EC, and OC at participants' addresses in the six MESA cities. Different colors represent quintiles of the range of concentrations ($\mu\text{g}/\text{m}^3$), shown in inset boxes, for a component in each city: blue, green, yellow, orange, and red display 1st, 2nd, 3rd, 4th, and 5th quintiles, respectively. The numbers on the axes indicate the X and Y map coordinates in kilometers.

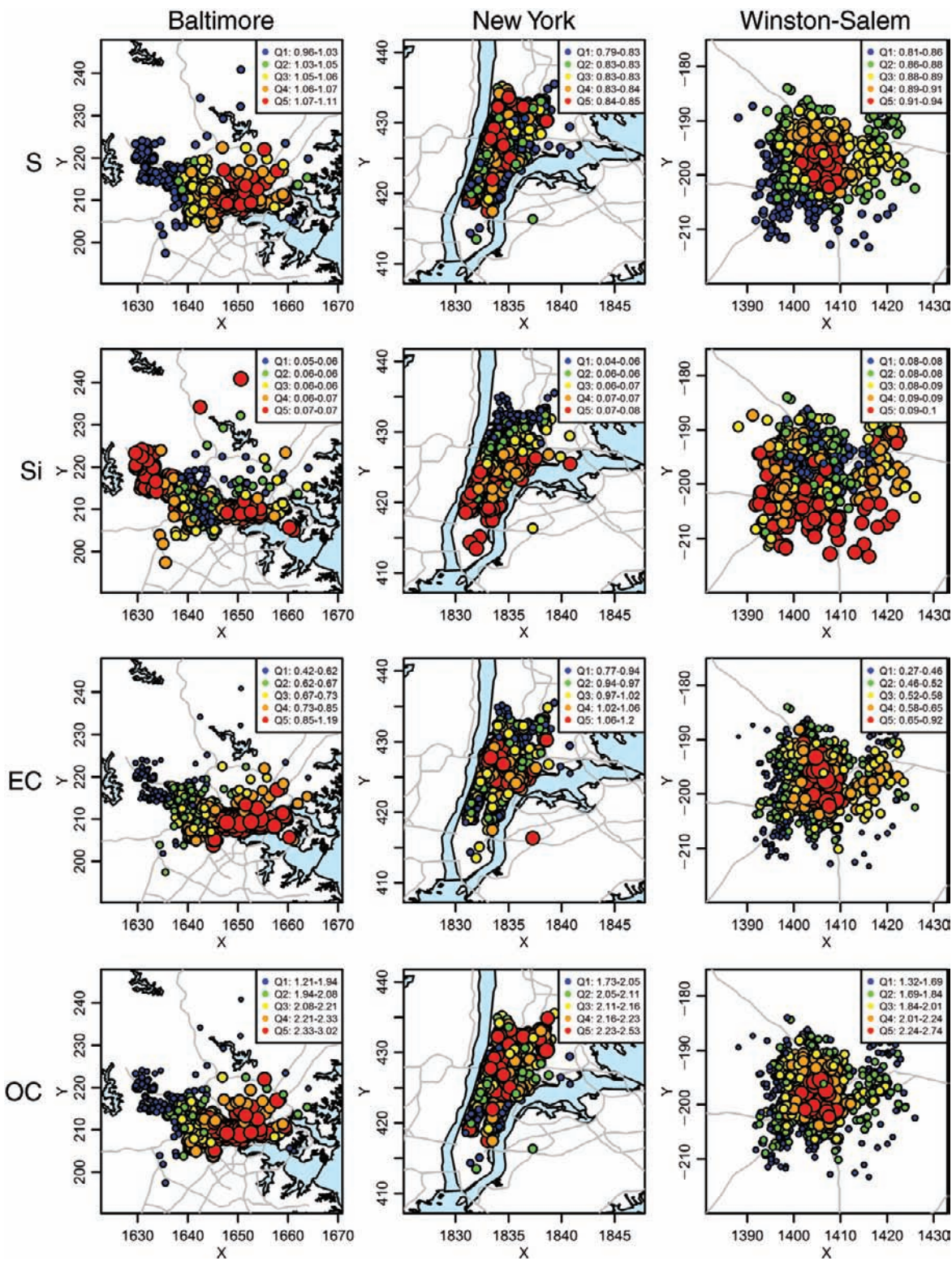


Figure 25 (Continued).

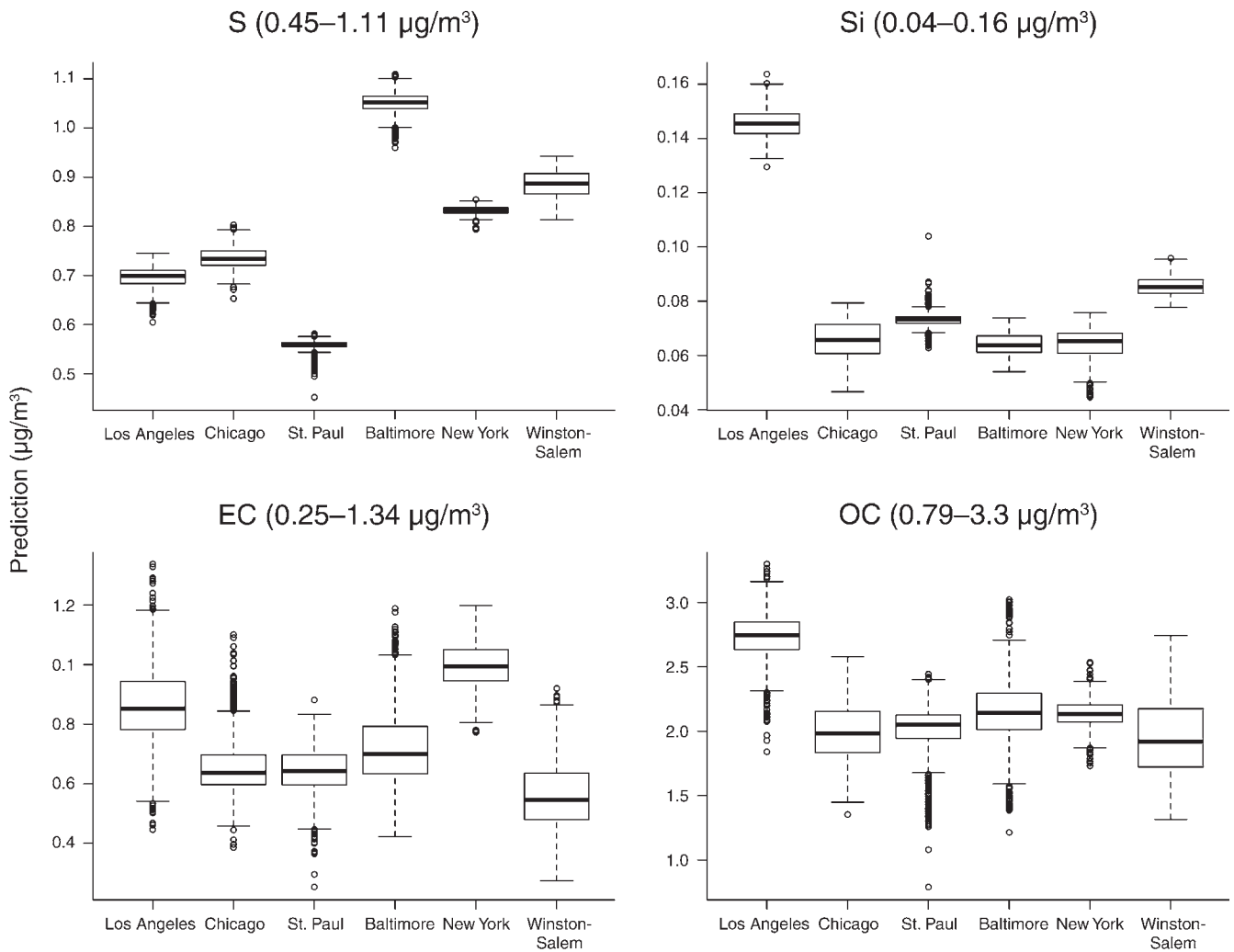


Figure 26. Box plots of predicted long-term concentrations (from the national spatial model) of sulfur, silicon, EC, and OC at participants' addresses in the six MESA cities. Boxes outline 25th to 75th percentile, with middle bar showing the median. Dotted lines represent the 5th to 95th percentile, with outliers shown as circles above and below. The concentration measurements in parentheses represent the full range for all cities.

Table 35. PM_{2.5} Component Predictions (Mean ± SD) at 5820 MESA Air Participant Addresses from 2000 to 2002 Within 10 km of Any MESA Air Monitor for the Two Primary and Three Secondary Prediction Models^a

Pollutant / City	n	Primary Models		Secondary Models		
		Spatio-temporal	National Spatial	Citywide Average	Nearest-Monitor	IDW
S						
Los Angeles	1056	1.13 ± 0.04	0.70 ± 0.02	1.20	1.20 ± 0.02	1.21 ± 0.00
Chicago	1042	1.24 ± 0.06	0.73 ± 0.02	1.24	1.23 ± 0.06	1.23 ± 0.03
St. Paul	910	0.81 ± 0.01	0.56 ± 0.01	0.85	0.85 ± 0.01	0.85 ± 0.00
Baltimore	890	1.67 ± 0.06	1.05 ± 0.03	1.65	1.65 ± 0.06	1.64 ± 0.03
New York	970	1.46 ± 0.13	0.83 ± 0.01	1.41	1.39 ± 0.05	1.40 ± 0.01
Winston-Salem	952	1.69 ± 0.08	0.89 ± 0.03	1.64	1.63 ± 0.02	1.64 ± 0.01
Si						
Los Angeles	1056	0.14 ± 0.02	0.15 ± 0.00	0.14	0.15 ± 0.01	0.15 ± 0.00
Chicago	1042	0.11 ± 0.01	0.07 ± 0.01	0.11	0.12 ± 0.01	0.12 ± 0.01
St. Paul	910	0.10 ± 0.01	0.07 ± 0.00	0.11	0.11 ± 0.00	0.11 ± 0.00
Baltimore	890	0.09 ± 0.01	0.06 ± 0.00	0.09	0.08 ± 0.01	0.08 ± 0.01
New York	970	0.12 ± 0.01	0.06 ± 0.01	0.13	0.13 ± 0.02	0.13 ± 0.00
Winston-Salem	952	0.10 ± 0.01	0.09 ± 0.00	0.09	0.09 ± 0.00	0.10 ± 0.00
EC^b						
Los Angeles	1056	1.98 ± 0.34	0.87 ± 0.14	1.68 ± 0.02	1.95 ± 0.15	1.77 ± 0.08
Chicago	1042	1.40 ± 0.20	0.66 ± 0.10	1.35 ± 0.03	1.28 ± 0.11	1.31 ± 0.06
St. Paul	910	0.85 ± 0.08	0.64 ± 0.08	0.78 ± 0.04	0.70 ± 0.08	0.74 ± 0.06
Baltimore	890	1.35 ± 0.21	0.72 ± 0.15	1.29 ± 0.09	1.33 ± 0.27	1.29 ± 0.13
New York	970	2.38 ± 0.44	0.99 ± 0.08	2.52 ± 0.17	2.67 ± 0.34	2.56 ± 0.21
Winston-Salem	952	1.10 ± 0.08	0.56 ± 0.12	1.17 ± 0.01	1.29 ± 0.20	1.22 ± 0.06
OC						
Los Angeles	1056	2.33 ± 0.28	2.73 ± 0.20	2.05	2.42 ± 0.12	2.13 ± 0.00
Chicago	1042	1.92 ± 0.28	1.97 ± 0.21	1.89	1.82 ± 0.12	1.82 ± 0.00
St. Paul	910	1.73 ± 0.13	2.01 ± 0.19	1.72	1.63 ± 0.13	1.62 ± 0.00
Baltimore	890	2.19 ± 0.38	2.14 ± 0.28	2.15	2.09 ± 0.16	1.88 ± 0.00
New York	970	2.18 ± 0.38	2.13 ± 0.12	1.89	1.91 ± 0.04	1.92 ± 0.00
Winston-Salem	952	2.63 ± 0.15	1.96 ± 0.29	2.52	2.55 ± 0.05	2.44 ± 0.00

^a IDW indicates inverse-distance weighting.

^b SD of citywide EC is not zero in each city, because citywide EC averages of participants were calculated using all monitors within each city area when participant home addresses were within 100 m from A1 and A2 roads or 50 m from A3 roads.

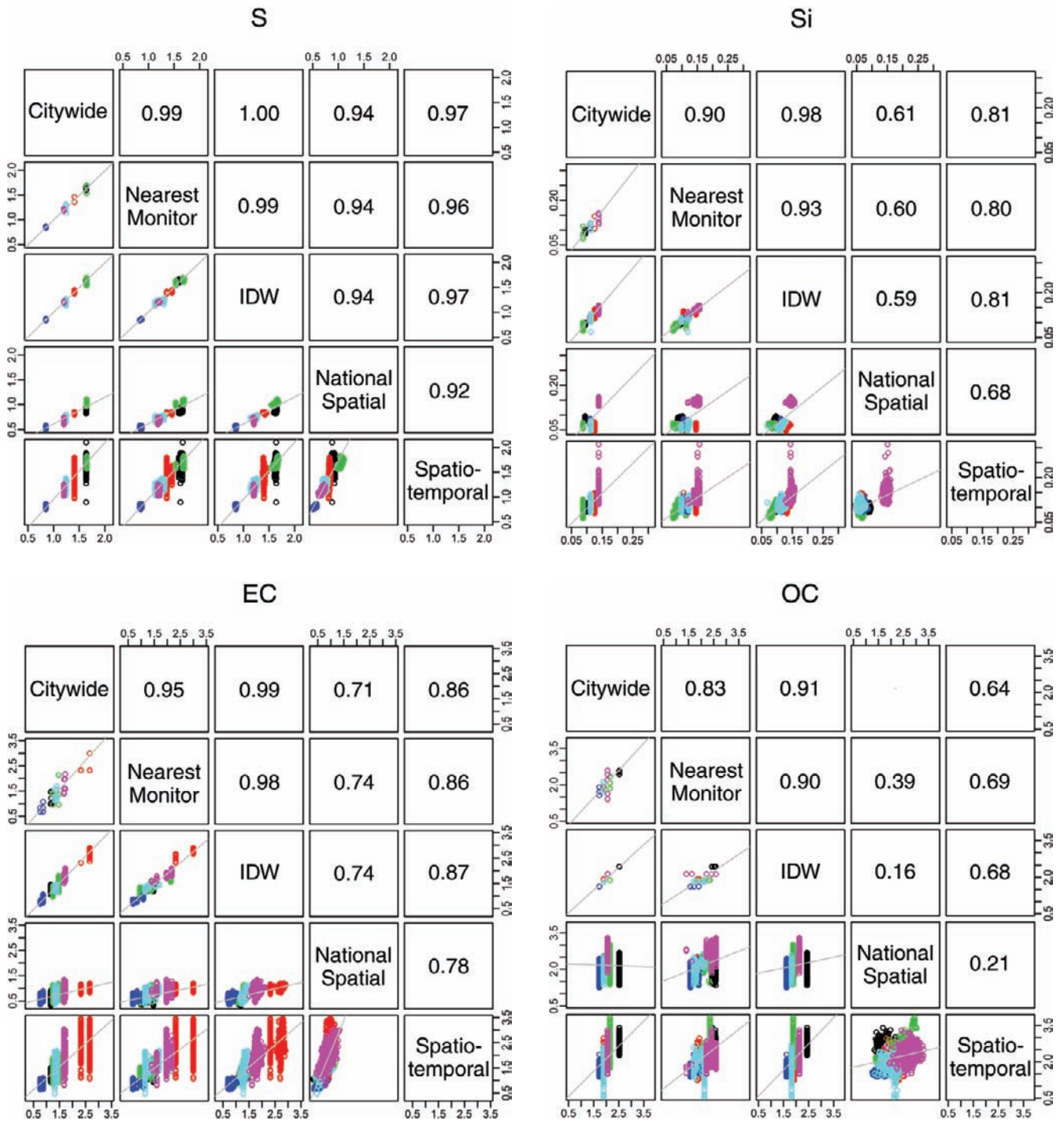
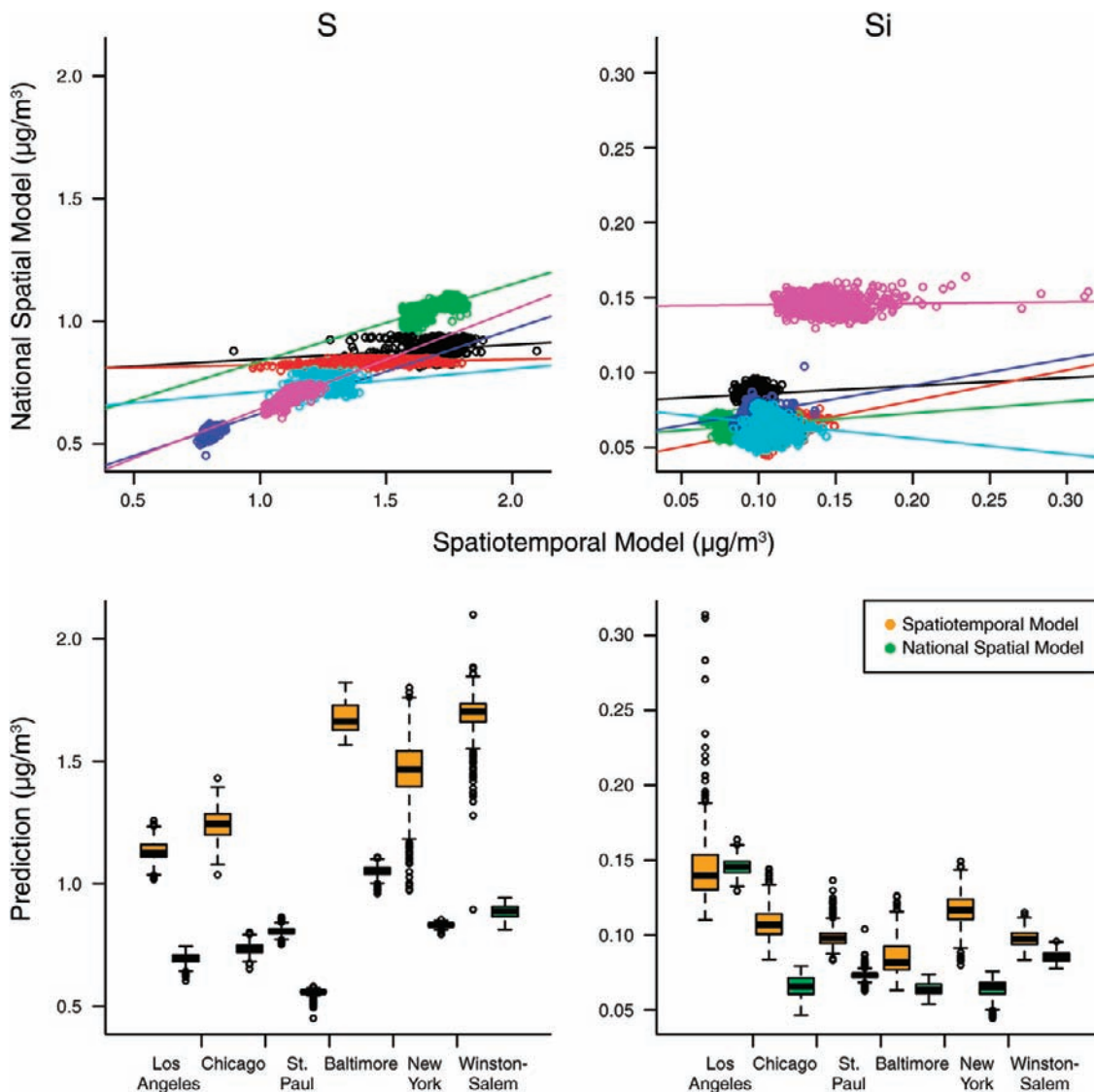


Figure 27. Scatter plots and correlation coefficients for predicted concentrations ($\mu\text{g}/\text{m}^3$) of sulfur, silicon, EC, and OC between the citywide average, nearest-monitor, IDW, national spatial, and spatiotemporal models for MESA participants' addresses at exam 1 within 10 km of any MESA Air monitor in the six cities. For the scatter plots, black indicates Winston-Salem; red, New York; green, Baltimore; blue, St. Paul; light blue, Chicago; and pink, Los Angeles.



(Figure continues on next page.)

Figure 28. Scatter plots and box plots of predicted sulfur, silicon, EC, and OC concentrations from the spatiotemporal and national spatial models. For the scatter plots, black indicates Winston-Salem; red, New York; green, Baltimore; blue, St. Paul; light blue, Chicago; and pink, Los Angeles. For lower graphs, boxes outline 25th to 75th percentile, with middle bar showing the median. Dotted lines represent the 5th to 95th percentile, with outliers shown as circles above and below.

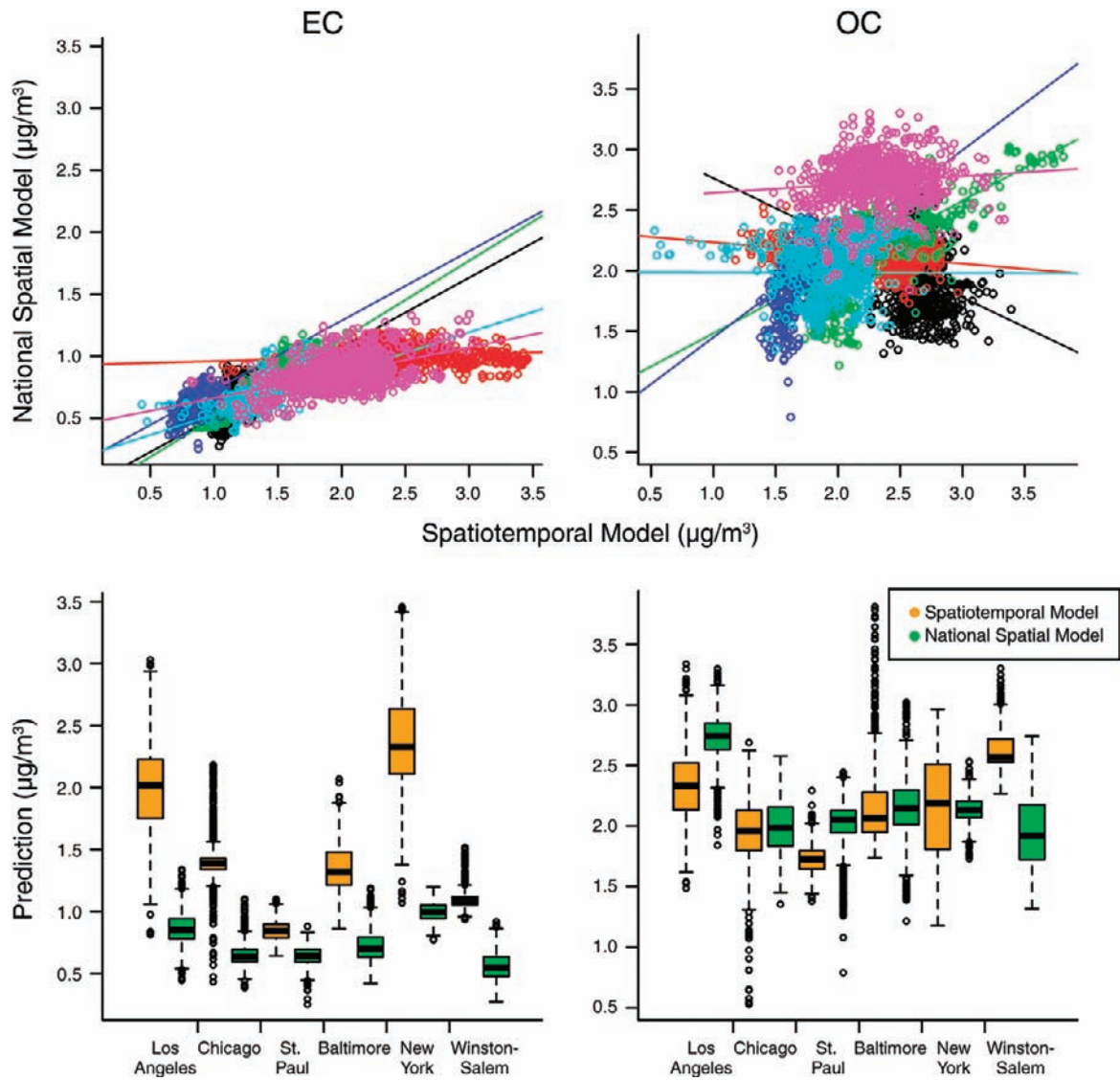


Figure 28 (Continued).

The covariates were chosen on the basis of previous scientific findings for CAC and CIMT. From the full list of chosen covariates, we selected progressive sets of confounders for adjustment by grouping the same features of variables and using a statistical approach to selection. The details are described below under “Results Using National Spatial Model Predictions” and in Appendix G (available on the HEI Web site).

Estimation is done using software for mixed-effects models, specifically lme4 in R, version 2.12.2 (R Development Core Team 2011).

Relative Risk Regression In our data set about half of the participants’ Agatston CAC scores were zero. Furthermore, the positive scores tended to be highly skewed. Thus, we focused on the binary outcome of presence or absence of CAC. A standard approach of fitting a logistic regression model produces estimates of odds ratios, and there is a common tendency to interpret the odds ratio as an estimate of the relative risk at all times. However, since the frequency of CAC being greater than zero was high, the rare disease assumption required for the odds ratio calculated from our statistical models to be a valid approximation of the relative risk was not met. To adjust for this, we therefore used relative risk regression to estimate the exposure effect parameter and obtain a direct estimate of the relative risk parameter of interest. Lumley and colleagues have described methods for estimating the relative risk using standard software (Lumley et al. 2006). We used a logarithmic transformation of the expected outcome along with a Gaussian error model.

Relationship Between the Cross-Sectional and Longitudinal Models We performed cross-sectional analyses for all outcomes and longitudinal analyses for CIMT to examine the relationship between long-term averages of $PM_{2.5}$ components and subclinical outcomes of atherosclerosis. For the primary analyses, we computed long-term averages from the MESA Air/NPACT spatiotemporal model predictions. In parallel analyses, we substituted exposure predictions from the national spatial model, and in secondary exposure analyses, we used exposure estimates based on citywide average, nearest monitor, and IDW. Although the longitudinal model also allowed us to estimate cross-sectional effects, we initially conducted separate cross-sectional analyses using only baseline data, in part because CAC endpoints were not analyzed longitudinally. In the following sections, we show estimated associations of $PM_{2.5}$ and $PM_{2.5}$ components with both CAC and CIMT in cross-sectional analyses and with only CIMT in longitudinal analyses.

Results Using Spatiotemporal Model Predictions

Cross-Sectional Analyses Long-term average concentrations of sulfur, silicon, OC, and EC were computed for MESA participants using the predicted 2-week concentrations from the MESA Air/NPACT spatiotemporal model described above under “Exposure Predictions: Distributions, Model Fit, and Validation.” We restricted the population for analysis to participants living within 10 km of any MESA Air monitor. For comparison with the $PM_{2.5}$ component predictions, we also examined predictions for the long-term average concentration of $PM_{2.5}$ mass between 2007 and 2008 from a MESA Air spatiotemporal model (Sampson et al. 2011) and for 2000 from a national spatial model (MESA Air Data Team 2013).

CIMT and CAC were chosen as subclinical atherosclerosis outcomes. CIMT was quantified in millimeters as the thickness of the far right wall of the carotid measured during exam 1. CAC measurements were Agatston units. Nonzero Agatston scores were log-transformed to improve the distribution of this measure. Since approximately half of the Agatston values were zero, we also calculated the binary variable indicating the presence of CAC, based on Agatston score greater than zero, or the absence of CAC.

Tables 36 and 37 show summary statistics of $PM_{2.5}$ and $PM_{2.5}$ components, CAC, CIMT, and other individual characteristics for 5493 MESA participants who resided within the prediction area and had both CAC and CIMT measurements at exam 1, out of 6266 who consented to use of their address. Mean long-term concentrations of $PM_{2.5}$, sulfur, silicon, EC, and OC were 13.80, 1.32, 0.11, 1.52, and 2.16 $\mu\text{g}/\text{m}^3$, respectively. These participants had a mean age of 62 years; 52% were female; 40%, white; 26%, African American; 22%, Hispanic; and 12%, Chinese American. Forty-four percent had hypertension, 12% had diabetes, and 15% used a statin drug. The mean CIMT was 0.68 mm, and average $\log(\text{CAC})$ was 4.32 logged Agatston units for the 2684 participants with nonzero CAC values (summary statistics for CIMT and CAC by sex and race or ethnicity are presented in Table 1 of Appendix H, available on the HEI Web site).

For the cross-sectional analysis model, we used relative risk regression for presence of CAC and linear regression for log-transformed CAC and CIMT. We examined six confounder models to assess the relationship of long-term $PM_{2.5}$ mass and $PM_{2.5}$ component concentrations with CAC and CIMT (Table 38). These models are intended to show the impact of confounding variables; they progress from minimal to full adjustment (see Appendix G, available on the HEI Web site). Model 1 is the minimally

Table 36. PM_{2.5} Long-Term Concentrations, Subclinical Atherosclerosis Outcomes, and Individual Characteristics of 5493 MESA Participants at Exam 1: Continuous Variables

Variable	<i>n</i>	Minimum	Median	Maximum	Mean	SD	IQR	RBT ^a
Exposure (µg/m³)								
PM _{2.5}	5493	10.27	14.04	17.27	13.80	1.44	1.51	0.89
S	5493	0.76	1.27	2.10	1.32	0.32	0.51	1.18
Si	5493	0.06	0.10	0.31	0.11	0.02	0.02	0.80
EC	5493	0.48	1.37	3.45	1.52	0.58	0.89	0.97
OC	5493	0.58	2.13	3.81	2.16	0.41	0.69	0.61
Outcome								
Log(CAC) ^b	2684	-0.25	4.45	8.71	4.32	1.83	2.62	
CIMT (mm)	5493	0.32	0.64	2.85	0.68	0.19	0.22	
Individual Characteristics^c								
Age	5493	44.00	62.00	84.00	61.88	10.14	17.00	
Weight (lb)	5493	71.60	170.00	314.40	172.93	37.46	50.20	
Height (cm)	5493	123.80	166.20	202.50	166.59	10.00	14.50	
Waist (cm)	5492	33.50	97.00	193.50	97.78	14.10	17.73	
Body surface area	5493	1.04	1.85	2.63	1.86	0.22	0.31	
BMI (kg/m ²)	5493	15.35	27.49	54.50	28.19	5.31	6.54	
SBP (mm Hg)	5491	67.00	123.00	230.50	125.87	21.09	28.50	
DBP (mm Hg)	5491	41.00	71.50	115.50	71.81	10.23	13.50	
HDL (mg/dL)	5476	15.00	49.00	138.00	51.05	14.72	19.00	
LDL (mg/dL)	5410	12.00	116.00	315.00	117.29	31.05	40.00	
Triglycerides (mg/dL)	5478	23.00	111.00	2256.00	130.76	85.21	82.00	
Creatinine (mg/dL)	5479	0.40	0.90	4.10	0.95	0.23	0.30	
Log(CRP) (mg/L)	5458	-1.90	0.62	4.58	0.63	1.16	1.61	

^a RBT: ratio of variability of between-city exposures to total variability.

^b Measured by Agatston score units. The number of participants for log(CAC) is much smaller than the total number of participants because 51% of participants have an Agatston score of zero.

^c BMI indicates body mass index; SBP, systolic blood pressure; DBP, diastolic blood pressure; HDL, high-density lipoprotein; LDL, low-density lipoprotein; CRP, C-reactive protein.

Table 37. Subclinical Atherosclerosis Outcome and Individual Characteristics of 5493 MESA Participants at Exam 1: Discrete Variables

Variable	Value	n (%)
Outcome (presence of CAC)	No	2809 (51.1)
	Yes	2684 (48.9)
Sex	Female	2872 (52.3)
	Male	2621 (47.7)
Race	White	2179 (39.7)
	Chinese American	673 (12.3)
	African American	1452 (26.4)
	Hispanic	1189 (21.6)
Site	Winston-Salem	892 (16.2)
	New York	856 (15.6)
	Baltimore	775 (14.1)
	St. Paul	898 (16.3)
	Chicago	999 (18.2)
	Los Angeles	1073 (19.5)
Education	Incomplete high school	908 (16.5)
	Complete high school	989 (18.0)
	Some college	1568 (28.5)
	Complete college	2015 (36.7)
	Missing	13 (0.2)
Income	<\$12,000	563 (10.2)
	\$12,000–\$24,999	1016 (18.5)
	\$25,000–\$49,999	1534 (27.9)
	\$50,000–\$74,999	903 (16.4)
	>\$75,000	1279 (23.3)
	Missing	198 (3.6)
Smoking status	Never	2765 (50.3)
	Former	2021 (36.8)
	Current	695 (12.7)
	Missing	12 (0.2)
Current alcohol use	No	1340 (24.4)
	Yes	3106 (56.5)
	Missing	1047 (19.1)
Hypertension	No	3101 (56.5)
	Yes	2392 (43.5)
Diabetes	Normal	4083 (74.3)
	Impaired fasting glucose	746 (13.6)
	Untreated diabetes	139 (2.5)
	Treated diabetes	511 (9.3)
	Missing	14 (0.3)
Gum disease	No	3958 (72.1)
	Yes	1466 (26.7)
	Missing	69 (1.3)
Hypertensive medication	No	3500 (63.7)
	Yes	1990 (36.2)
	Missing	3 (0.1)
Statin use	No	4673 (85.1)
	Yes	817 (14.9)
	Missing	3 (0.1)

Table 38. Cross-Sectional and Longitudinal Analysis Models

Model	Variable	
1	Cross-sectional	Age, sex, race
	Longitudinal	Sex, race
2	Cross-sectional	Model 1 + education + income + waist circumference + body surface area
	Longitudinal	Sex, race
3 ^a	Cross-sectional	Model 2 + DBP + hypertension + statin use
	Longitudinal	Sex, race, DBP, hypertension, statin use
4	Cross-sectional	Model 3 + diabetes, HDL, LDL, triglycerides, log(CRP), creatinine, hypertensive medication, gum disease, alcohol use, smoking status
	Longitudinal	All cross-sectional variables
5	Cross-sectional	Model 3 + site (city)
	Longitudinal	Sex, race, DBP, hypertension, statin use, site (city)
6	Cross-sectional	Model 4 + site (city)
	Longitudinal	All cross-sectional variables

^a Primary model.

adjusted model and includes terms for age, sex, and race or ethnicity. Model 2 adds terms for education, income, waist circumference, and body surface area. Model 3, our primary model, adds terms for hypertension, diabetes, statin use, and diastolic blood pressure to the terms included in model 2. Variables considered as potential confounders in model 3, but not chosen, were included in model 4. In models 5 and 6, we further controlled for study site (city) using all other covariates for models 3 and 4, respectively, as a sensitivity analysis. We also performed analyses adjusted for gaseous pollutants such as NO₂ and SO₂. In addition, we examined the sensitivity of our findings to the size of the prediction area. Besides participants living within 10 km of all fixed and home-outdoor monitoring sites, we considered more restricted subsets of participants living within 5 km or 2 km of any monitor. Table 39 and Figure 29 show estimated effects of an IQR increase in the PM_{2.5} components on the presence of CAC, as well as log(CAC) and CIMT, for different degrees of confounder

Table 39. Cross-Sectional Associations for Presence of CAC, Log(CAC), and CIMT in MESA Participants at Exam 1 with an IQR Increase in Predicted PM_{2.5} and PM_{2.5} Component Concentrations from the Spatiotemporal Model in Six Cross-Sectional Models^{a,b}

Pollutant / Model	Presence of CAC RR (95% CI)	Log(CAC) exp(β) (95% CI)	CIMT β (95% CI)
PM_{2.5}			
1	0.997 (0.973 to 1.021)	0.966 (0.901 to 1.036)	0.007 (0.002 to 0.012)
2	1.007 (0.982 to 1.031)	0.964 (0.897 to 1.036)	0.008 (0.003 to 0.013)
3	1.003 (0.979 to 1.028)	0.957 (0.891 to 1.028)	0.007 (0.002 to 0.012)
4	1.003 (0.977 to 1.029)	0.928 (0.857 to 1.004)	0.006 (0.000 to 0.012)
5	1.040 (0.991 to 1.093)	0.992 (0.860 to 1.144)	0.000 (-0.010 to 0.010)
6	1.032 (0.976 to 1.092)	0.935 (0.793 to 1.102)	-0.003 (-0.014 to 0.009)
S			
1	0.988 (0.951 to 1.027)	1.044 (0.932 to 1.170)	0.022 (0.014 to 0.031)
2	0.991 (0.953 to 1.031)	1.054 (0.938 to 1.184)	0.023 (0.014 to 0.031)
3	0.980 (0.943 to 1.019)	1.027 (0.914 to 1.153)	0.021 (0.012 to 0.029)
4	0.992 (0.951 to 1.034)	1.013 (0.892 to 1.150)	0.023 (0.014 to 0.032)
5	1.057 (0.900 to 1.240)	0.844 (0.523 to 1.360)	0.029 (-0.005 to 0.062)
6	1.020 (0.860 to 1.210)	0.927 (0.545 to 1.575)	0.038 (0.002 to 0.074)
Si			
1	1.011 (0.984 to 1.038)	0.941 (0.869 to 1.020)	0.006 (0.000 to 0.011)
2	1.014 (0.987 to 1.042)	0.930 (0.857 to 1.009)	0.005 (-0.001 to 0.011)
3	1.018 (0.991 to 1.045)	0.932 (0.859 to 1.011)	0.005 (0.000 to 0.011)
4	1.008 (0.977 to 1.041)	0.947 (0.860 to 1.043)	0.003 (-0.004 to 0.010)
5	1.045 (1.007 to 1.084)	1.002 (0.886 to 1.132)	-0.001 (-0.010 to 0.008)
6	1.030 (0.984 to 1.079)	1.065 (0.914 to 1.242)	-0.006 (-0.017 to 0.006)
EC			
1	0.981 (0.944 to 1.019)	0.886 (0.795 to 0.989)	0.002 (-0.006 to 0.009)
2	0.989 (0.951 to 1.028)	0.894 (0.800 to 0.999)	0.003 (-0.004 to 0.011)
3	0.984 (0.947 to 1.023)	0.884 (0.791 to 0.988)	0.003 (-0.005 to 0.011)
4	0.979 (0.938 to 1.021)	0.874 (0.772 to 0.989)	0.002 (-0.006 to 0.010)
5	1.088 (1.006 to 1.176)	0.739 (0.592 to 0.923)	-0.004 (-0.019 to 0.012)
6	1.051 (0.963 to 1.147)	0.677 (0.527 to 0.871)	-0.007 (-0.024 to 0.010)
OC			
1	1.015 (0.978 to 1.054)	1.008 (0.906 to 1.122)	0.027 (0.019 to 0.035)
2	1.023 (0.985 to 1.062)	0.993 (0.891 to 1.106)	0.026 (0.018 to 0.034)
3	1.019 (0.982 to 1.058)	0.977 (0.877 to 1.089)	0.025 (0.017 to 0.033)
4	1.023 (0.981 to 1.066)	0.952 (0.841 to 1.078)	0.024 (0.015 to 0.033)
5	1.066 (1.011 to 1.124)	1.003 (0.862 to 1.167)	0.004 (-0.007 to 0.015)
6	1.053 (0.992 to 1.118)	0.969 (0.813 to 1.155)	0.001 (-0.011 to 0.013)

^a See Table 38 for description of the six models.

^b Effect estimates (RR and β coefficients) and 95% CIs are presented per IQR increase: 1.51, 0.51, 0.02, 0.89, and 0.69 $\mu\text{g}/\text{m}^3$ for PM_{2.5}, S, Si, EC, and OC, respectively.

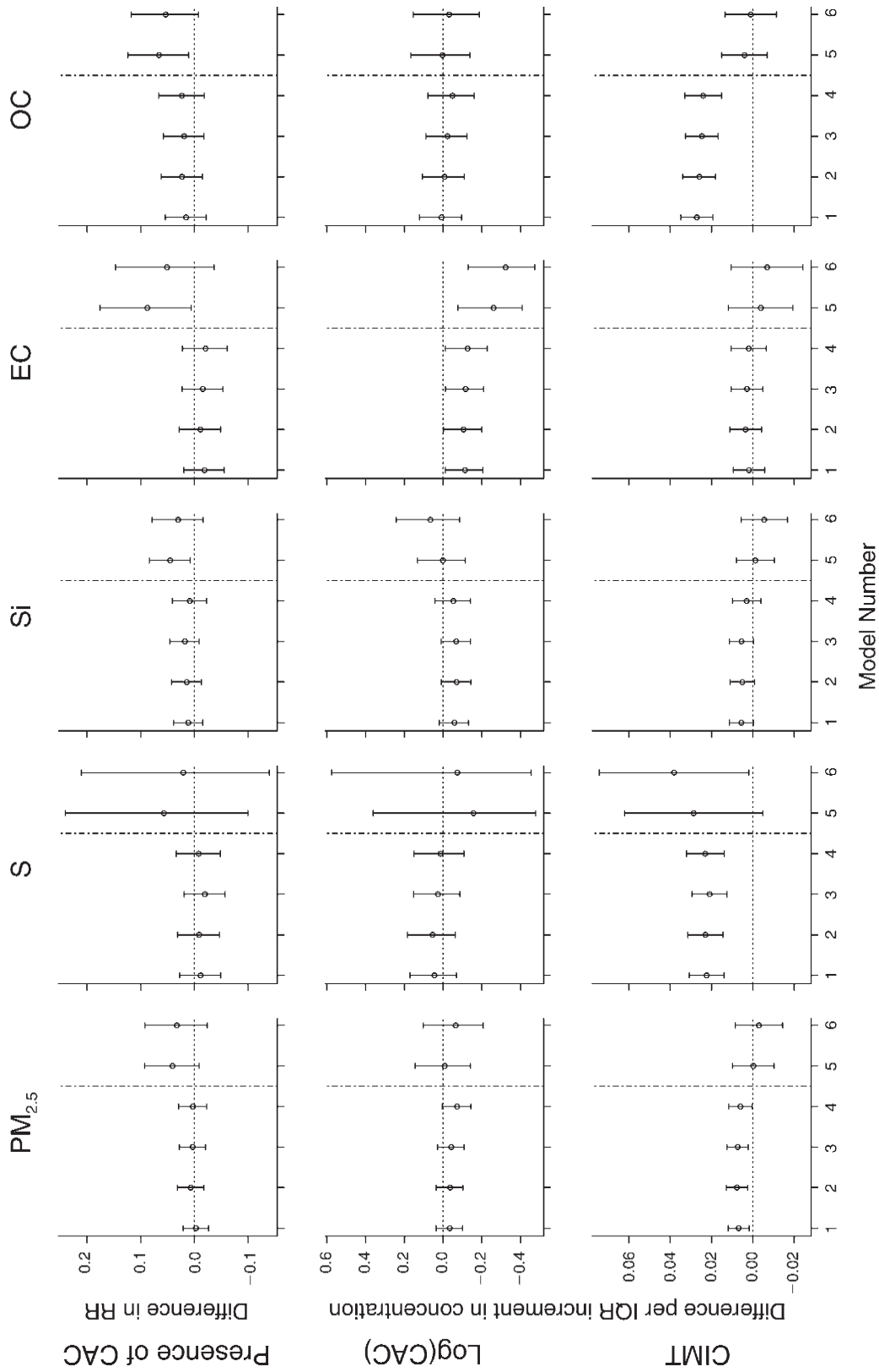


Figure 29. Cross-sectional associations between presence of CAC, log(CAC), and CIMT in MESA participants at exam 1 and IQR increments in predicted PM_{2.5} and PM_{2.5} component concentrations from the spatiotemporal model in six cross-sectional models with 95% CIs. IQR increments were 1.51, 0.51, 0.02, 0.89, and 0.69 µg/m³ for PM_{2.5}, sulfur, silicon, EC, and OC, respectively. The dotted vertical line separates models 1 through 4 that did not control for city from models 5 and 6 that controlled for city (see Table 38 for descriptions of the six models).

adjustment. In our primary model (model 3), IQR increases of 1.51, 0.51, and 0.69 $\mu\text{g}/\text{m}^3$ in $\text{PM}_{2.5}$, sulfur, and OC, respectively, were associated with increases in CIMT of 0.007 (95% CI, 0.002 to 0.012) mm, 0.021 (0.012 to 0.029) mm, and 0.025 (0.017 to 0.033) mm, respectively, while an IQR increase of 0.02 $\mu\text{g}/\text{m}^3$ in silicon was associated with a borderline increase of 0.005 (95% CI, 0.000 to 0.011) mm. There were no associations between the CAC measures and $\text{PM}_{2.5}$ or the four $\text{PM}_{2.5}$ components in our primary model, apart from a negative association between EC and $\log(\text{CAC})$ in those participants with measurable CAC.

Longitudinal Analyses We used health data for MESA participants at exams 1, 2, and 3 from 2000 through 2005 for longitudinal analysis. Estimated long-term $\text{PM}_{2.5}$ component concentrations of study participants were the same as the annual averages used in the cross-sectional analyses, except for participants who moved during the study period. For participants who moved, we calculated the weighted annual averages across home addresses. The CIMT measurement used was the thickness of the far wall of the right carotid artery, which was the only CIMT measure read in a consistent manner across the three exams. A MESA ancillary study used a consistency protocol for the baseline exam and follow-up exams 2 and 3 (Polak et al. 2011), allowing use of standardized measurements in the longitudinal analysis. A follow-up exam was carried out once at either exam 2 or exam 3, so only two CIMT measurements were available for each participant in the longitudinal analysis. No longitudinal analysis of CAC measurements was performed.

The statistical model for our longitudinal analysis of CIMT is described above under “Models for Effects on CIMT and CAC” and in Appendix G (available on the HEI Web site). We assessed longitudinal relationships between long-term $\text{PM}_{2.5}$ and $\text{PM}_{2.5}$ component concentrations and progression of CIMT using the six models outlined in Table 38, with model 3 as the primary model. Both cross-sectional and longitudinal effects were estimated in the same models. The selected adjustment variables for the cross-sectional effect terms in the longitudinal analysis were the same as those used in our cross-sectional analysis. Adjustment variables for the longitudinal part of the model were chosen by the selection process described in Appendix G.

For the 5224 study participants who resided within the prediction area, visited a study clinic at exam 1 as well as exam 2 or 3, and had CIMT measurement at exam 1, 2, or 3, mean baseline CIMT was 0.68 mm and the mean progression rate for CIMT was 0.016 mm per year over a mean follow-up period of 2.5 years. Individual characteristics at

follow-up exams were not much different than those at the baseline exam (Table 40). In the longitudinal analysis, we found that higher concentrations of at least three $\text{PM}_{2.5}$ components were cross-sectionally associated with greater CIMT (Table 41, Figure 30) in the primary model (model 3). Cross-sectional associations in the longitudinal analyses were consistent with those estimated in the cross-sectional analyses, except there was no longer evidence of an association for silicon. None of the four components showed evidence of longitudinal effects.

Results Using National Spatial Model Predictions

Table 42 and Figure 31 show analysis results from a cross-sectional model for associations of $\text{PM}_{2.5}$ and the four $\text{PM}_{2.5}$ components with the presence of CAC, $\log(\text{CAC})$, and CIMT. Similar to the results of the analysis using the MESA Air/NPACT spatiotemporal model predictions, $\text{PM}_{2.5}$, sulfur, silicon, and OC were associated with CIMT in the analysis using the national spatial model predictions. IQR increases of 2.19, 0.18, 0.02, and 0.39 $\mu\text{g}/\text{m}^3$ in $\text{PM}_{2.5}$, sulfur, silicon, and OC, respectively, were associated with increases in CIMT of 0.007 (95% CI, 0.003 to 0.011) mm, 0.010 (0.004 to 0.016) mm, 0.008 (0.005 to 0.012) mm, and 0.009 (0.004 to 0.015) mm in model 3. In addition, using national spatial model predictions, a 0.39 $\mu\text{g}/\text{m}^3$ increase in OC was associated with a 3.3% increase in relative risk of CAC (95% CI, 0.4% to 6.2%). Findings for silicon and CIMT in our primary model were particularly sensitive to adjustment for city, as noted when compared with findings from models 5 and 6. In the longitudinal analysis, we found cross-sectional relationships similar to those estimated in the cross-sectional analysis (Table 43 and Figure 32). No component predictions from the national spatial model were associated with progression of CIMT in the primary model (Table 43 and Figure 32).

Cross-validation statistics were calculated and health effects were estimated for SO_4 , NO_3 , SO_2 , and NO_2 (presented in Appendix H, available on the HEI Web site) and for nickel, vanadium, and copper (presented in Appendix N, available on the HEI Web site). Effect estimates for SO_4 and SO_2 mirrored those for sulfur. There was little evidence for associations with NO_2 , NO_3 , nickel, or vanadium. There was good evidence for associations of copper with CIMT, however, and suggestive evidence for associations with presence of CAC.

Measurement Error Corrections

The difference between true exposures and the values predicted by our national spatial or spatiotemporal exposure models results in measurement error that may

Table 40. Summary Statistics of CIMT and Individual Characteristics of 5224 MESA Participants at Exams 1, 2, and 3 for Longitudinal Analysis^a

	Exam 1					Exam 2				
	<i>n</i>	Minimum	Median	Maximum	Mean ± SD	<i>n</i>	Minimum	Median	Maximum	Mean ± SD
Time (yrs) ^b	5202	0.0	0.0	0.0	0.0 ± 0.0	2617	0.5	1.7	3.3	1.8 ± 0.5
CIMT (mm)	5202	0.32	0.64	2.85	0.68 ± 0.19	2617	0.32	0.72	2.80	0.75 ± 0.21
CIMT increase ^c						1523	0.01	0.07	1.14	0.09 ± 0.09
CIMT decrease ^d						963	-0.49	-0.06	-0.01	-0.08 ± 0.07
Weight (lb)	5202	71.6	170.5	314.4	173.1 ± 37.6	2616	72.2	169.0	310.0	172.3 ± 37.4
Height (cm)	5202	123.8	166.3	202.5	166.7 ± 10.0	2616	123.5	165.7	198.0	166.1 ± 9.7
Waist (cm)	5201	33.5	97.0	193.5	97.7 ± 14.1	2616	62.0	96.5	166.3	97.6 ± 14.2
Body surface area	5202	1.0	1.9	2.6	1.9 ± 0.2	2616	1.0	1.9	2.6	1.9 ± 0.2
BMI (kg/m ²)	5202	15.4	27.5	54.5	28.2 ± 5.3	2616	15.2	27.5	55.9	28.2 ± 5.5
SBP (mm Hg)	5200	67.0	123.0	230.5	125.8 ± 21.0	2615	60.0	120.0	214.0	123.4 ± 21.0
DBP (mm Hg)	5200	41.0	71.5	115.5	71.8 ± 10.2	2615	38.0	70.0	114.0	70.1 ± 10.1
HDL (mg/dL)	5185	15.0	49.0	138.0	51.1 ± 14.7	2602	23.0	50.0	161.0	52.0 ± 15.2
LDL (mg/dL)	5122	12.0	116.0	284.0	117.3 ± 30.9	2581	28.0	112.0	377.0	113.7 ± 32.2
Triglycerides (mg/dL)	5187	23.0	111.0	2256.0	130.2 ± 85.3	2604	26.0	113.0	1090.0	131.1 ± 77.4

	Exam 3				
	<i>n</i>	Minimum	Median	Maximum	Mean ± SD
Time (yrs) ^b	2584	1.9	3.1	5.0	3.2 ± 0.3
CIMT (mm)	2584	0.36	0.63	2.32	0.66 ± 0.16
CIMT increase ^c	2230	0.01	0.04	0.47	0.05 ± 0.05
CIMT decrease ^d	223	-0.60	-0.02	-0.01	-0.04 ± 0.07
Weight (lb)	2583	85.2	169.0	332.0	172.5 ± 38.5
Height (cm)	2583	137.0	166.0	196.0	166.2 ± 10.2
Waist (cm)	2582	60.0	97.0	164.8	98.1 ± 14.4
Body surface area	2583	1.2	1.8	2.6	1.9 ± 0.2
BMI (kg/m ²)	2583	15.8	27.5	53.8	28.2 ± 5.4
SBP (mm Hg)	2583	64.5	121.0	202.0	123.7 ± 20.5
DBP (mm Hg)	2583	37.0	69.5	115.0	69.9 ± 10.0
HDL (mg/dL)	2560	17.0	50.0	145.0	51.7 ± 14.8
LDL (mg/dL)	2524	8.0	111.0	323.0	112.3 ± 32.1
Triglycerides (mg/dL)	2561	26.0	107.0	2265.0	128.5 ± 91.6

^a BMI indicates body mass index; DBP, diastolic blood pressure; HDL, high-density lipoprotein; LDL, low-density lipoprotein; SBP, systolic blood pressure.

^b Time to follow-up visit since baseline visit.

^c Participants who had CIMT at exam 2 or 3 greater than CIMT at exam 1.

^d Participants who had CIMT at exam 2 or 3 smaller than CIMT at exam 1.

Table 41. Cross-Sectional and Longitudinal Associations for CIMT in MESA Participants with an IQR Increase in Predicted PM_{2.5} and PM_{2.5} Component Concentrations from the Spatiotemporal Model in Six Longitudinal Models^{a,b}

Pollutant/Model	Cross-Sectional β (95% CI)	Longitudinal β (95% CI)
PM_{2.5}		
1	0.006 (0.001 to 0.011)	0.000 (−0.001 to 0.001)
2	0.007 (0.002 to 0.013)	0.000 (−0.001 to 0.001)
3	0.007 (0.002 to 0.012)	0.000 (−0.001 to 0.001)
4	0.006 (0.000 to 0.012)	0.000 (−0.001 to 0.001)
5	0.003 (−0.007 to 0.013)	0.001 (−0.001 to 0.003)
6	0.000 (−0.011 to 0.012)	0.000 (−0.002 to 0.003)
S		
1	0.024 (0.015 to 0.033)	−0.002 (−0.004 to 0.000)
2	0.025 (0.016 to 0.033)	−0.002 (−0.003 to 0.000)
3	0.023 (0.014 to 0.031)	−0.002 (−0.003 to 0.000)
4	0.024 (0.015 to 0.034)	−0.002 (−0.004 to 0.000)
5	0.036 (0.001 to 0.071)	0.003 (−0.004 to 0.010)
6	0.046 (0.007 to 0.084)	0.001 (−0.007 to 0.009)
Si		
1	0.004 (−0.002 to 0.010)	0.000 (−0.001 to 0.001)
2	0.004 (−0.002 to 0.010)	0.000 (−0.001 to 0.001)
3	0.004 (−0.002 to 0.010)	0.000 (−0.001 to 0.001)
4	0.003 (−0.004 to 0.010)	0.000 (−0.001 to 0.001)
5	0.001 (−0.009 to 0.010)	0.001 (−0.001 to 0.003)
6	−0.002 (−0.014 to 0.010)	0.000 (−0.002 to 0.002)
EC		
1	0.002 (−0.005 to 0.010)	−0.001 (−0.003 to 0.001)
2	0.005 (−0.003 to 0.013)	−0.001 (−0.003 to 0.001)
3	0.004 (−0.003 to 0.012)	−0.001 (−0.003 to 0.001)
4	0.003 (−0.005 to 0.012)	0.000 (−0.002 to 0.002)
5	0.006 (−0.010 to 0.023)	0.004 (0.001 to 0.007)
6	0.001 (−0.017 to 0.020)	0.005 (0.002 to 0.009)
OC		
1	0.028 (0.020 to 0.036)	−0.001 (−0.002 to 0.001)
2	0.027 (0.019 to 0.035)	−0.001 (−0.002 to 0.001)
3	0.026 (0.018 to 0.034)	−0.001 (−0.002 to 0.001)
4	0.026 (0.016 to 0.035)	0.000 (−0.002 to 0.002)
5	0.008 (−0.004 to 0.019)	0.002 (−0.001 to 0.004)
6	0.004 (−0.009 to 0.017)	0.003 (0.000 to 0.006)

^a See Table 38 for description of the six models.

^b Effect estimates (β coefficients) and 95% CIs are presented per IQR increase: 1.51, 0.51, 0.02, 0.89, and 0.69 $\mu\text{g}/\text{m}^3$ for PM_{2.5}, S, Si, EC, and OC, respectively.

introduce bias or additional variability into our estimates of health effects. The measurement error is of a complex form, including Berkson-like error from smoothing the exposure surface by land-use regression and spatial modeling and classical-like error from uncertainty in estimating the parameters. In selected analyses we applied recently developed bootstrap methods to assess the impact of measurement error and derive corrected point estimates and CIs, as appropriate (Szpiro et al. 2011).

With predictions from the national spatial model in the cross-sectional analysis of CIMT for the MESA participants, measurement error correction did not change the point estimates or CIs for the associations with EC or OC. However, the standard errors for the associations with silicon and sulfur (and thus the 95% CIs) were markedly larger after accounting for measurement error. Without accounting for measurement error, sulfur was associated with an increase in CIMT of 0.010 (95% CI, 0.004 to 0.016) mm, whereas with adjustment for measurement error, it was associated with an increase of 0.010 (95% CI, 0.001 to 0.019) mm. Similarly, without accounting for measurement error, we found that silicon was associated with an increase in CIMT of 0.009 (95% CI, 0.005 to 0.012) mm, whereas with adjustment for measurement error, it was associated with an increase of 0.009 (95% CI, 0.003 to 0.014) mm. When spatiotemporal predictions were used with the same cross-sectional analysis of CIMT for the measurement error correction, effect estimates and standard errors were similar for all four components.

Sensitivity Analyses

In addition to our primary model, we performed several sensitivity analyses. In separate analyses, we adjusted for study city (models 5 and 6), for an extended set of covariates (models 4 and 6), for gaseous pollutants NO₂ and SO₂ (model 7 and model 8, respectively), and for other PM_{2.5} components in two-pollutant models; excluded statin users; used more-restricted prediction areas (5 km and 2 km); and estimated within-city and between-city effects. Associations of PM_{2.5} component concentrations with CIMT and CAC in the cross-sectional analysis, and with progression of CIMT in the longitudinal analysis, were consistent for different prediction areas (for CIMT, see Figure 4 in Appendix H, available on the HEI Web site; CAC and progression of CIMT results are not shown). Findings were unchanged when analysis was restricted to participants who did not use statins (results not shown). The effects of adjustments for other predictors, for NO₂ and SO₂, and for other PM_{2.5} components are described in the following sections.

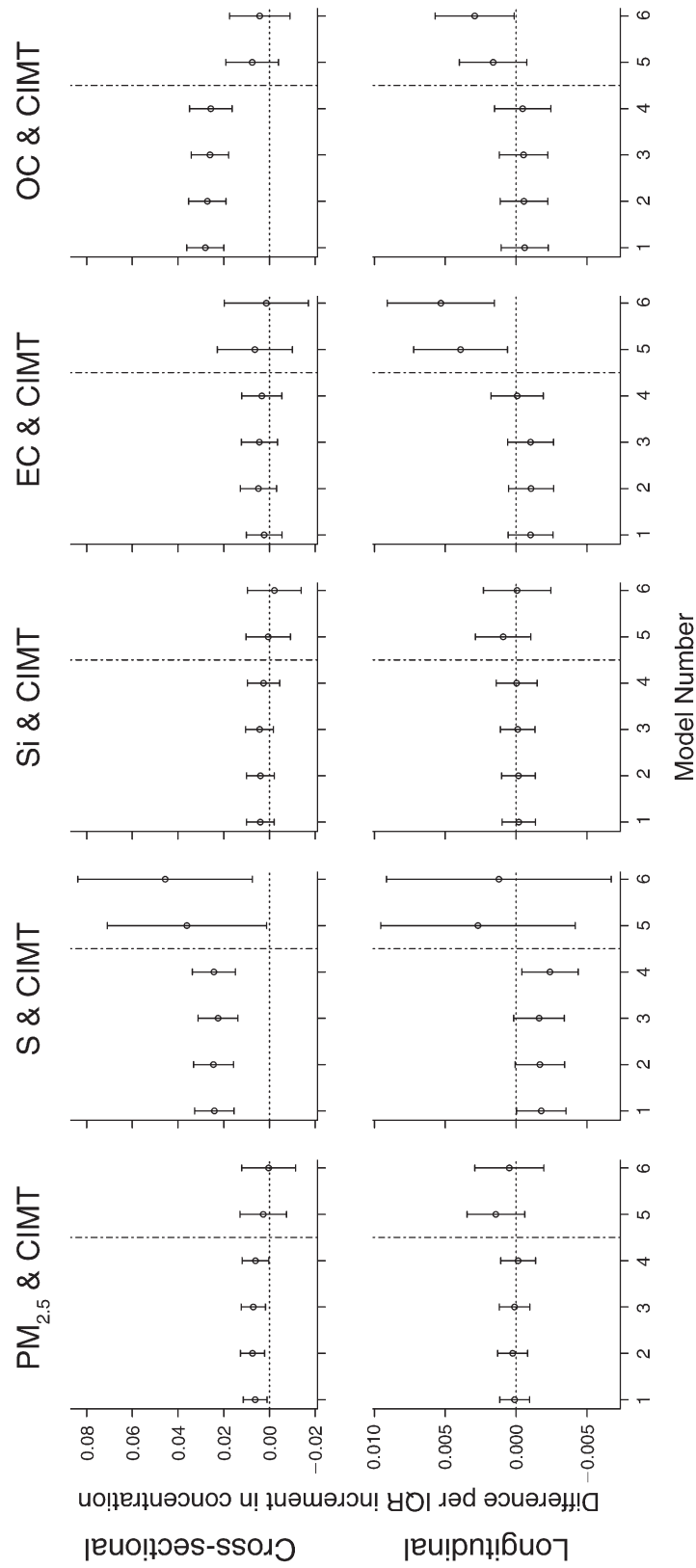


Figure 30. Cross-sectional and longitudinal associations between CIMT in MESA participants and IQR increments in predicted PM_{2.5} and PM_{2.5} component concentrations from the spatiotemporal model in six longitudinal models with 95% CIs. IQR increments were 1.51, 0.51, 0.02, 0.89, and 0.69 µg/m³ for PM_{2.5}, sulfur, silicon, EC, and OC, respectively. The dotted vertical line separates models 1 through 4 that did not control for city from models 5 and 6 that controlled for city (see Table 38 for descriptions of the six models).

Table 42. Cross-Sectional Effects on Presence of CAC, Log(CAC), and CIMT in MESA Participants at Exam 1 with an IQR Increase in Predicted PM_{2.5} Component Concentrations from the National Spatial Model in Six Cross-Sectional Models^{a,b}

Pollutant / Model	Presence of CAC RR (95% CI)	Log(CAC) exp(β) (95% CI)	CIMT β (95% CI)
PM_{2.5}			
1	1.004 (0.985 to 1.024)	0.965 (0.914 to 1.019)	0.007 (0.003 to 0.011)
2	1.011 (0.991 to 1.030)	0.959 (0.907 to 1.014)	0.007 (0.003 to 0.011)
3	1.009 (0.990 to 1.028)	0.956 (0.904 to 1.010)	0.007 (0.003 to 0.011)
4	1.008 (0.986 to 1.030)	0.931 (0.872 to 0.993)	0.006 (0.002 to 0.011)
5	1.025 (0.976 to 1.076)	0.965 (0.840 to 1.110)	0.002 (-0.008 to 0.011)
6	1.015 (0.960 to 1.072)	0.882 (0.752 to 1.034)	0.002 (-0.009 to 0.013)
S			
1	1.004 (0.977 to 1.032)	1.056 (0.974 to 1.146)	0.010 (0.004 to 0.017)
2	1.005 (0.977 to 1.034)	1.076 (0.990 to 1.169)	0.011 (0.005 to 0.017)
3	0.997 (0.969 to 1.025)	1.055 (0.972 to 1.146)	0.010 (0.004 to 0.016)
4	1.002 (0.973 to 1.032)	1.046 (0.957 to 1.144)	0.010 (0.004 to 0.017)
5	1.303 (1.060 to 1.603)	0.802 (0.442 to 1.457)	0.044 (0.003 to 0.086)
6	1.266 (1.009 to 1.589)	0.810 (0.415 to 1.581)	0.046 (0.000 to 0.092)
Si			
1	1.009 (0.991 to 1.026)	0.971 (0.924 to 1.021)	0.009 (0.005 to 0.012)
2	1.010 (0.992 to 1.028)	0.960 (0.913 to 1.010)	0.008 (0.004 to 0.011)
3	1.010 (0.992 to 1.027)	0.962 (0.915 to 1.011)	0.008 (0.005 to 0.012)
4	1.011 (0.991 to 1.032)	0.958 (0.902 to 1.017)	0.007 (0.003 to 0.012)
5	0.961 (0.873 to 1.059)	1.007 (0.761 to 1.333)	-0.014 (-0.033 to 0.006)
6	0.973 (0.875 to 1.082)	1.019 (0.744 to 1.394)	-0.018 (-0.040 to 0.003)
EC			
1	1.006 (0.969 to 1.043)	0.955 (0.858 to 1.062)	0.001 (-0.007 to 0.008)
2	1.007 (0.969 to 1.046)	0.961 (0.860 to 1.074)	0.000 (-0.008 to 0.008)
3	1.002 (0.965 to 1.041)	0.953 (0.854 to 1.065)	0.000 (-0.008 to 0.008)
4	0.995 (0.954 to 1.037)	0.973 (0.860 to 1.101)	0.000 (-0.009 to 0.009)
5	1.060 (1.004 to 1.120)	0.921 (0.784 to 1.082)	0.004 (-0.008 to 0.016)
6	1.045 (0.983 to 1.111)	0.915 (0.761 to 1.100)	0.006 (-0.007 to 0.019)
OC			
1	1.032 (1.005 to 1.060)	0.982 (0.909 to 1.062)	0.010 (0.005 to 0.016)
2	1.036 (1.007 to 1.065)	0.974 (0.899 to 1.056)	0.009 (0.003 to 0.015)
3	1.033 (1.004 to 1.062)	0.974 (0.898 to 1.055)	0.009 (0.004 to 0.015)
4	1.032 (1.000 to 1.065)	0.979 (0.893 to 1.073)	0.008 (0.001 to 0.014)
5	1.044 (1.002 to 1.087)	0.987 (0.876 to 1.113)	0.006 (-0.002 to 0.015)
6	1.041 (0.995 to 1.089)	0.975 (0.853 to 1.115)	0.007 (-0.002 to 0.016)

^a See Table 38 for description of the six models.

^b Effect estimates (RR and β coefficients) and 95% CIs are presented per IQR increase: 2.19, 0.18, 0.02, 0.28, and 0.39 $\mu\text{g}/\text{m}^3$ for PM_{2.5}, S, Si, EC, and OC, respectively.

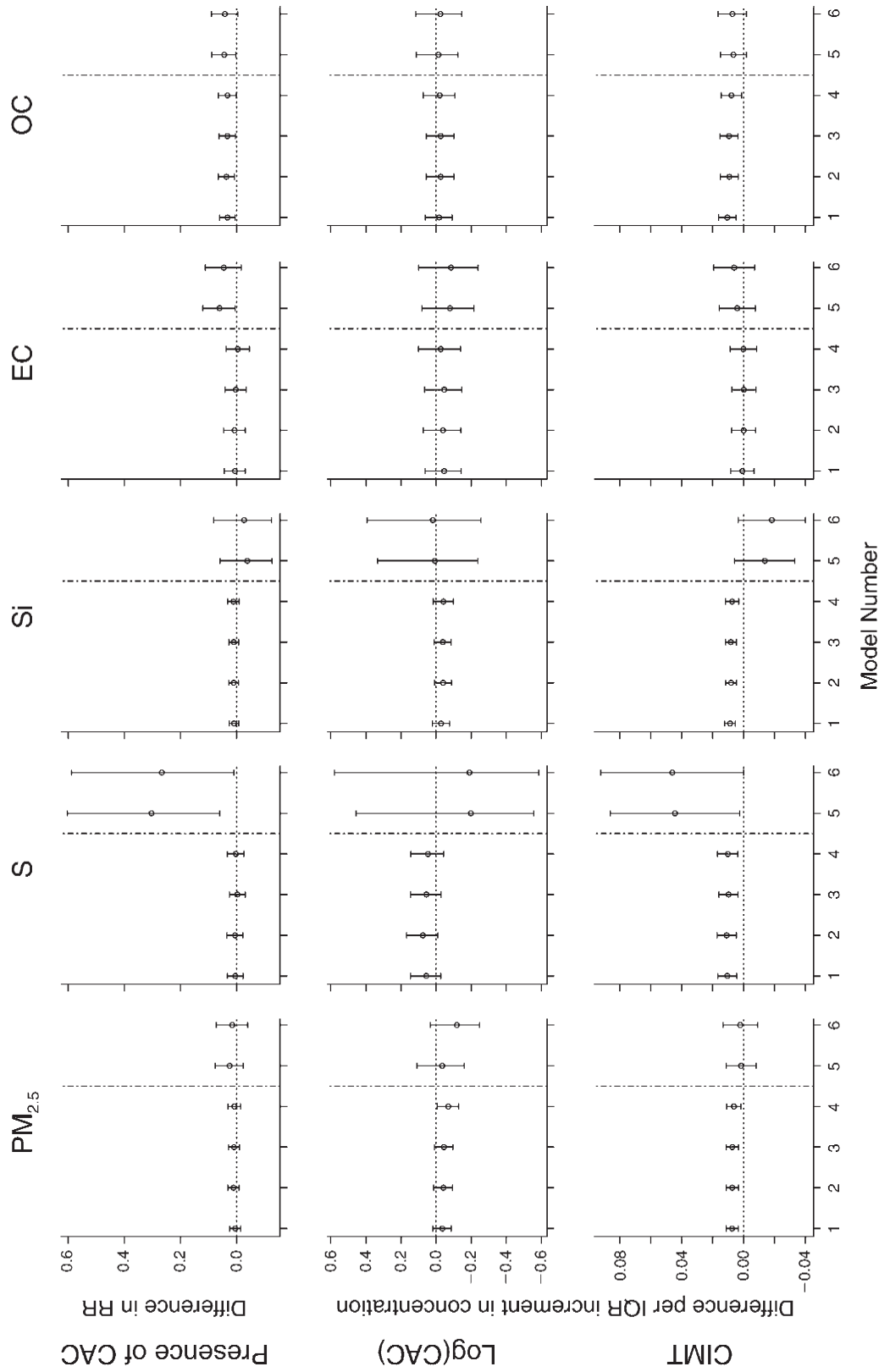


Figure 31. Cross-sectional associations between presence of CAC, log(CAC), and CIMT in MESA participants at exam 1 and IQR increments in predicted PM_{2.5} and PM_{2.5} component concentrations from the national spatial model in six cross-sectional models with 95% CIs. IQR increments were 2.19, 0.18, 0.02, 0.28, and 0.39 µg/m³ for PM_{2.5}, sulfur, silicon, EC, and OC, respectively. The dotted vertical line separates models 1 through 4 that did not control for city from models 5 and 6 that controlled for city (see Table 38 for descriptions of the six models).

Table 43. Cross-Sectional and Longitudinal Effects on CIMT in MESA Participants with an IQR Increase in Predicted PM_{2.5} Component Concentrations from the National Spatial Model in Six Longitudinal Models^{a,b}

Pollutant/Model	Cross-Sectional β (95% CI)	Longitudinal β (95% CI)
PM_{2.5}		
1	0.007 (0.003 to 0.011)	0.000 (−0.001 to 0.001)
2	0.007 (0.003 to 0.011)	0.000 (−0.001 to 0.001)
3	0.007 (0.003 to 0.011)	0.000 (−0.001 to 0.001)
4	0.006 (0.001 to 0.011)	0.000 (−0.001 to 0.001)
5	0.007 (−0.004 to 0.017)	0.001 (−0.001 to 0.003)
6	0.005 (−0.007 to 0.017)	0.001 (−0.001 to 0.004)
S		
1	0.012 (0.005 to 0.018)	−0.001 (−0.002 to 0.000)
2	0.012 (0.006 to 0.018)	−0.001 (−0.002 to 0.000)
3	0.011 (0.004 to 0.017)	−0.001 (−0.002 to 0.000)
4	0.011 (0.004 to 0.018)	−0.001 (−0.003 to 0.000)
5	0.045 (0.002 to 0.089)	0.000 (−0.008 to 0.008)
6	0.044 (−0.004 to 0.093)	−0.001 (−0.010 to 0.009)
Si		
1	0.007 (0.004 to 0.011)	0.000 (−0.001 to 0.001)
2	0.007 (0.003 to 0.010)	0.000 (−0.001 to 0.001)
3	0.007 (0.003 to 0.011)	0.000 (−0.001 to 0.001)
4	0.006 (0.002 to 0.011)	0.000 (−0.001 to 0.001)
5	−0.010 (−0.030 to 0.011)	0.002 (−0.002 to 0.006)
6	−0.016 (−0.039 to 0.007)	0.003 (−0.002 to 0.007)
EC		
1	0.000 (−0.008 to 0.008)	−0.001 (−0.003 to 0.000)
2	0.000 (−0.008 to 0.008)	−0.001 (−0.003 to 0.000)
3	0.000 (−0.008 to 0.008)	−0.001 (−0.003 to 0.000)
4	0.000 (−0.009 to 0.009)	−0.001 (−0.003 to 0.001)
5	0.007 (−0.006 to 0.019)	0.001 (−0.001 to 0.003)
6	0.007 (−0.007 to 0.021)	0.000 (−0.003 to 0.003)
OC		
1	0.009 (0.003 to 0.015)	0.000 (−0.001 to 0.001)
2	0.008 (0.002 to 0.014)	0.000 (−0.001 to 0.001)
3	0.008 (0.002 to 0.014)	0.000 (−0.001 to 0.001)
4	0.007 (0.000 to 0.014)	0.001 (−0.001 to 0.002)
5	0.008 (−0.001 to 0.017)	0.001 (−0.001 to 0.002)
6	0.007 (−0.002 to 0.017)	0.001 (−0.001 to 0.003)

^a See Table 38 for description of the six models.

^b Effect estimates (β coefficients) and 95% CIs are presented per IQR increase: 2.19, 0.18, 0.02, 0.28, and 0.39 $\mu\text{g}/\text{m}^3$ for PM_{2.5}, S, Si, EC, and OC, respectively.

Other Covariate Models In the cross-sectional analysis, the associations of CIMT with sulfur and with OC in our primary model using MESA Air/NPACT predictions persisted when we adjusted for the extended set of covariates in model 4, but the association with silicon did not (Table 39 and Figure 29). Some findings were sensitive to adjustment for city in models 5 and 6. The cross-sectional relationships in our longitudinal analysis were also generally similar to those in model 3 when the extended set of covariates was included in model 4. Adjusting for city altered the finding that there was no longitudinal effect of EC in the primary model. When the national spatial model predictions were used, the cross-sectional associations were largely unchanged with adjustment for the extended set of covariates. However, findings were again sensitive to adjustment for city.

Accounting for Gaseous Copollutants and Other PM_{2.5} Components In models 7 and 8, we examined the results of adding a term for NO₂ and SO₂, respectively, to the primary model 3 for estimating effects of PM_{2.5} components (Figures 11 to 14 in Appendix H, available on the HEI Web site). Compared with the results of the primary model, the relationship between silicon and CIMT was not sensitive to control for NO₂ and SO₂ in the cross-sectional analysis with models 7 and 8 (1% increase; 95% CI, 0.5% to 1.6%). Similarly, in the longitudinal analysis, the cross-sectional effects of the four PM_{2.5} components were not sensitive to control for NO₂ and SO₂, nor was the borderline longitudinal effect of silicon.

We used a two-pollutant model to assess the sensitivity of PM_{2.5} component effects on CIMT to the addition of another PM_{2.5} component term in the primary longitudinal model (model 3). In this longitudinal model sulfur and OC were cross-sectionally associated with CIMT when analyzed as single components. When exposure predictions from the spatiotemporal model (Figure 33) were used, the estimated cross-sectional effect of sulfur on CIMT was not sensitive to inclusion of silicon or EC, but was attenuated by the addition of OC to the analysis. The estimated cross-sectional effect of OC on CIMT was also attenuated by the addition of sulfur to the analysis. When exposure predictions from the national spatial model (Figure 34) were used, the effects of sulfur and silicon were not sensitive to inclusion of terms for any one of the other PM_{2.5} components. The cross-sectional effect of OC was sensitive only to the inclusion of a silicon term. In general, using the spatiotemporal model predictions, the cross-sectional effects of OC and sulfur in the longitudinal model were most robust to addition of terms for the other PM_{2.5} components, while using the national spatial model predictions, the sulfur and silicon effects were most robust.

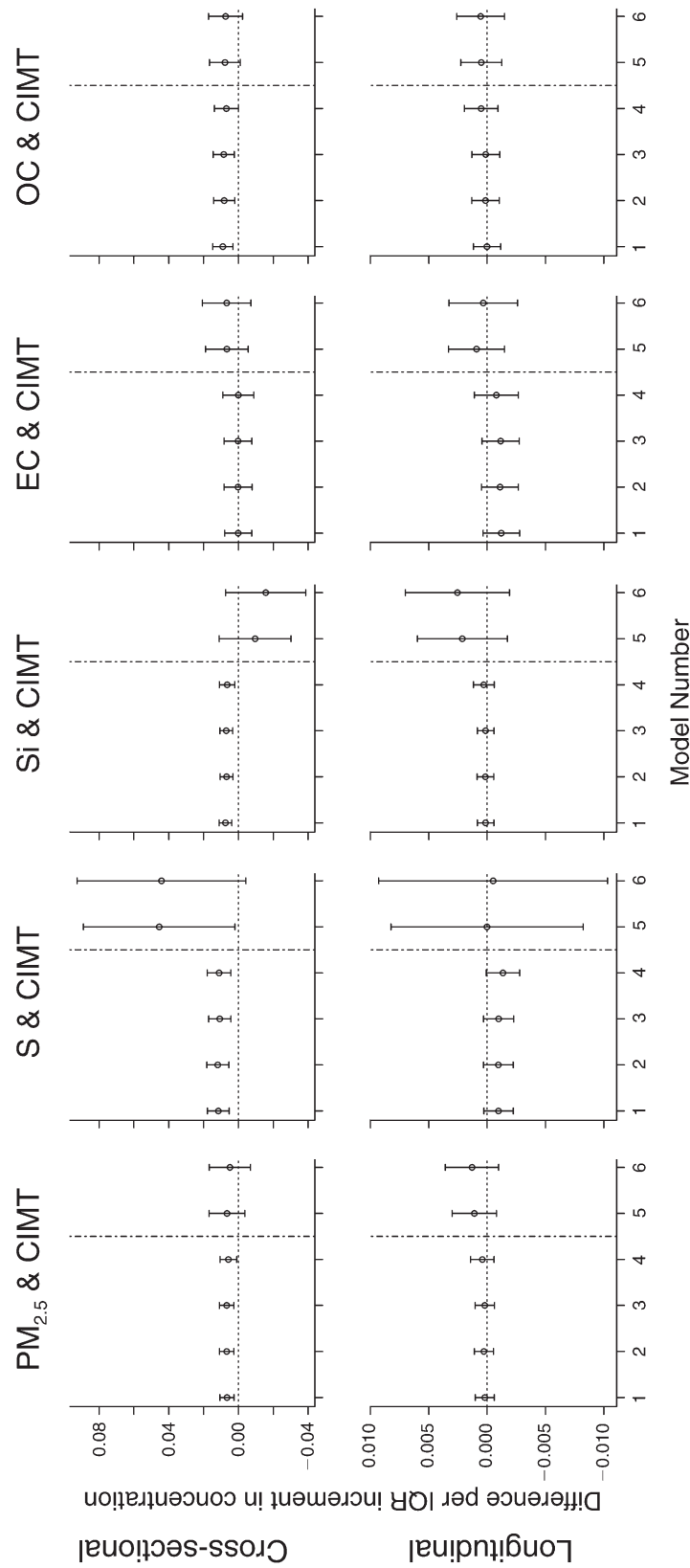


Figure 32. Cross-sectional and longitudinal associations between CIMT in MESA participants and IQR increments in predicted $PM_{2.5}$ and $PM_{2.5}$ component concentrations from the national spatial model in six longitudinal models with 95% CIs. IQR increments were 2.19, 0.18, 0.02, 0.28, and 0.39 $\mu g/m^3$ for $PM_{2.5}$, sulfur, silicon, EC, and OC, respectively. The dotted vertical line separates models 1 through 4 that did not control for city from models 5 and 6 that controlled for city (see Table 38 for descriptions of the six models).

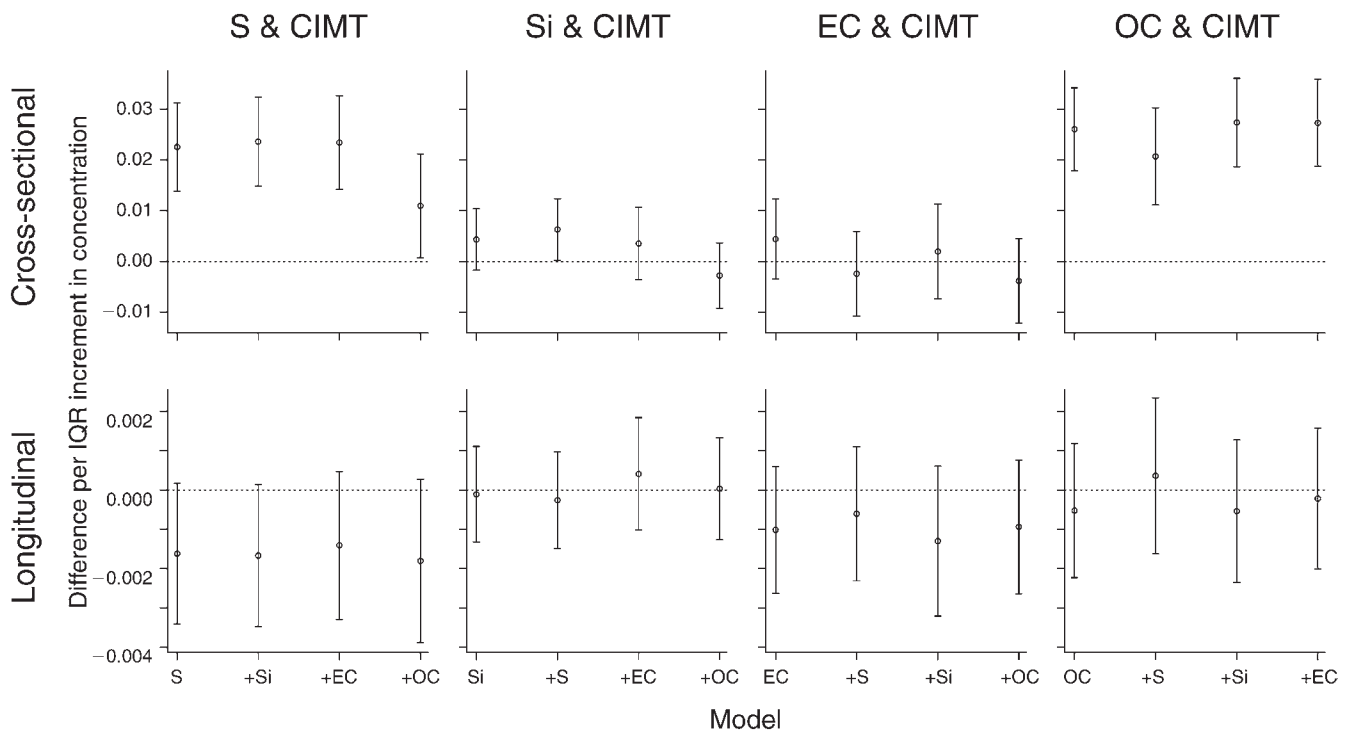


Figure 33. Sensitivity of cross-sectional and longitudinal associations between IQR increments in $PM_{2.5}$ component concentrations and CIMT to addition of another $PM_{2.5}$ component in the primary longitudinal model 3 using spatiotemporal model predictions. IQR increments were 0.51, 0.02, 0.89, and 0.69 $\mu\text{g}/\text{m}^3$ for sulfur, silicon, EC, and OC, respectively (see Table 38 for description of the model).

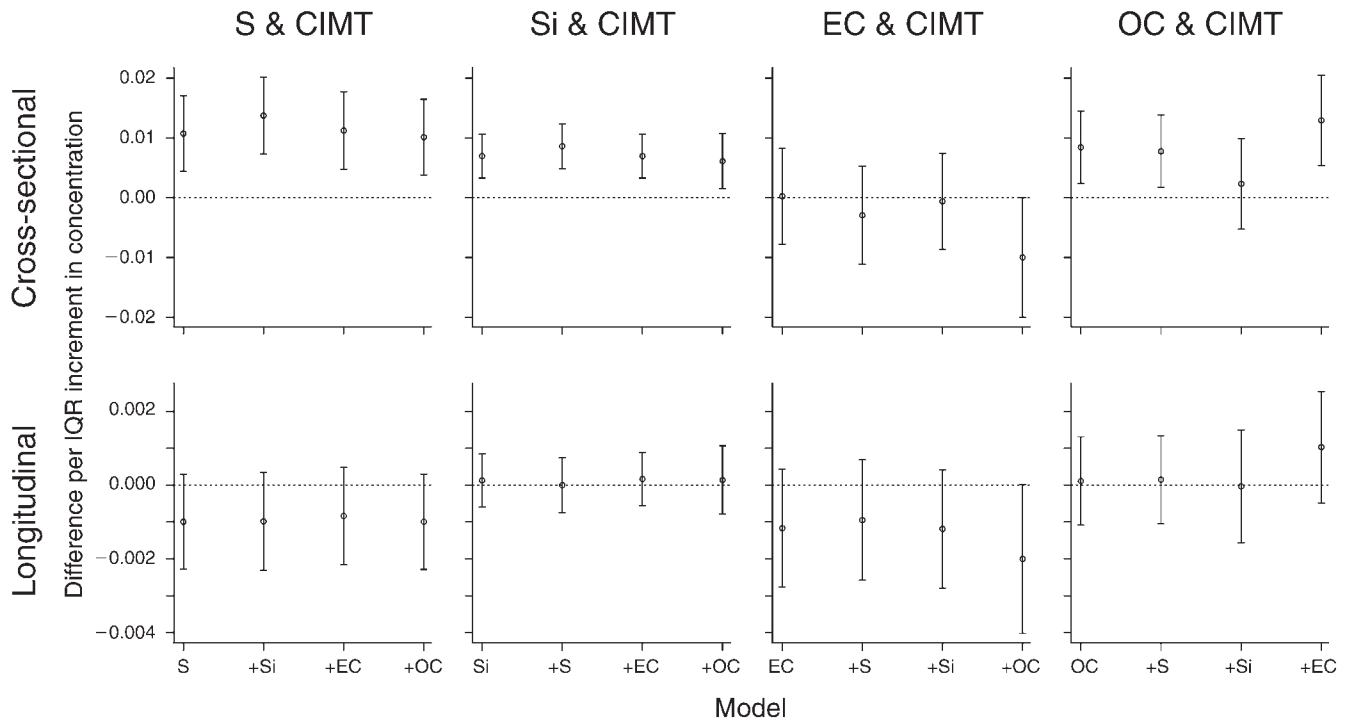


Figure 34. Sensitivity of cross-sectional and longitudinal associations between IQR increments in $PM_{2.5}$ component concentrations and CIMT to addition of another $PM_{2.5}$ component in the primary longitudinal model 3 using national spatial model predictions. IQR increments were 0.18, 0.02, 0.28, and 0.39 $\mu\text{g}/\text{m}^3$ for sulfur, silicon, EC, and OC, respectively (see Table 38 for description of the model).

Table 44. Within-City and Between-City Effects on Cross-Sectional and Longitudinal Associations for CIMT in MESA Participants with an IQR Increase in Predicted PM_{2.5} Component Concentrations from the Spatiotemporal Model in the Primary Longitudinal Model^a

Pollutant/ Model	Cross-Sectional β (95% CI)	Longitudinal β (95% CI)
S		
Within-city	0.034 (0.000 to 0.069)	0.003 (-0.004 to 0.010)
Between-city	0.022 (0.013 to 0.031)	-0.002 (-0.004 to 0.000)
Si		
Within-city	0.002 (-0.008 to 0.012)	0.001 (-0.001 to 0.003)
Between-city	0.006 (-0.002 to 0.013)	-0.001 (-0.002 to 0.001)
EC		
Within-city	0.007 (-0.009 to 0.024)	0.004 (0.000 to 0.007)
Between-city	0.004 (-0.005 to 0.012)	-0.002 (-0.004 to 0.000)
OC		
Within-city	0.008 (-0.003 to 0.020)	0.002 (-0.001 to 0.004)
Between-city	0.044 (0.032 to 0.056)	-0.003 (-0.005 to 0.000)

^a Effect estimates (β coefficients) and 95% CIs are presented per IQR increase: 0.51, 0.02, 0.89, and 0.69 $\mu\text{g}/\text{m}^3$ for S, Si, EC, and OC, respectively.

Within-City and Between-City Associations Table 44 shows the estimated within-city and between-city effects of PM_{2.5} component concentrations predicted using the spatiotemporal model on CIMT in the primary longitudinal analysis model 3. The effect estimates for the cross-sectional associations were similar for sulfur, silicon, and EC, but differed greatly for OC. The within-city effect estimates were generally similar to those in model 5 with city adjustment, while the between-city effect estimates were generally consistent with those estimated in model 3 (Table 41).

Analyses Using Secondary Estimates of PM_{2.5} Component Exposure

Health endpoints for the MESA participants were also examined using estimates of exposure to PM_{2.5} components based on three secondary approaches to exposure estimation, nearest neighbor, IDW, and citywide average

(detailed descriptions are provided in Appendix H, available on the HEI Web site). For the analysis of these secondary approaches, we chose the nearest-neighbor (nearest-monitor) approach a priori as our primary approach, and findings based on this approach were given the greatest interpretive weight. The same set of covariates was used in these health models as for the health models that used exposure predictions from the spatiotemporal or national spatial models. Also, as for other analyses, we considered model 3 as our primary model.

In the cross-sectional analysis using nearest-monitor exposure assignments, as in the analysis using the spatiotemporal model predictions, PM_{2.5}, sulfur, and OC were associated with CIMT, with effect estimates for sulfur and OC being the largest (Table 4 in Appendix H, available on the HEI Web site). However, using nearest-monitor exposure assignments, there was an association between EC and CIMT, but no association between silicon and CIMT, whereas the opposite was seen using the spatiotemporal model. Findings were similar using the IDW approach to assigning exposure. No cross-sectional associations of any PM_{2.5} component with either presence of CAC or change in amount of CAC were seen (Tables 5 and 6 in Appendix H).

THE WHI-OS ANALYSES

INTRODUCTION AND STUDY DESIGN

The Women's Health Initiative is a study of postmenopausal women that is supported by the National Institutes of Health. It has two components, Clinical Trials (WHI-CT) and the Observational Study (WHI-OS). As the primary objective of WHI-CT was to assess the effect of hormone therapy on risk of CVD, the study design and study resources focused primarily on assessment and characterization of health outcomes and events (including deaths) specific to CVD in the randomized clinical trial. Similarly, in WHI-OS researchers planned to study, within the context of an observational study design, the risk factors associated with development of precisely defined classes of CVD and incidence of CVD events and deaths and employed most of the same high-quality infrastructure to measure risk factors and outcomes as in the clinical trial.

The WHI cohorts have served as the focus of previous air pollution research. Through an ancillary study initially funded by the EPA through the UW's Particulate Matter Center, UW investigators analyzed incidence of CVD events in relation to exposure to fine PM (PM_{2.5}) in women of the WHI-OS cohort without a prior history of

CVD. At that time address information for participants was limited to their ZIP code at the time of recruitment, and exposure models were limited to use of the nearest population-based exposure monitor. Since that time, address history information has been organized, and addresses have been geocoded. The prior WHI ancillary study was continued and extended to include work funded in the NPACT study. The careful characterization of CVD events, large sample size, availability of high-quality information on important covariates, and length of follow-up make this cohort especially well suited for a study of the incidence of CVD events.

THE WHI-OS COHORT

Recruitment and Follow-Up

In this study we used the population of the large observational study (WHI-OS) exclusively. The WHI-OS population consists of 93,676 postmenopausal women recruited from study centers located in 46 cities in the continental United States and Hawaii. Women in the cohort underwent an initial evaluation between 1994 and 1998 and were followed annually for incidence of fatal and nonfatal cardiovascular events and to obtain updated information related to risk factors and health. At enrollment into WHI-OS, 20,582 of the women had a history of CVD, while 73,094 were free from clinically diagnosed CVD (Table 45).

Participants’ residential histories were available from the date of enrollment, or shortly before. Because the

national spatial model of exposure to PM_{2.5} and its components was developed only within the lower 48 U.S. states, those WHI-OS participants who lived elsewhere (chiefly residents of Hawaii) could not be included in most analyses in this study.

A rich suite of individual-level measures for cardiovascular risk factors was obtained at baseline, with many of the measurements updated annually. The original study officially ended in 2005. The study design and population characteristics have been described in detail elsewhere (Women’s Health Initiative Study Group 1998; Langer et al. 2003). Briefly, the women were 50 to 79 years of age, postmenopausal, and resided within commuting distance of a WHI Clinical Center or satellite clinic located in 36 U.S. Metropolitan Statistical Areas (MSAs). Eligible participants planned to remain in the area and were free from conditions that might preclude participation in follow-up surveys, such as alcoholism, mental illness, or dementia.

Our primary study population was restricted to women without a history of physician-diagnosed CVD, including prior myocardial infarction (MI), congestive heart failure, coronary revascularization, or stroke, at baseline (*N* = 73,094), but a sensitivity analysis was conducted including women with prior CVD. In secondary analyses of citywide average exposure, we included women only if they had not changed clinics before 2002, in order to establish a stable primary residence during follow-up. Institutional review boards of the UW, the Fred Hutchinson Cancer Research Center, and the WHI Clinical Centers approved the study.

Table 45. Exclusions from the WHI-OS Cohort for This Study

Cohort Exclusions	Number Excluded	Percent Excluded	Number Remaining	Percent Remaining
Total WHI-OS cohort	—	—	93,676	—
Without prior CVD ^a	—	—	73,094	100.0
Residence outside lower 48 states	2,141	2.9	70,953	97.1
Baseline address not geocodable	3,765	5.2	67,188	91.9
Not geocoded to street level	5,830	8.0	61,358	83.9
GIS covariates not available; can’t assign exposure to location	344	0.5	61,014	83.5
Never completed any follow-up questionnaire	274	0.4	60,740	83.1
Missing covariates for demographics, risk factors, or confounders; includes missing income	6,623	9.1	54,117	74.0
Income value unknown; not missing	1,590	2.2	52,539	71.9
Total excluded	20,561	28.1	52,539	71.9

^a Those without history of physician-diagnosed cardiovascular disease, including prior MI, congestive heart failure, coronary revascularization, or stroke, at baseline.

Health Endpoint and Covariate Data

Baseline questionnaires assessed demographics, lifestyle characteristics, cardiovascular risk factors, medical history, and use of medications; informed consent was obtained from participants. Anthropometric and blood pressure measurements were made at baseline (Langer et al. 2003). Subsequently, questionnaires mailed to subjects annually were used to update subject characteristics. Specific risk factors and characteristics that may modify the relationship between air pollution and CVD are as follows: age, BMI, smoking status (current smoker, former smoker, never smoked), years of smoking and cigarettes smoked per day, hypertension, hypercholesterolemia, diabetes, education, income, race and ethnicity, environmental exposure to tobacco smoke, occupation, physical activity, time spent outdoors, waist circumference, waist-to-hip ratio, medical history (especially prior diagnosis of CVD), medications, and family history of CVD. Among women without prior CVD whose baseline address was geocoded and assigned exposure concentrations, we further excluded 274 (0.4%) who never completed any follow-up questionnaire, 6623 (9.1%) who had missing values for any of the demographic characteristics, risk factors, or confounders included in the health models, and 1590 (2.2%) who reported not knowing their income, leaving 52,539 women (71.9% of those without prior CVD) for the primary analyses (Table 45).

Detailed definitions of the cardiovascular outcomes and descriptions of the adjudication procedures have been presented elsewhere (Miller et al. 2007, online supplement). Briefly, all outcomes were reported via questionnaire and assessed via physician-adjudicator review of medical records following established protocols (Curb et al. 2003; Heckbert et al. 2004). A detailed description of outcomes data, adjudication, and definitions follows. Note that codes from the International Classification of Diseases (ICD) were not used in the WHI-OS, because the investigators sought to achieve more precise categorization of CVD.

Medical records reviewed were hospital discharge codes, discharge summary, laboratory studies, electrocardiograms, diagnostic test reports, and procedure reports. Participants who had died were identified by proxy reports, supplemented by searches of the National Death Index. For adjudication of deaths, the most recent outpatient, emergency room, or emergency medical services reports, last hospitalization records, autopsy reports, coroner's reports, and death certificates were reviewed, as available. Nonfatal events were only adjudicated if the diagnosis was made during an overnight hospital stay, with the exception of revascularizations, which also

included procedures performed in an outpatient facility since August 1997.

MI is defined as the death of part of the myocardium due to an occlusion of a coronary artery from any cause, including spasm, embolus, thrombus, or the rupture of a plaque. MI is classified with an algorithm using standard criteria and incorporating medical history information, electrocardiogram readings, and results of cardiac enzyme or troponin determination (Langer et al. 2003). Coronary revascularization includes coronary artery bypass graft (CABG), percutaneous transluminal coronary angioplasty (PTCA), or coronary stent or atherectomy. Stroke is defined as rapid onset of a persistent neurologic deficit that is attributed to an obstruction or rupture of the brain arterial system and lasts more than 24 hours, without evidence of another cause.

In WHI-OS cardiovascular deaths are subclassified as definite or possible coronary heart disease (CHD) death, cerebrovascular death, other cardiovascular death, or unknown cardiovascular death. A CHD death is defined as death consistent with CHD as the underlying cause and preterminal hospitalization with MI within 28 days of death, or previous angina or MI, with no known, potentially lethal, noncoronary disease process, or as death resulting from a procedure related to coronary artery disease, such as CABG or PTCA (includes deaths consistent with ICD 9th revision [ICD-9] codes CM 410–414 or 427.5). CHD death is categorized as *definite* if (1) there was no known nonatherosclerotic cause, and (2) chest pain occurred within 72 hours of death, or there was a history of chronic ischemic heart disease (in the absence of valvular heart disease or nonischemic cardiomyopathy). CHD death is categorized as *possible* if there was no known nonatherosclerotic cause and the death certificate was consistent with CHD as the underlying cause. Cerebrovascular death is defined to include deaths consistent with ICD-9 codes CM 430–438, which include but are not limited to ischemic stroke and hemorrhagic stroke.

Other cardiovascular death, used in a secondary analysis, is defined as (1) a presumed MI or other presumed CHD cause that did not meet criteria for MI diagnosis, along with a death certificate consistent with MI or other CHD cause without other underlying or immediate cause, or (2) a presumed sudden or rapid unexplained death with either a previous history of MI or an autopsy report of severe atherosclerotic coronary artery disease without acute MI (includes deaths consistent with ICD-9 codes CM 415–429 or 440–452, with the exception of 427.5). Unknown cardiovascular death, also used in a secondary analysis, includes deaths for which there was some evidence (such as from a death certificate) that the underlying cause

involved the cardiovascular system, but there was insufficient detail to classify it more specifically.

In WHI, the reliability of self-reported cardiovascular outcomes compared with adjudicated outcomes was judged to be almost perfect for coronary bypass, substantial for angioplasty, MI, and stroke or transient ischemic attack, but only fair to moderate for angina or congestive heart failure (Curb et al. 2003; Heckbert et al. 2004). Similarly, comparisons of ICD-9 hospital discharge codes to adjudicated outcomes, or of local adjudication to central adjudication, found less agreement for angina, congestive heart failure, or transient ischemic attack, and strongest agreement for coronary bypass, angioplasty, stroke, or MI.

In this study, we considered definite CHD death (renamed as atherosclerotic cardiac death during subsequent follow-up of the WHI-OS cohort), possible CHD death, and cerebrovascular death as the main fatal outcomes of interest, and we refer to them jointly as CVD death. Our primary outcome event is the first occurrence during follow-up of MI, stroke, atherosclerotic cardiac death, possible CHD death, or cerebrovascular death.

Among the 52,539 women in WHI-OS with no prior CVD and complete data for all analytic variables, 2532 cardiovascular and cerebrovascular events and 445 cardiovascular and cerebrovascular deaths occurred through 2005 (Table 46). Compared with this group, the women without prior CVD but with some missing covariates ($n = 20,555$) were more likely to be Asian or Pacific Islander (7.5% versus 1.4%), owing to the exclusion of Hawaii from national exposure modeling. Furthermore, the women with some missing covariates were more likely to report not knowing their income (12.1% versus 0%), which was used as an adjustment variable. Women with a history of prior CVD were older, less likely to have a bachelor's degree, reported lower household income, had higher BMI, and were more likely to have a history of smoking, hypertension, diabetes mellitus, and hypercholesterolemia.

NATIONAL SPATIAL MODEL PREDICTIONS

Geocoding Results for Baseline Addresses

Out of 93,676 WHI-OS participants, address information was available for 93,605, and the baseline residential address was successfully geocoded for 88,308 (94%). Of these, 80,584 (91%) were geocoded to the more precise street level, while 7724 (9%) were geocoded to the ZIP code centroid level. Geocoding was not successful for 5297 (6%) of the 93,605 baseline addresses.

Among the addresses not geocoded, 5246 (99%) were previously identified as an invalid mailing address, while the validity of the address was unknown for 37 (0.7%),

and the address was classified as valid for only 14 (0.3%). In contrast, for addresses geocoded to the centroid level, only 1 (0.01%) was previously identified as an invalid mailing address, while the validity of the address was unknown for 1921 (25%), and the address was classified as valid for 5802 (75%). For addresses geocoded to street level, 5 (0.01%) had been identified as invalid, while the validity of the address was unknown for 12,729 (16%), and the address was classified as valid for 67,850 (84%).

Assignment of Exposure Predictions to Participants' Addresses

Out of 93,605 total study participants with address information, 2113 (2%) were excluded because of residence location outside the lower 48 U.S. states. Exposure predictions were not assigned to the 5297 addresses (6%) that could not be geocoded. Due to software computational issues in the GIS processing of geographic covariates at the locations of certain addresses, exposure predictions could not be assigned to 555 (0.6%) of the participants. Modeled exposure predictions were successfully assigned to 85,640 women (91.5%) for all baseline exposures. Among those assigned exposure, 78,251 (91.4%) had been geocoded to the street level, while 7389 (8.6%) were geocoded to the ZIP code centroid level.

Among women free of CVD at baseline, 70,953 resided within the lower 48 U.S. states at their baseline address (Table 45). Of these, 3765 (5.2%) had baseline addresses that could not be geocoded, another 5830 (8.0%) had baseline addresses that could not be geocoded to the desired precision of the street level, and a further 344 (0.5%) could not be assigned exposure because the GIS covariates used to predict exposure were unavailable at the location of the subject's residence. Thus, we successfully assigned baseline exposure to 61,014 (83.5%) of the 73,094 women without prior CVD.

Exposure Predictions for the WHI-OS Cohort

Figures 35 through 38 show the distributions of EC, OC, sulfur, and silicon concentrations at WHI-OS cohort addresses across the United States predicted from the national spatial model. These distributions and that of $PM_{2.5}$ are summarized in Table 47.

The approach to building a national spatial model for $PM_{2.5}$ exposure was generally similar to that carried out in MESA Air, with AQS and IMPROVE network data used to obtain an annual average for the year 2000. Cross-validated R^2 for the $PM_{2.5}$ model was 0.86. We used predictions from this model in the analyses of health effects in the WHI-OS cohort.

Table 46. Characteristics of Study Subjects and Events in WHI-OS^{a,b}

Characteristic	No Prior CVD, No Missing Covariates (<i>n</i> = 52,539)	No Prior CVD, Some Missing Covariates (<i>n</i> = 20,555)	Prior CVD (<i>n</i> = 20,582)
Cardiovascular and cerebrovascular events (<i>n</i> [%]) ^c	2532 (4.8)	984 (4.8)	2645 (12.9)
Cardiovascular and cerebrovascular deaths (<i>n</i> [%])	445 (0.8)	187 (0.9)	657 (3.2)
Age (yrs, mean ± SD)	63.0 ± 7.3	63.3 ± 7.3	65.5 ± 7.3
Race or ethnic group (%) ^d			
American Indian	0.4	0.6	0.6
Asian or Pacific Islander	1.4	7.5	1.9
Black	7.1	9.7	9.4
Hispanic	3.8	4.5	3.5
White	86.5	76.2	83.3
Other	0.9	1.7	1.3
Education (%)			
Not high-school graduate	4.0	6.8	7.0
Graduate of high school or trade school or GED	25.1	26.7	28.0
Some college or associate degree	26.6	26.1	27.7
Bachelor's degree or higher	44.4	40.4	37.4
Household income (%)			
<\$20,000	13.8	14.6	21.5
\$20,000–\$49,999	43.2	37.1	43.5
≥\$50,000	43.0	36.2	31.6
Respondent did not know	0	12.1	3.5
BMI (kg/m ² , mean ± SD)	27.1 ± 5.7	27.1 ± 5.8	27.9 ± 6.3
Smoking history (%)			
Former smoker	41.7	44.4	44.2
Current smoker	6.2	6.1	6.7
SBP (mm Hg, mean ± SD)	126.0 ± 17.7	127.1 ± 17.9	129.3 ± 18.5
Hypertension (%)	29.2	30.5	47.6
Diabetes mellitus (%)	4.1	5.4	10.0
Hypercholesterolemia (%)	12.3	13.3	24.3

^a Percentages may not total 100 because of rounding. GED indicates general equivalency diploma.

^b BMI indicates body mass index; CVD, cardiovascular disease; GED, general education development test; SBP, systolic blood pressure.

^c Events include MI, revascularization, stroke, and death from CHD or cerebrovascular disease.

^d Race or ethnic group was reported by the subjects.

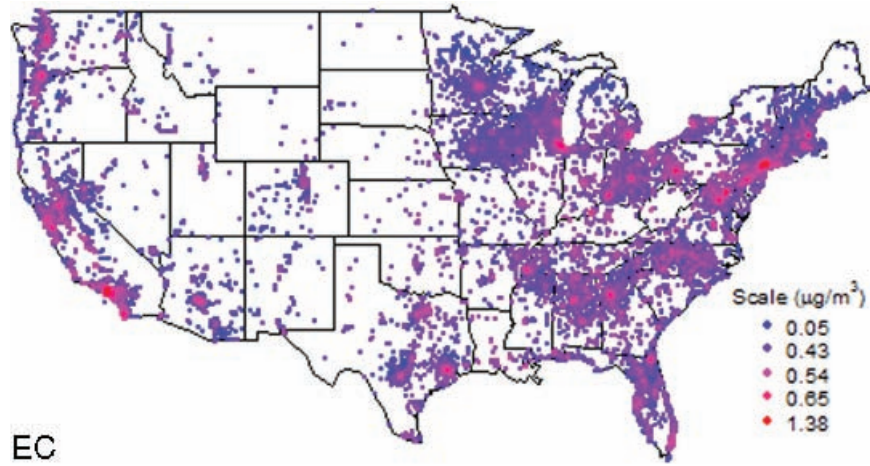


Figure 35. National spatial model predictions for EC concentrations at WHI-OS cohort addresses.

Description of Assigned Baseline Exposures

Summary statistics of the exposures assigned using addresses geocoded to street level for study participants with no prior CVD and no missing covariates (that is, those included in primary health analyses) are given in Table 47. The mean annual average predicted baseline PM_{2.5} concentration was 12.9 µg/m³ (SD, 2.8) with an IQR of 3.9. In order from largest to smallest, the mean annual average predicted concentrations (SD, IQR) for the components were as follows: OC, 1.94 µg/m³ (0.45, 0.64); sulfur, 0.69 µg/m³ (0.22, 0.25); EC, 0.56 µg/m³ (0.16, 0.21); and silicon, 0.10 µg/m³ (0.07, 0.07). Subjects without complete covariates or with prior CVD generally had marginally higher predicted exposure concentrations, except that the

predicted exposure to sulfur was not higher in those with prior CVD (Table 48).

The pairwise correlation coefficients for all baseline exposure measures are shown in Table 49. The strongest correlations were between EC and OC (0.78), total PM_{2.5} mass and sulfur (0.63), EC and PM_{2.5} (0.55), and OC and PM_{2.5} (0.51). Weak to no correlation existed between sulfur and silicon (-0.24), EC and sulfur (0.23), PM_{2.5} and silicon (-0.13), EC and silicon (-0.08), OC and silicon (-0.07), and OC and sulfur (0.08).

SECONDARY EXPOSURE ESTIMATES

PM_{2.5} component exposure was also estimated for the WHI-OS cohort using citywide average concentrations

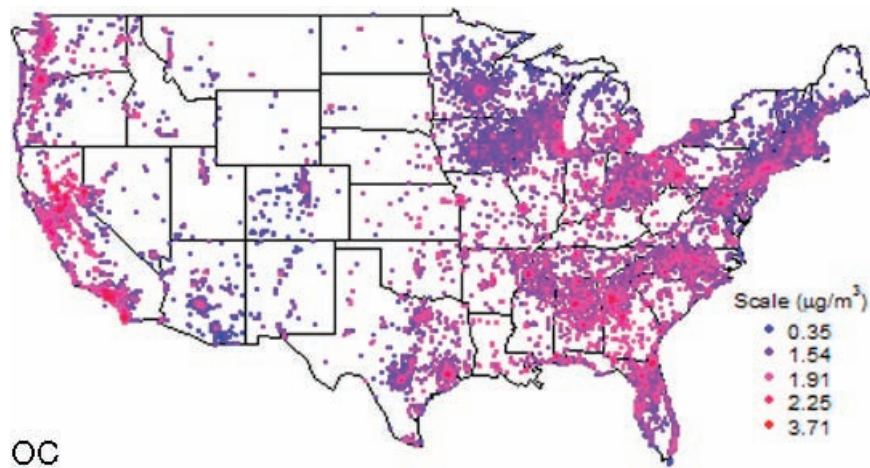


Figure 36. National spatial model predictions for OC concentrations at WHI-OS cohort addresses.

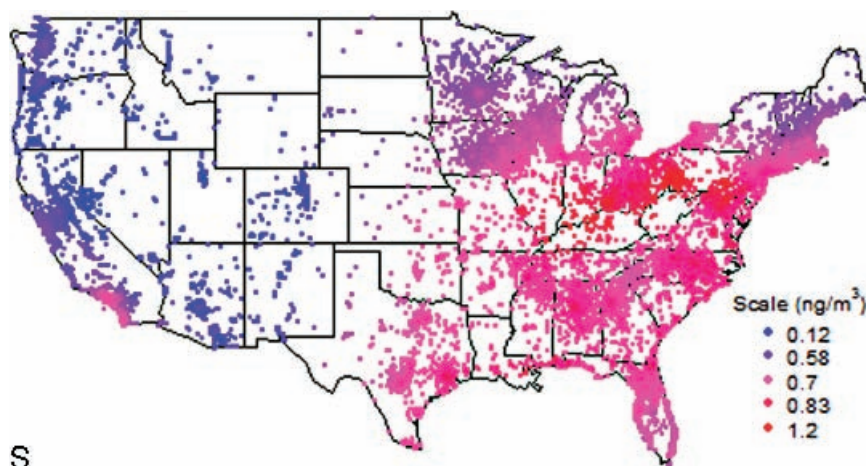


Figure 37. National spatial model predictions for sulfur concentrations at WHI-OS cohort addresses.

(detailed descriptions of this analysis and distributions of the results are provided in Appendix I, available on the HEI Web site).

Summary statistics of the exposures by distance to roadway are given in Table 47 for study participants with baseline addresses geocoded to street level. Among those with no prior CVD and no missing covariates (that is, those included in the primary health analyses), 17.4% were living within either 100 m of an A1 or A2 roadway or 50 m of an A3 roadway, while 3.6% lived within 100 m of an A1 or A2 roadway. Those without complete covariates or with prior CVD tended to live slightly closer to major roadways according to both categorical definitions, that is, within either 100 m of an A1 or A2 roadway or 50 m of an A3 roadway, or within 100 m of an A1 or A2 roadway (Table 48).

ANALYSIS OF HEALTH EFFECTS

Statistical Methods and Data Analysis

Cox proportional-hazards regression was used to estimate the HR and 95% CI for time to first CVD event or time to CVD death associated with a $10\text{-}\mu\text{g}/\text{m}^3$ increase in $\text{PM}_{2.5}$, EC, OC, sulfur, or silicon, or for proximity to a major roadway (yes/no), as previously defined. Factors hypothesized a priori to potentially confound the relationship between air pollution and CVD were included in all models; these included age, BMI, smoking status, cigarettes smoked per day and years of smoking, systolic blood pressure, history of hypertension, hypercholesterolemia, history of diabetes,

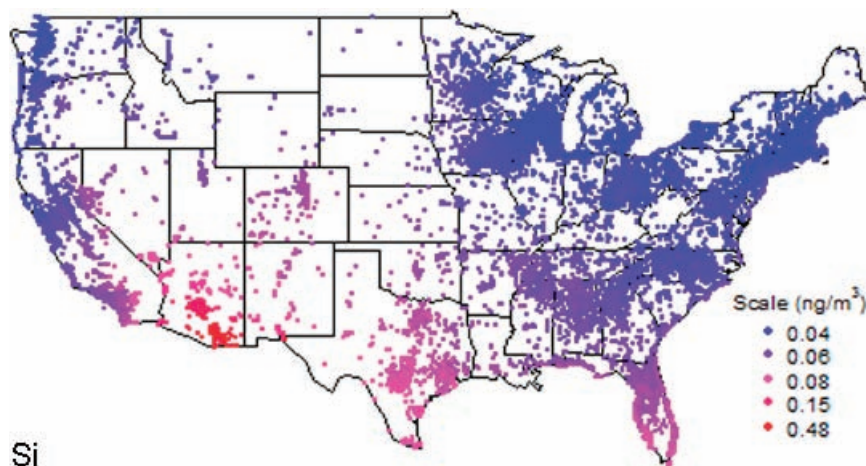


Figure 38. National spatial model predictions for silicon concentrations at WHI-OS cohort addresses.

Table 47. Distributions of Predicted PM_{2.5} and PM_{2.5} Component Concentrations and Distance to Roadways Using Baseline Addresses Geocoded to Street Level for WHI-OS Participants with No Prior CVD and No Missing Covariates^a

Pollutant	n	25th			75th		Mean ± SD
		Minimum	Percentile	Median	Percentile	Maximum	
Total PM _{2.5} mass	52,539	3.9	10.9	12.7	14.8	30.6	12.9 ± 2.8
EC	52,533	0.11	0.45	0.56	0.66	1.29	0.56 ± 0.16
OC	52,533	0.50	1.63	1.97	2.27	3.57	1.94 ± 0.45
S	52,533	0.12	0.59	0.70	0.84	1.19	0.69 ± 0.22
Si	52,533	0.04	0.06	0.08	0.13	0.48	0.104 ± 0.07
Distance to roadway		<i>n</i> (%)					
A1 or A2 < 100 m or A3 < 50 m	52,539	9154 (17.4)					
A1 or A2 < 100 m	52,539	1895 (3.6)					

^a Data are expressed in µg/m³.

Table 48. Distributions of Predicted PM_{2.5} and PM_{2.5} Component Concentrations and Distance to Roadways Using Baseline Addresses Geocoded to Street Level for WHI-OS Participants With or Without Prior CVD^a

Pollutant	No Prior CVD, No Missing Covariates (n = 52,539)			No Prior CVD, Some Missing Covariates (n = 20,555)			Prior CVD (n = 20,582)		
	n	Median	Mean ± SD	n ^b	Median	Mean ± SD	n ^b	Median	Mean ± SD
Total PM _{2.5} mass	52,539	12.7	12.9 ± 2.8	8483	12.9	13.0 ± 2.8	17,238	12.8	13.0 ± 2.8
EC	52,533	0.56	0.56 ± 0.16	8481	0.57	0.57 ± 0.16	17,237	0.57	0.57 ± 0.16
OC	52,533	1.97	1.94 ± 0.45	8481	1.97	1.95 ± 0.45	17,237	1.99	1.96 ± 0.46
S	52,533	0.70	0.69 ± 0.22	8481	0.71	0.70 ± 0.21	17,237	0.70	0.69 ± 0.23
Si	52,533	0.08	0.10 ± 0.07	8481	0.08	0.110 ± 0.08	17,237	0.08	0.109 ± 0.08
Distance to roadway		<i>n</i> (%)			<i>n</i> (%)			<i>n</i> (%)	
A1 or A2 < 100 m or A3 < 50 m	52,539	9154 (17.4)		8483	1542 (18.2)		17,238	3142 (18.2)	
A1 or A2 < 100 m	52,539	1895 (3.6)		8483	333 (3.9)		17,238	661 (3.8)	

^a Data are expressed in µg/m³.

^b n less than totals due to absence of exposure data for participants who had an address that either could not be geocoded at all or could not be geocoded to street level, or for which some GIS covariates were unavailable, or who resided outside the lower 48 U.S. states.

Table 49. Correlations of Predicted PM_{2.5} and PM_{2.5} Component Concentrations and Distance to Roadways Using Baseline Addresses Geocoded to Street Level^a

	PM _{2.5}	EC	OC	S	Si
Total PM _{2.5} mass	1	0.55	0.51	0.63	-0.13
EC		1	0.78	0.23	-0.08
OC			1	0.08	-0.07
S				1	-0.24
Si					1

^a Addresses for 52,539 WHI-OS participants with no prior CVD and no missing covariates.

education, household income level, and race; models were stratified with separate baseline hazards for diabetes status, age, and BMI.

Analyses were restricted to addresses geocoded to street level, effectively excluding those addresses geocoded to ZIP code centroid level only. All of the WHI-OS health analyses based on national spatial model exposure predictions in this report used the baseline address, defined as the address where the participant lived the longest during the initial 12 months of study follow-up, except for a sensitivity analysis that used a time-varying exposure based on address histories and national spatial model predictions (described in Appendix I, available on the HEI Web site). All of the WHI-OS health analyses presented in this report used outcomes occurring during the same time range, with a maximum of 11 years' duration — that is, from study entry at enrollment, which happened on a rolling basis between 1994 and 1998, until the cessation of the original WHI-OS follow-up in 2005.

In sensitivity analyses, PM_{2.5} components found to be significantly associated with outcomes in models with single exposure variables were included in models with two or more exposure variables. Analyses for time to CVD death were repeated with inclusion of women who had a history of prior CVD at baseline. Analysis of roadway proximity was repeated restricting the analysis to women living within the boundaries of an MSA at baseline; those living outside MSAs were presumably in more rural locations. Further sensitivity analyses examined associations with the categories of other CVD death and unknown CVD death, where there was less evidence for an atherosclerotic cause. Methodologies used for the additional analyses of within-city and between-city health effects and for analyses incorporating random effects are described separately.

The time axis used in survival analysis is time since enrollment. Data were analyzed using the statistical package SAS versions 9.2 and 9.3 (SAS, Cary, NC).

Results Using National Spatial Model Predictions

Associations between PM_{2.5} exposure from national spatial model predictions at the baseline address and all categories of CVD events and CVD deaths are presented in Table 50. The number of participants who had no prior CVD at baseline, had returned at least one follow-up questionnaire, had a baseline address that could be geocoded to street level, and were not missing data for any of the covariates included in the primary Cox regression model was 52,539. Among these women, there were 2532 CVD events available, of which 445 were deaths. Approximately two thirds of the events (1764) were CHD events, while the others were cerebrovascular disease events (863). The results are shown per 10- $\mu\text{g}/\text{m}^3$ increments of PM_{2.5} mass to facilitate comparison with previous studies and per IQR to facilitate comparisons between PM components (Table 50).

The estimated HR per 10- $\mu\text{g}/\text{m}^3$ increase in PM_{2.5} with time to first CVD event was 1.25, with 95% CI from 1.09 to 1.44 (Table 50). Both CHD events (HR, 1.20; 95% CI, 1.01 to 1.42) and cerebrovascular disease events (HR, 1.41; 95% CI, 1.12 to 1.79) were associated with increased PM_{2.5} concentration. For CVD deaths, the magnitude of the estimated association was increased, but was not statistically significant (HR, 1.31; 95% CI, 0.94 to 1.83). The largest HR was observed for death from atherosclerotic cardiac disease (HR, 1.61; 95% CI, 0.84 to 3.10).

When the analysis was not restricted to addresses geocoded to street level but also included those geocoded to centroid level, the total number of participants with available data increased to 57,488 and the total number of CVD events was 2779 (data not shown). In this sensitivity analysis, the overall association between PM_{2.5} and first CVD event was only slightly weaker (HR, 1.23; 95% CI, 1.07 to 1.40).

The associations between predictions for total PM_{2.5} mass and EC, OC, sulfur, and silicon from the national spatial model at the baseline address and all categories of CVD events are presented in Table 51; findings for selected categories are shown in Figures 39 and 40. An IQR increase in PM_{2.5} was associated with a 9% increased risk of incidence of a CVD event (HR, 1.09; 95% CI, 1.03 to 1.15). Similarly, an IQR increase in sulfur was associated with a 9% increased risk of incidence of a CVD event (HR, 1.09; 95% CI, 1.05 to 1.14). There was little evidence that the components EC, OC, and silicon were associated with CVD events in total. However, Figure 40 and Table 51

Table 50. Estimated Hazard Ratios for Time to First CVD Event and CVD Death Associated with a 10- $\mu\text{g}/\text{m}^3$ Unit Increase of Baseline Total $\text{PM}_{2.5}$ Mass Exposure Using National Spatial Model Predictions^a

Event	<i>n</i>	HR (95% CI) per 10 $\mu\text{g}/\text{m}^3$	HR (95% CI) per IQR (3.9 $\mu\text{g}/\text{m}^3$)
CVD event ^b	2532	1.25 (1.09 to 1.44)	1.09 (1.03 to 1.15)
Coronary heart disease ^c	1764	1.20 (1.01 to 1.42)	1.07 (1.01 to 1.14)
Cerebrovascular disease ^d	863	1.41 (1.12 to 1.79)	1.14 (1.04 to 1.25)
Myocardial infarction	800	1.09 (0.85 to 1.40)	1.03 (0.94 to 1.14)
Coronary revascularization	1285	1.21 (0.994 to 1.47)	1.08 (0.998 to 1.16)
Stroke	800	1.48 (1.15 to 1.89)	1.16 (1.06 to 1.28)
CVD death ^e	445	1.31 (0.94 to 1.83)	1.11 (0.98 to 1.26)
Atherosclerotic cardiac disease or possible CHD deaths	254	1.53 (0.99 to 2.38)	1.18 (0.996 to 1.40)
Atherosclerotic cardiac disease death	120	1.61 (0.84 to 3.10)	1.20 (0.94 to 1.55)
Possible CHD death	134	1.46 (0.81 to 2.64)	1.16 (0.92 to 1.46)
Cerebrovascular death	191	1.06 (0.64 to 1.75)	1.02 (0.84 to 1.24)

^a Total participants included = 52,539; events through year 2005 included. All estimates adjusted for age, ethnicity, education, household income, smoking, diabetes, hypertension, SBP, BMI, and hypercholesterolemia.

^b MI, coronary revascularization, stroke, atherosclerotic cardiac disease death, possible CHD death, and cerebrovascular death.

^c MI, coronary revascularization, atherosclerotic cardiac disease death, and possible CHD death.

^d Stroke, cerebrovascular death.

^e Atherosclerotic cardiac disease death, possible CHD death, and cerebrovascular death.

Table 51. Estimated Hazard Ratios for Time to First CVD Event Associated with an IQR Increase of Baseline Exposure Using National Spatial Model Predictions^a

Pollutant	IQR ($\mu\text{g}/\text{m}^3$)	CVD Event ^b (<i>n</i> = 2532) HR (95% CI)	CHD ^c (<i>n</i> = 1764) HR (95% CI)	Cerebrovascular Disease ^d (<i>n</i> = 863) HR (95% CI)	MI (<i>n</i> = 800) HR (95% CI)	Coronary Revascularization (<i>n</i> = 1285) HR (95% CI)	Stroke (<i>n</i> = 800) HR (95% CI)
Total $\text{PM}_{2.5}$ mass	3.9	1.09 (1.03 to 1.15)	1.07 (1.01 to 1.14)	1.14 (1.04 to 1.25)	1.03 (0.94 to 1.14)	1.08 (0.998 to 1.16)	1.16 (1.06 to 1.28)
EC	0.21	0.99 (0.94 to 1.05)	0.98 (0.92 to 1.05)	1.04 (0.95 to 1.14)	0.94 (0.85 to 1.03)	0.96 (0.89 to 1.03)	1.03 (0.94 to 1.14)
OC	0.64	1.03 (0.97 to 1.09)	1.00 (0.94 to 1.07)	1.13 (1.03 to 1.24)	0.98 (0.89 to 1.09)	0.98 (0.91 to 1.06)	1.13 (1.02 to 1.24)
S	0.25	1.09 (1.05 to 1.14)	1.11 (1.05 to 1.17)	1.07 (0.995 to 1.16)	1.08 (1.001 to 1.17)	1.14 (1.07 to 1.22)	1.10 (1.01 to 1.19)
Si	0.07	0.97 (0.93 to 1.01)	0.99 (0.94 to 1.04)	0.92 (0.86 to 0.99)	0.93 (0.86 to 1.01)	0.98 (0.92 to 1.04)	0.92 (0.85 to 0.99)

^a Total participants included = 52,539; events through year 2005 included. All estimates adjusted for age, ethnicity, education, household income, smoking, diabetes, hypertension, SBP, BMI, and hypercholesterolemia.

^b MI, coronary revascularization, stroke, atherosclerotic cardiac disease death, possible CHD death, and cerebrovascular death.

^c MI, coronary revascularization, atherosclerotic cardiac disease death, and possible CHD death.

^d Stroke, cerebrovascular death.

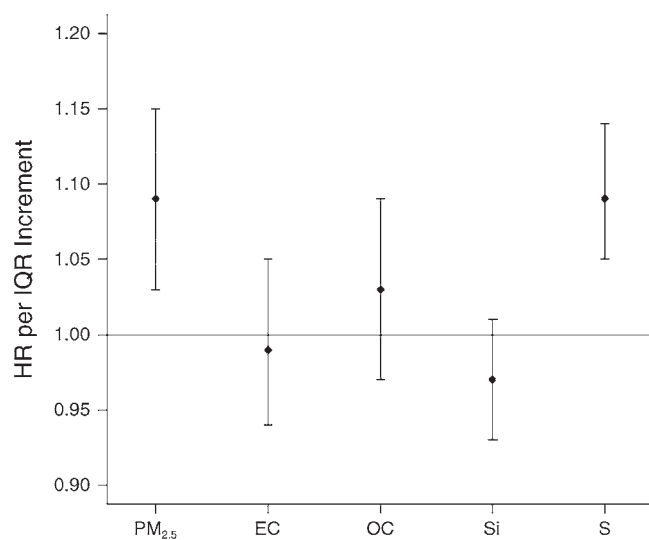


Figure 39. Estimated HR per IQR increment in PM_{2.5} and PM_{2.5} components for CVD events (95% CI). See Table 51 for details.

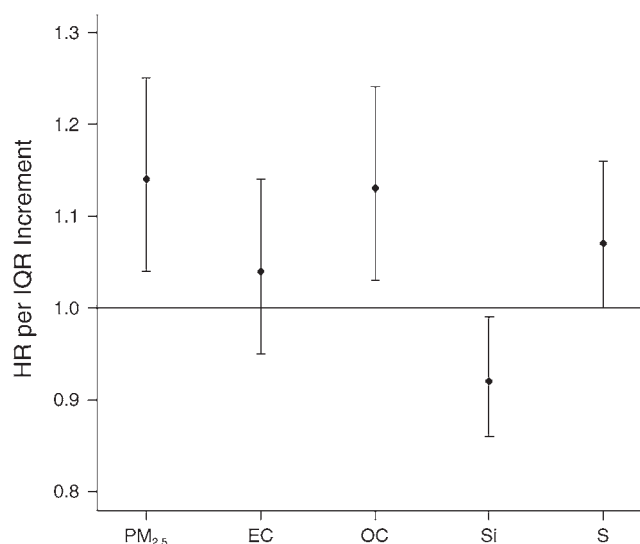


Figure 40. Estimated HR per IQR increment in PM_{2.5} and PM_{2.5} components for cerebrovascular disease events (95% CI). See Table 51 for details.

show that OC was positively associated with cerebrovascular events (HR, 1.13; 95% CI, 1.03 to 1.24) and silicon was negatively associated with cerebrovascular events (HR, 0.92; 95% CI, 0.86 to 0.99).

The associations between predictions for total PM_{2.5} mass, EC, OC, sulfur, and silicon from the national spatial model at the baseline address and all categories of CVD deaths are presented in Table 52; findings for selected categories are shown in Figures 41 and 42. OC had the

strongest association with time to CVD death. An IQR increase in OC was associated with a 23% increased risk (HR, 1.23; 95% CI, 1.07 to 1.41). An IQR increase in either PM_{2.5} mass or EC was associated with an 11% increased risk of CVD death (HR, 1.11; 95% CI, 0.98 to 1.26 for each). In contrast to CVD events, sulfur was not associated with CVD deaths, although an association was suggested between sulfur and death from atherosclerotic cardiac disease alone (HR, 1.23; 95% CI, 0.99 to 1.51). Neither was

Table 52. Estimated Hazard Ratios for Time to CVD Death Associated with an IQR Increase of Baseline Exposure Using National Spatial Model Predictions^a

Pollutant	IQR (μg/m ³)	CVD Death ^b (n = 445) HR (95% CI)	Atherosclerotic Cardiac Disease or Possible CHD Death (n = 254) HR (95% CI)	Atherosclerotic Cardiac Disease Death (n = 120) HR (95% CI)	Possible CHD Death (n = 134) HR (95% CI)	Cerebrovascular Death (n = 191) HR (95% CI)
Total PM _{2.5} mass	3.9	1.11 (0.98 to 1.26)	1.18 (0.996 to 1.40)	1.20 (0.94 to 1.55)	1.16 (0.92 to 1.46)	1.02 (0.84 to 1.24)
EC	0.21	1.11 (0.98 to 1.26)	1.17 (0.99 to 1.38)	1.27 (0.99 to 1.61)	1.08 (0.86 to 1.36)	1.03 (0.85 to 1.26)
OC	0.64	1.23 (1.07 to 1.41)	1.21 (1.01 to 1.46)	1.34 (1.02 to 1.75)	1.12 (0.88 to 1.43)	1.25 (1.01 to 1.53)
S	0.25	1.01 (0.92 to 1.12)	1.05 (0.91 to 1.20)	1.23 (0.999 to 1.51)	0.91 (0.76 to 1.09)	0.97 (0.83 to 1.14)
Si	0.07	1.03 (0.94 to 1.12)	1.08 (0.97 to 1.21)	0.92 (0.76 to 1.13)	1.18 (1.03 to 1.35)	0.96 (0.83 to 1.11)

^a Total participants included = 52,539; events through year 2005 included. All estimates adjusted for age, ethnicity, education, household income, smoking, diabetes, hypertension, SBP, BMI, and hypercholesterolemia.

^b Atherosclerotic cardiac disease death, possible CHD death, and cerebrovascular death.

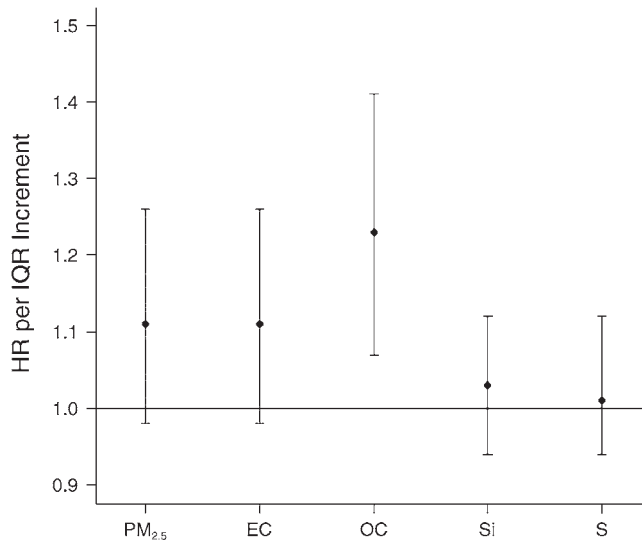


Figure 41. Estimated HR per IQR increment in PM_{2.5} and PM_{2.5} components for CVD death (95% CI). See Table 52 for details.

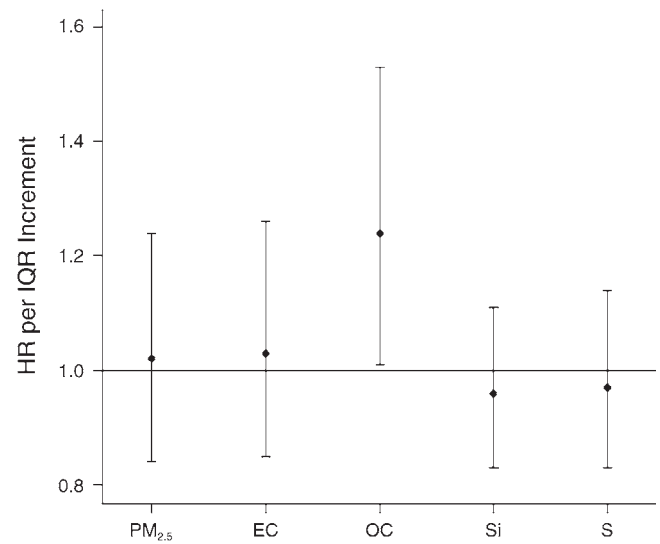


Figure 42. Estimated HR per IQR increment in PM_{2.5} and PM_{2.5} components for death from cerebrovascular disease (95% CI). See Table 52 for details.

any association observed between silicon exposure and all CVD deaths, although it was associated with possible CHD death alone (HR, 1.18; 95% CI, 1.03 to 1.35). There was some evidence for an association between EC and atherosclerotic cardiac disease death (HR, 1.27; 95% CI, 0.99 to 1.61), but less evidence to suggest that EC was associated with other categories of CVD death. OC was most strongly associated with atherosclerotic cardiac disease death (HR, 1.34; 95% CI, 1.02 to 1.75) and was also associated with death from cerebrovascular disease (HR, 1.25; 95% CI, 1.01 to 1.53).

Within-City and Between-City Analysis

For this analysis, the subject’s baseline address was assigned to an MSA code based on census year 2000 definitions; the MSA is referred to herein as “city.” In addition to exclusions noted in Table 45, subjects who lived outside MSA boundaries were not assigned to a city. Further, any MSA with fewer than 20 women (who had no missing covariates and were otherwise eligible for the primary health analysis) was excluded, yielding 45,980 women included in the within-city and between-city analysis (Table 53). In contrast to the methodology used previously (Miller et al. 2007), MSA was assigned according to the participant’s residential address, rather than the clinic location, and MSAs were never grouped into a Combined Metropolitan Statistical Area.

The methodology described below is for the within-city and between-city analysis of PM_{2.5} mass; identical statistical methods were used for each PM_{2.5} component. First,

exposures assigned to all subjects in a city were averaged to estimate a “city mean” exposure (\bar{X}_j). We then subtracted the city mean (\bar{X}_j) from the exposure assigned to each subject (X_{ij}), to estimate the difference between each individual exposure and the city mean ($X_{ij} - \bar{X}_j$).

The basic stratified Cox proportional-hazards model in equation (1) estimates the overall PM_{2.5} (or PM_{2.5} component) effect (β).

$$\lambda_{ij}(t) = \lambda_0(t) \exp(\beta X_{ij} + \gamma Z_i) \tag{1}$$

The model in equation (2) represents a reparameterization of the exposure variable but is otherwise identical. It simultaneously estimates the between-city (β_B) and within-city (β_W) PM_{2.5} mass (or PM_{2.5} component) effects. Note that because city is taken into account, the within-city estimates are effectively controlled for city-level PM_{2.5} mass (or PM_{2.5} component).

$$\lambda_{ij}(t) = \lambda_0(t) \exp[\beta_B \bar{X}_j + \beta_W (X_{ij} - \bar{X}_j) + \gamma Z_i] \tag{2}$$

Overall PM_{2.5} mass (and PM_{2.5} component) effects were estimated using equation (1), and within-city and between-city PM_{2.5} mass (and PM_{2.5} component) effects were estimated using equation (2). In both cases, stratified Cox proportional-hazards regression was performed to estimate HR and 95% CI for time to first CVD event associated with an IQR unit ($\mu\text{g}/\text{m}^3$) difference in PM_{2.5}.

The estimated health effects for the between-city analysis are reported for the same IQR increments as in the overall analysis because the overall IQRs and the citywide

Table 53. Distributions of Predicted PM_{2.5} and PM_{2.5} Component Concentrations Using Baseline Addresses Geocoded to Street Level^a

Pollutant / Analysis	<i>n</i> ^b	Minimum	25th Percentile	Median	75th Percentile	Maximum	Mean ± SD
Total PM _{2.5} mass							
Individual exposure	45,980	3.9	11.1	12.8	14.8	30.6	13.0 ± 2.7
Citywide average exposure	45,980	6.7	11.2	12.6	14.8	18.3	13.0 ± 2.5
Difference between individual exposure and citywide average exposure	45,980	-9.54	-0.60	0.07	0.63	12.76	0.00 ± 1.05
EC							
Individual exposure	45,978	0.13	0.47	0.57	0.66	1.29	0.57 ± 0.15
Citywide average exposure	45,978	0.30	0.49	0.58	0.62	0.90	0.57 ± 0.10
Difference between individual exposure and citywide average exposure	45,978	-0.57	-0.08	0.01	0.08	0.58	0.00 ± 0.12
OC							
Individual exposure	45,978	0.50	1.67	1.99	2.27	3.57	1.97 ± 0.44
Citywide average exposure	45,978	1.10	1.76	1.99	2.22	2.58	1.97 ± 0.30
Difference between individual exposure and citywide average exposure	45,978	-1.40	-0.21	0.04	0.23	1.33	0.00 ± 0.31
S							
Individual exposure	45,978	0.12	0.60	0.72	0.84	1.18	0.70 ± 0.22
Citywide average exposure	45,978	0.17	0.62	0.72	0.83	1.12	0.70 ± 0.22
Difference between individual exposure and citywide average exposure	45,978	-0.44	-0.02	0.01	0.02	0.80	0.00 ± 0.03
Si							
Individual exposure	45,978	0.037	0.058	0.075	0.125	0.462	0.104 ± 0.073
Citywide average exposure	45,978	0.049	0.060	0.073	0.129	0.414	0.104 ± 0.073
Difference between individual exposure and citywide average exposure	45,978	-0.214	-0.004	-0.001	0.004	0.368	0.000 ± 0.008

^a Data are expressed in µg/m³.^b Only WHI-OS participants with no prior CVD, no missing covariates, and living within boundaries of an MSA are included.

Table 54. Estimated Hazard Ratios for Time to First CVD Event Associated with an IQR Increase of Between-City Baseline Exposure Using National Spatial Model Predictions^a

Pollutant	IQR ^b (µg/m ³)	CVD Event ^c (n = 2246) HR (95% CI)	CHD ^d (n = 1562) HR (95% CI)	Cerebrovascular Disease ^e (n = 766) HR (95% CI)	MI (n = 714) HR (95% CI)	Coronary Revascularization (n = 1133) HR (95% CI)	Stroke (n = 708) HR (95% CI)
Total PM _{2.5} mass	3.9	1.07 (0.999 to 1.14)	1.05 (0.97 to 1.13)	1.11 (0.99 to 1.24)	0.99 (0.89 to 1.12)	1.08 (0.99 to 1.19)	1.12 (0.997 to 1.25)
EC	0.21	0.92 (0.85 to 1.01)	0.90 (0.81 to 1.01)	1.00 (0.86 to 1.17)	0.77 (0.66 to 0.91)	0.91 (0.80 to 1.03)	0.98 (0.83 to 1.15)
OC	0.64	1.02 (0.94 to 1.11)	0.96 (0.87 to 1.07)	1.19 (1.03 to 1.38)	0.93 (0.80 to 1.08)	0.97 (0.86 to 1.09)	1.16 (0.997 to 1.35)
S	0.25	1.06 (1.01 to 1.12)	1.08 (1.02 to 1.15)	1.03 (0.95 to 1.12)	1.04 (0.96 to 1.14)	1.12 (1.05 to 1.20)	1.06 (0.97 to 1.15)
Si	0.07	0.95 (0.91 to 0.995)	0.98 (0.93 to 1.03)	0.92 (0.85 to 0.99)	0.94 (0.87 to 1.01)	0.97 (0.91 to 1.03)	0.92 (0.85 to 0.99)

^a Total participants included = 45,980; events through year 2005 included. All estimates adjusted for age, ethnicity, education, household income, smoking, diabetes, hypertension, SBP, BMI, and hypercholesterolemia.

^b IQRs represent overall variation in exposure to pollutants; between-city variations were very similar (see Table 53).

^c MI, coronary revascularization, stroke, atherosclerotic cardiac disease death, possible CHD death, and cerebrovascular death.

^d MI, coronary revascularization, atherosclerotic cardiac disease death, and possible CHD death.

^e Stroke, cerebrovascular death.

average IQRs are very similar (Table 53). However, as the IQRs for the difference between individual exposure and citywide average exposure (Table 53) were much smaller than the overall IQRs, within-city health effects estimates are scaled based on the increment of the median of the city-specific IQRs of the difference between individual exposure and citywide average exposure (values given in Tables 54 and 55).

The distributions of the exposures assigned to subjects in the within-city and between-city analysis from overall exposure, from citywide average exposure, and from the

difference between individual exposure and citywide average exposure can be compared (Table 53). The distributions of overall exposure and citywide average exposure were similar for PM_{2.5} mass and for each of the PM_{2.5} components. As expected, the means were identical and the range was smaller for the citywide average exposure. The median of the citywide average was slightly smaller for PM_{2.5} mass and for silicon, but was slightly larger for EC, and was not different for OC or for sulfur. The IQRs for citywide averages were slightly smaller, except for silicon, which was slightly larger. The citywide average

Table 55. Estimated Hazard Ratios for Time to First CVD Event Associated with an IQR Increase of Within-City Baseline Exposure Using National Spatial Model Predictions^a

Pollutant	IQR ^b (µg/m ³)	CVD Event ^c (n = 2246) HR (95% CI)	CHD ^d (n = 1562) HR (95% CI)	Cerebrovascular Disease ^e (n = 766) HR (95% CI)	MI (n = 714) HR (95% CI)	Coronary Revascularization (n = 1133) HR (95% CI)	Stroke (n = 708) HR (95% CI)
Total PM _{2.5} mass	1.04	1.01 (0.97 to 1.05)	1.01 (0.96 to 1.07)	1.02 (0.94 to 1.09)	1.02 (0.95 to 1.10)	0.99 (0.94 to 1.06)	1.02 (0.95 to 1.10)
EC	0.133	1.00 (0.96 to 1.05)	1.02 (0.96 to 1.07)	1.00 (0.92 to 1.08)	1.02 (0.94 to 1.11)	1.00 (0.94 to 1.07)	1.00 (0.92 to 1.08)
OC	0.401	1.01 (0.95 to 1.06)	1.04 (0.97 to 1.11)	0.99 (0.90 to 1.08)	1.04 (0.94 to 1.15)	1.03 (0.95 to 1.11)	0.99 (0.90 to 1.09)
S	0.033	1.02 (0.97 to 1.06)	1.02 (0.96 to 1.08)	1.04 (0.96 to 1.13)	1.05 (0.97 to 1.14)	1.01 (0.95 to 1.07)	1.05 (0.96 to 1.14)
Si	0.007	1.03 (0.99 to 1.07)	1.03 (0.98 to 1.07)	1.03 (0.97 to 1.11)	1.04 (0.97 to 1.11)	1.01 (0.96 to 1.07)	1.03 (0.96 to 1.11)

^a Total participants included = 45,980; events through year 2005 included. All estimates adjusted for age, ethnicity, education, household income, smoking, diabetes, hypertension, SBP, BMI, and hypercholesterolemia.

^b IQRs represent within-city variation in exposure to pollutants; within-city variation is smaller than overall or between-city variation (see Table 53).

^c MI, coronary revascularization, stroke, atherosclerotic cardiac disease death, possible CHD death, and cerebrovascular death.

^d MI, coronary revascularization, atherosclerotic cardiac disease death, and possible CHD death.

^e Stroke, cerebrovascular death.

SD values were identical for sulfur and silicon, slightly smaller for PM_{2.5} mass, and noticeably smaller for EC and for OC, suggesting that EC and OC had relatively smaller between-city variability, while sulfur and silicon had relatively larger between-city variability.

In the rows showing the distribution of values for the difference between individual exposure and citywide average exposure (Table 53), the mean value is zero for PM_{2.5} mass and for each of the PM_{2.5} components, as expected, since this exposure metric is centered on the citywide average exposure. Similarly, the median values are close to zero. Furthermore, for PM_{2.5} mass and for each of the PM_{2.5} components, the range and IQR are substantially smaller than for either overall exposure or citywide average exposure. This difference is most pronounced for sulfur and silicon, indicating that these components have relatively smaller within-city variability than EC or OC or PM_{2.5} mass.

Interpretation of the health effects results is limited by the smaller number of subjects that could be included in the between-city and within-city analyses (Tables 54 through 57) compared with the analysis using overall exposure. Interpretation is also complicated by the difference in scaling factors used; the between-city estimates used the overall IQR increments as in the primary analyses, while the within-city estimates used the smaller within-city IQR increments. For between-city exposure and CVD events (Table 54), the pattern of associations generally paralleled results for overall exposure (Table 51), but HRs were often smaller. In between-city analyses and events, the strongest evidence was for sulfur, where the greatest

portion of variance was also between cities rather than within cities. No significant associations were observed between within-city exposure variation and CVD events (Table 55), which may not be surprising given that for the components that had been most strongly associated with events in the overall analysis, a larger portion of the overall variance was from between-city contrasts than from within-city contrasts.

For between-city exposure and CVD deaths (Table 56), the pattern of associations also generally paralleled results for overall exposure (Table 52), but HRs were often smaller, with a few exceptions. Consistent with the overall analysis, the most substantial evidence was found for OC and CVD deaths (HR, 1.17; 95% CI, 0.96 to 1.44), atherosclerotic cardiac disease death (HR, 1.16; 95% CI, 0.78 to 1.74), and cerebrovascular death (HR, 1.29; 95% CI, 0.94 to 1.76). For within-city exposure and CVD deaths, the strongest evidence was seen for sulfur and OC, although EC was as strongly associated with death from atherosclerotic cardiac disease (Table 57).

Sensitivity Analyses

Secondary Covariates We conducted an analysis using two or more exposure measures in a common Cox proportional-hazards model for CVD events (Table 4 in Appendix I, available on the HEI Web site). First, total PM_{2.5} mass (HR, 1.09 per IQR; 95% CI, 1.03 to 1.15) was associated with CVD events in a model including distance to roadway (living within 100 m of an A1 or A2 roadway). The overall pattern observed was that associations

Table 56. Estimated Hazard Ratios for Time to CVD Death Associated with an IQR Increase of Between-City Baseline Exposure Using National Spatial Model Predictions^a

Pollutant	IQR ^b (µg/m ³)	CVD Death ^c (n = 398) HR (95% CI)	Atherosclerotic Cardiac Disease or Possible CHD Death (n = 227) HR (95% CI)	Atherosclerotic Cardiac Disease Death (n = 108) HR (95% CI)	Possible CHD Death (n = 119) HR (95% CI)	Cerebrovascular Death (n = 171) HR (95% CI)
Total PM _{2.5} mass	3.9	1.08 (0.92 to 1.26)	1.08 (0.88 to 1.33)	1.21 (0.89 to 1.63)	0.99 (0.74 to 1.31)	1.06 (0.84 to 1.34)
EC	0.21	1.06 (0.86 to 1.31)	1.08 (0.82 to 1.44)	1.10 (0.73 to 1.66)	1.06 (0.72 to 1.57)	1.02 (0.73 to 1.41)
OC	0.64	1.17 (0.96 to 1.44)	1.09 (0.83 to 1.43)	1.16 (0.78 to 1.74)	1.03 (0.72 to 1.49)	1.29 (0.94 to 1.76)
S	0.25	0.98 (0.88 to 1.10)	0.99 (0.85 to 1.15)	1.23 (0.99 to 1.54)	0.81 (0.67 to 0.995)	0.98 (0.83 to 1.16)
Si	0.07	1.02 (0.93 to 1.12)	1.07 (0.95 to 1.20)	0.90 (0.73 to 1.11)	1.18 (1.03 to 1.36)	0.96 (0.83 to 1.12)

^a Total participants included = 45,980; events through year 2005 included. All estimates adjusted for age, ethnicity, education, household income, smoking, diabetes, hypertension, SBP, BMI, and hypercholesterolemia.

^b IQRs represent overall variation in exposure to pollutants; between-city variations were very similar (see Table 53).

^c Atherosclerotic cardiac disease death, possible CHD death, and cerebrovascular death.

Table 57. Estimated Hazard Ratios for Time to CVD Death Associated with an IQR Increase of Within-City Baseline Exposure Using National Spatial Model Predictions^a

Pollutant	IQR ^b ($\mu\text{g}/\text{m}^3$)	CVD Death ^c ($n = 398$) HR (95% CI)	Atherosclerotic Cardiac Disease or Possible CHD Death ($n = 227$) HR (95% CI)	Atherosclerotic Cardiac Disease Death ($n = 108$) HR (95% CI)	Possible CHD Death ($n = 119$) HR (95% CI)	Cerebrovascular Death ($n = 171$) HR (95% CI)
Total PM _{2.5} mass	1.04	1.05 (0.95 to 1.17)	1.10 (0.96 to 1.26)	1.06 (0.87 to 1.30)	1.12 (0.92 to 1.37)	0.99 (0.85 to 1.17)
EC	0.133	1.05 (0.94 to 1.18)	1.12 (0.97 to 1.30)	1.25 (1.003 to 1.55)	1.01 (0.83 to 1.24)	0.96 (0.81 to 1.14)
OC	0.401	1.10 (0.96 to 1.26)	1.18 (0.98 to 1.42)	1.26 (0.97 to 1.66)	1.10 (0.86 to 1.42)	1.00 (0.81 to 1.23)
S	0.033	1.12 (1.00 to 1.26)	1.17 (1.02 to 1.34)	1.26 (1.04 to 1.52)	1.08 (0.88 to 1.33)	1.06 (0.89 to 1.26)
Si	0.007	1.04 (0.95 to 1.13)	1.04 (0.93 to 1.17)	1.01 (0.83 to 1.22)	1.07 (0.93 to 1.23)	1.03 (0.90 to 1.19)

^a Total participants included = 45,980; events through year 2005 included. All estimates adjusted for age, ethnicity, education, household income, smoking, diabetes, hypertension, SBP, BMI, and hypercholesterolemia.

^b IQRs represent within-city variation in exposure to pollutants; within-city variation is smaller than overall or between-city variation (see Table 53).

^c Atherosclerotic cardiac disease death, possible CHD death, and cerebrovascular death.

identified previously in models with only one component were robust to inclusion of multiple components or roadway proximity, even to the extreme of a model with all four components plus roadway proximity, in which persistent associations were observed for sulfur (HR per IQR, 1.11; 95% CI, 1.06 to 1.16). In addition, in the last model OC became statistically significant for total CVD events (HR, 1.12 per IQR; 95% CI, 1.03 to 1.23).

Another analysis was conducted using two or more exposure measures in a common Cox proportional-hazards model for CVD deaths (Table 5 in Appendix I, available on the HEI Web site). For CVD deaths, similar to the situation for CVD events, associations identified previously in models with only one PM_{2.5} component were generally robust to inclusion of multiple components or roadway proximity, even to the extreme of a model with all four components and roadway proximity. Chiefly, OC was always significantly associated with CVD death, and compared with the previous model that did not include other components, the magnitude of the association was larger in a model also adjusting for EC, sulfur, silicon, and roadway proximity (HR per IQR, 1.32; 95% CI, 1.08 to 1.62).

Previous CVD When women with a history of prior CVD at baseline were included, the number of study participants available for analysis increased to 66,270 and the number of CVD deaths nearly doubled to 883 (Table 58). There were few large or unexpected differences between the results of this analysis and those of the primary analysis, from which women with prior CVD were excluded (Table 52). In general, the precision of the associations

mostly increased, while the magnitude of the estimated HR was often slightly smaller. In contrast to results of the primary analysis, statistically significant associations were found for atherosclerotic cardiac disease deaths and possible CHD deaths combined with PM_{2.5} mass (HR per IQR, 1.16; 95% CI, 1.03 to 1.30) and with EC (HR per IQR, 1.13; 95% CI, 1.01 to 1.26), as well as for possible CHD deaths alone with PM_{2.5} mass (HR per IQR, 1.22; 95% CI, 1.03 to 1.44). While the association of OC with cerebrovascular deaths alone was no longer statistically significant, both the magnitude and precision of its association with atherosclerotic cardiac disease deaths or possible CHD deaths, either alone or combined, increased, while the precision (but not the magnitude) of the association of OC with total CVD deaths ($n = 883$) increased. As before, the only component significantly associated with CVD death was OC, which continued to have the largest estimate of effect of all PM_{2.5} components (HR per IQR, 1.21; 95% CI, 1.10 to 1.33). Furthermore, EC was significantly associated with deaths from CHD (atherosclerotic cardiac disease deaths and possible CHD deaths combined) (HR per IQR, 1.13; 95% CI, 1.01 to 1.26), but not with deaths from cerebrovascular disease. Results for the analysis of the effect of living near a major roadway that included women with prior CVD are given in Table 59. No significant associations were found between any of the roadway measures and any type of CVD death. The strongest evidence was for death from cerebrovascular disease, with similar associations for living within 100 m of an A1 or A2 roadway or within 50 m of an A3 roadway (HR, 1.26; 95% CI, 0.97 to 1.63) and for living within 100 m of an A1 or A2 roadway (HR, 1.30; 95% CI, 0.79 to 2.12).

Table 58. Estimated Hazard Ratios for Time to CVD Death Associated with an IQR Increase of Baseline Exposure Using National Spatial Model Predictions Including Women with Prior CVD^a

Pollutant	IQR ($\mu\text{g}/\text{m}^3$)	CVD Death ^b (<i>n</i> = 883) HR (95% CI)	Atherosclerotic Cardiac Disease or Possible CHD Death (<i>n</i> = 560) HR (95% CI)	Atherosclerotic Cardiac Disease Death (<i>n</i> = 301) HR (95% CI)	Possible CHD Death (<i>n</i> = 259) HR (95% CI)	Cerebrovascular Death (<i>n</i> = 323) HR (95% CI)
Total PM _{2.5} mass	3.9	1.07 (0.98 to 1.17)	1.16 (1.03 to 1.30)	1.11 (0.94 to 1.29)	1.22 (1.03 to 1.44)	0.93 (0.80 to 1.08)
EC	0.21	1.08 (0.99 to 1.18)	1.13 (1.01 to 1.26)	1.12 (0.96 to 1.31)	1.14 (0.97 to 1.34)	1.00 (0.86 to 1.16)
OC	0.64	1.21 (1.10 to 1.33)	1.26 (1.11 to 1.42)	1.35 (1.14 to 1.59)	1.18 (0.99 to 1.40)	1.14 (0.97 to 1.33)
S	0.25	1.01 (0.94 to 1.08)	1.05 (0.96 to 1.15)	1.10 (0.97 to 1.25)	1.00 (0.88 to 1.15)	0.93 (0.83 to 1.05)
Si	0.07	1.03 (0.96 to 1.09)	1.04 (0.97 to 1.13)	0.97 (0.87 to 1.09)	1.11 (1.001 to 1.23)	1.00 (0.90 to 1.11)

^a Total participants included = 66,270; events through year 2005 included. All estimates adjusted for age, ethnicity, education, household income, smoking, diabetes, hypertension, SBP, BMI, and hypercholesterolemia.

^b Atherosclerotic cardiac disease death, possible CHD death, and cerebrovascular death.

Table 59. Estimated Hazard Ratios for Time to CVD Death Associated with Living Near a Major Roadway at Baseline Including Women with Prior CVD^a

Model / Variable	CVD Death ^b HR (95% CI)	Atherosclerotic Cardiac Disease or Possible CHD Death HR (95% CI)	Atherosclerotic Cardiac Disease Death HR (95% CI)	Possible CHD Death HR (95% CI)	Cerebrovascular Death HR (95% CI)
No restriction per MSA ^c					
Number of deaths	883	560	301	259	323
A1 or A2 < 100 m or A3 < 50 m	1.06 (0.90 to 1.25)	0.95 (0.77 to 1.17)	1.01 (0.76 to 1.35)	0.87 (0.63 to 1.20)	1.26 (0.97 to 1.63)
A1 or A2 < 100 m	0.88 (0.63 to 1.24)	0.68 (0.43 to 1.09)	0.70 (0.37 to 1.32)	0.65 (0.32 to 1.32)	1.30 (0.79 to 2.12)
Only women living inside an MSA ^d					
Number of deaths	799	507	273	234	292
A1 or A2 < 100 m or A3 < 50 m	1.07 (0.90 to 1.27)	0.97 (0.78 to 1.21)	1.08 (0.80 to 1.44)	0.86 (0.62 to 1.20)	1.25 (0.95 to 1.64)
A1 or A2 < 100 m	0.90 (0.63 to 1.29)	0.72 (0.44 to 1.16)	0.78 (0.41 to 1.48)	0.63 (0.30 to 1.35)	1.28 (0.76 to 2.17)

^a Events through year 2005 included. All estimates adjusted for age, ethnicity, education, household income, smoking, diabetes, hypertension, SBP, BMI, and hypercholesterolemia.

^b Atherosclerotic cardiac disease death, possible CHD death, and cerebrovascular death.

^c Total participants included = 66,270.

^d Total participants included = 58,782; women with baseline address outside of all MSA boundaries excluded.

Random Effects A sensitivity analysis was conducted including random effects for city, specified as the MSA of the participant’s baseline residential address. The methodology for identifying the MSA is the same as described previously for the sensitivity analyses except that MSAs with fewer than 20 subjects were included in the random effects analysis. The Cox regression model including a random effect is termed a frailty model and was fit with SAS statistical software version 9.3 using the penalized partial likelihood approach in which the variance of the error term is assumed to follow the normal distribution. Adjusted Wald-type tests were performed after penalized frailty modeling to evaluate the contribution of the random effect. The adjusted Wald *P* values for the random effects were significant for all models of CVD events but not for CVD deaths. Including an MSA-level random effect term had little effect on the estimated HR values or 95% CIs (Table 60): for all exposures and all outcomes, the CIs were widened slightly and the estimated HRs were often unchanged or changed only slightly in the random effects model. This suggests that little residual variance remained in our data after fitting our primary model for health effects without the random effect. Results from this sensitivity analysis were consistent with the primary analysis: our initial findings were robust to the inclusion of a frailty (random effect) term in the models. When comparing the estimated effects from the pairs of models, it should be noted that the interpretation of parameters from models with fixed effects and random effects are not identical, regardless of the statistical significance of the random

effect terms (or other terms). In short, inclusion of the random effect in the frailty model does not change the conclusions of our primary analyses in the nonfrailty models.

Time-Varying Exposure We also conducted an analysis using time-varying exposure based on national spatial model predictions and the participant’s residential history (described in Appendix I, available on the HEI Web site). The exposures studied were 1-year and 2-year averages before the CVD event or death. Findings for CVD events were essentially unchanged from findings using baseline addresses and national spatial model exposure predictions. For CVD deaths, findings differed somewhat from those obtained using baseline addresses. Chiefly, the time-varying approach identified more evidence for an effect of EC on death. In the analysis using a 1-year average, EC showed significant effects on CVD deaths and on atherosclerotic cardiac disease death, which were 40% to 45% larger than effects observed using baseline exposure. The effect of PM_{2.5} mass on CVD deaths also increased, but the effect of OC did not. In the time-varying analysis using a 2-year average, EC had a significant effect on death from atherosclerotic cardiac disease alone.

Results Using Secondary Estimates of Exposure

Citywide Average Estimates of Exposure When health endpoints were analyzed in the WHI-OS cohort using estimates of exposure to PM_{2.5} components based on citywide means (described in Appendix I, available on the HEI Web

Table 60. Nonfrailty and Frailty Models for Estimated Hazard Ratios for Time to CVD Event or CVD Death Associated with an IQR Increase of Baseline Exposure Using National Spatial Model Predictions and Only Women Who Lived Within an MSA^a

Pollutant	IQR (µg/m ³)	CVD Event ^b (n = 2276)		CVD Death ^d (n = 403)	
		Nonfrailty HR (95% CI)	Frailty ^c HR (95% CI)	Nonfrailty HR (95% CI)	Frailty ^c HR (95% CI)
Total PM _{2.5} mass	3.9	1.06 (1.001 to 1.13)	1.07 (0.99 to 1.15)	1.09 (0.95 to 1.26)	1.10 (0.94 to 1.29)
EC	0.21	0.97 (0.91 to 1.03)	0.98 (0.92 to 1.05)	1.07 (0.93 to 1.23)	1.07 (0.93 to 1.25)
OC	0.64	1.02 (0.96 to 1.08)	1.02 (0.95 to 1.09)	1.18 (1.01 to 1.36)	1.17 (1.002 to 1.37)
S	0.25	1.07 (1.02 to 1.12)	1.07 (1.003 to 1.14)	1.00 (0.90 to 1.12)	1.00 (0.88 to 1.14)
Si	0.07	0.96 (0.92 to 1.00)	0.97 (0.92 to 1.02)	1.02 (0.93 to 1.11)	1.02 (0.91 to 1.13)

^a Total participants included = 46,586; events through year 2005 included. All estimates adjusted for age, ethnicity, education, household income, smoking, diabetes, hypertension, SBP, BMI, hypercholesterolemia.

^b MI, coronary revascularization, stroke, atherosclerotic cardiac disease death, possible CHD death, and cerebrovascular death.

^c Frailty model includes random effect term for MSA of subject baseline residence.

^d Atherosclerotic cardiac disease death, possible CHD death, and cerebrovascular death.

site), findings differed somewhat from findings based on individual-level predictions made using the national spatial model. For CVD events, in addition to an effect of $PM_{2.5}$, the only $PM_{2.5}$ component that showed an effect was SO_4 (Table 10 in Appendix I), in keeping with the national spatial model exposure analysis (Table 50). For CVD deaths specifically, SO_4 was the only component that showed no effect. Only EC had an effect on deaths from atherosclerotic cardiac disease specifically. Using the national spatial model exposure estimates, only OC showed statistically significant effects on CVD deaths, although smaller, nonsignificant effects of EC were also seen (Table 52). Citywide average nickel concentrations were also calculated for these analyses, but nickel exposure showed no effect on either total CVD events or CVD deaths.

Traffic Exposure Measures The associations between measures of proximity to roadway, estimated using baseline addresses, and time to first CVD event are given in Table 61, and those with time to CVD death are shown in Table 62. For the first dichotomous measure of living within 100 m of an A1 or A2 roadway, or within 50 m of an A3 roadway, versus living farther from these roadways, the HR associated with incidence of CVD events was positive, but not statistically significant (HR, 1.06; 95% CI, 0.96 to 1.17), with similarly consistent results for each individual CVD event category.

For the second dichotomous measure of living within 100 m of an A1 or A2 roadway versus living farther from these roadways, HRs were generally larger. Associations that were positive, but not statistically significant, were found for incidence of CVD events (HR, 1.18; 95% CI, 0.98 to 1.42), CHD (HR, 1.12; 95% CI, 0.89 to 1.41), cerebrovascular disease (HR, 1.26; 95% CI, 0.92 to 1.71), coronary revascularization (HR, 1.26; 95% CI, 0.97 to 1.63), and stroke (HR, 1.30; 95% CI, 0.94 to 1.78).

Restriction of the analysis to women living within the boundaries of an MSA at baseline, effectively excluding women living in the most rural areas, reduced the number of subjects from 52,539 to 46,411. Results for living within 100 m of an A1 or A2 roadway or within 50 m of an A3 roadway and all CVD events were similar to results without the restriction. However, results for the second measure proved to be sensitive to the restriction. Among women who resided inside the boundaries of an MSA, living within 100 m of an A1 or A2 roadway versus living farther from these roadways significantly increased risk of all CVD events (HR, 1.23; 95% CI, 1.01 to 1.50), cerebrovascular disease (HR, 1.40; 95% CI, 1.02 to 1.92), and stroke (HR, 1.44; 95% CI, 1.04 to 2.00).

Interpretation of the results for time to CVD death was limited by wide CIs. The largest HRs were for living within 100 m of an A1 or A2 roadway and CVD death (HR, 1.06; 95% CI, 0.68 to 1.67), atherosclerotic cardiac disease death

Table 61. Estimated Hazard Ratios for Time to First CVD Event Associated with Living Near a Major Roadway at Baseline^a

Model / Variable	CVD Event ^b HR (95% CI)	CHD ^c HR (95% CI)	Cerebrovascular Disease ^d HR (95% CI)	MI HR (95% CI)	Coronary Revascularization HR (95% CI)	Stroke HR (95% CI)
No restriction per MSA ^e						
Number of events	2532	1764	863	800	1285	800
A1 or A2 < 100 m or A3 < 50 m	1.06 (0.96 to 1.17)	1.08 (0.96 to 1.21)	1.09 (0.92 to 1.29)	1.07 (0.90 to 1.27)	1.12 (0.97 to 1.28)	1.13 (0.95 to 1.34)
A1 or A2 < 100 m	1.18 (0.98 to 1.42)	1.12 (0.89 to 1.41)	1.26 (0.92 to 1.71)	0.99 (0.69 to 1.43)	1.26 (0.97 to 1.63)	1.30 (0.94 to 1.78)
Only women living inside an MSA ^f						
Number of events	2276	1580	779	725	1145	721
A1 or A2 < 100 m or A3 < 50 m	1.07 (0.96 to 1.18)	1.09 (0.96 to 1.24)	1.09 (0.91 to 1.30)	1.03 (0.86 to 1.24)	1.12 (0.97 to 1.30)	1.13 (0.94 to 1.35)
A1 or A2 < 100 m	1.23 (1.01 to 1.50)	1.14 (0.89 to 1.45)	1.40 (1.02 to 1.92)	1.00 (0.69 to 1.46)	1.28 (0.97 to 1.68)	1.44 (1.04 to 2.00)

^a Events through year 2005 included. All estimates adjusted for age, ethnicity, education, household income, smoking, diabetes, hypertension, SBP, BMI, and hypercholesterolemia.

^b MI, coronary revascularization, stroke, atherosclerotic cardiac disease death, possible CHD death, and cerebrovascular death.

^c MI, coronary revascularization, atherosclerotic cardiac disease death, and possible CHD death.

^d Stroke, cerebrovascular death.

^e Total participants included = 52,539.

^f Total participants included = 46,411; women with baseline address outside of all MSA boundaries excluded.

Table 62. Estimated Hazard Ratios for Time to CVD Death Associated with Living Near a Major Roadway at Baseline^a

Model/Variable	CVD Death ^b HR (95% CI)	Atherosclerotic Cardiac Disease or Possible CHD Death HR (95% CI)	Atherosclerotic Cardiac Disease Death HR (95% CI)	Possible CHD Death HR (95% CI)	Cerebrovascular Death HR (95% CI)
No restriction per MSA ^c					
Number of deaths	445	254	120	134	191
A1 or A2 < 100 m or A3 < 50 m	0.92 (0.72 to 1.17)	0.89 (0.64 to 1.24)	1.07 (0.68 to 1.68)	0.75 (0.47 to 1.20)	0.94 (0.65 to 1.36)
A1 or A2 < 100 m	1.06 (0.68 to 1.67)	0.80 (0.41 to 1.57)	1.20 (0.52 to 2.76)	0.49 (0.15 to 1.54)	1.45 (0.78 to 2.68)
Only women living inside an MSA ^d					
Number of deaths	403	228	108	120	175
A1 or A2 < 100 m or A3 < 50 m	0.95 (0.74 to 1.22)	1.00 (0.72 to 1.39)	1.23 (0.78 to 1.96)	0.81 (0.50 to 1.32)	0.88 (0.60 to 1.31)
A1 or A2 < 100 m	1.07 (0.66 to 1.72)	0.80 (0.39 to 1.63)	1.34 (0.58 to 3.09)	0.37 (0.09 to 1.49)	1.48 (0.78 to 2.83)

^a Events through year 2005 included. All estimates adjusted for age, ethnicity, education, household income, smoking, diabetes, hypertension, SBP, BMI, and hypercholesterolemia.

^b Atherosclerotic cardiac disease death, possible CHD death, and cerebrovascular death.

^c Total participants included = 52,539.

^d Total participants included = 46,411; women with baseline address outside of all MSA boundaries excluded.

(HR, 1.20; 95% CI, 0.52 to 2.76), and cerebrovascular death (HR, 1.45; 95% CI, 0.78 to 2.83). When analysis was restricted to those women living within an MSA, these ratios increased, as in the analysis of CVD events, but estimates remained imprecise (Table 62).

DISCUSSION

MAIN HEALTH EFFECTS FINDINGS

The epidemiologic work described in this section of the report culminated in a spectrum of observational analyses of the health effects of exposure to components of ambient PM_{2.5}. In the MESA cohort, the focus was on subclinical measures of atherosclerosis, specifically CIMT and CAC, while in the WHI-OS cohort, the focus was on both general and more specific time-to-event cardiovascular endpoints. Our intent at the outset was to investigate effects of selected PM_{2.5} components and compare effects across several classes of components. To this end, we focused the analyses on EC and OC as reflecting a variety of combustion processes, as well as secondary organic aerosols in the case of OC. Our working hypothesis was that PM_{2.5} components produced from combustion processes would be associated with more cardiovascular effects than other PM_{2.5} components. Silicon and SO₄ (with sulfur used as a

surrogate for SO₄ in MESA Air) were selected as PM_{2.5} components that reflect other sources and processes, specifically airborne crustal matter and secondary inorganic aerosols, respectively.

Results of the health effects analyses only partly supported the working hypothesis. In the MESA cohort, findings of the cross-sectional analysis were different for CIMT and CAC. Regardless of the approach used for predicting exposure, there was evidence of overall cross-sectional associations between OC and CIMT (Figures 29 and 31). In the longitudinal analysis, which was limited by the short follow-up period, in particular, there was little evidence that OC was associated with CIMT progression. There was little evidence that OC was associated with the presence or magnitude of CAC (among participants with nonzero Agatston scores), although findings using OC predictions from the national spatial model were suggestive of an association between OC and the presence of CAC.

In the WHI-OS cohort, when CVD events, including deaths, were analyzed, there was good evidence that estimated exposure to OC was associated with morbidity and mortality related to cerebrovascular disease and stroke, but not with other CVD event categories (Table 51). In the analysis of CVD deaths alone, however, there was good evidence that OC was associated with deaths from CVD in

general and with several subcategories, including deaths from atherosclerotic cardiovascular disease and deaths from cerebrovascular disease (Table 52).

Compared with results for OC, there was much less evidence for associations between estimated exposure to EC and either CIMT or CAC in the MESA cohort; with the MESA Air/NPACT spatiotemporal model predictions, there was a suggestion that EC was protective against $\log(\text{CAC})$ among individuals with nonzero Agatston scores. In the WHI-OS cohort, there was also little evidence for associations of EC with total CVD events, but somewhat better evidence for associations with CVD deaths, except for death from cerebrovascular disease, for which the evidence was weak.

Interestingly, there was also evidence of some associations between cardiovascular endpoints and the $\text{PM}_{2.5}$ components we chose to reflect noncombustion sources or processes (silicon and sulfur). In the MESA cohort, using predictions from both the spatiotemporal model and the national spatial model, the evidence that sulfur was associated cross-sectionally with CIMT was as good as that for OC. In the WHI-OS cohort, there was good evidence that estimated exposure to sulfur was associated with CVD events in general and with all of the CVD event subsets. The evidence for an association between sulfur and CVD deaths, however, was weaker. Evidence for associations of the cardiovascular endpoints with silicon was weaker overall, with some evidence for a cross-sectional association with CIMT, but not with CAC, in the MESA cohort, but little evidence for associations with CVD events or CVD deaths in the WHI-OS cohort.

Comparing estimated health effects across pollutants on the IQR scale, we found little evidence that the associations with the $\text{PM}_{2.5}$ components were stronger than those with $\text{PM}_{2.5}$ itself. The one exception was the CIMT effects estimated using the spatiotemporal model, for which the estimated effects of OC and sulfur were larger than the $\text{PM}_{2.5}$ effect estimate. In other cases, such as that of deaths from stroke in the WHI-OS cohort, for which the estimated effect of OC was much larger than that of $\text{PM}_{2.5}$, the width of the respective CIs precluded drawing firm conclusions about the relative sizes of the effects.

The pattern of results in the MESA analyses was generally similar for the health effects estimated using exposure predictions from the spatiotemporal model and the national spatial model. There were two exceptions: first, the evidence for an association of silicon with CIMT was weaker with exposure predictions from the spatiotemporal model, owing to wider CIs; and second, there was suggestive evidence of an association between OC and the presence of CAC using exposure predictions from the

national spatial model, but comparatively less evidence using predictions from the spatiotemporal model, again owing to wider CIs.

Sensitivity analyses in the MESA cohort produced results that were robust to some model specifications, but sensitive to others. There was little sensitivity of findings to more extended covariate models or to control for NO_2 or SO_2 . In contrast, many findings were sensitive to adjustment for city, which resulted in wider CIs, as expected, and some notable changes in effect estimates as well. For instance, in the city-adjusted cross-sectional analyses of $\text{PM}_{2.5}$ and OC in single-pollutant models using exposure predictions from the spatiotemporal model, effect estimates for CIMT were greatly attenuated, whereas effect estimates for the presence of CAC became larger. In models including two $\text{PM}_{2.5}$ components, findings for an association with CIMT were generally insensitive to the addition of the second $\text{PM}_{2.5}$ component. Notable exceptions were the weakening of the cross-sectional association with sulfur when OC was added to the analysis using predicted exposures from the spatiotemporal model (Figure 33) and the weakening of the estimated cross-sectional association with OC when silicon was added to the analysis using predicted exposures from the national spatial model (Figure 34). Control for the other $\text{PM}_{2.5}$ components in health analyses in the WHI-OS cohort showed that findings were generally robust, in particular, the OC association with CVD deaths and the OC and sulfur associations with CVD events. Finally, in limited analyses, correction for exposure measurement errors did not suggest that the use of predicted exposures had much impact on effect estimates, although there was loss of precision in some instances.

Analyses for MESA participants of predicted exposure to some $\text{PM}_{2.5}$ components and gaseous pollutants other than those of primary interest showed CIMT associations with SO_4 , as expected from the findings for sulfur, and with copper. There was comparatively less evidence for associations with NO_3 , SO_2 , and nickel, and little evidence for associations with NO_2 or vanadium.

ESTIMATION OF EXPOSURE

In order to complete the analyses of health effects described here involving the MESA and WHI-OS cohorts, we undertook a large monitoring and modeling effort to estimate individual exposures to $\text{PM}_{2.5}$ components. We based our approach on the premise that estimating exposure at the individual level would reduce exposure measurement error compared with other approaches that either assigned exposure at larger spatial scales or involved more ad hoc models (such as nearest-monitor models), and that this reduction in measurement error would result

in more valid (that is, less biased) and precise estimates of health effects. This premise, which also guided the approach to exposure estimation in the parent MESA Air study, allowed us to exploit the approach to exposure modeling used in that study.

Our proposed approach in the MESA analyses, specifically, was to use the intensive MESA Air/NPACT monitoring campaign to provide a data set that was more spatially dense than is typically available in monitoring networks that are used for regulatory purposes or designed specifically for research studies. To this end, monitors were employed at several fixed sites in each city to capture information on within-city temporal trends over space, and a rotating set of home-outdoor monitors was used to capture information with finer spatial resolution in each city. For the $PM_{2.5}$ components, concentrations of metals and other elements were obtained from Teflon filters and so were available over the entire time period of MESA Air monitoring, up to 4 years (Figure 3). The monitoring using quartz-fiber filters, from which EC and OC concentrations were obtained, took place over a shorter period of slightly more than 1 year. In addition to our relatively rich monitoring data, our exposure models made use of state-of-the-art methods for modeling spatiotemporal data utilizing an extensive set of geographic data and geostatistical spatial modeling.

We hoped that such an intensive monitoring campaign, coupled with our spatiotemporal modeling approach, would allow us to build models for exposure to $PM_{2.5}$ components that would provide better exposure predictions and result in better health effects estimates than studies with exposure predictions based on less-rich monitoring data. We assessed the validity of the exposure predictions for both the spatiotemporal model of exposure to $PM_{2.5}$ components and the national spatial model by using cross-validation methods to generate performance statistics for assessing the models' predictive ability. Cross-validation is an approximation to out-of-sample assessment. We relied partly on R^2 values for this purpose, but realize that R^2 is sensitive to the degree of variability in the data. Furthermore, the performance statistics do not account for potentially important differences in the monitoring network designs. The monitors in the MESA Air/NPACT network, for example, are aligned more closely with the study population than those in the CSN and IMPROVE networks.

Based on our overall cross-validated R^2 estimates, the predictive ability of the MESA Air/NPACT spatiotemporal model was generally good to excellent within each city, with variations depending on the city and the $PM_{2.5}$ component (Table 29); the overall R^2 statistics showed strong

predictive ability when summarized over all six cities. Although it is not yet clear how to best remove the role of time from these assessments, we did not aim for our model performance statistics to reflect our ability to predict temporal trends, since a goal of NPACT is to obtain good predictions of long-term exposure averages. Our attempts at calculating temporally adjusted R^2 values produced generally poorer performance statistics, but they tended to be better when summarized across the MESA cities, since these include the differences in concentrations across the cities.

The predictive ability of the national spatial model, which utilized only existing data from the CSN and IMPROVE monitoring networks, was modest to excellent across the continental United States, depending on the $PM_{2.5}$ component. Although it was difficult to adequately restrict the assessment of the national spatial model to the same MESA areas used in the spatiotemporal model, when we restricted the cross-validation to monitors within 200 km of each MESA city, the R^2 statistics were generally not much changed, apart from worsened predictions for silicon and improved predictions for nickel. We could not do a true out-of-sample comparison of the two models because the national spatial model could not be validated against the NPACT or snapshot data; not only did the two models rely on data from different networks, but also both the NPACT and snapshot data were 2-week measurements, while the national spatial model was restricted to annual average concentrations. Thus, we are unable to make a completely fair comparison of the predictive abilities of the MESA Air/NPACT spatiotemporal model and the national spatial model.

Our spatiotemporal model represents a state-of-the-art approach to modeling pollution exposure that directly uses all available space-time data. It has the advantage of being able to use highly imbalanced space-time data, such as that collected in the MESA Air study, in which the number of sites with measurements available over long time periods was limited. To obtain good estimates from this sophisticated model, appropriate high-quality inputs are needed: in particular, well-measured pollutant concentrations, a monitoring design that provides data that are rich in space and time and is tuned to the important sources of variation in the region of interest, geographic covariate data that have been appropriately selected and are accurate, and an underlying pollutant field that is sufficiently variable to be amenable to modeling. In the NPACT study, in comparison with the parent MESA Air study, several limitations with respect to these qualities potentially adversely affected the performance of the spatiotemporal model. Most important were the more

limited specialized sampling of $PM_{2.5}$ components done for the NPACT study and our inability to combine MESA Air data with the regulatory monitoring data, which affected the temporal and spatial coverage of our model. The NPACT sampling also presented difficulties in obtaining precise measurements of some components, particularly the carbon measures, and was not focused heavily on non-traffic-related sources that were needed for modeling some of the components. For most of these limitations, we can only speculate on their impact on our work.

First, the limited specialized sampling may have affected the quality of our results. For instance, because we were unable to combine MESA Air/NPACT data with regulatory monitoring data in our analysis, there were very few fixed-site monitors in each of the MESA cities. In addition, the monitoring period for EC and OC was relatively short. Thus, we had limited data with which to estimate the spatial-temporal trends or the variability over space of pollutant concentrations. By necessity, we limited our temporal trend model to have only one covariate and no spatial variability.

Second, unlike the data sets used to predict $PM_{2.5}$ and NO_x in MESA Air, there were very few NPACT sites that could provide any pure (that is, temporally unconfounded) estimates of spatial variation. The lack of any rich source of pure spatial information in our data sets, from either long-term average concentrations or spatial snapshots, hampered our ability to separate spatial variation from temporal variation.

Third, because the spatial area of the fixed and home-outdoor monitoring sites in MESA Air/NPACT was relatively restricted, the areas covered by the spatiotemporal model for $PM_{2.5}$ components were much smaller than those covered by the MESA Air model for $PM_{2.5}$ and NO_x . Smaller areas have inherently less spatial variability, and it is more difficult to develop models in the presence of less predictable variability.

Fourth, the quality of the monitoring data could also affect the predictive ability of the exposure model. In exploratory work not reported here, we compared spatiotemporal exposure modeling and predictions for EC and LAC. We found that the model performed somewhat better for LAC than for EC, even when we restricted the LAC data to the shorter time period and spatial intensity of monitoring that were available for EC. The relationship between the NPACT LAC measurements and the CSN EC measurements was less variable than that between the NPACT and CSN EC measurements (Appendix L, available on the HEI Web site), suggesting that relatively poor precision of the monitoring data could adversely affect the performance of spatiotemporal model predictions. We do

not yet know how this might influence model predictions for the other PM components.

A supplemental monitoring study (Appendix F, available on the HEI Web site) was carried out in NPACT to assess the correspondence between CSN monitoring data for the $PM_{2.5}$ components and MESA Air/NPACT data. Specifically, the aim was to assess the importance of the MESA Air/NPACT monitoring equipment and sampling schedule on concentration measurements. The effect of equipment was assessed by mimicking the AQS sampling cycle of 1 day in 3 days using the MESA Air/NPACT monitoring equipment. The effect of the sampling schedule was assessed by comparing, using the MESA Air/NPACT monitoring equipment, 2-week averages obtained with the sampling cycle of 1 day in 3 days with the 2-week sampling cycle. The data generated with the two different sets of monitoring equipment and under the two different monitoring schedules were generally well correlated. However, while there was good correspondence for total carbon measurements, the MESA Air measurements tended to give somewhat higher concentrations for EC and lower concentrations for OC than the CSN measurements (Figures 7 and 8 in Appendix K, available on the HEI Web site).

Uncertainties in the measurement of EC and OC from the 2-week MESA Air/NPACT monitoring campaign have no bearing on the predictions made using the national spatial model and are therefore not relevant to either the MESA health effects analyses conducted with exposure predictions from that model or the WHI-OS health effects analyses. They could, however, have an effect on the MESA health effects analyses conducted using the predictions made with the spatiotemporal model. To attempt to gain insight into the effect of the differences in the CSN and NPACT measurements of EC and OC, we adjusted values of EC and OC by calibrating our total carbon measurements against the CSN total carbon measurements from collocated monitors and our MESA Air LAC measurements against the CSN EC measurements. The differences between these adjusted total carbon and LAC values (now as EC) were then used to obtain adjusted values for OC. Spatiotemporal model predictions were then obtained for the adjusted EC and OC values. In Appendix Q (available on the HEI Web site), we provide cross-validation statistics for these adjusted measurements, compare the adjusted predictions for the MESA cohort with our original predictions, and present the findings of a sensitivity analysis in which we replace our original spatiotemporal model predictions of EC and OC with predictions of the adjusted measurements. The results of the sensitivity analysis were reassuring in that the general pattern of associations between health effects and EC and OC was unchanged.

The estimated effect of OC on CIMT, however, was attenuated, due in large part to inclusion of data from New York, in which there was little correlation between the original and adjusted OC or EC values. In short, even though there were differences between the AQS measurements and our MESA/NPACT EC and OC measurements, these differences did not change our overall conclusions.

Finally, the set of geographic covariates we considered could also have affected our modeling results. Though we used a very large set of geographic data in our models, the data may not have been highly relevant for some of the PM_{2.5} components, particularly silicon and sulfur. Lack of good geographic predictors may explain the relatively poor performance of some of the sulfur and silicon models in some of the areas (Table 28), or the distribution of monitoring sites may not have adequately reflected the geographic variability of these PM_{2.5} components in the study areas. Variability in the adequacy of the geographic predictors and the distribution of monitoring sites across the six cities may also partly explain why the accuracy of predictions for all four of the primary PM_{2.5} components analyzed varied across the six cities, being generally best in Los Angeles and worst in Winston-Salem.

The time period of exposure that is most important in determining the cardiovascular effects of PM exposure is not known, so it is not possible to specify the most relevant period of exposure. It would be preferable to use exposure estimates that precede measurement of the health outcome, or that precede or overlap with the period of time over which longitudinal outcomes are measured. In the MESA cohort, CIMT and CAC were measured between 2000 and 2002, with follow-up measurements obtained up to approximately 3 years later. Monitoring in MESA Air took place from 2005 to 2009 (Figure 8). In the WHI-OS cohort, accrual of events began in 1994 to 1998, and the rate of accrual accelerated with time as the cohort aged through mid-2005. We based the national spatial model on monitoring data from 2009. In both cohorts, then, monitoring data were obtained after the health outcome data.

Using PM_{2.5} predictions, we were able to conduct one set of sensitivity analyses to directly assess the importance of the lack of temporal correspondence in our exposure and health data. We compared the differences in PM_{2.5} predictions from MESA Air's spatiotemporal model for the year 2000 (Sampson et al. 2011) and the more recent time periods that we used in our spatiotemporal and national spatial models (shown in Appendix M, available on the HEI Web site). The PM_{2.5} level in 2000 was higher across all locations, but there was relatively little systematic difference in the relationship between PM_{2.5} concentrations in the two time periods across most sites.

The exception was Los Angeles, where there was relatively more PM_{2.5} in the locations with higher concentrations in 2000. For PM_{2.5} we found relatively little change in our health effects estimates from the two time periods, although in general the PM_{2.5} predictions from 2000, the more temporally aligned exposure time period, gave somewhat higher effect estimates with narrower CIs. We were unable to make this direct comparison for PM_{2.5} components, but we hypothesize that the relationships are similar.

Another important issue to consider in addressing the utility of basing the exposure models on monitoring data that are temporally misaligned is the possibility that the spatial relationships between the geographic variables that play a central role in our exposure estimation models and the PM_{2.5} component concentrations have changed, and that these changes differ by location. For example, emissions from individual motor vehicles, both gasoline-powered and diesel-powered, have declined over time. For a given degree of traffic intensity, the relationship between a measure of traffic intensity and, for example, EC concentration at the time of our monitoring may be different from that at a previous time period of interest, which would result in increased exposure measurement error. Although we have not been able to directly address the potential impact of such error in our health effects models for the PM_{2.5} components, the findings for PM_{2.5} provide some reassurance that the impact is likely to be small.

Change of residence could introduce another source of exposure measurement error. We did not incorporate change of residential address during the follow-up period into the primary WHI-OS analyses; rather, we assumed that the address at enrollment into the cohort adequately reflected exposure throughout the follow-up period. Obviously, this assumption is incorrect for study participants who moved during follow-up. In a sensitivity analysis, we assigned exposure at the address of each participant for both the 1- and 2-year periods before a CVD event and repeated the health analyses. There was no meaningful change in these findings from those of the primary analysis (shown in Appendix I, available on the HEI Web site), apart from stronger evidence for an association of EC with, specifically, CVD deaths. For the MESA cohort, we have data on all residential addresses since enrollment and for 15 years preceding enrollment. The exposure estimates we used in the longitudinal analysis incorporated individual residential history since enrollment. A cumulative measure of exposure that incorporates a time-weighted estimate for any specified time window of exposure could also be calculated and used as an alternative exposure estimate. Such modifications in exposure estimation could potentially reduce exposure measurement error.

INTERPRETATION AND LIMITATIONS OF THE FINDINGS

Of the PM_{2.5} components considered in this study, OC and sulfur exhibited the most consistent associations with health effects in the analyses of the MESA and WHI-OS cohorts, as summarized above under “Main Health Effects Findings.” There was comparatively little evidence of such associations for EC, the other combustion-related PM_{2.5} component. OC is a complex mixture of multiple organic compounds in primary emissions from many combustion sources, as well as organic compounds formed secondarily in the atmosphere, the secondary organic aerosols. The findings regarding OC raise several questions, including whether there are certain classes of organic compounds that are particularly toxic, whether primary organic emissions are more toxic than secondary organic aerosols, whether organic compounds in the vapor phase and semi-volatile organic compounds, in general, contribute to or drive the toxicity, and whether some feature of our monitoring and measurement campaign or prediction modeling approaches, or both, were driving the results for OC. These questions are being addressed by currently ongoing research and will likely frame future research hypotheses. The source apportionment provided insight into the sources of OC in the MESA analyses. OC showed strong correlations with a single factor related to secondary formation processes, or primary gasoline and biomass emissions, or both. In Los Angeles, Chicago, and New York, emissions from gasoline-powered vehicles appeared to be important contributors to the OC levels, whereas in St. Paul, Winston-Salem, and Baltimore, there was evidence of important contributions from biomass combustion.

Of the other three primary PM_{2.5} components analyzed, sulfur exhibited the most notable associations with health effects in the MESA and WHI-OS cohorts. We used sulfur as an indicator of SO₄, a secondary aerosol. In the source apportionment, sulfur was correlated with a single factor, which also contained some OC in all cities except St. Paul. This factor contributed to the total PM_{2.5} mass primarily in the summer, and these contributions were nearly equal across all fixed monitoring sites within each city except Los Angeles, where there was an additional contribution from regional sources associated with oil combustion.

Sulfur was used as a surrogate measure of SO₄, for which there were no direct measurements available from MESA Air/NPACT monitoring. Sulfur was used in the national spatial model in order to be consistent with the MESA Air/NPACT spatiotemporal model. Because SO₄ measurements were available from both of the data sources for the national spatial model (the CSN and IMPROVE networks), we used the national spatial model to generate

SO₄ exposure predictions for the MESA participants and conducted a sensitivity analysis to determine the impact of these exposure predictions on health endpoints. The associations between health effects and estimated SO₄ exposure in the MESA participants were nearly identical to those for sulfur. This suggests that it was reasonable to consider sulfur to be a good measure of SO₄ also in the analyses utilizing exposure predictions from the spatiotemporal model, for which SO₄ estimates were not available.

The evidence that exposure to secondary SO₄ has direct adverse effects on health is weak (Grahame and Schlesinger 2005). However, in both the MESA and WHI-OS cohorts, the evidence indicating associations between health effects and SO₄ (or sulfur) was as strong as the evidence for OC. Because SO₄ is present in the ambient air as part of a complex and highly correlated mixture of pollutants, it is not possible to implicate exposure to SO₄ itself as underlying the associations that were observed. The Integrated Discussion (Section 3 of this report) attempts to make use of the findings from the parallel animal toxicology study (Section 2 of this report), in which the effects of SO₄ can be directly assessed, in concert with the epidemiologic findings of this study, to gain insight into the question of SO₄ effects.

There was comparatively less evidence that silicon was associated with the health endpoints. Silicon was selected as a reflection of PM_{2.5} related to crustal sources. Findings from the source apportionment supported that contention in five of the six cities, but less so in Chicago, where several sources were major silicon contributors, including industrial emissions.

We found little evidence of associations between the health endpoints and EC, which is traditionally taken to reflect emissions largely from diesel engines and biomass combustion. The source apportionment indicated that EC was moderately correlated with primary emissions from vehicles in all cities, but no strong correlations with any particular factor were evident in any of the cities.

To interpret our findings regarding OC and EC, issues relating to the monitoring and measurement of these components and the exposure modeling must be considered. First, the sensitivity analysis using predictions for EC and OC that were adjusted to be more in line with AQS measurements showed a pattern of results in keeping with the original analyses, suggesting that differences in the monitoring and measurements were not critical. Second, the reasonable consistency between the health effects findings in MESA analyses based on exposure predictions from the spatiotemporal model and the predictions based on the national spatial model also suggests that the uncertainties in our OC and EC measurements and modeling did not

have a great effect on the health effects estimates. Third, as discussed further below, results of health effects analyses using our secondary exposure estimates in the MESA cohort that did not make use of spatiotemporal prediction modeling were consistent with those that used the spatiotemporal model predictions. Finally, the findings from our WHI-OS analyses also showed the strongest evidence for associations of health effects with OC and sulfur, but relatively little evidence for associations with EC. Findings from analyses of some components included in our secondary analyses may also be helpful in interpreting our findings relating to EC. Like EC, NO₂ is often used as a marker of traffic. As summarized under “Estimation of Exposure” above, traffic variables (CALINE predictions and distance to roadways) contributed to NO₂ predictions. Copper is also a marker of traffic, as indicated by the source apportionment. Correlations between EC and NO₂ exposure predictions were stronger than those between copper and either EC or NO₂ (Figure 8 in Appendix N, available on the HEI Web site). As for EC, the evidence for associations of NO₂ with the cardiovascular endpoints in the MESA analyses was generally weak. There was good evidence that copper, however, was associated with CIMT and suggestive evidence for an association with the presence of CAC (Figure 2 in Appendix N). The findings for NO₂ are in line with our findings for EC. Copper had a different spatial distribution within the MESA cities than EC and NO₂ (Appendix H, available on the HEI Web site), and it reflects somewhat different aspects of traffic.

This NPACT epidemiologic study presented the opportunity to assess consistency of findings across two cohorts. Regarding exposure estimation, although MESA Air/NPACT spatiotemporal model predictions of PM_{2.5} components could not be made for the WHI-OS cohort, national spatial model predictions were made for both cohorts. The general approach for both models was to utilize monitoring data, a host of geographic variables, and geostatistical smoothing to generate predictions. This approach was common to the two models, even though the input data and some features of the modeling were different. Regarding the health endpoints, while the subclinical measures of atherosclerosis used in MESA (CIMT and CAC) are not perfect measures of atherosclerosis, both predicted, in the MESA cohort, the occurrence of cardiovascular events, which are the endpoints in WHI-OS (Folsom et al. 2008). Therefore, despite marked differences in the study populations and in the health endpoints, a reasonable case can be made for expecting consistency in the results for the two cohorts.

As noted above, associations of OC and sulfur demonstrated the most consistency across the two cohorts. Of the

PM_{2.5} components, OC and sulfur had the strongest evidence for associations with CIMT. Similarly, OC and sulfur had the best evidence for associations with CVD deaths and CVD events, respectively.

Interestingly, there was little consistency of associations between the two subclinical outcomes in the MESA analyses. There was only weak evidence for an association of OC with CAC, and little evidence for an association of sulfur with CAC. CIMT and CAC tend to be only moderately correlated within individuals (Folsom et al. 2008), but each is an independent predictor of CVD events, so each provides some information that the other does not. CIMT, for the most part, does not measure vessel plaque, whereas CAC is typically part of a plaque. Obviously, CIMT reflects the status of carotid arteries most directly, but it also tends to correlate strongly with intima-media thickness in other arterial beds. Being in coronary arteries themselves, CAC reflects some aspects of plaque in the vessels that are directly involved in cardiac ischemia and infarction.

Health effects analyses were also carried out with less-sophisticated, but commonly used approaches to estimating exposure. In the MESA analyses, both nearest-monitor and IDW approaches were used. The nearest-monitor and IDW exposure predictions were strongly correlated, and these, in turn, were strongly correlated with spatiotemporal model and national spatial model exposure predictions for sulfur and EC, but generally less so for silicon and OC (Figure 27). In general, correlations were better with exposure predictions from the spatiotemporal model than with those from the national spatial model, likely due to the source monitoring data. The nearest-monitor and IDW cross-sectional estimates of health effects were similar (Appendix H, available on the HEI Web site), and these, in turn, were similar to the effect estimates obtained using the spatiotemporal model exposure predictions, all showing that OC and sulfur had the strongest associations with CIMT. There was somewhat more evidence for associations with silicon when nearest-monitor and IDW exposure predictions were used, and less for EC, whereas the opposite was the case using the spatiotemporal model predictions. There was somewhat less consistency with the health effects estimates obtained using the national spatial model.

In the WHI-OS analyses, health effects were estimated using the citywide average exposure based on CSN monitoring data, in addition to exposure averages based on national spatial model predictions (Appendix I, available on the HEI Web site). Comparison of these health effects estimates was hampered by some differences in the data used for the respective analyses. Citywide average exposure estimates were based on 2004 CSN data, while the

national spatial model estimates were based on CSN and IMPROVE data from 2009; study subjects who could not be geocoded to baseline residence were excluded from the national spatial model analysis, but not from the analysis using citywide average exposures; and the health effects estimates based on citywide average exposures were standardized to cross-city IQRs of PM_{2.5} components, while those based on the national spatial model exposure estimates were standardized to IQRs of exposure prediction distributions for the study subjects. Despite these differences, there was considerable consistency between the two sets of findings for total CVD events. Both analyses found evidence for associations of PM_{2.5} and sulfur (SO₄) with CVD, CHD, and cerebrovascular disease events and associations of OC with cerebrovascular disease events. They found limited evidence of associations of EC or silicon with CVD events. For CVD deaths, there was somewhat less consistency between the two analyses. While both analyses found evidence that OC was associated with deaths from CVD, atherosclerotic cardiac disease, and cerebrovascular disease, the evidence that EC was also associated with CVD deaths and atherosclerotic cardiac disease deaths was better in the citywide average analyses than in the national spatial model analyses. Also, in the citywide average analyses, there was evidence that silicon was associated with deaths from CVD, atherosclerotic cardiac disease, and cerebrovascular disease, while there was little evidence for this in the national spatial model analyses.

Because there is no gold standard for comparing health findings based on the less-sophisticated approaches for estimating exposure with those based on the more-sophisticated approaches we used, it is not possible to draw firm conclusions about the validity of the different sets of health effects estimates. To the extent that the agreement in the findings among the approaches is less than complete, it suggests that the findings are somewhat dependent on the approach to estimating exposure to PM_{2.5} components.

For the MESA cohort, both cross-sectional and longitudinal analyses of CIMT were performed. In the longitudinal analysis, there was little evidence for associations of the PM_{2.5} components with CIMT progression. This may not be surprising considering the short follow-up period: each study participant had only two measures of CIMT, separated by either approximately 2 years (exam 2) or 4 years (exam 3), with a mean follow-up of 2.5 years. Nevertheless, a study using the longitudinal CIMT data employed in our study reported that CIMT progression predicted incidence of stroke (Polak et al. 2011), suggesting that even this short follow-up period has value.

Although CIMT data from exam 5 are not yet available, incorporating them in the analysis in the future should allow a better assessment of longitudinal effects, in addition to cross-sectional effects, because of the longer follow-up period of up to 10 years.

We elected not to attempt a longitudinal analysis of CAC endpoints, primarily because we did not consider it reasonable to expect much change in CAC over such a short follow-up period and we were concerned about the comparability of CT scanners on repeated examinations. A new scoring system was developed at the MESA Coordinating Center that facilitates the longitudinal analysis of CAC (Liang et al. 2012). The new system provides scores for the approximately 50% of study participants that currently have no identified CAC by Agatston scoring, so future analysis of the continuous CAC endpoint using the new scoring system will have more statistical power to detect effects of exposure to PM_{2.5} components, if they are present.

We limited our primary analyses to four of the many PM_{2.5} components that were measured in the MESA Air/NPACT monitoring campaign and that are available on a national scale from the CSN and IMPROVE monitoring networks. The selection was motivated by a desire to limit our analyses to components that reflect important sources of PM_{2.5} emissions and PM_{2.5} formation processes and to allow a focused and hypothesis-driven set of analyses to be carried out. We have, however, included in Appendices H and N (available on the HEI Web site) findings for MESA participants obtained using national spatial model exposure predictions for a set of secondary PM_{2.5} components: nickel, vanadium, SO₄, NO₃, and copper. This selection was motivated in part by interests and findings of the other NPACT study by the New York University team (Lippmann et al. 2013), and to allow further integration with the parallel animal toxicology study carried out by the other part of our NPACT team at the Lovelace Respiratory Research Institute (Section 2 of this report). In summary, there was strong evidence for a cross-sectional association of copper with CIMT, as there was for OC and sulfur, but weak evidence for associations of nickel, vanadium, or NO₃ with CIMT. The findings for SO₄, as expected, paralleled those for sulfur.

Overall, in the MESA analyses, there was little sensitivity of the health effects estimates to progressive addition of covariates to the models, with the exception of adjustment for city. Although not included in our primary models, inclusion of terms for city in the analyses always produced larger CIs and sometimes resulted in large changes in the effect estimates for PM_{2.5} components, especially for effects on CIMT. In particular, adjustment for city greatly

attenuated the cross-sectional estimate for OC effects on CIMT based on the exposure predictions of the spatiotemporal model. This was not the case when the exposure predictions of the national spatial model were used.

The motivation for adding terms for city (models 5 and 6) was to control for unmeasured potential confounders associated with the city, and therefore associated with exposure. The primary disadvantage to controlling for city is that it substantially reduced variability in exposure estimates. Figures 20 and 26 present the distributions of predicted exposure concentrations across the six MESA cities for the spatiotemporal model predictions and the national spatial model predictions, respectively, showing the contrast in variability in predicted concentrations between cities and within cities. The CIs of the effect estimates in the models that include terms for city are generally wider, reflecting the reduction in exposure variability. By choosing model 3 as our primary model, we placed the most interpretive weight on a model without control for city. However, more work is needed to determine the best covariate model. Because of the possibility of residual between-city confounding in our primary analysis, the sensitivity of effect estimates to control for city somewhat qualifies the conclusions that can be drawn regarding associations observed for some $PM_{2.5}$ components.

If the adverse effects of $PM_{2.5}$ are due, at least in part, to its chemical composition, one could argue that because $PM_{2.5}$ consists of a mixture of components, the health effects of some specific $PM_{2.5}$ components would be expected to be larger than those of the $PM_{2.5}$ mass. To make this comparison, we have standardized effect estimates to IQR. Because the monitoring data used for total $PM_{2.5}$ mass in the spatiotemporal model are much richer (in space and time) than those used for the $PM_{2.5}$ components, it could be argued that uncorrected comparisons of health effects estimates based on these two different types of exposure measures might not be very meaningful. Regardless, we presented $PM_{2.5}$ health effects estimates for both MESA and WHI-OS participants. On the national scale, where the $PM_{2.5}$ monitoring data used for generating predictions are still more rich than those for $PM_{2.5}$ components, the model's prediction ability for $PM_{2.5}$ (cross-validated $R^2 = 0.85$) is not dramatically different from that for $PM_{2.5}$ components (cross-validated $R^2 = 0.61$ to 0.95 , depending on the component). As noted earlier, in the MESA analyses, using the IQR scale for comparisons, there was little evidence that associations of $PM_{2.5}$ components with CIMT and CAC were stronger than those of $PM_{2.5}$ itself, with the exception of the effects on CIMT estimated using the spatiotemporal model exposure predictions (but not the national spatial model predictions),

where there was evidence that OC, and especially sulfur, had larger effects than $PM_{2.5}$ (Figure 29). In other cases, the width of the respective CIs precluded drawing firm conclusions about the relative sizes of the effects.

Similarly, in the WHI-OS analyses, it is difficult to argue persuasively that the estimated health effect of any $PM_{2.5}$ component was greater than that of $PM_{2.5}$, with the possible exceptions of the OC associations with deaths from CVD, atherosclerotic cardiac disease, or cerebrovascular disease (Tables 52 and 58), although even for these results the 95% CIs often overlap. On the basis of these findings, then, and following the above line of reasoning, the question of whether any $PM_{2.5}$ component has more pronounced effects on CVD than those attributable to $PM_{2.5}$ mass itself is still open.

Distance-to-roadway effects were only assessed in the WHI-OS cohort. There was some evidence that residing within 100 m of a larger roadway (A1 or A2 road) was associated with increased risk of CVD events, but not with CVD deaths, for which we had relatively limited power to detect associations. There is no strict correspondence between the federal CFCC roadway classifications (A1, A2, and A3) and the amount of traffic that these roadways experience. For example, in MESA cities, average daily traffic counts in A1-designated roadways varied from a high of 144,100 in Chicago to 41,300 in Winston-Salem. There was, however, generally good correspondence between the roadway classification and traffic within any given city. The variability across cities, however, complicates the use of the CFCC roadway classification as a measure of traffic exposure by introducing a type of exposure measurement error that has not been well characterized. This complication may motivate investigators to focus on within-city exposure contrasts when using this exposure measure in cohort studies.

The focus of NPACT on long-term exposure effects, rather than short-term effects, is a distinction that sometimes gets blurred. The subclinical endpoints evaluated in the MESA analyses do not lend themselves to being considered as anything but effects of long-term exposures, although there can be short-term changes in CIMT. Cardiovascular events, including deaths, can result from short-term exposures, but the effects of short-term exposure have not been considered here. To say that effects are due to long-term exposure does not imply that they are due to constant exposure to relatively stable concentrations. The effects of long-term exposure could be due to an accumulation of multiple short-term injuries, possibly through short-term peaks in exposure. We are unable to address this possibility, in part, because of the way in which we have estimated exposure.

We had originally planned to incorporate a measure of the oxidative potential of $PM_{2.5}$ as an exposure variable in the health effects models, similar to the way in which we incorporated $PM_{2.5}$ components. In light of the relatively poor models for estimating dithiothreitol (DTT) exposure (Appendix E, available on the HEI Web site), we abandoned this plan. This would have first entailed estimating DTT for every filter sample as a function of the $PM_{2.5}$ components on the filter, which would have been done with substantial uncertainty, and then building a spatiotemporal model to predict DTT for every participant's residence. The chain of prediction seemed overly tenuous for the results to be meaningful. We therefore limited our objective to the generation of DTT prediction models. The limitation of potential predictors of DTT to the $PM_{2.5}$ components for which we had data undoubtedly was the reason for our relatively poor DTT models. A larger suite of components, and in particular a large set of organic compounds, would most likely have resulted in better modeling of DTT. Much better models for DTT were obtained in southern California using organic compounds as predictors (Ntziachristos et al. 2007).

$PM_{2.5}$ components were specified as main effect terms in our health effects models, as is typically done for single pollutants. Each $PM_{2.5}$ component was considered as a pollutant, and effects were estimated for incremental increases in the component concentration. Another approach to specifying $PM_{2.5}$ component effects springs from considering that $PM_{2.5}$ components are part of the $PM_{2.5}$ mass and not separate pollutants. Arguably, a more relevant question to ask in such a context is whether differences in the chemical composition of $PM_{2.5}$ modify its effects. Specifying $PM_{2.5}$ component effects, then, might take the form of interaction terms (or product terms) involving PM and the $PM_{2.5}$ components. Regression coefficients of the interaction terms then address whether the $PM_{2.5}$ effect is modified by composition. We have not used this specification of $PM_{2.5}$ component effects in our health effects models, but it could be a fruitful approach to take in future analyses. Another issue relating to model specification is whether some or all of the $PM_{2.5}$ component effects, especially for components that make up larger proportions of the $PM_{2.5}$ mass, simply reflect effects of $PM_{2.5}$ itself. One way of addressing this issue would be to include a term for $PM_{2.5}$ in each model assessing effects of the $PM_{2.5}$ components (Mostofsky et al. 2012).

CONCLUSIONS

Our approach to estimating exposure was based on the premise that estimating exposure at the level of the

individual would reduce measurement error compared with other approaches that assign exposure at larger spatial scales, and that this reduction in measurement error would result in better estimates of the health effects of $PM_{2.5}$ components. A large monitoring and modeling effort was undertaken to obtain individual-level predictions of exposure to the $PM_{2.5}$ components that were used in the MESA and WHI-OS health analyses. We were successful in monitoring ambient concentrations of PM components that affected our target cohorts and had reasonable success in predicting exposures within the MESA cities. The success varied across components and cities, with results being somewhat limited by the quantity and quality of the data, along with limited temporal and spatial coverage. Predictions of overall exposure for the six MESA cities together, however, were considerably better, thanks to the large inherent differences across the six cities. Predictions made on a national scale using existing monitoring data, which were used in both the MESA and WHI-OS analyses, were generally very good from a model assessment perspective, but the monitoring data on which these predictions were based were not well aligned with the locations of study participants.

Results of the health effects analyses employing individual-level exposure estimates only partly support the working hypothesis that combustion-related $PM_{2.5}$ components are more toxic than noncombustion components. Of the components selected to reflect combustion emissions, among the most consistent findings obtained across the exposure and health models, across the health endpoints, and across the cohorts were for OC, although there were some exceptions. There was little evidence that estimated exposure to EC, also a reflection of combustion-related $PM_{2.5}$, was associated with health effects. There was also evidence that components selected to reflect noncombustion emissions were associated with cardiovascular outcomes, with the evidence for sulfur being particularly strong. The evidence for silicon was considerably weaker.

In this study the use of two different cohorts, for whom individual-level exposures were estimated using a common approach, allowed for investigation of the effects of exposure to $PM_{2.5}$ components on an array of subclinical and clinical endpoints and for an assessment of the consistency of effects that would not otherwise have been possible. The findings regarding OC and SO_4 should prompt further study of the health effects of OC sources and of specific organic compounds and classes of compounds, as well as secondary organic and inorganic aerosols, although effects of other sources and components remain of interest.

ACKNOWLEDGMENTS

The Multi-Ethnic Study of Atherosclerosis (MESA) is supported by contracts from the National Heart, Lung and Blood Institute (N01-HC-95159 through N01-HC-95165 and N01-HC-95169). The Multi-Ethnic Study of Atherosclerosis and Air Pollution (MESA Air) is supported by grant RD836197 from the U.S. Environmental Protection Agency Science to Achieve Results (STAR) program; additional assistance was provided by STAR grant R833741. Min Sun was supported by a scholarship from the China Scholarship Council (CSC). The Women's Health Initiative (WHI) program is funded by the National Heart, Lung and Blood Institute.

REFERENCES

- Abdi H. 2003. Partial Least Squares (PLS) regression. In: *The SAGE Encyclopedia of Social Sciences Research Methods* (Bryman A, Futing T, Lewis-Beck M, eds). SAGE Publications, Inc., Thousand Oaks, CA.
- Allen R, Box M, Liu LJ, Larson TV. 2001. A cost-effective weighing chamber for particulate matter filters. *J Air Waste Manag Assoc* 51:1650–1653.
- Ault A, Moore M, Furutani H, Prather KA. 2009. Impact of emissions from the Los Angeles Port region on San Diego air quality during regional transport events. *Environ Sci Technol* 43:3500–3506.
- Bild DE, Bluemke DA, Burke GL, Detrano R, Diez Roux AV, Folsom AR, Greenland P, Jacob DR Jr, Kronmal R, Liu K, Nelson JC, O'Leary D, Saad MF, Shea S, Szklo M, Tracy RP. 2002. Multi-Ethnic Study of Atherosclerosis: Objectives and design. *Am J Epidemiol* 156:871–881.
- Cheng Y, He KB, Duan FK, Zheng M, Ma YL, Tan JH, Du ZY. 2010. Improved measurement of carbonaceous aerosol: Evaluation of the sampling artifacts and inter-comparison of the thermal-optical analysis methods. *Atmos Chem Phys* 10:8533–8548.
- Cohen MA, Adar SD, Allen RW, Avol E, Curl CL, Gould T, Hardie D, Ho A, Kinney P, Larson TV, Sampson P, Sheppard L, Stukovsky KD, Swan SS, Liu LJS, Kaufman JD. 2009. Approach to estimating participant pollutant exposures in the Multi-Ethnic Study of Atherosclerosis and Air Pollution (MESA Air). *Environ Sci Technol* 43:4687–4693.
- Curb JD, McTiernan A, Heckbert SR, Kooperberg C, Stanford J, Nevitt M, Johnson KC, Proulx-Burns L, Pastore L, Criqui M, Daugherty S; WHI Morbidity and Mortality Committee. 2003. Outcomes ascertainment and adjudication methods in the Women's Health Initiative. *Ann Epidemiol* 13:S122–S128.
- Eldred RA, Cahill TA, Pitchford M, Malm WC. 1988. IMPROVE: A New Remote Area Particulate Monitoring System for Visibility Studies. Annual Meeting of the APCA, Dallas, TX, 1988.
- Folsom AR, Kronmal RA, Detrano RC, O'Leary DH, Bild DE, Bluemke DA, Budoff MJ, Liu K, Shea S, Szklo M, Tracy RP, Watson KE, Burke GL. 2008. Coronary artery calcification compared with carotid intima-media thickness in the prediction of cardiovascular disease incidence: The Multi-Ethnic Study of Atherosclerosis (MESA). *Arch Intern Med* 168:1333–1339.
- Frank N. 2012. Recommendations to Users of CSN and IMPROVE Speciation Data Regarding Sampling Artifact Correction for PM_{2.5} Organic Carbon. EPA Air Quality Analysis Group, Office of Air Quality and Standards, Research Triangle Park, NC. Available from www.epa.gov/ttnnaqs/standards/pm/data/20120614Frank.pdf.
- Geitl JK, Lawrence R, Thorpe AJ, Harrison RM. 2010. Identification of brake wear particles and derivation of a quantitative tracer for brake dust at a major road. *Atmos Environ* 44:141–146.
- Gill EA, Curl CL, Adar SD, Allen RW, Auchincloss AH, O'Neill MS, Park SK, Van Hee VC, Diez Roux AV, Kaufman JD. 2011. Air pollution and cardiovascular disease in the Multi-Ethnic Study of Atherosclerosis. *Prog Cardiovasc Dis* 53:353–360.
- Grahame TJ, Schlesinger RB. 2005. Evaluating the health risk from secondary sulfates in eastern North American regional ambient air particulate matter. *Inhal Toxicol* 17:15–27.
- Heckbert SR, Kooperberg C, Safford MM, Psaty BM, Hsia J, McTiernan A, Gaziano JM, Frishman WH, Curb JD. 2004. Comparison of self-report, hospital discharge codes, and adjudication of cardiovascular events in the Women's Health Initiative. *Am J Epidemiol* 160:1152–1158.
- Ito K, Mathes R, Ross Z, Nádas A, Thurston G, Matte T. 2011. Fine particulate matter constituents associated with cardiovascular hospitalizations and mortality in New York City. *Environ Health Perspect* 119:467–473.
- Kessler SH, Nah T, Daumit KE, Smith JD, Leone SR, Kolb CE, Worsnop DR, Wilson KR, Kroll JH. 2012. OH-initiated heterogeneous aging of highly oxidized organic aerosol. *J Phys Chem A* 116:6358–6365.

- Langer RD, White E, Lewis CE, Kotchen JM, Hendrix SL, Trevisan M. 2003. The Women's Health Initiative Observational Study: Baseline characteristics of participants and reliability of baseline measures. *Ann Epidemiol* 13: S107–S121.
- Liang CJ, Budoff MJ, Kaufman JD, Kronmal RA, Brown ER. 2012. An alternative method for quantifying coronary artery calcification: The Multi-Ethnic Study of Atherosclerosis (MESA). *BMC Med Imaging* 12:14.
- Lindström J, Szpiro AA, Sampson PD, Bergen S, Oron A. 2011a. SpatioTemporal: Spatio-Temporal Model Estimation R-package. Available from <http://cran.r-project.org/web/packages/SpatioTemporal/index.html>. Accessed 01/31/2013.
- Lindström J, Szpiro AA, Sampson PD, Sheppard L, Oron A, Richards L, Larson T. 2011b. A Flexible Spatio-Temporal Model for Air Pollution: Allowing for Spatio-Temporal Covariates. UW Biostatistics Working Paper Series, Working Paper 370. Available from <http://biostats.bepress.com/uwbiostat/paper370/>.
- Lippmann M, Chen L-C, Gordon T, Ito K, Thurston GD. 2013. National Particle Component Toxicity (NPACT) Initiative: Integrated Epidemiologic and Toxicologic Studies of the Health Effects of Particulate Matter Components. Research Report 177. Health Effects Institute, Boston, MA.
- Lumley T, Kronmal R, Ma S. 2006. Relative Risk Regression in Medical Research: Models, Contrasts, Estimators, and Algorithms. UW Biostatistics Working Paper Series, Working Paper 293. Available from <http://bepress.com/uwbiostat/paper293>.
- MESA Air Data Team. 2013. Data organization and operating procedures. Available from <http://www.uwchsc.org/MESAAP/Documents/MESAAirDOOP.pdf>.
- Miller KA, Siscovick DS, Sheppard L, Shepherd K, Sullivan JH, Anderson GL, Kaufman JD. 2007. Long-term exposure to air pollution and incidence of cardiovascular events in women. *N Engl J Med* 356:447–458.
- Mostofsky E, Schwartz J, Coull BA, Koutrakis P, Wellenius GA, Suh HH, Gold DR, Mittleman MA. 2012. Modeling the association between particle constituents of air pollution and health outcomes. *Am J Epidemiol* 176:317–326.
- Norris G, Vedanthan R, Duvall R, Wade K, Brown S, Prouty J, Bai S, Dewinter J. 2010. EPA Positive Matrix Factorization (PMF) 4.1 Fundamentals and User Guide. Draft Version. EPA Office of Research and Development, Washington, DC.
- Ntziachristos L, Froines JR, Cho AK, Sioutas C. 2007. Relationship between redox activity and chemical speciation of size-fractionated particulate matter. Part Fibre Toxicol 4:5.
- Ogulei D, Hopke PK, Zhou L, Pancras JP, Nair N, Ondov JM. 2006. Source apportionment of Baltimore aerosol from combined size distribution and chemical composition data. *Atmos Environ* 40:S396–S410.
- Ostro B, Lipsett M, Reynolds P, Goldberg D, Hertz A, Garcia C, Henderson KD, Bernstein L. 2010. Long-term exposure to constituents of fine particulate air pollution and mortality: Results from the California Teachers Study. *Environ Health Perspect* 118:363–369.
- Ostro B, Lipsett M, Reynolds P, Goldberg D, Hertz A, Garcia C, Henderson KD, Bernstein L. 2011. Erratum: Assessing long-term exposure in the California Teachers Study. *Environ Health Perspect* 119:A242–A243.
- Ostro B, Roth L, Malig B, Marty M. 2009. The effects of fine particle components on respiratory hospital admissions in children. *Environ Health Perspect* 117:475–480.
- Paatero P. 1999. The multilinear engine: A table-driven, least squares program for solving multilinear problems, including the n-way parallel factor analysis model. *J Computational Graphical Stat* 8:854–888.
- Peltier RE, Hsu SI, Lall R, Lippmann M. 2009. Residual oil combustion: A major source of airborne nickel in New York City. *J Expo Sci Environ Epidemiol* 19:603–612.
- Peltier RE, Lippmann M. 2010. Residual oil Combustion: 2. Distributions of airborne nickel and vanadium within New York City. *J Exp Sci Environ Epidemiol* 20:342–350.
- Peng RD, Bell ML, Geyh AS, McDermott A, Zeger SL, Samet JM, Dominici F. 2009. Emergency admissions of cardiovascular and respiratory diseases and the chemical composition of fine particle air pollution. *Environ Health Perspect* 117:957–963.
- Polak JF, Pencina MJ, O'Leary DH, D'Agostino RB. 2011. Common carotid artery intima-media-thickness progression as a predictor of stroke in Multi-Ethnic Study of Atherosclerosis. *Stroke* 42:3017–3021.
- R Development Core Team. 2011. R: A language and environment for statistical computing. 2.12.2 ed. R Foundation for Statistical Computing, Vienna, Austria.
- Sampson PD, Szpiro AA, Sheppard L, Lindström J, Kaufman JD. 2011. Pragmatic estimation of a spatio-temporal air quality model with irregular monitoring data. *Atmos Environ* 45:6593–6606.

Subramanian R, Khlystov AY, Robinson AL. 2006. Effect of peak inert-mode temperature on elemental carbon measured using thermal-optical analysis. *Aerosol Sci Tech* 40:763–780.

Szpiro AA, Sheppard L, Lumley T. 2011. Efficient measurement error correction with spatially misaligned data. *Biostatistics* 12:610–623.

Thorpe A, Harrison RM. 2008. Sources and properties of non-exhaust particulate matter from road traffic: A review. *Sci Total Environ* 400:270–282.

Thurston G, Burnett R, Krewski D, Shi YL, Turner M, Ito K, Lall R, Jerrett M, Calle E, Tunne M, Pope CA. 2009. Ischemic heart disease mortality associations with long-term exposure to PM_{2.5} components [abstract]. *Epidemiology* 20:S80–S81.

Tibshirani R. 1996. Regression shrinkage and selection via the lasso. *J R Stat Soc* 58:267–288.

U.S. Census Bureau. 2007. TIGER/Line Shapefiles Technical Documentation. Geography Division of U.S. Census Bureau, reissued May 2008. Available from www.census.gov/geo/www/tiger/tgrshp2007/tgrshp2007.html.

U.S. Environmental Protection Agency. 2010. General Information. Technology Transfer Network Ambient Monitoring Technology Information Center. Available from www.epa.gov/ttnamt1/specgen.html. Accessed 01/31/2013.

U.S. Environmental Protection Agency. 2009. Integrated science assessment for particulate matter. EPA/600/R-08/139F. Office of Research and Development, Research Triangle Park, NC. Available from <http://cfpub.epa.gov/ncea/cfm/recordisplay.cfm?deid=216546>.

U.S. Environmental Protection Agency. 1999. Method IO-3.3: Determination of metals in ambient particulate matter using x-ray fluorescence (XRF) spectroscopy. In: *Compendium of Methods for the Determination of Inorganic Compounds in Ambient Air*. EPA/625/R-96/010a. U.S. Environmental Protection Agency, Center for Environmental Research Information, Office of Research and Development, Cincinnati, OH.

U.S. Environmental Protection Agency. 1998. Quality Assurance Guidance Document 2.12. Monitoring PM_{2.5} in Ambient Air Using Designated Reference or Class I Equivalent Methods. National Exposure Research Laboratory, Research Triangle Park, NC. Available from www.epa.gov/ttn/amtic/files/ambient/pm25/qa/m212covd.pdf.

Watson JG, Chow JC, Chen L-WA. 2005. Summary of organic and elemental carbon/black carbon analysis methods and intercomparisons. *Aerosol Air Qual Res* 5:65–102.

Women's Health Initiative Study Group. 1998. Design of the Women's Health Initiative clinical trial and observational study. *Control Clin Trials* 19:61–109.

Zhou J, Ito K, Lall R, Lippmann M, Thurston G. 2011. Time-series analysis of mortality effects of fine particulate matter components in Detroit and Seattle. *Environ Health Perspect* 119:461–466.

Zhu Y, Hinds WC, Kim S, Sioutas C. 2002. Concentration and size distribution of ultrafine particles near a major highway. *J Air Waste Manag Assoc* 52:1032–1034.

APPENDIX A. HEI Quality Assurance Statement

The conduct of this study was subjected to independent audit by Abt Associates Inc. The audit team consisted of Dr. Sue Greco, who has over 10 years of experience with human health risk assessment, including exposure to fine PM, and Mr. Jose Vallarino, who has overseen quality assurance programs for the last 15 years. Another member of the audit team was Dr. Jin Huang, who assisted with data regeneration. The audit consisted of two on-site visits to the University of Washington School of Public Health in Seattle, a data-regeneration exercise, and a review of the final report.

April 6–8, 2009

The first on-site audit conducted by the auditors at the University of Washington School of Public Health was a technical systems audit. The audit consisted of a review of the organizational structure, data-gathering methods, data management, and data quality programs for the study. The auditors' recommendations were mainly related to improving the study's documentation.

December 6–7, 2011

The auditors conducted a second on-site audit at the University of Washington School of Public Health, which consisted of a review of the draft final report. The UW researchers led the auditors through the steps required to generate selected tables and figures starting from raw data. The auditors identified some items that required correction, but nothing was discovered that would adversely affect the findings of the report. The auditors recommended central archiving of the final report's tables and figures.

March 2011–March 2012

The auditors regenerated a portion of the x-ray fluorescence data for the first half of 2008 for pollutant samples

obtained at both fixed and home-outdoor monitoring sites, starting with raw data and using instructions provided by the UW researchers. The vast majority of the regenerated concentrations (555 samples, with up to 48 elements in each sample) matched the concentrations in the final data set provided by the researchers. Of the 27 calculated concentrations that differed from the final data set by more than 5%, only 3 had positive nonzero concentrations in both data sets. The remaining 24 concentrations were zero or negative in the final data set and in the regenerated data.

December 2012

The auditors reviewed a revised copy of the final report to evaluate whether the previous recommendations had been addressed. Overall, the auditors found the UW researchers to be well organized and cooperative during the audits. The quality assurance audit demonstrated that the study procedures, analysis steps, and data storage were systematic, consistent, and well designed to manage the various and complex data and analytical streams necessary to complete the study.



Sue Greco, Sc.D.



Jose Vallarino, M.Sc.

APPENDICES AVAILABLE ON THE WEB

Appendices B–Q contain supplemental material not included in the printed report. They are available on the HEI Web site, <http://pubs.healtheffects.org>.

- Appendix B. CSN Monitoring Sites and Protocols
- Appendix C. Building and Validating the MESA Spatial and Spatiotemporal Models
- Appendix D. The NO₂ Model
- Appendix E. Oxidative Potential
- Appendix F. Supplemental Monitoring Campaign
- Appendix G. Data Analysis Plan for CIMT Longitudinal Analysis
- Appendix H. MESA Exposure and Health Analysis: Additional Text, Tables, and Figures
- Appendix I. WHI Exposure and Health Analysis: Additional Text and Tables
- Appendix J. Source Apportionment Literature Review for the Six MESA Cities

- Appendix K. NPACT Monitoring Data QA/QC
- Appendix L. NPACT Monitoring Data QA/QC: Supplemental Study
- Appendix M. Comparison of PM_{2.5} Annual Averages Between 2000 and 2007–8
- Appendix N. Prediction Model and Health Effect Analysis for Nickel, Vanadium, and Copper Analyses
- Appendix O. CAC QA/QC
- Appendix P. CIMT QA/QC (Right Common Carotid)
- Appendix Q. Adjusted EC and OC Findings

ABOUT THE AUTHORS

Sverre Vedal, M.D., M.Sc., is a professor in the Department of Environmental and Occupational Health Sciences at the University of Washington. He earned his M.D. from the University of Colorado and his M.Sc. in epidemiology from the Harvard School of Public Health. His research interests include investigation of the health effects of exposure to ambient air pollution and occupational lung disease. He is a member of the EPA Clean Air Scientific Advisory Committee panels on particulate matter and ozone and directs the University of Washington Center for Clean Air Research, one of the EPA Clean Air Research Centers. Dr. Vedal was the principal investigator of the University of Washington NPACT initiative and contributed most directly to the exposure modeling and health effects analyses of the MESA and WHI-OS cohorts.

Sun-Young Kim, Ph.D., is a research scientist in the Department of Environmental and Occupational Health Sciences at the University of Washington. She earned her Ph.D. in the Department of Epidemiology and Biostatistics at the Seoul National University School of Public Health in Seoul, Korea. Dr. Kim's research focuses on the influence of exposure prediction models on health effects estimation and health effects analysis of air pollution. Dr. Kim developed the MESA spatiotemporal exposure prediction models for PM_{2.5} components and performed health effects analyses for the MESA cohort under the guidance of Drs. Lianne Sheppard and Sverre Vedal.

Kristin A. Miller, M.S., is a doctoral student at the University of Washington in the Department of Epidemiology. She earned her M.S. in epidemiology from the University of Washington and holds an A.B. in physics from Mount Holyoke College. Her research focuses on environmental epidemiology, primarily the relationship between air pollution exposure and cardiovascular disease. Ms. Miller was responsible for the health effects analyses of the WHI-OS cohort under the guidance of Drs. Joel Kaufman and Sverre Vedal.

Julie Richman Fox, Ph.D., M.H.S., is an exposure sciences postdoctoral fellow in the Department of Environmental and Occupational Health Sciences at the University of Washington. She earned her Ph.D. from the Johns Hopkins Bloomberg School of Public Health in the Division of Environmental Health Engineering. Dr. Fox's research focuses on development, validation, and optimization of inhalation exposure and biomarker dose characterization methods for application in health research. Dr. Fox generated and analyzed the positive matrix factorization models used in the source apportionment section of this report under the guidance of Dr. Timothy Larson.

Silas Bergen, B.S., is a Ph.D. student in the Department of Biostatistics at the University of Washington. He earned his B.S. in statistics from Winona State University in Winona, MN. Mr. Bergen's research focuses on air pollution exposure modeling and measurement error correction in subsequent epidemiologic modeling. Mr. Bergen generated and validated the national air pollution exposure models for PM_{2.5} using universal kriging and partial least squares and generated predictions at MESA locations, under the guidance of Dr. Adam Szpiro.

Timothy Gould, M.S., P.E., is a research scientist/engineer in the Department of Environmental Engineering at the University of Washington. He earned his M.S. degree from Carnegie Mellon University Departments of Civil & Environmental Engineering and Engineering & Public Policy. He helps design protocols and conducts air quality measurements and data characterization in support of health effects studies. Mr. Gould designed and coordinated the NPACT field sampling program for organic and elemental carbon particulate matter and worked on speciated particulate data characterization with Dr. Timothy Larson.

Joel D. Kaufman, M.D., M.P.H., is a professor in the Departments of Environmental and Occupational Health Sciences, Epidemiology, and Medicine at the University of Washington. He received his M.D. from the University of Michigan and his M.P.H. from the University of Washington. Dr. Kaufman's research integrates the disciplines of epidemiology, exposure sciences, toxicology, and clinical medicine with a primary focus on environmental factors in cardiovascular and respiratory disease. He is the principal investigator of MESA Air and a member of the EPA Clean Air Scientific Advisory Committee panel on NO_x. His primary contributions to NPACT were assisting in the health analyses of the MESA and WHI-OS cohorts.

Timothy V. Larson, Ph.D., is a professor in the Department of Civil and Environmental Engineering and in the Department of Environmental and Occupational Health Sciences

at the University of Washington. Dr. Larson holds a B.S. in chemical engineering from Lehigh University, and an M.S.Ch.E. and a Ph.D. from the University of Washington. His expertise and research focus is in characterization of urban air pollution, exposure assessment of airborne particles and gases, and source/receptor relationships of ambient air pollutants. He is a member of the EPA Clean Air Scientific Advisory Committee panels on SO_x and NO_x. Dr. Larson's primary contributions to NPACT were in supervising the PM component monitoring and analyses, as well as the source apportionment.

Paul D. Sampson, Ph.D., is a research professor in the Department of Statistics and Director of the Statistical Consulting Program at the University of Washington. He earned his Ph.D. in statistics from the University of Michigan. His primary statistical research is in spatial and spatiotemporal modeling of environmental data and, in particular, models for nonstationary spatial covariance structure. Professor Sampson was responsible for the statistical modeling framework for the exposure estimation work carried out in NPACT and consulted on a number of other components of the report.

Lianne Sheppard, Ph.D., is a professor in the Departments of Biostatistics, and Environmental and Occupational Health Sciences at the University of Washington. She received her Ph.D. from the University of Washington. Her research interests focus on statistical methods for environmental and occupational epidemiology and include study design, measurement error, exposure modeling and estimation, and estimation of environmental exposure effects. Dr. Sheppard is a Fellow of the American Statistical Association, a member of the EPA Clean Air Scientific Advisory Committee panel on NO_x, and a member of the Health Effects Institute Review Committee. Her primary contributions to NPACT were in directing the development of the MESA spatiotemporal models and the health effects analyses of the MESA cohort.

Christopher D. Simpson, Ph.D., is an associate professor and director of the Exposure Science program in the Department of Environmental and Occupational Health Sciences at the University of Washington. He earned his Ph.D. in environmental and analytical chemistry from the University of British Columbia, Canada. Dr. Simpson's research interests involve the application of analytical chemistry to the development of techniques for assessment of exposure to toxic chemicals, and the subsequent application of those techniques to investigate occupational and environmental exposures. Dr. Simpson had primary responsibility for measurement and interpretation of the oxidative potential of particulate matter extracts described in this report.

Adam A. Szpiro, Ph.D., is an assistant professor in the Department of Biostatistics at the University of Washington. He earned his Ph.D. from Brown University in the Division of Applied Mathematics. Dr. Szpiro's research focuses on spatial and spatiotemporal statistical methods with applications to air pollution and environmental epidemiology. His primary methodologic contributions to NPACT were in the exposure models and measurement error correction techniques for epidemiologic analyses.

CONTRIBUTORS

Sara Dubowsky Adar, Sc.D., M.H.S., is currently the John Searle Assistant Professor of Epidemiology at the University of Michigan School of Public Health. Dr. Adar earned an environmental engineering degree from the Massachusetts Institute of Technology, her M.Sc. from the Johns Hopkins School of Public Health, and a doctorate in environmental epidemiology from the Harvard School of Public Health. Dr. Adar's research focuses on the human health effects of air pollution, especially those from motor vehicles. She contributed to the NPACT MESA cohort health effects modeling initially as a senior fellow and then Assistant Professor in the Departments of Epidemiology and Environmental and Occupational Health Sciences at the University of Washington.

Cynthia L. Curl, M.S., is the project manager of MESA Air at the University of Washington, and a doctoral student in the Department of Environmental and Occupational Health Sciences. She earned her M.Sc. from the University of Washington, also in Environmental and Occupational Health Sciences. Ms. Curl contributed to the successful integration of the NPACT and MESA Air studies, helped to oversee the NPACT exposure monitoring campaign, and assisted in the description of the MESA cohort.

Amanda Gasset, B.S., is a Ph.D. student in the Department of Biostatistics at the University of Washington and a research scientist in the Department of Environmental and Occupational Health Sciences. She earned her B.S. degree from Lewis and Clark College in computer science and mathematics. Ms. Gasset was the primary liaison for technicians collecting samples in the field and was responsible for quality assurance for all of the data included in the NPACT report.

Anne Ho, M.S., was a staff biostatistician at the University of Washington in the Department of Environmental and Occupational Health Sciences. She earned her M.S. in biostatistics from the University of Michigan. Ms. Ho helped to develop the exposure monitoring and geographic covariate database, and to develop the geocoding procedures used to accurately locate residential addresses.

Krystle Jumawan, B.A., was an undergraduate student in the Department of Geography at the University of Washington. Her primary role on the NPACT study was to geocode participant residential locations to allow the calculation of geographic covariates for use in the air pollution exposure models. She has since graduated from the University of Washington with her B.A.

Hil Lyons, Ph.D., is a statistician currently with Intellectual Ventures. He obtained his Ph.D. from the University of Washington Department of Statistics. His research interests include global health modeling, spatial statistics, stochastic processes, and statistical consulting. Dr. Lyons contributed to the statistical analysis and interpretation of predictors of oxidative potential while working as a staff member at the Center for Statistical Consulting in the University of Washington Department of Statistics, under the guidance of Drs. Paul Sampson and Christopher Simpson.

Assaf Oron, Ph.D., M.Sc., is currently a staff statistician at Children's Hospital in Seattle, WA. He earned his Ph.D. from the University of Washington in the Department of Statistics. As a senior staff statistician at the University of Washington in the Department of Environmental and Occupational Health Sciences, Dr. Oron contributed to NPACT by generating the MESA spatiotemporal model for NO₂.

Michael Paulsen, M.S., is a research scientist at the University of Washington in the Department of Environmental and Occupational Health Sciences. He earned his M.S. in environmental health from the University of Washington. His research focuses on development and application of analytical methods to quantify environmental and occupational exposures to pollutants such as wood smoke and diesel exhaust, and to hazardous chemicals such as organophosphate pesticides. Mr. Paulsen's role on this project was to analyze PM samples for oxidative potential by measuring oxidation of DTT in extracts of PM.

Mark Richards, B.A., is currently a master's degree student in the Department of Applied Mathematics at the University of Washington. He attended the University of California, Berkeley, where he earned his B.A. in both statistics and applied mathematics. As a research scientist at the University of Washington in the Department of Environmental and Occupational Health Sciences, he had a leadership role in developing the exposure monitoring and geographic covariate database for the NPACT study, and contributed to the development of the national PM_{2.5} model under the guidance of Dr. Paul Sampson.

Min Sun, Ph.D., is currently a senior researcher at Tianjin Tasly Pharmaceutical Co., Ltd., in Tianjin, China. She was

a visiting Ph.D. student at the University of Washington from Tianjin Medical University from 2009 to 2011 and earned her Ph.D. in epidemiology and health statistics from Tianjin Medical University in 2013. Dr. Sun developed the PM_{2.5} component secondary exposure estimates in NPACT and carried out the MESA health effects analyses using these secondary exposure estimates.

OTHER PUBLICATIONS RESULTING FROM THIS RESEARCH

Bergen S, Sheppard L, Sampson PD, Kim S-Y, Richards M, Vedal S, Kaufman JD, Szpiro AA. 2013. A national prediction model for PM_{2.5} component exposures and measurement error-corrected health effect inference. *Environ Health Perspect* 121:1017–1025.

Sun M, Kaufman JD, Kim S-Y, Larson TV, Gould TR, Polak JF, Budoff MJ, Diez Roux AV, Vedal S. 2013. Particulate matter components and subclinical atherosclerosis: Common approaches to estimating exposure in a Multi-Ethnic Study of Atherosclerosis cross-sectional study. *Environ Health* 12:39 (doi:10.1186/1476-069X-12-39).

ABBREVIATIONS AND OTHER TERMS

AQS Air Quality System
 BMI body mass index
 CABG coronary artery bypass graft
 CAC coronary artery calcium
 CFCC Census Feature Class Code
 CHD coronary heart disease
 CI confidence interval
 CIMT carotid intima-media thickness
 CRP C-reactive protein
 CSN Chemical Speciation Network
 CT computed tomography
 CVD cardiovascular disease
 DBP diastolic blood pressure
 DTT dithiothreitol
 EBCT electron beam computed tomography
 EC elemental carbon
 EPA U.S. Environmental Protection Agency
 FRM Federal Reference Method
 GIS geographic information system
 HDL high-density lipoprotein
 HPEM Harvard personal environmental monitor

HR hazard ratio
 IC ion chromatography
 ICD International Classification of Diseases
 IDW inverse-distance weighting
 IMPROVE Interagency Monitoring of Protected Visual Environments
 IQR interquartile range
 LAC light absorption coefficient
 LDL low-density lipoprotein
 MDCT multi-detector computed tomography
 MESA Multi-Ethnic Study of Atherosclerosis
 MESA Air MESA Air Pollution Study
 MI myocardial infarction
 MRI magnetic resonance imaging
 MSA Metropolitan Statistical Area
 MSE mean squared error
 NDVI Normalized Difference Vegetation Index
 NIOSH National Institute of Occupational Safety and Health
 NO₂ nitrogen dioxide
 NO₃ nitrate
 NO_x oxides of nitrogen
 NPACT National Particle Component Toxicity (initiative)
 O₃ ozone
 OC organic carbon
 PLS partial least squares
 PM particulate matter
 PM₁₀ particulate matter ≤ 10 μm in aerodynamic diameter
 PM_{2.5} particulate matter ≤ 2.5 μm in aerodynamic diameter
 PMF positive matrix factorization
 PTCA percutaneous transluminal coronary angioplasty
 RMSE root mean squared error
 RMSEP root mean squared error of the predictions
 SBP systolic blood pressure
 SO₂ sulfur dioxide
 SO₄ sulfate
 S/N signal-to-noise ratio
 STN Speciation Trends Network
 SVD singular value decomposition

TC	total carbon	In	indium
TOR	thermal-optical reflectance	Ir	iridium
TOT	thermal-optical transmittance	K	potassium
UK	universal kriging	La	lanthanum
UW	University of Washington	Mg	magnesium
WHI	Women's Health Initiative	Mn	manganese
WHI-CT	Women's Health Initiative Clinical Trials	Mo	molybdenum
WHI-OS	Women's Health Initiative–Observational Study	Na	sodium
XRF	x-ray fluorescence	Nb	niobium

ELEMENTS

Ag	silver	P	phosphorus
Al	aluminum	Pb	lead
As	arsenic	Rb	rubidium
Au	gold	S	sulfur
Ba	barium	Sb	antimony
Br	bromine	Sc	scandium
Ca	calcium	Se	selenium
Cd	cadmium	Si	silicon
Ce	cerium	Sm	samarium
Cl	chlorine	Sn	tin
Co	cobalt	Sr	strontium
Cr	chromium	Ta	tantalum
Cs	cesium	Tb	terbium
Cu	copper	Ti	titanium
Eu	europium	V	vanadium
Fe	iron	W	tungsten
Ga	gallium	Y	yttrium
Hf	hafnium	Zn	zinc
Hg	mercury	Zr	zirconium

Section 2: NPACT Animal Toxicologic Study of Cardiovascular Effects of Mixed Vehicle Emissions Combined with Non-vehicular Particulate Matter

Matthew J. Campen, Amie K. Lund, Steven K. Seilkop, and Jacob D. McDonald

ABSTRACT

BACKGROUND

The goal of this work was (1) to provide further insight into biologic mechanisms explaining associations observed in the parallel epidemiologic study and (2) to identify potency differences among contrasting atmospheres generated in a laboratory that simulated different pollutant mixtures in the environment, with an emphasis on using mixed vehicular engine emissions (MVE*) (a combination of gasoline engine exhaust [GEE] and diesel engine exhaust [DEE]). The working hypothesis was that important environmental effects on the cardiovascular system are driven by exposure to vehicle-derived pollutants, including both GEE and DEE. MVE (at high and low concentrations) was used as a benchmark against other non-vehicular particulate matter (PM), including sulfate (S; combined neutralized and acidic sulfate as assessed by the contribution of ammonium sulfate to total PM), ammonium nitrate (N), and paved road dust (RD), which are all major contributors to the PM mixture but are poorly characterized for potential cardiovascular toxicity.

METHODS

We placed hypercholesterolemic male apolipoprotein E-null (ApoE^{-/-}) mice (6–8 wk old) on a high cholesterol and fat diet at the initiation of each exposure study. Mice were exposed by inhalation for 6 hr/day, 7 days/wk for a period of 50 days to MVE, MVE from which PM was removed (i.e., MVE gases, or MVEG), non-vehicular particles (i.e., S, N, or RD) and non-vehicular particles combined with MVEG. We reduced the size of the RD aerosol

to less than 2.5 μm to ensure it was respirable for a rodent. Vasoconstriction and endothelium-dependent vasorelaxation were assessed myographically to determine whether exposure to any of these components resulted in altered vascular function. To measure exposure-induced oxidative stress, we assessed aortic lipid peroxidation, plasma oxidized lipoproteins (oxLP), and aortic heme oxygenase (HO)-1 expression by real-time polymerase chain reaction (RT-PCR). We analyzed exposure-mediated alterations in nitric oxide (NO)-related pathways through messenger ribonucleic acid (mRNA) expression of endothelial nitric oxide synthase (eNOS), inducible NOS (iNOS), dihydrofolate reductase (DHFR), and guanosine 5'-triphosphate cyclohydrolase (GTPCH), as determined by RT-PCR. To assess endothelin-1 (ET-1) and matrix metalloproteinase (MMP) expression, we used RT-PCR to determine aortic expression of ET-1 and MMP-2, -3, -7, and -9 mRNA, as well as gelatinase activity through in situ zymography of histologic sections of aorta. Additional endpoints measured were vascular expression of MMP tissue inhibitors, tissue inhibitor of matrix metalloproteinases 1 and 2 (TIMP-1 and -2), and tissue factor, as well as coagulation assays. Finally, to quantify monocyte/macrophage (MOMA) infiltration into the plaque region, we utilized MOMA-2 immunohistochemistry. We evaluated the results by both analysis of variance (ANOVA) and multivariate approaches.

RESULTS

When mice were exposed to the various atmospheres, we observed several interesting trends that suggested a possible interaction between particles and gases. This was most evident in terms of aortic lipid peroxidation, where MVE led to potent increases in lipid peroxidation that were diminished with PM filtration. Furthermore, non-vehicular PM induced minimal or no effects, but non-vehicular PM combined with MVE gases induced more substantial effects than either component alone. MVE and MVEG combined with non-vehicular PM were also noted as promoting increased vascular inflammation, gelatinase activity, plaque size, and vasoreactivity. Analysis of aorta sections revealed increased vascular MMP-2 and -9 activity in ApoE^{-/-} mice exposed to MVE and N + MVEG_{High}. Oxidized lipoproteins were significantly increased with

This section is one part of Health Effects Institute Research Report 178, which also includes a section covering the epidemiology portion of this study, a Commentary by the NPACT Review Panel, an HEI Statement about the research project, and a Synthesis relating this report to Research Report 177. Correspondence concerning the Investigators' Report may be addressed to Dr. Matthew Campen, University of New Mexico College of Pharmacy, Dept. of Pharmaceutical Sciences MSC09 5360, 1 University of New Mexico, Albuquerque, NM 87131; mcampen@salud.unm.edu.

For authors' affiliations, see About the Authors at the end of this section.

* A list of abbreviations and other terms appears at the end of this section.

MVE exposure, which was even further elevated in animals exposed to S + MVE_{Low}, N + MVE_{Low}, and RD + MVE_{Low}. Lastly, vascular reactivity assays revealed that MVE and S-containing exposures resulted in enhanced phenylephrine (PE)-induced vasoconstriction in the vasculature of ApoE^{-/-} mice. No significant difference was observed in acetylcholine (ACh)-mediated vasodilation across exposure groups when compared with animals exposed to filtered air. A multivariate statistical analysis revealed possible underlying concentration–response relationships between vascular lipid peroxides and inflammation and individual chemical components of the exposure mixtures. However, after a statistical evaluation of the consistency of results among endpoints and the relative strength of the concentration–response relationships, we concluded that there was significant uncertainty in the associations and that these associations are inconclusive, although they may merit further study.

CONCLUSIONS

The findings suggest that components of vehicle-generated pollutants may drive key mechanistic pathways in atherosclerosis, such as vascular MMP expression and activity, endothelial dysfunction indicated by enhanced vasoconstriction, and increased reactive oxygen species (ROS) and circulating oxLP. Results indicate a substantial independent effect of emission-source gas-phase components, but addition of PM to the mixture was frequently associated with greater toxicity. The implications of this study may (1) provide motivation to consider specific components and mixtures of vehicle-related pollutants in future regulatory efforts and (2) help identify at-risk individuals who may be susceptible to cardiovascular effects of specific pollutant mixtures, in order to minimize the public health impact of ambient air pollution.

INTRODUCTION

There is ample evidence that both acute coronary events (Burnett et al. 1995; Schwartz and Morris 1995) and the incidence of ischemic heart disease (Pope et al. 2004) are associated with the chronic effects of air pollution. More recently, studies have implicated MVE as a main driver of adverse cardiac health effects, primarily by using roadway proximity as a surrogate of exposure (Peters et al. 2004; Pope et al. 2004; Hoffman et al. 2007; Künzli et al. 2010). This is consistent with our previous studies showing both chronic and acute cardiovascular effects of GEE and DEE (Lund et al. 2007, 2009; Campen et al. 2010b).

Atherosclerosis is a disease of the vasculature characterized by arterial plaque formation manifested by lipid

deposition and influx of macrophages into the arterial intima, vascular endothelial dysfunction, and altered vaso-reactivity; it has a multifactorial etiology that includes behavioral, genetic, and environmental influences. Numerous studies have shown that exposure to components of air pollution contributes to the progression of atherosclerosis, as demonstrated by impaired vascular endothelial function (Knuckles et al. 2008), increased plaque cell turnover and lipid concentration in aortic plaque lesions (Suwa et al. 2002; Campen et al. 2010b), altered vasomotor tone associated with increased vascular inflammation (Sun et al. 2005), upregulated expression of ET-1 and vascular MMP expression (Lund et al. 2007), and induced vascular ROS and circulating oxidized low-density lipoprotein (Lund et al. 2009, 2011). We reported recently that circulating inflammatory factors can be induced acutely following diesel exhaust inhalation in humans, leading to activation of endothelial cell adhesion molecules, which is one of the earliest steps in the development of atherosclerotic lesions (Channell et al. 2012). Notably, a principal component of diesel exhaust, nitrogen dioxide (NO₂), also induced this effect. While these studies describe a clear causative relationship between exposure to vehicle-generated air pollutants and deleterious effects on the cardiovascular system, the underlying mechanisms have not yet been fully elucidated. Furthermore, few studies have investigated in a systematic manner whether these responses occur after exposure to other major sources of ambient air pollutants such as S, N, and RD.

Several signaling pathways have been identified as being involved in the progression of atherosclerosis and the onset of clinical cardiovascular events such as heart attack and stroke. A hallmark of atherosclerosis is inappropriate vascular remodeling, which under pathologic conditions is mediated by extracellular matrix degradation by the MMP family of endopeptidases (Galis et al. 2002). In addition to atherogenesis (McMillan et al. 1995), MMP expression and activity are also associated with the destabilization of advanced plaques, resulting in plaque rupture (Newby 2005). Importantly, MMPs — specifically MMP-9 — have been reported to be upregulated during clinical cardiovascular events and may even serve as a novel predictor of cardiovascular mortality (Blankenberg et al. 2003). Many diverse stimuli — including ROS, which are upregulated in animal models of vehicle-generated air pollution exposure (Lund et al. 2007) — can upregulate MMPs in the vasculature (Rajagopalan et al. 1996; Lund et al. 2007, 2009; Zalba et al. 2007). MMPs are regulated on multiple levels: transcriptionally, translationally, through inhibition by binding to their TIMPs, and through enzymatic cleavage from their zymogen to active form.

The imbalance in expression of vascular factors, including ET-1 and NO, produced by the endothelium is also known to contribute to the onset and to mediate the progression of atherosclerosis. ET-1 is a secreted vasoactive peptide that signals through two main receptor subtypes in the vasculature: ET_A and ET_B. Signaling of ET-1 through the ET_A receptor mediates vasoconstriction and mitogenic pathways, while signaling through the ET_B receptor predominantly mediates vasodilation and ET-1 clearance. ET-1 is reported to be significantly upregulated in atherosclerotic vessels (Ihling et al. 2001) and has also been shown to induce MMP expression and activity in cardiovascular pathologies (Ergul et al. 2003). Additionally ET-1 may further aggravate atherosclerosis pathophysiology through its ability to stimulate ROS via nicotinamide adenine dinucleotide phosphate (NAD(P)H) oxidase (Griendling et al. 2000). NO, another vasoactive compound associated with atherosclerosis, is produced by the constitutive eNOS or iNOS in endothelial cells that line the vasculature. NO acts as a vasodilator in the vasculature, dysregulation of which has been demonstrated in atherosclerotic vessels in multiple animal models and in humans (Föstermann et al. 1988; Chester et al. 1990). eNOS can be downregulated in atherosclerosis or functionally impaired by the presence of oxygen radicals (Chatterjee et al. 2008). Upregulation of iNOS may reflect an inflammatory state in the entire vessel, not limited to endothelium, but the NO generated from this protein is not involved in homeostatic control of vasodilation and platelet inhibition, unlike eNOS-derived NO (Chatterjee et al. 2008). Also of importance is that NO can be oxidized in the presence of ROS, producing peroxynitrite (ONOO⁻). ONOO⁻ is a highly reactive molecule in the vasculature responsible for cell damage through promotion of lipid peroxidation (Rubbo and O'Donnell 2005).

The tunica media layer of the arterial wall is predominantly composed of smooth muscle cells, which actively respond to stimuli from the autonomic nervous system, from humoral factors, and from vasoactive factors (such as ET-1 and NO) secreted by the vascular endothelial layer. Altered vasomotor tone, as assessed by vasoreactivity, is closely linked to the development of atherosclerosis and is believed to play an integral role in the pathophysiology of myocardial ischemia in humans with coronary artery disease. (The most accepted measurement of vasomotor tone in rodent models is through the use of myography, which allows for the measurement of changes in arterial luminal diameter when challenged with vasoconstrictive [e.g., PE] or vasodilatory [e.g., ACh] stimuli.) Human atherosclerotic coronary artery segments have been shown to release less active NO (Chester et al. 1990) and, in general, to display increased vasomotor tone as a result of this loss

of NO function (Badimon et al. 1992; Lüsher 1993). Additionally, tissue and plasma levels of ET-1 are known to be upregulated in patients with atherosclerosis (Lerman et al. 1991; Bacon et al. 1996), and ET-1-mediated vasoconstriction is reported to be enhanced in atherosclerotic vessels (Lerman et al. 1991). Therefore, it is important to assess any alterations in vessel reactivity in both vasoconstriction and vasodilatory responses in atherosclerotic vessels.

The key initiating events in atherosclerosis are the retention and oxidation of low-density lipoprotein (LDL) in the vascular wall. The lipid oxLP is also known to play an important role in atherogenesis (Berliner and Heinecke 1996) mainly through binding to cell surface receptors such as the lectin-like oxLP (LOX)-1 receptor, CD36, SR-A, and SR-B1, among others (Steinbrecher 1999; Terpstra et al. 2000), and is found to be highly upregulated in humans with atherosclerosis (Witztum and Steinberg 2001). Notably, ox-LDL signaling has been shown to upregulate expression of monocyte adhesion molecules, including monocyte chemoattractant protein (MCP)-1, intracellular adhesion molecule (ICAM)-1, and vascular cell adhesion molecule (VCAM)-1 (Li and Mehta 2000; Chen H et al. 2003; Chen K et al. 2005). The interactions among atherosclerotic contributors oxLP, ET-1, and vascular MMP likely play an important role in the progression of atherosclerosis, as both oxLP and ET-1 have been shown to increase MMP-9 activity (Ergul et al. 2003; Li et al. 2003). While there are many components of vehicular emissions that might account for an increase in production of oxLP with exposure, at least one main component, diesel PM, has been reported to increase oxidative modification of LDL in vitro (Ikeda et al. 1995).

Recent findings in our laboratory suggest that whole combustion emissions, especially GEE and DEE, have a greater cardiovascular effect than particles alone (Lund et al. 2007; Campen et al. 2010b). The present study offers a platform from which to better assess the potential contributions from particulate and gaseous components of MVE to cardiovascular toxicity, taking into consideration the mechanistic insights that can be inferred from many of the molecular pathways described above. In the current study, we exposed ApoE^{-/-} mice, a mouse model known to be susceptible to pollution exposure. A number of studies have found that pathways related to atherosclerosis are promoted by PM and various other pollutants in this mouse model (Sun et al. 2005; Araujo et al. 2008; Campen et al. 2010b). However, we did not aim to show the severity of biologic effects, but rather to conduct quantitative comparisons among pollutant mixtures.

The aim of the present study was to provide a basis for comparing pathophysiological and molecular endpoints in

animals with results from the parallel human study (described in Section 1 of this report), which uses data from the Multi-Ethnic Study of Atherosclerosis (MESA) Air cohort. For example, results of vascular reactivity responses in animal studies are comparable to measurements of large and small artery compliance in humans using ultrasound and pulse waves (Joannides et al. 2006). The working hypothesis was that important environmental effects on the cardiovascular system are driven by exposure to vehicular pollutants, including both GEE and DEE. This hypothesis considered that the public health importance of traffic exposure is linked both to the potential for enhanced exposure because of commuting or proximity to roadways and to the potency of vehicular emissions, which may be more toxic than other components of ambient air.

Our approach was to generate laboratory exposure atmospheres that simulated different pollutant mixtures in the environment, with an emphasis on benchmarking MVE against other sources of PM, taking into consideration the importance of gaseous copollutants. MVE included both GEE and DEE, combined in proportions that represent potential exposure scenarios in the environment. We selected a combination of the two types of engine exhaust, as exposure to these pollutants rarely occurs in isolation. The other pollutants included S, N, and RD, all of which account for a large portion of PM and are poorly characterized regarding their cardiovascular toxicity (e.g., Seinfeld and Pandis 1998). Furthermore, the relative proportions of each of these pollutants vary in different regions of the United States, with N having higher proportions in Western cities such as Los Angeles, California, S having higher proportions in the Northeast, and RD having higher proportions generally in the Southwestern/Western regions in combination with fugitive (resuspended or windblown) dust from other sources. Differences in the toxic potencies of these varied PM samples may help explain regional variability in the observed risk of cardiopulmonary morbidity and mortality.

We conducted comparative studies of cardiovascular toxicity in mice, with identical protocols applied across exposure atmospheres to facilitate comparisons of toxicity for contrasting pollutants and chemical components. To the extent feasible, the biologic responses studied complemented the classes of epidemiologic measurements being conducted in the parallel study in humans (see Section 1 of this report), with an additional goal of including invasive measurements that were not possible in the epidemiologic study.

For example, we quantified MMPs in vascular tissue, which dovetails with an endpoint of the MESA Air cohort: to quantify MMP expression on monocytes. We also

examined several other cardiovascular endpoints that we hoped would provide a foundation for translating animal models of inhaled air pollution exposure to those measured and observed in human exposure models.

SPECIFIC AIMS

The aims of this study were to conduct toxicologic laboratory tests to provide further insight into mechanisms explaining biologic associations related to cardiovascular morbidity and mortality observed in the parallel epidemiologic study (see Section 1 of this report) and to inform potential regional contrasts in epidemiologic findings. The underlying assumption was that animal toxicology models could be used to reveal biologic sensitivity to inhalation atmospheres of different composition and that these data could help inform and interpret associations of cardiovascular endpoints in epidemiologic studies. The overarching hypotheses were that most of the morbidity seen in the epidemiologic study would be associated with MVE exposure and that other, more regional, pollutants would demonstrate less biologic potency. We examined the biologic responses in the cardiovascular system in ApoE^{-/-} mice exposed for 6 hr/day, 7 days/wk for 50 days to mixtures of MVE, S, N, RD, or combinations of these pollutants created in the laboratory. We selected biologic response indicators in this study that complemented the cardiovascular focus of the epidemiologic study and focused primarily on physiologic alterations in vascular function, as well as regulation of the expression of vascular factors associated with the progression of atherosclerosis and/or onset of a clinical cardiovascular event (and associated mortality in humans), including ROS, MMP, ET-1, NO, and oxLP.

METHODS AND STUDY DESIGN

EXPOSURE ATMOSPHERES

The exposure atmospheres in this study were MVE (including both GEE and DEE), S, N, and RD (Table 1). We studied MVE at two different exposure concentrations, defined as “high” (300 µg/m³ PM) and “low” (100 µg/m³ PM). We also investigated the role of the gas phase in causing or potentiating biologic effects of MVE, S, N, and RD by removing the PM from the MVE using filtration and then examining the MVE gases only (MVEG) either alone or in combination with S, N, and RD. We added MVEG to the S, N, or RD atmospheres at the high concentration, proportional to that in the MVE_{High} atmosphere. We further evaluated the potential for PM interactions with combinations of pollutants by employing mixtures of RD + MVE_{Low},

Table 1. Target exposure atmospheres for NPACT Toxicology Study

Exposure Atmosphere	Target Concentrations			
	PM ($\mu\text{g}/\text{m}^3$)	NO _x (ppm)	CO (ppm)	NMVOC (mg/m^3)
Atmospheres				
MVE _{High}	300	30	100	15
MVE _{Low}	100	10	33	5
RD	300	0	0	0
S	300	0	0	0
N	300	0	0	0
Gaseous Atmospheres and Non-vehicular PM + Gases				
MVEG _{High}	0	30	100	15
MVEG _{Low}	0	10	33	5
RD + MVEG _{High}	300	30	100	15
S + MVEG _{High}	300	30	100	15
N + MVEG _{High}	300	30	100	15
Non-vehicular PM + Whole Emissions^a				
RD + MVE _{Low}	200 + 100	10	33	5
S + MVE _{Low}	200 + 100	10	33	5
N + MVE _{Low}	200 + 100	10	33	5

^a PM concentration given as RD + MVE_{Low}, S + MVE_{Low}, and N + MVE_{Low}.

N + MVE_{Low}, and S + MVE_{Low}. In order to evaluate the interactions, we combined MVE at the low exposure target ($100 \mu\text{g}/\text{m}^3$ PM) with non-vehicular PM (S, N, or RD at $200 \mu\text{g}/\text{m}^3$) to result in the same PM concentration as the high exposure levels for the single pollutants (i.e., $300 \mu\text{g}/\text{m}^3$ total). Exposures were conducted for 6 hr/day for 50 days. We were unable to conduct all exposures in parallel because of the number of exposure chambers and how many animals could be housed in them and since S and N were created using the same system. Therefore, a batched approach (A–D) was implemented. In the first batch of exposures, the following atmospheres were generated: filtered air, MVE_{High}, MVEG_{High}, S, and S + MVEG_{High}. In the second batch, the following atmospheres were generated: filtered air, MVE_{Low}, MVEG_{High}, N, and N + MVEG_{High}. In the third batch, the following atmospheres were generated: filtered air, MVE_{High}, MVEG_{Low}, MVEG_{High}, RD, and RD + MVEG_{High}. In the fourth batch, the following atmospheres were generated: filtered air, MVE_{High}, S + MVE_{Low}, N + MVE_{Low}, and RD + MVE_{Low}.

Development of Atmosphere Combinations

Figure 1 provides a schematic of the exposure atmosphere generation and dilution system for the creation of

the NPACT study atmospheres. (The aerosol generation technique for each of the individual atmospheric components or mixtures is described below.) To combine these mixtures, we took a combination of approaches. We began generation of MVE by collecting exhaust from both a gasoline engine and a diesel engine. The exhausts were immediately diluted as they entered separate stainless steel dilution tunnels, and then extracted via eductor pumps to a 2-m^3 secondary mixing chamber where they were combined. The secondary mixing chamber provided a residence time of approximately 4 minutes to ensure complete mixing prior to further dilution and transit to the exposure chambers. After the mixing chamber, MVE transited to a distribution plenum; it was then further diluted from the plenum and delivered to several whole-body inhalation chambers. MVEG was produced by placing an 8-inch \times 10-inch high-efficiency particulate filter after the distribution plenum and prior to the whole-body chamber. We examined MVEG either alone at the same dilution as MVE or in combination with N, S, or RD (see Table 1).

The mixing of either MVEG or MVE with N, S, or RD occurred at an intersection just prior to the specific inhalation chamber. The mixture was then added to the exposure chamber. We monitored the relative proportions of MVEG or MVE when combined with the N, S, or RD atmospheres and controlled them based on the concentrations of carbon monoxide (CO) and nitrogen oxides (NO_x) measured in real time in the exposure chamber (relative to the targeted concentrations). This was possible because the ratio of these gases to the relative proportions of PM in MVE was consistent throughout the exposure.

Motor Vehicle Exhaust Table 2 defines the approximate proportion of the exhaust mixtures, accounting for the concentrations of PM, NO_x, CO, and nonmethane volatile organic compounds (NMVOCs) attributed to GEE or DEE. We selected these relative proportions based on the maximum concentration of PM that could be obtained from GEE without adding excess heat and humidity to the chambers. The GEE was diluted approximately 10:1 from the tailpipe. DEE was then added in a concentration that achieved the target of $300 \mu\text{g}/\text{m}^3$ of total PM. A similar procedure was followed to achieve $100 \mu\text{g}/\text{m}^3$ of MVE, using a dilution of 1:30 of GEE mixed with DEE to reach $100 \mu\text{g}/\text{m}^3$. Only about 20% of PM was derived from GEE, whereas GEE accounted for most of the CO and NMVOC in the exposure atmosphere.

Diesel Engine Exhaust DEE was produced from a single-cylinder, 5500-watt, Yanmar diesel engine generator using No. 2 diesel certification fuel (Phillips Chemical Company, Borger, TX) and 40-weight motor oil (Rotella T, Shell,

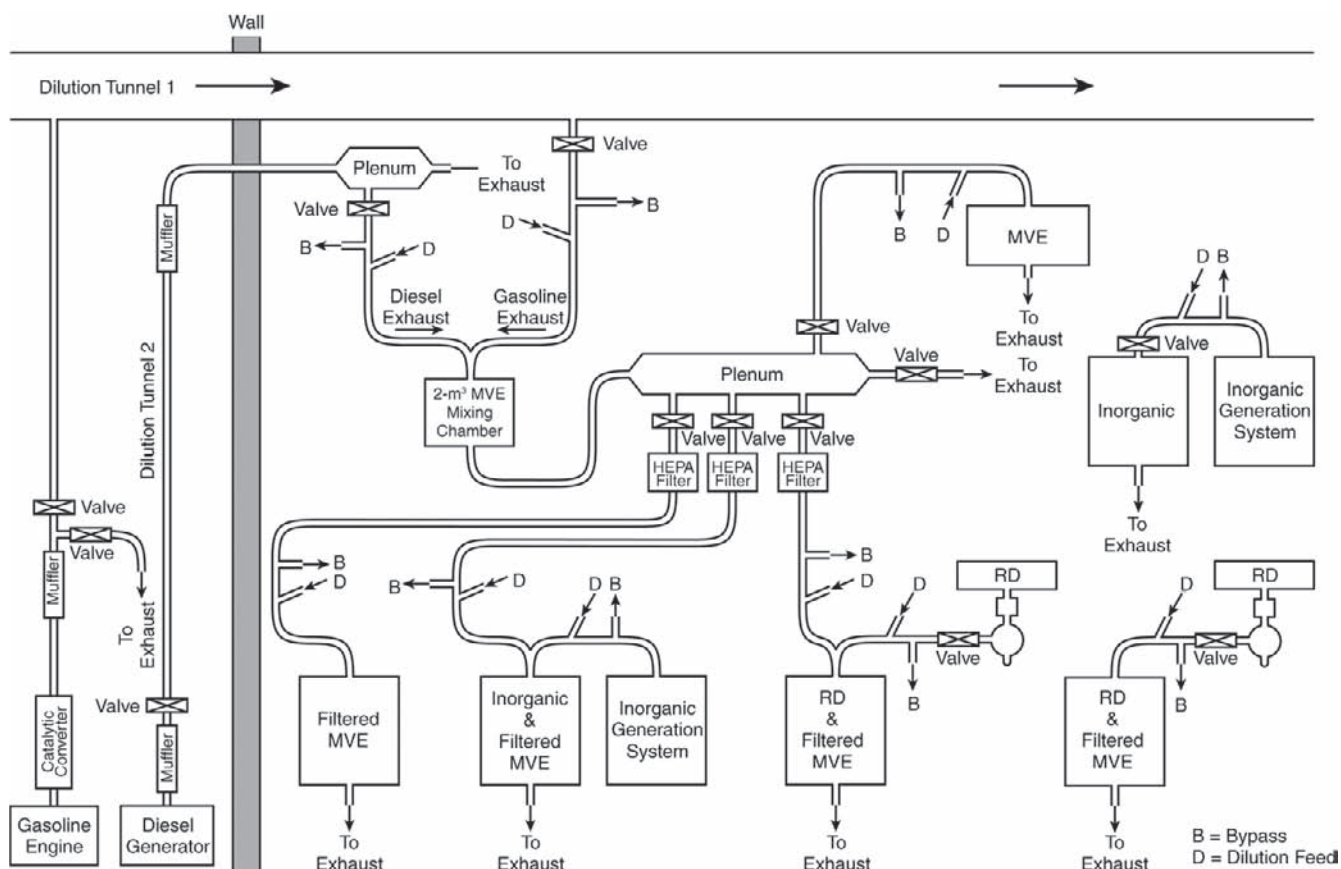


Figure 1. Schematic of the NPACT inhalation exposure facility. GEE and DEE were generated in an adjacent engine laboratory. Exhaust from each dilution tunnel was extracted and combined into a 2-m³ mixing chamber before diversion to a secondary distribution plenum. During transition, aerosols were diluted by a combination of an aerosol bypass (B) that would remove air from the system and a dilution feed (D) that would add clean dilution air into the system. The two smaller systems on the right represent the generators of the S and N atmospheres (top) and the RD atmosphere (bottom).

Table 2. Target Proportions of GEE and DEE in MVE Exposure Atmospheres

Exposure Atmosphere	Target Concentrations			
	PM (µg/m ³)	NO _x (ppm)	CO (ppm)	NMVO (mg/m ³)
MVE _{High}				
GEE	50	25	97	14
DEE	250	5	2.2	1
MVE _{Low}				
GEE	16.6	8.3	32.3	4.7
DEE	83.3	1.7	0.7	0.3

Houston, TX) as described in a study by McDonald and colleagues (2004b). Electrical current was pulled from the engine to provide a constant load (90%) during operation. Desired concentrations were attained by diluting the direct exhaust with filtered air; the clean control air and diesel-dilution air were pretreated by passing them through a carbon-impregnated filter to remove volatile organic compounds (VOCs) and through a high-efficiency particulate air (HEPA) filter to remove PM.

Gasoline Engine Exhaust We generated GEE using the method described by McDonald and colleagues (2007), with the exception that only one engine was used during a 6-hour exposure period instead of two. In brief, exhaust was generated from a 1996 General Motors 4.3 L V6 gasoline engine (approximate mileage, 150,000) equipped with

a stock exhaust system (including muffler and catalyst). The engine was connected to an eddy current dynamometer (Model Alpha 240, Zöllner, Kiel, West Germany) linked to a dynamometer interface (Type DTC-1, Dyne Systems Co., Germantown, WI) that was controlled by a custom software program (Cell Assistant, Dyne Systems Co.). The engine was fueled with gasoline obtained from a local station in Albuquerque, New Mexico. The fuel was obtained during the non-winter months to avoid ethanol as a component. The crankcase oil (10W-30, Pennzoil Products Company, Houston, TX) and the oil filter (Duraguard PF52, AC Delco, Detroit, MI) were changed every 122 hours (equivalent to 3000 miles) of engine operation. Exhaust was immediately diluted at the tailpipe in a dilution/exposure system, as previously described.

Sulfate and Nitrate We generated S and N aerosols from an evaporation–condensation aerosol generation system. The system was designed to re-create a bimodal sulfate size distribution within the fine particle ($\leq 2.5 \mu\text{m}$) PM fraction as it exists in the atmosphere (Seinfeld and Pandis 1998). The evaporation–condensation system started with nebulization of a dilute sulfate (5%) solution. The nebulized S was subsequently dried by passage through a diffusion drier filled with silica gel (Wilkerson, Englewood, CO). The dried aerosol was heated to 150°C and subsequently chilled to approximately 5°C through a counter-current heat exchanger and an aerosol bypass/dilution leg. Flow through the S-generation unit was at 2 L/min. The same system was used to create the N exposure atmosphere, starting with a 10 mg/mL solution.

Road Dust We collected RD from roadway surfaces on residential streets in Phoenix and Tucson, Ariz. We selected sampling locations based on proximity to populations that are part of the MESA Air cohort studied in Section 1 of this report. Material was vacuumed from street surfaces with a commercially available, standardized, low-volume surface sampler (CS3, Inc., Sandpoint, ID). The sampler removed material $>10 \mu\text{m}$ during collection. Once obtained, the material was sieved through an orbital shaker, and the finest fraction (bulk material with a diameter $<38 \mu\text{m}$) was kept. To prevent growth of biologic organisms, the sieved material was stored at -80°C until aerosolization. RD aerosol was generated using a Wright Dust Feeder (CH Technologies, Westwood, NJ) coupled to a $\text{PM}_{2.5}$ Cyclone (URG Corp., Chapel Hill, NC) on the effluent stream to remove particles $>2.5 \mu\text{m}$. We limited particle size to ensure the material was in the respirable range for a rodent.

Dilution Systems

We diluted the exhaust with tempered ($\approx 15\text{--}20^\circ\text{C}$) ambient air, filtered using charcoal (to remove volatile contaminants) and HEPA (to remove PM) filters. Our general approach was to dilute the GEE and DEE immediately after combustion to ensure that particle nucleation events were quenched rapidly and to the greatest extent possible. However, because the atmospheres passed through a mixing chamber that allowed approximately 4 minutes of aging, the preservation of the primary exhaust particles was not considered feasible for this study. When choosing dilution rates, we had to balance a need to conserve material for the highest exposure concentration with a need for maximum dilution to reduce exhaust temperature. For GEE, achievable PM exposure concentrations were dictated by the dilution required to reach chamber temperatures low enough to be compatible with animal welfare ($\approx 20\text{--}27^\circ\text{C}$). We used an in-line, flow-through muffler on each exhaust line to reduce exposure chamber noise levels to less than 85 dB.

Exposure Chambers

We conducted the exposures in whole-body rodent inhalation chambers (2 m^3) (Lab Products, Maywood, NJ). Inside the chambers, there were six tiers of cage units. Each cage unit contained multiple individual wire cages and had an excreta catch pan lined with absorbent paper, which was cleaned both before and after daily exposures. Chambers were washed and sterilized weekly.

The chambers were ventilated with the exposure atmospheres at approximately 500 L/min, yielding a residence time within the chamber of about 4 minutes. These chambers were designed to enhance the uniformity of the aerosol distribution throughout the exposure (Cheng and Moss 1995; McDonald et al. 2004b). The chambers contained sampling ports above each cage unit to facilitate characterizing the spatial homogeneity of the exposures and to provide multiple sample locations for exposure characterization.

Atmosphere Characterization

We conducted exposure atmosphere characterization as described in previous studies (McDonald et al. 2004a, 2004b, 2006, 2008). We provide a summary of the types of measurements in Table 3 and describe the methods in further detail in Appendix R (available on the HEI Website). In brief, we have developed sample collection strategies to capture and measure gas-phase, particle-phase, and

Table 3. Summary of Types of Exposure Atmosphere Characterization Measurements and Measurement Conditions^a

Measurement	Collection Device	Collection Media	Collection Point	Sampling Flow Rate (L/m)	Analytical Instrument	Analysis Location
Gravimetric mass	Aluminum in-line filter holder	TIGF	Chamber/plenum	4	MB	LRRRI
Continuous mass	DustTrak nephelometer	NA	Chamber	2	NA	LRRRI
NO _x	Chemiluminescence analyzer	NA	Chamber	0.4	NA	LRRRI
Particle size	Fast-mobility particle sizer/aerodynamic particle sizer	NA	Chamber	10	NA	LRRRI
CO/CO ₂ /THC	Photoacoustic analyzer	NA	Chamber	1	NA	LRRRI
THC	Flame ionization detector	NA	Chamber	1	NA	LRRRI
Organic/elemental carbon	Aluminum in-line filter holder	Quartz filter (1)	Plenum	20	TOR	DRI
Ions (sulfate/nitrate/ammonium)	Aluminum in-line filter holder	Quartz filter (2)	Plenum	20	IC, AC	DRI
Metals and other elements	Teflon in-line filter holder	Teflon filter (2)	Plenum	20	XRF	DRI
NMVOCs (C ₁ –C ₁₂)	Volatile organic sampler	Electropolished canister	Chamber	0.1	GC/MS; GC/FID	DRI
Volatile carbonyls	Volatile organic sampler	DNPB cartridge	Chamber	0.3	LC/MS	LRRRI
Semivolatile/fine particle organics	Tisch environmental PUF sampler	Quartz filter/PUF/XAD-4/PUF	Plenum	80	GC/MS	DRI

^a AC indicates automated colorimetry; DNPB, dinitrophenylhydrazine; DRI, Desert Research Institute; GC/FID, gas chromatography/flame ionization detection; GC/MS, gas chromatography/mass spectrometry; IC, ion chromatography; LC/MS, liquid chromatography/mass spectrometry; LRRRI, Lovelace Respiratory Research Institute; MB, microbalance; NA, not applicable; NMVOC, nonmethane volatile organic compound; PUF, polyurethane foam; THC, total hydrocarbons; TIGF, Teflon-impregnated glass fiber filter; TOR, thermal/optical reflectance; XAD, polyaromatic adsorbing resin; XRF, X-ray fluorescence.

semivolatile organic compounds (SVOCs) for a broad spectrum of chemical classes. We analyzed gases by chemiluminescence (for NO_x), infrared spectroscopy (for CO), and gas chromatography/mass spectrometry (for VOCs) after collection into SUMMA canisters (EMSL Analytical, Cinnaminson, NJ). Particle chemistry was determined from material collected on quartz filters for analysis of carbon (elemental carbon [EC] and organic carbon [OC]) by thermal/optical reflectance (Chow et al. 1993) and inorganic ions (S, N, and ammonium) by ion chromatography after aqueous extraction (Chow et al. 1999). OC was normalized to organic mass by multiplying the measured value by 1.2 to account for unmeasured hydrogen and other elements.

Metals were analyzed by X-ray fluorescence on ultra-clean Teflon-membrane filters. SVOCs and particle-phase organic compounds were extracted using Teflon-coated glass-fiber filters, followed by 10 g of XAD-4 resin (Sigma-Aldrich, St. Louis, MO) and analyzed by gas chromatography/mass spectrometry. Particle size distribution was measured with a fast-mobility particle sizer (TSI, St. Paul, MN) for the approximately 5 to 500 nm size range and an aerodynamic particle sizer (TSI) for the 0.5 to 20 μm size range. Particle mass concentration by gravimetric analysis of Teflon-membrane filters at the inlet of and inside the exposure chamber was conducted once a week at each exposure level.

To analyze the polar SVOCs, we spiked filters and XAD-4 cartridges with deuterated internal standards (hexanoic acid-d₁₁, benzoic acid-d₃, adipic acid-d₁₀, suberic acid-d₁₂, homovanillic, 2,2-d₂ acid, tetradecanoic acid-d₂₄, eicosanoic acid-d₃₉, myristic acid-d₂₇, succinic acid-d₄, and phthalic-3,4,5,6-d₄ acid). We extracted samples with approximately 170 mL of dichloromethane (CH₂Cl₂) using the Dionex ASE system (Thermo Scientific) for 15 minutes per cell at 1500 psi and at 80°C, followed by another extraction using approximately 170 mL of acetone under the same conditions. We concentrated the extracts to approximately 1 mL by rotary evaporation at 35°C under gentle vacuum, filtering them through a 0.2 µm polytetrafluoroethylene (PTFE) disposable filter device (Whatman Puradisc 25 TF) and rinsing the flask three times with 1 mL dichloromethane and acetone (50/50 by volume) each time. We collected filtrate in a 4 mL amber glass vial for a total volume of approximately 4 mL.

The polar compounds, including alkanolic acids, phenols, and aromatic acids, were analyzed in dichloromethane extracts from filters (Pall-Gelman, Port Washington, NY) and XAD-4 sorbents. We added 200 µL of acetonitrile to the dichloromethane and concentrated the samples under high purity nitrogen to 100 to 200 µL. We used a mixture of bis(trimethylsilyl)trifluoroacetamide (BSTFA) with 1% trimethylchlorosilane (TMCS) and pyridine to convert the polar compounds into their trimethylsilyl derivatives for analysis of the species of interest. We analyzed the samples employing the electron impact gas chromatography/mass spectrometry technique, using a Varian CP-3800 GC equipped with a CP-8400 AutoSampler and interfaced to a Varian 4000 Ion Trap mass spectrometer. Injections were 1 µL in the splitless mode onto a 5% phenylmethyl-silicone-fused silica capillary column (J&W Scientific DB-5ms) (30 m × 0.25 mm × 0.25 mm). We identified and quantified the analytes using the selected ion storage technique, by monitoring the molecular ions of each analyte and each deuterated analyte.

BIOLOGIC ENDPOINTS

Table 4 provides a summary of the biologic endpoints measured. Methods for each of the measures are described below.

Animals

All studies used male ApoE^{-/-} mice obtained from a commercial vendor (Taconic) at 6 to 8 weeks of age and placed in quarantine for 2 weeks after arrival. A high fat/high cholesterol diet (Harlan Teklad 88137) was begun

Table 4. Experimental Endpoints for Animal Exposure Studies

Biologic Pathways	Specific Assays ^a
General vascular toxicity: oxidative/nitrosative stress	HO-1, GSH (mRNA) Lipid peroxides (TBARS) ET-1 (mRNA) iNOS (mRNA)
Atherosclerosis: vascular remodeling and lipid accumulation	MMP-2, -9 activity MMP/TIMP (mRNA) Lesion staining (lipids, macrophages) ox-LP in plasma
Coronary artery disease: nitric oxide synthase impairment	Dilation/constriction eNOS (mRNA) DHFR, GTPCH (mRNA)

^a All assays were performed in aortic tissues, unless otherwise indicated.

concomitant with the onset of the 50-day exposures. Food and water were available ad libitum except during exposures, when food was removed from the chambers (water was available continuously). Mice were housed under conditions approved by the Association for Assessment Accreditation of Laboratory Animal Care for temperature (20–25°C), relative humidity (40–60%), and light cycle (12h:12h, light:dark). We exposed mice for 6 hr/day, 7 days/wk to the exposure atmospheres described in Table 1. Because of the high number of animals (see under each assay subhead for numbers), exposures were staggered in time. After completion of the exposure, the mice were euthanized by humane methods (pentobarbital overdose), and biologic specimens were collected immediately. Blood was spun in ethylenediaminetetraacetic acid (EDTA) tubes to collect plasma and then immediately frozen. With the exception of aortas for vascular function studies, all organs were snap-frozen in liquid nitrogen and stored in a –80°C freezer until utilized. All studies were approved by the Lovelace Respiratory Research Institute (LRRRI) Animal Care and Use Committee.

Vascular Function

We harvested aortas ($n = 8$) fresh from mice the day after the 50-day exposures and placed them immediately in ice-cold physiologic saline solution (PSS). They were rapidly cleaned of perivascular fat and residual adventitia and trimmed to even-length rings (one per vessel, $n = 8$ vessels per group), which were then mounted on a wire myograph

(Model 620M; Danish Myo Technology A/S) and submerged in a heated (37°C) and aerated PSS. Rings were allowed 60 minutes to recover from the harvesting and develop spontaneous tone. We used a high potassium (60 and 120 mM) challenge to test the viability of the rings by adding a potassium PSS solution to each ring bath for 5 minutes twice, followed each time by a washout.

We then treated each viable vessel ring (one per animal) with increasing concentrations of PE to test constriction. Concentrations ranged from 10^{-9} M to $10^{-4.5}$ M in half-molar steps. Constriction was observed until plateau, which occurred after approximately 5 minutes for each concentration step. After the PE curves were generated, the vessels were allowed to rest for 30 minutes in regular PSS. We then precontracted them to approximately 50% to 70% of maximal PE constriction and subsequently added ACh in increasing concentrations to generate a dilation curve.

Because of the large numbers of exposures and animals needed for these assays, the exposures occurred over the course of several years involving different personnel. For the most part, the PE response curves were highly consistent among the results from the people performing the assays. However, the magnitude and shape of the ACh curves varied substantially.

Lipid Peroxidation Assay

Using a different set of mice, we harvested aortas ($n = 8$ per group per exposure block) immediately after killing the animals, cleaned them of perivascular fat, and then homogenized them. We then measured lipid peroxidation by a thiobarbituric acid reactive substances (TBARS) assay using a standard kit (ZeptoMetrix), according to the manufacturer's directions. Results are reported as equivalents of malondialdehyde (MDA), from which the standard curve was generated (per manufacturer's instructions).

Histopathology

MMP Activity With another set of mice, we determined MMP activity by incubating aorta cryosections (6 μ m thick) with 45 μ L of 10- μ g/mL dye-quenched (DQ) gelatin (EnzChek, Molecular Probes, Invitrogen, Carlsbad, CA) and 1- μ g/mL DAPI (4',6-diamidino-2-phenylindole nuclei stain; Invitrogen). We added coverslips and chilled the cryosections for 5 minutes at 4°C in 1% UltraPure low-melting-point agarose (Invitrogen) and then incubated them for 6 hours in a dark, humid chamber at 37°C. Negative control slides were co-incubated with a specific gelatinase inhibitor (MMP-2, -9 inhibitor type IV, Chemicon, Millipore, Temecula, CA) to determine the selectivity of the assay. We analyzed the slides using fluorescence

microscopy, calculated densitometry using white/black images, and quantified the images using ImageJ software (National Institutes of Health, Bethesda, MD) (performed on 6 sections per sample, 3 regions per section, 6 animals per group). We subtracted the background fluorescence (fluorescence present in the total image outside of the vessel) from each section before making statistical comparisons between groups.

Plaque Area Using the same set of mice, we determined plaque area at the aortic outflow tract on aorta cryosections stained for MOMA-2 (monocyte/macrophage selective marker), using hematoxylin counterstaining. MOMA-2 staining density was assessed on 4 sections per animal on 3 animals per exposure group by a trained, blinded reader, with the following exceptions: 6 per group (MVEG_{High}), 9 per group (MVE_{High}), and 12 per group (filtered-air controls). Slides were all analyzed at the same time using standard histopathologic techniques. The plaque area was determined by tracing the entire area and normalizing that value based on the luminal area using imaging software (ImageJ) (Campen et al. 2010b).

Real-time Polymerase Chain Reaction

We assessed specified endpoint mRNA in aortas using RT-PCR, as described in an earlier study (Lund et al. 2007). Briefly, we isolated total RNA from the aortic arch (including the ascending thoracic and a small portion of descending thoracic) using RNeasy Fibrous Tissue Mini Kit (Qiagen, Valencia, CA) ($n = 8$ for each exposure group). We synthesized complementary deoxyribonucleic acid (cDNA) from total RNA in a 20- μ L final reaction volume, per the manufacturer's instructions (iScript Select cDNA Synthesis Kit, Bio-Rad, Hercules, CA). We heated the mixture at 42°C for 1 hour and then cooled it to 4°C. We performed RT-PCR using the appropriate primers (500 nM concentration for forward and reverse), an iCycler (Bio-Rad), and an ABI 7500 RT-PCR system (Applied Biosystems, Foster City, CA). We ran control reactions without reverse transcriptase or without RNA to verify the absence of contaminated DNA or primer dimerization, respectively. PCR amplification was carried out in a 25- μ L volume containing 0.25 ng of cDNA, 500 nM each of forward and reverse primers, 12.5 μ L iQ SYBR Green Supermix (Bio-Rad), and 9.5 μ L water. The PCR process consisted of heating the mixture at 95°C for 10 minutes and then running 40 cycles of heating at 95°C for 30 seconds and at 60°C for 30 seconds. We used the following primer sequences to analyze the genes: MMP-2 (forward) 5'-ACCAGGTGAAGGATGTGAAGCA-3', (reverse) 5'-ACCAGGTGAAGGAGAAGGCTG; MMP-3 (forward) 5'-AGA

AGGAGGCAGCAGAGAACC-3', (reverse) 5'-GCAATGGGT AGGATGAGCACAC-3'; MMP-7 (forward) 5'-CTATGCAGC TCACCCTGTTCTG-3', (reverse) 5'-GCCTGTCCCCACTGA TGTGC-3'; MMP-9 (forward) 5'-GACAGGCACTTCACC GGCTA-3', (reverse) 5'-CCCGACACACAGTAAGCATT CTG-3'; TIMP-2 (forward) 5'-CTTCAAGCATCCAGGCTG AGC-3', (reverse) 5'-TCATCAGTTTGTGCAAAAGAGGGA-3'; ET-1 (forward) 5'-AAGACCATCTGTGTGGCTTCTAC-3', (reverse) 5'-CAGCCTTTCTTGAATGTTTGGAT-3'; HO-1 (forward) 5'-TTCTGGTATGGGCCTCACTGG-3', (reverse) 5'-ACCTCGTGAGACGCTTTACA-3'; iNOS (forward) 5'-GGCAGCCTGTGAGACCTTTG-3', (reverse) 5'-TGCATT GCAAGTGAAGCGTTT-3'; eNOS (forward) 5'-CTGGCC CAGAAATACCTGGTT-3', (reverse) 5'-ACCGAACGAAGT GACACAATCC-3'; DHFR (forward) 5'-AATCCTAGCGTG AAGGCTGTA-3', (reverse) 5'-GGCGACGATGCAGTTC AAT-3'; guanosine 5'-triphosphate cyclohydrolase (GTPCH) (forward) 5'-CGCAGCGAGGAGGAAAAC-3', (reverse) 5'-CGAGAGCAGAATGGACCAGTAA-3'; and housekeeping gene glyceraldehyde-3-phosphate dehydrogenase (GAPDH) (forward) 5'-CATGGCCTTCCGTGTTTCTTA-3', (reverse) 5'-GCGGCACGTCAGATCCA-3'.

To confirm the presence of a single amplification product, we subjected the PCR products to a melt curve analysis. We ran samples in triplicate and calculated mean normalized gene expression, as described in an earlier study (Lund et al., 2007).

oxLP Assays

We quantified total cholesterol and oxLP in plasma ($n = 8/\text{group}$), as described in previous studies (Lund et al., 2007, 2011). Briefly, we transferred 150 μL of plasma to a microcentrifuge tube containing 2 μL of 1 mM butylated hydroxytoluene (BHT), centrifuged at 13.2g for 10 minutes at 4°C. We then transferred 100 μL of the infranant to a clean tube, added 100 μL of LDL precipitating reagent (Pointe Scientific), mixed it by inversion, and centrifuged it for 5 minutes at 13.2g at 4°C. The remaining pellet was resuspended (using 1 mM EDTA and 0.01 mM BHT) and processed through both a TBARS assay (200 μL), per the manufacturer's instructions (Zeptomatrix), and a cholesterol assay (Cell BioLabs), using cholesterol detection reagent (2 μL sample + 40 μL reagent, incubated for 5 minutes at 37°C and read at an optical density wavelength of 520 nm). The oxLP values were reported as TBARS per microgram of cholesterol.

Statistical Analysis

Statistical Analysis Comparing Experimental Groups

While a multifactorial analysis could be considered appropriate for many of the assays, we opted to use a more

conservative one-way ANOVA with the Dunnett test for post hoc comparisons to control for experiment-wise error in inferences from multiple comparisons against controls across pollutant atmospheres. To investigate gas-particle interaction effects, we assessed F-test contrasts from the ANOVA for specific differences between experimental group means (e.g., the difference in responses between $\text{MVEG}_{\text{High}} + \text{S}$ and $\text{MVEG}_{\text{High}}$ alone) using a Newman-Keuls test. However, we used a two-way ANOVA to analyze vascular contraction by PE because the addition of the PE concentration factor required a two-way approach to allow for an appropriate comparison between atmospheres.

Some data were normalized to control (filtered-air) values to accommodate the batched nature of the study design. That is, since we did not conduct N exposures at the same time as S exposures and since there was often substantial evidence of differences between control values between batches of animals at different measurement times, we compared the magnitude of specific responses (especially PCR-related endpoints) to the unique filtered-air controls (i.e., one control group for each exposure batch) that were run for each project. We did this using either ratios (values divided by the means of batch control groups) or deviations (differences of the values from batch control means). For all data, this approach was considered relative to pooling the raw data from control groups. P values less than 0.05 were considered significant. Data in graphs are presented as means \pm SEM. The output of the statistical tests is provided in Appendix S (available on the HEI Web site).

Statistical Analysis to Identify Components of Exposures Related to Biologic Responses

We performed a Multiple Additive Regression Tree (MART) analysis, similar to that conducted by Seilkop and colleagues (2012) on data across the 14 different exposure combinations and based on 36 different chemical components (Table 5). In brief, the MART analysis uses the full complexity of the exposure atmosphere by pairing concentrations of individual components (e.g., organic carbon or metals) with the obtained measurements of the biologic endpoints, going beyond the comparisons of endpoints with each exposure atmosphere (i.e., complex mixtures). The strength of the associations between components and endpoints is then assessed, yielding a ranking of components called "predictor values." The endpoints that were analyzed were those that showed consistent evidence of statistically significant responses relative to controls (TBARS, MMP-2/-9, MOMA-2 staining, and plaque area). The TBARS, MMP-2/-9, and plaque area data were first normalized relative to their respective batch controls (as a ratio [TBARS] and as deviations [MMP-2/-9 and plaque area] relative to control mean values).

Table 5. Chemical Component Predictor Variables Used in MART Analysis

Exposure Atmosphere Components	Designation
Particle component	
Particle mass	PM
Ammonium	AMMONIUM
Elements	ELEMENTS
Nitrate	NITRATE
Sulfate	SULFATE
Elemental carbon	EC
Organic carbon	OC
Particle phase organic component	
Organic acids	POACID
Organic phenols	POPHEN
Organic sterols	POSTERO
Organic sugars	POSUG
Organic hopanes	POHOP
Organic steranes	POSTER
Organic PAHs	POPAH
Organic nitro-PAHs	PONPAH
Organic alkanes	POALK
Gases	
Carbon monoxide	CO
Nitrogen monoxide	NO
Nitrogen dioxide	NO ₂
Sulfur dioxide ^a	SO ₂
Non-methane volatile organic compounds	
Alkanes	NMVOALKA
Alkenes	NMVOALKE
Aromatics	NMVOARO
Volatile carbonyl organic compounds	
Alkanals	CARBALKA
Alkenals	CARBALKE
Aromatic aldehydes	CARBARO
Ketones	CARBKET
Vapor phase semivolatile organic compounds	
Acids	SVOACID
Phenols	SVOPHEN
Sterols	SVOSTERO
Sugars	SVOSUG
Hopanes	SVOHOP
Steranes	SVOSTER
PAHs	SVOPAH
Nitro-PAHs	SVONPAH
Alkanes	SVOALK

^aSO₂ was not measured in the original experiment, but subsequently was measured at 2620 µg/m³ for MVE_{High}; the same concentration was assumed for MVE_{High}, and 2620/3 = 873 µg/m³ was assumed for MVE_{Low} and MVE_{Low}, as well as for combinations including these atmospheres.

Partial dependence plots depict how the MART-estimated concentration–response relationship for each biologic outcome is affected by a predictor after accounting for the average effects of all the other chemical predictors across their experimental exposure ranges. These functions show major features of the nature of the concentration–response function for a given predictor (approximate linearity vs. substantial nonlinearity, threshold-like response, etc.). They are shown in this report as deviations from the predicted overall mean across all observations (centered on 0) to facilitate comparisons of the estimated magnitudes of concentration–response gradients across predictor variables.

QUALITY ASSURANCE

This research was conducted in a manner that is consistent with many of the standards developed for Good Laboratory Practices, although full compliance with Good Laboratory Practices was not a requirement of the protocol. Quality control (QC) consisted of the conduct of all work according to the approved protocols and standard operating procedures, the inclusion of verified QC standards for the calibration of the certification of system performance, and third-party verification of all data before submission to the statistician for analysis. These QC processes applied to all aspects of the study, including the test and evaluation of engine performance, the verification of fuel and oil composition, the receipt and husbandry of animals, the analysis of test atmospheres, the evaluation of clinical signs, and the evaluation of changes in tissue or other biologic responses in animals. Animal activities involving receipt and husbandry were tracked through a validated software system (Provantis, Instem).

For each of the analytical tools applied to test atmospheres, calibration or “span” checks were conducted each time of use. There was a wide array of biologic assays employed for this study. The sensitivity and range of the assays varied and may have not been optimal for the ranges required for this study. They were, however, internally consistent with the standards of operation and matched well against historical control data. Most of the assays did not have “positive controls” to verify their ability to detect a change if there were to be a biologic effect, as this is not standard practice at LRRI for the assays that were employed.

RESULTS

EXPOSURE ATMOSPHERE COMPOSITION

Table 6 provides the mean and standard deviation of the atmospheric component concentrations monitored

Table 6. Target and Actual Mean Exposure Concentrations

Exposure Atmosphere	Target Concentrations (Actual \pm SD) ^a			
	PM ($\mu\text{g}/\text{m}^3$)	NO _x (ppm)	CO (ppm)	NMVOC (mg/m^3)
Core Atmospheres				
MVE _{High}	300 (310.1 \pm 69.9)	30 (31.3 \pm 6.8)	100 (101.5 \pm 16.6)	15 (15.2 \pm 1.5)
MVE _{Low}	100 (102.5 \pm 20.9)	10 (5.3 \pm 1.8)	33 (34.2 \pm 6.5)	5 (4.6 \pm 0.5)
RD	300 (346.3 \pm 130.6)	0 (0.1 \pm 0.1)	0 (0.2 \pm 0.4)	0 (0.1 \pm 0.1)
S	300 (324.5 \pm 28.2)	0 (0.1 \pm 0.1)	0 (0.2 \pm 0.4)	0 (0.1 \pm 0.1)
N	300 (316.3 \pm 47.0)	0 (0.1 \pm 0.1)	0 (0.2 \pm 0.4)	0 (0.1 \pm 0.1)
Gaseous Atmospheres and Non-vehicular PM + Gases				
MVE _{High}	0 (11.9 \pm 3.6)	30 (30.6 \pm 3.9)	100 (105.8 \pm 8.2)	15 (16.8 \pm 0.8)
MVE _{Low}	0 (10.0 \pm 8.8)	10 (8.7 \pm 1.9)	33 (32.6 \pm 4.6)	5 (4.8 \pm 0.2)
RD + MVE _{High}	300 (332.1 \pm 50.8)	30 (25.1 \pm 4.6)	100 (102.7 \pm 9.8)	15 (13.1 \pm 0.7)
S + MVE _{High}	300 (316.4 \pm 30.5)	30 (17.3 \pm 5.5)	100 (99.6 \pm 25.6)	15 (16.8 \pm 0.8)
N + MVE _{High}	300 (321.0 \pm 47.0)	30 (19.5 \pm 5.6)	100 (97.3 \pm 20.2)	15 (16.8 \pm 0.8)
Non-vehicular PM + Whole Emissions				
RD + MVE _{Low}	300 (307.8 \pm 45.9)	10 (9.1 \pm 2.2)	33 (35.6 \pm 6.5)	5 (3.8 \pm 0.4)
S + MVE _{Low}	300 (311.8 \pm 50.7)	10 (14.1 \pm 3.1)	33 (36.7 \pm 5.6)	5 (6.6 \pm 0.6)
N + MVE _{Low}	300 (326.5 \pm 69.8)	10 (12.8 \pm 2.9)	33 (35.7 \pm 5.9)	5 (5.3 \pm 0.5)

^a Values in parentheses are average \pm SD or the detection limit if not detected.

daily compared with their target values. These averages represent the concentrations during the 50-day monitoring period for each atmosphere. The average concentrations of PM and CO, which were the primary dilution and atmosphere combination indicators, were within about 15% of their targets.

Figures 2 and 3 summarize the composition of the atmospheres as the percentage of total measured mass for each chemical class. Figure 2 shows the exposure atmospheres: MVE_{High}, S, N, RD, and MVE_{High}, alone or in combination with S, N, or RD. Figure 3 shows MVE_{Low} and MVE_{Low}, as well as the atmosphere combinations, where MVE_{Low} was mixed with S, N, or RD to create a total PM concentration (300 $\mu\text{g}/\text{m}^3$) equal to the exposure atmospheres. All other results of the atmospheric composition characterization are reported in Appendix R (available on the HEI Web site).

As Figures 2 and 3 show, NO, NO₂, and CO accounted for most of the mass of the measured components of the exposure atmospheres that included MVEG. As a fraction of total mass, PM was a small component. Of interest is that even in atmospheres where no MVEG was added, CO and NO_x still accounted for a considerable proportion of the mass of the exposure. NMVOCs accounted for approximately 10% of the mass for all of the exposure groups. It

is noteworthy that this result indicates that the animals contributed a considerable portion of the NMVOCs measured in the MVE_{Low}, MVEG_{Low}, N, S, and RD atmospheres. This is consistent with previous reports of detailed characterizations of animal exposure chambers (e.g., McDonald et al. 2004a, 2006, 2008).

The PM from all of these atmospheres varied substantially in composition, which was by design. The S atmosphere consisted primarily of un-neutralized sulfuric acid droplets, with approximately 10% of the S neutralized to ammonium sulfate. The MVE consisted of approximately 60% EC, which can be ascribed to the large contribution of DEE to the PM component of that atmosphere. The PM composition from this specific diesel engine was previously characterized as approximately 70% EC (McDonald et al. 2004a), while PM from GEE contain lower proportions of EC (McDonald et al. 2008). RD consisted of approximately 85% elements, or crustal-derived metal oxides and other metals. Some metals (elements) were also identified in the MVE atmospheres, and measurable but lower amounts were identified in the MVEG_{High} atmosphere. The concentrations of metals were low enough that many approached those measured in control air. The remaining mass of RD consisted of OC. As expected, the addition of gases did not have an impact on the overall composition of PM.

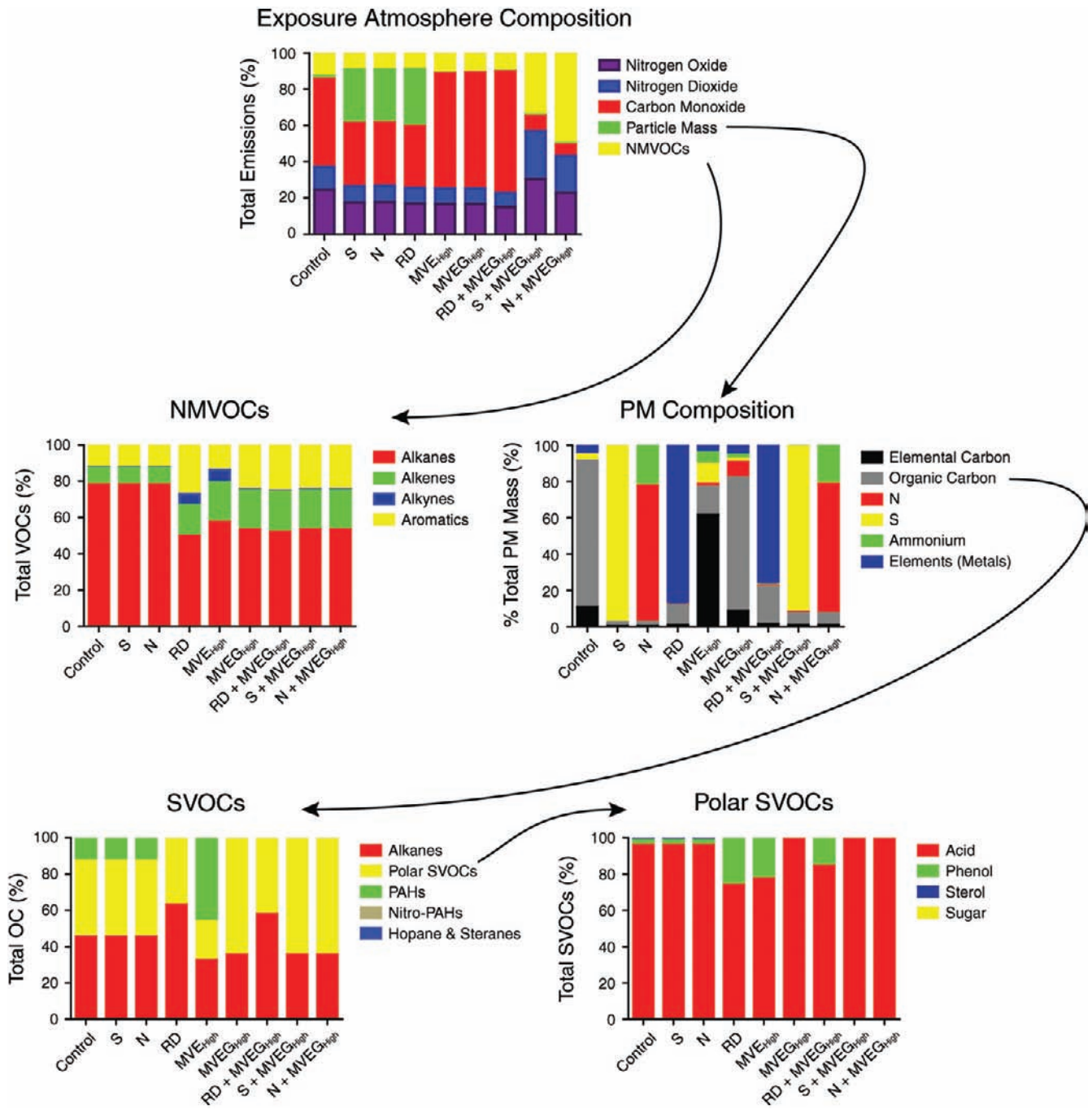


Figure 2. Fractional composition of the exposure atmospheres and their combinations with MVEG_{High}.

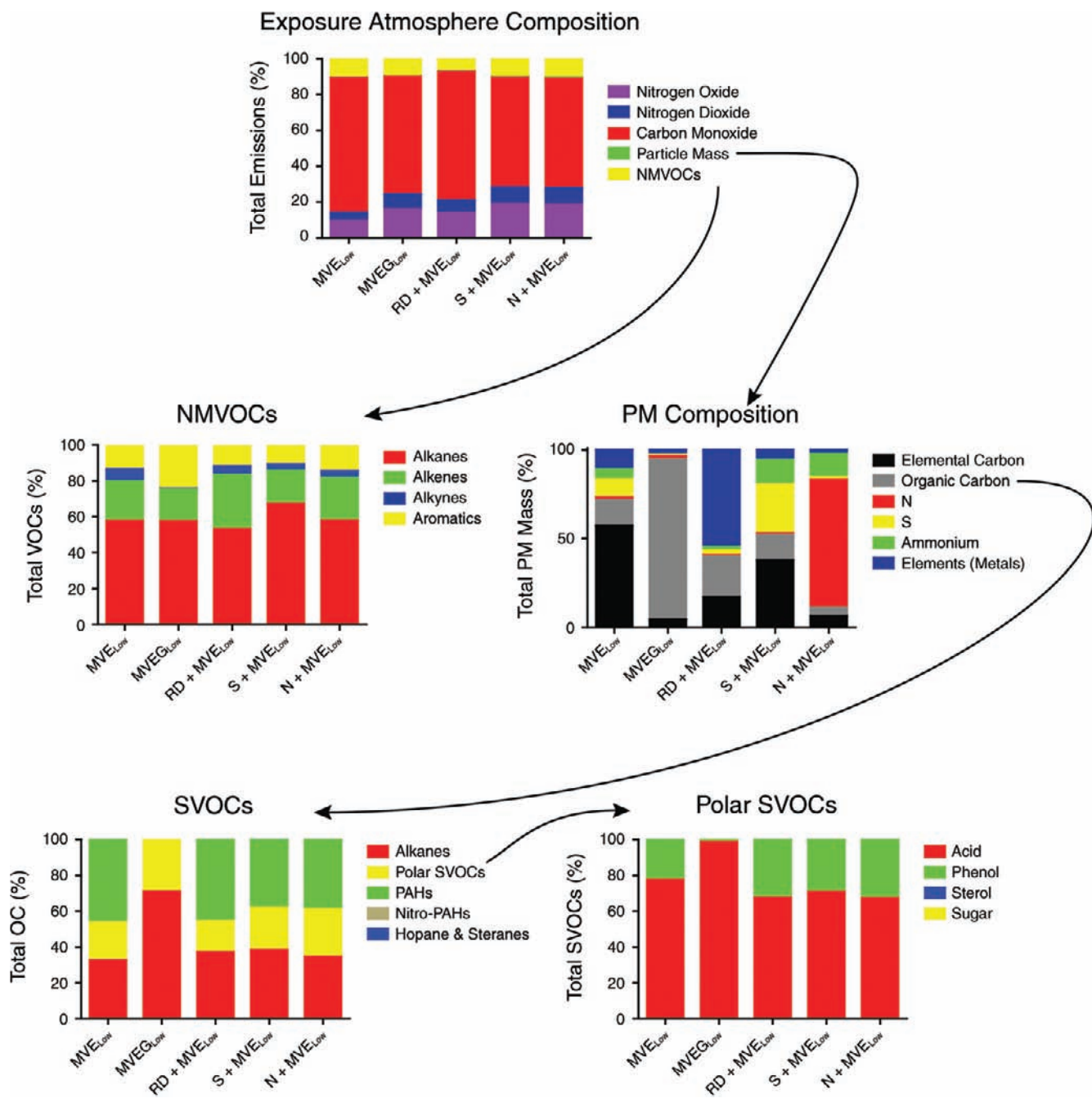


Figure 3. Fractional composition of the exposure atmospheres for MVE_{Low} , $MVEG_{Low}$, and the combination of MVE_{Low} and RD, S, or N.

Determination of the potential impact of the gases on the surface chemistry of the PM was not part of this study.

In addition to the significant contrast in atmospheres by design, we observed differences in the concentrations of many of the minor constituents among the atmospheres. For example, the concentrations of polycyclic aromatic hydrocarbons (PAHs) and some metals varied from day to day and among atmospheres that included MVE as a constituent. We mostly attributed these variances to day-to-day variation (detailed exposure measurements were made only in one atmosphere per day), but also attributed them in part to measurement error. It is also possible that some of the combination atmospheres' constituents may interact with the MVE in different ways, contributing to the measured differences in composition.

The particle number size distribution (shown in Appendix R) had a median size of approximately 60 nm for each of the atmospheres except RD; the only notable difference was the amount of particles present at each exposure level. The RD atmosphere had significantly lower numbers of particles in the smallest size range compared with N, S, and MVE_{High} (see Figure R.8 compared with Figures R.2, R.4, and R.6). MVE had the highest particle number count, followed by S.

Particle mass size distribution showed a median of approximately 2 μm for RD, and approximately 1 μm for the other atmospheres (see figures in Appendix R). The RD particle size was typical of what would be observed within the 2.5- μm -size cut of ambient air samples. However, in aggregate, the RD particle size in these atmospheres was smaller than what is typical for measurements of ambient air when a 10- μm -size cut is used. The smaller size was used by design to ensure the particles were respirable for rodents, because large particles are filtered out in the nasal passages and thus do not enter the lung.

As expected, the NMVOC concentrations were substantially different in the MVE, S, N, and RD exposure atmospheres. These substantial differences in contribution are not reflected in the normalized plots shown in Figures 2 and 3 because of the low concentrations of other gases in control atmospheres. The NMVOC concentrations in the MVE_{High} and MVEG_{High} atmospheres and in atmospheres where MVEG_{High} was added to the inorganic ions (S and N) were approximately 15 mg/m³, compared with less than 0.1 mg/m³ in the control atmosphere. The NMVOC contribution was made primarily by GEE and not DEE, as determined by prestudy assessments of the two sources. As a result, the NMVOCs were similar in both magnitude and composition to what was previously reported from the same GEE test system at the same dilution of approximately

10:1 (McDonald et al. 2008). This composition includes significant contributions from the lower-molecular-weight alkanes and alkenes, with lesser contributions from aromatic compounds such as benzene, toluene, and other alkylated benzenes (Figure 2). Alkynes consisted primarily of acetylene, which occurred in varying amounts in several of the atmospheres.

Among the measured SVOCs, the alkanes, PAHs, and polar organic compounds had significant contributions to the MVE atmosphere (Figure 2). The levels of some organic compounds identified in the control atmosphere were substantially lower than in the treatment exposure atmospheres (Appendix R). The PAH contributions to MVE were reduced substantially in any of the atmospheres that were HEPA-filtered to make MVEG (Figures 2 and 3). These data suggest that the PAHs, in contrast with the other compound classes, such as alkanes, were scrubbed by the HEPA filter. The PAH concentrations reported here include both the semivolatile and particle phases. It is noteworthy that the majority of the mass of PAHs in these atmospheres is present in the gas phase.

Hopanes and steranes and nitro-PAH concentrations were substantially lower than all other compound classes in each of the atmospheres, as expected (McDonald 2004a, 2008). The very low concentrations of hopanes and steranes in MVE indicated a negligible contribution from lubrication oil. Of interest is that the proportion of hopanes and steranes was highest in RD (Table R.2), suggesting that the organic component of that atmosphere contained oil that may have leaked from vehicles onto roadways. The polar organic compounds consisted primarily of acids (mostly aliphatic and aromatic, and likely from oxidation of the parent compounds present in the fuel generating the MVE exhaust) and phenolic compounds. The RD atmosphere contained considerable concentrations of phenols and alkanes, which were likely associated with vegetative detritus. Overall, detailed organic analysis revealed significant contributions of organic compounds in the MVE and RD atmospheres, with minimal to no organic compounds in the N and S atmospheres, as expected. The RD atmosphere contained limited or no PAHs, but was rich in polar organic compounds and alkanes.

BIOLOGIC RESPONSES

We evaluated the toxicologic data statistically by comparing differences in biologic responses between exposure groups and filtered-air control groups, as well as employing a MART analysis (discussed later) to evaluate relationships between specific components of exposure atmospheres and biologic responses.

Aortic Lipid Peroxidation

Our central research question was whether mixtures of air pollutants have differential or interactive effects in driving vascular oxidative stress. As a primary means of addressing this, we examined lipid peroxides in the aortas of ApoE^{-/-} mice, as we have found lipid peroxides (as assessed by the TBARS method) to be a consistent and reproducible biologic indicator. We used aortas from mice following a 50-day whole-body inhalation exposure to the atmospheres described in the Methods section.

Figure 4 shows the absolute aortic lipid peroxide levels, raw (top) and normalized to batched controls (bottom), for each pollutant atmosphere after the 50-day exposures. Mice exposed to MVE incurred a dramatic and exposure-dependent increase in aortic lipid peroxide levels. When particles were filtered from the MVE, this effect was significantly reduced ($P < 0.01$) but not eliminated: mice exposed to MVEG_{High} still exhibited increased aortic lipid levels. Similar to results from previous studies with non-vehicle-derived PM (Campen et al. 2010a; McDonald et al. 2010), we saw no significant effect from PM exposure alone (i.e., S, N, or RD). Although the addition of MVE_{Low} and MVEG_{High} to the N, S, and RD atmospheres led to increased effects relative to controls (Figure 4, bottom), these effects, apart from S, were of the same magnitude as those observed for MVEG_{High} and MVE_{Low} alone (Table 7). For S, there was evidence that its effect may be potentiated by mixing with MVEG. Additionally, using Newman-Keuls post hoc multiple comparison test, we noted that pooled MVE_{High} was significantly greater than pooled MVEG_{High} ($P < 0.001$), as well as N + MVEG_{High} and RD + MVEG_{High} ($P < 0.01$), but not significantly greater than S + MVEG.

Aortic Gelatinase Activity

We measured vascular gelatinase (MMP-2/-9) activity in aortas from subgroups of all the exposure groups. As seen in previous studies of gasoline emissions, we observed a significant upregulation of MMP-2/-9 activity after exposure that was both localized to the intimal region and also diffusely elevated throughout the medial region (Figure 5). The level of gelatinase activity appeared elevated after exposure to most atmospheres, including N alone (Figure 6). There was little evidence that the addition of particles to MVE_{Low} or MVEG_{High} resulted in elevated activity beyond that associated with the combustion exposures alone (Table 7). However, there were difficulties in quantifying the net fluorescence of the cleaved DQ-gelatin against the autofluorescent components in the medial lamellar structures, as well as a negative concentration–response pattern

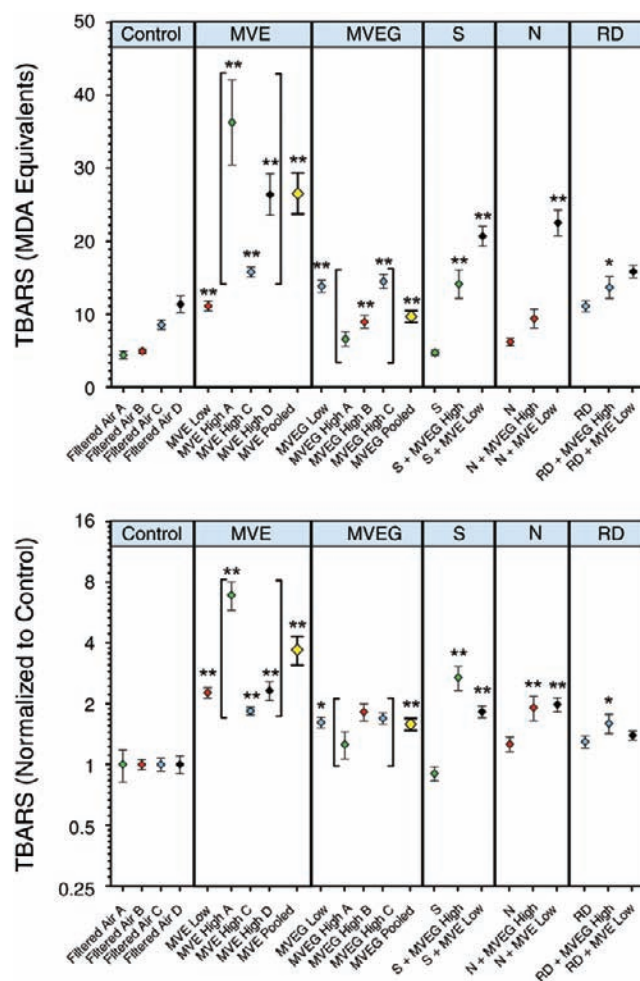


Figure 4. Absolute aortic lipid peroxide levels (mean \pm SEM of MDA equivalents, using TBARS assay) following 50-day exposures to each pollutant atmosphere. Colors represent the exposure batch (green = batch A; red = batch B; blue = batch C; black = batch D; yellow = pooled batches, encompassing batches within brackets). Because controls from each batch were not identical, raw data (top) were normalized (bottom) in order to compare groups' proportional change relative to control values. ANOVA was performed, and given the strong evidence of differences between experimental groups ($P < 0.001$), a Dunnett multiple comparison test was used to compare all treated groups with controls. Asterisks denote statistically significant difference from pooled control groups (* $P < 0.05$, ** $P < 0.01$). (MVE indicates mixed vehicular engine emissions; MVEG, mixed vehicular engine emissions with particulate matter filtered out, gases only; N, nitrate; RD, road dust; S, sulfate.)

for MVE and a lack of activity for mixtures of MVE_{Low} and MVEG_{High} with RD. These considerations led us to be cautious in interpreting the results.

Aortic Plaque Growth and Inflammation

We made cryosections of the aortic outflow tract for MOMA-2 staining to evaluate plaque area growth. Because blood vessels in ApoE^{-/-} mice on a high fat diet are

Table 7. Specific A Priori Comparisons of Results of Biologic Response Testing^a

Experimental Group	Aortic Lipid Peroxidation (TBARS)		Gelatinase Activity (MMP-2/-9)		MMP-9 mRNA Expression		Plaque Area		Vascular Inflammation (MOMA-2)	
	MVE _{Low}	MVEG _{High}	MVE _{Low}	MVEG _{High}	MVE _{Low}	MVEG _{High}	MVE _{Low}	MVEG _{High}	MVE _{Low}	MVEG _{High}
MVEG _{Low}	—	ns	—	↑↑	—	ns	—	ns	—	ns
MVE _{High}	↑↑	↑↑	↓↓	ns	ns	ns	ns	ns	ns	ns
S + MVEG _{High}	—	↑↑	—	ns	—	↑↑	—	↓	—	ns
S + MVE _{Low}	ns	—	↓	--	ns	—	ns	—	ns	—
N + MVEG _{High}	—	ns	—	↑↑	—	ns	—	ns	—	ns
N + MVE _{Low}	ns	—	↓↓	—	ns	—	ns	—	ns	—
RD + MVEG _{High}	—	ns	—	ns	—	ns	—	ns	—	ns
RD +MVE _{Low}	↓↓	—	↓↓	—	ns	—	ns	—	↓	—

^a ↑ indicates $P < 0.05$ increase in effect relative to group in column heading; ↑↑, $P < 0.01$ increase in effect relative to group in column heading; ↓, $P < 0.05$ decrease in effect relative to group in column heading; ↓↓, $P < 0.01$ decrease in effect relative to group in column heading; ns, not statistically significant relative to group in column heading; —, not tested.

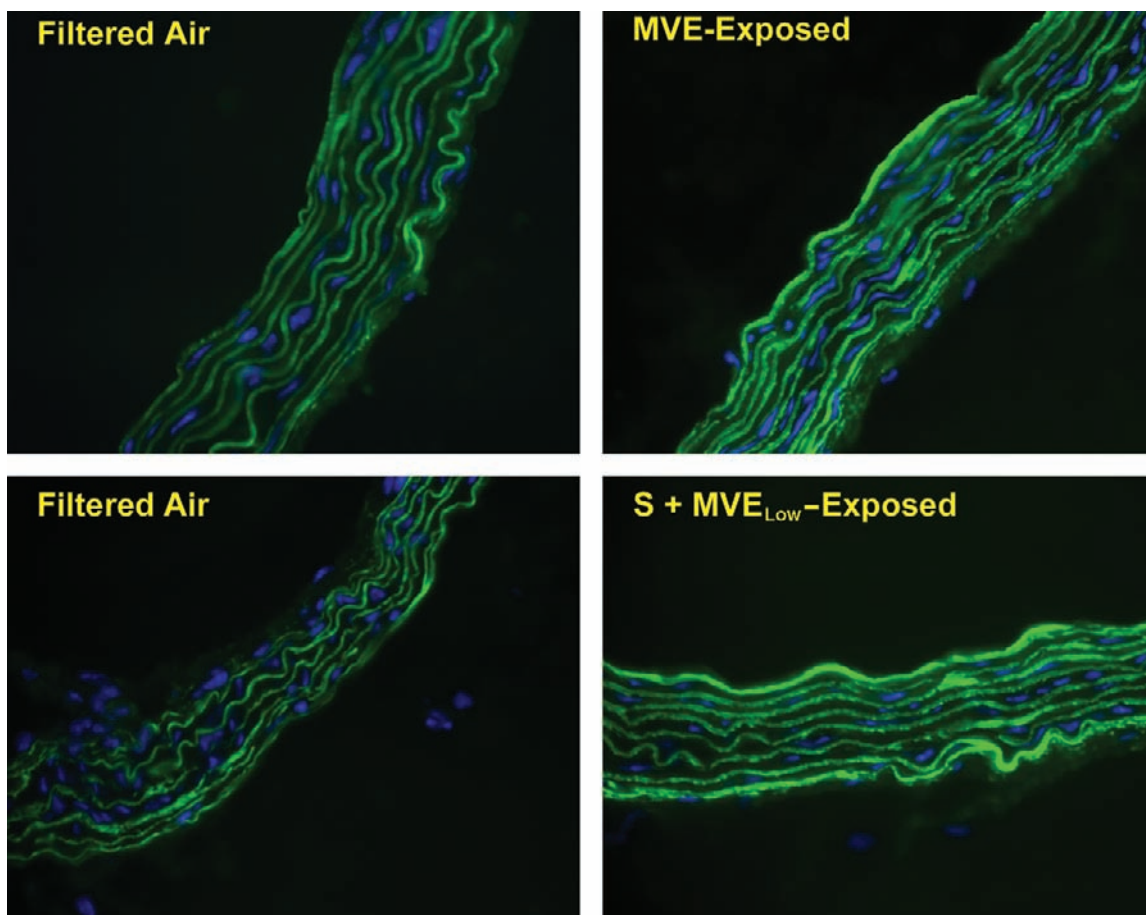


Figure 5. Example images of aortic gelatinase activity (assessed by in situ zymography) from mice exposed to filtered air (control), MVE, and S + MVE_{Low}.

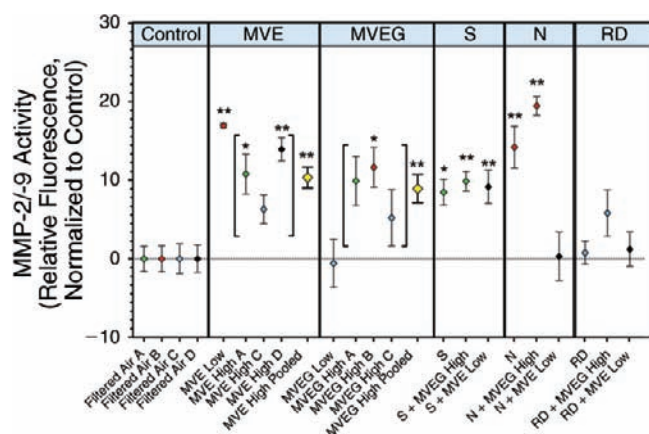


Figure 6. Aortic gelatinase activity (means \pm SEM, using MMP-2/-9 assay) revealed by in situ zymography. Quantification included autofluorescent background values, reducing ability to separate qualitative changes in the in situ zymography. Colors represent the batch of exposures (green = batch A; red = batch B; blue = batch C; black = batch D; yellow = pooled batches, encompassing batches within brackets). ANOVA was performed, and given the strong evidence of differences between experimental groups ($P < 0.001$), a Dunnett multiple comparison test was used to compare all treated groups with controls. Asterisks denote statistically significant differences from pooled control group (* $P < 0.05$, ** $P < 0.01$). (MVE indicates mixed vehicular engine emissions; MVEG, mixed vehicular engine emissions with particulate matter filtered out, gases only; N, nitrate; RD, road dust; S, sulfate.)

relatively pro-atherogenic, positive staining was noted in nearly all animals (including controls). We determined the density of staining separately from the plaque size. A blinded observer determined the range of densities and assigned scores from 1 to 4 (for light to heavy staining, respectively) for each slide. An example of the range of staining density is shown in Figure 7.

Exposure to the various atmospheres almost universally elevated staining for monocyte infiltration (Figure 8, top panel), although not always statistically significantly: only MVE_{High}, MVE_{Low}, S + MVEG_{High}, and N + MVEG_{High} induced statistically significant vascular inflammation scores, relative to controls. However, the small sample sizes ($n = 3$) reduced statistical power in comparisons with controls as well as those among experimental groups, and there was no substantial evidence to suggest gas-particle interactions.

In contrast to monocyte infiltration, plaque area generally did not appear to be dramatically altered by the 50-day exposures (Figure 8, lower panel), which is consistent with previous work on diesel emissions (Campen et al. 2010b). However, with the larger number of exposure groups in the present study, we saw a more distinct trend toward increased plaque size than previously reported. With the exception of three groups (S + MVEG_{High}, RD, and RD + MVEG_{High}), all group means were above that of the

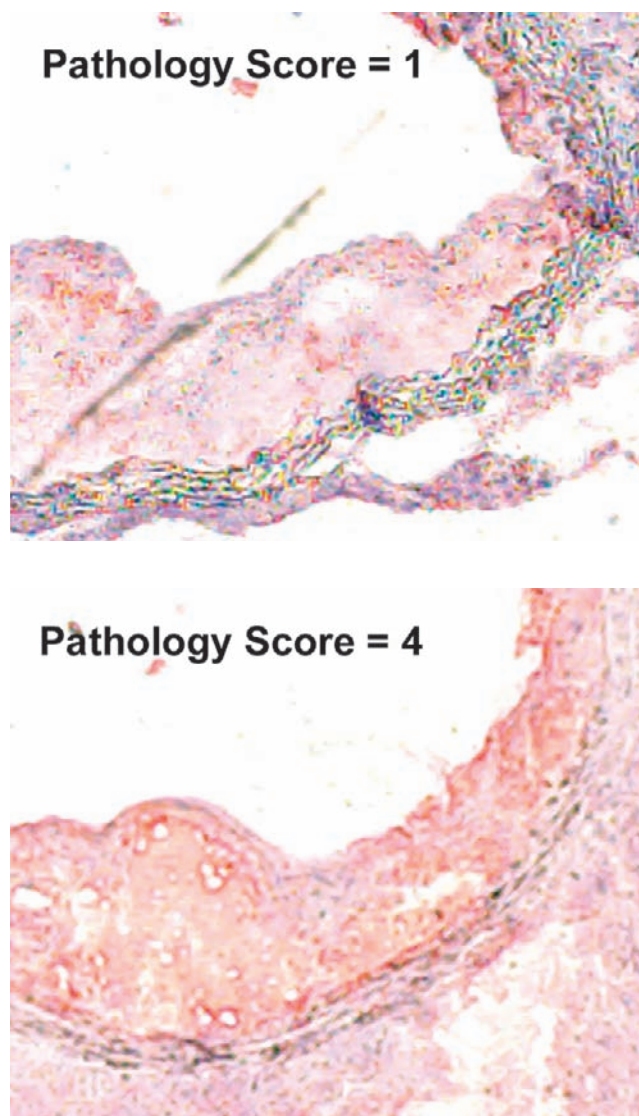


Figure 7. Representative aortic outflow tract plaque images from ApoE^{-/-} mice showing range of staining density (scored from 1 to 4). Sections were labeled with an antibody specific for MOMA-2 and counterstained with hematoxylin and eosin.

filtered-air control group. In addition, using ANOVA, we observed that N and N + MVEG_{High} were statistically significantly elevated compared with control.

Aortic Gene Expression Changes

To assess potential effects on pathways that regulate vascular function and remodeling, we measured aortic gene expression of a number of biologic markers related to NO pathways and metalloproteinases, along with HO-1 and ET-1, using RT-PCR. For NO-related pathways,

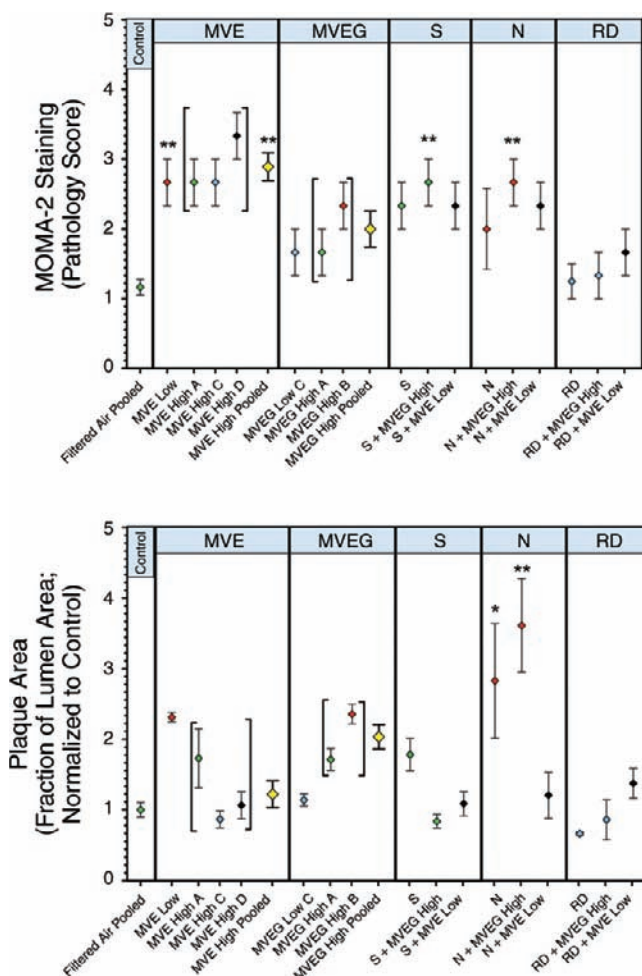


Figure 8. Quantification (means ± SEM) of vascular inflammation (MOMA-2 staining) (top) and plaque area (bottom) from the aortic leaflet regions in ApoE^{-/-} mice exposed to the various atmospheres. Colors represent the exposure batch (green = batch A; red = batch B; blue = batch C; black = batch D; yellow = pooled batches, encompassing batches within brackets). ANOVA was performed on these data, and given the strong evidence of differences between experimental groups ($P < 0.001$), a Dunnett multiple comparison test was used to compare all treated groups with controls. Asterisks denote statistically significant differences from pooled control groups (* $P < 0.05$, ** $P < 0.01$). (MVE indicates mixed vehicular engine emissions; MVEG, mixed vehicular engine emissions with particulate matter filtered out, gases only; N, nitrate; RD, road dust; S, sulfate.)

we examined expression of eNOS, iNOS, DHFR, and GTPCH. The last two enzymes are crucial for maintaining levels of tetrahydrobiopterin, an essential cofactor that keeps nitric oxide synthase (NOS) dimerized and functionally coupled.

Among these four gene markers (shown in Figure 9), eNOS, iNOS, and DHFR were not significantly altered by any pollutant atmosphere. Only GTPCH mRNA expression was significantly different among experimental groups

after analysis using ANOVA ($P = 0.0468$). Using a Newman-Keuls post hoc comparison of the GTPCH data, it appeared that no two groups were statistically significantly different; however, the N + MVEG_{High} and RD + MVEG_{High} groups were the most quantitatively different from one another. In the absence of significant trends, we are cautious not to over-interpret the data, but we noted that two groups (MVEG_{Low} and N + MVEG_{High}) did show some degree of consistency in elevated gene expression for DHFR and GTPCH.

We then assessed changes in gene expression of four MMPs, namely, MMP-2, -3, -7, and -9 (Figure 10). Aortic MMP-3 and -7 were not significantly altered by any pollutant atmosphere. Because the zymography revealed increased activity of gelatinases in MMP-2/-9 and we had previously observed an increase in MMP-9 in several studies (Lund et al. 2007; Campen et al. 2010b), these endpoints were of substantial interest. However, MMP-2 and -9 showed only modest changes, and an ANOVA test revealed only two statistically significant changes across the entire profile of pollutant atmospheres. MMP-2 was significantly elevated in the S + MVE_{Low} group, while MMP-9 was significantly elevated in the S + MVEG_{High} group. Of note, MMP-2 and MMP-9 were somewhat (i.e., not always statistically significantly) elevated in all atmospheres containing S compared with filtered-air controls, indicating a potential commonality related to the S component.

Figure 11 shows aortic gene expression of three additional markers: ET-1, HO-1, and TIMP-2. For all three markers, only the MVEG_{Low} concentration group revealed significant increases over filtered-air controls. ET-1 gene expression varied considerably between groups (e.g., MVEG_{Low} was significantly elevated compared with N + MVE_{Low}), but was not statistically significantly different from filtered-air controls. There were significant decreases seen for HO-1 with the N + MVE_{Low} and RD + MVE_{Low} atmospheres, and there was a downward trend for TIMP-2 with the RD + MVEG_{High} and RD + MVE_{Low} atmospheres.

Vascular Function by Myography

To measure vascular reactivity and function, we used a wire myograph to assess changes in vascular contraction to PE and vascular relaxation with application of ACh after pollution exposures. The results of these analyses are presented in Figures 12 and 13. One difficulty arose in finding qualified individuals to conduct these technically challenging protocols. Because of this, the personnel varied, resulting in inter-observer differences in the outcomes

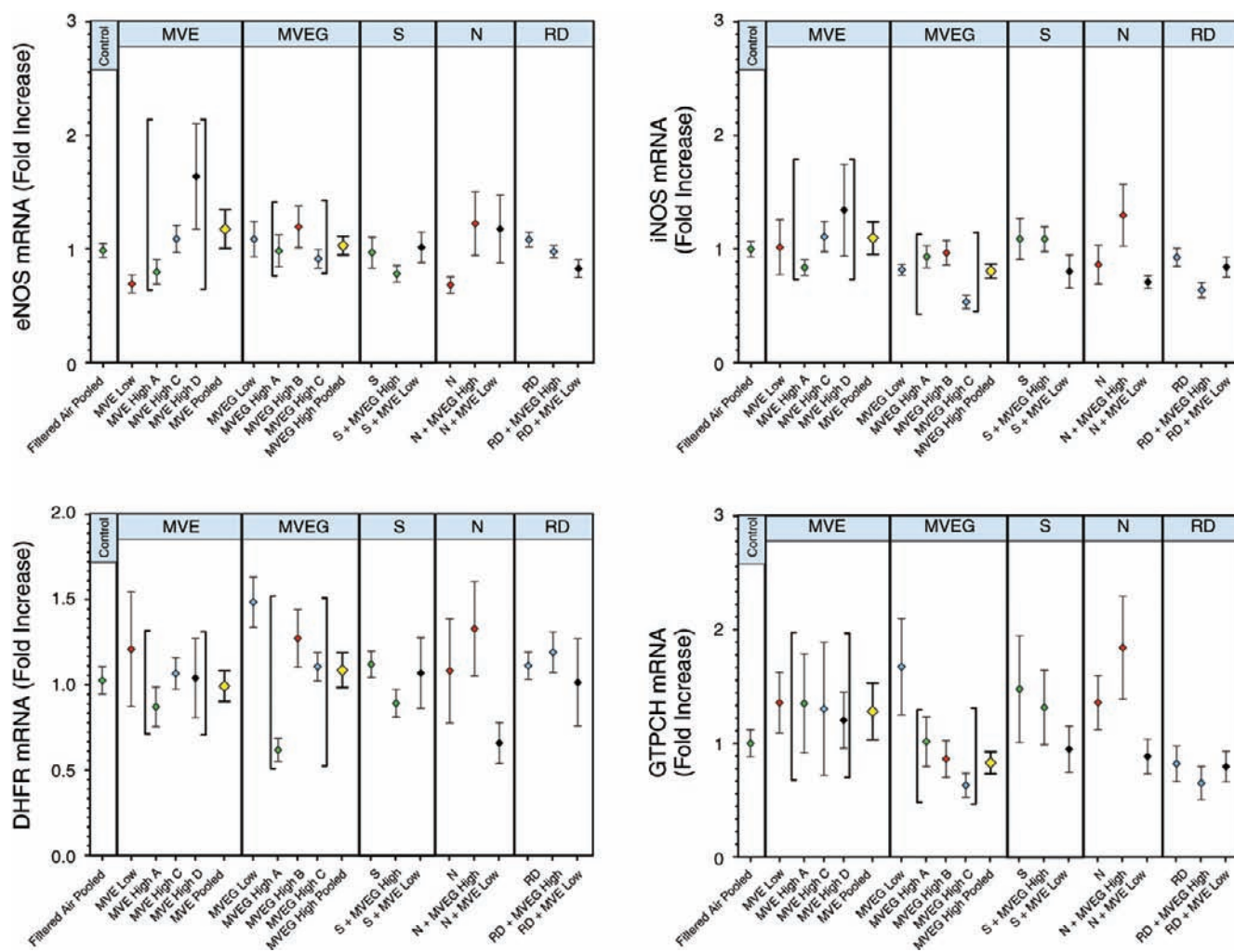


Figure 9. Aortic gene expression changes (means ± SEM) in eNOS, iNOS, DHFR, and GTPCH. Colors representing the exposure batch (green = batch A; red = batch B; blue = batch C; black = batch D; yellow = pooled batches, encompassing batches within brackets). ANOVA was performed on these data, and given the strong evidence of differences between experimental groups ($P < 0.001$), a Dunnett multiple comparison test was used to compare all treated groups with controls. Asterisks denote statistically significant differences from pooled control groups. (MVE indicates mixed vehicular engine emissions; MVEG, mixed vehicular engine emissions with particulate matter filtered out, gases only; N, nitrate; RD, road dust; S, sulfate.)

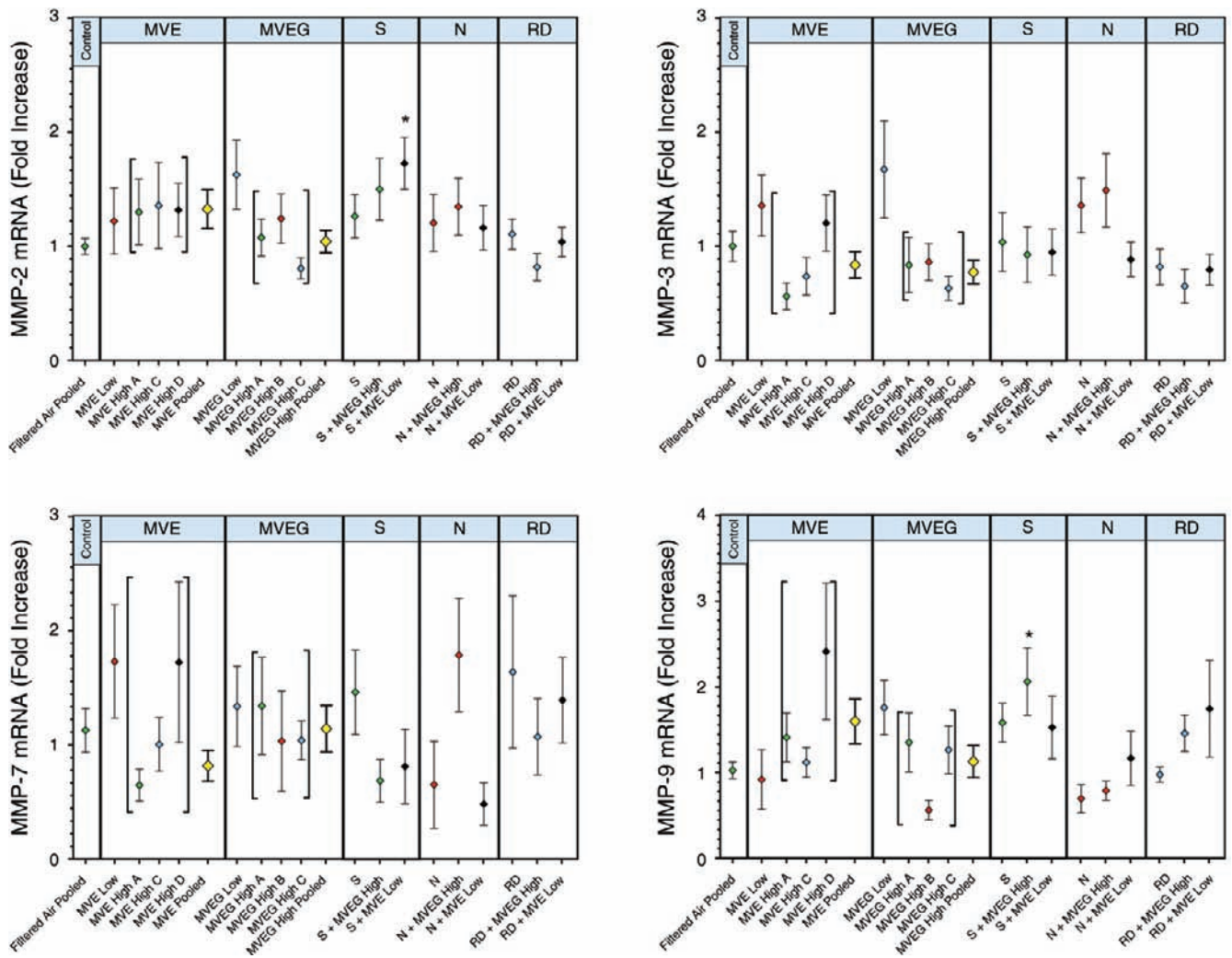


Figure 10. Aortic gene expression changes (means \pm SEM) in MMP-2, -3, -7, and -9. Colors represent the exposure batch of (green = batch A; red = batch B; blue = batch C; black = batch D; yellow = pooled batches, encompassing batches within brackets). ANOVA was performed on these data, and given the strong evidence of differences between experimental groups ($P < 0.001$), a Dunnett multiple comparison test was used to compare all treated groups with controls. Asterisks denote statistically significant differences from pooled control groups (* $P < 0.05$, ** $P < 0.01$). (MVE indicates mixed vehicular engine emissions; MVEG, mixed vehicular engine emissions with particulate matter filtered out, gases only; N, nitrate; RD, road dust; S, sulfate.)

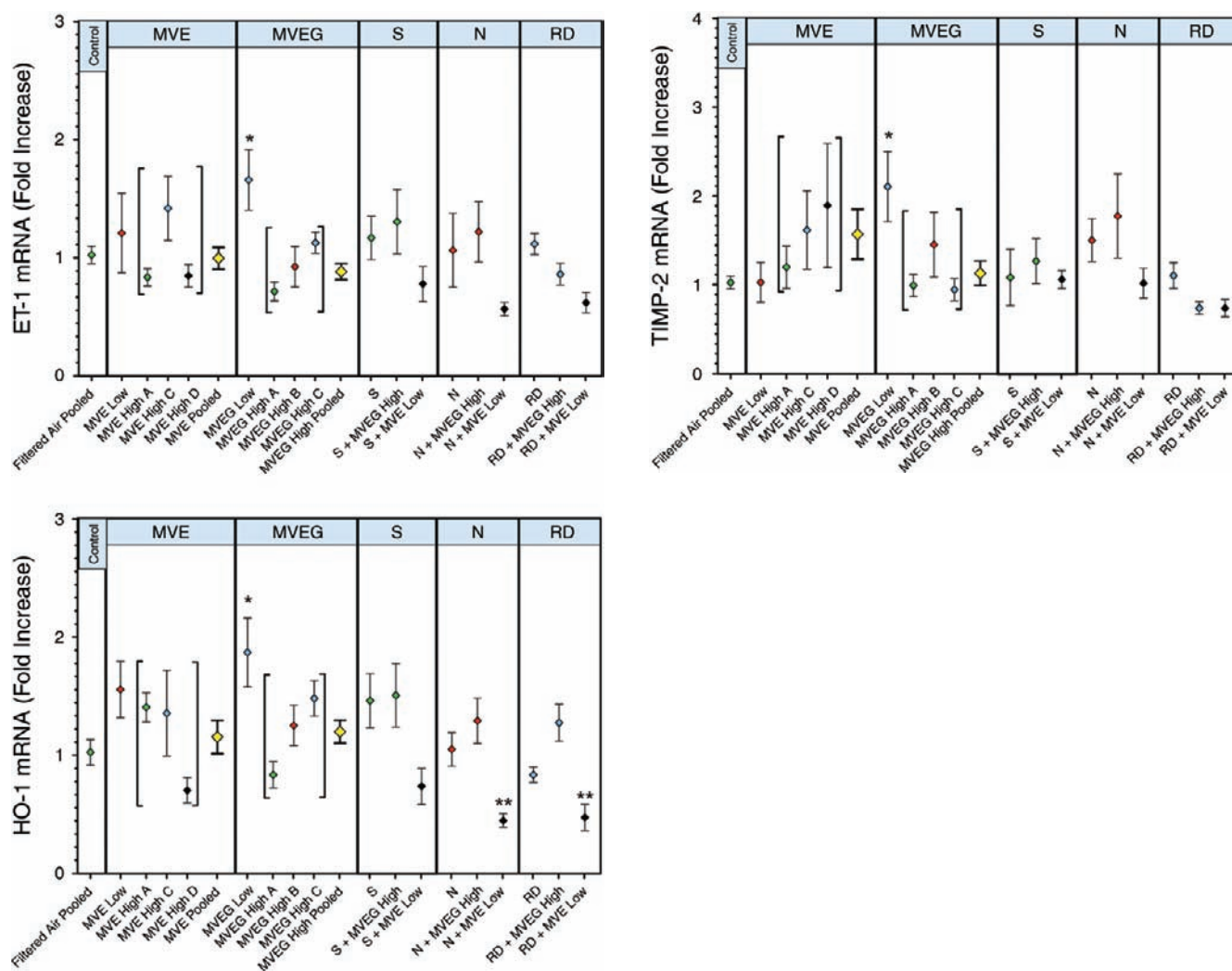


Figure 11. Aortic gene expression changes (means \pm SEM) in ET-1, HO-1, and TIMP-2. Colors represent the exposure batch (green = batch A; red = batch B; blue = batch C; black = batch D; yellow = pooled batches, encompassing batches within brackets). ANOVA was performed on these data, and given the strong evidence of differences between experimental groups ($P < 0.001$), a Dunnett multiple comparison test was used to compare all treated groups with controls. Asterisks denote statistically significant differences from pooled control groups (* $P < 0.05$, ** $P < 0.01$). (MVE indicates mixed vehicular engine emissions; MVEG, mixed vehicular engine emissions with particulate matter filtered out, gases only; N, nitrate; RD, road dust; S, sulfate.)

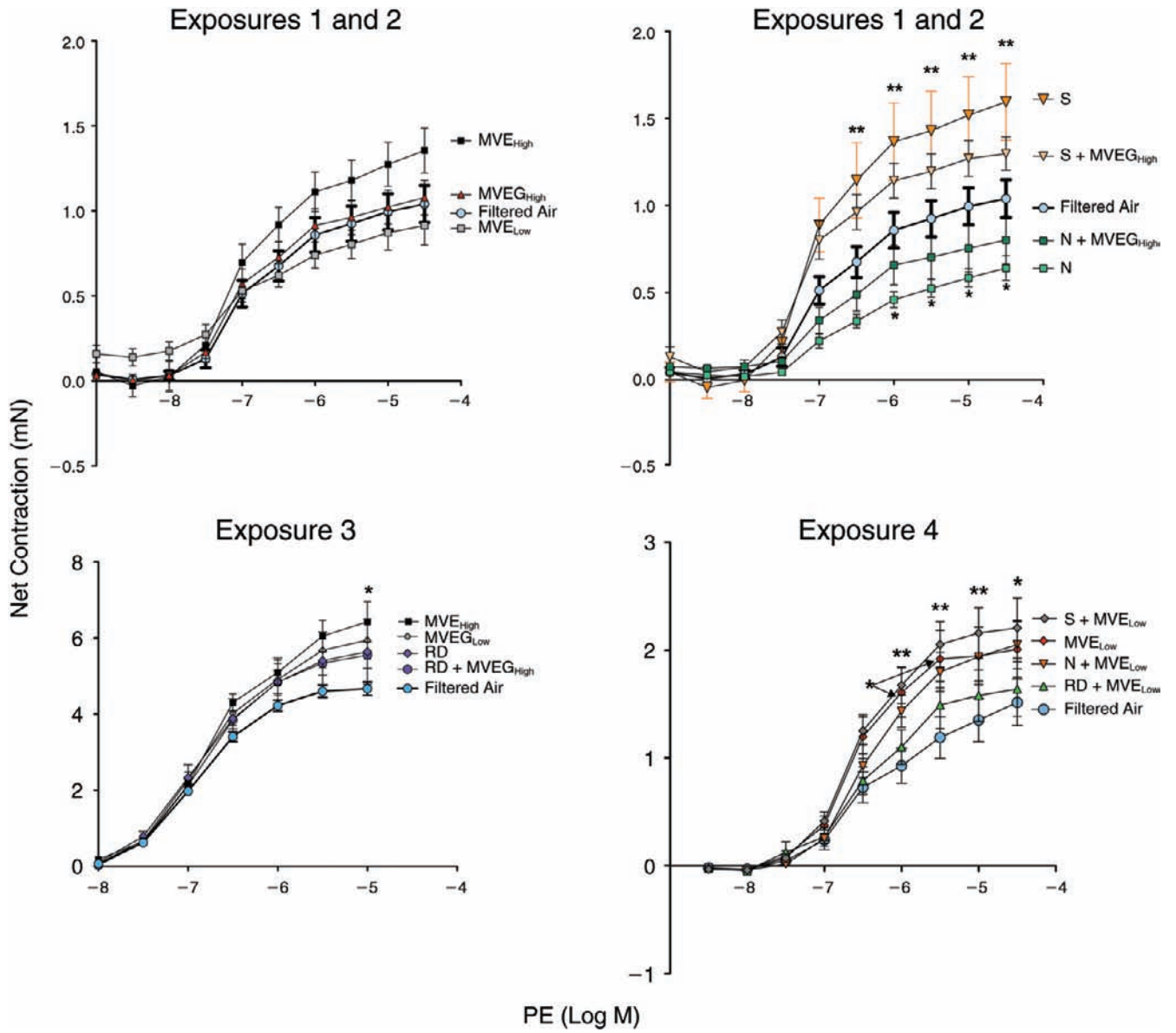


Figure 12. PE-induced contraction in mouse aortas following 50-day exposures. Asterisks indicate statistically significant differences from control by two-way ANOVA (* $P < 0.05$; ** $P < 0.01$). Control data from exposure batches 1 and 2, which were performed by the same technician, were pooled, and all groups within those batches were compared. Exposure batches 3 and 4 (which were performed by a second and third technician, respectively) were compared separately.

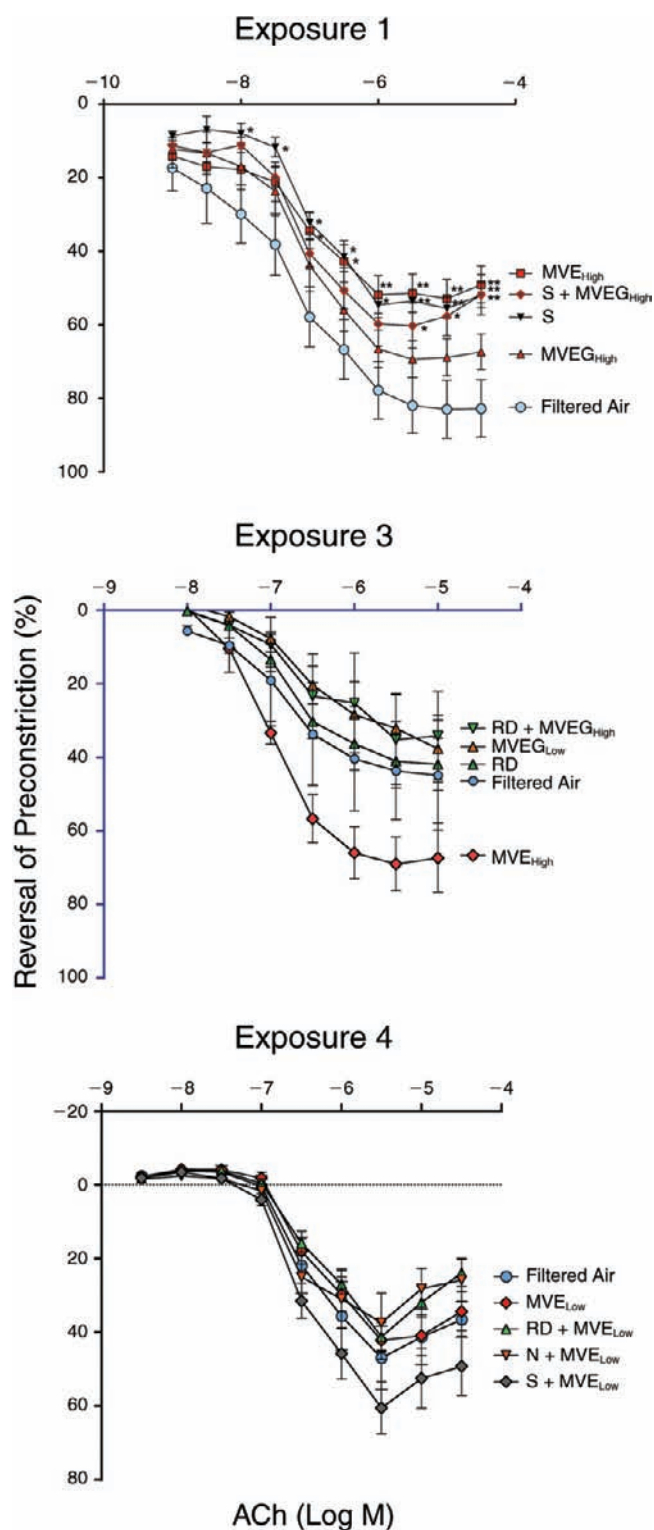


Figure 13. ACh-induced reversal of precontraction in mouse aortas following 50-day exposures. Asterisks indicate statistically significant differences from control by a two-way ANOVA (* $P < 0.05$; ** $P < 0.01$). Data from Exposure 2 were discarded because of an unexplained absence of response to ACh in all groups.

of the vascular function testing. We began the first two batches of exposures using a protocol developed by Sun and colleagues (2005), with mean contractions of approximately 1 millinewton for filtered-air control aortas (see top panels in Figure 12). Subsequently, a highly trained vascular physiologist at LRRRI applied slightly different techniques that optimized vascular contraction in the third NPACT exposure batch. As a result of the optimization, contraction magnitude increased dramatically (6-fold) (see bottom left panel of Figure 12), but it became difficult to directly combine data from the different exposure batches. When we returned in part to the original protocol, we observed slightly more robust contractions than in the first and second exposure batches but not as pronounced as contractions in the third batch (see bottom right panel of Figure 12).

In spite of these concerns, when we examined the data relative to the controls in the same batch, we observed very similar trends in aortas from mice exposed to different pollutant mixtures with respect to contraction from PE (Figure 12). The aortas of mice exposed to MVE exhibited a consistent, if not always significant, enhancement in PE-induced contraction compared with controls exposed to filtered air. S induced similar effects, and possibly to a greater degree. Interestingly, exposure to N reduced the vascular contraction to PE. Trends revealed a hyperconstrictive phenotype common to most exposures except for N with or without MVEG. With application of ACh, there was a reversal of precontraction in the aortas (Figure 13). Because we employed different technicians, it was difficult to evaluate effects across exposure batches. In Exposure 1, filtered-air-exposed mice exhibited greater ACh-mediated dilation than those from the MVE, S, and S + MVEG_{High} groups. In Exposures 3 and 4, no significant effects were observed.

oxLP Assays

In an effort to elucidate pathways that may be involved in pollutant-mediated effects from emissions generated by vehicles on the progression of atherosclerosis, as well as to quantify endpoints that serve as markers for comparing animal studies to human studies of exposure, we quantified oxLP levels in circulating plasma from all animals in all exposure groups. We observed a significant induction of oxLP in ApoE^{-/-} mice exposed to MVE_{High}, S + MVE_{Low}, N + MVE_{Low}, and RD + MVE_{Low} (Figure 14), which is close to the results obtained from the TBARS assay in aortas from these animals (see Figure 4). Additionally, we measured a slight — but not significant — increase of oxLP with MVEG_{Low}, S, S + MVEG_{High}, and RD + MVEG_{High} exposures, as shown in Figure 14.

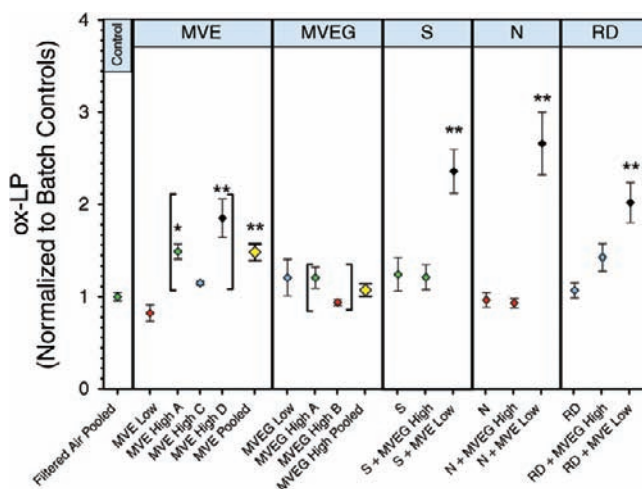


Figure 14. Plasma ox-LP levels (means \pm SEM) in the exposed vs. control groups. Colors represent the exposure batch (green = batch A; red = batch B; blue = batch C; black = batch D; yellow = pooled batches, encompassing batches within brackets). Asterisks indicate statistically significant changes ($*P < 0.05$; $**P < 0.01$) compared with filtered-air controls observed in MVE high, S + MVE_{Low}, N + MVE_{Low}, and RD + MVE_{Low}. Data were pooled across exposure batches. (MVE = mixed vehicular engine emissions; MVEG = mixed vehicular engine emissions with particulate matter filtered out, gases only; N = nitrate; RD = road dust; S = sulfate.)

MULTIPLE ADDITIVE REGRESSION TREE ANALYSIS

To provide additional insight into the role of the mixture compositions (i.e., going beyond the mixture effects themselves), we used MART analysis to associate specific components of the exposure atmospheres with biologic endpoints. The output of the MART analysis is a set of “predictors” that represent (classes of) exposure components and ranks them by the strength of their associations with each biologic marker. The relative importance scores for these predictors calculated using MART are shown in Table 8. For TBARS, the first and third strongest predictors are non-particulate engine combustion components (non-methane volatile organic alkanes [NMVOALK] and CO), while the second most important predictor is particulate SULFATE.* Notably, in a previous study, CO was tested in a similar biologic model, albeit with a shorter exposure duration, but did not drive increases in aortic TBARS levels in that study (Campen et al. 2010a). Particulates

* In this report, particulate SULFATE is spelled in all caps to distinguish it from the exposure mixture (referred to as “S”). This nomenclature applies also to all PM components found in Table 5.

(AMMONIUM, SULFATE, and PM) are the strongest predictors for the other endpoints, along with volatile carbonyl ketone (CARBKET).

Partial dependence plots for the four endpoints illustrated in Figure 15 show the MART-estimated concentration–response patterns in the data. Of the four endpoints, only the TBARS assay demonstrated monotonically increasing concentration–response functions for its top three predictors. Conversely, the other endpoints exhibited counter-intuitive evidence of decreasing predictive concentration–response functions for at least one of their top three predictors. For MMP-2/-9, the decreasing concentration–response function for the second strongest predictor (volatile CARBKET) was particularly surprising as it was the opposite of the concentration–response function for the strongest predictor (AMMONIUM).

Graphs of the normalized data provide insight into the reliability of the MART-predicted concentration–response functions (i.e., partial dependencies) of the predictors. Specifically, Figure 16 shows reasonably compelling evidence of an increase in the response observed in the TBARS assay associated with both NMVOALKA and CO. There is also general evidence of a positive association with particulate SULFATE exposure at low concentrations, but less so at the higher concentrations ($\approx 300 \mu\text{g}/\text{m}^3$). At this concentration, animals exposed to S alone showed no evidence of an increased response, but those with additional exposure to MVEG_{High} exhibited a significantly ($P < 0.01$) increased response. This could potentially be interpreted as gas–particle interaction, with a significantly higher response in animals exposed to S + MVEG_{High} than in those exposed to MVEG_{High} alone ($P < 0.01$).

There was little evidence of an increased response in MMP-2/-9 activity associated with an increase in pollutant concentrations among the MART-identified top predictors for these endpoints (Figure 17). In particular, there was a substantial lack of consistency in response to the top predictor, AMMONIUM, at the highest concentrations ($>70 \mu\text{g}/\text{m}^3$). In this concentration range, N and N + MVEG_{High} showed a similar increase in response for AMMONIUM, but N + MVE_{Low} showed no evidence of a response. This might indicate a gas–N particle interaction, due to the higher level of gases in the N + MVEG_{High} exposure. However, the similar magnitude of response increase in animals exposed to MVE_{Low} casts doubt on this interpretation. Overall, these results do not provide a compelling causal exposure-related explanation of the observed pattern of MMP-2/-9 responses.

Table 8. Relative Importance Scores for Predictors in the MART Analysis by Assay^a

TBARS		MMP-2/-9		MOMA-2		Plaque Area	
NMVOALKA	100	AMMONIUM	100	SULFATE	100	AMMONIUM	100
SULFATE	64	CARBKET	97	AMMONIUM	98	PM	81
CO	51	PM	62	CARBKET	61	SULFATE	78
CARBKET	48	SULFATE	57	PM	53	ELEMENTS	58
AMMONIUM	42	ELEMENTS	52	NITRATE	47	SVOACID	46
EC	40	CO	47	ELEMENTS	43	CO	44
PM	36	CARBALKA	46	PONPAH	37	POACID	43
POSUG	31	POALK	38	CO	37	POSTERO	42
PONPAH	28	NO ₂	37	POSTERO	30	NO ₂	41
CARBALKA	26	SVOHOP	32	CARBALKA	28	SVOHOP	40
NO ₂	26	POSTERO	27	SVOHOP	28	OC	33
OC	25	NITRATE	26	POALK	26	POSUG	31
POSTERO	24	NMVOALKA	25	NO ₂	26	CARBALKA	28
NMVOALKE	23	POSUG	21	OC	23	CARBKET	25
NITRATE	22	SVOALK	16	NMVOALKA	23	POPAH	25
ELEMENTS	20	SVOACID	15	SVOSTER	20	POALK	24
POPHEN	19	NMVOALKE	14	POSUG	18	NITRATE	24
SVOHOP	16	OC	13	POPHEN	17	SVOPHEN	21
SVOPAH	13	EC	12	EC	17	CARBARO	21
POALK	12	POACID	10	CARBARO	16	EC	21
SVOSTER	12	POPHEN	9	NMVOARO	16	POHOP	19
CARBARO	9	POPAH	7	POPAH	15	NMVOALKA	17
NMVOARO	8	SVOPAH	6	POHOP	11	POSTER	17
POACID	7	POSTER	6	SVOACID	11	POPHEN	16
POPAH	7	CARBARO	6	NMVOALKE	9	SVOSTER	15
POHOP	6	CARBALKE	4	POSTER	7	CARBALKE	14
SVOACID	5	SVOPHEN	4	POACID	6	PONPAH	13
SVOSUG	4	POHOP	4	SVOSUG	4	SVOALK	7
POSTER	2	SVOSTER	3	CARBALKE	2	NMVOALKE	7
SVOPHEN	0	NMVOARO	0	SVOPHEN	0	SVOSUG	5
SO ₂	0	PONPAH	0	SO ₂	0	SVOPAH	0
NO	0	NO	0	SVOPAH	0	NMVOARO	0
SVOALK	0	SVOSUG	0	NO	0	NO	0
SVOSTERO	0	SVOSTERO	0	SVOSTERO	0	SVOSTERO	0
SVONPAH	0	SVONPAH	0	SVONPAH	0	SVONPAH	0
CARBALKE	0	SO ₂	0	SVOALK	0	SO ₂	0

^a See Table 5 for abbreviations.

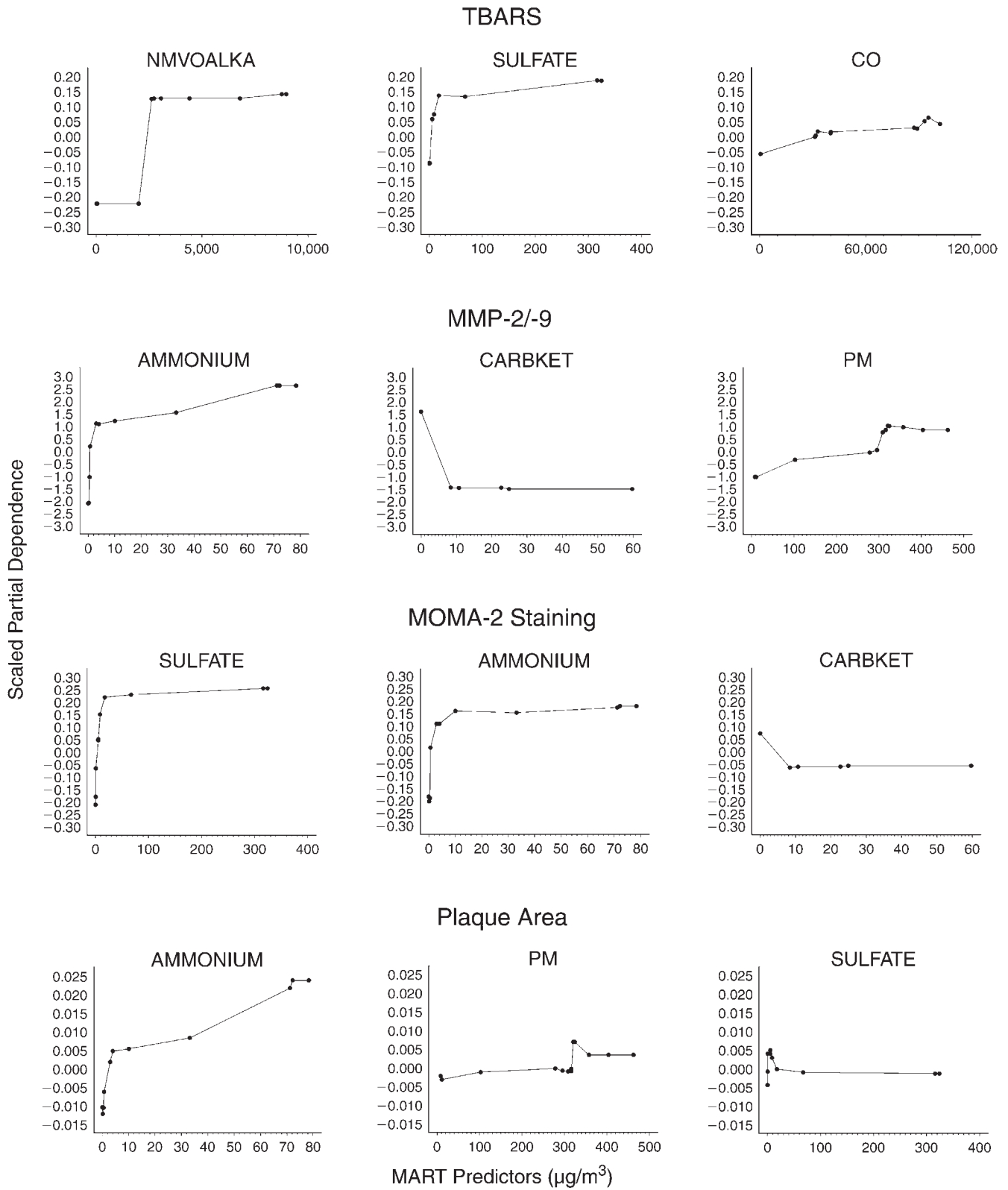


Figure 15. Partial dependence of top three predictors for four biologic endpoints in MART analysis.

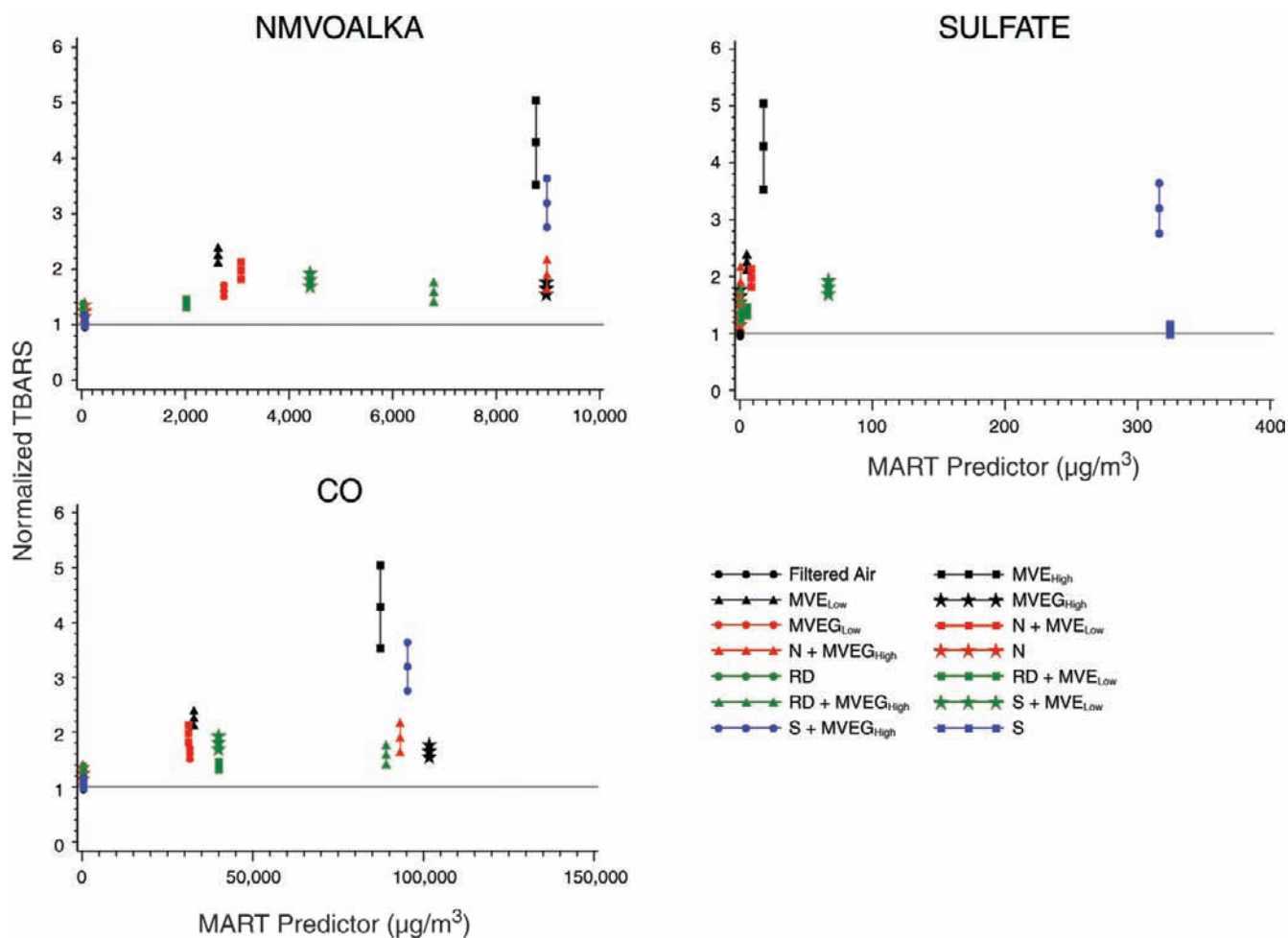


Figure 16. Observed lipid peroxide levels (means and SEs) using TBARS assay relative to MART-identified top predictors.

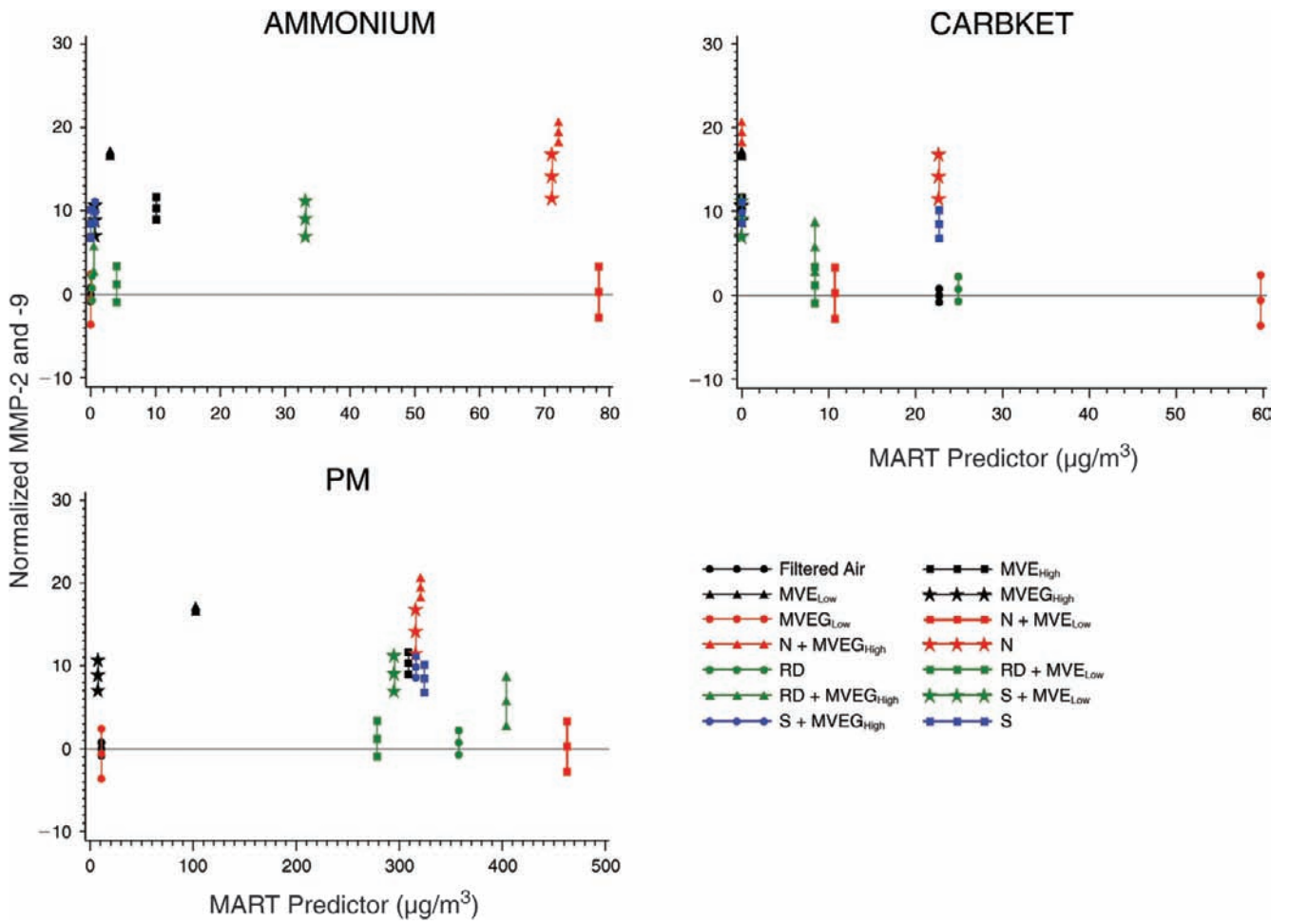


Figure 17. Observed MMP-2 and -9 expression (means and SEs) relative to MART-identified top predictor.

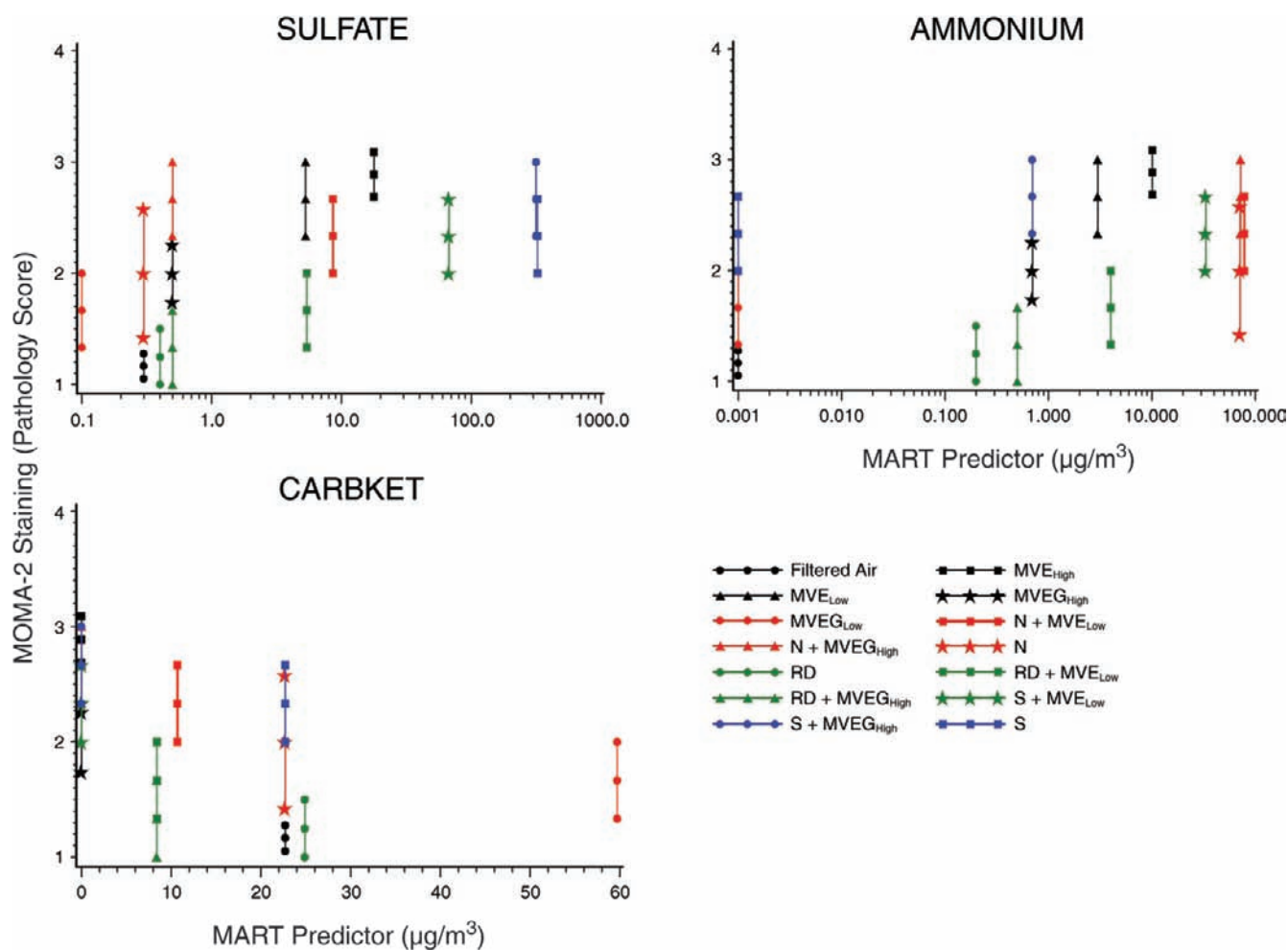


Figure 18. Observed vascular inflammation results using MOMA-2 staining (means and SEs) relative to MART-identified top predictors.

As indicated by MOMA-2 staining, there was evidence of an increase in vascular inflammation response associated with SULFATE, but less evidence, at least superficially, for an increasing response associated with AMMONIUM (Figure 18). However, the apparent lack of an association of vascular inflammation with AMMONIUM was primarily due to the increased response in the S group, which had no AMMONIUM exposure. Similarly, the apparent strength of the SULFATE concentration–response relationship is challenged by the apparent high responses in the N and N + MVE_{High} groups (at low SULFATE concentrations). When the MOMA-2 data are plotted relative to both AMMONIUM and SULFATE concentrations

(Figure 19), both components appear to be related to the concentration–response pattern, which provides further evidence of possible underlying causal concentration–response relationships between the two particulates and vascular inflammation.

Figure 20 illustrates plaque area data relative to the top three MART predictors. There is little, if any, evidence to suggest concentration–response relationships in these data; we observed particularly strong variability in response patterns in experimental groups at the highest concentrations of particulate AMMONIUM and SULFATE. Thus, the evidence for underlying causal concentration–response relationships for these particulates is weak, at best.

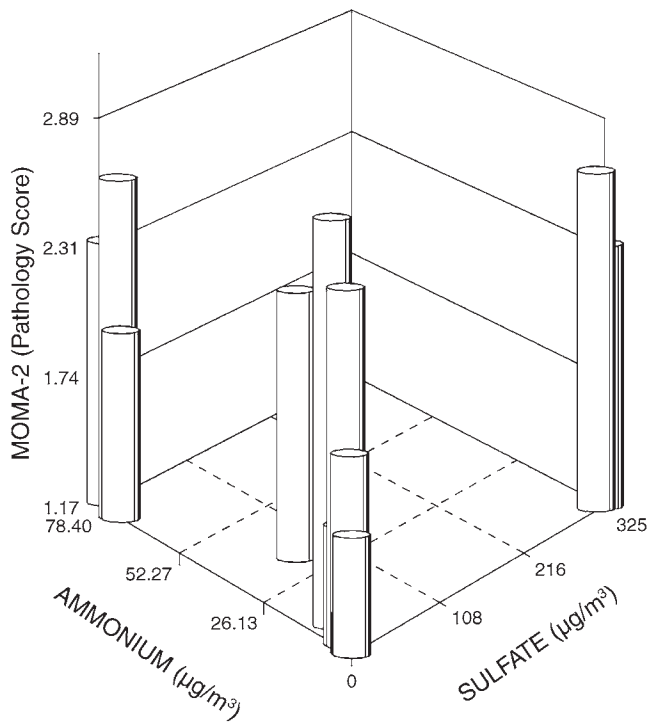


Figure 19. Observed mean MOMA-2 values relative to AMMONIUM and SULFATE exposure.

DISCUSSION

The goal of this work was (1) to provide further mechanistic insight into biologic associations observed in the accompanying epidemiologic study and (2) to identify potency differences among contrasting atmospheres of environmental relevance. The working hypothesis was that important environmental effects on the cardiovascular system are driven by exposures to pollutants derived from vehicles, including both GEE and DEE. Table 9 summarizes the major biologic responses that were measured in the animal toxicology study. In general, MVE was found to have a significant effect on most of the responses, either alone or in combination with other particle atmospheres (S, N, and RD) (data not shown). For several biologic outcomes, MVEG alone was sufficient to induce statistically significant changes compared with the filtered-air control groups, which is consistent with several previous reports of the effects of gasoline and diesel emissions (Lund et al. 2007; Campen et al. 2010b). Further, it was noteworthy that in several cases the addition of MVEG_{High} to other PM atmospheres (S, N, and RD) enhanced or caused effects that did not exist in the absence of the gases; for example, this was observed for lipid peroxidation and vascular inflammation and to a lesser extent for aortic gelatinase activity and MMP expression. Two responses appeared specific to PM, more so than for the gaseous components: the generation of circulating oxLP was likely driven by exposure to PM, and vasoconstriction by exposure to MVE and S.

These studies utilized laboratory-generated atmospheres to enable investigators to make a comparative study of contrasting compositions that may be present in ambient air, specifically how composition affects the potency to

Table 9. Summary of Key Vascular Findings^{a,b}

	MVE	MVEG	S	S+MVEG	N	N+MVEG	RD	RD+MVEG
Lipid peroxidation	++++	+++	0	+++	0	+++	0	++
Plaque area	+	+	+	0	+++	+++	0	0
Vascular inflammation	+++	+	+	+++	+	+++	0	0
Aortic gelatinase activity	++	++	+	+	+	++	0	0
NO pathways	0	0	0	0	0	0	0	0
MMP expression	+	+	+	++	0	+	0	0
Vasoconstriction	++	0	+++	++	-	0	+	+
ox-LP generation	+++	0	0	0	0	0	0	0

^a Changes all compared with control (filtered air). - indicates statistically significant reduction; 0 indicates no apparent effect; + indicates nonsignificant increasing trends; ++ to ++++ indicate clear statistically significant effects, increasing strength.

^b MVE indicates mixed vehicular engine emissions; MVEG, mixed vehicular engine emissions with PM filtered out, gases only; N, nitrate; RD, road dust; S, sulfate.

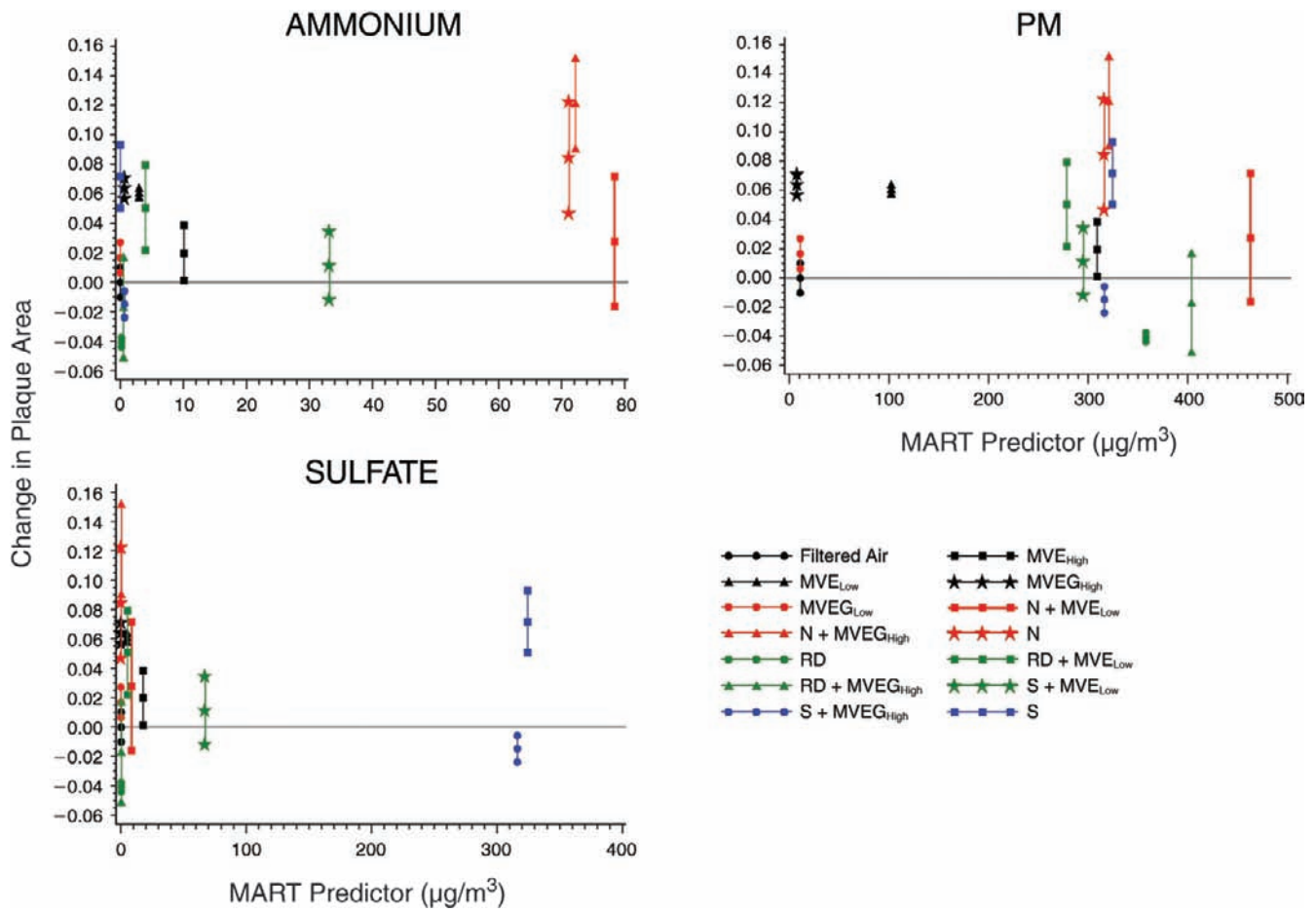


Figure 20. Observed plaque area growth (means and SEs) relative to MART-identified top predictors. Net change from control values is expressed as a fraction of lumen area (i.e., maximum of 1.0).

induce adverse biologic effects. An alternative approach would be to conduct studies using concentrated ambient PM in regions that have varying compositions of ambient air pollutants (as was done in the NPACT study at NYU [Chen and Lippmann 2013]). The advantage of the studies using concentrated ambient PM is that they employ real-world PM exposures, which account for the complexity of exposures as they exist in the environment, including the myriad sources that contribute to ambient air, as well as atmospheric transformation of pollutants that may affect the potency of the PM. The disadvantage of that approach is that the PM composition and concentration vary from day to day, so that it may be difficult to attribute biologic effects to specific components or sources that may be critical for driving longer-term effects. In addition, because the atmospheres are difficult to reproduce exactly, results cannot be easily replicated.

We chose to use laboratory-generated atmospheres because that approach simplifies the complexity of working with ambient air and allows controlled exposure atmospheres to be reproduced consistently, enabling policy-relevant assessments of important contributors to ambient air. Another important advantage of the approach used here was the inclusion of gaseous copollutants derived from mixed diesel and gasoline emissions in the exposure atmospheres. Based on the results of the present study, along with previous reports (Lund et al. 2007; Campen et al. 2010b), we conclude that the MVE gases are independent drivers of cardiovascular toxicity.

In addition, we conclude from the results of the present study that particles and gases may have an important interaction that could potentiate systemic vascular oxidative stress. What we observed in the first exposure batch implied a synergistic relationship (i.e., more than additive), although collectively the results suggest additivity of the effects of MVE emissions and gases. More specifically, the combination of GEE (which has a low mass PM concentration and a high gas contribution) and DEE (which has a high PM mass concentration and relatively low concentration of gases) resulted in a more potent lipid peroxidation response than either type of emissions alone, as demonstrated in a previous study (Lund et al. 2011). In another earlier study (Campen 2010b), DEE with PM concentrations 3.3-fold greater did not elicit as large an increase in aortic TBARS as compared with the combined DEE plus GEE (MVE) in the present work. In the current study, we noted that the addition of MVEG to non-vehicular PM led to an increase in some outcomes, such as lipid peroxidation measured with TBARS after exposure to S + MVEG_{High} and N + MVEG_{High} (compared with S and N alone, respectively) and to a lesser extent RD + MVEG_{High} (compared

with RD alone), or MMP-2/-9 activity after exposure to N + MVEG_{High} (compared with N alone). However, this observation was inconsistent.

Our analysis of circulating oxLP in exposure groups suggested that MVE was the sole determinant of lipoprotein oxidation. MVEG atmospheres, non-vehicular PM, and the combinations thereof failed to induce a significant effect on this endpoint. We observed a significant induction of oxLP in Apo E^{-/-} mice exposed to MVE_{High}, S + MVE_{Low}, N + MVE_{Low}, and RD + MVE_{Low} (all atmospheres with PM concentrations of 300 µg/m³), which was reasonably consistent across MVE exposure batches (Figure 14). Restricted analysis of select groups revealed a potential effect in the RD + MVEG_{High} group; however, MVEG_{High} alone or in combination with the other particle types simply did not elicit the response of atmospheres that contained motor-vehicle-derived particulates. Since S, N, and RD in combination with MVEG did not induce changes while S, N, and RD combined with MVE did, it is difficult to ascribe an effect to the non-vehicular PM as opposed to whole MVE. A factor that may explain the relative potency of the MVE atmosphere is particulate surface area, which is quite high on the complex diesel particles compared with the non-vehicular PM (S, N, and RD). This enhanced surface area affords a greater substrate for reactivity with molecules in the lung and also adsorbance of SVOCs and NMVOCs, which are typically at high levels in the exhaust from gasoline engines. The EC in the DEEPM may have also contributed to greater interaction between the MVE gases and PM. Thus, the new approach of mixing DEE with GEE may show enhanced toxicity (compared with DEE or GEE alone) by combining the PM derived from DEE with the SVOCs and NMVOCs derived from GEE. As we were unable to examine this relationship in greater mechanistic detail, our conclusions in this regard are speculative.

In an earlier study, we reported that a 7-day exposure to MVE resulted in a statistically significant increase in oxLP-LOX-1 signaling in Apo E^{-/-} mice, which is associated with increased MMP-2/-9 activity in the vessel wall and plaque regions (Lund et al. 2011). Since oxLP is known to be a key mediator of atherogenesis and to exert its effects in the vasculature mainly through binding to cell surface receptors such as LOX-1 (Steinbrecher 1999; Terpstra et al. 2000), the combined evidence from our previous and current studies provides a basis for further investigation into the expression of and signaling through oxLP receptors in response to exposure to components of vehicle-generated air pollutants. Furthermore, ox-LDL signaling has been shown to upregulate expression of monocyte adhesion molecules, including MCP-1, ICAM-1,

and VCAM-1 (Li and Mehta 2000; Chen H et al. 2003; Chen K et al. 2005), which may also account for the increased monocyte/macrophage sequestration and infiltration into the vascular wall observed with some of the exposure groups in these studies (using MOMA-2 staining).

Our approach to laboratory atmosphere generation considered MVE to be a critical atmosphere, and S, N, and RD to be important copollutants that may modify MVE toxicity. This study evaluated combined GEE and DEE in combination for the first time, which can be considered an advantage because it provides a more environmentally relevant exposure composition compared with evaluating either source on its own. As described in this study, this combination created compelling data on the role of gas and particle interactions in terms of the toxic potency of pollutant mixtures, as discussed earlier.

The MVE atmosphere, however, does have limitations in its suitability as a representation of contemporary traffic exposures. Both the DEE and GEE generation systems have been described in detail previously (McDonald et al. 2004a, 2008), including assessments of the relevance of those emissions to on-road exhaust. In both cases, the exhausts are outdated compared with emissions from contemporary vehicle fleets in the United States. The GEE was derived from a 1996 engine and aftertreatment system, and the DEE exhaust composition resembled that of engines manufactured before 2007. We must take into account that contemporary engines in compliance with current EPA standards emit far less PM, NO_x, and CO, along with most other gaseous subspecies, than the systems used in this study. We generated S, N, and RD in this study to create the composition and particle sizes that mirror what is observed in ambient air for each of these atmospheres, and in general, this was accomplished. The only exception was for S, which was only partially neutralized and, depending on the presence of ammonia, which we would have expected to have been more completely neutralized as seen in many geographic regions (Seinfeld and Pandis 1998). (It should also be noted that the RD atmosphere was restricted to PM smaller than 2.5 μm and thus did not include the larger particles that are commonly associated with road dust.)

A recent study in humans noted an important protective effect afforded by removal of the PM from diesel exhaust (Lucking et al. 2011), although the engine exhaust used in that study was notably lower in gas concentrations (especially VOCs) than the combined engine exhausts used in the present study. However, in the present study, filtration of PM from the MVE atmosphere was effective only in attenuating a few vascular effects measured in the present study, such as an increase in oxLP and vascular inflammation (MOMA-2 staining). Other studies (Lund

et al. 2007; Campen et al. 2010b) from our laboratory confirm modest but statistically significant effects from exposure to the gas phase from PM-filtered GEE and DEE. Thus, we can conclude that the gas phase of emissions is an independent driver of systemic vascular effects.

When examining the effects of non-vehicular PM and MVE on the expression of MMP mRNA, we found few significant changes. Aortic MMP-2 and -9 mRNA were the only statistically significantly elevated genes in exposed groups compared with control, but this effect was observed for only one exposure atmosphere each (Figure 10). We observed a small increase in MMP-9 expression in the MVEG_{Low} group, but it was not notably different from MVE alone. Compared with controls, the enzymatic activity of MMP-2/-9 (measured by in situ zymography) was more noticeably increased in the vasculature of ApoE^{-/-} mice exposed to MVE, MVEG, S, S + MVEG_{High}, S + MVE_{Low}, N, and N + MVEG_{High} (see Table 7). Overall the expression and activity data did not correlate well among groups, but the factors driving mRNA expression and activation of the protein are numerous and complex. Since TIMP-2 preferentially inhibits MMP-2 (Olson et al. 1997), it stands to reason that an induction of TIMP-2 would result in decreased ability for cleaving the MMP-2 zymogen to its active form. As TIMP-1 is the primary inhibitor of MMP-9, it may be interesting to determine the effects of PM and MVE on its expression in future studies.

Vascular constriction in response to various atmospheres may have been the most robust outcome in terms of providing a “fingerprint” for the exposures. Most atmospheres appeared to enhance the constrictive effects of PE, most notably those containing S. As enhanced vasoconstriction has been reported in human atherosclerotic coronary arteries (Lerman et al. 1991; Badimon et al. 1992; Lüscher 1993; Bacon et al. 1996), it may serve as an air-pollution-mediated physiologic pathway involved in the progression of atherosclerosis. Enhanced vasoconstriction can lead to states of hypertension, which can also have deleterious effects on the cardiovascular system. Interestingly, in this study N had the opposite effect, exhibiting a subtle blunting of constriction (see Figure 12). It is plausible that this may be due, at least in part, to the ability of N to act as a nitrogen donor in the vascular system and thus contribute to NO production and to conditions of increased oxidative stress if NO is subsequently converted to ONOO⁻, a highly reactive protein-damaging oxidant (Gryglewski et al. 1986). Decreased bioavailability of NO is known to alter vasoreactivity and mediate endothelial dysfunction, which is also associated with altered HO-1 and MMP production (Rajagopalan et al. 1996; Bonetti et al. 2003; Amiri et al. 2004; Lund et al. 2009).

The MART analysis revealed possible underlying concentration–response relationships between individual chemical components and biologic endpoints, in particular vascular lipid peroxides and vascular inflammation. This analysis showed evidence of an association between an increase in lipid peroxides (using a TBARS assay) and both volatile alkanes (NMVOALKA) and CO, and a positive but inconsistent association with SULFATE. Although the initial findings are intriguing, the results should not be over-interpreted. With only 14 distinct exposure combinations and 36 components (i.e., MART predictor variables), the method can, at best, provide only suggestive evidence relative to causality. The strength of the interpretation of the results is further limited by the substantial variability in the response data across exposure batches (especially for gene expression) and by the small experimental group sizes (as low as three) for MOMA-2 and plaque area measurements. In addition, it is important to note that the MART analysis does not reflect sensitivity to uncertainties in exposure characterization for the individual chemical components.

This study demonstrated that (1) subchronic exposure to MVE results in statistically significant increases in a number of vascular markers, including lipid peroxidation, circulating oxLP, vascular MMP expression and activity, and enhanced vasoconstriction in ApoE^{-/-} mice; and (2) exposure to N, S, and RD alone does not appear to drive the statistically significant effects observed in the cardiovascular system unless they are combined with MVE_{Low} or MVEG_{High}. These findings reveal some of the causative components of motor-vehicle-generated pollutants, as well as key mechanistic pathways involved in the progression of cardiovascular disease and onset of acute clinical events such as heart attack and stroke. Additionally, our findings suggest an important role for the interaction of PM and gaseous pollutants in complex air pollution mixtures in the sequelae of cardiovascular effects. The gaseous components were implicated in the multivariate statistical analysis as determining the response, but the responses observed were generally higher when the MVE gases were combined with non-vehicular PM. The implications of these findings may provide guidance for future regulatory oversight of the role of MVE in the context of other important ambient air pollutants and point to the importance of both the gaseous components of ambient air and PM in aggregate.

IMPLICATIONS OF FINDINGS

This is the first study to evaluate the biologic responses of mice to subchronic inhalation of a mixture of GEE and DEE, as well as other non-vehicular PM present in

ambient air (N, S, and RD) alone or in combination with the mixed engine emissions. The most compelling observation from this study was a possible gas–particle interaction that may lead to enhanced vascular toxicity. Interactive effects among pollutants have not been extensively studied, as most research projects are of smaller scope; programmatic efforts such as the present study enable these unprecedented head-to-head comparisons. While the initial observations of a synergistic interaction between PM and gas components (Lund et al. 2011) did not hold up in repeated exposures, the consistency of MVE potency, compared with previous work on GEE or DEE alone, lends support to the notion that there may be some additivity of the effects of engine emissions with those of copollutants. In terms of the regulatory implications of these findings, the interactive effects of gases and particles clearly argue for implementation of a multipollutant framework that addresses ambient air quality issues from a mixture point of view rather than addressing one pollutant at a time.

The MART analysis revealed possible underlying concentration–response relationships between lipid peroxides and vascular inflammation and individual chemical components—primarily in the gas phase. However, our statistical evaluation of the consistency among endpoints and the relative strength of the concentration–response relationships revealed considerable uncertainty in the associations and suggested that these associations are inconclusive, although they may merit further study. Further, it was noted that the atmospheres appeared more potent by standard statistical analyses when both the PM and gas phases were included.

Additionally, the findings of the present study clearly demonstrated that (1) subchronic exposure to vehicle-related mixed emissions results in statistically significant increases in lipid peroxidation, circulating oxLP, vascular MMP expression and activity, and enhanced vasoconstriction in ApoE^{-/-} mice, each of which is associated with progression of atherosclerosis and clinical cardiovascular events; and (2) exposure to N, S, and RD alone did not appear to drive any of the statistically significant effects observed in the cardiovascular system. These findings in mice on molecular and physiologic endpoints may provide a foundation for comparison to current (such as the analysis obtained from the MESA Air cohort in Section 1 of this report) and future integrative analysis of human endpoints. We hope such translatable comparisons will also provide a foundation for understanding the mechanisms of cardiovascular effects, which will allow for more effective preventative and therapeutic options. In addition, such comparisons may help in identifying corresponding causative components of environmental air pollutants (both gaseous and PM), including those generated from

vehicle-related sources that may require future regulatory monitoring or emission limits. In aggregate, the findings further extend observations of the importance to health of the carbonaceous components of ambient air PM and of gaseous pollutants in combination with PM, and further support the importance of MVE in context of other pollutants.

ACKNOWLEDGMENTS

The authors would like to thank Drs. Vijay Naik, Jean-Clare Seagrave, and Joe Mauderly, and Mark Guana, Terry Zimmerman, Joann Lucero, Selita Lucas, Jennifer Buntz, and Richard White for their technical and intellectual contributions to this study.

REFERENCES

- Amiri F, Viridis A, Neves MF, Iglarz M, Seidah NG, Touyz RM, Reudelhuber TL, Schiffrin EL. 2004. Endothelium-restricted overexpression of human endothelin-1 causes vascular remodeling and endothelial dysfunction. *Circulation* 110:2233–2240.
- Araujo JA, Barajas B, Kleinman M, Wang X, Bennett BJ, Gong KW, Navab M, Harkema J, Sioutas C, Lusk AJ, Nel AE. 2008. Ambient particulate pollutants in the ultrafine range promote early atherosclerosis and systemic oxidative stress. *Circ Res* 102:589–596.
- Bacon CR, Cary NRB, Davenport AP. 1996. Endothelin peptide and receptors in human atherosclerotic coronary arteries and aorta. *Circ Res* 79:794–801.
- Badimon L, Chesebro JH, Badimon JJ. 1992. Thrombus formation on ruptured atherosclerotic plaques and rethrombosis on evolving thrombi. *Circulation* 86:SI174–SI185.
- Berliner JA, Heinecke JW. 1996. The role of oxidized lipoproteins in atherogenesis. *Free Radic Biol Med* 20:707–727.
- Blankenberg S, Rupprecht HJ, Poirier O, Bickel C, Smieja M, Hafner G, Meyer J, Cambein F, Tiret L; AtheroGene Investigators. 2003. Plasma concentrations and genetic variation of matrix metalloproteinase 9 and prognosis of patients with cardiovascular disease. *Circulation* 107:1579–1585.
- Bonetti PO, Lerman LO, Lerman A. 2003. Endothelial dysfunction: A marker of atherosclerotic risk. *Arterioscler Thromb Vasc Biol* 23:168–175.
- Burnett RT, Dales R, Krewski D, Vincent R, Dann T, Brook JR. 1995. Associations between ambient particulate sulfate and admissions to Ontario hospitals for cardiac and respiratory diseases. *Am J Epidemiol* 142:15–22.
- Campen MJ, Lund AK, Doyle-Eisele M, McDonald JD, Knuckles TL, Rohr A, Knipping E, Mauderly JL. 2010a. A comparison of vascular effects from complex and individual air pollutants indicates a toxic role for monoxide gases. *Environ Health Perspect* 118:921–927.
- Campen MJ, Lund AK, Knuckles TL, Conklin DF, Bishop B, Young D, Sielkop SK, Seagrave JC, Reed MD, McDonald JD. 2010b. Inhaled diesel emissions alter atherosclerotic plaque composition in ApoE^{-/-} mice. *Toxicol Appl Pharmacol* 242:310–317.
- Channell MC, Aragon M, Paffett ML, Devlin R, Campen MJ. 2012. Circulating factors induce coronary endothelial cell activation following exposure to inhaled diesel exhaust and nitrogen dioxide in humans: Evidence from a novel translational in vitro model. *Toxicol Sci* 127:179–186.
- Chatterjee A, Black SM, Catravas JD. 2008. Endothelial nitric oxide (NO) and its pathophysiologic regulation. *Vascul Pharmacol* 49:134–140.
- Chen H, Li D, Chen J, Roberts GJ, Saldeen T, Mehta JL. 2003. EPA and DHA attenuate ox-LDL-induced expression of adhesion molecules in human coronary artery endothelial cells via protein kinase B pathway. *J Mol Cell Cardiol* 35:769–775.
- Chen K, Chen J, Liu Y, Xie J, Li D, Sawamura T, Hermonat PL, Mehta JL. 2005. Adhesion molecule expression in fibroblasts: Alterations in fibroblast biology after transfection with LOX-1 plasmid. *Hypertension* 46:622–627.
- Chen L-C, Lippmann M. 2013. Study 1. Subchronic Inhalation Exposure of Mice to Concentrated Ambient PM_{2.5} from Five Airsheds. In: National Particle Component Toxicity (NPACT) Initiative: Integrated Epidemiologic and Toxicologic Studies of the Health Effects of Particulate Matter Components. Research Report 177. Health Effects Institute, Boston, MA.
- Cheng Y-S, Moss OR. 1995. Part 2: Inhalation exposure. In: *Concepts in Inhalation Toxicology* (McClellan RO, ed.). Taylor & Francis, Washington, DC.
- Chester AH, O'Neil GS, Moncada S, Tadjkarimi S, Yacoub MH. 1990. Low basal and stimulated release of nitric oxide in atherosclerotic epicardial coronary arteries. *Lancet* 336:897–900.
- Chow JC, Watson JG, Green MC, Lowenthal DH, DuBois DW, Kohl SD, Egami RT, Gillies JA, Rogers CF, Frazier CA,

- Cates W. 1999. Middle- and neighborhood-scale variations of PM₁₀ source contributions in Las Vegas, Nevada. *J Air & Waste Manage Assoc* 49:641–654.
- Chow JC, Watson JG, Lowenthal DH, Soloman PA, Magliano KL, Ziman SD, Richards LW. 1993. PM₁₀ and PM_{2.5} compositions in California's San Joaquin Valley. *Aerosol Sci Technol* 18:105–128.
- Ergul A, Portik-Dobos V, Giulumian AD, Molero MM, Fuchs LC. 2003. Stress upregulates arterial matrix metalloproteinase expression and activity via endothelin A receptor activation. *Am J Physiol Heart Circ Physiol* 285:H2225–H2232.
- Föstermann U, Mugge A, Alheid U, Haverich A, Frölich JC. 1988. Selective attenuation of endothelium-mediated vasodilation in atherosclerotic human coronary arteries. *Circ Res* 62:185–190.
- Galis ZS, Khatri JJ. 2002. Matrix metalloproteinases in vascular remodeling and atherosclerosis: The good, the bad and the ugly. *Circ Res* 90:251–262.
- Griendling KK, Sorescu D, Ushio-Fukai M. 2000. NAD(P)H oxidase: Role in cardiovascular biology and disease. *Circ Res* 86:494–501.
- Gryglewski RJ, Palmer RM, Moncada S. 1986. Superoxide anion is involved in the breakdown of endothelium-derived vascular relaxing factor. *Nature* 320:454–456.
- Hoffmann B, Moebus S, Mohlenkamp S, Stang A, Lehmann N, Dragano N, Schmermund A, Memmesheimer M, Mann K, Erbel R, Jöckel KH; Heinz Nixdorf Recall Study Investigative Group. 2007. Residential exposure to traffic is associated with coronary atherosclerosis. *Circulation* 116:489–496.
- Ihling C, Szombathy T, Bohrmann B, Brockhaus M, Schaefer HE, Loeffler BM. 2001. Coexpression of endothelin-converting enzyme-1 and endothelin-1 in different stages of human atherosclerosis. *Circulation* 104:864–869.
- Ikeda M, Shitashige M, Yamasaki H, Sagai M, Tomita T. 1995. Oxidative modification of low density lipoprotein by diesel exhaust particles. *Bio Pharm Bull* 18:866–871.
- Joannides R, Bellien J, Thuillez C. 2006. Clinical methods for the evaluation of endothelial function: A focus on resistance arteries. *Fundam Clin Pharmacol* 20:311–320.
- Knuckles TL, Lund AK, Lucas SN, Campen MJ. 2008. Diesel exhaust exposure enhances venoconstriction via uncoupling of eNOS. *Toxicol Appl Pharmacol* 230:346–351.
- Künzli N, Jerrett M, Garcia-Esteban R, Basagaña X, Beckermann B, Gilliland F, Medina M, Peters J, Hodis HN, Mack WJ. 2010. Ambient air pollution and the progression of atherosclerosis in adults. *PLOS ONE* 5:e9096.
- Lerman A, Edwards BS, Hallet JW, Heublein DM, Sandberg S, Burnett JC. 1991. Circulating and tissue endothelin-1 immunoreactivity in advanced atherosclerosis. *N Engl J Med* 325:997–1001.
- Li D, Liu L, Chen H, Sawamura T, Ranganathan S, Mehta JL. 2003. LOX-1 mediates oxidized low-density lipoprotein-induced expression of matrix metalloproteinases in human coronary artery endothelial cells. *Circulation* 107:612–617.
- Li D, Mehta JL. 2000. Antisense to LOX-1 inhibits oxidized LDL-mediated upregulation of monocyte chemoattractant protein-1 and monocyte adhesion to human coronary artery endothelial cells. *Circulation* 101:2889–2895.
- Lucking AJ, Lundbäck M, Barath SL, Mills NL, Sidhu MK, Langrish JP, Boon NA, Pourazar J, Badimon JJ, Gerlofs-Nijland ME, Cassee FR, Boman C, Donaldson K, Sandstrom T, Newby DE, Blomberg A. 2011. Particle traps prevent adverse vascular and prothrombotic effects of diesel engine exhaust inhalation in men. *Circulation* 123:1712–1728.
- Lund AK, Knuckles TL, Obat Akata C, Shohet R, McDonald JD, Seagrave JC, Campen MJ. 2007. Exposure to gasoline exhaust results in alterations of pathways involved in atherosclerosis. *Toxicol Sci* 95:485–494.
- Lund AK, Lucero J, Harman M, Madden MC, McDonald JD, Seagrave JC, Campen MJ. 2011. The oxidized low density lipoprotein receptor mediates vascular effects of inhaled vehicular emissions. *Amer J Respir Crit Care Med* 184:82–91.
- Lund AK, Lucero J, Lucas S, Madden M, McDonald J, Campen MJ. 2009. Vehicular emissions induce vascular MMP-9 expression and activity associated with endothelin-1 mediated pathways. *Arterioscler Thromb Vasc Biol* 29:511–517.
- Lüscher TF. 1993. The endothelium as a target and mediator of cardiovascular disease. *Eur J Clin Invest* 23:607–685.
- McDonald JD, Barr EB, White RK. 2004a. Design, characterization, and evaluation of a small-scale diesel exhaust exposure system. *Aerosol Sci Technol* 38:62–78.
- McDonald JD, Barr EB, White RK, Chow JC, Schauer JJ, Zielinska B, Grosjean E. 2004b. Generation and characterization of four dilutions of diesel engine exhaust for

- a subchronic inhalation study. *Environ Sci Technol* 38: 2513–2522.
- McDonald JD, Barr EB, White RK, Kracko D, Chow JC, Zielinska B, Grosjean E. 2008. Generation and characterization of gasoline engine exhaust inhalation exposure atmospheres. *Inhal Toxicol* 20:1157–1168.
- McDonald JD, Doyle-Eisele M, Campen MJ, Seagrave J, Holmes T, Lund A, Surratt JD, Seinfeld JH, Rohr AC, Knipping EM. 2010. Cardiopulmonary response to inhalation of biogenic secondary organic aerosol. *Inhal Toxicol* 22:253–265.
- McDonald JD, Reed MD, Campen MJ, Barrett EG, Seagrave J, Mauderly JL. 2007. Health Effects of Inhaled Gasoline Engine Emissions. *Inhal Toxicol* 19:107–116.
- McDonald JD, White RK, Barr EB, Zielinska B, Chow JC, Grosjean E. 2006. Generation and characterization of hardwood smoke inhalation exposure atmospheres. *Aerosol Sci Technol* 40:573–584.
- McMillan WD, Patterson BK, Keen RR, Shively VP, Cipollone M, Pearce WH. 1995. In situ localization and quantification of mRNA for 92-kd type IV collagenase and its inhibitor in aneurismal, occlusive, and normal aorta. *Arterioscler Thromb Vasc Biol* 15:1139–1144.
- Newby AC. 2005. Dual role of matrix metalloproteinases (matrixins) in intimal thickening and atherosclerotic plaque rupture. *Physiol Rev* 85:1–31.
- Olson MW, Gervasi DC, Mobashery S, Fridman R. 1997. Kinetic analysis of the binding of human matrix metalloproteinase-2 and -9 to tissue inhibitors of metalloproteinase (TIMP)-1 and TIMP-1. *J Biol Chem* 272:29975–29983.
- Peters A, von Klot S, Heier M, Trentinaglia I, Hörmann A, Wichmann HE, Löwel H; Cooperative Health Research in the Region of Augsburg Study Group. 2004. Exposure to traffic and the onset of myocardial infarction. *N Engl J Med* 351:1721–1730.
- Pope CA III, Burnett RT, Thruston GD, Thun MJ, Calle EE, Krewski D, Godleski JJ. 2004. Cardiovascular mortality and long-term exposure to particulate air pollution: Epidemiological evidence of general pathophysiology pathways of disease. *Circulation* 109:71–77.
- Rajagopalan S, Meng XP, Ramasamy S, Harrison DG, Galis ZS. 1996. Reactive oxygen species produced by macrophage-derived foam cells regulate the activity of vascular matrix metalloproteinases in vitro. Implications for atherosclerotic plaque stability. *J Clin Invest* 98: 2572–2579.
- Rubbo H, O'Donnell V. 2005. Nitric oxide, peroxynitrite and lipoxygenase in atherogenesis: Mechanistic insights. *Toxicol* 208:305–317.
- Schwartz J, Morris R. 1995. Air pollution and hospital admissions for cardiovascular disease in Detroit, Michigan. *Am J Epidemiol* 142:23–35.
- Seilkop SK, Campen MJ, Lund AK, McDonald JD, Mauderly JL. 2012. Identification of chemical components of common air pollutants that affect indicators of atherosclerosis. *Inhal Toxicol* 24:270–287.
- Seinfeld JH, Pandis SN. 1998. *Atmospheric Chemistry and Physics: From Air Pollution to Climate Change*. John Wiley & Sons, New York, NY.
- Steinbrecher UP. 1999. Receptors for oxidized low density lipoprotein. *Biochim Biophys Acta* 1436:279–298.
- Sun Q, Wang A, Jin X, Natanzon A, Duquaine D, Brook RD, Aguinaldo JG, Fayad ZA, Fuster V, Lippmann M, Chen LC, Rajagopalan S. 2005. Long-term air pollution exposure and acceleration of atherosclerosis and vascular inflammation in an animal model. *JAMA* 293:3003–3010.
- Suwa T, Hogg JC, Quinlan KB, Ohgami A, Vincent R, van Eeden SF. 2002. Particulate air pollution induces progression of atherosclerosis. *J Am Coll Cardiol* 39:935–942.
- Terpstra V, van Amersfoort ES, van Velzen AG, Kuiper J, van Berkel TJ. 2000. Hepatic and extrahepatic scavenger receptors: Function in relation to disease. *Arterioscler Thromb Vasc Biol* 20:1860–1872.
- Witztum JL, Steinberg D. 2001. The oxidative modification hypothesis of atherosclerosis: Does it hold for humans? *Trends Cardiovasc Med* 11:93–102.
- Zalba G, Fortuño A, Orbe J, San José G, Moreno MU, Belzunce M, Rodríguez JA, Beloqui O, Páramo JA, Díez J. 2007. Phagocytic NADPH oxidase dependent superoxide production stimulates matrix metalloproteinase-9: Implications for human atherosclerosis. *Arterioscler Thromb Vasc Biol* 27:587–593.

APPENDICES AVAILABLE ON THE WEB

Appendices R and S contain supplemental material not included in the printed report. They are available on the HEI Web site at <http://pubs.healtheffects.org>.

Appendix R: Characterization of NPACT Animal Toxicologic Exposure Atmospheres

Appendix S: Statistical Results for NPACT Animal Toxicologic Exposure Atmosphere Composition

ABOUT THE AUTHORS

Matthew J. Campen, Ph.D., M.S.P.H., is currently an associate professor in the Department of Pharmaceutical Sciences at the University of New Mexico, Albuquerque. His laboratory is broadly interested in the cross-talk of the cardiovascular and respiratory system in health and disease. His primary research focus involves the impact of inhaled toxicants, especially common air pollutants, on vascular function and injury, but has expanded to explore the role of ubiquitin ligases in modulating pathologic vascular growth and response to injury. Campen was trained in environmental health at the University of North Carolina School of Public Health, Chapel Hill, followed by a post-doctoral fellowship in the Johns Hopkins University School of Medicine, Baltimore, Maryland. Prior to his current appointment, he worked as an independent scientist at the LRRRI in Albuquerque, New Mexico. His laboratory has received funding from the U.S. Environmental Protection Agency, HEI, and the National Institutes of Health. Campen has published more than 50 peer-reviewed articles. He has recently been appointed as an associate editor of *Toxicological Sciences* and *Cardiovascular Toxicology*, and also contributes to the editorial board of *Inhalation Toxicology*. Campen served as co-principal investigator on the animal toxicology component of the NPACT project.

Amie K. Lund, Ph.D., is an associate scientist in the Environmental Respiratory Health Program at LRRRI in Albuquerque, New Mexico. She received her Ph.D. in biomedical sciences, with an emphasis in cardiovascular toxicology from the University of New Mexico, Albuquerque. Her current research interests are in investigating the effects of inhaled air pollutants on both the systemic and cerebral vasculature, with an emphasis on elucidating pathways and molecular targets involved in the progression of atherosclerosis and signaling pathways involved in the onset of clinical cardiovascular events. Lund currently has more than 20 peer-reviewed publications and has authored and coauthored several book chapters. She also serves on committees for the American Heart Association and the Society of Toxicology (Inhalational Respiratory Specialty Section). Lund served as an investigator on the animal toxicology component of the NPACT project from 2009 to 2011.

Steven K. Seilkop, M.S., is a consulting biostatistician (SKS Consulting Services, Siler City, North Carolina) with more than 30 years of experience in the analysis of toxicologic, epidemiologic, biomedical, pharmaceutical, and environmental data. He has worked in governmental, industrial, and academic settings, and is currently an

adjunct scientist at LRRRI in Albuquerque, New Mexico. Seilkop specializes in the application and development of statistical methodology for carcinogenicity testing, toxicity testing, and risk assessment. He served as biostatistician for the animal toxicology study component of the NPACT project, which included responsibility for conducting the MART analyses and interpreting their results.

Jacob D. McDonald, Ph.D., received his doctorate in environmental chemistry with an emphasis in atmospheric chemistry from the University of Nevada–Reno. McDonald is director of the Chemistry and Inhalation Exposure Program and director of the Environmental Respiratory Health Program at LRRRI in Albuquerque, New Mexico. He oversees exposure assessment and exposure atmosphere generation, inhalation toxicology, pharmacokinetics, and analytic/bioanalytic chemistry. McDonald served as a co-principal investigator for the animal toxicology component of the NPACT project.

OTHER PUBLICATION RESULTING FROM THIS RESEARCH

Lund AK, Lucero J, Harman M, Madden MC, McDonald JD, Seagrave JC, Campen MJ. 2011. The oxidized low-density lipoprotein receptor mediates vascular effects of inhaled vehicular emissions. *Am J Resp Crit Care Med* 184:82–91.

ABBREVIATIONS AND OTHER TERMS

ACh	acetylcholine
ANOVA	analysis of variance
ApoE ^{-/-}	apolipoprotein E null
BHT	butylated hydroxytoluene
cDNA	complementary deoxyribonucleic acid
CO	carbon monoxide
DEE	diesel engine exhaust
DHFR	dihydrofolate reductase
EC	elemental carbon
EDTA	ethylenediaminetetraacetic acid
eNOS	endothelial nitric oxide synthase
ET-1	endothelin-1
GAPDH	glyceraldehyde-3-phosphate dehydrogenase
GEE	gasoline engine exhaust
GTPCH	guanosine 5'-triphosphate cyclohydrolase
HEPA	high-efficiency particulate air

HO-1	heme oxygenase-1	NOS	nitric oxide synthase
ICAM	intracellular adhesion molecule	NO _x	nitrogen oxides
iNOS	inducible nitric oxide synthase	OC	organic carbon
LDL	low-density lipoprotein	ONOO ⁻	peroxynitrite
LOX	lectin-like oxidized low-density lipoprotein receptor	ox-LDL	oxidized low-density lipoprotein
LRRI	Lovelace Respiratory Research Institute	oxLP	oxidized low-density lipoprotein
MART	multiple additive regression tree	PAHs	polycyclic aromatic hydrocarbons
MCP	monocyte chemoattractant protein	PE	phenylephrine
MDA	malondialdehyde	PM	particulate matter
MMP	matrix metalloproteinase	PSS	physiologic saline solution
MOMA	monocyte/macrophage	QC	quality control
mRNA	messenger ribonucleic acid	RD	road dust
MVE	mixed vehicular engine emissions	ROS	reactive oxygen species
MVEG	mixed vehicular engine emissions with particulate matter filtered out, gases only	RT-PCR	real-time polymerase chain reaction
N	nitrate	S	sulfate
NAD(P)H	nicotinamide adenine dinucleotide (phosphate)	SO ₂	sulfur dioxide
NMVOC	nonmethane volatile organic compound	SVOC	semivolatile organic compound
NO	nitric oxide	TBARS	thiobarbituric acid reactive substances
NO ₂	nitrogen dioxide	THC	total hydrocarbons
		TIMP	tissue inhibitor of matrix metalloproteinases
		VCAM	vascular cellular adhesion molecule
		VOC	volatile organic compound

Section 3: Integrated Discussion

Sverre Vedal and Matthew J. Campen

INTEGRATING THE EPIDEMIOLOGIC AND TOXICOLOGIC STUDIES

There are several reasons for viewing epidemiologic and toxicologic studies in concert. In an idealized view, toxicologic studies might be said to test in an experimental setting the findings from epidemiologic and other observational studies that, in spite of all efforts, remain at the level of associations. In another idealized view, toxicologic studies might be said to identify the effects of exposures that could actually occur in humans and the mechanisms that cause these effects, and epidemiologic studies subsequently test whether the effects in fact occur. These two idealized views help focus attention on the aspects of human observational and animal experimental studies that could enhance their value when both types of studies are examined together, compared with their value when examined separately.

The value of examining epidemiologic and toxicologic studies together could be further enhanced if the studies were designed in the first place with an eye to the eventual integration of their findings. The epidemiologic and toxicologic studies described in this report were intended to complement each other, with the epidemiologic studies providing evidence in humans in real-world settings and the toxicologic study allowing direct assessment of exposures to mixtures and individual compounds in mice. In addition, our findings presented opportunities for assessing coherence between the observational human evidence and the experimental animal evidence.

In the two epidemiologic studies described in this report, the PM_{2.5}* components were selected to reflect emissions from combustion and noncombustion sources and secondary organic and inorganic aerosols. The observational endpoints ranged from markers of atherosclerosis to clinical cardiovascular events in two population cohorts, MESA and WHI-OS. In the toxicologic study, the exposure atmospheres included various combinations and concentrations

of emissions from combustion and noncombustion sources and non-vehicle-derived inorganic aerosols. The experimental endpoints reflected processes involved in the progression of atherosclerosis and the triggering of clinical cardiovascular events.

TOXICOLOGIC AND EPIDEMIOLOGIC EXPOSURES

With the exception of the pure sulfate and nitrate atmospheres, all of the exposure atmospheres used in the toxicologic study were mixtures of emissions or of combinations of emissions and PM components (sulfate, nitrate, or road dust). The source mixtures included MVE atmospheres, MVEG atmospheres (in which the particles had been filtered out), and road-dust atmospheres. The combinations of emissions and PM components included atmospheres of MVE or MVEG mixed with sulfate, nitrate, or road dust.

In the two epidemiologic studies, by contrast, terms for exposure to PM_{2.5} components were used in the health effect models. These exposure terms were predictions intended to represent the spatial distribution of PM_{2.5} component concentrations within and between the six MESA cities and nationally. The PM_{2.5} components measured in the dedicated PM_{2.5} component monitoring campaign in the MESA cities, or included in the CSN or IMPROVE national monitoring networks, were either specific elements (e.g., the transition metals) or groups of compounds that shared some operationally defined features (e.g., EC and OC). The PM_{2.5} components EC, OC, sulfur, and silicon were chosen to be the primary focus of the studies and to reflect both sources and processes. EC and OC are associated with combustion sources, and OC is also associated with secondary organic aerosol. Sulfur was used as a surrogate for sulfate, a secondary inorganic aerosol generated largely from photochemical oxidation of combustion products of sulfur-containing fuels. Silicon is associated with crustal sources. Each of these four components also makes up a large proportion of the PM_{2.5} mass; together they make up the majority of PM_{2.5} mass. Individual-level exposure models were generated for each of these components.

In addition to the PM components of primary interest, we also generated limited exposure predictions for a heterogeneous group of other PM_{2.5} components and gaseous

* A list of abbreviations and other terms appears at the end of this section.

This section is one part of Health Effects Institute Research Report 178, which also includes sections on the epidemiology and toxicology portions of this study, a Commentary by the HEI NPACT Review Panel, an HEI Statement about the research project, and a Synthesis relating this report to Research Report 177. Correspondence concerning the Research Report may be addressed to Dr. Sverre Vedal, 4225 Roosevelt Way NE, #100, Department of Environmental and Occupational Health Sciences, University of Washington School of Public Health, Seattle, WA 98105; svedal@uw.edu.

pollutants. Nickel and vanadium were selected as components of interest by the New York University team that carried out another set of studies funded under HEI's NPACT initiative (Lippmann et al. 2013); they were interested in nickel and vanadium as markers of residual-oil combustion. The selection of sulfate and nitrate made possible direct comparisons with specific components used in the exposure atmospheres in the toxicologic study. Copper was selected as a marker of brake wear and traffic. SO₂ and NO₂ were selected primarily to allow the assessment of their potential confounding effects on associations between PM_{2.5} components and health effect endpoints. NO₂ also served as a marker of traffic.

Understanding which sources and processes are indicated by EC, OC, sulfur, and silicon (as well as the pollutants of secondary interest) informed our interpretation of the exposure effect estimates in the health effect models used in the epidemiologic study. Also, because many of the experimental exposure atmospheres used in the toxicologic study were combinations of emissions and other PM, an understanding of the sources that contributed to the PM_{2.5} components used in the epidemiologic studies was important for integrating the findings of the epidemiologic and toxicologic studies. We used receptor-based source-apportionment methods to exploit the temporal and spatial distributions and correlations among the many measured PM_{2.5} components in order to gain insight into the components that best reflected specific sources and processes and into the sources and processes that contributed to specific PM_{2.5} components. Positive matrix factorization, one of several such source apportionment methods, was used to group components that are correlated over space and time into factors. Based on the components that contributed to these factors, it was possible to discern some reasonable linkages between the individual factors and specific air pollution sources and processes. However, this entailed some guesswork; we therefore referred to many of the source factors as source-like (e.g., biomass-like) to reflect these uncertainties. We know of no other health study in which a source apportionment has been attempted to aid in the interpretation of effect estimates associated with long-term exposure to PM.

Source apportionment helped integrate the findings of our epidemiologic studies with those of the toxicologic studies. We also made use of the detailed chemical composition measurements of the experimental exposure atmospheres in the toxicologic studies. A multiple additive regression tree (MART) analysis is a method applied to the prediction of endpoints that combines or pools ("boosts") a series of individual classification trees to generate a classification that performs better than any individual tree.

"Predictor variables" are ranked according to their relative importance in classifying the endpoints. In our case, the potential predictor variables were the 36 chemical components measured in each of the 14 exposure atmospheres, and the endpoints were the cardiovascular endpoints in the toxicologic study. For each of the four cardiovascular endpoints selected (TBARS, MMP-2 and -9, plaque inflammation, and plaque area), the MART analysis generated a ranking of the relative importance of the chemical components in classifying the endpoints. With this information in hand, further integration with the results of the epidemiologic study, which focused on four PM_{2.5} components rather than source mixtures, was possible. As a point of caution, with 14 distinct exposures and only 36 component variables, care must be taken in interpreting the findings of the MART analysis.

Some of the barriers to integrating the findings of the two types of studies were the other obvious differences in the respective exposures rather than differences caused by the use of source mixtures and components. The "exposures" considered in the epidemiologic studies were actually predicted outdoor concentrations at cohort members' home addresses. A number of steps are required to get from these predicted concentrations to estimates of true exposure, and these steps result in variable degrees of error in the final estimates of exposure. The exposure prediction models are imperfect, as can be seen from the model performance statistics derived from cross-validations (see Section 1, Tables 30, 34, and 35). Residential outdoor concentrations, in turn, are only relevant for the time people spend at home; further, they might not correlate well with ambient contributions to indoor PM-component concentrations, further degrading our exposure predictions as estimates of true exposures.

Although the exposure atmospheres used in the toxicologic study produced well-characterized exposures in animals, these exposures were not typical of ambient exposures because the exposure atmospheres included particle and gas concentrations that were substantially higher than those found in ambient air in the U.S. For example, PM_{2.5} concentrations were approximately 10 to 20 times those found in typical ambient settings that one might expect in the cohort studies, and concentrations of gases (such as NO_x) were approximately 200 times higher. Although human exposures to concentrations of these magnitudes do occur in occupational settings or in microenvironments for short time periods, they are rare. The high exposure concentrations used in the toxicologic study were selected to produce responses that could be compared across exposure groups. Based on our previous experience, we expected that lower exposure concentrations would yield a

smaller biologic response that would be difficult to distinguish from the inherent variability of the biologic model. Furthermore, the toxicologic study was conducted with genetically modified mice that have enhanced sensitivity to inhaled materials compared with wild-type mice of the same genetic background. Integration of the toxicologic and epidemiologic findings depended partly on finding some common biologic mechanisms that underlie both the observational associations reported for ambient exposure conditions and the toxicologic effects reported for considerably different exposure conditions. To the extent that these mechanisms differ, the integration of epidemiologic and toxicologic findings remains challenging.

TOXICOLOGIC AND EPIDEMIOLOGIC ENDPOINTS

As noted above, the endpoints examined in the toxicologic study reflected processes involved in the progression of atherosclerosis and the triggering of clinical cardiovascular events, whereas the health outcomes of the epidemiologic studies included a range of subclinical markers of atherosclerosis (CIMT and CAC) and clinical cardiovascular events. Increased CIMT is considered to be an early manifestation of atherosclerosis and is associated with cardiovascular disease risk factors and events (Karim et al. 2008; Nair et al. 2012). Although CIMT is measured specifically in the carotid arteries, it is strongly associated with measures of atherosclerosis in other arterial vascular beds (Karim et al. 2008). CAC is a measure of calcified plaque in coronary arteries and, as with CIMT, is associated with cardiovascular disease risk factors and events as well as with measures of atherosclerosis in other arterial vascular beds (Karim et al. 2008). Of the toxicologic study's endpoints, those that might relate best to atherosclerosis are plaque growth and inflammation, MMP activity and expression in the aorta, and concentrations of oxidized low-density lipoprotein in the blood. Many of the toxicologic study endpoints could reflect processes involved in the occurrence of clinical cardiovascular events, which are the endpoints in the WHI-OS cohort study. Plaque growth and inflammation, lipid peroxidation in the aorta, and MMP expression and activity (as reflections of plaque instability) might be the most relevant endpoints.

INTEGRATING EPIDEMIOLOGIC AND TOXICOLOGIC FINDINGS

How, then, does jointly examining the findings from our epidemiologic and toxicologic studies help in interpreting these findings? In the epidemiologic studies, of the four

PM_{2.5} components chosen to be of primary interest, the evidence of associations for both subclinical measures of atherosclerosis and clinical events was strongest for sulfur (our surrogate for sulfate) and OC and less strong for EC and silicon (Integrated Discussion Table 1). From the more limited assessments of the components and pollutants of secondary interest, including nitrate, nickel, vanadium,

Integrated Discussion Table 1. Strength of the Evidence for Associations of PM_{2.5} Components and Other Pollutants with Subclinical Measures of Atherosclerosis and Cardiovascular Disease Events^{a,b}

	MESA Cohort ^c		WHI-OS Cohort ^d					
			CVD Events			CVD Deaths		
	CIMT	CAC	CVD ^e	MI	Stroke	CVD ^f	ACD	Stroke
PM _{2.5}	+++	0	+++	0	+++	+	++	0
EC	0	+	0	0	0	+	++	0
OC	++++	++	0	0	+++	+++	+++	+++
Sulfate	++++	0	+++	++	+++	0	++	0
Si	+++	+	0	0	0	0	0	0
Ni	+	+						
V	0	0						
Cu	++	+						
Nitrate	0	0/+						
SO ₂	+ / ++	0						
NO ₂	0	0						

^a CIMT indicates carotid intima-media thickness; CAC, coronary artery calcium; CVD, cardiovascular disease; MI, myocardial infarction; and ACD, atherosclerotic cardiac disease.

^b 0 indicates little evidence (effect estimates were close to or below the null; 95% CIs covered the null or they did not cover the null, but effect estimates were below the null); +, some evidence (effect estimates were above the null; 95% CIs covered the null); ++, fair evidence (effect estimates were above the null; some of the 95% CIs might have covered the null); +++, good evidence (effect estimates were above the null; 95% CIs generally did not cover the null); +++++, strong evidence (effect estimates were above the null; 95% CIs did not cover the null).

^c In assessments for the MESA cohort, results of the cross-sectional analyses and effect estimates and 95% CIs from models 1 through 4 as defined in Section 1, Table 38, were considered. Assessments were based on data from Section 1, Figure 29 (spatiotemporal exposure predictions), and Section 1, Figure 31 (national spatial model exposure predictions), for PM_{2.5}, EC, OC, silicon, and sulfur; from Figure 9 in Appendix H (available on the HEI Web site) for sulfate, nitrate, SO₂, and NO₂; and from Figure 6 in Appendix N (available on the HEI Web site) for Ni, V, and Cu. Good evidence (+++) and strong evidence (++++) require consistency in results obtained using predictions from the two exposure models. Some evidence (+) is assigned if no criteria for this category are met except in models 5 and 6, which include adjustment for city, as defined in Section 1, Table 38.

^d Assessments for the WHI-OS cohort were based on data from Section 1, Table 51 (CVD events), and Section 1, Table 52 (CVD deaths). Because only one set of models was considered, evidence levels for this cohort could not be greater than good (+++).

^e MI, coronary revascularization, stroke, ACD death, possible coronary heart disease death, and cerebrovascular disease death, combined.

^f ACD death, possible coronary heart disease death, and cerebrovascular disease death, combined.

Integrated Discussion Table 2. Strength of the Evidence for Effects of Experimental Atmospheres on Cardiovascular Endpoints^a

	TBARS (Lipid Peroxidation)	Plaque Area	Vascular Inflammation	Gelatinase Activity	Nitric Oxide Pathways Components	MMP Expression	Vaso-constriction	Oxidized Lipoprotein (oxLP)
MVE	++++	+	+++	++	0	+	++	+++
MVEG	+++	+	+	++	0	+	0	0
Sulfate	0	+	+	+	0	+	+++	0
Sulfate PM with MVEG	+++	0	+++	+	0	++	++	0
Nitrate	0	+++	+	+	0	0	–	0
Nitrate PM with MVEG	+++	+++	+++	++	0	+	0	0
Road Dust	0	0	0	0	0	0	+	0
Road Dust with MVEG	++	0	0	0	0	0	+	0

^a – indicates statistically significant reduction; 0, no apparent effect; +, nonsignificant increasing trend; ++ to +++++, clear significant effects with increasing strength.

copper, NO₂, and SO₂, the evidence was strongest for copper. The evidence from the toxicologic study is summarized in Integrated Discussion Table 2 as a cross-tabulation of the degree of strength of the evidence by exposure atmosphere and cardiovascular marker. MVE-containing atmospheres generally produced more effects than other atmospheres. We begin with a discussion of sulfate and nitrate, two components with direct counterparts in both types of studies, followed by a discussion of MVE, road dust and crustal sources, OC, and SO₂.

SULFATE

In the source apportionment, the largest contribution to sulfur in all of the MESA cities except Los Angeles was from a secondary sulfate-like factor that was also enriched in arsenic and selenium. Predicted exposure to sulfur (as a marker for sulfate) in the MESA study was associated with CIMT and with cardiovascular events. Although this association might indicate that sulfate was the component directly (and possibly causally) responsible for the observed cardiovascular associations, it is at least as likely that either sulfate was exerting its effects in combination with other pollutants in the pollutant mix or other pollutants in the mix were solely responsible for the effects. These alternatives could not be evaluated given the limitations of the epidemiologic data.

Good arguments have been made that sulfate is a relatively nontoxic component of PM (Grahame and Schlesinger 2005). Our toxicologic study findings, however,

showed effects of sulfate both alone and in combination with the MVE-containing mixtures. Of all the pollutant atmospheres, an atmosphere of pure sulfate caused the most substantial changes in aortic vasoreactivity. Changes in aortic vasoreactivity were also noted for sulfate combined with MVEG, though to a lesser extent. There was also a suggestion that the atmosphere of pure sulfate increased plaque area and plaque inflammation. Other than these effects, sulfate had effects only when combined with mixtures containing MVE. In the MART analysis, sulfate was ranked — based on the strength of the association — among the top 4 of the 36 components and pollutants considered in analyses of each of the four endpoints. In light of these findings from the toxicologic study, it is possible that sulfate itself — rather than its presence in a complex mixture or some other compounds in the mix — is responsible for the associations found in the epidemiologic study. In the only other cohort study that included spatial exposure contrasts for sulfate, the California Teachers Study (Ostro et al. 2010), sulfate was associated with cardiopulmonary and ischemic heart disease mortality.

In order to attempt to provide an epidemiologic counterpart to the toxicologic observations that sulfate in combination with MVE produced effects on some endpoints, we performed an exploratory analysis that assessed whether the sulfate associations in the MESA cohort were modified by exposure to traffic emissions. Our analysis used the distance to a major roadway and predicted outdoor NO₂ concentration at a MESA participant’s home

address as indicators of exposure to traffic emissions. We assessed modifications of the sulfate associations with CIMT and CAC by including traffic–sulfate interaction terms in the health effect models. Because of the uncertainty in specifying both traffic exposure and exposure to sulfate, which is aggravated when these estimated exposures are coupled in an interaction analysis, and the limited power to assess interaction effects with this approach, we do not place great weight on these findings. At face value, however, we found little evidence that the sulfate effect was modified by our estimated traffic exposures (Appendix H, Table 8, available on the HEI Website) and thus were unable to find support in the epidemiologic study results for the effects of the sulfate–MVE mixture seen in the toxicologic study results.

NITRATE

In the epidemiologic studies, associations with nitrate were addressed using only data from the MESA cohort and only exposure predictions from the national spatial model. There was little evidence for associations of nitrate with CIMT or CAC, with the exception of a marginal association with CIMT progression (Appendix H, Figure 10, available on the HEI Web site). As discussed in Section 1 (“Discussion and Conclusions/Interpretation and Limitations of the Findings”), because of the short follow-up period we did not place much interpretive weight on our findings on CIMT progression. Because nitrate was not measured at residential locations for the MESA cohort, our source apportionment did not include nitrate. In the toxicologic study, nitrate alone had an effect on plaque area, and there were suggestions of an effect on plaque inflammation. Nitrate did not increase aortic vasoreactivity. As with sulfate, nitrate in combination with MVEG had effects as well. In the MART analysis, nitrate ranked consistently lower than sulfate for all endpoints.

The toxicologic study provided more support for nitrate effects than did the epidemiologic cohort studies. However, the epidemiologic cohort studies’ assessment of nitrate effects was relatively limited, because, again, we used data only from the MESA cohort and used only national spatial model exposure predictions. In the California Teachers Study (Ostro et al. 2010) nitrate was associated with cardiopulmonary and ischemic heart disease mortality. Previous assessments of the evidence on nitrate concluded that there were very few epidemiologic data on nitrate effects, and toxicologic data did not support much of a role for nitrate in causing health effects (Reiss et al. 2007). Therefore, although there were indications that nitrate itself might have adverse cardiovascular effects, the data in support of this association remain limited.

MIXED VEHICULAR ENGINE EMISSIONS

The toxicologic study found that the MVE exposure atmosphere caused the most consistent effects across all endpoints. The epidemiologic studies had no direct correlate of MVE. Based on the source apportionment, none of the four PM_{2.5} components of primary interest in the epidemiologic analyses seemed to be influenced largely by MVE. Of these components, EC has traditionally been used as a marker of exposure to MVE (specifically diesel exhaust). The source apportionment indicated that our EC measure reflected a complex mix of sources, although the diesel exhaust/brake wear–like feature contributed to EC to some degree in every MESA city, with contributions ranging from 6% to 36%, depending on the city. To the extent that EC was an indicator of MVE exposure, the epidemiologic studies did not find much support for a role for MVE in atherosclerosis or in cardiovascular events. In contrast, in both the California Teachers Study (Ostro et al. 2010) and the Netherlands Cohort Study on Diet and Cancer (NLCS) (Brunekreef et al. 2009), EC and black carbon, respectively, were associated with cardiovascular mortality. In neither study was information provided on the extent to which NO₂ or black carbon were markers of exposure to MVE.

Other potential markers of exposure to MVE in the epidemiologic studies were NO₂ and copper. The source apportionment indicated that the diesel exhaust/brake wear–like feature also contributed to NO₂, arguably to a greater extent than to EC, with contributions ranging from 1% to 46% across the MESA cities. Because NO₂ (along with nitrate) was of secondary interest, our health analyses of NO₂ were completed only in the MESA cohort and then only using the spatiotemporal model exposure predictions. In those analyses, we found little evidence that NO₂ was associated with our endpoints. Again, in contrast, NO₂ was associated with cardiovascular mortality in the NLCS (Brunekreef et al. 2009).

The diesel exhaust/brake wear–like feature from the source apportionment was a larger contributor to copper than to the other components we studied. For copper, the contributions of the diesel exhaust/brake wear–like feature ranged from 32% to 57% across the MESA cities. Because copper was a pollutant of secondary interest, our health analyses of copper were completed only in the MESA cohort and used only the national spatial model exposure predictions. We did not know whether the sources that contributed to the spatial distribution of copper based on the national monitoring network were qualitatively or quantitatively similar to those that contributed to the spatial distribution based on MESA monitors. Therefore, whether a diesel exhaust/brake wear–like feature contributed as strongly to the spatial distribution of copper

nationally was not known. In these relatively limited exposure and health analyses, copper was associated with both CIMT and the presence of CAC.

The epidemiologic studies, then, at best provided mixed support for the primary finding from the toxicologic study about MVE. To the extent that exposure to MVE was reflected by either EC or NO₂—and we suggest that in this context these are not particularly good markers of MVE exposure—the epidemiologic studies found little evidence to support a role for MVE. Copper, however, might be a better marker of exposure to MVE than either EC or NO₂. Our epidemiologic findings for copper, although limited in scope, suggest that exposure to MVE could be important in the development of atherosclerosis.

ROAD DUST AND CRUSTAL SOURCES

The toxicologic study found little evidence that the fine fraction of road dust itself had an effect on any of the toxicologic endpoints. Road dust mixed with MVE gases showed an effect on TBARS but not on other endpoints. As with MVE, no measure of road dust exposure was used in the epidemiologic studies, although arguably copper (with contributions from a brake wear–like feature) could have served in this capacity. As expected, silicon did not have substantial contributions from a road dust–like feature (which had been identified by the source apportionment as contributing to silicon in only two of the six MESA cities). The crustal-like feature, however, contributed to silicon in all of the MESA cities, with contributions ranging from 12% to 54%. Silicon was associated with CIMT in the MESA data, but there was little evidence that it was associated with any of the cardiovascular events in the WHI-OS data. A pure crustal-source atmosphere was not included in the toxicologic study. Because the direct effects of road dust could only be assessed in the toxicologic study and the associations with crustal sources could only be assessed in the epidemiologic study, the evidence for cardiovascular effects of road dust and crustal sources from these studies was limited.

ORGANIC CARBON

In the epidemiologic study, predicted exposure to OC was associated with CIMT and cardiovascular events, especially cardiovascular deaths. The source apportionment indicated that, although there were contributions to OC from multiple sources, a secondary aerosol–like contribution was prominent in every MESA city (with contributions ranging from 26% to 48%), a prominent biomass–like contribution was identified in four of the six cities (with contributions ranging from 15% to 45%; see Section 1, Figures 5, 6, 9, and 10), and a diesel exhaust/brake

wear–like contribution was identified in five of the six cities (with contributions ranging only from 3% to 23%; see Figures 5–10). The toxicologic study did not include atmospheres of secondary organic aerosols or biomass emissions, so these effects could not be assessed experimentally. Although the separate effects of OC could not be addressed directly by the toxicologic study, OC concentrations were measured in all of the experimental exposure atmospheres and thus could be included in the MART analysis. Although OC consistently ranked in the top half of all components for all of the four endpoints in the MART analysis, it was not one of the highest-ranking components. Some specific classes of organic compounds were ranked among the very top components in the MART analysis, but these were more likely to be volatile or semivolatile organic compounds rather than particle-phase organic compounds. For plaque area, however, particle-phase and semivolatile organic acids ranked high.

SULFUR DIOXIDE

SO₂ was not of primary interest in the epidemiologic studies. We did, however, include it in the sensitivity analyses to assess possible confounding of the PM component effects. Our health analyses of SO₂ were completed only for the MESA cohort and used only the exposure predictions from the national spatial model. There was little evidence of associations of SO₂ with CIMT or CAC. Although SO₂ was not included in the toxicologic study as an exposure atmosphere, SO₂ concentrations were measured in all of the experimental exposure atmospheres and thus could be included in the MART analysis. SO₂ ranked among the lowest of the 36 components in the MART relative-importance analysis for all of the four endpoints. Although we are mindful of the limitations of the MART analysis, the findings of the epidemiologic and toxicologic studies were consistent in providing little evidence to support cardiovascular effects of exposure to SO₂.

SUMMARY AND SUGGESTIONS FOR IMPROVING INTEGRATION

From these parallel epidemiologic and toxicologic studies, we assessed evidence and attempted to draw conclusions. These assessments were sharpened, strengthened, weakened, or made more complicated by considering the evidence from all three studies as a whole. Our conclusions can be summarized as follows:

- Results from all three studies refocus attention on acidic secondary inorganic aerosols, and on sulfate in particular.

- Assessing the role of MVE was more complicated. The toxicologic effects of MVE atmospheres were among the most clear, whereas the epidemiologic evidence was mixed because the markers of traffic emissions considered in the studies (primarily EC and secondarily copper and NO₂) represented MVE to different degrees, and their associations with the health endpoints appeared to differ.
- The epidemiologic findings encourage additional focus on the OC fraction of fine PM and possibly secondary organic aerosols in future studies; the toxicologic study did not directly assess the effects of OC. In secondary analyses, the toxicologic study did provide stronger evidence associated with effects associated with some semivolatile and volatile organic compounds than effects associated with particle-phase organic compounds.
- The evidence for cardiovascular effects of road dust and crustal dust was limited in the epidemiologic studies; we were unable to incorporate combined evidence from all three studies because the study designs were different.
- Although assessment of the effects of gaseous pollutants was not the focus of this work, our limited findings provided little evidence for cardiovascular effects for either NO₂ or SO₂ (although the evidence was marginally stronger for SO₂).

The source apportionment in the MESA study allowed us to better link the PM_{2.5}-component associations in this epidemiologic study to the source exposures used in the toxicologic study. The source apportionment also provided insight into the use of PM_{2.5} components as tracers of pollution sources in cohort studies, in which the exposure contrasts are spatial. The spatial distribution of EC, for example, was such that we could not assume that the weak epidemiologic evidence on EC pertained largely to vehicular emissions, as is commonly assumed. In contrast, we had more confidence that the evidence on other components, such as sulfate, silicon, and even copper, was more indicative of sources such as secondary inorganic aerosols, crustal sources, and roadway emissions, respectively.

How could our linked epidemiologic and toxicologic studies have been designed to allow better integration than was possible here? We offer the following suggestions:

- First, more attention to the selection of exposure atmospheres and ambient PM_{2.5}-component measurements would allow for more direct comparison and integration. For example, the addition of specific biomass combustion or secondary organic aerosol exposure atmospheres or data on ambient concentrations of high-molecular-weight organic acids might have allowed us to refine our conclusions relating to OC. Future analyses estimating exposure to and effects of other PM_{2.5}-component tracers (e.g., potassium) might also be helpful.
- Second, better integration of the cardiovascular endpoints might be useful. For example, aortic vascular reactivity, measured in the toxicology study, had no direct counterpart in the epidemiologic studies. Future analyses of data on additional endpoints for which data are available in the MESA cohort, such as flow-mediated dilation, might improve integration with toxicologic studies.
- Third, the toxicologic exposures were characterized as subchronic and were intended to provide insight into effects of exposures and mechanisms operating at medium time scales (i.e., months). Although the extent to which longer exposures to laboratory atmospheres would have better mimicked human chronic exposures is not known, it is possible that longer exposures would allow for more meaningful comparisons.

The toxicologic and epidemiologic evidence generated in concert proved to be useful in gaining a more complete understanding of PM_{2.5} component and source effects and in pointing to future research directions. Even greater attention to integrating laboratory and estimated population exposures, as well as experimental and observational endpoints, should further enhance the utility of combined toxicologic and epidemiologic studies.

REFERENCES

- Brunekreef B, Beelen R, Hoek G, Schouten L, Bausch-Goldbohm S, Fischer P, Armstrong B, Hughes E, Jerrett M, van den Brandt P. 2009. Effects of Long-Term Exposure to Traffic-Related Air Pollution on Respiratory and Cardiovascular Mortality in the Netherlands: The NLCS-AIR Study. Research Report 139. Health Effects Institute, Boston, MA.
- Grahame TJ, Schlessinger RB. 2005. Evaluating the health risk from secondary sulfates in eastern North American regional ambient air particulate matter. *Inhal Toxicol* 17: 15–27.
- Karim R, Hodis HN, Detrano R, Liu CR, Liu CH, Mack WJ. 2008. Relation of Framingham risk score to subclinical atherosclerosis evaluated across three arterial sites. *Am J Cardiol* 102:825–830.

Lippmann M, Chen L-C, Gordon T, Ito K, Thurston GD. 2013. National Particle Component Toxicity (NPACT) Initiative: Integrated Epidemiologic and Toxicologic Studies of the Health Effects of Particulate Matter Components. Research Report 177. Health Effects Institute, Boston, MA.

Nair SB, Malik R, Khattar RS. 2012. Carotid intima-media thickness: Ultrasound measurement, prognostic value and role in clinical practice. *Postgrad Med J* 88:694–699.

Ostro B, Lipsett M, Reynolds P, Goldberg D, Hertz A, Garcia C, Henderson KD, Bernstein L. 2010. Long-term exposure to constituents of fine particulate air pollution and mortality: Results from the California Teachers Study. *Environ Health Perspect* 118:363369. [Erratum: Ostro B et al. 2011. Assessing long-term exposure in the California Teachers Study. *Environ Health Perspect* 119:A242–243.]

Reiss R, Anderson EL, Cross CE, Hidy G, Hoel D, McLellan R, Moolgavkar S. 2007. Evidence of health impacts of sulfate- and nitrate-containing particles in ambient air. *Inhal Toxicol* 19:419–449.

ABBREVIATIONS AND OTHER TERMS

CAC coronary artery calcium
CIMT carotid intima-media thickness
CSN Chemical Speciation Network
EC elemental carbon

IMPROVE Interagency Monitoring of Protected Visual Environments
LDL low-density lipoprotein
MART multiple additive regression tree
MESA Multi-Ethnic Study of Atherosclerosis
MMP matrix metalloproteinase
MVE mixed vehicular engine emissions
MVEG mixed vehicular engine emissions with particulate matter filtered out, gases only
NLCS Netherlands Cohort Study on Diet and Cancer
NO₂ nitrogen dioxide
NO_x oxides of nitrogen
NPACT National Particle Component Toxicity
OC organic carbon
PM particulate matter
PM_{2.5} particulate matter ≤ 2.5 μm in aerodynamic diameter
PMF positive matrix factorization
SO₂ sulfur dioxide
TBARS thiobarbituric acid reactive substances
WHI-OS Women's Health Initiative–Observational Study

Research Report 178, *National Particle Component Toxicity (NPACT) Initiative Report on Cardiovascular Effects*, S. Vedal et al.

INTRODUCTION

Extensive epidemiologic evidence supports the association between air pollution and adverse health effects worldwide (Dockery et al. 1993; Samet et al. 2000; Aga et al. 2003; HEI 2003; Pope and Dockery 2006; Krewski et al. 2009; Brook et al. 2010). Exposure to particulate air pollution has been reported to increase the risk for a number of health outcomes, in particular cardiovascular disease (CVD*) (Pope et al. 2004; Miller et al. 2007). Hence, exposure to air pollution is currently regarded as an important but modifiable risk factor that has the potential to affect large numbers of people around the globe (Lim et al. 2012). However, there are few data on the health effects of the chemical components of particulate matter (PM), and it is unclear whether exposure to PM with different chemical compositions is associated with different levels of risk, in particular cardiovascular risk. Additionally, the biologic mechanisms underlying these associations are not well understood. Although regulations to address air quality over the past decades have focused on PM mass concentrations, scientists have hypothesized that the composition and other characteristics of PM, such as its size or surface properties, are potentially important as they might act through different biologic pathways to induce pathophysiologic effects. With a better understanding of the components of PM and their varying health impacts, it might be possible to focus regulatory efforts on those PM sources that contribute the most toxic components.

As outlined in the Preface, HEI funded the National Particle Components Toxicity (NPACT) initiative to develop a better understanding of which toxic components of the

PM mixture might be responsible for toxicity that contributes to human health effects. The NPACT initiative consisted of coordinated epidemiologic and toxicologic studies conducted in multiple cities to evaluate the toxicity and health effects related to different chemical and physical properties of PM, while taking into account the contribution of gaseous copollutants. Given the strong associations between ambient PM concentrations and cardiovascular mortality and morbidity, and because of a need to better understand the mechanisms underlying these associations, the NPACT studies focused on CVD outcomes. The two studies were spearheaded by Morton Lippmann (New York University) and Sverre Vedal (University of Washington). For the current report, the epidemiology section was led by Vedal and the toxicology section by Matthew Campen (University of New Mexico) and Jacob McDonald (Lovelace Respiratory Research Institute). For the Lippmann team, individual studies were led by Lung-Chi Chen and Terry Gordon (toxicology) and Kazuhiko Ito and George Thurston (epidemiology), all of New York University. Additional information for both studies is available in the Preface to this report.

Although air pollution is a complex mixture of compounds in gaseous (e.g., ozone, carbon monoxide [CO], sulfur oxides [SO_x], and nitrogen oxides [NO_x]) and particle phases, the cardiovascular effects have mostly been ascribed to the PM components of air pollution (Bhatnagar 2006; Araujo and Nel 2009). Nevertheless, data on the cardiovascular effects of the chemical components of PM are limited, and it is unclear whether exposure to PM with different chemical composition is associated with different levels of CVD risk. Additionally, the biologic mechanisms underlying these associations are not well understood. Furthermore, epidemiologic data suggest that the gaseous components of air pollution might play a more important role than previously supposed (Mustafic et al. 2012; Shah et al 2013), and animal experimental data have suggested that the gaseous components of engine emissions might be responsible for a substantial portion of their toxicity (Lund et al. 2007, 2009, 2011; Campen et al. 2010). Several studies support the notion that components of engine exhaust might be important promoters of adverse cardiovascular effects, especially the progression of atherosclerotic disease (Peters et al. 2004; Pope et al. 2004; Hoffmann et al. 2007; Künzli et al. 2010). Thus, in the

Dr. Vedal's 4-year study, "Integrated epidemiologic and toxicologic cardiovascular studies to identify toxic components and sources of fine particulate matter," began in February 2007. Total expenditures were \$3,412,130. The draft Investigators' Report from Vedal and colleagues was received for review in November 2011. A revised report, received in March 2012, was accepted for publication in October 2012. During the review process, the NPACT Review Panel and the investigators had the opportunity to exchange comments and to clarify issues in both the Investigators' Report and the NPACT Review Panel's Commentary.

This document has not been reviewed by public or private party institutions, including those that support the Health Effects Institute; therefore, it may not reflect the views of these parties, and no endorsements by them should be inferred.

* A list of abbreviations and other terms appears at the end of this Commentary.

toxicologic component of the current study, Drs. Campen and McDonald and colleagues exposed animals to whole engine exhaust (i.e., from diesel and gasoline engines combined; known as mixed vehicular emissions [MVE]) or to exhaust from diesel and gasoline engines with the PM filtered out (known as mixed vehicular emissions, gases only [MVE gases]). The researchers also exposed animals to MVE or MVE gases mixed with non-vehicular particle pollutants to better delineate the contributions of engine exhaust and its components to the observed toxicity of ambient particle pollution. For the epidemiologic component of the study, Vedal and colleagues set out to identify which of the diverse components of $PM \leq 2.5 \mu m$ in aerodynamic diameter ($PM_{2.5}$), also known as fine PM, contributed to the adverse cardiovascular effects, particularly atherosclerosis, of ambient air pollution in two relatively large cohorts.

This Commentary is intended to aid the sponsors of HEI and the public by highlighting both the strengths and limitations of the study and by placing the Investigators' Report into scientific and regulatory perspectives.

SCIENTIFIC AND REGULATORY BACKGROUND

In 1997, the U.S. Environmental Protection Agency (EPA) issued the National Ambient Air Quality Standards (NAAQS) for $PM_{2.5}$ based on epidemiologic evidence showing that particles in this size fraction were associated with adverse human health effects. Soon afterward, the U.S. Congress directed the EPA to undertake a major research program to answer key scientific questions, relevant to regulatory decisions, about the basis for the toxicity of PM. Reviews by the Committee on Research Priorities for Airborne Particulate Matter established by the National Research Council (NRC) identified critical research needs for assessing the role of PM and its components in contributing to adverse health effects (NRC 1998). Further reviews conducted by HEI (2002) and the NRC (2001, 2004) found that, even though much progress had been made in understanding the role that PM characteristics might play in explaining the relationships between PM and health effects, these advances had been uneven among technical disciplines. Toxicologic evidence from animal and in vitro studies was predominant, with a strong focus on metals and a growing emphasis on the ultrafine fraction of PM (particulate matter $\leq 0.1 \mu m$ in aerodynamic diameter). Some components (e.g., organic compounds) had received less research attention than others (NRC 2004).

In 2000, the EPA created the Speciation Trends Network (currently known as the Chemical Speciation Network [CSN]) to monitor the chemical composition of $PM_{2.5}$ more widely. Over the next 5 years, the network was gradually

expanded to include more than 200 $PM_{2.5}$ speciation monitoring sites across the continental United States and Puerto Rico. This network made it possible to conduct larger-scale epidemiologic studies of the associations between PM composition and health effects (Franklin et al. 2009; Ostro et al. 2009, 2010; Zanobetti et al. 2009; Bell 2012).

Establishing the relative cardiovascular toxicity of various PM components could facilitate more targeted regulations through the identification of specific sources that contribute to the presence of these PM components in ambient air. However, attributing cardiovascular toxicity to individual PM components is difficult because of the complexities associated with the identification and characterization of PM components and with their unique spatiotemporal variability, as well as the attribution of their origin to specific sources. Vedal and colleagues used source tracer methods (see Source Apportionment text box) to identify likely source categories that might be contributing most to the CVD risks associated with exposure to PM. The researchers employed positive matrix factorization (PMF) to test the appropriateness of the preselected markers they used to represent sources, but source factors were not used in the epidemiologic models.

Complexities associated with source identification are compounded by the numerous cardiovascular responses elicited by PM exposure, which could plausibly be affected differentially by different types of PM and pollutant mixtures. Both epidemiologic and experimental studies have shown a range of PM-induced changes in cardiovascular function and health, including changes in heart rate variability (HRV), thrombosis, endothelial function, atherogenesis, myocardial susceptibility to ischemia, and changes in circulating levels of cardiovascular progenitor cells (U.S. EPA ISA 2009). Hence, it is difficult to evaluate the cardiovascular toxicity of a specific PM component in relation to one specific cardiovascular function or disease state alone. In addition, such evaluations are made more difficult by the incomplete understanding of the mechanisms that increase cardiovascular risk and lead to adverse cardiovascular events.

PM CHARACTERISTICS, COMPONENTS, AND SOURCES

Ambient PM is a complex mixture of solid and liquid particles suspended in air. The size, chemical composition, and other physical and biologic properties of particles vary with location and time. In addition, variability in pollutant concentrations derives from variability in pollutant sources. The sources might be natural, such as forest fires, or the result of human activities, such as driving vehicles and operating manufacturing or power-generating

Source Apportionment

As part of their research, both the Lippmann and Vedal teams used source apportionment, a method for quantifying how individual sources (or groups of sources) of pollution contribute to concentrations of air pollutants at a certain location. Typically, researchers apply source apportionment techniques to investigate how emissions from specific sources and source categories contribute to PM in the atmosphere, although such techniques have also been applied to gaseous pollutants. The techniques generally focus on pollution from combustion (from both mobile and stationary sources), other industrial activities, and dust (from natural soil or resuspension of road dust, which may include material from vehicle brakes and tires).

Most PM source apportionment techniques are “receptor-oriented” and use observed concentrations of PM components measured at a monitoring station (“the receptor”) to calculate how much of the total PM can be attributed to specific sources. Generally, the underlying assumption is that the composition of different PM emissions can be used to trace them back to their sources because the sources have unique emissions “fingerprints.” In particular, most of the methods assume a chemical mass balance (i.e., the mass of all chemical components combined is accounted for in the model) and state that the observed PM concentration at a given location represents the sum of the contributions from individual sources. Thus:

$$c_i = \sum f_{ij} S_j,$$

where c_i is the concentration of the measured component i at the receptor; f_{ij} is the fraction of total PM emissions from source j that is component i ; and S_j , the variable of interest, is the total PM concentration at the receptor coming from source j .

A second type of source apportionment technique is “source-based.” Techniques in this category mathematically track emissions from sources in an air quality model, to estimate the contribution of the sources at one or more locations (e.g., a person’s home). Such models typically do not use measured concentrations directly.

Given that it is impossible to measure all source contributions, neither approach can be directly evaluated for its accuracy, although the source-based methods can use measured concentrations to evaluate the model’s performance, and receptor models can be compared with other models and estimated emissions. Various hybrids of source- and receptor-based methods are being developed. Both the Lippmann and Vedal studies used receptor modeling approaches — in particular, factor analysis.

Solving the chemical mass balance model using measured concentrations (c_i) to find source contributions (S_j) requires either knowing the compositions of the various source emissions (f_{ij}) or being able to estimate them from the data. The latter approach typically relies on factor analysis (receptor modeling), a method that calculates the source fingerprints and source contributions together. According to

this model, the source fingerprints are called “factors,” and the source contributions are more appropriately referred to as “factor contributions” because the factors do not necessarily correspond to a specific source. Instead, the characteristics of the factors (i.e., which PM chemical components comprise a given factor) are associated with sources by comparing the composition of the factors (e.g., the dominant chemical components) with what is known about the composition of various source emissions that may be present and may affect the concentrations at the receptor site.

Factor analysis approaches are applied widely because they do not make assumptions about which actual sources contribute to a factor, and they are able to address the issue that source composition may vary spatially and often changes between the source and the receptor. On the other hand, it should be understood that factor analysis results are based on interpretations of how specific factors relate to sources (or to atmospheric formation processes, in the case of secondary PM components) and on operational judgments, such as how many factors to include in an analysis and how to treat uncertainties and detection limits. Some studies have used multiple source apportionment methods side by side and have generally found them to produce similar results (Hopke et al. 2006; Sarnat et al. 2008; Thurston et al. 2005), even when the various source apportionment outputs were used to estimate exposures for epidemiologic analyses (Thurston et al. 2005; Sarnat et al. 2008).

Three of the Lippmann studies (Study 1 by Chen and Lippmann, Study 2 by Gordon et al., and Study 3 by Ito et al.) used basic factor analysis methods to estimate source contributions from component concentration data. Study 4 by Thurston and colleagues further apportioned $PM_{2.5}$ mass using absolute principal component analysis (APCA). APCA is a factor analysis technique that assesses portions of the mass associated with the identified factors that can then be regressed on the concurrent $PM_{2.5}$ concentrations to apportion $PM_{2.5}$ mass to source categories. This makes it possible to determine the fraction of mass attributable to the individual factors and the identified source categories that they are assumed to be associated with (Thurston and Spengler 1985; Hopke et al. 2006).

Vedal and colleagues used positive matrix factorization (PMF), a method that is widely used with software available from the EPA. PMF employs regression methods to constrain all factors to be positive and takes into account uncertainty in the measurements for each chemical component in the data set, which allows for weighting measurements that may have less measurement error (Hopke et al. 2006). In contrast with the Lippmann team, Vedal and colleagues did not use the source apportionment results directly in their health analyses. Instead, they used source apportionment to support their hypothesis that their selected indicators (EC, OC, silicon, and sulfur) are associated with their assumed sources, such as EC and OC with traffic-related emissions.

facilities. Reactive chemical species in the atmosphere can also combine to generate secondary particles, such as sulfates, nitrates, and organics, that often make up a significant fraction of total PM (i.e., generally more than 50% of PM mass in most locations).

Ambient PM concentrations in any particular location are affected by local emissions, ambient mixtures of gaseous pollutants, weather, geography, and seasonal variations in sources and atmospheric processes. Many gaseous pollutants (ozone, CO, sulfur dioxide [SO₂], and NO_x in particular) derive from the same sources as PM, and they can have health effects of their own as well as in concert with PM. Any consideration of the health effects of various components and sources of PM should also take into account how the co-occurring gaseous pollutants might affect the toxicity of the PM components and the overall toxicity of the pollutant mixture to which the population is exposed.

For large studies, PM_{2.5} exposure assessment is often carried out using central monitors, and exposures are assigned according to city of residence. This approach typically results in relatively low exposure misclassification, because PM_{2.5} concentrations in many cities tend to be relatively uniform across the metropolitan area (compared with pollutants, such as nitrogen dioxide [NO₂], that exhibit high spatial variation). PM_{2.5} concentrations also commonly exhibit similar hour-to-hour and day-to-day variations across a metropolitan area. For studies of short-term effects, which compute effect estimates based on differences in exposures and outcomes on different days, PM_{2.5} concentrations measured at a central monitor are usually sufficient to represent time-based fluctuations in concentration across a metropolitan area. For studies of longer-term effects, this spatial uniformity in most cities allows researchers to estimate associations based on differences in PM_{2.5} concentrations among cities.

For PM_{2.5} components, there is some evidence that concentrations of some components are more spatially and temporally variable than others, and more variable than PM_{2.5} mass itself (Bell 2011), but this was not as well studied in 2005, when the current study commenced. More sophisticated exposure assessment methods, such as land-use regression (LUR), kriging, and inverse-distance weighting, that attempt to resolve within-city exposure contrasts were available by 2005. However, these approaches would have been very difficult to implement and validate using additional measurements for all of the components, gaseous variables, and source factors in studies of, say, 100 or 150 cities. Thus the current NPACT studies are primarily based on differences in exposures and outcomes between cities (although the MESA study attempted to capture within-city variation in pollutant concentrations).

Because PM_{2.5} components were the main focus of all of the NPACT studies — given that national speciation data were only available for the PM_{2.5} size fraction — only one of the three toxicology studies (the Gordon study found in Lippmann et al. 2013) and none of the four epidemiology studies addressed the question of the relative toxicity of PM sizes. Gordon and colleagues evaluated PM with an aerodynamic diameter ≤ 10 μm (PM₁₀) and the subset of PM with an aerodynamic diameter between 2.5 and 10 μm (PM_{10-2.5}, also known as coarse PM) in vitro; these two size classes are of interest because of the various sources and health effects associated with them. Coarse particles tend to derive from resuspension or mechanical processes; PM_{2.5} tends to be formed primarily from combustion and secondary formation while being transported over quite long distances. Some scientists have hypothesized that even smaller particles (PM with an aerodynamic diameter < 0.1 μm, also known as ultrafine PM), which dominate in terms of number of particles in ambient air, might be particularly toxic (Utell and Frampton 2000; Oberdörster 2001), but to date no definitive answers about the relative toxicity of ultrafine and fine PM have emerged (Lippmann et al. 2013).

Specific components of PM that were a focus of the NPACT studies include trace elements (including metals); organic compounds; ions, such as sulfate, nitrate, and ammonium; and organic carbon (OC) and elemental carbon (EC). In addition, an initial goal of the NPACT studies was to include gaseous copollutants, such as NO₂, ozone, and SO₂, to attempt to differentiate PM-related health effects from those related to gases. However, because of the limited number of cities where gaseous pollutant data were available and the potential for high correlations between concentrations of gases and some components and sources, this aspect of the NPACT initiative remained less developed.

EPIDEMIOLOGIC EVIDENCE

Earlier epidemiologic efforts in U.S. and European cities have contributed valuable insights to our understanding of health effects associated with PM and its components (Schwartz et al. 1996; Samet et al. 2000; Laden et al. 2000; Metzger et al. 2004; Peel et al. 2005). However, various study limitations — such as relatively short study periods, modest sized study populations, and high correlations among pollutants in any one city — have hindered the ability either to detect statistically significant pollution effects associated with specific PM components or to discriminate among the effects of different pollutants. Furthermore, major questions remained about the specificity of the markers used to define particular pollutant sources.

At the time the NPACT studies were funded in 2006, time-series studies had found associations of daily mortality and morbidity with short-term exposure to PM mass that varied seasonally and regionally (Samet et al. 2000; Peng et al. 2005). A number of studies found stronger associations for fine or ultrafine particles compared to those for coarse particles or PM₁₀ (Schwartz et al. 1996). Another time-series study published before the NPACT initiative, the Aerosol Research and Inhalation Epidemiology Study in Atlanta, Georgia, found PM_{2.5}, PM₁₀, NO₂, and CO to be associated with emergency department visits for respiratory health effects (Peel et al. 2005) and PM_{2.5}, NO₂, and CO with cardiovascular endpoints (Metzger et al. 2004). Some epidemiologic studies also found no differences in the associations of different size fractions with mortality (Wichmann et al. 2000) or with respiratory effects in children with asthma (Lippmann et al. 2000; Pekkanen et al. 1997; Peters et al. 1997).

Prior to the funding of the Vedal NPACT study, two key cohort studies found associations between cardiovascular mortality and long-term exposure to fine particulate; these associations were stronger for PM_{2.5} than for PM₁₀ or PM₁₅ (particulate matter $\leq 15 \mu\text{m}$ in aerodynamic diameter). Analyses of the American Cancer Society (ACS) Cancer Prevention Study II (CPS-II) prospective cohort data found all-cause, cardiovascular, and lung cancer mortality to be more strongly associated with long-term exposure to sulfate and PM_{2.5} than with coarse particles (HEI 2000; Pope et al. 2002). Similar associations between PM_{2.5}, sulfate particulate, and mortality were reported for a reanalysis of the Harvard Six Cities Study, a long-term exposure cohort with pollution monitoring specifically designed for health studies (HEI 2000). A sensitivity analysis of the ACS-CPS-II cohort also reported regional differences in the magnitude of risk estimates associated with a 10- $\mu\text{g}/\text{m}^3$ increase in PM_{2.5} concentrations (HEI 2000), implying that differences in the composition of PM_{2.5} might result in different PM_{2.5} toxicity.

Other studies attempted to associate health effects directly with source profiles (Clarke et al. 2000; Laden et al. 2000; Riediker et al. 2004). The statistical approaches in these studies, which included factor analysis, principal component analysis, and tracer methods (see Source Apportionment text box), were based on assumptions about the groups of elements and compounds that characterize an emission source. Laden and colleagues (2000), for example, used atmospheric markers for various sources to examine relationships between those sources and all-cause mortality. They found no evidence of associations with crustal sources and fairly robust associations with markers for coal, motor vehicles, and residual oil combustion.

Lippmann and colleagues (2006) found that excess daily mortality risk was associated with short-term changes in

nickel (Ni) and vanadium (V) concentrations measured in fine particle samples from the National Morbidity, Mortality, and Air Pollution Study. Additionally, reductions in concentrations of SO₂, Ni, and V were associated with decreased monthly mortality counts in a study conducted in Hong Kong after the introduction of low-sulfur fuel (Hedley et al. 2002). By the time NPACT was initiated, several studies attributed both acute and chronic cardiovascular and respiratory health effects to motor-vehicle-related pollution (Künzli et al. 2005; Schwartz et al. 2005). Prior epidemiologic studies have also found health effects associated with exposures to the particulate as well as the gaseous components of vehicle emissions (Peters et al. 2004; Pope et al. 2004). In addition, Hoffmann and colleagues (2007) found greater risk of coronary artery calcium (CAC) deposits associated with living near a busy road, with greater risks at closer proximities. The adverse effects associated with exposure to traffic were summarized by the World Health Organization (2005) and more recently HEI (2010).

TOXICOLOGIC EVIDENCE

At the time the current study was funded, many toxicologic studies had investigated the types of particles that might cause adverse health effects, and much of the evidence suggested that exposure to several kinds of PM triggers acute events such as oxidative stress, inflammatory events, and cell injury both *in vitro* and *in vivo* (U.S. EPA 2004).

Geographic and seasonal differences in the toxicologic effects of PM and its components had been assessed in few previous studies. Given the variation in ambient aerosols within and between locations and time periods, some researchers focused on controlled-exposure studies of animals to specific source mixtures, such as diesel exhaust, gasoline exhaust, wood combustion, and coal combustion (McDonald et al. 2004). At the time the NPACT initiative began, such studies had found that the effects on vasoconstriction and inflammation were driven by the gaseous rather than the particulate components of diesel exhaust (Campen et al. 2005). Inflammatory effects of diesel exhaust were also found in human controlled-exposure studies (Salvi et al. 1999; Holgate et al. 2003); animal studies reported similar inflammatory effects of wood smoke (Tesfaigzi et al. 2002). Earlier work by Campen and colleagues (2001) also showed some immediate and delayed cardiac effects, including arrhythmias, in mice exposed to V and Ni sulfate particles, with time course of response varying by element. Different sources of PM, such as diesel exhaust and wood smoke, might also have unique inflammatory effects in different systems (Salvi et al. 1999; Tesfaigzi et al. 2002).

In an effort to understand the potential underlying mechanisms for the adverse cardiovascular outcomes observed in epidemiologic studies, Lippmann and colleagues (2005) conducted animal studies using fine concentrated ambient particles (CAPs) and found effects on heart rate (HR) and HRV measures in normal and atherosclerotic mice based on subchronic exposures to PM_{2.5}-apportioned sources of fine CAPs, defined as secondary sulfate, resuspended soil, and residual oil combustion, measured over several months in Sterling Forest State Park in Tuxedo, New York (Lippmann et al. 2005). The Ni source factor was associated with an upwind Ni smelter using back-trajectory analysis (Lippmann et al. 2006). Additionally, other studies of these subchronically exposed mice have shown CAPs exposures to be associated with inflammation or increased atherogenesis (Maciejczyk and Chen 2005; Sun et al. 2005).

Properties other than size, such as solubility, are also likely to play an important role in particle effects (Leikauf et al. 2001). Compared on a mass basis, smaller particles have been shown to induce more inflammatory effects than did larger particles (Oberdörster et al. 2000; Li et al. 2003). These and the studies discussed above have provided important and useful information about the physicochemical characteristics of particles that might induce adverse effects (U.S. EPA 2004).

INTEGRATING EPIDEMIOLOGIC AND TOXICOLOGIC APPROACHES IN NPACT

Although there is a large body of epidemiologic and toxicologic evidence of the effects of PM on health, few studies have combined both types of evidence in a coordinated way. The NPACT initiative was designed to provide a systematic approach to the study of PM components, size fractions, and sources by using complementary epidemiologic and toxicologic approaches to evaluate related, primarily cardiovascular endpoints. The study designs (described briefly in the Preface) anticipated points of comparison both between and across the two studies from each research center (the Vedal study as described in this report and the Lippmann study as described in HEI Research Report 177 [Lippmann et al. 2013]). Vedal and colleagues assessed the effects of PM components and gases on subclinical markers of atherosclerosis and clinical cardiovascular events in two cohort studies. Similarly, in studies with atherosclerotic mice, Campen and McDonald and colleagues assessed effects of particulate and gaseous components of vehicle emissions in combination with non-vehicular PM on biomarkers of oxidative stress, vascular effects, and inflammation in an effort to understand biologic pathways from exposures.

SPECIFIC AIMS

Vedal and colleagues listed the following primary specific aim and three hypotheses:

- Specific Aim: To identify the chemical components of ambient PM that contribute to the effects of long-term PM exposure on the development and progression of atherosclerosis and the incidence of cardiovascular events.
- Hypothesis 1: PM_{2.5} chemical components in primary motor vehicle exhaust emissions have more long-term cardiovascular toxicity, as reflected in cardiovascular mortality, incident cardiovascular events, atherosclerosis, and cardiac dysfunction, than PM composed of either secondary inorganic aerosols or crustal components.
- Hypothesis 2: The cardiovascular effects of long-term exposure attributed to the toxic PM components are not caused or modified by chemical components in the gaseous or vapor phase of vehicular emissions or to other pollutant gases in the ambient pollutant mix.
- Hypothesis 3: PM oxidant potential (a) is greater in PM from motor vehicular sources than from secondary PM or crustal PM and (b) is associated with cardiovascular mortality, incident cardiovascular events, and atherosclerosis.

Vedal and colleagues explored Hypothesis 1 in Section 1 of this report by evaluating associations between estimated exposures to a selected group of PM_{2.5} components (OC, EC, silicon, and sulfate) and cardiovascular outcomes from the Multi-Ethnic Study of Atherosclerosis (MESA) and the Women's Health Initiative–Observational Study (WHI-OS) cohorts.

In Section 2 of this report, Campen and colleagues elaborated on Hypothesis 2. Their primary aim was to “provide a basis for comparing pathophysiologic and molecular endpoints in animals with results from the parallel human study.” The researchers' working hypothesis was that “important environmental effects on the cardiovascular system are driven by exposure to vehicular pollutants, including both GEE and DEE. This hypothesis considered that the public health importance of traffic exposure is linked both to the potential for enhanced exposure because of commuting or proximity to roadways and to the potency of vehicular emissions, which may be more toxic than other components of ambient air.” Their approach was to expose mice to atmospheres that contained vehicle emissions with and without PM and assess biologic effects in these mice.

Dr. Vedal's research on Hypothesis 3 included an evaluation of oxidative potential of PM collected on filters. This information is included in Appendix E (“Oxidative

Potential,” available on the HEI Web site at www.healtheffects.org at the recommendation of the Panel, because it could not be used directly for interpreting the epidemiology or toxicology studies.

In the following sections, the studies conducted by Vedal and colleagues at the University of Washington (Section 1)

and Campen and colleagues at the University of New Mexico and Lovelace Respiratory Research Institute (LRRRI) (Section 2) are described and discussed separately. An overview of these two sections is presented in Commentary Table 1. In addition, an overall evaluation of the studies is presented at the end of this Commentary.

Commentary Table 1. Overview of Studies^a

	Section 1		Section 2
	MESA Cohort	WHI-OS Cohort	LRRRI/UNM
Principal investigator	Vedal	Vedal	Campen
Study type	Epidemiology	Epidemiology	Toxicology
Study design	Cohort	Cohort	Inhalation study
Species	Human	Human	ApoE knockout mice, high-fat/high-cholesterol diet
Geographic location	Six U.S. cities	United States	n/a
Exposure duration	n/a	n/a	50 days
Exposure atmosphere	n/a	n/a	MVE or MVE gases, and combinations of MVE or MVE gases with non-vehicular PM (sulfate, nitrate, or road dusts)
PM size class	PM _{2.5}	PM _{2.5}	PM _{2.5}
Exposure characterization	Spatiotemporal: XRF for sulfur, Si, and other elements; TOR for EC and OC National spatial: CSN and IMPROVE monitoring data	CSN and IMPROVE monitoring data	Detailed analysis of gas, semivolatile, and particle phases (~500 compounds)
Exposure modeling	Land-use regression with kriging Spatiotemporal data: collected Aug. 2005–Aug. 2009 (sulfur and Si) and Mar. 2008–Aug. 2009 (EC and OC); average estimated for May 2007–Apr. 2008 National spatial data: see WHI-OS	Land-use regression with kriging National spatial data: CSN and IMPROVE average for 2009 (sulfur and Si) or May 2009–April 2010 (EC and OC)	n/a
Source apportionment	PMF	PMF	MART analysis (alternative to source apportionment)
Follow-up period	2000–2007	1998–2005	n/a
Endpoints	CIMT and CAC	Cardiovascular and cerebrovascular events and deaths	Aortic tissue: lipid peroxidation, vascular function and remodeling, plaque growth, and vascular inflammation

^a ApoE indicates apolipoprotein E; CSN, Chemical Speciation Network; IMPROVE, Interagency Monitoring of Protected Visual Environments; MART, multiple additive regression tree; MVE, mixed vehicular emissions; n/a, not applicable; TOR, thermal/optical reflectance (IMPROVE method); XRF, X-ray fluorescence.

SECTION 1: EPIDEMIOLOGY STUDY

INTRODUCTION

Because of associations found between long-term exposure to PM_{2.5} concentrations and CVD in reports from large cohort studies noted in the previous section, the epidemiologic component of the NPACT initiative focused on associations between concentrations of selected PM_{2.5} components and cardiovascular outcomes. The outcomes included clinical as well as subclinical measures of cardiovascular atherosclerosis, which are considered to be linked to the underlying pathology for most cardiovascular events, and cardiovascular and cerebrovascular disease events and deaths. Vedal and colleagues used data from MESA and WHI-OS, two cohorts established by the National Heart, Lung, and Blood Institute. The MESA cohort comprised approximately 6800 participants (initial ages 45 to 84 years) selected from four ethnic groups living in six U.S. cities. The WHI-OS cohort comprised approximately 90,000 postmenopausal women (initial ages 50 to 79 years) living in 45 U.S. cities. The investigators used pollutant concentration data for sulfur, OC, EC, and silicon obtained from CSN monitors in participant cities to model long-term concentrations for participants in both studies. These four components were selected for exposure assignment because they were hypothesized to be indicators of different types of PM_{2.5} or different sources of PM_{2.5}. The investigators also used data from dedicated measuring campaigns in the MESA cities instead of the CSN monitoring data in order to model spatially and temporally resolved concentrations at the participants' residences in the MESA cities.

The following section of the Commentary focuses on the epidemiologic study by Vedal and colleagues. Because the elements of the exposure assessments were common to both cohort studies, it begins with a description of the methods used to assign concentrations to cohort participants, followed by a description of the source apportionment methods used to understand the relationships between sources and the PM_{2.5} component concentrations. It next provides separate descriptions and evaluations of the WHI-OS and MESA cohort studies.

EXPOSURE MODELING FOR THE MESA AND WHI-OS STUDIES

Two separate models were developed to characterize spatial contrasts in exposure. For the MESA study, a detailed spatiotemporal model was developed based on measurement campaigns conducted specifically for this purpose as part of NPACT in the MESA cities. For the

WHI-OS study it was necessary to use the existing CSN and Interagency Monitoring of Protected Visual Environments (IMPROVE) monitoring data of PM_{2.5} component concentrations to construct the national spatial model, because the WHI-OS cohort was distributed across multiple cities across the United States. The national spatial model was also used for the MESA cities.

MESA Spatiotemporal Model

To assess the effects of PM_{2.5} components on subclinical atherosclerosis in the MESA participants, the investigators used data from multiple ambient and home-outdoor monitoring sites in the six cities studied in MESA. These concentrations were then used as inputs into a spatiotemporal model to estimate concentrations of the components outside each individual's home. The investigators' goal was to reduce the measurement error that is typical in large-scale epidemiologic studies, which have generally been unable to account for significant spatial variability in PM_{2.5} and its components.

Data used for the MESA epidemiologic spatiotemporal study included only the air quality data collected as part of the Multi-Ethnic Study of Atherosclerosis and Air Pollution (MESA Air) study, an ancillary study funded in 2004 by the EPA that included monitoring at three additional locations: along the coast in Los Angeles, California; inland in Riverside, California; and in Rockland County, New York, a suburban area outside New York City. MESA Air monitoring data consisted of 2-week monitoring at three to seven sites in each city. PM_{2.5} and its elemental components, including light-absorbing carbon, were measured at each site in addition to passive sampling of NO_x and NO₂. Two-week integrated samples were also collected in each city at the home locations of approximately 50 participants from the original MESA cohort. This sampling was repeated in two seasons. At home locations without outdoor measurements, concentrations were modeled using home-address data, land-use information, and data from the monitors in the city. Additional funding provided under the NPACT initiative allowed comparison of results from collocated MESA and CSN monitors. The number of samples collected for the elemental analyses at these supplemental monitors ranged from more than 70 at each of seven sites in Los Angeles to approximately 50 at the site in Rockland County.

The full MESA-Air and supplemental NPACT monitoring data sets that the investigator constructed for the spatiotemporal model consisted of data from 5493 participants (Section 1, Table 36). Samples were collected at various cities, locations, and time periods between August 2005 and July 2009. Figures 3 and 4 of Section 1 list

the sample sizes and dates of collection for the monitoring efforts.

Additional monitoring was conducted as part of the NPACT initiative to determine the quality and comparability of the MESA Air data with those collected by state and federal agencies. This entailed collection of PM_{2.5}, EC, and OC samples using the MESA monitoring system collocated at the CSN monitoring sites. The results of this quality assurance study based on these additional sampling data showed that the MESA Air and NPACT data could not be combined with the CSN and IMPROVE data for further statistical analysis; thus, the spatio-temporal models used to assign exposure for the MESA cohort analyses were based on the supplemental monitoring data alone.

National Spatial Model

The investigators constructed a national spatial model capable of predicting exposures outside each individual's home using CSN and IMPROVE data from more than 250 monitoring sites around the country. This model was used to estimate exposure in both the MESA and WHI-OS cohort analyses. At CSN sites, 24-hour samples are generally collected by state agencies on a schedule of 1 in 3 or 1 in 6 days. The IMPROVE monitoring network, which is overseen by a consortium of federal agencies, measures PM_{2.5} and components as well as gaseous copollutants at national parks and wilderness areas within the United States on a schedule of 1 in 3 days. The full national spatial models were cross-validated with data from CSN or IMPROVE sites located within 200 km of a MESA city. For this analysis, CSN data were used from approximately 70 sites nationally. Most IMPROVE sites are located far from MESA cities, but data from 17 IMPROVE sites were included in the investigators' cross-validation because of their proximity to a MESA city.

Source Apportionment

A full source apportionment analysis using PMF was conducted to evaluate factors potentially contributing to concentrations of PM_{2.5} components in the cities; however, indicator components, not factors (e.g., EC, but not "traffic factor"), were used in the epidemiologic analyses. The PMF results were used primarily to determine how well the indicator components coincided with the factors determined from the PMF analysis, thereby demonstrating that these indicator components were appropriate. Elements included in the source-apportionment analysis were those that were measured above the detection limit in approximately 50% of samples. The final list of pollutants that met the full inclusion criteria varied somewhat

by city, but the following were included in the factor analysis: PM_{2.5}, Al, As, Ba, Br, Ca, Cr, Cu, Fe, K, Mg, Mn, Mo, Na, Ni, Pb, sulfur, Se, silicon, Sr, Ti, V, Zn, and Zr as well as EC, OC, NO₂, NO_x, and SO₂ (Section 1, Table 7). The factors identified were also correlated to individual elements, and their source contributions in terms of mass were assessed as well.

As a result of their PMF source apportionment analysis, the investigators concluded that the four indicator components assessed in this study (EC, OC, silicon, and sulfur) broadly represented four source categories: local combustion sources including traffic; primary gasoline/biomass combustion and secondary OC formation; crustal/soil; and secondary sulfate formation, respectively.

Quality Assurance

The investigators conducted detailed quality assurance evaluations. These included collecting more than 100 simultaneous 2-week samples of NO₂, NO_x, and SO₂ in each city. These "snapshot" samples were repeated over three seasons that are generally marked by low, medium, or high ozone concentrations, with the intention of measuring the spatial variability of these pollutants, particularly around roadways, while controlling for temporal trends in the pollutants. A second snapshot quality assurance comparison was conducted in 2009 in three cities — Chicago, Illinois, St. Paul, Minnesota, and Winston-Salem, North Carolina. This monitoring campaign included simultaneous home-outdoor measurements of silicon and sulfur (as well as all other elements) at approximately 30 homes in each city over two seasons. The results from this study were then used to validate silicon and sulfur spatiotemporal models.

The MESA Air samplers were also collocated with monitors at seven CSN sites for side-by-side comparisons across methods between January and August 2009 (see Appendix F, "Supplemental Monitoring Campaign," available on the Web at www.healtheffects.org). For OC and EC samples, the comparison with CSN data indicated that OC concentrations reported for the MESA Air and NPACT sampling campaigns, were lower, potentially caused by volatilization of organics over the 2-week monitoring period.

Exposure Assignment Methods

Home-outdoor concentrations for each participant in the MESA study were estimated using a spatiotemporal model based on data from the field monitoring program as well as geographic factors. For the four indicator components (EC, OC, silicon, and sulfur), the log of the 2-week average component concentration was estimated from a model that included the long-term mean of the component, a single temporal trend in each city, and a spatiotemporal error

term. Because of limited PM_{2.5} component data, the final spatiotemporal models estimated for EC, OC, sulfur, and silicon were more limited than those for NO₂, which was based on a much larger sample size.

Geographic variables in the spatiotemporal models included distance to a busy road, land-use type, longitude and latitude, distance to a major source, emission of criteria pollutants, vegetation cover, percent impervious surface, elevation, and distance to nearest residual-oil-burning boiler (grade 4 or 6 oil). The exact geographic indicators included in the spatiotemporal models varied by pollutant and city, but all models included geographic variables from two to five categories. Separate spatiotemporal models were run for each indicator component — EC, OC, sulfur, and silicon. Both mean and variance models were estimated for each pollutant and city, taking into account season, number of monitoring sites, and number of observations. Variable selection included selection of site-specific temporal trends. Spatiotemporal modeling was conducted using the SpatioTemporal procedure from the R statistical program developed by the investigators (Lindstrom 2011).

Cross-validation was conducted for final model selection by dividing the home-outdoor data into ten subsets, then fitting ten models to those while leaving out one subset at a time. Temporally adjusted R^2 and values for mean squared error were calculated, and those models with the highest temporally adjusted R^2 values were selected. As a result, the final spatiotemporal models varied somewhat by city and PM_{2.5} component (Section 1, Table 28). As mentioned above, sulfur and silicon snapshot campaign samples were used to validate the spatiotemporal model, but the model was found to be limited in terms of predicting spatial variability of these components in Chicago, St. Paul, and Winston-Salem, where this snapshot campaign was carried out.

For the national spatial exposure model, the analysis focused on the same indicator component as for the spatiotemporal exposure model — EC, OC, sulfur, and silicon — in addition to SO₂, Ni, V, Cu, nitrate, and sulfate. Annual averages from all of 2009 or from May 2009 to April 2010 were included in the models for EC and OC, which were measured at 157 IMPROVE and 98 CSN sites. For sulfur and silicon, monitoring was conducted from January through December 2009 at 155 IMPROVE and 89 CSN sites. The results from the national spatial model were used in the health effects models and were compared with the exposure estimates from the spatiotemporal model.

The national spatial model used partial least squares regression (PLS) to group collinear geographic variables into scores that could then be used as inputs to a universal

kriging model to spatially smooth the data. The investigators transformed the long-term average component concentrations by taking the square root in order to reduce the skewness of the distributions. In an approach similar to that used in the spatiotemporal model, they performed a cross-validation by removing one of ten data sets at a time to compare results for PLS alone and PLS with universal kriging. The model-fitting process above was also used for sulfate, SO₂, nitrate, Ni, V, and Cu, except that Ni and Cu concentrations were log transformed instead of square-root transformed. Finally, a similar modeling method was also used to develop a national spatial model for PM_{2.5}, explained in detail in the WHI-OS Cohort Overview below.

To determine the ability of the national spatial model to predict exposures sufficiently for health effects studies of MESA participants, the investigators compared the result from the spatiotemporal exposure model with results from the national spatial model when modeling data for the national model were restricted to monitoring sites within 200 km of a MESA city. Similar R^2 values were found for both groups of models for all pollutants except silicon and Cu, implying that the overall performance summary for the national spatial model applies to the MESA cohort. Additional tests of the models were conducted by comparing exposure model predictions using the spatiotemporal model and the national spatial model with estimates obtained from models using citywide averages, nearest monitoring site, and inverse-distance weighting.

EVALUATION OF THE MESA AND WHI-OS EXPOSURE ASSESSMENT

In its independent assessment of Section 1, the NPACT Review Panel thought that the investigators had conducted thorough and extensive exposure assessments. They not only used the CSN and IMPROVE data to construct a nationwide spatial model of exposure for both the MESA and WHI-OS health effects analyses, but also conducted extensive additional sampling and built a sophisticated model intended to account for local variations in the spatial and temporal distribution of key indicator components (EC, OC, sulfur, and silicon). They attempted to characterize exposures in a systematic fashion and conducted the analyses in the two cohorts in a manner which, to the extent feasible, facilitated comparison between the two sets of results.

PMF was applied to the ambient pollutant data to understand potential sources of the PM_{2.5} in the MESA cities. However, the primary way that potential sources were linked to the analysis of epidemiologic associations in MESA and WHI-OS was through focusing on single

indicator components known to be indicative of certain sources or atmospheric formation processes. For this purpose sulfur, silicon, EC, and OC were selected. The Panel thought that these components were logical choices and that the strategy of using indicator components brought simplicity and elegance to the study. The primary role of PMF was to explore the validity of this initial strategy and to help verify the connection between these components and their assumed primary source(s). One major difficulty, however, is the complexity of PM_{2.5} — from its formation processes to its spatial and temporal variability. Not surprisingly, PMF provided reassurance that the selected indicator components did have a tendency to co-vary with the expected factors (e.g., silicon with crustal PM and sulfur with secondary formation products in regional air masses), but the selected components also linked to more than one factor, and this varied by city and season. Thus, it must be recognized that considerable ambiguity remains and that more detailed analyses will be required. Furthermore, none of the components were unequivocally linked to vehicle emissions, and thus relying on them significantly limited the ability to explicitly test the study's overarching hypothesis regarding the relative importance of traffic-related pollutants in causing health effects in the two cohorts. Fortunately, the data assembled for MESA and WHI-OS cohorts are extensive, and thus there is considerable promise that more analysis will yield further understanding.

The ability to accurately determine individual exposures to several different pollutants was essential to the study. A key part of the study therefore was to develop long-term exposure models that could predict the spatial variability in outdoor sulfur, silicon, EC, and OC (as well as Cu, Ni, V, nitrate, sulfate, and SO₂) in multiple cities across the country and at the resolution of home addresses. This involved a multiyear, multisite monitoring effort and the development of new methods. Primarily, the investigators developed two different models referred to as spatiotemporal and national spatial, which used different data sets and methods and emphasized different spatial and temporal scales. In particular, work with the MESA cohort had the advantage of considering two different exposure model estimates as well as direct use of measurements through nearest-monitor, citywide average, and inverse-distance weighting approaches (see below). In contrast, the WHI-OS analysis considered just the national spatial model for exposure. Because the nearest monitor approach was the method used in earlier studies of this cohort (Miller et al. 2007), the national spatial model used here was expected to be an improvement. Of importance to note is that the national spatial model was developed using only one year of data collected around 2009, whereas health data collection during the WHI-OS follow-up took

place considerably earlier. Historical trends in spatial patterns, which are likely to have occurred given the known trends in PM_{2.5} and its components from 1990 to 2010, add uncertainty to the accuracy of the national spatial model exposure “surface” (the modeled concentrations across the geographic area) compared with the population and disease being studied. For the MESA cohort, the 2009 pollution data collection period is a closer match to the period during which measurements of baseline carotid intima media thickness (CIMT) and CAC were made, although the relevant exposure window for plaque development or altered CIMT could have happened many years before these preclinical outcomes were evaluated.

Nonetheless, the multiple exposure estimates used in MESA Air have provided a good opportunity to gain new insight into how the choice of exposure model affects the results. As the investigators recognized, assessing which exposure model provides more or stronger associations with the selected health endpoints is not a good way to evaluate an exposure model and determine which model performs better. Ideally, this determination needs to be made independent of the health data. The Panel identified several important issues about the development and evaluation of the MESA Air exposure model. First, there were considerable differences in the ability to develop reliable models for each of the selected indicator components given the available data and methods. Second, some approaches to evaluating model fit can be misleading, particularly given the combination of multiple within-city measurements and multiple contrasting cities present in this study. The ability of the models to predict national-scale patterns in concentrations when cities are in distinctly different regions with distinctly different exposure sources does not necessarily translate into an ability of the models to predict patterns within a city. These two different demands on the model were decoupled in the study; this decoupling revealed that — depending on which pollutant was modeled — either the national or the within-city variation would dominate and that developing a reliable model was generally more difficult and hence less successful for pollutants with high within-city variation. Furthermore, although bringing in results generated from more than one exposure model can help add to the weight of evidence, it can also complicate interpretation, especially when the models have different strengths and/or emphasize a different aspect of the air pollution exposure signal.

OVERVIEW OF THE MESA COHORT STUDY

The primary hypothesis tested in the MESA study was that chemical components of PM_{2.5} associated with primary motor vehicle exhaust have greater effects on subclinical

markers of atherosclerosis than do other $PM_{2.5}$ components, particularly secondary inorganic or crustal species. The National Heart, Lung, and Blood Institute's MESA health-monitoring cohort study was initiated in 2000 and enrolled 6814 participants without known heart disease during the recruitment period between 2000 and 2002. Study participants were primarily from four major ethnic or racial categories — white non-Hispanic, African American, Chinese American, and Hispanic. Participants lived in and around six major cities: New York City, New York, Los Angeles, California, Chicago, Illinois, Winston-Salem, North Carolina, St. Paul, Minnesota, and Baltimore, Maryland.

MESA study participants ranged from 45 to 84 years of age at the start of the study. The cohort included in the NPACT analysis consisted of 6266 individuals from the original cohort who agreed to the geocoding of their home address for use in further statistical analysis or home-outdoor air quality monitoring. To augment the original MESA study, the EPA established the MESA Air study in 2004 to allow assessment of the long-term effects of air pollutants on the cardiovascular endpoints measured in the larger MESA study. MESA Air included monitoring at three additional sites: one along the coast in Los Angeles, one inland in Riverside, California, and a third in Rockland County, a suburban area outside New York City. Although additional participants were recruited by the MESA study when these sites were added, the lack of the required baseline health measures for these more recently recruited participants led Vedal and colleagues to exclude them from the analyses in the current study.

Outcomes

Because the participants had no clinically observable heart disease at the time of recruitment, subclinical measures of atherosclerosis were the focus of the MESA analysis. Two measures of atherosclerosis were used as the primary endpoints of interest: CIMT, which was measured using ultrasound imaging of the carotid artery, and CAC, which was measured using computed tomography (CT) scans of the chest. CIMT is a measure (in mm) of the thickness of the carotid artery wall, a measure of generalized atherosclerosis, and CAC is a measure of calcium in the coronary arteries, a measure of coronary atherosclerosis and predictive of clinically evident cardiovascular events. The MESA participants filled out lifestyle questionnaires and underwent detailed health examinations, including tests for blood and urine biomarkers, blood pressure in arms and legs, electrocardiograms, magnetic resonance imaging, and endothelial function tests, as well as artery imaging.

CIMT was measured using a two-dimensional ultrasound scanner (GE Logiq model) at all of the participating MESA study centers; the protocol was to measure the common carotid artery at the same location on the neck for all participants. CAC was measured using one of two methods: a cardiac-gated electron beam CT or a multi-detector CT scanner. The mean Agatston score of two scans was used as the endpoint for CAC. An Agatston score is a measure of coronary artery calcification; a score greater than 0 indicates the presence of calcification (van der Bijl et al. 2010). Because the distribution of the Agatston scores was skewed, values greater than 0 were log-transformed for linear regression analysis. Because more than half of participants had Agatston scores of 0, scores were converted to binary outcomes of 0 or 1, indicating presence or absence of CAC for relative risk regression.

Exposure Assignment

Outdoor air pollution concentrations for each participant's geocoded home address in the MESA Air study were estimated using the spatiotemporal model described above. Geocoded home addresses at the time of the baseline assessments were also used for assigning exposures for each participant based on the national spatial model, also described above.

Statistical Analysis

The health outcome variables used in the models were presence of CAC, the natural log of the CAC score (log-CAC), and CIMT. CAC was modeled both as a binary outcome and as the log of the scores. For $PM_{2.5}$ and the four indicator components (EC, OC, sulfur, and silicon), long-term averages were computed from the MESA spatiotemporal model estimates (built for the NPACT study) and were estimated from the national spatial model and applied to the address obtained at the baseline exam for each participant.

CAC was modeled using relative risk regression (Lumley et al. 2006); log-CAC and CIMT were modeled using linear regression. Both cross-sectional and longitudinal analyses were conducted. The cross-sectional analyses were conducted on binary CAC, log-CAC, and CIMT from the baseline assessment. The baseline and follow-up assessments were included in longitudinal mixed models that predicted the effect on CIMT of an interquartile range increase in $PM_{2.5}$, sulfur, silicon, EC, or OC. The cross-sectional and longitudinal analyses were conducted using random slopes and intercepts mixed models, using the lme4 package in R statistical software (version 2.12.2, R Development Core Team, 2011).

In addition to the geographic measures discussed above for the exposure assessment, the health effects models included adjustments for many demographic and health factors. The adjustments included age, sex, race, education, income, waist circumference, body surface area, diastolic blood pressure, hypertension, statin use, diabetes, high-density lipoproteins (HDL), low-density lipoproteins (LDL), triglycerides, log C-reactive protein, creatinine, hypertensive medication, gum disease, alcohol use, smoking status, and city. Six models that included differing covariates were tested with PM_{2.5}, sulfur, silicon, EC, or OC as the predictor and binary CAC, log-CAC, or CIMT as the outcome variable. The model that was preferred by the investigators, known as model 3, included age, sex, race, education, income, waist circumference, body surface area, diastolic blood pressure, hypertension, and statin use as cross-sectional variables. Sex, race, diastolic blood pressure, hypertension, and statin use were also treated as longitudinal variables in the selected model. A full specification of the covariates for each of the six tested models is shown in Section 1, Table 38.

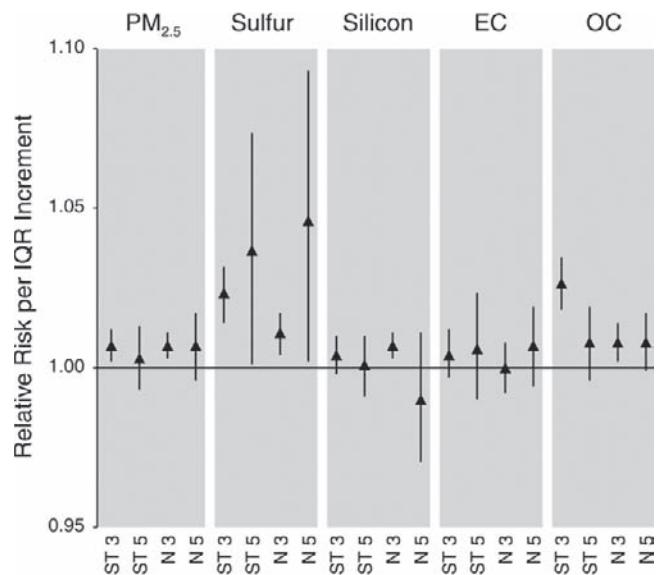
Sensitivity Analyses

Sensitivity analyses were conducted using variations of the primary model outlined above (Model 3). Of the six models, the investigators presented results from four, chiefly for comparison with the primary model, including two that evaluated the sensitivity of the model to the inclusion of additional health measures and two that evaluated the effect of city. Additional factors were also evaluated, including gaseous pollutants (NO₂ and SO₂), statin use, limiting the cohort to participants living within 2 or 5 km of a MESA Air monitor, and between- versus within-city effects. Between-city model estimates were determined using the primary model's longitudinal and cross-sectional parameter estimates and comparing those results to within-city effects determined from models that also included a variable controlling for city. The six models were also run using exposure estimates from the national spatial model as well as exposure estimates from citywide averages, nearest monitoring site, and inverse-distance weighting.

KEY RESULTS FOR THE MESA COHORT

CIMT Analysis

Selected results for the associations found between estimated air pollution concentrations and CIMT are presented in Commentary Figure 1. These results are for the cross-sectional analysis, in which each featured pollutant was assigned by both the spatiotemporal and national spatial



Commentary Figure 1. Associations found in data from the MESA cohort between selected pollutants and CIMT. Data shown are RR estimates with 95% CIs for an IQR increment in predicted PM_{2.5} and PM_{2.5} component concentrations, for various combinations of pollutants and exposure models. ST indicates spatiotemporal model, N indicates national spatial model, IQR denotes interquartile range, and 3 and 5 indicate covariate models 3 and 5, respectively (as defined in Section 1, Table 38). Note that the IQR varied by pollutant and by exposure model: the IQRs (in µg/m³) for the spatiotemporal and national spatial models were, respectively, 1.51 and 2.19 for PM_{2.5}, 0.51 and 0.18 for sulfur, 0.02 and 0.02 for silicon, 0.89 and 0.28 for EC, and 0.69 and 0.39 for OC. From data in Section 1, Tables 41 and 43.

models. (Values shown in Commentary Figure 1 have been exponentiated from the coefficient data in the investigators' report tables to obtain risk estimates and confidence intervals that are visually more comparable with those reported for the other outcomes in the report.) Results are included for Model 3 (the model preferred by the investigators) and Model 5, which included the same covariates as Model 3 with an additional city variable (as explained in Sensitivity Analyses, below).

Spatiotemporal Model Results When pollutant concentrations were assigned using the spatiotemporal model, relative risk estimates for CIMT associated with PM_{2.5}, sulfur, and OC were elevated and statistically significant in the results from analyses using Model 3 covariates. Only the relative risks for sulfur and CIMT analyzed using Model 5 covariates were statistically significant. Relative risks reported for sulfur and OC were both substantially higher than those reported for PM_{2.5}.

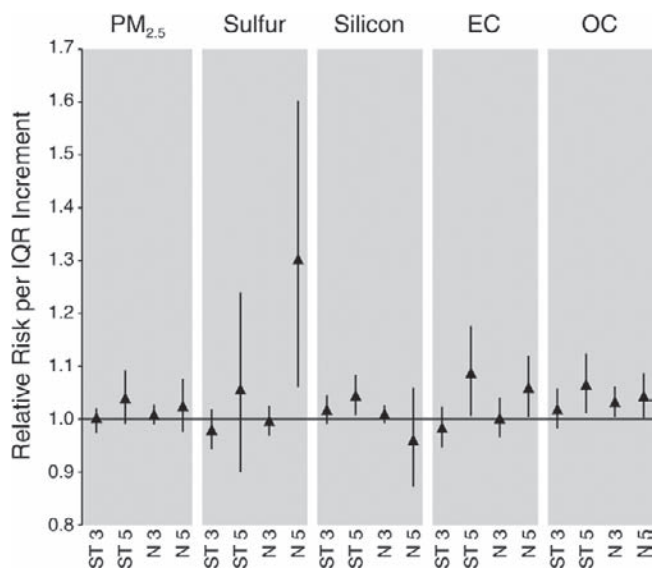
National Spatial Model Results When pollutant concentrations were assigned using the national model, significant relative risk estimates were likewise reported for

PM_{2.5}, sulfur, silicon and OC analyzed with Model 3 covariates and sulfur with Model 5 covariates. Results were similar to those for analyses of pollutant concentrations assigned with the spatiotemporal model, with the exception of silicon, which was statistically significant in the analysis with Model 3 covariates, but strongly reduced by the addition of the city variable (Model 5). With the exception of the results for sulfur using the Model 5 covariates, the reported relative risks for components were quite similar to those reported for PM_{2.5}.

CAC Analysis

Selected results for the associations between estimated air pollutant concentrations and CAC are presented in Commentary Figure 2. These results are for the cross-sectional analysis, in which the featured pollutants were assigned by both the spatiotemporal and national spatial models. Again, results are shown for Model 3 and Model 5.

Spatiotemporal Model Results When analyzed using Model 3 covariates, the relative risks for the presence of CAC associated with PM_{2.5} and the four components were all close to the null and not statistically significant. When a city variable was added (Model 5), the effect estimates for sulfur, EC, and OC increased and became significant.



Commentary Figure 2. Associations found in data from the MESA cohort between selected pollutants and CAC. Data shown are RR estimates with 95% CIs for an IQR increment in predicted PM_{2.5} and PM_{2.5} component concentrations, for various combinations of pollutants and exposure models. ST indicates spatiotemporal model, N indicates national spatial model, IQR denotes interquartile range, and 3 and 5 indicate covariate Models 3 and 5, respectively (as defined in Section 1, Table 38). Note that the IQR varied by pollutant and by exposure model (see Commentary Figure 1). From data in Section 1, Tables 39 and 42.

National Spatial Model Results For the Model 3 analyses, the relative risk for the presence of CAC associated with OC was significantly elevated, but the estimates for PM_{2.5}, EC, sulfur, and silicon were close to the null. In the analysis with Model 5 covariates, statistically significant risks for sulfur, EC, and OC were reported. The estimate for sulfur, in particular, was substantially elevated and statistically significant in the analysis with the Model 5 covariates compared with the null result in the analysis with Model 3 covariates, and notably higher than the estimate for PM_{2.5}.

Sensitivity Analyses

Effects of Including the Participant's City in the Model

As noted above, Model 5 included the same covariates as Model 3, with the addition of an indicator for city of residence. By including the city, it is possible to assess the potential for confounding by city resulting from unknown and unmeasured factors specific to cities that could influence health outcomes. Dramatic differences in estimates of relative risks between models that do and do not include a variable for city of residence can indicate unresolved confounding issues attributable to such between-city differences. Commentary Figure 1 shows estimated relative risks for CIMT, and Commentary Figure 2 shows estimated relative risks for the presence of CAC for Models 3 and 5 for both the national spatial and spatiotemporal models.

For the CIMT analyses, the addition of a city variable to the model widened the CIs for the relative risks associated with concentrations of PM_{2.5} and the four components. More notably, the addition of a city variable markedly increased the relative risk and CIs associated with sulfur concentrations assigned using both the spatiotemporal and national spatial models. Adding the city variable also reduced the magnitude of the relative risks associated with silicon concentrations determined by the national spatial model and with OC concentrations determined by the spatiotemporal model.

In the CAC analyses, the addition of a city variable produced a similar pattern of changes in relative risks and CIs. The estimated relative risk for the presence of CAC associated with sulfur concentrations determined by the national spatial model increased dramatically when the city variable was added and became statistically significant despite much larger CIs. The relative risk estimate associated with silicon determined by the spatiotemporal model increased and became statistically significant when the city variable was added, but the opposite was true for the analyses using concentrations from the national spatial model. For associations between the presence of CAC

and EC concentrations determined by both the spatiotemporal and national spatial models, the relative risks both increased and became statistically significant when the analyses included the city variable. For sulfur (using the national spatial model) and EC (using both spatiotemporal and national spatial models), the relative risk estimates were notably higher than those for the corresponding PM_{2.5} analyses when the city variable was included.

Effects of Alternate Exposure Assignment Methods The investigators experimented with different methods of exposure assignment, comparing the assigned concentrations with those generated using the spatiotemporal and national spatial models (Section 1, Table 35). Across the six cities, for the four indicator components, the mean values and standard deviations for the spatiotemporal model were, for the most part, consistent with values generated using citywide averaging, nearest-monitor assignment, and inverse-distance weighting. Some of the largest differences were seen when comparing the national spatial model to the spatiotemporal and secondary models, particularly for sulfur and EC.

EVALUATION OF THE MESA COHORT STUDY

The Panel thought that Vedal and colleagues' epidemiologic analyses of data from the MESA cohort (and also from the WHI-OS cohort, described below) were wide-ranging and innovative contributions to air pollution epidemiology. The research was well motivated and well conducted, and the specific aims and hypotheses were laid out explicitly. Additionally, the use of subclinical markers of cardiovascular disease — a complex and labor-intensive approach — was potentially a very useful approach for evaluating the cardiovascular health of otherwise healthy individuals.

For the MESA cohort study, the investigators did a large amount of work in modeling and estimating exposures, as discussed above. However, the Panel noted, this was not always paralleled by a similar level of effort in the analyses of health outcomes. The investigators evaluated the associations of air pollution with two different markers of subclinical atherosclerosis, namely, CIMT and CAC. However, the MESA cohort data included many other important outcomes, including vascular reactivity, markers of inflammation and coagulation, lipid oxidation, and adhesion molecules that could have been evaluated and may have supported the main epidemiologic findings. Effects of those markers could be further explored in future health effects assessment.

For the health outcome analyses, the investigators applied two different exposure models (the spatiotemporal

model and the national spatial model) that both had specific merits with respect to their ability to explore between-city and within-city variations in exposure in the health effects analyses. The investigators concluded that the most consistent effects on subclinical atherosclerosis measures were seen for OC — generally considered to be a marker of secondary aerosol — and that, contrary to their original hypothesis, the classic traffic-related pollutant EC showed only inconsistent and weak associations. By contrast, sulfur showed strong associations with CIMT in some analyses. These results were based on generally sophisticated methods and adequate sensitivity analyses; however, the Panel identified several additional considerations that should be taken into account when interpreting the overall results. These considerations pertain to the within- and between-city variability of exposures, the choice of statistical models (including issues concerning multipollutant models), and the availability and quality of the outcome data. Overall, the Panel interpreted the findings in a slightly different way than the investigators did, shifting the weight of evidence somewhat more toward EC (as explained in the following sections).

R^2 for Spatiotemporal Models of Exposure

The Panel thought that the study had very carefully reported the quality of the measurements conducted to develop the exposure models and concluded that the statistical methodology was sound. However, the spatiotemporal models did not perform well for within-city comparisons (or analyses), as was acknowledged by the investigators. The model performance for all components differed remarkably across the cities. The low city-specific R^2 values were understandable for sulfur, which is largely dominated by regional variation, but were problematic for EC, which has well-documented large within-city variation. The spatiotemporal models for EC performed well only in Los Angeles. Reasons for the low R^2 are not well understood but are possibly related to the limited quantity of monitoring data available for the analysis coupled with the unbalanced space-time monitoring design; the availability of geographic information system (GIS) predictors (e.g., the investigators did not include traffic intensity data); the fact that other sources were not well characterized using GIS (e.g., wood smoke); the precision of EC measurements; and the modest variability of EC at the monitoring sites used to develop the models. These design features could therefore have contributed to the variable performance of models predicting within-city variations of EC concentrations. The R^2 values were somewhat better for the national spatial model than for the spatiotemporal model for most components.

Spatial Clustering and Confounding

The design of the MESA cohort required that the possibility of spatial clustering be taken into account. The investigators used a nonrepresentative sampling procedure because population-based random sampling was not feasible. While the use of community-based cohorts is both common and understandable, it is likely to aggravate the problem of spatial clustering (in which observations for individual cohort members are not independently measured) and can lead to clustering of pollution observations at participant residences even beyond the clustering within the six cities. Given that relevant neighborhood effects on subclinical atherosclerosis in the MESA study were shown previously (Murray et al. 2010) and that relevant effects of adjustment for neighborhood SES on air pollution estimates in the ACS-CPS-II cohort were reported (Krewski et al. 2009), the Panel thought that it would have been useful if the investigators had evaluated the possibility of additional confounding by neighborhood-level socioeconomic status in the main analysis of the study. The Panel realized that it was not feasible to include city-level contextual variables with data from only six cities but thought that the effects of the (probably more relevant) smaller-scale neighborhood contextual variables could have been assessed in the model, as was done in models built for the ACS-CPS-II studies (Krewski et al. 2009).

Moreover, differences among the MESA cities could have produced confounding by city. The investigators acknowledged the potential problem of confounding by city and chose to adjust for city in the analyses using indicator variables (Model 5, above). Although this adjustment was probably justified and necessary, it unfortunately removed the exposure contrast between cities; the analysis was thus essentially based on the relatively poorly modeled small-scale within-city exposure contrasts. However, in the discussion section, the investigators put their strongest interpretive emphasis on the city-unadjusted estimates, which show the highest effects for OC. In these analyses, city-level confounding was one important potential explanation for the observed effects. The city-adjusted models produced findings that are much weaker and less convincing and indicated effects that in most cases were not clearly above the null — while the EC effects became more prominent (which further supports the Panel's conclusions, noted above, that the spatiotemporal model did not fully model the variability of EC within MESA cities). It is true that the precision of the effect estimates decreased in the city-adjusted models, but this is appropriate and reflects the greater uncertainty with which the associations could be estimated because of the loss of the between-city exposure differences. Thus, there is a trade-off between potential bias (confounding by city) and both

the strength of association and lack of precision (because of the reduction of exposure contrast). For OC in particular, Section 1, Table 44 indicates that the associations resulted primarily from between-city variation. Consequently, in the city-adjusted models, the effects of OC are substantially less precise. It is therefore impossible to separate the effects of city-specific factors from an effect of OC, precluding a strong statement about the role of OC on subclinical atherosclerosis.

Adjustment for Noise

Chronic noise exposure is a known risk factor for hypertension, and long-term exposure to traffic-related ambient noise has been shown to elevate blood pressure and raise the risk for myocardial infarctions (MIs). At the same time, hypertension is an important risk factor for subclinical atherosclerosis. The Panel was concerned that the MESA study did not include data on chronic noise exposure. (Because air pollution and traffic noise have in part overlapping sources, it was not possible in the current study to separate the effects of these two potential environmental risk factors for subclinical atherosclerosis.) Future studies should consider applying traffic noise models as a first step in attempting to control for noise.

Other Covariates

The Panel noted that variables specified in the preferred model (Model 3) and the other models evaluated could show “overlap” in disease pathways — that is, either they are both on the same pathway for atherosclerosis or they convey the same kind of information as other variables in the model (i.e., they are not independent risk factors). Model 3, for example, included both hypertension and diastolic blood pressure, as well as diabetes. Hypertension and diastolic blood pressure are clearly related (even if the forms of the variables were not correlated), and all three possibly share pathologic mechanisms in the development of heart disease, thus making it unlikely they are independent risk factors in developing heart disease. The inclusion of variables for blood pressure and diabetes in a model predicting the development of heart disease could lead to substantial bias in the model, and inclusion of variables containing nonindependent risk factors could result in statistical problems caused by strong correlations between the predictive variables.

Outcome Measurement

The Panel identified a potential issue with the quality of the main outcome measure regarding the baseline CIMT values (see Section 1, Table 40). It was surprising that the

median increase in CIMT was much larger between exams 1 and 2 than between exams 2 and 3, especially because the time period was longer for the second interval. In addition, the quality assurance report for the CIMT data showed high systematic bias of approximately -0.1 mm for one person who read the scanned images compared with the other two readers, which is 10 times greater than the median overall yearly change of 0.01 mm. By contrast, CAC was measured with much better reproducibility; the Panel was therefore of the opinion that, in light of these CIMT measurement issues, at least equal weight should be given to the CAC analyses.

Considering the issues discussed above — the probability of confounding by city, the dedicated measurement campaign in MESA designed to assess within-city exposure differences, and the higher quality and reproducibility of the CAC measurements compared with the CIMT measurements — the Panel thought that more interpretive weight should be given to the city-adjusted models and the CAC analyses. In that case, there would be more evidence for EC than OC.

It should be noted that the investigators pointed out that the results were contrary to their original hypothesis, which stated that traffic-related exposures would be more strongly associated with health outcomes than would non-traffic-related exposures. Based on the Panel's evaluation, the analyses of the MESA cohort at present provide little evidence that any one component or source is more strongly related to health effects than total $PM_{2.5}$ or that any one single component is more important than the others. The observed associations for OC should be interpreted cautiously, considering the specific limitations and strengths of the study, particularly the fact that these associations are only apparent in the analyses that were not adjusted for city. The Panel recommends that more analyses be conducted to confirm or refute a specifically strong effect of OC on subclinical atherosclerosis.

WHI-OS COHORT OVERVIEW

The specific aim of the current WHI-OS study was to identify the chemical components of ambient PM that contribute to the incidence of cardiovascular events. The principal hypothesis to be tested was that primary emissions of $PM_{2.5}$ components from motor vehicles have a greater effect on long-term cardiovascular outcomes than do secondary inorganic or crustal components. Using the cardiovascular events recorded for the WHI-OS cohort, the investigators assessed associations with $PM_{2.5}$ and the four indicator components — sulfur, silicon, EC, and OC — using the national spatial model of exposure.

The WHI-OS is a large-scale cohort study, funded by the National Institutes of Health, of postmenopausal women that measured baseline risk factors for cardiovascular disease between 1994 and 1998 and included annual updates for most measures through 2005. The WHI study included annual updates of fatal and nonfatal cardiovascular incidents, risk factors, and health measures for 93,676 women from 46 U.S. cities. Physical measurements, including height, weight, waist and hip circumference, heart rate, and blood pressure, were obtained at baseline for all WHI participants. In addition, blood samples were collected for the majority of WHI-OS participants; most samples were stored for future analysis. The participants completed questionnaires about demographic and lifestyle factors, medical history, dietary intake, residential address throughout the study period, and medication and vitamin use. The 73,094 participants without CVD at baseline were included in the current NPACT analyses of the WHI-OS data, and the 20,582 with CVD at baseline were included only in the sensitivity analyses. The final cohort size for the current analyses was 52,539, after excluding individuals living outside the continental United States and those with missing geographic, follow-up, or covariate data.

Outcomes

The outcomes studied in the WHI-OS analysis were cardiovascular events defined as MI, stroke, mortality caused by CVD or cerebrovascular causes, hospitalization for coronary heart disease (CHD) or angina pectoris, and coronary revascularization procedures including bypass and angioplasty. Both ischemic and hemorrhagic strokes were included in CVD deaths. Information on health outcomes was obtained from participants through questionnaires followed by physician-conducted medical record reviews (including death certificates) for incident cases and negative reports from participants. The CHD deaths were further classified as “definite” or “possible” based on definitions outlined in the study design. CHD deaths were determined to be definite if a review of the records indicated a likely underlying CHD cause in addition to one of the following criteria: hospitalization for MI within 28 days preceding death, history of angina or MI, no other life-threatening noncardiovascular medical condition, death resulting from bypass or angioplasty procedures, or chest pain in the 72 hours prior to death. CHD deaths were determined to be possible if death certificates and a review of medical records showed no other non-CHD cause and pointed to CHD as the most likely cause. Some additional analyses included “other cardiovascular deaths” and “unknown cardiovascular deaths.” Other cardiovascular deaths were classified as those where MI or other CHD

causes were likely but did not meet the study's definitions or where there was sudden death without another potential underlying cause. Unknown cardiovascular deaths were classified as those where evidence was limited but pointed to an underlying cardiovascular cause, as determined by a review of medical records or death certificates.

Exposure Assessment Using the National Spatial Model

PM_{2.5} as well as sulfur, silicon, EC, and OC were used in the national spatial model to estimate concentrations at the home addresses of the WHI-OS participants. The current WHI-OS analysis used the same national spatial model as was used for the MESA analyses, discussed previously. A similar model was also used for PM_{2.5} and the WHI-OS cohort, using 2000 data from Air Quality System (AQS) and IMPROVE monitoring sites. Cardiovascular events measured in WHI-OS occurred beginning in 1994. Consequently, data for exposures and health outcomes were collected over different time periods.

Home addresses at the time of the baseline assessments were geocoded for 94% of the 93,676 participants in WHI-OS. Modeled exposures were assigned for the 60,014 participants without preexisting CVD, but the final sample size used for statistical models including health outcomes was 52,539. Some factors that reduced the sample size included prior diagnosis of CVD, unavailable or invalid home address, home located outside of continental United States, and missing covariate data.

In addition to the modeled exposures discussed above, several additional exposure estimates were also evaluated in health effects analyses and compared with results from the national spatial models. These exposure estimates included use of (1) citywide averages from 2004 in lieu of modeled home address exposures and (2) distance of the home to a busy road to indicate proximity to traffic. Distance to a busy road was based on census roadway classifications for "unseparated roadways" (A1, primary highway with limited access; A2 primary road without limited access [also includes a tunnel]; and A3, secondary connecting road [also includes an underpass]). One of the two dichotomous distance variables represented homes located within "100 m of an A1 or A2 class roadway" or "within 50 m of an A3 roadway" versus all other home locations. The other dichotomous distance variable split the data into those homes located less than or more than 100 m from an A1 or A2 roadway.

Statistical Analyses

Because the health outcome was defined as time to first cardiovascular event or death, the health effect analyses estimated hazard ratios using Cox proportional-hazards regression models. These models used regression to estimate

time to CVD-related illness or death for a particular increase in a pollutant concentration, generally 10 µg/m³ of PM_{2.5} or the interquartile range (IQR) for PM_{2.5} or a PM component. For the models using proximity to roadway variables, the hazard ratios were estimated using the category of home location. Potential confounders included as covariates in all models were age, body mass index, smoking factors, diabetes, blood pressure, hypertension, hypercholesterolemia, education, household income, and race. The models also assumed different strata of diabetes, age, and body mass index for the baseline hazards (a component of the Cox proportional-hazards models). Models were run for all CVD events combined as well as specifically for each health outcome, as described above in the Outcomes section of the WHI-OS Cohort Overview. The Cox proportional-hazards models used SAS statistical software (versions 9.2 and 9.3, SAS Institute, Cary, NC).

Analyses of within- and between-city effects were also conducted with city defined as home location within a metropolitan statistical area (MSA). The city also had to have at least 20 participants with homes in that MSA to be included in the analysis, resulting in a reduction in the number of participants to 45,980. To estimate within- and between-city effects of pollution measures on CVD event or death, modified Cox proportional-hazards models were run that incorporated the mean of PM_{2.5} or a component for a given city (the between-city effects) as well as the participant-specific exposure subtracted from the city mean (the within-city effects). Hazard ratios were determined for each pollutant and CVD category for both within- and between-city effects.

Sensitivity Analyses

Sensitivity analyses were conducted to evaluate the stability of models, taking into account a number of factors: (1) PM components found to have statistically significant associations with health measures in single-pollutant models were run in multipollutant models; (2) hazard index models were evaluated for their sensitivity to pre-existing heart disease by adding participants with prior CVD to the analyses and comparing results with those from models run without these individuals; (3) distance to a busy roadway was evaluated by restricting to participants living only within a designated MSA at baseline, which likely reduced the numbers of rural home locations in those models; (4) health effects models were run separately for deaths classified as "other CVD" and "unknown CVD," because atherosclerosis was not necessarily the actual cause of death for these cases, and the results were compared with all CVD deaths; (5) the effects on model results of measuring exposures and health effects during different time periods were assessed by comparing results from spatiotemporal

models using PM_{2.5} measured in 2007–2008 with results from models using PM_{2.5} data from 2000; and (6) a further effect of city in the Cox proportional-hazards models was also tested by adding a random city term to the models, which were then called frailty models, to determine if the term was responsible for a significant portion of the variance found in the health effect analyses.

KEY RESULTS FROM THE WHI-OS COHORT

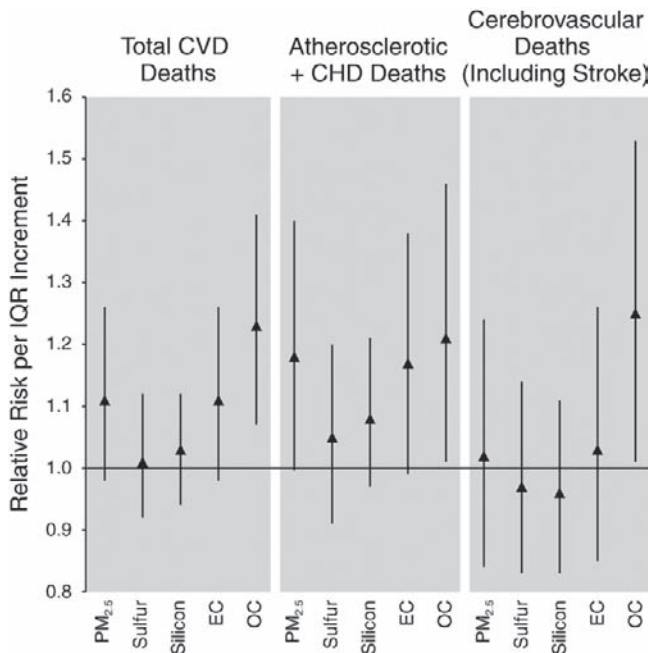
Main Analyses Using the National Spatial Model

Cardiovascular Disease Deaths The investigators analyzed all CVD deaths, as well as deaths from subsets of CVD, including atherosclerotic cardiac disease, cerebrovascular disease, “atherosclerotic cardiac disease or possible CHD death,” and “possible CHD death” according to WHI-OS records. Associations found between PM_{2.5}, sulfur, silicon, EC, or OC and selected causes are shown in Commentary Figure 3.

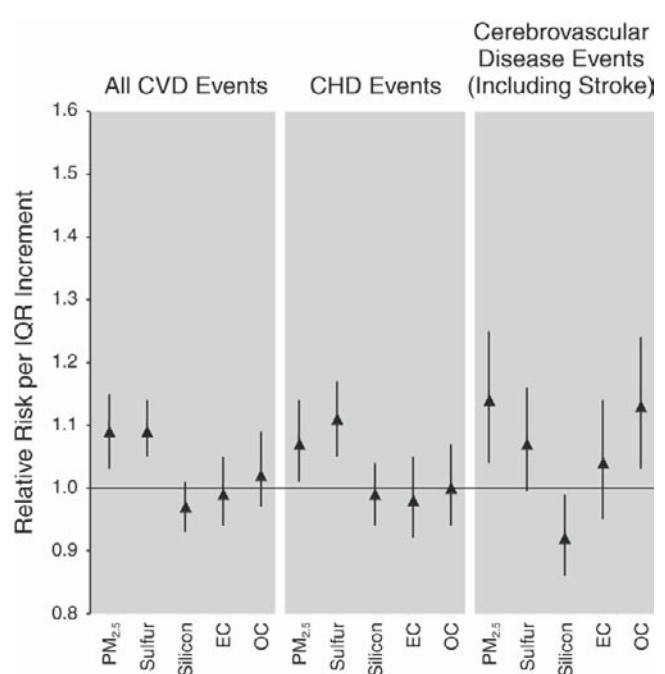
For all CVD deaths, the strongest association was with concentrations of OC; associations with PM_{2.5} and EC were marginal. Atherosclerotic death associations showed

a similar pattern, with a statistically significant association with OC and marginal associations with PM_{2.5} and EC. Cerebrovascular death associations also showed a statistically significant association with OC, but were not associated with PM_{2.5} or any other component.

Cardiovascular Disease Events The investigators analyzed all CVD events, including deaths, as well as events related to subsets of CVD, including CHD, cerebrovascular disease, stroke, MI, and coronary revascularization, according to WHI-OS records. Associations found between PM_{2.5}, sulfur, silicon, EC, or OC, and selected events are shown in Commentary Figure 4. RRs for the analyses of events showed slightly different patterns than those found for the analysis of deaths, though with tighter CIs. Associations between all CVD events and concentrations of PM_{2.5} and sulfur were small but statistically significant, whereas a negative and statistically significant association was found for silicon. The only notable associations for CHD events were with sulfur and PM_{2.5}. Cerebrovascular disease events were significantly associated with PM_{2.5} and OC, marginally associated with sulfur, and negatively and significantly associated with silicon.



Commentary Figure 3. Associations found in data from the WHI-OS cohort between total and cause-specific CVD mortality and selected pollutants. Data shown are RR estimates with 95% CIs associated with an IQR increment of baseline exposure using national spatial model predictions. Note that the IQR (in µg/m³) varied by pollutant (i.e., 3.9 for PM_{2.5}, 0.25 for sulfur, 0.07 for silicon, 0.21 for EC, and 0.64 for OC). From data in Section 1, Table 52.



Commentary Figure 4. Associations found in data from the WHI-OS cohort between all CVD events, CHD events, and cerebrovascular disease events (including stroke) and selected pollutants. Data shown are RR estimates with 95% CIs associated with an IQR increment of baseline exposure using national spatial model predictions. Note that the IQR varied by pollutant (see Commentary Figure 3). Based on Section 1, Table 51.

Commentary Table 2. Comparisons of Selected Results for Analyses Based on Within- and Between-City Baseline Exposures in the WHI-OS Cohort^a

Component	Outcome	Between-City RR (95% CI)	IQR ($\mu\text{g}/\text{m}^3$)	Within-City RR (95% CI)	IQR ($\mu\text{g}/\text{m}^3$)
Sulfur	CVD deaths	0.98 (0.88–1.10)	0.25	1.12 (1.00–1.26)	0.033
EC	Atherosclerotic disease deaths	1.10 (0.73–1.66)	0.21	1.25 (1.00–1.55)	0.13
OC	Atherosclerotic disease deaths	1.16 (0.78–1.74)	0.64	1.26 (0.97–1.66)	0.40
PM _{2.5}	CVD events	1.07 (1.00–1.14)	3.9	1.01 (0.97–1.05)	1.04
Sulfur	CVD events	1.06 (1.01–1.12)	0.25	1.02 (0.97–1.06)	0.033
Sulfur	CHD events	1.08 (1.02–1.15)	0.25	1.02 (0.96–1.08)	0.033
OC	Cerebrovascular disease events	1.19 (1.03–1.38)	0.64	0.99 (0.90–1.08)	0.40
Sulfur	Coronary revascularization events	1.12 (1.05–1.20)	0.25	1.01 (0.95–1.07)	0.033
PM _{2.5}	Coronary revascularization events	1.08 (0.99–1.19)	3.9	0.99 (0.94–1.06)	1.04
OC	Stroke events	1.16 (1.00–1.35)	0.64	0.99 (0.90–1.09)	0.40
PM _{2.5}	Stroke events	1.12 (1.00–1.25)	3.9	1.02 (0.95–1.10)	1.04

^a Boldface indicates statistical significance (lower CI \geq 1.00).

Sensitivity Analyses

Within- and Between-City Analyses Because the main analyses with data from the WHI-OS cohort did not include any variables identifying the residence city for each of the participants, the Panel requested an analysis of the separate effects of within- and between-city variance on the results. Of all the associations between deaths or events and concentrations of PM_{2.5} and components shown in Section 1 of the Investigators' Report in Tables 54, 55, 56, and 57, there were a few notable differences (Commentary Table 2).

The association between CVD deaths and sulfur in the between-city analysis was null but was much stronger in the within-city analysis, particularly when considering the smaller within-city IQR over which the association was evaluated. Similarly, the associations between atherosclerotic deaths and an IQR change in EC and OC in the between-city analysis were positive but far from statistically significant; these associations were also stronger in the within-city analysis.

A different pattern of associations was found when the between- and within-city analyses of events (Section 1, Tables 54 and 55) were compared. Although the additional number of cases in the analyses of events yielded tighter CIs for the risk estimates than those for the analyses of deaths, the within-city analysis did not report any significant associations for any of the cause categories. However, the between-city analysis reported significant associations between CVD events and PM_{2.5} and sulfur; CHD events and sulfur; cerebrovascular disease events and OC;

coronary revascularization events and PM_{2.5} and sulfur; and stroke events and both PM_{2.5} and OC.

Frailty Analysis The investigators also performed what they termed a frailty analysis, in which a city variable was included as a random-effect variable in the analytic model used to estimate associations between CVD deaths and events and concentrations of PM_{2.5} and the four components. The results, shown in Section 1, Table 60, show only trivial differences in the relative risks for the frailty and non-frailty (standard Cox) models, with slightly wider CIs for the estimates from the frailty models (resulting from the additional uncertainty of the inclusion of the random-effect variable).

Living Near a Major Roadway In order to investigate their central hypothesis about motor vehicle emissions, the investigators analyzed the relationships between CVD events and deaths in the WHI-OS cohort and the distance between participant residences and roadways of various types (Section 1, Tables 61 and 62). Although some elevated relative risks were reported for the various categories of CVD deaths and living either within 100 m of an A1 or A2 roadway or within 50 m of an A3 roadway, the CIs were very wide, and no findings approached significance. When this cohort was restricted to participants living within the boundaries of an MSA or within 100 m of an A1 or A2 roadway, the results were similarly inconclusive.

Given the larger number of events compared with deaths, the results for a parallel analysis of CVD events and residential distance to roadways had greater statistical power

and less uncertainty. RRs were elevated and nearly significant for all CVD, cerebrovascular disease, coronary revascularization, and stroke events for participants living within 100 m of an A1 or A2 roadway and statistically significant for all CVD events (RR, 1.40; 95% CI, 1.01–1.50), cerebrovascular disease events (RR, 1.23; 95% CI, 1.02–1.92), and stroke events (RR, 1.44; 95% CI 1.04–2.00) when that same group was further restricted to those living within an MSA.

EVALUATION OF THE WHI-OS COHORT STUDY

In its evaluation of the WHI-OS cohort analysis, the Panel noted that the study had a number of strengths. The cohort data featured thorough and specific case ascertainment; deaths and health events verified by death certificates and annual questionnaires, and non-respondents tracked through proxies. Follow-up was excellent, with an annual response rate of more than 94%. At the end of the close-out period in 2005, 4.1% of the initial cohort were lost to follow-up or had stopped follow-up, and 6.1% were deceased (Fred Hutcherson Cancer Research Center Web site; accessed April 8, 2013).

The Panel noted that the investigators were experienced and had competently performed the statistical analyses, employing well-established techniques for long-term cohort study analyses. Their national spatial model for exposure assessment represented a thorough and ambitious effort to accurately estimate pollutant concentrations at the home address (at enrollment) of every cohort member included in the study. In this section of the commentary, the Panel outlines several issues regarding the data analyses and interpretation of results, followed by a section that compares this cohort study to previous PM component studies.

Challenges in the Exposure Data

Although the WHI-OS data set included data on deaths and events for the period 1999 through 2005, the investigators used data on $PM_{2.5}$ and $PM_{2.5}$ components collected in 2009 to build the national spatial model used to represent concentrations of pollutants at participants' residences at the time of the baseline assessment for the health effects analyses. There is some evidence that changes in measured $PM_{2.5}$ concentrations during long follow-up periods (i.e., decades) occur in a spatially uniform manner (Krewski et al. 2009; Pope et al. 2009), meaning that mean concentrations for the current and previous years at a fixed location will very likely retain their relative magnitudes compared with those at other fixed locations, even if overall concentrations have decreased or increased. However, there have not been similar investigations of the

spatiotemporal behavior of $PM_{2.5}$ components, which have spatial distribution characteristics that are different from $PM_{2.5}$ and each other (Bell 2011). The use of data for component concentrations that were collected in a year that was not represented in the health effects follow-up might introduce bias in the results. In addition, exposures were assigned to the participant's residence address as recorded at the beginning of the study in the mid-1990s, resulting in potential misclassification of exposure for some members of the cohort if they later moved to a different city with different exposure levels.

Furthermore, there are some known technical issues with using $PM_{2.5}$ data from the year 2009 that need to be considered when assessing the results. $PM_{2.5}$ concentrations recorded in 2009 are known to have been unusually low (compared with, for example, the 1999–2005 time frame for the WHI-OS follow-up) because of reductions in industrial output related to an economic downturn and anomalous weather conditions affecting the North American continent. It is entirely possible that concentrations of the components of $PM_{2.5}$ were not only similarly low in 2009, but that concentrations of specific components might have been low compared with others. For example, if the reduction in $PM_{2.5}$ resulted from reductions in secondary aerosols but not reductions in metals or EC, then the 2009 concentrations could represent a skewed mixture of components compared with those measured at the time of the follow-up.

These reduced $PM_{2.5}$ concentrations and potentially non-proportional reductions in $PM_{2.5}$ component concentrations in 2009 have some implications for effect estimates. If health events were recorded during a time of higher exposure than is represented by the component concentration data used to estimate and assign exposure, then the relative risks associated with an IQR increase in concentrations could be overestimated. Similarly, if some component concentrations were low in 2009 compared with the 1999–2005 follow-up for the cohort, relative risks could be overestimated for those components. These possibilities need to be considered when interpreting the results.

The Panel also noted — as it did for the MESA cohort study, above — that the national spatial model of exposure used for the WHI-OS cohort likely underestimated the within-city variation in concentrations for all components. This is due to the national spatial model's sole reliance on the CSN and IMPROVE networks, which may have only a single monitoring station in a given city (and only rarely more than two monitors in a metropolitan area). This underestimation of within-city spatial concentration variation is of particular importance for components such as EC, which have concentrations with high spatial variation

relative to components with regionally uniform concentrations, such as sulfur and OC. Thus the WHI-OS cohort study dependence on the national spatial model likely resulted in more robust estimates for health effect associations with sulfur or OC than with EC.

Adjustment for Total PM_{2.5} Mass

Although the Panel appreciated the need to reduce complexity, it noted that the analyses of associations with health outcomes focused overwhelmingly on single-pollutant models. The Panel was unconvinced that such models adequately addressed the objectives of the NPACT initiative—to investigate whether health effects are driven by specific chemical components rather than by overall PM_{2.5} mass concentration. Associations of outcomes with single components from such models can be confounded by each other. Also, single-pollutant models allow only qualitative evaluation of the extent to which higher RRs per IQR for one component compared with another component (or total PM_{2.5}) could have been caused by chance. The multi-pollutant models shown as sensitivity analyses (Appendix H, Table 4, available on the HEI Web site) were helpful in addressing the issue of mutual confounding but did not provide a clear approach to quantifying the strength of the evidence provided by one relative risk being higher than another (excluding chance). The Panel was in particular disappointed that the investigators did not explore models that included each component together with total PM_{2.5} mass or similar models. Mostofsky and colleagues (2012) recently reviewed such models and elaborated on how they can help clarify whether a particular component is better than total PM_{2.5} at explaining variations in the outcomes.

Between- and Within-City Models

Although these methods can be used to assess pollution effects at the community level as well as the individual level, they do not completely account for city effects. As an alternative method, Miller and colleagues (2007) used a fixed-effect model for city, adjusting for city with an indicator variable for each city. In the current study, investigators included a random effect variable for city. Jerrett and colleagues (2008) included in the Cox proportional-hazards model a random effect variable for city, as well as a citywide mean concentration and a “difference variable” representing the difference between the city-mean concentrations and the individually assigned exposures. The Panel believes that the use of such approaches would have produced results that were more directly comparable with earlier studies and would have reduced the effects of city-level bias in the results.

In the WHI-OS study, analyses of associations with cardiovascular events analyses were mostly limited to between-city effects (Section 1, Table 54 and Table 55). The between-city analyses yielded several statistically significant or nearly significant estimates (especially for silicon and EC) that might have been caused by uncontrolled confounding by city. The within-city analyses overall did not show significant results, although the point estimates were in the expected direction. Conversely, the within-city analyses of deaths showed positive associations for cause-specific mortality for sulfur (although with a very small IQR) and one positive association for EC. One conclusion from these results is that the component concentrations were correlated with important city-specific confounders but that it was not possible to tease apart the effects of component and city. The analyses of cardiovascular deaths alone might also lack sufficient statistical power for a definitive analysis of within- and between-city differences and PM_{2.5} components.

Another possibly striking result was the difference between the cohort restrictions for the analyses of living near a major roadway (see Section 1, Table 61). In the “A1 or A2 < 100 m” model, the point estimates were slightly elevated, but not significant when all participants were included, whereas in the model restricted to participants living in MSAs, the estimates increased, with estimates for CVD, cerebrovascular disease, MI, and stroke event all becoming significant. This difference points to potential confounding by city, because the same presumed exposures to roadways resulted in different risk estimates when non-urban participants are omitted.

For the frailty analysis, where a random-effect variable was used to include city of residence in one model and compared with the results from the classic Cox model, the authors reported that “including an MSA-level random effect term had little effect on the estimated HR values or 95% CIs (Table 60): for all exposures and all outcomes, the CIs were widened slightly and the estimated HRs were often unchanged or changed only slightly in the random effects model. . . . In short, inclusion of the random effect in the frailty model does not change the conclusions of our primary analyses in the nonfrailty models.” Thus the results from the random-effects sensitivity analysis showed very similar results when comparing nonfrailty and frailty models and therefore were reassuring, especially given the findings of the within- and between-city analyses, where many noteworthy associations between components and CVD events were driven by between-city contrasts in exposure. However, given the inherent underestimation of within-city concentration variations by the national spatial model of exposure, it is

unlikely that any sensitivity analysis designed to compare the effects of within- and between-city variation in the WHI-OS study could demonstrate any notable effect of within-city variability.

Comparison with Selected Literature on PM_{2.5} Components

The literature on PM_{2.5} components includes studies of long-term and short-term relationships between component concentrations and outcomes, with relatively fewer long-term studies because of the somewhat recent availability of speciated PM_{2.5} data and the multiple-year time frames demanded by cohort analysis methods. Ostro and colleagues (2010) conducted one such long-term exposure study in a cohort of nearly 45,000 female teachers in Southern California, followed from June 2002 to July 2007. The researchers restricted their sampling to participants living within either 8 km (7,888 participants) or 30 km (44,847 participants) of a monitoring station. For the 30-km analyses, the associations found between ischemic heart disease (IHD) mortality was strongest for sulfate (RR, 2.39; 95% CI, 1.93–2.97), followed by OC (RR, 2.03; 95% CI, 1.79–2.29), PM_{2.5} (RR, 1.91; 95% CI, 1.65–2.21), and EC (RR, 1.41; 95% CI, 1.14–1.74). Similar results were reported for those living within 8 km of a monitor. In two-pollutant models with OC and EC or with sulfate and EC, the addition of EC had little impact on effect estimates. Two-pollutant models with OC and sulfate showed a modest increase in effect estimates for both components. These findings by Ostro and colleagues (2010) for associations between IHD and long-term exposures to OC and sulfate, which were stronger than those for PM_{2.5} and EC, support similar findings reported by Vedal and colleagues — although the current study covers a far larger geographic area.

Although not directly comparable, the results of some short-term analyses with multiple components can also be informative. In one recent meta-analysis using Medicare data from 119 counties in the United States, Levy and colleagues (2012) analyzed the short-term associations between hospital admissions and short-term changes in PM_{2.5} and selected PM_{2.5} component concentrations (EC, OC, sulfate, and nitrate) measured by way of the CSN network. Each county was analyzed separately, and findings were aggregated using a Bayesian multivariate normal hierarchical model that permitted calculation of posterior probabilities of toxicity from two-pollutant models (expressed as a change in beta coefficient per unit change in concentration). For both the national and regional analyses, variations in EC concentrations were much more highly associated with hospital admissions for CVD than were variations in sulfate, nitrate, OC, and PM_{2.5} mass.

When EC was paired with OC, sulfate or PM_{2.5}, a posterior probability of 1.000 was found. In the analysis of hospital admissions for respiratory disease, however, posterior probabilities for OC were quite high when OC was paired with sulfate, nitrate, and PM_{2.5}, and OC was nearly equivalent to EC (EC posterior probability = 0.576) in toxicity in the two-pollutant model. Although the long-term exposure assessment and chronic disease outcomes in the current study make it difficult to compare the findings with those from Levy and colleagues (2012), the contrast between these consistent findings for EC and CVD admissions on a short-term basis and the current findings for OC in the MESA and WHI-OS cohorts raise some interesting scientific questions about both mechanisms of effect (e.g., Is EC the best indicator of the pollution mixture or sources that trigger short-term effects, while OC is an indicator for the mixture that poses a greater risk for longer-term systemic effects leading to CVD?) and the possibility that OC in the current study is a proxy for another component or for PM_{2.5} itself.

Stanek and colleagues (2011) recently published a review of research on PM_{2.5} components and health effect outcomes. The studies in the review cited multiple factors and elements that were associated with cardiovascular mortality, including crustal, soil (Al, Ca, Fe, and silicon), salt, sulfate, traffic, motor vehicle exhaust (Mn, Fe, Zn, Pb, OC, EC, CO, and NO₂), Cu smelter, combustion (Cr, Cu, Fe, Mn, and Zn), vegetative burning (OC and K), and an unnamed factor (Br, Cl, and Pb). The findings by Vedal and colleagues for OC and sulfur (a marker for sulfate) — and, in some sensitivity analyses, EC — contribute to this lengthy list of components associated with deaths from CVD. More important, the findings from Vedal and colleagues contribute evidence from a long-term cohort study that analyzed a large quantity of exposure and mortality data from multiple cities to the still rather sparse evidence from long-term epidemiologic studies.

Comparison with PM_{2.5} Results for the WHI-OS Cohort

Many readers of this report will be aware of the report by Miller and colleagues (2007) on the association of PM_{2.5} exposure with the same outcomes in the same cohort. Although the primary objective of the current report was to explore the role of PM_{2.5} components, it would clearly have been interesting to compare the current results for PM_{2.5} with those reported by Miller and colleagues.

In the report by Miller and colleagues, the hazard ratios per 10 µg/m³ PM_{2.5} were 1.24 (95% CI, 1.09–1.41) for any CVD event and 1.76 (95% CI, 1.25–2.47) for CVD deaths. In the current report, the relative risk for any CVD event

was similar, at 1.25 (95% CI, 1.09–1.44), but the relative risk for CVD deaths was considerably attenuated, at 1.31 (95% CI, 0.94–1.83) (Section 1, Table 50). A possible reason for the difference in the results for CVD deaths was the addition of deaths in the later years of follow-up in the current report (1998–2005 versus 1994–2003 in the paper by Miller and colleagues). The number of CVD deaths increased from 261 to 445, but the number of CVD events increased proportionally less, from 1816 to 2532. Another possible reason is that the IQR for the distribution of PM_{2.5} exposures reported by Miller and colleagues was 6.7 µg/m³, while the IQR reported for the present study was only 3.9 µg/m³. This difference between the exposure ranges indicates that potential differences in exposure estimates may have contributed to the observed differences in results. Without results for analyses using similar exposure assignment methods and follow-up periods, we cannot distinguish among these — or other — possible explanations for the difference in estimates.

The two reports also differ markedly in the extent to which associations between CVD events and air pollution were apparent in contrast between the within- and between-city analyses. The results reported by Miller and colleagues provided clear evidence of associations in both of these analyses, although the hazard ratio estimates were stronger for within-city, at 1.64 (95% CI, 1.24–2.18), than for between-city, at 1.15 (95% CI, 0.99–1.32). The within- and between-city hazard ratio estimates (rescaled to per 10 µg/m³ for comparability) in the current report were 1.10 (95% CI, 0.74–1.60) and 1.19 (95% CI, 0.997–1.40), respectively. Again, without further analyses it is impossible to narrow down possible reasons for this difference.

WHI-OS STUDY CONCLUSIONS

This well-conducted epidemiology study by Vedal and colleagues represents an admirable effort to advance the state of the science and has added to the relatively limited evidence about long-term exposure to particulate air pollution and its components and cardiovascular events and mortality. Although the study examined a limited number of PM_{2.5} components, they were chosen deliberately to represent the dominant components and prevailing sources (resulting in fewer statistical tests, which reduced potential problems associated with multiple testing). In the context of previously published results for long- and short-term exposures (as well as the minor internal inconsistencies in the current report), the relative importance of traffic versus other sources of PM remains unclear. The current report emphasized results for OC; however, it is important to note that a lack of significant associations (as was generally observed for the other PM_{2.5} components) is

not necessarily evidence of no associations, as reflected in the investigators' discussion of the findings in terms of greater or lesser evidence of effect. Confidence intervals for effect estimates from specific pollutants frequently overlapped. Furthermore, measurement error that varies across the examined pollutants could easily lead to the attenuation of effects for the components with the largest measurement errors; this could be especially important for within-city effects, which would likely be magnified by the larger number of within-city measurements from a larger number of sampling locations and devices. With these uncertainties, together with the often high correlations among pollutants in the current report and elsewhere (e.g., between EC and OC) and the multiple sources of some components (e.g., OC), interpretations about specific components and sources are still limited.

SECTION 2: TOXICOLOGY STUDY

SPECIFIC AIMS

The specific aims of the toxicology study were (1) to provide mechanistic insight into biologic associations in the epidemiology studies and (2) to identify differences in the toxic potency of various atmospheres of environmental relevance. The working hypothesis was that “important environmental effects on the cardiovascular system are driven by exposures to vehicle-derived pollutants, including both gasoline engine exhaust (GEE) and diesel engine exhaust (DEE).”

Campen and colleagues' general approach was to expose animals by whole-body inhalation to laboratory-generated atmospheres of mixed diesel and gasoline engine exhaust (i.e., MVE) and other non-vehicular particles at physiologically relevant concentrations. The study was designed to complement the epidemiology study by Vedal and colleagues by attempting to tease apart the contribution to toxicity of ambient PM in MVE compared with that of other pollutant mixtures.

APPROACH

The experimental design consisted of an extensive evaluation of several cardiovascular endpoints in male ApoE knockout mice that were fed a high-cholesterol and high-fat diet and are prone to developing atherosclerosis. Groups of mice were exposed for 50 days to a variety of exposure atmospheres that aimed to simulate various exposures in the environment. The investigators used MVE as a basic component and combined it with other particle

atmospheres to represent ambient mixtures with secondary pollutants. The MVE exposure consisted of a combination of GEE and DEE in a 1:5 ratio based on PM concentration, at a maximum concentration of 300 $\mu\text{g}/\text{m}^3$ to reflect real-world exposures under certain highly polluted conditions. The diesel engine was a single-cylinder, 5500-watt Yanmar diesel generator, and the gasoline engine was a 1996 General Motors 4.3-L V6 engine equipped with a stock exhaust system. Both engines were used in previous studies conducted at LRRRI for the National Environmental Respiratory Center, although not with combined exhaust as in the current study.

The investigators generated a large number of exposure conditions (see Commentary Table 3). Basic atmospheres included two concentrations of MVE (100 $\mu\text{g}/\text{m}^3$ and 300 $\mu\text{g}/\text{m}^3$) and two concentrations of MVE gases — with PM removed — at the same exhaust dilutions as MVE. Concentrations of MVE gases were 10 ppm NO_x , 33 ppm CO, and 5 ppm nonmethane volatile organic compounds (NMVOCs) for the low concentration and 30 ppm NO_x , 100 ppm CO, and 15 ppm NMVOCs for the high concentration.

Commentary Table 3. Overview of Exposure Atmospheres and Target Concentrations of Major Components^a

Atmosphere	Target Concentrations			
	PM ($\mu\text{g}/\text{m}^3$)	NO_x (ppm)	CO (ppm)	NMVOC ($\mu\text{g}/\text{m}^3$)
MVE _{Low}	100	10	33	5
MVE _{High}	300	30	100	15
MVE gases _{Low}	0	10	33	5
MVE gases _{High}	0	30	100	15
S	300	0	0	0
S + MVE _{Low} ^b	300	10	33	5
S + MVE gases _{High} ^c	300	30	100	15
N	300	0	0	0
N + MVE _{Low} ^b	300	10	33	5
N + MVE gases _{High} ^c	300	30	100	15
RD	300	0	0	0
RD + MVE _{Low} ^b	300	10	33	5
RD + MVE gases _{High} ^c	300	30	100	15

^a MVE was generated by combining emissions from a gasoline engine and a diesel generator at a 1:5 ratio. All PM (including non-vehicular PM) was in the fine particle range. (S indicates sulfate; N, nitrate; RD, road dust.)

^b Combined atmospheres with MVE contained 100 $\mu\text{g}/\text{m}^3$ of MVE plus 200 $\mu\text{g}/\text{m}^3$ of non-vehicular PM (N, S, or RD). Thus, those atmospheres contained a low concentration of MVE gases.

^c Combined atmospheres with MVE gases contained 300 $\mu\text{g}/\text{m}^3$ of non-vehicular PM (N, S, or RD) plus the high concentration of MVE gases.

In addition, there were three atmospheres with non-vehicular $\text{PM}_{2.5}$ (i.e., sulfate, nitrate, and road dust at 300 $\mu\text{g}/\text{m}^3$). The sulfate and nitrate atmospheres were generated by aerosolizing ammonium sulfate and ammonium nitrate solutions, respectively, using an evaporation and condensation system. Because the same instrument was used to generate the sulfate and nitrate atmospheres, the exposures to these atmospheres were done in sequential batches. The road dust was collected from residential arterial roadways in Phoenix and Tucson, Arizona, in proximity to the populations included in the MESA Air cohort that were evaluated in the epidemiology study. The road dust was filtered to remove coarse PM, stored, and subsequently aerosolized. A cyclone was used to remove all PM larger than 2.5 μm to limit the exposures to fine PM ($\text{PM}_{2.5}$), because rodents are not capable of inhaling coarse PM.

Finally, additional atmospheres were generated by combining the MVE or MVE gases with sulfate, nitrate, or road dust. To achieve a final concentration of 300 $\mu\text{g}/\text{m}^3$ of total PM, 200 $\mu\text{g}/\text{m}^3$ of non-vehicular PM was added to 100 $\mu\text{g}/\text{m}^3$ of MVE (i.e., with a low concentration of MVE gases). When non-vehicular PM was combined with MVE gases only, the high concentration of MVE gases was used. All atmospheres were characterized in detail, including chemical analyses of PM for a large number of elements, NMVOCs, ions, and carbon (see Section 2, Table 3, for a full list of measurements).

After the 50-day exposures, blood and aortic tissues were collected from the mice and evaluated for measures of oxidative and nitrosative stress, vascular reactivity, and atherosclerotic plaque formation (see Section 2, Table 4). Measures reflecting oxidative and nitrosative stress and impairment of nitric oxide synthase (NOS) included the following endpoints: lipid peroxides (using a thiobarbituric acid reactive substances [TBARS] assay) in homogenized aortic tissue, mRNA expression of heme-oxygenase-1 (HO-1), endothelin-1 (ET-1), eNOS (endothelial NOS), iNOS (inducible NOS), DHFR (dihydrofolate reductase), GTPCH (guanosine 5'-triphosphate cyclohydrolase), and GAPDH (glyceraldehyde 3-phosphate dehydrogenase) in aortic branches using real-time polymerase chain reaction (RT-PCR). The investigators also assessed vascular reactivity in aortic rings in vitro, using a wire myograph and adding phenylephrine to induce contraction or acetylcholine to induce dilation.

Finally, the investigators conducted histopathologic analyses of aortic cryosections to assess the development of atherosclerosis, including monocyte/macrophage (MOMA)-2 staining to evaluate the macrophage content of the plaques. MOMA-2 staining density was reported as a

pathology score of 1 to 4, from light to heavy staining, on each slide assigned by a blinded observer. In addition, the plaque area was determined as a fraction of the total luminal area and normalized to controls by tracing the stained area using imaging software. Additional evaluation of vascular remodeling included mRNA expression of the matrix metalloproteinases (MMP) (i.e., MMP-2, -3, -7, and -9), as well as the tissue inhibitor of metalloproteinases 2 (i.e., TIMP-2) in homogenized aortic branches using RT-PCR. They also determined the activity of the MMP enzyme (referred to as “gelatinase activity,” which covers both MMP-2 and -9) in aortic tissue using in situ zymography, a fluorescent electrophoretic technique that visualizes enzyme activity in the tissue (see Section 2, Figure 5). In addition, concentrations of total cholesterol and oxidized lipoproteins (oxLP) were determined in plasma. OxLP reflects the degree of lipoproteins containing oxidatively modified apolipoprotein B (the main component of LDL) and was measured as TBARS per μg of cholesterol.

The large volume of data was initially analyzed by exposure atmospheres, using one-way analyses of variance (ANOVA) to compare the exposed groups with the unexposed group. To evaluate gas-particle interactions, the investigators followed up with selected pairwise comparisons using the F-test contrast from the ANOVA. They specifically compared the MVE low versus high concentrations; the MVE gases low versus high concentrations; sulfate, nitrate, or road dust plus MVE gases versus MVE gases at the high concentration; and sulfate, nitrate, or road dust plus MVE versus MVE at the low concentration. The investigators did not pursue other pairwise comparisons in order to avoid issues with multiple testing of the same data.

Because the exposures were conducted sequentially in different batches of mice, some exposures were repeated. Some of the data analyses included results for individual batches (each normalized to its own batch control group). In other analyses, results were averaged across batches, and data from all control groups were also combined.

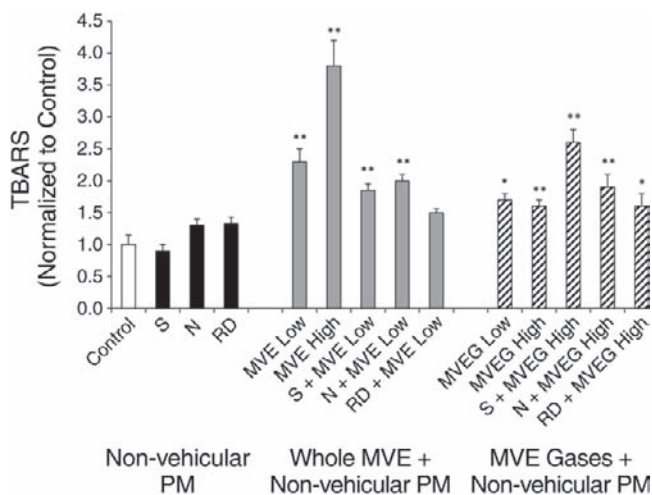
The investigators conducted additional analyses using the results of the detailed exposure characterizations, in which they related the biologic responses to the concentrations of specific components in the exposure atmospheres. This was done using a multiple additive regression tree (MART) approach as described by Seilkop and colleagues (2012). The MART analysis identified so-called predictors, which reflected PM components that were ranked according to how strongly they were associated with a specific endpoint. It was based on 36 chemical components that were measured across the 14 exposure atmospheres. The endpoints analyzed were those four for

which the initial ANOVA had shown a significant difference between exposed and control mice (i.e., TBARS, MMP enzyme activation, MOMA-2 staining of plaques, and plaque area).

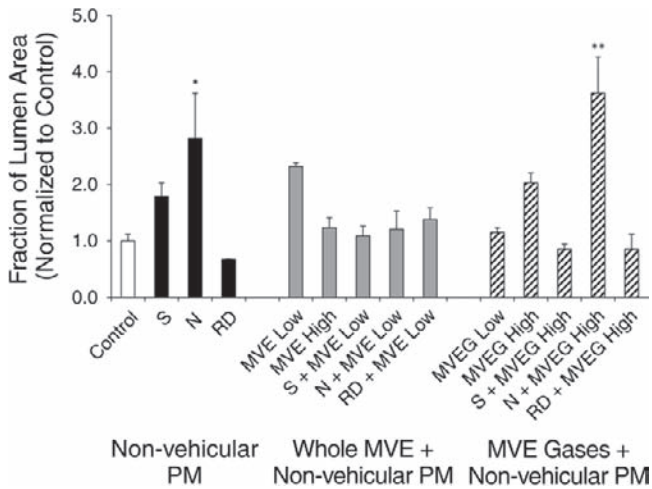
SUMMARY OF KEY TOXICOLOGIC RESULTS

Aortic lipid peroxidation (measured as TBARS), an indication of the generation of reactive oxygen species (ROS), was found to have increased after exposure to various atmospheres. MVE led to the largest increase (Commentary Figure 5). Removing the particles from the atmosphere reduced these effects but did not fully eliminate them. Atmospheres that contained MVE or MVE gases combined with non-vehicular PM showed some effects as well. In contrast, exposures to the non-vehicular PM atmospheres alone did not produce an effect.

The investigators also reported a significant induction of oxLP (measured as TBARS per μg cholesterol) in plasma of mice exposed to atmospheres containing MVE — MVE at the high concentration as well as MVE combined with sulfate, nitrate, or road dust — but not in plasma of mice exposed to MVE at the low concentration, to non-vehicular PM alone, or to MVE gases with or without sulfate, nitrate, or road dust (Section 2, Figure 14).

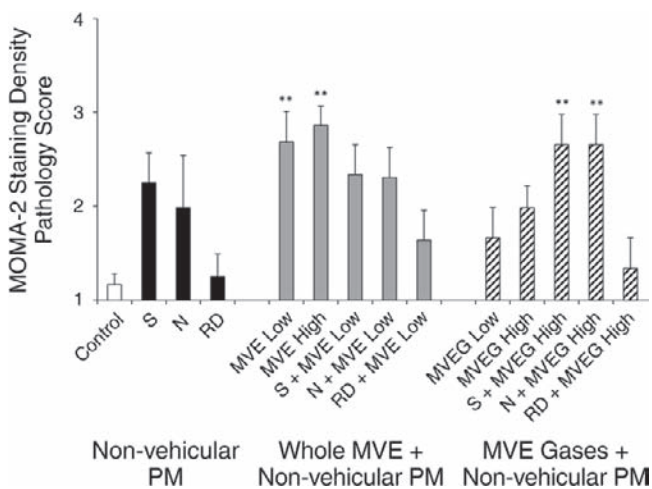


Commentary Figure 5. Lipid peroxidation in aortic tissue of mice exposed to MVE, MVE gases, or non-vehicular PM atmospheres, assessed by TBARS assay and normalized to control (1.0). White bars: mice exposed to filtered air. Black bars: mice exposed to non-vehicular PM (sulfate, nitrate, or road dust). Dark gray bars: mice exposed to MVE (at either of two concentrations) or to MVE at the low concentration plus non-vehicular PM. Hatched bars: mice exposed to MVE gases (at either of two concentrations) or to MVE gases at the high concentration plus non-vehicular PM. Asterisks indicate significantly different from control using ANOVA followed by the Dunnett test (* $P < 0.05$, ** $P < 0.01$). From data in Section 2, Figure 4, bottom panel.



Commentary Figure 6. Atherosclerotic plaque area in aortic tissue of mice exposed to MVE, MVE gases, or non-vehicular PM atmospheres, assessed by determining the size of the MOMA-2-stained area (in aortic-tissue cross-sections) compared with the total lumen area and normalized to control. See Commentary Figure 5 caption for details. From data in Section 2, Figure 8, bottom panel.

Atherosclerotic plaque formation increased after exposure to nitrate alone and nitrate combined with MVE gases but not to the other atmospheres (Commentary Figure 6). In contrast, macrophage infiltration of plaques (measured as MOMA-2 staining density) increased after exposure to low and high concentrations of MVE and to MVE gases combined with either sulfate or nitrate (Commentary Figure 7).

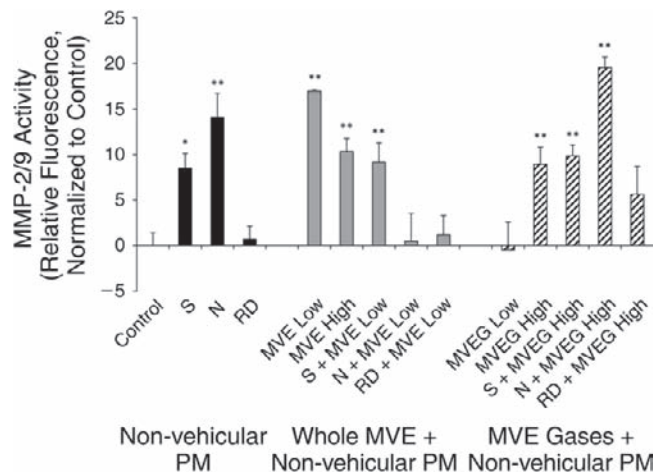


Commentary Figure 7. Macrophage infiltration of atherosclerotic plaques in aortic tissue of mice exposed to MVE, MVE gases, or non-vehicular PM atmospheres, assessed by scoring the density of MOMA-2 staining (in aortic-tissue cross-sections) on a scale of 1 to 4. See Commentary Figure 5 caption for details. From data in Section 2, Figure 8, top panel.

The investigators evaluated the expression of genes involved in oxidative and nitrosative stress and vascular inflammation in aortic tissues. There were no consistent changes in mRNA expression in aortic tissue for the metalloproteinases MMP-2, -3, -7, and -9 or for other inflammatory markers, such as HO-1, ET-1, TIMP-2, iNOS, and eNOS. However, the investigators reported increased MMP enzyme activity in aortic tissues — an indication of vascular remodeling — after exposure to all atmospheres except those containing road dust or MVE gases at the low concentration (see Section 2, Figure 6; and Commentary Figure 8).

The investigators reported some changes in vascular reactivity, that is, increased constriction (in response to phenylephrine) as well as decreased dilation (in response to acetylcholine) after exposure to MVE, sulfate, and MVE plus sulfate (Section 2, Figures 12 and 13). They did not observe other changes in vascular reactivity except for decreased constriction after exposure to nitrate, the opposite response of that observed for MVE and sulfate. An overview of the changes is shown in Commentary Table 4 (last two columns). The table includes a comparison of previous studies conducted at the same laboratory using exposures to DEE or GEE. A discussion of the comparisons is provided in the Evaluation section.

The investigators applied the advanced MART statistical analysis to the four endpoints that showed significance in the initial ANOVA (i.e., TBARS, MMP enzyme activity, macrophage infiltration, and plaque area). Based on the predictor relative importance scores (see Section 2, Table 8),



Commentary Figure 8. Metalloproteinase (MMP-2/9) activity in aortic tissue of mice exposed to MVE, MVE gases, or non-vehicular PM atmospheres, assessed by in situ zymography. See Commentary Figure 5 caption for details. From data in Section 2, Figure 6.

Commentary Table 4. Comparison of Biological Endpoints Across LRRRI Studies Using Single or Combined GEE and DEE Atmospheres^a

	Lund et al. 2007		Lund et al. 2009	Campen et al. 2010		Lund et al. 2009, 2011	Lund et al. 2011	Campen et al. 2013 (NPACT Study)	
Species	Mice	Mice	Mice	Mice	Mice	Humans	Mice	Mice	Mice
Engine exhaust type ^b	GEE	GEE	GEE	DEE	DEE	DEE	MVE	MVE	MVE
Exhaust composition (PM versus gases)	Whole exhaust	Gases only	Whole exhaust	Whole exhaust	Gases only	Whole exhaust	Whole exhaust	Whole exhaust	Gases only
Exposure duration	50 days	50 days	7 days	50 days	50 days	2 hr	7 days	50 days	50 days
PM (µg/m ³)	61	2	61	1012.3	27.5	106	300	310.1	11.9
NO _x (ppm)	19	18	19	35.4	33.5	3.9	18	31.3	30.6
CO (ppm)	80	80	80	30.9	30.9	9	104	101.5	105.8
Histology in Aortic Tissue									
Valve/leaflet lesion area	—	—	—	n.s.	n.s.	—	—	n.s.	n.s.
Macrophage infiltration (MOMA-2 staining)	—	—	—	Up	n.s.	—	Up	Up	n.s.
Valve collagen content (Sirius red staining)	—	—	—	Up	n.s.	—	—	—	—
Smooth muscle (actin staining)	—	—	—	n.s.	n.s.	—	—	—	—
Lipids (oil red staining)	—	—	—	Down	Down	—	—	—	—
Nitrotyrosine	Up	Up	—	—	—	—	—	—	—
MMP-9	Up	Up	—	—	—	—	—	—	—
Gene Expression in Aortic Tissue									
MMP-2	—	—	Up	—	—	—	—	n.s.	n.s.
MMP-3	Up	Up	—	n.s.	n.s.	—	—	n.s.	n.s.
MMP-7	Up	Up	—	n.s.	n.s.	—	—	n.s.	n.s.
MMP-8	—	—	—	Down	Down	—	—	—	—
MMP-9	Up	Up	Up ^c	Up	Up	—	Up	n.s.	n.s.
MMP-12	n.s.	n.s.	—	n.s.	n.s.	—	—	—	—
MMP-13	—	—	—	Down	Down	—	—	—	—
TIMP-1	n.s.	n.s.	n.s.	n.s.	n.s.	—	Up	—	—
TIMP-2	Up	Up	Up	Up	Up	—	Up	n.s.	Up ^d
ET-1	Up	Up	—	Up	Up	—	Up	n.s.	Up ^d
HO-1	Up	Up	—	n.s.	n.s.	—	—	n.s.	Up ^d
LOX-1	Up	—	—	—	—	—	Up	—	—
VEGF ^e	—	—	n.s.	—	—	—	—	—	—
eNOS	—	—	—	—	—	—	—	n.s.	n.s.
iNOS	—	—	—	—	—	—	—	n.s.	n.s.
DHFR	—	—	—	—	—	—	—	n.s.	n.s.
GTPCH	—	—	—	—	—	—	—	n.s.	n.s.

(Table continues on next page)

^a All measurements were made in aortic tissue except when indicated otherwise. Up and down indicate a significant decrease and increase, respectively, compared with results for mice exposed to filtered air. The abbreviation n.s. indicates not significant (compared with results for mice exposed to filtered air); — indicates that no results were reported.

^b GEE in Lund et al. (2007 and 2009) was from a 1996 General Motors 4.3 L, V6 gasoline engine. DEE in Campen et al. (2010) was from a 2000 Cummins 5.9-L, ISB turbo light-duty diesel engine. DEE in Lund et al. (2011) was from a Cummins 5.9-L, 205-hp light-duty diesel engine (for a human exposure study conducted at the U.S. EPA in North Carolina). MVE in Lund et al. (2009) and Campen et al. (2013) was generated by mixing GEE from a 1996 General Motors 4.3-L, V6 gasoline engine with DEE from a 5500-watt Yanmar diesel generator at a 1:5 ratio.

^c Significant increase in protein concentration as well as mRNA expression measured in aorta.

^d Increase was observed only with MVE gases at the low concentration.

^e VEGF indicates vascular endothelial growth factor.

^f sLOX indicates soluble lectin-like oxidized LDL receptor.

Commentary Table 4 (Continued). Comparison of Biological Endpoints Across LRRRI Studies Using Single or Combined GEE and DEE Atmospheres^a

	Lund et al. 2007		Lund et al. 2009	Campen et al. 2010		Lund et al. 2009, 2011	Lund et al. 2011	Campen et al. 2013 (NPACT Study)	
Other Assays in Aortic Tissue									
MMP-2/9 enzyme activity	—	—	Up	—	—	—	Up	Up	Up
Vascular reactivity	—	—	—	—	—	—	—	Up	n.s.
TBARS	Up	Up	Up	Up	Up	—	Up	Up	Up
Superoxide	—	—	Up	—	—	—	—	—	—
Other Assays in Plasma									
TBARS	n.s.	n.s.	—	—	—	—	—	—	—
oxLDL or oxLP	—	—	—	n.s.	n.s.	—	Up	Up	n.s.
sLOX ^f	—	—	—	—	—	Up	Up	—	—
MMP-9 protein	—	—	Up	—	—	Up	—	—	—
ET-1 protein	—	—	Up	—	—	Up	—	—	—
NO _x	—	—	Up	—	—	Up	—	—	—

^a All measurements were made in aortic tissue except when indicated otherwise. Up and down indicate a significant decrease and increase, respectively, compared with results for mice exposed to filtered air. The abbreviation n.s. indicates not significant (compared with results for mice exposed to filtered air); — indicates that no results were reported.

^b GEE in Lund et al. (2007 and 2009) was from a 1996 General Motors 4.3 L, V6 gasoline engine. DEE in Campen et al. (2010) was from a 2000 Cummins 5.9-L, ISB turbo light-duty diesel engine. DEE in Lund et al. (2011) was from a Cummins 5.9-L, 205-hp light-duty diesel engine (for a human exposure study conducted at the U.S. EPA in North Carolina). MVE in Lund et al. (2009) and Campen et al. (2013) was generated by mixing GEE from a 1996 General Motors 4.3-L, V6 gasoline engine with DEE from a 5500-watt Yanmar diesel generator at a 1:5 ratio.

^c Significant increase in protein concentration as well as mRNA expression measured in aorta.

^d Increase was observed only with MVE gases at the low concentration.

^e VEGF indicates vascular endothelial growth factor.

^f sLOX indicates soluble lectin-like oxidized LDL receptor.

the strongest predictors of biologic effects were gaseous components, such as non-methane volatile organic alkanes (the first predictor for TBARS), CO (the third predictor for TBARS), and volatile carbonyl ketones (the second predictor for MMP enzyme activity and the third for macrophage infiltration). Particulate components (ammonium, PM mass, and sulfate) constituted the top three predictors for plaque area and were included in the remaining top three positions for the three other endpoints as well. (Note that in these analyses, sulfate is a component measured in all the exposure atmospheres, that is, it is different from the laboratory-generated sulfate particles used to expose animals.)

The investigators also constructed plots that suggested stronger exposure–response patterns for TBARS (non-methane volatile organic alkanes and CO) and macrophage infiltration (sulfate and ammonium) and were relatively weaker for the other endpoints (see Section 2, Figure 15). Graphs of concentrations of the top three MART predictors against the four biologic responses showed reasonable evidence of a dose–response relationship

between TBARS and both non-methane volatile organic alkanes and CO (see Section 2, Figures 15 and 16) but less convincing or no evidence for dose–response relationships between the other endpoints and their top three predictors.

EVALUATION OF THE TOXICOLOGY STUDY

In its independent evaluation, the Panel noted that Campen and colleagues had conducted a complex study with an impressive number of single and combined exposure atmospheres. A novel feature was the use of MVE, in which exhausts from a diesel and a gasoline engine were combined. The investigators also included atmospheres with MVE gases only (without PM), to specifically address the toxicity of gases versus particles and to evaluate possible particle–gas interactions. They were successful in generating a variety of complex atmospheres; the concentrations achieved were close to the targeted concentrations (see Section 2, Table 6). The MVE exposure system was developed recently at LRRRI; results from short-term

exposures of ApoE knockout mice to MVE, assessing endpoints similar to those in the current study, were published recently (Lund et al. 2011).

The following section of the Commentary first discusses the findings and compares them with earlier work conducted at LRRRI using single DEE and GEE exposures and then discusses some limitations of and uncertainties about the approaches and techniques used. Finally, it discusses the role of the composition of the exposure atmospheres in causing possible health effects.

Lipid Peroxidation in Aortic Tissue

Lipid peroxidation (measured as TBARS) increased significantly after exposure to a number of atmospheres, specifically those that contained MVE or MVE gases; non-vehicular PM alone did not have an effect. Exposure to MVE led to the largest increase in aortic TBARS; this response was significantly larger than the response to MVE gases. As noted by the investigators, filtering the particles from the exhaust significantly reduced the effects but did not eliminate them. These results were different from those of previous studies conducted at LRRRI with separate DEE and GEE exposures (Commentary Table 4); in those studies, the lipid peroxidation responses increased similarly in mice exposed to whole DEE versus filtered DEE (Campen et al. 2010) and also increased similarly in mice exposed to GEE versus filtered GEE (Lund et al. 2007), indicating that the gaseous components were responsible for the TBARS responses in those two studies. The Panel thought that the current study challenged this hypothesis, because a significantly larger TBARS response was observed for MVE versus MVE gases (see Section 2, Table 7), suggesting that the particulate component played a significant role in the induction of aortic lipid peroxidation in addition to the effects observed after exposure to MVE gases.

Overall, these results suggest that both MVE particles and gases play a significant role in the induction of aortic lipid peroxidation: the MVE gas exposure (without PM) had an effect by itself, but exposure to whole MVE (PM plus gases) had a significantly larger effect. The non-vehicular PM did not have any effects on its own but did when MVE or MVE gases were added. TBARS levels, for example, did not change after exposure to sulfate alone but increased after exposure to sulfate plus MVE gases; this increase was significantly larger than that observed after exposure to MVE gases alone.

However, in the absence of exposures using MVE particles alone (i.e., without the gases, which is technically difficult to do), it remains unclear whether MVE particles would affect aortic lipid peroxidation independently.

One interesting possibility is that the GEE component of the MVE contains particles that might have different toxicity than the particles in DEE, but more research is needed to determine whether this is indeed the case.

Oxidation of Lipoproteins in Plasma

The investigators found that there was a significant increase of oxLP in the plasma of mice exposed to atmospheres containing MVE; they reported that this result was in agreement with the aortic lipid peroxidation results. However, the Panel noted that atmospheres containing MVE gases induced aortic lipid peroxidation but did not induce any changes in oxLP, whether or not other non-vehicular PM was present (see Section 2, Figure 14). Therefore, only atmospheres that contained both MVE particles and gases led to increased levels of oxLP in the exposed mice.

The investigators suggested that “a factor that may explain the relative potency of the MVE atmosphere is particulate surface area, which is quite high on the complex diesel particles compared with non-vehicular PM [sulfate, nitrate, and road dust].” It has been hypothesized that greater surface area, a characteristic of smaller particles, could result in greater biologic reactivity of the particles (Tran et al. 2000; Brown et al. 2001; Donaldson et al. 2002; Araujo and Nel 2009). The investigators did observe some differences in particle sizes among atmospheres. Particles in the MVE atmosphere had a slightly lower number mean aerodynamic diameter (NMAD) of 74 nm compared with an NMAD of 83 nm for road dust, but a larger NMAD than that of the nitrate particles, at 52 nm (see Appendix Table R.2). Despite some differences in particle sizes among atmospheres, it was not apparent that the slightly smaller PM consistently exerted larger biologic effects. Although it remains unclear whether smaller PM with a larger surface area is more toxic, it could be argued that the smaller particles present in the MVE atmospheres were sufficient to boost the toxicity of otherwise inert road dust.

Atherosclerotic Plaque Area and Inflammation

The investigators found that exposure to nitrate alone or nitrate plus MVE gases led to significant increases of atherosclerotic plaque area, but none of the other atmospheres caused a change in plaque area (Section 2, Figure 8, lower panel). Campen and colleagues (2010) did not find an increase in aortic valve lesion area in ApoE knockout mice exposed for 50 days to DEE at a higher PM_{2.5} concentration (~1,000 µg/m³), which is in line with the lack of effect for exposures to MVE or MVE gases in the current study (see also Commentary Table 4).

In contrast, macrophage infiltration of plaques, a pro-inflammatory effect, was affected by exposure to MVE and to MVE gases plus sulfate or nitrate (see Section 2, Figure 8, upper panel). The fact that only whole MVE or atmospheres with MVE gases plus sulfate or nitrate increased macrophage infiltration suggests that the combination of particles and gases is essential for the inflammatory effects, because neither MVE gases nor PM alone increased macrophage infiltration. The increased macrophage infiltration after MVE exposure is consistent with results reported in the investigators' previous study of DEE exposure (Campen et al. 2010), although the dose-response relationship reported in the previous study was not observed in the current study. This could have been caused by the fact that the PM concentrations used in the current study (100 and 300 $\mu\text{g}/\text{m}^3$) were less than a third of the high concentration ($\sim 1000 \mu\text{g}/\text{m}^3$) used in the previous study.

Interestingly, the combination of nitrate and MVE gases (at the high concentration) led to significant proatherogenic or proinflammatory effects, whereas the combination of nitrate with whole MVE (i.e., with gases at the low concentration) did not (see Section 2, Figure 8, upper panel). These data are of potential interest because they suggest that a specific component of secondary aerosols (nitrate) might be more potent than other components of the air pollutant mixture in affecting plaque size. The investigators observed other interesting differences between the results for plaque area and macrophage infiltration of plaques. For example, MVE at the low and high concentrations increased macrophage infiltration but did not affect the plaque area. On the other hand, exposure to nitrate alone increased the plaque area but did not affect macrophage infiltration. This dissociation is consistent with previous findings showing that DEE induced an increase in the macrophage component of plaques but did not increase plaque area (Campen et al. 2010).

The Panel thought that there are several caveats that suggest a cautious interpretation of these results. First, to calculate plaque area, the investigators normalized the data to the luminal area. This measurement could be subject to variability because of the sample collection procedures (luminal area varies depending on the state of contraction of the aorta). Because the aorta samples were collected fresh rather than after perfusion and fixation with formaldehyde, the vascular tone could have changed during tissue collection and thus affected the results.

Second, the investigators reported large variability in macrophage infiltration results (Section 2, Figure 8) that might in part be the result of small group size, which was for some groups only three mice. The same issue applies

to the plaque area results. There might thus have been insufficient power to distinguish a statistically significant effect. Third, the estimation of the pathology scores to quantify the density of MOMA-2 staining of macrophages was semiquantitative and could be considered somewhat subjective. It is unclear whether the pathology scores reflected only the intensity of the staining or if they also included an assessment of the size of the stained areas. Even though the investigators tried to standardize the scoring by mixing batches during staining and using the same observer, the results might have been affected by variations in the intensity of immunohistochemical staining because of technical issues during the staining procedures (e.g., duration of staining and washing cycles) and thus not be an accurate representation of the macrophage content of the plaques.

Metalloproteinases and Other Biologic Markers in Aortic Tissue

The investigators reported increased activity of the MMP enzyme in aortic tissue after exposure to most of the atmospheres compared with controls exposed to filtered air (Section 2, Figure 6). This increase was not confirmed by mRNA expression of MMP-2 and MMP-9 in aortic tissue; the mRNA expression did not significantly change (Section 2, Figure 10). The investigators reported earlier that metalloproteinase mRNA expression was affected by exposure to GEE (Lund et al. 2007, 2009), DEE (Campen et al. 2010), or MVE (Lund et al. 2011) (Commentary Table 4). Interestingly, the responses with whole GEE and DEE were the same as when the PM was removed, indicating that the gaseous components were the main driver of the metalloproteinase response in aortic tissue (Lund et al. 2007; Campen et al. 2010). It is not clear why the current study failed to find increases in mRNA expression of metalloproteinases; the investigators mentioned some technical difficulties in performing the assays, which limits the interpretation of the current results.

There was also no significant upregulation of HO-1 or ET-1 in the current study (Section 2, Figure 11), in contrast with the previous studies in which both ET-1 and HO-1 were upregulated by exposure to GEE (Lund et al. 2007); ET-1 but not HO-1 was upregulated by exposure to DEE (Campen et al. 2010); and ET-1 was upregulated by exposure to MVE (Lund et al. 2011) (Commentary Table 4). One possibility for this is that aortic gene expression depends on the specific concentrations of either pure GEE or DEE or the specific proportion of gasoline and diesel in MVE. For instance, upregulation of these genes in previous studies mostly occurred at the highest concentration of DEE (1000 $\mu\text{g}/\text{m}^3$) (Campen et al. 2010). An even larger number

of changes was observed with GEE ($60 \mu\text{g}/\text{m}^3$) (Lund et al. 2007). Shorter-term exposures of mice for 7 days to GEE ($60 \mu\text{g}/\text{m}^3$) or MVE ($300 \mu\text{g}/\text{m}^3$) also led to increases in MMP and ET-1 (Lund et al. 2009, 2011). This might indicate that GEE is equally or possibly more potent than DEE in affecting metalloproteinases and other inflammatory markers in aortic tissue. The more pronounced results obtained with the short-term GEE exposures might also be an indication that there could have been an adaptive response for longer-term exposures.

It is interesting, however, that although the levels of MMP-2 and MMP-9 mRNA were not affected in the current study, MMP enzyme activity did increase. Perhaps MMP protein levels or their functional status remained elevated after 50 days of exposures, when mRNA expression might already have returned to normal. However, the investigators did not assess MMP protein levels in aortic tissue in the current study. The fact that mRNA expression remained elevated after 50-day exposures to GEE (Lund et al. 2007) but not after 50-day exposures to MVE (in the current study) remains unexplained.

Vascular Reactivity

The investigators noted significantly increased vascular constriction and decreased dilation after exposure to MVE, sulfate, or MVE plus sulfate (Section 2, Figure 12). Other atmospheres had no significant effects except for nitrate, which had the opposite effect, reducing constriction in response to phenylephrine. The increased vasoconstriction after exposure to MVE is in line with the observation of diminished forearm blood flow in humans exposed to DEE ($300 \mu\text{g}/\text{m}^3$) for 1 or 2 hours (Mills et al. 2005, 2011); this effect was not seen with filtered exhaust (Mills et al. 2011). Other studies found contradictory evidence when exposing mouse aortic rings in vitro to resuspended diesel exhaust particles. Although a fairly consistent impairment of vasodilation was observed, constriction either increased (Campen et al. 2005), did not significantly change (Miller et al. 2009), or decreased (Mills et al. 2011). At the same time, the finding of effects with exposure to sulfate alone is a relatively novel toxicologic finding; additional analyses to confirm this would be valuable.

One possible explanation for the observed discrepancies is that the evaluation of vascular function is technically challenging. The variability in baseline responses of aortic rings to phenylephrine or acetylcholine stimulation among three technicians in the current study and the fact that the results of one batch were found to be invalid attest to these challenges and meant that data from different batches could not be combined. In addition, the investigators found an opposite effect for nitrate exposures that was

difficult to explain. They suggested that this could have been caused by the “ability of [nitrates] to act as a nitrogen donor in the vascular system and thus contribute to NO production.” The Panel thought this suggestion was premature, because exposure to nitrate plus MVE did not cause significant changes in vasoconstriction. Although it is possible that the presence of gases and other PM could counter the attenuating effect of nitrate, the lack of consistency and reproducibility among various experiments warrants caution in interpreting these results.

Biologic Responses and Exposure Composition

As noted in the results and discussion above, the effects of exposure atmospheres varied across the biologic responses. The differences between the atmospheres with and without particles are of special interest, providing insight into the role of particles and gases and how they might interact and possibly enhance the effects. Nitrate and sulfate, for example, had no biologic effects by themselves, but effects were observed when either of them was combined with MVE (e.g., TBARS and oxLP). Even more striking, MVE gases, sulfate, or nitrate alone had no effect on macrophages but did when they were combined. The investigators interpreted these results as suggestive evidence for gas–particle interactions. Of note, the top three predictors for plaque area were all particulate components (ammonium, PM, and sulfate), unlike the predictors for TBARS, which were gaseous components (non-methane volatile organic alkanes and CO) as well as sulfate. However, the lack of consistent exposure–response patterns in the MART analysis, together with the small sample size of aortic sections analyzed per mouse, prevent firm conclusions based on these data.

The investigators also hypothesized that the EC component of DEE PM might have contributed to greater interaction between gases and particles in the various atmospheres. This is a plausible hypothesis because EC particles contain sites with unpaired electrons that are likely to react with other molecules, such as oxygen, hydrogen, and nitrogen, during secondary PM formation in exhaust (Chang et al. 1982). Indeed, MVE at the high concentration and all three combinations of non-vehicular PM and MVE led to increased levels of oxLP in plasma, whereas neither MVE at the low concentration, which had substantially lower levels of EC, nor the atmospheres with non-vehicular PM, which did not have EC, did (see Section 2, Figure 14). This not only supports the notion that EC might have contributed to these effects, but it also suggests that there could be a threshold, that is, a minimum concentration of EC required before a response is observed.

Exposure Characterization

The investigators conducted an extensive characterization of aerosol components in each exposure atmosphere. This not only strengthened their experimental protocol but enabled them to extend their analyses and attempt to dissect the contributions of specific components to the overall toxicity of the PM and gaseous mixtures. However, the absence of an MVE particle-only exposure atmosphere (at two PM concentrations but without MVE gases) limited the extent to which the independent role of particles could be assessed. Isolating MVE particles for such studies remains technically challenging.

The exposure data indicated that the target conditions were achieved, representing a wide range of mixtures. The various atmospheres that were generated for the 50-day exposures represented a range of model atmospheric compositions that the investigators hoped would provide new insights into the roles of various particle types and sources in toxicity, in particular, cardiovascular effects.

The inclusion of MVE (a mixture of GEE and DEE) combined with sulfate, nitrate, or road dust was a novel aspect of the study, taking a step toward representing real-world atmospheric mixtures and addressing the question of whether typical combinations of the major chemical components of fine PM have different effects than do single components or sources of PM. Nonetheless, it should be kept in mind that these laboratory-generated atmospheres were less complex than real-world atmospheres. In addition, although the major components were — by design — dramatically different from atmosphere to atmosphere, detailed compositional data on the various gases and particle components, such as trace metals, suggested that differences among the trace components in the various atmospheres might have been less pronounced.

Exposure Atmosphere Composition

The study results have provided some unique insights into the potential health effects of urban, near-roadway exposures that would be interesting to pursue in future research. They indicate that combining MVE with freshly generated non-vehicular PM (sulfate, nitrate, or road dust) changes the chemical composition of the MVE particles. Specifically, the PM composition of these combined atmospheres appears to be considerably different from the simple sum of their parts. This is illustrated by the PM composition of MVE and sulfate atmospheres separately (Appendix Table R.2, available on the HEI Web site) compared with that of the two combined (Appendix Table R.1). This points to the uptake onto the non-vehicular particle surfaces of gaseous compounds originating from the MVE that were likely organic in nature. To a lesser extent,

this also appears to be the case for the combination of MVE gases and the non-vehicular particles.

The Panel noted that in the case of combining MVE gases with non-vehicular particles, the semivolatile organic compounds that are most likely to be taken up by the particles are removed when the exhaust is filtered to remove the MVE particles. Technical advances are needed in order to correctly generate such gaseous combination atmospheres, because particle filtration does more than simply remove particles. However, in the real world, MVE gases do not occur in isolation, and thus the combination of the MVE with sulfate, nitrate, or road dust was more realistic. The results of the current study clearly point to the need for more toxicology research that uses such combination atmospheres.

The investigators applied MART analysis to explore the potential effects of various component concentrations among atmospheres (as opposed to comparing the atmospheres themselves without taking into account their detailed composition). The Panel thought that this was an interesting approach but that there were two factors that limited the interpretation. First, as noted by the investigators, the number of independent atmospheres was small compared with the number of components measured. This decreased the statistical power to identify components that might pose the greatest cardiovascular risk. Not surprisingly, some unexpected rankings were observed, such as the high importance of ammonium. Second, it appeared that the detailed exposure characterization was conducted on a few occasions only; thus it remains unknown what the variability in composition from day to day might have been or how well the reported averages reflected the composition over the 50-day exposure period.

Key exposure parameters, such as continuous PM mass, engine operation, proportions of gasoline and diesel exhaust versus dilution air, and fuel composition were monitored daily and were likely sufficiently stable. However, there might have been variations in the concentrations of many of the trace components because of the fact that the exposure-generation equipment was stopped and restarted each day. If the cardiovascular responses were dependent on these trace components, which is what the MART analysis was meant to assess, then variation in the true average 50-day exposure composition might have influenced the results. On the other hand, it would be impractical and cost-prohibitive to conduct daily analysis of such detailed inorganic and organic particle and gaseous chemical speciation. Furthermore, measuring the detailed composition of a large number of exposures on a daily basis is not guaranteed to provide the desired answers. Given such limitations, the Panel noted that the

level of compositional detail that the investigators provided was impressive and was probably at the limit of what is currently feasible.

Overall, the results from the current study underscore the importance of investigating mixtures that better reflect real-world conditions. These exposures, although imperfect in that they involved laboratory-generated PM components and no aging of the materials before exposure, did allow for pre-existing sulfate, nitrate, and road dust to be mixed constantly with fresh vehicle exhaust, thus better approximating the constant mixing in the near-road urban environment. The current results also suggest that semivolatile organic compounds might be taken up from fresh exhaust by the non-vehicular particles, which partitioning theory, atmospheric chemistry, and recent experimental evidence (Li et al. 2011) would indicate is possible. The implication would be that these compounds might exist on or near the particle surface and might thus be more readily available for uptake once deposited in the lungs.

Overall Interpretation

The investigators drew two main conclusions from their toxicologic study: (1) subchronic exposure to vehicle-related mixed emissions results in statistically significant increases in lipid peroxidation, circulating oxLP, vascular MMP expression and activity, and enhanced vasoconstriction in ApoE knockout mice, each of which is associated with progression of atherosclerosis and clinical cardiovascular events; and (2) exposure to nitrate, sulfate, or fine road dust alone did not appear to drive any of the statistically significant effects observed in the cardiovascular system.

The Panel agrees with the investigators' first conclusion. The current study, in which ApoE knockout mice were exposed for 50 days to MVE, significantly extended the investigators' previous study, in which 7-day exposures of mice to MVE led to similar biologic responses (Lund et al. 2011). Although the current findings suggest an important contribution by gaseous components, they differ from those of the investigators' previous studies in that the particulate components were also important in the induction of biologic effects (e.g., TBARS), suggesting that gas-particle interactions might be important. It was interesting to note that nitrate or nitrate plus MVE gases increased plaque area, whereas exposure to MVE (in the current study) or DEE for 50 days (in Campen et al. 2010) showed no effect on atherosclerotic lesions. This suggests that nitrate might be more proatherogenic than all of the other PM atmospheres that were not enriched in nitrate, which would contradict the investigators' second conclusion.

The effects of exposure to nitrate are more similar to the proatherogenic effects induced by markedly longer exposures (5 months) to DEE at 438 $\mu\text{g}/\text{m}^3$ in a study at Tuxedo, New York (Quan et al. 2010), although it should be noted that the response was even stronger with CAPs in the companion study at NYU (Chen and Lippmann 2013).

A caveat, however, is that in the MART analyses nitrate was only the 17th predictor for plaque, with a relatively low score of 24 (out of a maximum of 100). Given the small number of samples and the large variability in the biologic data, it would be important to repeat these exposures in the future to confirm whether emissions rich in nitrate can indeed increase atherogenesis. Another caveat concerns the animal model used. Although the current study and the studies at NYU (Quan et al. 2010; Chen and Lippmann 2013) both used ApoE knockout mice, an important difference between them was that in the current study at LRRRI the mice were fed a high-fat/high-cholesterol diet, whereas in the NYU studies they were fed normal chow. This might have led to a higher level of atherosclerosis in the mice exposed to filtered air in the current study, which could have obscured the possible effects caused by exposure to MVE.

The Panel wishes to highlight the following additional observations:

1. Different components appeared to be associated with different endpoints, even though several of the endpoints are thought to reflect various aspects of the same disease process, namely, atherogenesis. This result was relatively unexpected and raises the question of whether some of the evaluated outcomes reflected true pathogenic mediators or whether they merely served as markers of exposure or of effect.
2. Gaseous components were strong drivers of lipid peroxidation in the vasculature, as suggested by the MART analysis, in which two of the three top predictors consisted of gaseous components (non-methane volatile organic alkanes and CO). Thus, TBARS in aortic tissue did not increase after exposure to any of the non-vehicular PM components alone but did increase after exposure to the MVE, MVE gases, and combined atmospheres. This result was consistent with the investigators' previous studies, in which removing DEE particles did not alter the responses induced by whole DEE. However, the investigators did not include an important control, namely, MVE particles without gases, which admittedly is technically difficult to achieve. Low concentrations of particles remained present in the MVE gases atmospheres, likely in part due to particles produced by the animals. Conversely, some gases are removed in the process of filtering the particles. Although the data in the

current study are suggestive of gas–particle interactions, the evidence remains ambiguous.

3. Various atmospheres influenced aortic TBARS and oxLP differently. This was intriguing, because both endpoints equally reflect lipid peroxidation — although in different settings, that is, in the vascular wall (TBARS) and in circulating blood (oxLP). It was noteworthy that, despite the differences observed, both endpoints appeared to be affected by both gaseous and particulate components.
4. The actual development of atherosclerotic plaques could be driven primarily by particulate components, because the top two MART predictors for macrophage infiltration were particulate components (sulfate and ammonium), and none of the gaseous atmospheres promoted atherogenesis. Sulfate and ammonium were among the top predictors for three out of the four endpoints analyzed by MART; in addition, the only non-vehicular PM that had an effect on atherogenesis was nitrate, which has a high concentration of ammonium. Although these data require further validation, they suggest that particulate components are the most predictive of outcomes that are more closely related to plaque formation (plaque area and macrophage infiltration).

In summary, this is an interesting study with impressive and comprehensive head-to-head comparisons among various exposure atmospheres. The results support the notion that both particulate and gaseous components have a role in the induction of various cardiovascular outcomes. However, although suggestive, the data are not conclusive for the presence of particle–gas interactions in the induction of proatherogenic effects. Further studies are required to elucidate this and to confirm some of the novel findings of this study.

OVERALL EVALUATION OF THE VEDAL REPORT

In Section 1 of this report, Vedal and colleagues' overall objective was to identify the chemical components of ambient PM that contribute to the cardiovascular effects associated with long-term PM exposure, including progression of atherosclerosis, cardiovascular events, and deaths. The investigators' hypothesis was that PM_{2.5} components derived from motor vehicle exhaust emissions are associated with more long-term cardiovascular effects than are PM_{2.5} components derived from crustal or secondary organic sources. In Section 2, Campen and colleagues' overall objective was to conduct laboratory toxicology

studies, evaluating the cardiovascular impacts in mice of the inhalation of atmospheres of various compositions, that could serve to inform the regional and source-related contrasts noted in epidemiologic findings about cardiovascular morbidity and mortality.

In the final section of the Commentary (below), the Panel discusses the research detailed in Sections 1 and 2 of the report and evaluates the results in light of the overall objectives. In addition, the Panel evaluates the integrated discussion in Section 3 of the report and assesses the overall findings with regard to key questions on the role of PM_{2.5} mass and PM_{2.5} components in contributing to adverse health outcomes — questions that reflect back to the original goals of the NPACT initiative.

PM_{2.5} COMPONENTS AND CARDIOVASCULAR OUTCOMES IN HUMANS

The MESA and WHI-OS epidemiology study by Vedal and colleagues, presented in Section 1 of the report, represents one of the first focused attempts at assessing the long-term human health effects of selected particle components. The MESA study had the interesting feature of investigating the effects of long-term exposure to PM_{2.5} and selected components on the development of sub-clinical manifestations of atherosclerosis in a human population. The WHI-OS study also investigated the relationships between long-term exposures and initial cardiovascular events, including stroke and coronary revascularization procedures. The studies also attempted to estimate long-term exposure to selected PM components on a within-city spatial scale, in contrast with previous city-based studies that relied solely on CSN monitors and exposure gradients across larger geographic domains.

However, many of the results of the overall study by Vedal and colleagues were less conclusive than the Panel would have liked. The uncertainty in the within-city exposure assessments caused by the supplemental monitoring campaigns (2-week samples) and the sheer technical difficulty of the modeling tasks complicated the exposure assessment. Short follow-up times in the MESA study for CAC and CIMT limited the assessment of progression, resulting in the investigators' main conclusions being primarily based on one baseline measure of the degree of subclinical atherosclerosis. Further follow-up data on atherosclerosis progression would allow better interpretation of associations, and an analysis of additional available MESA cohort outcomes (e.g., data on vascular reactivity, markers of inflammation and coagulation, lipid oxidation, and adhesion molecules) will allow a much more comprehensive assessment of health effects and further complement the toxicology study.

The Vedal study did produce some interesting information on associations between the selected components and cardiovascular health effects versus the associations reported for $PM_{2.5}$. Although the initial hypothesis was that components of $PM_{2.5}$, such as sulfur (sulfate), OC, and EC, would potentially be more toxic than the mixture of components measured as $PM_{2.5}$ mass, the epidemiologic results were mixed when component effect estimates were compared directly for the outcomes in the two cohorts. In the MESA study, CIMT and CAC were more strongly associated with sulfur than with $PM_{2.5}$ in some models. In the WHI-OS study, OC was equally or more strongly associated with all CVD deaths, atherosclerotic deaths, and both cerebrovascular events and deaths than was $PM_{2.5}$ mass. These results suggest that the OC and sulfur components in $PM_{2.5}$ might be of greater concern for human health than $PM_{2.5}$ mass alone, but they will require additional studies to confirm, particularly given that both components account for a high percentage of total $PM_{2.5}$ mass.

The primary models used in these epidemiologic studies involved comparing epidemiologic results among pollutants according to their driving source of variability (i.e., within- vs. between-city). The precision of the modeled effect estimates varied by pollutant when all cities were combined, which led to results that were difficult to interpret and made it difficult to draw conclusions about the overall study hypothesis. Furthermore, although including results from more than one exposure model can help add to the weight of evidence, it can also complicate interpretation, especially when the models differed in the quality of their inputs and construction or emphasized a different aspect of the air pollution exposure signal. In the case of this study, the spatiotemporal and spatial models did just this, and thus it is difficult to know how to interpret both the similarities and the differences in the associations that were found.

Previous epidemiologic studies have found associations between secondary sulfate arising from regional, photochemically aged air masses and health effects. The associations found in the MESA and WHI-OS studies support earlier findings that adverse health effects are associated with these aged air masses. In the WHI-OS study, there was consistency across endpoints showing sulfur was positively associated. But because sulfur was also strongly correlated with $PM_{2.5}$, such consistency among the associations makes it difficult to distinguish among effects. In addition, sulfur was consistently associated with CIMT in the MESA study.

Arguably the most noteworthy results in this work were the associations found for OC (e.g., with CIMT in the

MESA study) and the lack of significant associations for EC, which has less ambiguous sources (i.e., combustion sources typically linked to traffic). That OC had effects was not unexpected; it consists of thousands of species, several of which are known to trigger biologic responses, and it is commonly found among the particles associated with vehicle exhaust. That OC was found to be associated with endpoints using both the spatiotemporal and spatial models, which are not well correlated, is more difficult to interpret.

What do these different predicted exposure surfaces (i.e., modeled concentrations across geographic areas) represent, and are there some similarities that lead to OC being associated with CIMT in both models? The study compared MESA Air 2-week OC measurements (used to develop the spatiotemporal model) with standard CSN and IMPROVE 24-hour measurements (used to develop the national spatial model) and showed that there was reasonable agreement between these measurements, but also some disagreement. OC detected from a quartz filter sampled at a slow flow rate for 2 weeks is likely to contain both OC that landed on the filter during sampling and OC resulting from the aging of more volatile carbon compounds. Indeed, the MESA Air 2-week OC measurements were biased low compared with the standard measurements, which also have their own limitations. The net result is that the OC concentration data set used to develop the spatiotemporal model was less likely to represent the very dynamic OC that exists in equilibrium with gases and other particle surfaces in areas of fresh emissions (i.e., OC in this study was less likely to be a strong indicator of motor vehicle emissions). In contrast, EC, being from combustion and generally inert in the atmosphere, should be a good indicator of fresh emissions. Given the richer spatial coverage in the MESA Air monitoring data set, the spatiotemporal model predicted considerably greater EC exposures and much more variability among participants compared with those of the national spatial model. This behavior suggests that the spatiotemporal model exposures for EC were more realistic; this was likely also the case for the OC predictions from this model. However, the difference between the OC exposures predicted by the two models was not as large as the difference for EC, although the spatiotemporal OC model did predict greater variability among participants.

It is also interesting to compare the large-scale pattern in OC from the two models. It reveals that there was a clear concentration gradient across cities (i.e., St. Paul, Chicago, Baltimore, New York, Los Angeles, Winston-Salem from lowest to highest, based on median OC predicted by the spatiotemporal model). Notably, the national spatial model, built on national monitoring data, suggested a different gradient (Winston-Salem, Chicago, St. Paul,

Baltimore, New York, Los Angeles) and was less able to predict within-city variability. Then how is it possible that the OC exposures assigned from the spatiotemporal model led to positive associations with CIMT, but only when the effect of city was not included in the models? This question remains to be answered, as does the question of what this model behavior tells us about which aspects of OC and, more important, which source(s) of OC might be driving the associations. The effects of accounting for city in the model are potentially telling. With such an adjustment for city, OC assigned using the spatiotemporal model no longer has an effect on CIMT, which is similar to the effect of EC. On the other hand, when city is accounted for (using the spatiotemporal model), significant associations are found between OC or EC and CAC. When more emphasis is placed on CAC — which is arguably better linked to atherosclerosis progression — a different story emerges, one that is potentially better linked to the main study hypothesis that particles related to motor vehicles are more toxic than other particles.

More consistency also emerges between the findings for the MESA and WHI-OS cohorts. In particular, the analysis of the WHI-OS endpoints using the national spatial model also found some associations with EC but generally only after isolating the effect of within-city exposure differences. This suggests that even though the national spatial model was not optimal for small-scale changes, its predictions for EC at this scale had some validity, which is further supported by the results of the comparisons reported in the study for EC exposures estimated for each city using spatiotemporal versus national spatial models.

MVE AND PM_{2.5} COMPONENTS AND CARDIOVASCULAR OUTCOMES IN MICE

The toxicology study provided some insights into the effects of exposures to complex atmospheres on vascular endpoints in ApoE knockout mice. The investigators drew two main conclusions from their study: (1) subchronic exposure to vehicle-related mixed emissions results in statistically significant increases in lipid peroxidation, circulating oxLP, vascular MMP expression and activity, and enhanced vasoconstriction in ApoE knockout mice, each of which is associated with progression of atherosclerosis and clinical cardiovascular events; and (2) exposure to nitrate, sulfate, or road dust alone did not appear to drive any of the statistically significant effects observed in the cardiovascular system.

The study has thus confirmed previous evidence on the toxicity of DEE and GEE and has provided relatively new evidence that similar effects are seen with combinations of these two types of engine exhaust. The study also

confirmed that exposure to MVE gases alone has some effects, although they were not as large as those of MVE. The relative roles of particles and gases in causing these effects remain somewhat unclear, however, and further research is recommended, in particular because of the absence of a control group exposed to MVE particles without the gases.

The study collected a wealth of information on exposure atmosphere composition, analyzing close to 500 individual compounds. Using MART statistical analyses, the investigators explored the role of composition, but this wealth of data could be further investigated.

SUMMARY AND CONCLUSIONS FOR THE VEDAL REPORT

Although the epidemiologic (Section 1) and toxicologic (Section 2) studies were in theory designed to complement one another, there are reasons why a joint interpretation of their results must be undertaken with some caution. The toxicology study, for example, found clear adverse effects of exposure to engine exhaust, that is, traffic-related pollutants, whereas the epidemiology study found some evidence for adverse effects of OC but less for EC, a component that has traditionally been associated with traffic exposure.

One important consideration is that the mice in the toxicology study were exposed to relatively high concentrations of PM_{2.5} and components (100 and 300 µg/m³), an order of magnitude higher than the highest concentrations in the MESA and WHI-OS epidemiology studies. Although such concentrations of PM occur in ambient air under certain conditions and in occupational settings, it remains unclear whether they might activate somewhat different mechanistic pathways in mice compared with the humans in the MESA and WHI-OS cohorts.

The toxicology and epidemiology studies also had very different study designs. Whereas the mice were exposed to MVE, non-vehicular PM from three sources, and mixtures of MVE or MVE gases and the non-vehicular particles, the human cohort members were exposed to more complicated ambient atmospheres at varying pollution concentrations. Although the endpoints assessed in the mouse and human studies were cardiovascular in nature, they were not closely matched for possible mechanisms of effect. The measurement of CIMT in the MESA cohort was closest to the measured endpoints in mice, but measurement error and a short follow-up period meant that the uncertainty of the estimates of pollutant effects would make comparisons with the toxicology results difficult. In addition, the Panel was surprised by the missed opportunity to match outcomes. The MESA study had additional

data on clinical markers, such as vascular reactivity, markers of inflammation and coagulation, lipid oxidation, and adhesion molecules, that were better matched to the markers measured in the toxicology study. It would be of value if the investigators were to pursue additional analyses of the MESA data, beyond the effects on CIMT and CAC only, in which they would evaluate these additional markers.

Finally, the Panel noted that the toxicology results in the mice had a much lower degree of uncertainty than the epidemiology results in the humans, because the toxicology study was conducted in a controlled environment, and there was less uncertainty in the measurements of biologic markers. This difference in levels of certainty in the results makes it more difficult to compare the toxicology and epidemiology results directly.

In summary, it is clear that the study has produced some interesting new results but that more detailed research and integration of epidemiologic and toxicologic findings are required to reach more definitive conclusions about the roles of PM mass versus PM components in contributing to adverse health effects. In addition, the contribution of the gaseous pollutants to the adverse effects of air pollution remains understudied. The value of the study is that it took perhaps the closest look yet at the effects on health of chronic exposure to OC and EC, two plausible components or indicators directly related to the components responsible for causing health effects associated with PM_{2.5} mass. In particular, the work on OC is novel and invites replication in other settings as well as new studies on associations of OC with other endpoints.

At the outset, it was recognized that the investigators were tackling a very complex problem, and it remains important to recognize the complexity of PM and the major challenge of disentangling which PM components might be more harmful than others. Combining epidemiologic and toxicologic studies is an appropriate path forward, but there are limits to how much detailed knowledge on specific components and sources and on the myriad of adverse outcomes can ultimately be obtained. Nonetheless, this study and its companion NPACT study by Lippmann and colleagues (2013) have added significantly to the information base and represent a valuable platform for more detailed exploration in the future.

ACKNOWLEDGMENTS

The Health Review Committee thanks the NPACT Review Panel for its help in evaluating the scientific merit of the Investigators' Report. The Committee is also grateful to Geoffrey Sunshine and Katherine Walker for their oversight of the study; to Kate Adams, Annemoon van Erp, and

Kathleen Ward Brown for their assistance in preparing its Commentary; to Mary Brennan, Genevieve MacLellan, and Hilary Selby Polk for science editing of this Research Report and its Commentary; and to Barbara Gale, Hope Green, Fred Howe, and Bernard Jacobson for their roles in preparing the report for publication.

REFERENCES

- Aga E, Samoli E, Touloumi G, Anderson HR, Cadum E, Forsberg B, Goodman P, Goren A, Kotesovec F, Kriz B, Macarol-Hiti M, Medina S, Paldy A, Schindler C, Sunyer J, Tittanen P, Wojtyniak B, Zmirou D, Schwartz J, Katsouyanni K. 2003. Short-term effects of ambient particles on mortality in the elderly: Results from 28 cities in the APHEA2 project. *Eur Respir J Suppl* 40:28s–33s.
- Araujo JA, Nel AE. 2009. Particulate matter and atherosclerosis: Role of particle size, composition and oxidative stress. *Part Fibre Toxicol* 6:24.
- Bell ML. 2012. Assessment of the Health Impacts of Particulate Matter Characteristics. Research Report 161. Health Effects Institute, Boston, MA.
- Bell ML, Ebiscu K, Peng RD. 2011. Community-level spatial heterogeneity of chemical constituent levels of five particles and implications for epidemiological research. *J Expo Sci Environ Epidemiol* 21:372–384.
- Bhatnagar A. 2006. Environmental cardiology: Studying mechanistic links between pollution and heart disease. *Circ Res* 99:692–705.
- Brook RD, Rajagopalan S, Pope CA III, Brook JR, Bhatnagar A, Diez-Roux AV, Holguin F, Hong Y, Luepker RV, Mittleman MA, Peters A, Siscovick D, Smith SC Jr, Whitsel L, Kaufman JD; on behalf of the American Heart Association Council on Epidemiology and Prevention, Council on the Kidney in Cardiovascular Disease, and Council on Nutrition, Physical Activity and Metabolism. 2010. Particulate matter air pollution and cardiovascular disease: An update to the scientific statement from the American Heart Association. *Circulation* (doi: CIR.0b013e3181dbeece1)
- Brown DM, Wilson MR, MacNee W, Stone V, Donaldson K. 2001. Size-dependent proinflammatory effects of ultrafine polystyrene particles: A role for surface area and oxidative stress in the enhanced activity of ultrafines. *Toxicol Appl Pharmacol* 175:191–199.
- Campen MJ, Babu NS, Helms GA, Pett S, Wernly J, Mehran R, McDonald JD. 2005. Nonparticulate components of diesel exhaust promote constriction in coronary arteries from ApoE^{-/-} mice. *Toxicol Sci* 88(1):95–102.

- Campen MJ, Lund AK, Knuckles TL, Conklin DJ, Bishop B, Young D, Seilkop S, Seagrave J, Reed MD, McDonald JD. 2010. Inhaled diesel emissions alter atherosclerotic plaque composition in ApoE^{-/-} mice. *Toxicol Appl Pharmacol* 242:310–317.
- Campen MJ, Nolan JP, Schladweiler MC, Kodavanti UP, Evansky PA, Costa DL, Watkinson WP. 2001. Cardiovascular and thermoregulatory effects of inhaled PM-associated transition metals: A potential interaction between nickel and vanadium sulfate. *Toxicol Sci* 64(2):243–252.
- Chang SG, Brodzinsky R, Gundel LA, Novakov T. 1982. Chemical and catalytic properties of elemental carbon. In: *Particulate Carbon: Atmospheric Life Cycle*, pp 159–181 (Wolff GT, Klimisch RL, eds.). Plenum, New York, NY.
- Chen L-C, Lippmann M. 2013. NPACT Study 1. Subchronic Inhalation Exposure of Mice to Concentrated Ambient PM_{2.5} from Five Airsheds. In: *National Particle Component Toxicity (NPACT) Initiative: Integrated Epidemiologic and Toxicologic Studies of the Health Effects of Particulate Matter Components*. Research Report 177. Health Effects Institute, Boston, MA.
- Clarke RW, Coull B, Reinisch U, Catalano P, Killingsworth CR, Koutrakis P, Kavouras I, Krishna Murthy GG, Lawrence J, Lovett E, Wolfson JM, Verrier RL, Godleski JJ. 2000. Inhaled concentrated ambient particles are associated with hematologic and bronchoalveolar lavage changes in canines. *Environ Health Perspect* 108:1179–1187.
- Dockery DW, Pope CA III, Xu X, Spengler JD, Ware JH, Fay ME, Ferris BG, Speizer FE. 1993. An association between air pollution and mortality in six U.S. cities. *N Engl J Med* 329:1753–1759.
- Donaldson K, Brown D, Clouter A, Duffin R, MacNee W, Renwick L, Tran L, Stone V. 2002. The pulmonary toxicology of ultrafine particles. *J Aerosol Med* 15:213–220.
- Franklin M, Vora H, Avol E, McConnell R, Lurmann F, Liu F, Penfold B, Berhane K, Gilliland F, Gauderman WJ. 2012. Predictors of intra-community variation in air quality. *J Expo Sci Environ Epidemiol* 22:135–147.
- Health Effects Institute. 2000. Reanalysis of the Harvard Six Cities Study and the American Cancer Society Study of Particulate Air Pollution and Mortality. A Special Report of the Institute's Particle Epidemiology Reanalysis Project. Health Effects Institute, Cambridge, MA.
- Health Effects Institute. 2003. Revised Analyses of Time-Series Studies of Air Pollution and Health. Special Report. Health Effects Institute, Boston, MA.
- Health Effects Institute. 2002. Understanding the Health Effects of Components of the Particulate Matter Mix: Progress and Next Steps. HEI Perspectives. Health Effects Institute, Boston, MA.
- Hedley AJ, Wong CM, Thach TQ, Ma S, Lam TH, Anderson HR. 2002. Cardiorespiratory and all-cause mortality after restrictions on sulphur content of fuel in Hong Kong: An intervention study. *Lancet* 360:1646–1652.
- HEI Panel on the Health Effects of Traffic-Related Air Pollution. 2010. *Traffic-Related Air Pollution: A Critical Review of the Literature on Emissions, Exposure, and Health Effects*. Special Report 17. Health Effects Institute, Boston, MA.
- Hoffmann B, Moebus S, Möhlenkamp S, Stang A, Lehmann N, Dragano N, Schmermund A, Memmesheimer M, Mann K, Erbel R, Jöckel KH; Heinz Nixdorf Recall Study Investigative Group. 2007. Residential exposure to traffic is associated with coronary atherosclerosis. *Circulation* 116:489–496.
- Holgate ST, Devlin RB, Wilson SJ, Frew AJ. 2003. Part II. Healthy subjects exposed to concentrated ambient particles. In: *Health Effects of Acute Exposure to Air Pollution*. Research Report 112. Health Effects Institute, Boston, MA.
- Hopke PK, Ito K, Mar T, Christensen WF, Eatough DJ, Henry RC, Kim E, Laden F, Lall R, Larson TV, Liu H, Neas L, Pinto J, Stölzel M, Suh H, Paatero P, Thurston GD. 2006. PM source apportionment and health effects: 1. Inter-comparison of source apportionment results. *J Expo Sci Environ Epidemiol* 16:275–286.
- Jerrett M, Shankardass K, Berhane K, Gauderman WJ, Künzli N, Avol E, Gilliland F, Lurmann F, Molitor JN, Molitor JT, Thomas DC, Peters J, McConnell R. 2008. Traffic-related air pollution and asthma onset in children: A prospective cohort study with individual exposure measurement. *Environ Health Perspect* 116:1433–1438.
- Krewski D, Jerrett M, Burnett RT, Ma R, Hughes E, Shi Y, Turner MC, Pope CA III, Thurston G, Calle EE, Thun MJ. 2009. Extended Follow-Up and Spatial Analysis of the American Cancer Society Study Linking Particulate Air Pollution and Mortality. Research Report 140. Health Effects Institute, Boston, MA.
- Künzli N, Jerrett M, Garcia-Esteban R, Basagaña X, Beckermann B, Gilliland F, Medina M, Peters J, Hodis HN, Mack WJ. 2010. Ambient air pollution and the progression of atherosclerosis in adults. *PLOS ONE* 5:e9096.
- Künzli N, Jerrett M, Mack WJ, Beckerman B, LaBree L, Gilliland F, Thomas D, Peters J, Hodis HN. 2005. Ambient

air pollution and atherosclerosis in Los Angeles. *Environ Health Perspect* 113(2):201–206.

Laden F, Neas LM, Dockery DW, Schwartz J. 2000. Association of fine particulate matter from different sources with daily mortality in six U.S. cities. *Environ Health Perspect* 108:941–947.

Leikauf GD, McDowell SA, Wesselkamper SC, Miller CR, Hardie WD, Gammon K, Biswas PP, Korfhagen TR, Bachurski CJ, Wiest JS, Willeke K, Bingham E, Leikauf JE, Aronow BJ, Prows DR. 2001. Pathogenomic Mechanisms for Particulate Matter Induction of Acute Lung Injury and Inflammation in Mice. Research Report 105. Health Effects Institute, Boston, MA.

Levy JI, Diez D, Dou Y, Barr CE, Dominici F. 2012. A meta-analysis and multisite time-series analysis of the differential toxicity of major fine particulate matter constituents. *Am J Epidemiol* 175:1091–1099.

Li N, Sioutas C, Cho A, Schmitz D, Misra C, Sempf J, Wang M, Oberley T, Froines J, Nel A. 2003. Ultrafine particulate pollutants induce oxidative stress and mitochondrial damage. *Environ Health Perspect* 111:455–460.

Li S-M, Liggio J, Graham L, Lu G, Brook J, Stroud C, Zhang J, Makar P, Moran MD. 2011. Condensational uptake of semivolatile organic compounds in gasoline engine exhaust onto pre-existing inorganic particles. *Atmos Chem Phys* 11:10157–10171.

Lim SS, Vos T, Flaxman AD, Danaei G, Shibuya K, Adair-Rohani H, et al. 2012. A comparative risk assessment of burden of disease and injury attributable to 67 risk factors and risk factor clusters in 21 regions, 1990–2010: A systematic analysis for the Global Burden of Disease Study 2010. *Lancet* 380(9859):2224–2260.

Lindstrom J, Szpiro AA, Sampson PD, Sheppard L, Oron A, Richards M, Larson T. 2011. A flexible spatio-temporal model for air pollution: Allowing for spatio-temporal covariates. UW Biostatistics Working Paper Series. Working Paper 370. <http://biostats.bepress.com/uwbiostat/paper370/>.

Lippmann M, Chen L-C, Gordon T, Ito K, Thurston GD. 2013. National Particle Component Toxicity (NPACT) Initiative: Integrated Epidemiologic and Toxicologic Studies of the Health Effects of Particulate Matter Components. Research Report 177. Health Effects Institute, Boston, MA.

Lippmann M, Hwang J-S, Maciejczyk P, Chen LC. 2005. PM source apportionment for short-term cardiac function changes in ApoE^{-/-} mice. *Environ Health Perspect* 113:1575–1579.

Lippmann M, Ito K, Hwang JS, Maciejczyk P, Chen LC. 2006. Cardiovascular effects of nickel in ambient air. *Environ Health Perspect* 114(11):1662–1669.

Lippmann M, Ito K, Nádas A, Burnett RT. 2000. Association of Particulate Matter Components with Daily Mortality and Morbidity in Urban Populations. Research Report 95. Health Effects Institute, Cambridge, MA.

Lumley T, Kronmal R, Ma S. 2006. Relative Risk Regression in Medical Research: Models, Contrasts, Estimators, and Algorithms. UW Biostatistics Working Paper Series. Working Paper 293. www.bepress.com/uwbiostat/paper293.

Lund AK, Knuckles TL, Obot Akata C, Shohet R, McDonald JD, Gigliotti A, Seagrave JC, Campen MJ. 2007. Gasoline exhaust emissions induce vascular remodeling pathways involved in atherosclerosis. *Toxicol Sci* 95:485–494.

Lund AK, Lucero J, Harman M, Madden MC, McDonald JD, Seagrave JC, Campen MJ. 2011. The oxidized low-density lipoprotein receptor mediates vascular effects of inhaled vehicle emissions. *Am J Respir Crit Care Med* 184:82–91.

Lund AK, Lucero J, Lucas S, Madden MC, McDonald JD, Seagrave JC, Knuckles TL, Campen MJ. 2009. Vehicular emissions induce vascular MMP-9 expression and activity associated with endothelin-1-mediated pathways. *Arterioscler Thromb Vasc Biol* 29:511–517.

Maciejczyk PB, Chen LC. 2005. Effects of subchronic exposures to concentrated ambient particles (CAPs) in mice. VIII. Source-related daily variations in in vitro responses to CAPs. *Inhal Toxicol* 17:243–253.

McDonald JD, Barr EB, White RK, Chow JC, Schauer JJ, Zielinska B, Grosjean E. 2004. Generation and characterization of four dilutions of diesel engine exhaust for a subchronic inhalation study. *Environ Sci Technol* 38(9):2513–2522.

Metzger KB, Tolbert PE, Klein M, Peel JL, Flanders WD, Todd K, Mulholland JA, Ryan PB, Frumkin H. 2004. Ambient air pollution and cardiovascular emergency department visits. *Epidemiology* 15:46–56.

Miller KA, Siscovic DS, Sheppard L, Shepherd K, Sullivan JH, Anderson GL, Kaufman JD. 2007. Long-term exposure to air pollution and incidence of cardiovascular events in women. *N Engl J Med* 356:447–458.

Miller MR, Borthwick SJ, Shaw CA, McLean SG, McClure D, Mills NL, Duffin R, Donaldson K, Megson IL, Hadoke PW, Newby DE. 2009. Direct impairment of vascular function by diesel exhaust particulate through reduced

- bioavailability of endothelium-derived nitric oxide induced by superoxide free radicals. *Environ Health Perspect* 117:611–616.
- Mills NL, Miller MR, Lucking AJ, Beveridge J, Flint L, Boere AJ, Fokkens PH, Boon NA, Sandstrom T, Blomberg A, Duffin R, Donaldson K, Hadoke PW, Cassee FR, Newby DE. 2011. Combustion-derived nanoparticulate induces the adverse vascular effects of diesel exhaust inhalation. *Eur Heart J* 32:2660–2671.
- Mills NL, Törnqvist H, Robinson SD, Gonzalez M, Darnley K, MacNee W, Boon NA, Donaldson K, Blomberg A, Sandstrom T, Newby DE. 2005. Diesel exhaust inhalation causes vascular dysfunction and impaired endogenous fibrinolysis. *Circulation* 112:3930–3936.
- Mostofsky E, Schwartz J, Coull BA, Koutrakis P, Wellenius GA, Suh HH, Gold DR, Mittleman MA. 2012. Modeling the association between particle constituents of air pollution and health outcomes. *Am J Epidemiol* 176:317–326.
- Murray ET, Diez Roux AV, Carnethon M, Lutsey PL, Ni H, O’Meara ES. 2010. Trajectories of neighborhood poverty and associations with subclinical atherosclerosis and associated risk factors: The Multi-Ethnic Study of Atherosclerosis. *Am J Epidemiol* 171:1099–1108.
- Mustafic H, Jabre P, Caussin C, Murad MH, Escolano S, Tafflet M, Périer MC, Marijon E, Vernerey D, Empana JP, Jouven X. 2012. Main air pollutants and myocardial infarction: A systematic review and meta-analysis. *JAMA* 307:713–721.
- National Research Council (U.S.). 1998. Research Priorities for Airborne Particulate Matter: I. Immediate Priorities and a Long-Range Research Portfolio. Committee on Research Priorities for Airborne Particulate Matter. National Academy Press, Washington, DC.
- National Research Council (U.S.). 2001. Research Priorities for Airborne Particulate Matter: III. Early Research Progress. Committee on Research Priorities for Airborne Particulate Matter. National Academy Press, Washington, DC.
- National Research Council (U.S.). 2004. Research Priorities for Airborne Particulate Matter: IV. Continuing Research Progress. Committee on Research Priorities for Airborne Particulate Matter. National Academy Press, Washington, DC.
- Oberdörster G. 2001. Pulmonary effects of inhaled ultrafine particles. *Int Arch Occup Environ Health* 74:1–8.
- Oberdörster G, Finkelstein JN, Johnston C, Gelein R, Cox C, Baggs R, Elder ACP. 2000. Acute Pulmonary Effects of Ultrafine Particles in Rats and Mice. Research Report 96. Health Effects Institute, Cambridge, MA.
- Ostro B, Lipsett M, Reynolds P, Goldberg D, Hertz A, Garcia C, Henderson KD, Bernstein L. 2010. Long-term exposure to constituents of fine particulate air pollution and mortality: Results from the California Teachers Study. *Environ Health Perspect* 118:363–369.
- Ostro B, Roth L, Malig B, Marty M. 2009. The effects of fine particle components on respiratory hospital admissions in children. *Environ Health Perspect* 117:475–480.
- Peel JL, Tolbert PE, Klein M, Metzger KB, Flanders WD, Todd K, Mulholland JA, Ryan PB, Frumkin H. 2005. Ambient air pollution and respiratory emergency department visits. *Epidemiology* 16(2):164–174.
- Pekkanen J, Timonen KL, Ruuskanen J, Reponen A, Mirme A. 1997. Effects of ultrafine and fine particles in urban air on peak expiratory flow among children with asthmatic symptoms. *Environ Res* 74:24–33.
- Peng RD, Dominici F, Pastor-Barriuso R, Zeger SL, Samet JM. 2005. Seasonal analyses of air pollution and mortality in 100 U.S. cities. *Am J Epidemiol* 161(6):585–594.
- Peters A, von Klot S, Heier M, Trentinaglia I, Hörmann A, Wichmann HE, Löwel H; Cooperative Health Research in the Region of Augsburg Study Group. 2004. Exposure to traffic and the onset of myocardial infarction. *N Engl J Med* 351:1721–1730.
- Peters A, Wichmann HE, Tuch T, Heinrich J, Heyder J. 1997. Respiratory effects are associated with the number of ultra-fine particles. *Am J Respir Crit Care Med* 155:1376–1383.
- Pope CA III, Burnett RT, Thun MJ, Calle EE, Krewski D, Ito K, Thurston GD. 2002. Lung cancer, cardiopulmonary mortality, and long-term exposure to fine particulate air pollution. *JAMA* 287:1132–1141.
- Pope CA III, Burnett RT, Thurston GD, Thun MJ, Calle EE, Krewski D, Godleski JJ. 2004. Cardiovascular mortality and long-term exposure to particulate air pollution: Epidemiological evidence of general pathophysiological pathways of disease. *Circulation* 109:71–77.
- Pope CA III, Dockery DW. 2006. Health effects of fine particulate air pollution: Lines that connect. *J Air Waste Manage Assoc* 56:709–742.
- Pope CA III, Ezzati M, Dockery DW. 2009. Fine-particulate air pollution and life expectancy in the United States. *N Engl J Med* 360:376–386.

- Quan C, Sun Q, Lippmann M, Chen LC. 2010. Comparative effects of inhaled diesel exhaust and ambient fine particles on inflammation, atherosclerosis, and vascular dysfunction. *Inhal Toxicol* 22:738–753.
- R Development Core Team. 2011. R: A Language and Environment for Statistical Computing. R Development Core Team, Vienna, Austria. www.R-project.org.
- Riediker M, Devlin RB, Griggs TR, Herbst MC, Bromberg PA, Williams RW, Cascio WE. 2004. Cardiovascular effects in patrol officers are associated with fine particulate matter from brake wear and engine emissions. *Part Fibre Toxicol* 1:2.
- Salvi S, Blomberg A, Rudell B, Kelly F, Sandström T, Holgate ST, Frew A. 1999. Acute inflammatory responses in the airways and peripheral blood after short-term exposure to diesel exhaust in healthy human volunteers. *Am J Respir Crit Care Med* 159:702–709.
- Samet JM, Zeger SL, Dominici F, Curriero F, Coursac I, Dockery DW, Schwartz J, Zanobetti A. 2000. Part II. Morbidity and mortality from air pollution in the United States. In: *The National Morbidity, Mortality, and Air Pollution Study. Research Report 94*. Health Effects Institute, Cambridge, MA.
- Sarnat JA, Marmur A, Klein M, Kim E, Russell AG, Sarnat SE, Mulholland JA, Hopke PK, Tolbert PE. 2008. Fine particle sources and cardiorespiratory morbidity: An application of chemical mass balance and factor analytical source-apportionment methods. 2008. *Environ Health Perspect* 116:459–466.
- Schwartz J, Dockery DW, Neas LM. 1996. Is daily mortality associated specifically with fine particles? *J Air Waste Manage Assoc* 46(10):927–939.
- Schwartz J, Litonjua A, Suh H, Verrier M, Zanobetti A, Syring M, Nearing B, Verrier R, Stone P, MacCallum G, Speizer FE, Gold DR. 2005. Traffic related pollution and heart rate variability in a panel of elderly subjects. *Thorax* 60(6):455–461.
- Seilkop SK, Campen MJ, Lund AK, McDonald JD, Mauderly JL. 2012. Identification of chemical components of combustion emissions that affect pro-atherosclerotic vascular responses in mice. *Inhal Toxicol* 24:270–287.
- Shah AS, Langrish JP, Nair H, McAllister DA, Hunter AL, Donaldson K, Newby DE, Mills NL. 2013. Global association of air pollution and heart failure: A systematic review and meta-analysis. *Lancet*. Available at [www.thelancet.com/journals/lancet/article/PIIS0140-6736\(13\)60898-3/fulltext](http://www.thelancet.com/journals/lancet/article/PIIS0140-6736(13)60898-3/fulltext).
- Stanek LW, Sacks JD, Dutton SJ, Dubois J-JB. 2011. Attributing health effects to apportioned components and sources of particulate matter: An evaluation of collective results. *Atmos Environ* 45:5655–5663.
- Sun Q, Wang A, Jin X, Natanzon A, Duquaine D, Brook RD, Aguinaldo JG, Fayad ZA, Fuster V, Lippmann M, Chen LC, Rajagopalan S. 2005. Long-term air pollution exposure and acceleration of atherosclerosis and vascular inflammation in an animal model. *JAMA* 294(23):3003–3010.
- Tesfaigzi Y, Singh SP, Foster JE, Kubatko J, Barr EB, Fine PM, McDonald JD, Hahn FF, Mauderly JL. 2002. Health effects of subchronic exposure to low levels of wood smoke in rats. *Toxicol Sci* 65:115–125.
- Thurston GD, Ito K, Mar T, Christensen WF, Eatough DJ, Henry RC, Kim E, Laden F, Lall R, Larson TV, Liu H, Neas L, Pinto J, Stölzel M, Suh H, Paatero P, Hopke PK. 2005. The Workshop on the Source Apportionment of PM Health Effects: Inter-Comparison of Results and Implications. *Environ Health Perspect* 113:1768–1774.
- Thurston GD, Spengler JD. 1985. A quantitative assessment of source contributions to inhalable particulate matter pollution in metropolitan Boston. *Atmos Environ* 19:9–25.
- Tran CL, Buchanan D, Cullen RT, Searl A, Jones AD, Donaldson K. 2000. Inhalation of poorly soluble particles. II. Influence of particle surface area on inflammation and clearance. *Inhal Toxicol* 12:1113–1126.
- U.S. Environmental Protection Agency. 2004. Air Quality Criteria for Particulate Matter (Final Report). EPA 600/P-99/002aF-bF, 2004. U.S. EPA, Washington, DC.
- U.S. Environmental Protection Agency. 2009. Integrated Science Assessment for Particulate Matter (Final Report). EPA/600/R-08/139F, 2009. U.S. EPA, Washington, DC.
- Utell MJ, Frampton MW. 2000. Acute health effects of ambient air pollution: The ultrafine particle hypothesis. *J Aerosol Med* 13:355–359.
- van der Bijl N, Joemai RMS, Geleijns J, Bax JJ, Schuijff JD, de Roos A, Kroft LJM. 2010. Assessment of Agatston coronary artery calcium score using contrast-enhanced CT coronary angiography. *AJR* 195:1299–1305.
- Wichmann H-E, Spix C, Tuch T, Wölke G, Peters A, Heinrich J, Kreyling WG, Heyder J. 2000. Part I: Role of particle number and particle mass. In: *Daily Mortality and Fine and Ultrafine Particles in Erfurt, Germany. Research Report 98*. Health Effects Institute, Cambridge, MA.
- Women's Health Initiative Observational Study. www.nhlbi.nih.gov/whi/os.htm. Accessed April 8, 2013.

World Health Organization. 2005. Health Effects of Transport-Related Air Pollution (Krzyzanowski M, Kuna-Dibbert B, Schneider J, eds.). WHO Regional Office for Europe, Copenhagen.

Zanobetti A, Franklin M, Koutrakis P, Schwartz J. 2009. Fine particulate air pollution and its components in association with cause-specific emergency admissions. *Environ Health* 8:58.

ABBREVIATIONS AND OTHER TERMS

ACS	American Cancer Society	log-CAC	natural log of CAC score
ANOVA	analyses of variance	LRRI	Lovelace Respiratory Research Institute
AQS	Air Quality System	LUR	land-use regression
CAC	coronary artery calcium	MART	multiple additive regression tree
CAPs	concentrated ambient particles	MESA	Multi-Ethnic Study of Atherosclerosis
CHD	coronary heart disease	MESA Air	Multi-Ethnic Study of Atherosclerosis and Air Pollution
CI	confidence interval	MI	myocardial infarction
CIMT	carotid intima media thickness	MMP	matrix metalloproteinases
CO	carbon monoxide	MOMA	monocyte/macrophage
CPS-II	Cancer Prevention Study II	MSA	metropolitan statistical area
CSN	Chemical Speciation Network	MVE	mixed vehicular engine emissions
CT	computer tomography	NAAQS	National Ambient Air Quality Standards
CVD	cardiovascular disease	NMAD	number mean aerodynamic diameter
DEE	diesel engine exhaust	NM VOC	nonmethane volatile organic compounds
DHFR	dihydrofolate reductase	NO ₂	nitrogen dioxide
EC	elemental carbon	NOS	nitric oxide synthase
eNOS	endothelial NOS	NO _x	nitrogen oxides
ET-1	endothelin-1	NPACT	National Particle Components Toxicity (initiative)
EPA	U.S. Environmental Protection Agency	NRC	National Research Council
GADPH	glyceraldehyde 3-phosphate dehydrogenase	OC	organic carbon
GEE	gasoline engine exhaust	oxLP	oxidized lipoproteins
GIS	geographic information system	PCR	polymerase chain reaction
GTPCH	guanosine 5'-triphosphate cyclohydrolase	PLS	partial least squares regression
HDL	high-density lipoprotein	PM	particulate matter
HO-1	heme-oxygenase-1	PM _{0.1}	PM with an aerodynamic diameter ≤ 0.1 μm
HR	heart rate	PM _{2.5}	PM with an aerodynamic diameter ≤ 2.5 μm
HRV	heart rate variability	PM ₁₀	PM with an aerodynamic diameter ≤ 10 μm
IHD	ischemic heart disease	PM _{10-2.5}	PM with an aerodynamic diameter between 2.5 and 10 μm
IMPROVE	Interagency Monitoring of Protected Visual Environments	PM ₁₅	PM with an aerodynamic diameter ≤ 15 μm
iNOS	inducible NOS	PMF	positive matrix factorization
IQR	interquartile range	ROS	reactive oxygen species
LDL	low-density lipoprotein	SES	socioeconomic status
		SO ₂	sulfur dioxide
		SO _x	sulfur oxides
		TBARS	thiobarbituric acid reactive substance
		TIMP	tissue inhibitor of metalloproteinases
		WHI	Women's Health Initiative
		WHI-OS	Women's Health Initiative—Observational Study
		WHO	World Health Organization

ELEMENTS

Ag	silver	Mg	magnesium
Al	aluminum	Mn	manganese
As	arsenic	Mo	molybdenum
Ba	barium	Na	sodium
Br	bromine	Ni	nickel
Ca	calcium	Pb	lead
Cl	chlorine	Se	selenium
Cr	chromium	Sr	strontium
Cu	copper	Ti	titanium
Fe	iron	V	vanadium
K	potassium	Zn	zinc
		Zr	zirconium

Research Report 177, *National Particle Component Toxicity (NPACT) Initiative: Integrated Epidemiologic and Toxicologic Studies of the Health Effects of Particulate Matter Components*, Morton Lippmann, Lung-Chi Chen, Terry Gordon, Kazuhiko Ito, and George D. Thurston

Research Report 178, *National Particle Component Toxicity (NPACT) Initiative Report on Cardiovascular Effects*, Sverre Vedal, Matthew J. Campen, Jacob D. McDonald, Joel D. Kaufman, Timothy V. Larson, Paul D. Sampson, Lianne Sheppard, Christopher D. Simpson, and Adam A. Szpiro

INTRODUCTION

As outlined in the Preface, HEI funded the National Particle Component Toxicity (NPACT*) initiative to provide more insight into which components of the particulate matter (PM) mixture may be responsible for its toxicity and human health effects. The initiative consisted of coordinated epidemiologic and toxicologic studies conducted in multiple cities to evaluate the toxicity of different chemical and physical properties of PM and their associated health effects, while taking into account the contribution of gaseous copollutants. The NPACT initiative has spanned nearly a decade from its initial conception and the development of request for applications (RFA) 05-1, through the issuing of the RFA and study selection, to the conduct of research, submission of the final reports, and evaluation by the HEI NPACT Review Panel. It is important to take a broad look at the results of all the separate epidemiologic and toxicologic studies that were part of the two major research efforts and to consider them in the context of current scientific understanding of how particle components may affect health, and to what sources those components can be attributed.

This Synthesis looks broadly at the approaches and the results of the reports by Dr. Morton Lippmann at New York University (hereafter referred to as the Lippmann team, study, or report) and Dr. Sverre Vedal at the University of Washington (hereafter referred to as the Vedal team, study, or report). In this Synthesis, the HEI NPACT Review Panel considers whether there is coherence and

consistency in the epidemiologic and toxicologic results and discusses the larger scientific significance of the overall findings and their implications for future research into the health effects of particle components.

INITIAL OBJECTIVES OF THE NPACT INITIATIVE

The overall purpose of RFA 05-1 was “to develop a comprehensive research program to systematically address questions about the health effects related to different components” of the ambient PM mixture, and it specified several features of studies that would be considered for funding:

- Consideration of how gaseous pollutants may affect the toxicity of the PM components;
- A preference for studies that combined epidemiologic and toxicologic approaches; and
- A project plan that demonstrated a systematic comparative study design for the evaluation of PM characteristics that may be associated with toxicity.

At the time, several hypotheses regarding particle characteristics and toxicity were of interest, such as the possibility that some transition metals, sulfates, or certain organic compounds have stronger associations with adverse health effects than other PM components. In the interest of soliciting targeted research, RFA 05-1 specified that proposals “have a clear and defensible prior hypothesis to be tested, rather than involving large numbers of exploratory analyses.” The RFA also stated that investigators might use source apportionment in their investigations, but cautioned that “identifying sources responsible for toxic effects should be considered primarily as a step toward identifying the components and characteristics of the emissions from those sources that have toxic effects.”

This document has not been reviewed by public or private party institutions, including those that support the Health Effects Institute; therefore, it may not reflect the views of these parties, and no endorsements by them should be inferred.

* A list of abbreviations and other terms appears at the end of this Synthesis.

Synthesis Table 1. Broad Overview of NPACT Study Designs^a

Study Approach	Lippmann et al.	Vedal et al.
Exposure timescales	Short- and long-term	Long-term only
Health endpoints	Respiratory and cardiovascular	Cardiovascular only
Epidemiologic Studies		
Study design	Multicity time-series analysis and one cohort	Two cohorts
Health endpoints	Acute: respiratory and cardiovascular mortality and hospitalizations Chronic: mortality	Chronic: Subclinical markers of atherosclerosis; cardiovascular disease events (including mortality)
PM components and exposure assessment	EPA CSN monitors; MSA averages; sources	Cohort-specific and EPA CSN and IMPROVE monitors; individual-level exposure predictions; two exposure models; focus on OC, EC, silicon, and sulfur; included some evaluation of other pollutants and PM components
Source apportionment goal	Assessing exposure	Interpretation of exposure health effect estimates
Toxicologic Studies		
Study design	ApoE knockout mouse model (normal diet); 6-month exposures; FVB/N mice; 12-day and 100-day exposures	ApoE knockout mouse model (high-fat/high-cholesterol diet); 50-day exposure
Biologic endpoints	Cardiovascular effects and markers of oxidative stress and inflammation	Vascular effects and markers of oxidative stress and inflammation
Animal and cell culture exposures	Concentrated ambient particles (in vivo) and ambient particles collected on filters (in vitro and in vivo); five air sheds	Laboratory-generated complex mixtures: combinations of mixed vehicular engine emissions and non-vehicular primary particles (in vivo)

^a ApoE indicates apolipoprotein E; CSN, Chemical Speciation Network; EC, elemental carbon; EPA, U.S. Environmental Protection Agency; IMPROVE, Interagency Monitoring of Protected Visual Environments; MSA, metropolitan statistical area; OC, organic carbon; PM, particulate matter.

Both NPACT studies funded under this RFA* included a toxicology component, with in vivo exposures to laboratory-generated pollution mixtures in the Vedal report (the Campen study) and to concentrated ambient particles in the Lippmann report (the Chen study), and in vivo and in vitro exposures to particle extracts in the Lippmann report (the Gordon study). Both reports also included an epidemiology component, comprising a time-series study (the Ito study) and a cohort study (the Thurston study) in the Lippmann report and two cohort studies in the Vedal report (the Vedal epidemiologic study), investigating associations between particle composition and a variety of

health outcomes in short- and long-term settings. Synthesis Table 1 summarizes the various studies that were conducted by the two teams of investigators.

DATA AND STUDY DESIGN

In addition to its detailed reviews of each study, the NPACT Review Panel considered, and discusses here, some of the strengths and limitations encountered by both teams in the design of the studies, the availability of data, exposure assessment and exposure atmosphere generation, and possible approaches to linking PM components to specific sources.

PM COMPOSITION DATA

Both the Lippmann and the Vedal epidemiologic studies relied on PM composition data available from the Chemical Speciation Network (CSN), operated by the U.S.

* A third study, *Assessment of the Health Impacts of Particulate Matter Characteristics*, by Dr. Michelle L. Bell of Yale University, was published as HEI Research Report 161 in January 2012. This study was funded through RFA 04-2, *Walter A. Rosenblith New Investigator Award*. Because the topic was very relevant to the NPACT initiative, HEI decided to include this study under the umbrella of NPACT (although the study was reviewed separately and published earlier).

EPA, which to date is the most comprehensive effort in the world to systematically collect such data nationwide. In addition, the Vedal team augmented the CSN data with their own monitoring data. Although these studies could not have been undertaken without the availability of the CSN data, the Panel noted that they also highlight some of the limitations of that network. First, the network is relatively sparse, comprising only about 200 locations nationally, such that the finer-scale spatial gradients in chemical components within cities are not captured. Second, although taking samples more often than many other efforts to collect PM component data, most CSN locations collect samples only once every three or six days. This infrequency limits researchers' ability to evaluate associations of PM components with daily health outcomes in short-term study designs and (to a lesser extent) reduces the information available for long-term averaging in the longer cohort studies. Third, concentrations of many of the components measured in the CSN network, especially metals, are below their minimum detection limits (MDLs) on a large number of sampling days, limiting analyses to only those components that can be detected repeatedly and reliably. Fourth, the accuracy of measured concentrations of elemental carbon (EC) and organic carbon (OC) depends on the methods used to measure these components. Because the measurements are defined operationally (EC and OC are complementary fractions of total carbon, and their respective concentrations depend on the methods used for sampling and measuring carbonaceous material), there is considerable uncertainty associated with them, and comparing them across studies is difficult. These issues affect some of the chemical components most important to the NPACT studies.

The Vedal team addressed the sparseness of the monitoring network and non-continuous sampling by adding extra monitors in additional locations to measure EC, OC, and the other PM components measured by the CSN and by calculating average concentrations over longer (2-week) time periods. However, the Panel noted that they did not use the same measurement approach in their additional monitoring as was employed by the CSN, and their results did not agree well with measurements from collocated CSN monitors. Thus, although the increased spatial information provided by the additional monitoring might have reduced exposure measurement error, the different approach and sampling time used by the additional monitoring campaign might have actually enhanced such error.

In particular, the Panel considered the uncertainties in EC and OC measurements important because these components are used to help identify traffic as a source of PM. The Vedal team focused on these components in accordance with their hypothesis that traffic-related air

pollutants drive the effects of PM on health. Source apportionment analyses conducted by the Lippmann team were also sensitive to these two components, because they were used in the estimation of traffic-related source categories. In addition to being operationally defined (see above), EC and OC are known to be subject to strong spatial and temporal gradients, making it likely that the small number of observations made at central monitoring stations do not adequately represent the highly variable concentrations observed across an entire urban area. Nonetheless, EC and OC continue to be important components to characterize in studies that evaluate the health impacts of PM components, particularly when there is an interest in traffic-related effects.

On the other hand, sulfate (measured as elemental sulfur) is well captured by the CSN. Sulfur concentrations are typically well above detection limits, are measured with relatively high certainty, and have relatively low spatial variability. Therefore, exposure measurement error associated with sulfate is expected to be low. Selenium, arsenic, vanadium, and nickel, which are key components for identifying coal-burning and fuel-oil combustion, are often below the limit of detection in the CSN database. The low concentrations of those pollutants, which have been decreasing over the past decades, hinder assessment of how they might be linked to health impacts. However, as reported by the Lippmann team in the current and prior studies, in some locations (notably New York City) concentrations of vanadium and nickel are sufficiently high that it has been possible to identify associations of these elements with health outcomes. However, new local regulations in New York City that address fuels used for residential heating are expected to reduce concentrations of nickel and vanadium in ambient air.

LINKING PM COMPONENTS AND SOURCES TO HEALTH OUTCOMES

For their epidemiologic analyses, the two NPACT teams adopted somewhat different philosophies on the use of source apportionment to link health outcomes to PM components. The Lippmann team relied heavily on a source apportionment approach that they had developed previously to link source categories directly to health outcomes in their epidemiologic analyses, whereas the Vedal team used source apportionment to assist in the interpretation of their health effects estimates and to support their focus on OC, EC, silicon, and sulfur as markers of specific sources in their analyses of health outcomes. An underlying question is which approach provides better information about which sources of PM components most affect health risks: Is it better to use source apportionment results, which may

represent more accurately the combined effects of multi-pollutant atmospheres, but which require more effort and introduce additional uncertainties and assumptions, or is it better to simply use individual components that are typically linked to one or more specific sources? Each approach has its strengths, and there are strong reasons to use either method or both methods (as was done by the Lippmann team).

The Panel noted that all current source apportionment approaches (see the sidebar *Source Apportionment* in the Commentary) introduce uncertainty (Balachandran et al. 2012). Although some approaches may decrease uncertainty by reducing temporal variability, other approaches that produce source categories may increase temporal variability as compared with approaches using concentrations of individual components. For some approaches those potential errors can be quite large. In their analyses using an approach based on factor analysis methods that they had developed previously, the Lippmann team found differences among locations in terms of which components contributed to similar source categories, providing indications that source emissions vary spatially, that the factor analytic approaches are sensitive to measurement uncertainties, that there are temporal variations in the composition of the emissions, and that other factors may add uncertainty to this approach. Two of the limitations noted by the Panel were that the investigators did not account for how uncertainties in the component measurements affect the certainty of the source categories and that many of the concentrations were below the MDL. How their results might differ from those obtained using a different source apportionment technique and what the effect would have been of including measurement uncertainties and MDLs in the analyses remain unknown. Furthermore, it is not apparent which chemical components drive the associations between source categories and key health outcomes in the Lippmann report (which is a different issue from determining which components are contained in the source categories that they identified). It was reassuring, however, that the Lippmann team came to consistent interpretations when they did include individual components in their analyses. We refer readers to the Commentary accompanying the Lippmann report (HEI Research Report 177) for a more detailed discussion of these issues.

The Vedal team applied positive matrix factorization (PMF), a widely used source apportionment approach, to support their focus on EC, OC, silicon, and sulfur as key components in their analyses of health outcomes. The Panel thought that their approach was defensible. The PMF factors they identified were reasonably consistent with what was expected in terms of sources and were also generally

consistent with the source apportionment results of the Lippmann team. However, it would be of interest to compare the PMF results of the Vedal team directly with the source apportionment results of the Lippmann team in those cities that the two studies had in common.

The Panel thought that the question of how (or whether) to use source apportionment to identify which PM components have strong associations with adverse health outcomes is an important one. It is generally preferable to use both source categories and component concentrations directly in the health analyses, if the study design permits, with a focus on examining consistencies and differences between the two approaches. When source apportionment results are used for health analyses, researchers should recognize, discuss, and — if possible — address the uncertainties introduced by this method.

ESTIMATING EXPOSURE USING AIR QUALITY DATA

The Lippmann team approached the estimation of exposure from measured air pollutant concentrations in a straightforward fashion; they assumed that the monitored concentrations (or source apportionment results estimated for each city based on a single monitor or a few central monitors) can be used directly, with little additional spatial modeling to account for spatial gradients (e.g., variation due to different land uses and activities). The Vedal team, on the other hand, developed a more elaborate spatiotemporal exposure model, which estimated exposures at the individual level (i.e., the outdoor concentrations at participants' residences) for the Multi-Ethnic Study of Atherosclerosis (MESA) cohort. This approach was made possible by the intensive, dedicated monitoring conducted by the team in the six cities of the MESA study. The Vedal team also constructed a national spatial exposure model, which also estimated component concentrations at participants' homes for their analyses of both the MESA cohort and the Women's Health Initiative–Observational Study (WHI-OS) cohort.

The Panel thought that the initial formulation of the approach by the Vedal team was promising. However, the Panel noted that there were challenges associated with estimating EC and OC concentrations at the individual level. For instance, there were only small differences between EC concentrations measured at roadside locations and those at urban background locations, raising questions about the ability of the spatiotemporal model to accurately assign exposure at participant residences. The Panel identified additional concerns with the approach used by the Vedal team (as discussed in the Commentary accompanying the Vedal report), such as the varying R^2 values for the different

components across the models (an indication of model accuracy in model validation) and the potential loss of volatile components over the longer sampling period of 2 weeks. At the same time, the Panel noted the more general challenge facing the primary alternative to such spatiotemporal modeling, which is the reliance on observations from just a few sites to characterize potential populationwide intra-urban exposures to pollutants such as EC, OC, and other primary pollutants (in much the same way the Lippmann team proceeded). Although using one or a few sites to characterize individual and populationwide exposures to certain secondary PM components, such as sulfate, may be sufficiently accurate, using this approach to estimate exposures to primary pollutants — such as metals — introduces larger uncertainties, potentially biasing the results.

SINGLE-POLLUTANT AND MULTIPOLLUTANT MODELS

When associations of PM_{2.5} components and health outcomes are analyzed in single-pollutant models, potential interactions or high correlations between components could affect the analysis and lead to misidentification of which pollutants may be most strongly associated with the observed human and animal health effects. Furthermore, other constituents of inhaled atmospheres — such as gaseous pollutants — might complicate assessment of which associations may be causally related. The Lippmann team attempted to address these issues by employing source apportionment in all of their studies, two-pollutant models in time-series analyses in which they controlled for PM_{2.5} mass, and a total-risk-impact approach in their cohort study. The Vedal team made simple comparisons between the results for individual components and those for PM_{2.5} mass in their epidemiologic study and carried out sensitivity analyses involving two-pollutant models. They performed a more sophisticated analysis (i.e., a multiple additive regression tree [MART] analysis) in their toxicologic study (the Campen study), in which they related the hundreds of compounds measured in their complex exposure atmospheres to biologic markers. Although the Panel appreciated the efforts of both NPACT teams, they concluded that any future research using PM component data needs to more directly address appropriate analyses for multipollutant atmospheres in the statistical design.

APPROACHES TO ANIMAL INHALATION EXPOSURES

The two NPACT teams exposed apolipoprotein E (ApoE) knockout mice to exposure atmospheres with pollutant concentrations that were by design higher than typical North American ambient concentrations, although such

concentrations can be found in developing countries or occupational settings. The teams used different approaches to generate the pollutant mixtures, making it possible to compare responses to concentrated ambient PM and predetermined laboratory mixtures in a similar animal model. The Lippmann team (specifically the Chen study) used concentrators that pass ambient air through a cyclone that excludes particles larger than 2.5 µm, and then through a virtual impactor that concentrates particles between about 0.1 and 2.5 µm. The system does not exclude (or concentrate) gaseous pollutants or particles smaller than 0.1 µm (ultrafine PM). Thus, the resulting concentrated ambient particles (CAPs) exposure atmosphere is similar in pollutant composition to the ambient air, but the mixture is altered in terms of both particle concentration and relative composition. The Panel noted that this is an appropriate approach given the focus on PM components in the NPACT initiative and the fact that much of the mass of ambient PM is within the size range (PM_{2.5}) that is being concentrated and of great interest regarding its health effects. The approach used by the Vedal team in their toxicologic study (conducted at the Lovelace Respiratory Research Institute [LRRRI]) was to generate controlled atmospheres by mixing diluted and cooled exhaust from a gasoline and a diesel engine to provide a base pollutant mixture (i.e., mixed vehicular engine emissions, or MVE) and then removing PM from the mixture or adding different types of PM. This approach was driven by their general focus on PM components derived from traffic (vehicular) sources for both the epidemiologic and toxicologic studies. The Lippmann team measured about 30 components in the CAPs atmospheres, whereas LRRRI measured close to 500 compounds (metals and many organic compounds in the particle and gas phases) in their complex exposure atmospheres.

The inhalation exposures at LRRRI did not include secondary PM components that are formed by atmospheric processes (e.g., secondary organic aerosols). However, sulfate and nitrate ions, which are major PM components in ambient air, were added as primary particles, allowing the team to investigate the health effects of exposure to those components. In a typical city, secondary sulfate particles would form by oxidation of gaseous sulfur dioxide emissions from coal or oil burning, whereas secondary nitrate particles would be formed by oxidation of nitrogen oxides emitted by vehicles and other combustion sources. A unique feature of the Campen study was the addition of road dust particles in the fine fraction. In contrast, the animal exposure atmospheres used in the Chen study included secondary aerosols by design, although the extent to which this occurred likely varied by location (the West Coast of the United States versus the East Coast versus the Midwest). Exposure mixtures for both studies

contained PM: at LRRI, from engine emissions or added nitrate, sulfate, and road dust; for the Lippmann study, from general traffic sources. Gaseous pollutants in engine exhaust were included or excluded by design at LRRI, and ambient gaseous pollutants were present by default (but not concentrated) in the CAPs exposures in the Chen study. In addition to the animal inhalation exposures in the two studies, the Lippmann team also used intratracheal aspiration of particles collected on filters (in the Gordon study), which allowed them to investigate the differences in biologic responses in mice exposed to different PM size ranges. This approach excluded gaseous components altogether. The investigators analyzed endotoxin content of the filter samples and elemental composition, but did not analyze OC, EC, or other organic compounds.

Because the Lippmann team did not use specific source mixtures for the exposures but conducted inhalation studies in five locations with different ambient air pollution mixtures, they conducted source apportionment to link their exposures back to source categories, such as emissions from mobile and stationary sources. Therefore, the animal exposure strategies of both teams had the potential to link biologic endpoints to similar types of sources, such as traffic, power generation, and dust, as well as to secondary aerosols (sulfates and nitrates). Furthermore, the parallel epidemiologic studies used similar markers for mobile-source emissions (EC and OC), although the source apportionment methods typically used in epidemiologic studies encounter difficulties in separating PM derived from gasoline engines from PM derived from diesel engines based on EC and OC concentrations.

The Panel thought that MVE was a reasonable representation of mobile source emissions for toxicologic studies that allowed a more direct comparison of the toxicologic results with epidemiologic results for non-source-specific estimates of traffic-related exposures. On the other hand, the sulfate added to the MVE exposures at LRRI was a primary rather than secondary particle and did not include other components (e.g., selenium, arsenic, vanadium, or nickel) that are often found in emissions from sources that emit sulfur dioxide, and was thus less representative of real-world conditions.

COMPARING KEY FINDINGS ACROSS THE STUDIES

This section discusses the main findings in terms of what sources and PM components the teams found to play a role in the health outcomes they assessed, looking for consistency across the epidemiologic and toxicologic studies within and across the two main NPACT studies.

Overviews of the main findings of the epidemiologic and toxicologic studies are presented in Synthesis Table 2 and Synthesis Table 3, respectively.

The Lippmann team's time-series study (the Ito study) identified a fairly large number of PM components associated with daily hospitalizations due to cardiovascular disease (CVD) and daily all-cause and CVD mortality. Source categories attributed to primary vehicle exhaust and secondary sulfate aerosols were found to be important in some of these short-term associations. The long-term American Cancer Society cohort study (the Thurston study) also identified a number of PM components that could explain some of the mortality associations, including EC and sulfur. However, OC, silicon, and potassium (a marker for biomass combustion) were not associated with mortality in the cohort study. Source categories attributed to coal combustion and traffic pollution were found to be important in the associations with long-term effects, whereas little evidence was found for associations with source categories attributed to crustal sources or biomass combustion. There was minimal overlap between the PM_{2.5} components associated with short-term responses and those associated with long-term responses. Results for metals varied, but many effect estimates were highly uncertain (i.e., the confidence intervals were large), possibly due to the limited number of measurements above the limit of detection for metallic components in many cities.

The Vedal epidemiologic study focused primarily on EC and OC as markers of vehicle exhaust and other combustion emissions, on OC also as a marker of secondary organic aerosol, on silicon as a marker of crustal PM, and on sulfur as a marker of secondary PM. Results suggested that OC and sulfur were associated with several of the endpoints studied, but EC and silicon were not. The Panel agreed with the investigators that this suggests that traffic-related pollution and secondary PM could be playing a role in PM toxicity.

The Lippmann team's animal inhalation study (the Chen study) showed that a large number of components were positively or negatively associated with acute changes in heart rate and heart rate variability in mice. When the investigators tried to rank these components, they concluded that nickel, aluminum, EC, phosphorus, and sulfur had stronger associations with the cardiac endpoints than did PM_{2.5} mass. Effects of CAPs exposures on plaque progression in mice were primarily seen at Tuxedo, New York, Manhattan, New York, and East Lansing, Michigan, where the investigators deemed pollution mixtures to be more influenced by coal-fired power plant emissions than at Irvine, California, and Seattle, Washington. The Lippmann teams' *in vitro* and *in vivo* study of PM collected on filters

Synthesis Table 2. Approaches and Key Findings of the Epidemiologic Studies^{a,b}

	New York University/Ito	New York University/Thurston	University of Washington/Vedal ^c
Study design	Time series (short-term)	Cohort (long-term)	Cohort (long-term)
Population	U.S. MSAs	ACS CPS-II cohort	WHI-OS
Cities	150 cities	100 cities	45 cities
Participants	Population >100 million	~450,000 people	~90,000 people
Health endpoints	Hospitalization Mortality	Mortality	Time to first event (MI, stroke, cardiac procedures, and CVD deaths)
PM components and source categories associated with health outcomes	<p>Cold season: PM_{2.5}, NO₂, CO, EC, OC, and Cu</p> <p>Modified^d by PM_{2.5}; Cu, Ni, and V</p> <p>Sources: vehicle exhaust</p>	<p>Warm season: PM_{2.5}, NO₃, Fe, Pb, and EC</p> <p>Modified^d by PM_{2.5}: sulfate</p> <p>Sources: secondary aerosols</p>	<p>Best evidence for sulfur and less for OC; little evidence for EC or silicon</p> <p>Some evidence for OC only</p> <p>Best evidence for OC and sulfur; little evidence for EC or silicon; some evidence for Cu</p>
		Components: PM _{2.5} , As, Se, sulfur, Cl, Fe, Pb, and EC Not associated: OC, silicon, and K Source categories: coal combustion and possibly traffic; little evidence for soil or biomass combustion	Best evidence for OC and less for sulfur; little evidence for EC or silicon Some evidence for OC only Best evidence for OC and less for sulfur; little evidence for EC or silicon

^a ACS CPS-II indicates American Cancer Society Cancer Prevention Study II; As, arsenic; CAC, coronary artery calcification; Cl, chlorine; CIMT, carotid intima-media thickness; CO, carbon monoxide; Cu, copper; CVD, cardiovascular disease; EC, elemental carbon; Fe, iron; K, potassium; MESA, Multi-Ethnic Study of Atherosclerosis; MI, myocardial infarction; MSA, metropolitan statistical area; Ni, nickel; NO₂, nitrogen dioxide; NO₃, nitrate; OC, organic carbon; Pb, lead; PM, particulate matter; PM_{2.5}, particulate matter $\leq 2.5 \mu\text{m}$ in aerodynamic diameter; Se, selenium; V, vanadium; WHI-OS, Women's Health Initiative-Observational Study.

^b Epidemiologic studies at New York University were headed by George Thurston and Kazuhiko Ito and at the University of Washington by Sverre Vedal.

^c Source apportionment results supported the focus on four main components for evaluation in the Vedal study: EC and OC as markers of vehicle exhaust and other combustion emissions; OC also as a marker of secondary organic aerosol; silicon as a marker of crustal PM; and sulfur as a marker of secondary PM.

^d Risk estimates for these components were substantially modified when PM_{2.5} was included in a two-pollutant model.

Synthesis Table 3. Approaches and Key Findings of the Toxicologic Studies^{a,b}

	New York University / Chen		New York University / Gordon		University of Washington / Campen
Study design	Short-term (daily time-series)	Long-term (6 months)	Short-term (12 days)	Long-term (100 days)	Medium-term (50 days)
Exposures	Inhalation of CAPs at five locations (Manhattan, Tuxedo, East Lansing, Seattle, and Irvine)		Aspiration of PM collected on filters at five locations (Manhattan, Tuxedo, Ann Arbor, Seattle, and Los Angeles area); three size fractions		Inhalation of combinations of MVE or MVE gases with non-vehicular PM _{2.5} (sulfate, nitrate, or road dust)
PM concentrations	60–138 µg/m ³		In vitro: 50–100 µg/mL In vivo: 50 µg		100 or 300 µg/m ³
Model	ApoE knockout mice (normal diet)		FVB/N mice; epithelial cells, endothelial cells, cardiomyocytes	FVB/N mice	ApoE knockout mice (high-fat/high-cholesterol diet)
Biologic endpoints	Heart rate and heart rate variability	Aorta plaque growth; serum biomarkers; heart rate and heart rate variability	Mice: lung inflammation Cells: viability, ROS, inflammatory markers, beat frequency	Lung inflammation	Aorta: lipid peroxidation, vascular function and remodeling, plaque growth and inflammation
PM components and sources associated with biologic findings	Effects after exposure to Ni (residual oil combustion) > to Al, EC, and P (traffic) > to sulfur (coal combustion) > to PM _{2.5}	Plaque growth in Tuxedo, Manhattan, and East Lansing, but not in Irvine and Seattle; attributed to coal combustion	Complex interaction of particle size and composition (location and season); nothing ruled out	Source apportionment not reported	Effects after exposure to MVE > to MVE gases; fewer effects of nitrate and sulfate; no effects of road dust Effects after exposure to non-vehicular PM combined with MVE > non-vehicular PM without MVE

^a Al indicates aluminum; CAPs, concentrated ambient particles; MVE, mixed vehicular engine emissions; Ni, nickel; P, phosphorus; PM, particulate matter; ROS, reactive oxygen species.

^b Toxicologic studies at New York University were headed by Lung-Chi Chen and by Terry Gordon and for the University of Washington study by Matthew Campen at the University of New Mexico and Jacob McDonald at the Lovelace Respiratory Research Institute.

(the Gordon study) found that PM size and composition (determined by location and season) played a complex role in PM toxicity. The Panel noted that no size classes or components could be ruled out.

The toxicologic study conducted at LRRRI (the Campen study) used laboratory-generated atmospheres based on MVE and MVE gases combined with non-vehicular PM. Several combinations of particles and gases were found to affect different biologic markers in aortic tissues. The whole MVE mixture produced the largest changes, with MVE gases producing smaller and fewer changes. Fewer effects were observed with primary nitrate and sulfate particles, and none with fine road dust particles. Combining non-vehicular PM with MVE gases increased the effects over non-vehicular PM alone, but generally did not exceed the effects of MVE by itself. Thus there was little evidence of a more-than-additive effect when exposure atmospheres were combined. The results support the role of both particulate and gaseous components in the induction of various cardiovascular outcomes, but whether there are important particle–gas interactions remains unclear and requires further research.

REFLECTIONS ON THE MAIN FINDINGS

Both the Lippmann and Vedal studies found that adverse health outcomes were consistently associated with sulfur and sulfate (markers primarily of coal and oil combustion) and with traffic-related pollutants, although the relative importance of the latter remains unclear because exposure to traffic-related pollutants varies within metropolitan areas and thus is more subject to uncertainty than exposure to pollutants from other source categories. On the other hand, there were only small differences in EC concentrations measured at roadside locations compared with urban background locations, indicating either spatial homogeneity in concentrations or, as noted above, potentially high measurement error for EC due to the 2-week sampling protocol. The results for sulfur and sulfate may have been more consistent because their concentrations were more accurately estimated (due to their spatial homogeneity) than were concentrations of other pollutants.

Biomass combustion, crustal sources, and related components were not generally associated with short- or long-term epidemiologic findings in these studies, but there were only a few cities where these sources (and their attributed components) were likely to be measured consistently. The possibility remains that biomass combustion contributed to OC concentrations, and thus to the associations reported for OC and cardiovascular outcomes. There were few consistent associations with other components

or sources, although the Panel cautioned that is not conclusive evidence that these components and sources do not have adverse health effects. Further analyses of some of these sources are warranted.

With regard to the association of health effects with EC compared with those associated with OC, the differences in findings between the Lippmann and Vedal studies are surprising. In typical urban environments, mobile sources are expected to be the major source of EC and important contributors to OC. It is noteworthy that these studies report such prominent differences between the results for EC and OC, given the strong correlation between the two in many cities. Again, these differences may be due to the stronger spatial gradients between cities for OC than for EC, the exposure models and study designs, or the difficulties involved in measuring OC and EC.

One limitation of the CSN is that it is by design focused on PM_{2.5}, while it is becoming increasingly clear that coarse PM remains of interest. For example, the Lippmann team's *in vitro* and *in vivo* toxicologic evaluations (in the Gordon study) found stronger associations per unit mass between coarse PM, which is often associated with dust, and certain biologic endpoints than for fine PM. However, associations of silicon, a marker for dust, with health effects or clinical markers in the epidemiologic studies were often fairly weak (with the exception of CIMT in the Vedal epidemiologic study), as would be expected.

Both studies highlight how important the CSN is to research on the health effects of components of air pollution and to air quality management. Neither study could have been performed without CSN data, although the studies highlighted some limitations that suggest that further efforts would be helpful to characterize EC, OC, and metals (i.e., combustion- and traffic-related components); to lower the detection limits of some components; and to collect daily measurements. In summary, the Panel concluded that — except for the fairly consistent associations of many of the health outcomes with sulfur and sulfate, which may, in part, be due to better exposure assessment — associations with other components were mixed, and linkages to sources were not definitive.

How do these two major studies compare with the published literature? Quite a few investigators have performed smaller-scale studies and analyses to identify which PM components and sources are associated with a variety of adverse health outcomes. Not surprisingly, the results of those studies have been mixed, if only because of the differences in the selection of PM components and health outcomes of interest, study time frames (short- and long-term), and the imprecision of estimates because of the difficulties in obtaining truly large data sets on PM composition and sources.

In the third NPACT study (see earlier footnote), Bell (2012) used daily Medicare hospitalization data to evaluate the effects of short-term exposures to various components of the PM_{2.5} mixture on daily morbidity. She focused on the average values of seven PM_{2.5} components (those accounting for $\geq 1\%$ of PM_{2.5} mass in the CSN) in 187 U.S. counties, using national, regional, and seasonal models. For her all-year analysis of the entire United States, Bell reported strong and statistically significant increases in the association between cardiovascular hospitalizations and an interquartile range increase in EC, nickel, and vanadium (Bell 2012).

It is beyond the scope of this summary to provide a detailed review of the literature on the health effects of PM components and sources. A recent systematic review of the findings of animal toxicology, human chamber, and field epidemiology studies (Stanek et al. 2011) presents results from five epidemiologic studies on total mortality (see Table 3 of that paper), which among them found that soil, sea salt, local sulfur dioxide, secondary sulfate, motor vehicle emissions, coal burning, wood smoke, biomass combustion, copper smelter emissions, residual oil combustion, and incinerator emissions were associated with health outcomes. This is just one illustration of the variety of results reported in the literature.

Together, the two studies discussed here, as well as the study by Bell, follow the conclusion of Stanek and colleagues (2011) that “apportionment methods have linked a variety of health effects to multiple groups of PM components and sources of PM, but the collective evidence has not yet isolated factors or sources that would be closely and unequivocally related to specific health outcomes.”

Overall, this comprehensive and ambitious research program has shown that research on the toxicity of PM components is not likely to easily identify a single culprit PM component or source category or to identify a unique set of biomarkers that could be reliably used to monitor exposure. More work remains to be done to refine statistical methods for simultaneous modeling of multiple pollutants; to improve the representation of spatial contrasts in component concentrations, especially within cities; and to improve source identification and attribution. Further toxicologic studies are needed to connect particle components with physiologic mechanisms, to study the relative toxicity of particles and gaseous pollutants, to study atmospheric aging of complex mixtures to better reflect real-world conditions, and to provide more insight into the role of PM_{2.5} components in causing tissue injury and dysfunction.

The NPACT studies, which are to date the most systematic effort to combine epidemiologic and toxicologic analyses of these questions, found associations of secondary sulfate and, to a somewhat lesser extent, traffic sources with health effects. But the Panel concluded that the studies do not provide compelling evidence that any specific source, component, or size class of PM may be excluded as a possible contributor to PM toxicity. If greater success is to be achieved in isolating the effects of pollutants from mobile and other major sources, either as individual components or as a mixture, more advanced approaches and additional measurements will be needed so that exposure at the individual or population level can be assessed more accurately. Such enhanced understanding of exposure and health will be needed before it can be concluded that regulations targeting specific sources or components of PM_{2.5} will protect public health more effectively than continuing to follow the current practice of targeting PM_{2.5} mass as a whole.

ACKNOWLEDGMENTS

The Health Review Committee thanks the members of the NPACT Review Panel for their help in evaluating the scientific merit of the Investigators' Reports by Lippmann and colleagues and Vedal and colleagues and for preparing this Synthesis. The Committee is also grateful to Kate Adams and Annemoon van Erp for their assistance in preparing this Synthesis and to Virgi Hepner, Genevieve MacLellan, and Hilary Selby Polk for science editing of this Synthesis.

REFERENCES

- Balachandran S, Pachon JE, Hu Y, Lee D, Mulholland JA, Russell AG. 2012. Ensemble-trained source apportionment of fine particulate matter and method uncertainty analysis. *Atmos Environ* 61: 387–394.
- Bell ML. 2012. Assessment of the Health Impacts of Particulate Matter Characteristics. Research Report 161. Health Effects Institute, Boston, MA.
- Stanek LW, Sacks JD, Dutton SJ, Dubois JJB. 2011. Attributing health effects to apportioned components and sources of particulate matter: An evaluation of collective results. *Atmos Environ* 45:5655–5663.

ABBREVIATIONS AND OTHER TERMS

ACS	American Cancer Society	MDL	minimum detection limit
ApoE	apolipoprotein E	MESA	Multi-Ethnic Study of Atherosclerosis
CAPs	concentrated ambient particles	MVE	mixed vehicular engine emissions
CIMT	carotid intima-media thickness	NPACT	National Particle Component Toxicity (initiative)
CSN	Chemical Speciation Network	OC	organic carbon
CVD	cardiovascular disease	PM	particulate matter
EC	elemental carbon	PM _{2.5}	particulate matter $\leq 2.5 \mu\text{m}$ in aerodynamic diameter
EPA	Environmental Protection Agency	PMF	positive matrix factorization
LRRI	Lovelace Respiratory Research Institute	RFA	request for applications
MART	multiple additive regression tree	WHI-OS	Women's Health Initiative–Observational Study

RELATED HEI PUBLICATIONS: PARTICULATE MATTER AND DIESEL EXHAUST

Number	Title	Principal Investigator	Date
Research Reports			
177	National Particle Component Toxicity (NPACT) Initiative: Integrated Epidemiologic and Toxicologic Studies of the Health Effects of Particulate Matter Components	M. Lippmann	2013
174	Cardiorespiratory Biomarker Responses in Healthy Young Adults to Drastic Air Quality Changes Surrounding the 2008 Beijing Olympics	J. Zhang	2013
171	Multicity Study of Air Pollution and Mortality in Latin America (the ESCALA Study)	I. Romieu	2012
167	Assessment and Statistical Modeling of the Relationship Between Remotely Sensed Aerosol Optical Depth and PM _{2.5} in the Eastern United States	C.J. Paciorek	2012
166	Advanced Collaborative Emissions Study (ACES) Subchronic Exposure Results: Biologic Responses in Rats and Mice and Assessment of Genotoxicity		2012
164	Pulmonary Particulate Matter and Systemic Microvascular Dysfunction	T.R. Nurkiewicz	2011
161	Assessment of the Health Impacts of Particulate Matter Characteristics	M.L. Bell	2012
160	Personal and Ambient Exposures to Air Toxics in Camden, New Jersey	P. Lioy	2011
158	Air Toxics Exposure from Vehicle Emissions at a U.S. Border Crossing: Buffalo Peace Bridge Study	J.D. Spengler	2011
156	Concentrations of Air Toxics in Motor Vehicle-Dominated Environments	E.M. Fujita	2011
153	Improved Source Apportionment and Speciation of Low-Volume Particulate Matter Samples	J.J. Schauer	2010
152	Evaluating Heterogeneity in Indoor and Outdoor Air Pollution Using Land-Use Regression and Constrained Factor Analysis	J.I. Levy	2010
147	Atmospheric Transformation of Diesel Emissions	B. Zielinska	2010
145	Effects of Concentrated Ambient Particles and Diesel Engine Exhaust on Allergic Airway Disease in Brown Norway Rats	J.R. Harkema	2009
143	Measurement and Modeling of Exposure to Selected Air Toxics for Health Effects Studies and Verification by Biomarkers	R.M. Harrison	2009
142	Air Pollution and Health: A European and North American Approach (APHENA)	K. Katsouyanni	2009
140	Extended Follow-Up and Spatial Analysis of the American Cancer Society Study Linking Particulate Air Pollution and Mortality	D. Krewski	2009
139	Effects of Long-Term Exposure to Traffic-Related Air Pollution on Respiratory and Cardiovascular Mortality in the Netherlands: The NLCS-AIR Study	B. Brunekreef	2009
138	Health Effects of Real-World Exposure to Diesel Exhaust in Persons with Asthma	J. Zhang	2009

Continued

Copies of these reports can be obtained from HEI; pdf's are available for free downloading at <http://pubs.healtheffects.org>.

RELATED HEI PUBLICATIONS: PARTICULATE MATTER AND DIESEL EXHAUST

Number	Title	Principal Investigator	Date
129	Particle Size and Composition Related to Adverse Health Effects in Aged, Sensitive Rats	F.F. Hahn	2005
124	Particulate Air Pollution and Nonfatal Cardiac Events <i>Part I.</i> Air Pollution, Personal Activities, and Onset of Myocardial Infarction in a Case–Crossover Study <i>Part II.</i> Association of Air Pollution with Confirmed Arrhythmias Recorded by Implanted Defibrillators	A. Peters D. Dockery	2005
122	Personal, Indoor, and Outdoor Exposures to PM _{2.5} and Its Components for Groups of Cardiovascular Patients in Amsterdam and Helsinki	B. Brunekreef	2005
118	Controlled Exposures of Healthy and Asthmatic Volunteers to Concentrated Ambient Particles in Metropolitan Los Angeles	H. Gong Jr.	2003
112	Health Effects of Acute Exposure to Air Pollution <i>Part I.</i> Healthy and Asthmatic Subjects Exposed to Diesel Exhaust <i>Part II.</i> Healthy Subjects Exposed to Concentrated Ambient Particles	S.T. Holgate	2003
110	Particle Characteristics Responsible for Effects on Human Lung Epithelial Cells	A.E. Aust	2002
94	The National Morbidity, Mortality, and Air Pollution Study <i>Part II.</i> Morbidity and mortality from air pollution in the United States	J.M. Samet	2000
HEI Special Reports			
17	Traffic-Related Air Pollution: A Critical Review of the Literature on Emissions, Exposure, and Health Effects		2010
	Research Directions to Improve Estimates of Human Exposure and Risk from Diesel Exhaust	HEI Diesel Epidemiology Working Group	2002
	Diesel Emissions and Lung Cancer: Epidemiology and Quantitative Risk Assessment	HEI Diesel Epidemiology Expert Panel	1999
HEI Communication			
10	Improving Estimates of Diesel and Other Emissions for Epidemiologic Studies		2003
HEI Perspectives			
	Understanding the Health Effects of Ambient Ultrafine Particles		2013
	Understanding the Health Effects of Components of the Particulate Matter Mix: Progress and Next Steps		2002

Copies of these reports can be obtained from HEI; pdf's are available for free downloading at <http://pubs.healtheffects.org>.

HEI BOARD, COMMITTEES, and STAFF

Board of Directors

Richard F. Celeste, Chair *President Emeritus, Colorado College*

Sherwood Boehlert *Of Counsel, Accord Group; Former Chair, U.S. House of Representatives Science Committee*

Enriqueta Bond *President Emerita, Burroughs Wellcome Fund*

Purnell W. Choppin *President Emeritus, Howard Hughes Medical Institute*

Michael T. Clegg *Professor of Biological Sciences, University of California—Irvine*

Jared L. Cohon *President Emeritus and Professor, Civil and Environmental Engineering and Engineering and Public Policy, Carnegie Mellon University*

Stephen Corman *President, Corman Enterprises*

Gowher Rizvi *Vice Provost of International Programs, University of Virginia*

Linda Rosenstock *Dean Emerita and Professor of Health Policy and Management, Environmental Health Sciences and Medicine, University of California—Los Angeles*

Henry Schacht *Managing Director, Warburg Pincus; Former Chairman and Chief Executive Officer, Lucent Technologies*

Warren M. Washington *Senior Scientist, National Center for Atmospheric Research; Former Chair, National Science Board*

Archibald Cox, Founding Chair *1980–2001*

Donald Kennedy, Vice Chair Emeritus *Editor-in-Chief Emeritus, Science; President Emeritus and Bing Professor of Biological Sciences, Stanford University*

Health Research Committee

David L. Eaton, Chair *Dean and Vice Provost of the Graduate School, University of Washington—Seattle*

David Christiani *Elkan Blout Professor of Environmental Genetics, Harvard School of Public Health*

David E. Foster *Phil and Jean Myers Professor Emeritus, Department of Mechanical Engineering, Engine Research Center, University of Wisconsin—Madison*

Uwe Heinrich *Professor, Medical School Hannover; Executive Director, Fraunhofer Institute for Toxicology and Experimental Medicine, Hanover, Germany*

Grace LeMasters *Professor of Epidemiology and Environmental Health, University of Cincinnati College of Medicine*

Sylvia Richardson *Professor and Director, MRC Biostatistics Unit, Institute of Public Health, Cambridge, United Kingdom*

Allen L. Robinson *Raymond J. Lane Distinguished Professor and Head, Department of Mechanical Engineering, and Professor, Department of Engineering and Public Policy, Carnegie Mellon University*

Richard L. Smith *Director, Statistical and Applied Mathematical Sciences Institute, University of North Carolina—Chapel Hill*

James A. Swenberg *Kenan Distinguished Professor of Environmental Sciences, Department of Environmental Sciences and Engineering, University of North Carolina—Chapel Hill*

HEI BOARD, COMMITTEES, and STAFF

Health Review Committee

Homer A. Boushey, Chair *Professor of Medicine, Department of Medicine, University of California—San Francisco*

Ben Armstrong *Reader in Epidemiological Statistics, Public and Environmental Health Research Unit, Department of Public Health and Policy, London School of Hygiene and Tropical Medicine, United Kingdom*

Michael Brauer *Professor, School of Environmental Health, University of British Columbia, Canada*

Bert Brunekreef *Professor of Environmental Epidemiology, Institute of Risk Assessment Sciences, University of Utrecht, the Netherlands*

Mark W. Frampton *Professor of Medicine and Environmental Medicine, University of Rochester Medical Center*

Stephanie London *Senior Investigator, Epidemiology Branch, National Institute of Environmental Health Sciences*

Armistead Russell *Howard T. Tellepsen Chair of Civil and Environmental Engineering, School of Civil and Environmental Engineering, Georgia Institute of Technology*

Lianne Sheppard *Professor of Biostatistics, School of Public Health, University of Washington—Seattle*

Officers and Staff

Daniel S. Greenbaum *President*

Robert M. O’Keefe *Vice President*

Rashid Shaikh *Director of Science*

Barbara Gale *Director of Publications*

Jacqueline C. Rutledge *Director of Finance and Administration*

Helen I. Dooley *Corporate Secretary*

Kate Adams *Senior Scientist*

Hanna Boogaard *Staff Scientist*

Aaron J. Cohen *Principal Scientist*

Maria G. Costantini *Principal Scientist*

Philip J. DeMarco *Compliance Manager*

Hope Green *Editorial Assistant (part time)*

L. Virgi Hepner *Senior Science Editor*

Anny Luu *Administrative Assistant*

Francine Marmenout *Senior Executive Assistant*

Nicholas Moustakas *Policy Associate*

Hilary Selby Polk *Senior Science Editor*

Jacqueline Presedo *Research Assistant*

Sarah Rakow *Science Administrative Assistant*

Robert A. Shavers *Operations Manager*

Matt Storm *Staff Accountant*

Geoffrey H. Sunshine *Senior Scientist*

Annemoon M.M. van Erp *Managing Scientist*

Katherine Walker *Senior Scientist*



HEALTH
EFFECTS
INSTITUTE

101 Federal Street, Suite 500
Boston, MA 02110, USA
+1-617-488-2300
www.healtheffects.org

RESEARCH
REPORT

Number 178
October 2013